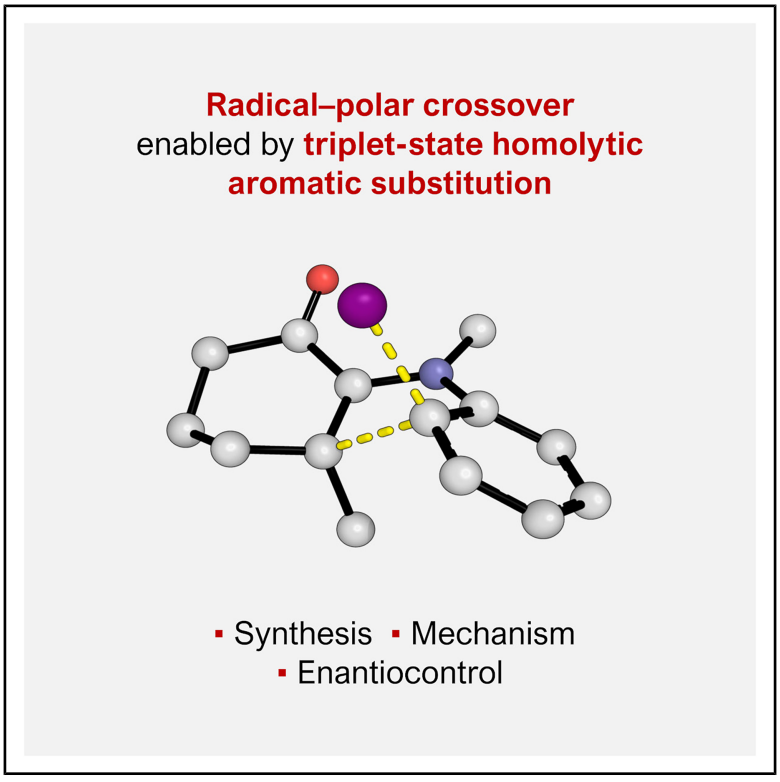
Chem

Article

A radical–polar crossover approach to complex nitrogen heterocycles via the triplet state

Graphical abstract



Authors

Zachariah Lockhart, Mihai V. Popescu, Juan V. Alegre-Requena, Jay Ahuja, Shaokang Chai, Robert S. Paton, Martin D. Smith

Correspondence

robert.paton@colostate.edu (R.S.P.), martin.smith@chem.ox.ac.uk (M.D.S.)

In brief

Precisely positioning a leaving group has been shown to divert certain alkene photocyclizations from isomerization—the usual result of this type of reaction—to iminium salt formation. Trapping this ionic intermediate with nucleophiles enables the rapid assembly of structurally complex and chemically diverse nitrogen-containing ring systems.

Highlights

- Visible-light excitation of *N*-(2-iodoaryl) enaminones yields iminium salts
- A homolytic aromatic substitution (HAS) mechanism prevails in the triplet state
- Electron donation into the σ^*_{C-I} orbital during cyclization dictates selectivity
- *S*-to-*C* chirality transfer occurs when an *ortho*-sulfinyl substituent is used

Lockhart et al., 2026, Chem *12*, 102904
July 9, 2026 © 2026 The Authors. Published by Elsevier Inc.
https://doi.org/10.1016/j.chempr.2025.102904

CellPress

Please cite this article in press as: Lockhart et al., A radical–polar crossover approach to complex nitrogen heterocycles via the triplet state, Chem (2026), https://doi.org/10.1016/j.chempr.2025.102904

Chem

CellPress
OPEN ACCESS

Article

A radical–polar crossover approach to complex nitrogen heterocycles via the triplet state

Zachariah Lockhart,[1] Mihai V. Popescu,[1,2] Juan V. Alegre-Requena,[2,3] Jay Ahuja,[1] Shaokang Chai,[1] Robert S. Paton,[2,*] and Martin D. Smith[1,4,*]

[1]Chemistry Research Laboratory, University of Oxford, 12 Mansfield Road, Oxford OX1 3TA, UK
[2]Department of Chemistry, Colorado State University, 1301 Center Ave., Ft. Collins, CO 80523-1872, USA
[3]Departamento de Química Inorgánica, Instituto de Síntesis Química y Catálisis Homogénea (ISQCH), CSIC-Universidad de Zaragoza, C/ Pedro Cerbuna 12, Zaragoza 50009, Spain
[4]Lead contact
*Correspondence: robert.paton@colostate.edu (R.S.P.), martin.smith@chem.ox.ac.uk (M.D.S.)
https://doi.org/10.1016/j.chempr.2025.102904

THE BIGGER PICTURE Triplet excited states typically undergo radical-like addition and recombination processes in a stepwise manner. Here, we introduce a new radical–polar crossover (RPC) method that integrates the one-electron (radical) reactivity of triplet excited states with the two-electron (polar) reactivity of nucleophiles, using alkenes as a chromophore instead of a radical acceptor or electron donor and affording complex three-dimensional heterocycles that are not available by other photochemical means. The mechanistic insights presented here into this "interrupted" photocyclization will inspire the development of other triplet-state reactions incorporating RPC. In time, broader application of triplet-mediated RPC methods could reduce the resource intensity of pharmaceutical, agrochemical, and materials development, aligning with sustainable chemistry goals such as responsible consumption and production (UN SDG 12).

SUMMARY

The transition from radical to ionic reactivity is a key design feature of many photochemical reactions, enabling complex transformations not possible under either mechanistic regime alone. Ground-state alkenes are common substrates in existing methods of this type, serving as radical acceptors to generate open-shell intermediates from which the radical–polar crossover (RPC) event is oxidatively or reductively triggered by a photocatalyst. Here, we describe an alternative RPC mechanism proceeding via an alkene triplet diradical. In this transformation, an iodine radical liberated during a homolytic aromatic substitution step functions as a single-electron oxidant to generate an iminium electrophile that can be intercepted en route to complex natural-product-like amines. An enantioselective variant of the reaction, enabled by an oxidatively installed sulfinyl leaving group, points to the generality of this underdeveloped pattern of diradical reactivity, paving the way for other triplet-state reactions that incorporate both one- and two-electron bond-forming processes.

INTRODUCTION

The addition of carbon-centered radicals to ground-state alkenes offers a versatile route for the formation of challenging carbon–carbon bonds, and also enables an increase in molecular complexity through the onward reaction of the subsequently formed radical. This intermediate is often trapped in a radical termination step but may also react via a polar (non-radical) step.[1] When the initial formation of radicals is mediated by an excited-state photocatalyst, these intermediates can undergo a single-electron oxidation (to generate a cationic intermediate) or a single-electron reduction (to generate an anionic intermediate).[2–5] These ionic species may then engage in two-electron reactions to yield diverse products (Figure 1A).

This radical–polar crossover (RPC) is the basis of many photoredox processes and has enabled a wide range of impactful transformations.[6–8,11–13] A conceptually related yet mechanistically distinct process is the reaction of alkene radical cations with nucleophiles to yield radical intermediates (Figure 1B). Notably, the Nicewicz laboratory has harnessed this reactivity to enable a wide array of photocatalytic anti-Markovnikov functionalizations of alkenes.[9] Although a radical termination step (such as hydrogen atom transfer) usually follows nucleophilic addition to alkene radical cations, RPC can also be integrated into reaction sequences comprising these intermediates. An impressive example of this reactivity was reported by Yoon and colleagues involving the cyclization of pendent heteroatom nucleophiles onto alkenes following single-electron oxidation

This is an open access article under the CC BY license (http://creativecommons.org/licenses/by/4.0/).

Please cite this article in press as: Lockhart et al., A radical–polar crossover approach to complex nitrogen heterocycles via the triplet state, Chem (2026), https://doi.org/10.1016/j.chempr.2025.102904

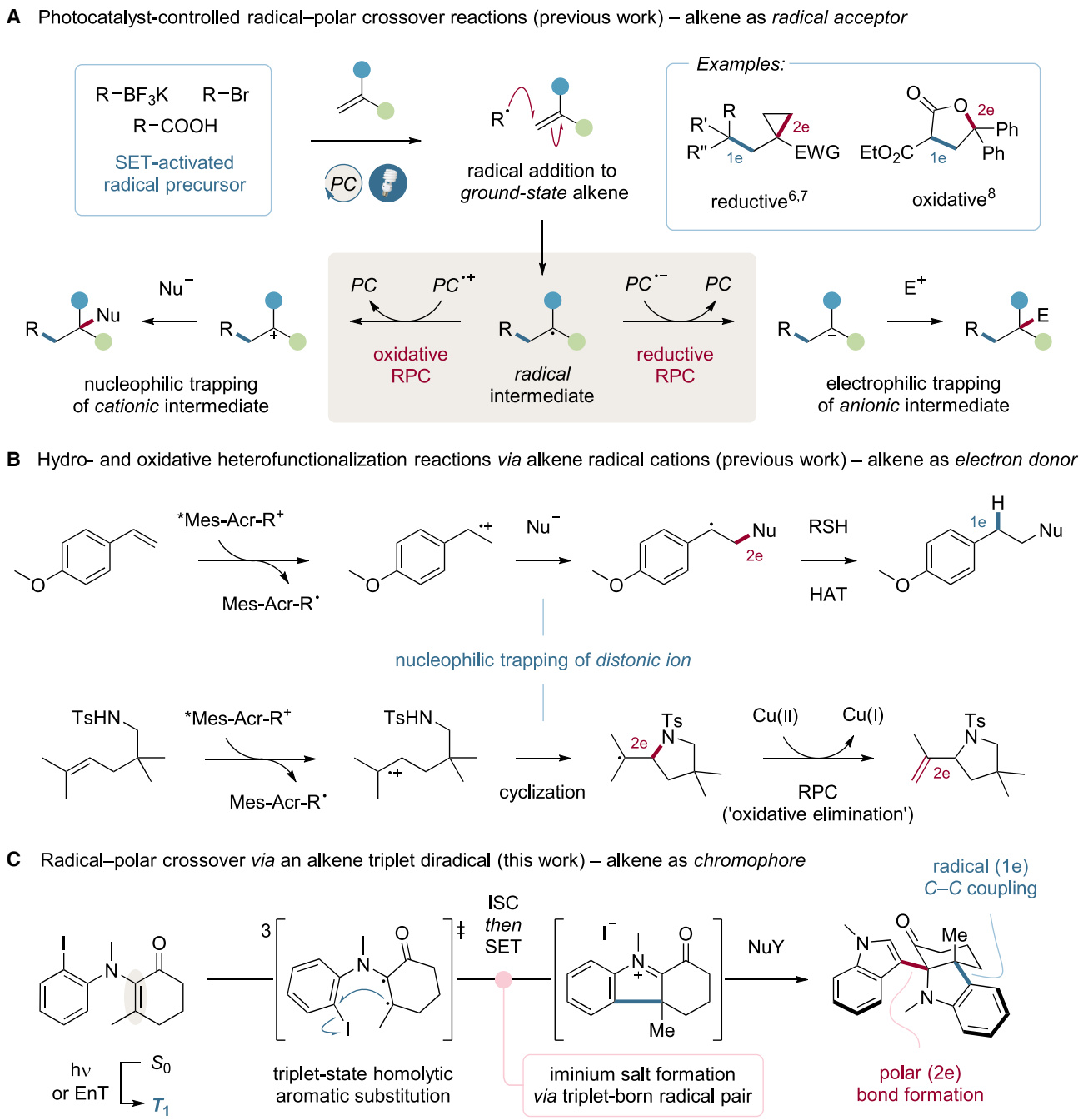


Figure 1. Photochemical approaches to RPC reactions

(A) Previous work: RPC can occur when alkenes function as radical acceptors; subsequent one-electron oxidation or reduction leads to intermediates that can be trapped in two-electron bond-forming processes. This reactivity can be exemplified in the reductive formation of cyclopropanes[6,7] and the oxidative generation of lactones[8] from alkenes under photoredox catalysis.

(B) Previous work: alkene radical cations react with nucleophiles to generate radical intermediates; they do not themselves display radical reactivity. Thiols are frequently used to reduce these intermediates via a radical hydrogen atom transfer (HAT) mechanism and facilitate turnover of the highly oxidizing photocatalyst required to activate the alkene substrate[9]; alternatively, when used in stoichiometric quantities, copper(II) salts can promote RPC, permitting two successive two-electron bond-forming processes.[10]

(C) This work: a transition from diradical to ionic reactivity occurring from the triplet excited state. Following a regioselective radical cyclization step, ISC and SET lead to an iminium salt that can be intercepted through a polar nucleophilic mechanism.

PC, photocatalyst; EWG, electron-withdrawing group; Mes-Acr, mesityl acridinium; EnT, energy transfer; NuY, nucleophile (e.g., 1-methylindole).

Please cite this article in press as: Lockhart et al., A radical–polar crossover approach to complex nitrogen heterocycles via the triplet state, Chem (2026), https://doi.org/10.1016/j.chempr.2025.102904

of the latter.[10] However, while this reaction incorporates an RPC step, the transition does not enable a merger of radical and polar reactivities; instead, the copper-mediated sequence consists of two successive two-electron bond-forming steps, the latter of which (elimination to form a C=C bond) does not contribute to an increase in molecular complexity.

In contrast, RPC reactions have not been exploited where alkenes act as a *chromophore* rather than a radical acceptor or electron donor. This approach could allow for the combination of polar reactivities, such as nucleophilic addition, with diradical reactivities characteristic of triplet states but not accessible to either free radicals or alkene radical cations, such as six-electron photocyclization. Here we introduce one such RPC strategy. Following photochemical activation of an alkene by direct excitation or triplet energy transfer, a homolytic aromatic substitution (HAS) mechanism takes place in the triplet state, effectively "interrupting"[14] a 6π-type photocyclization and giving rise to an iminium salt that can be trapped intra- or intermolecularly by diverse two-electron nucleophiles (Figure 1C). This photocyclization–cation trapping cascade[15,16] leads to the generation of complex three-dimensional templates containing an array of functional groups not present in the substrate, with high levels of both regio- (with respect to any arene *meta*-substituents) and diastereoselectivity (with respect to the fully substituted ring junction). Thus, the transformation also contrasts with traditional (typically UV-mediated) 6π photocyclizations,[17–21] which give rise to isomerization products via singlet diradical/zwitterionic intermediates, with minimal control over the direction of cyclization in unsymmetrical substrates and no obvious opportunities for vicinal difunctionalization of the mutating chromophore.

RESULTS AND DISCUSSION

We have previously examined the energy transfer-mediated[22] isomerization of *N*-aryl enaminones,[23] and observed that an outlier in their reactivity was that the *ortho*-iodinated substrate **1** led to the exclusive formation of indole **2** as a single regioisomer, without *ipso*-H diradical cyclization products **3** in detectable quantities (Figure 2A). It was hypothesized that this product arises from either the cyclization of a photolytically generated aryl radical onto the enone in a 5-*endo*-*trig*[24] fashion or a selective *ipso*-I substitution and net-eliminative cyclization process upon excitation of the enone to its triplet state.[25–27] Eliminative photocyclizations such as this have previously been applied in the generation of aromatic systems in natural products and the development of new materials.[28,29] We designed *N*-allyl substrate **4** to probe the formation of an aryl radical, reasoning that a 5-*exo*-*trig* mode would be competitive with any other cyclization (Figure 2B). In the presence of an iridium sensitizer and 467 nm light, **4** yielded indole **5** (86% yield), and bridged cyclobutane **6** (10% yield); 5-*exo*-*trig* cyclization products **7** were not observed. This result is consistent with energy transfer activation of the enone in **4** and subsequent *ipso*-I cyclization to yield **5**, with competitive [2+2] cycloaddition onto the *N*-allyl group to yield **6**.[30]

A control experiment in which **4** was reduced using a neutral organic super-electron donor[31] gave a mixture of 5-*exo*- and 5-*endo*-*trig* aryl radical cyclization products, demonstrating the viability of both cyclization modes whenever the aryl radical in question is generated thermally (see Section S3.3.1). Thus, the failure to observe 5-*exo*-*trig* products upon sensitized irradiation of **4** suggests that an aryl radical does not form under photochemical activation of this and related compounds. Instead, a mechanism involving the regioselective cyclization of an alkene triplet diradical is more likely (Figure 2C). We reasoned that such a process would lead initially to a radical pair, **8**, which could be expected, upon intersystem crossing (ISC) and single-electron transfer (SET), to form an iminium iodide salt, **9**. Thus, provided re-aromatization is prevented, it should be possible to effect a net-eliminative 1,2-difunctionalization of the alkene functional group in compounds such as **10** through the thermal trapping of this cationic photoproduct with different two-electron nucleophiles. This would represent a key strategic advance: typically, 6π-type photocyclizations do not allow for diversification through the nucleophilic (or electrophilic) trapping of an ionic intermediate (instead, the formation of singlet zwitterionic/diradical intermediates typically precedes hydrogen shift and/or proton transfer processes, as in our previous work[23,32]). Our triplet-state approach to iminium ion formation would also constitute a distinct but complementary strategy to existing RPC processes. To explore this possibility, substrate **10**, which absorbs weakly in the visible region and bears a methyl substituent at the enone β-position, was synthesized and irradiated with 427 nm light in an acetonitrile–water mixture. In the absence of a photocatalyst and the presence of potassium acetate, this yielded hemiaminal **11** in 89% yield as a single diastereoisomer. The observed product is consistent with *in situ* base-promoted hydrolysis of an iminium salt; this putative intermediate was formally generated and characterized by nuclear magnetic resonance (NMR) spectroscopy as enol species **12** by treating the hemiaminal product with trifluoroacetic acid in acetonitrile-d_3 solution.

With evidence in hand for the photochemical generation of an iminium cation, we sought to explore the scope of the reaction with respect to the nucleophilic coupling partner (Figure 3A). (Details of reaction optimization and considerations regarding the use of a photocatalyst can be found in Section S5.) Thus, irradiation of β-methyl substrate **10** with 427 nm light in the presence of *N*-methylindole in a polar solvent mixture gave the complex heterocycle **13** as a single diastereoisomer in 81% yield and >40:1 ratio of eliminative to non-eliminative cyclization. The *N*-substituent on the indole is not necessary for reactivity, and **14** can be isolated in 83% yield by the addition of 1*H*-indole as the nucleophile. Other π-rich heterocycles are also reactive: addition of 2,4-dimethylpyrrole yields **15** (68% yield), while 3-methoxythiophene affords **16** (44% yield) and 2-methylfuran leads to **17** (59% yield). Potassium trifluoroborate salts may also be used as nucleophiles in a process reminiscent of the borono-Petasis reaction,[33,34] enabling the formal addition of furan (**18**, 55% yield), styrenes (**19**, 66% yield), and alkynes (**20**, 53% yield). Reduction of the iminium cation through addition of triethylsilane led to **21** (80% yield); this process also enables the synthesis of the deuterated analog **22** (79% yield, >99% D). Addition of allyltrimethylsilane to form **23** was also successful (80% yield). The trimethylsilyl enol ether derived from acetophenone could be employed in anhydrous nitromethane solvent, in the presence of sodium trifluoroacetate, to generate

Please cite this article in press as: Lockhart et al., A radical–polar crossover approach to complex nitrogen heterocycles via the triplet state, Chem (2026), https://doi.org/10.1016/j.chempr.2025.102904

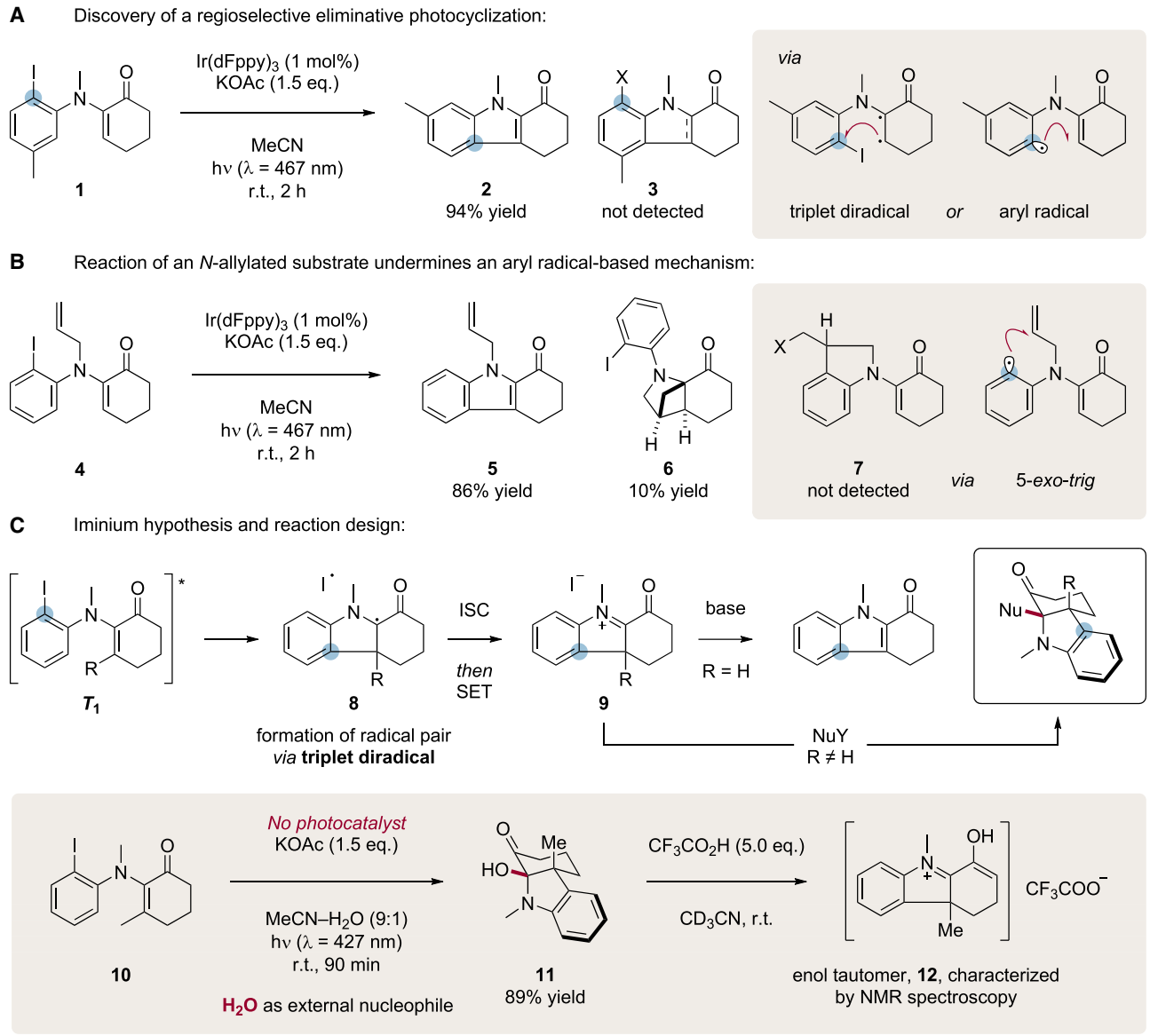


Figure 2. Overview of reaction development

(A) Observation of an unexpected product leads to the development of an eliminative alkene difunctionalization reaction.

(B) Tethering an alkene radical acceptor through nitrogen indicates that the intermediacy of an aryl radical is unlikely and that the observed reactivity is more consistent with a triplet-state mechanism. X = H or I.

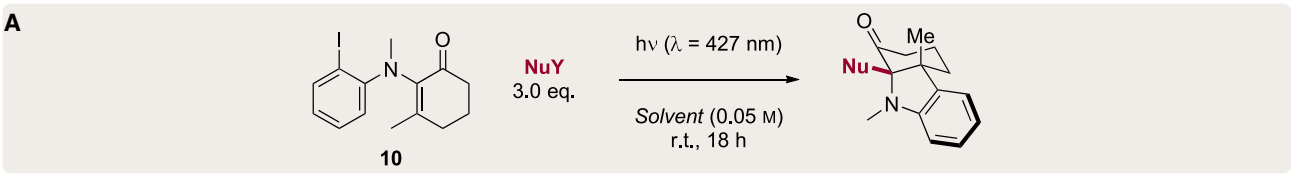
(C) Reaction design and validation: the formation of an iminium salt as the primary photoproduct of the reaction is supported by the isolation of hemiaminal **11** upon the direct irradiation of a β-methylated substrate, **10**, in which re-aromatization is prevented; treating the former compound with trifluoroacetic acid enables the identification of the putative iminium ion intermediate as enol **12**.

1,4-diketone **24** (57% yield), which was subsequently examined by single-crystal X-ray diffraction. Toluenesulfonylmethyl isocyanide (TosMIC) was added smoothly in aqueous acetonitrile to produce amide **25** in 74% yield and with complete diastereoselectivity. We were also able to move beyond the formation of carbon–carbon bonds. Performing the reaction in the presence of diethylphosphite led to the formation of aminophosphonate **26** in 57% yield as the *cis*-diastereomer (19:1 diastereomeric ratio). Water (to afford **11** in 89% yield) and methanol (to give **27** in 77% yield) are also proficient trapping agents in the presence of bases. The potential of this process to generate complex natural-product-like[35] heterocycles was demonstrated by tethering a nucleophile to enable intramolecular trapping. Irradiation of **28**, which bears a pendent carbamate functional group, led to the formation of bridged tetracycle **29** in 88% yield, the structure of which was confirmed through X-ray crystallography.

We were also able to install different substituents in the enone β-position with minimal impact on the efficiency of the cyclization

Please cite this article in press as: Lockhart et al., A radical–polar crossover approach to complex nitrogen heterocycles via the triplet state, Chem (2026), https://doi.org/10.1016/j.chempr.2025.102904

CellPress
OPEN ACCESS



13 81% yield
Y = H
MeCN–HFIP (9:1)

14 83% yield
Y = H
MeCN–HFIP (9:1)

15 68% yield
Y = H
MeCN–H_2O (9:1)

16[a] 44% yield
Y = H
MeCN–HFIP (9:1)

17 59% yield
Y = H
MeCN–HFIP (9:1)

18 55% yield
Y = BF_3K
MeCN–H_2O (3:1)

19[b] 66% yield
Y = BF_3K
MeCN–H_2O (3:1)

20[b] 53% yield
Y = BF_3K
MeCN–H_2O (3:1)

21[c] 80% yield
Y = $SiEt_3$
MeCN–H_2O (9:1)

22[c] 79% yield (>99% D)
Y = $SiEt_3$
MeCN–H_2O (9:1)

23 80% yield
Y = $SiMe_3$
MeCN–HFIP (9:1)

24 57% yield
NuY = $PhC(OSiMe_3)=CH_2$
CF_3COONa (1.0 eq.), $MeNO_2$

≡ CCDC 2243733

25 74% yield
NuY = TosMIC
MeCN–H_2O (9:1)

26 57% yield
Y = H
MeCN–H_2O (9:1)

11[d] 89% yield
KOAc (1.5 eq.)
MeCN–H_2O (9:1)

27[e,f] 77% yield
K_3PO_4 (1.5 eq.)
MeCN–MeOH (9:1)

29[g] 88% yield
MeCN–H_2O (9:1)

≡ CCDC 2243732 *from* **28**

B

30 – 64% yield

31 – 42% yield

32 – 42% yield

33 – 53% yield

34 – 57% yield

35 – 62% yield

36 – 58% yield

37 (R = NO_2)[a,h] – 29% yield (64%[i])
38 (R = NHCOMe) – 69% yield
39 (R = Br) – 79% yield
40 (R = I) – 72% yield

(legend on next page)

Please cite this article in press as: Lockhart et al., A radical–polar crossover approach to complex nitrogen heterocycles via the triplet state, Chem (2026), https://doi.org/10.1016/j.chempr.2025.102904

process. A β-ethyl substrate was irradiated in the presence of TosMIC to afford **30** in 64% yield (Figure 3B). An *N*-acyl piperidinyl substituent was also tolerated, producing **31** in 42% yield. Different *N*-substitution patterns are also possible: products bearing *N*-allyl **32** (alongside 6% of a competitive [2+2] product) and *N*-benzyl **33** groups were effectively generated in yields of 42% and 53%, respectively. Enaminones of varying ring sizes are likewise tolerated, as evidenced by the successful reaction to form fused cyclopentanone **34** in 57% yield. We were able to exemplify the regioselective nature of this transformation through the incorporation of substituents at either *meta*-position. The cyclization of a 5-chloro-2-iodo substrate and subsequent trapping with TosMIC afforded **35** (62% yield) without formation of the alternative regioisomer in detectable quantities. Similarly, a 3-methyl-2-iodo substrate cyclizes regioselectively to yield **36** (58% yield). The introduction of *para*-substituents on the aromatic ring is also possible. While *para*-nitro product **37** was generated in moderate yield (29%) with substantial starting substrate recovery, other groups in this position cyclize effectively: *para*-*N*-acetyl **38** (69% yield), *para*-bromo **39** (79% yield), and *para*-iodo **40** (72% yield) products were all formed efficiently.

Although we had satisfactorily demonstrated that the reaction does not proceed via an aryl radical, the origin of the underlying regioselectivity was challenging to interpret, and hence we applied a combination of experimental and computational techniques to address this problem. UV-visible absorption spectroscopy revealed a band centered at *ca.* 345 nm that extends above 400 nm for β-methyl substrate **10**; due to its weakly absorbing nature, this was assigned to an $n\pi^*$ transition between the ground and first excited singlet (S_1) state, in accordance with previous photophysical studies of cyclohexenones and their derivatives.[36–38] Since ISC from this state is known to be fast for cyclic enones,[39,40] we expect that bond formation proceeds via the T_1 state. This tenet is consistent with the substantial rate acceleration observed (without change in product distribution) for the photocyclization of **41** (triplet-state energy, $E_T \approx 48$ kcal mol^{-1}) in the presence of catalytic Ir(dFppy)$_3$ (E_T = 60.1 kcal mol^{-1}).[41] Upon irradiation with a 467 nm Kessil lamp in acetonitrile solution, indole **42** was formed in 99% yield under these conditions; in contrast, a significantly lower yield of 13% (14% conversion) was obtained in the photocatalyst's absence (Figure 4A). The iridium complex is not sufficiently oxidizing ($E_{1/2}[Ir^{III*}/Ir^{II}]$ = +0.39 V vs. Fc$^+$/Fc [ferrocenium/ferrocene]) or reducing ($E_{1/2}[Ir^{IV}/Ir^{III*}]$ = −1.23 V vs. Fc$^+$/Fc) in the excited state to activate **41** (whose half-wave oxidation and reduction potentials were measured as +0.73 V and −2.42 V, respectively, vs. Fc$^+$/Fc) by SET, implicating triplet energy transfer as the mode of catalysis. Moreover, Mulliken spin density calculations (see Section S4.5) suggest that single-electron oxidation of the enaminone substrates used here would yield what is essentially an amine radical cation with negligible radical character at the enone β-position, further undermining the possibility of cyclization via an alkene radical cation.

Additional evidence for triplet-state generation in the absence of sensitizer includes the observation of a competing [2+2]-photocycloaddition (known to be a fast triplet process)[42,43] in the reaction to form **32**, as well as a substantial reduction in conversion (and attendant formation of oxidative degradation products) observed when **10** was irradiated in the presence of oxygen[44,45]; see Sections S3.2.5, S3.2.6, and S3.2.7 for more detail.

We proceeded to study the reaction mechanism with density functional theory (DFT) at the M06-2X-D3/def2-QZVPP//M06-2X-D3/def2-TZVP level (Figures 4B and 4C). Once the triplet-state ^{3}**A** (which has an adiabatic triplet energy of 48.3 kcal mol^{-1}) is reached, a conrotatory ring-closure to form a new C–C bond can proceed either *ipso*- to the iodine substituent (via **TS-I** [TS, transition state] to furnish intermediate ^{3}**B**) or at the unsubstituted position (via **TS-II** leading to intermediate ^{3}**C**). Computation predicts selective attack at the carbon bearing the iodine substituent ($\Delta\Delta G^‡$ = −0.4 kcal mol^{-1}); this selectivity is maintained across several commonly employed DFT levels of theory, albeit to varying degrees (see Section S4.2). We further performed single-point corrections using multiconfiguration methods (NEVPT2:CASSCF(10,10)/Def2-TZVP) that indicated greater selectivity ($\Delta\Delta G^‡$ = −2.6 kcal mol^{-1}), suggesting that the competition between **TS-I** and **TS-II** is selective toward the formation of intermediate ^{3}**B** in an irreversible and highly exergonic fashion (−40.7 kcal mol^{-1}). Intrinsic reaction coordinate (IRC) calculations performed from **TS-I** revealed that the minimum energy path directly connects intermediate ^{3}**A** to ^{3}**B** without forming a stable σ-intermediate (Figure 4D). Natural bond orbital (NBO) analysis of **TS-I** revealed a Wiberg bond order (WBO) of 0.28 for the forming C–C bond, indicative of an early TS (Figure 4E). The WBO of the C–I bond is 0.90, and the natural spin density on iodine is 0.13, suggesting partial bond-breaking in the TS. That the *ipso*-I cyclization (via **TS-I**) is concerted is consistent with its lower activation energy (vs. **TS-II**): the partial breaking of the C–I bond in the transition structure enables the stabilization of one of the unpaired electrons on the iodine atom. Second-order perturbation theory analysis of natural bonding orbitals indicated that donation into the σ^*_{C-I} orbital from adjacent C–C σ and π bonds of the aromatic system is worth 14.6 kcal mol^{-1}, consistent with a direct and concerted radical *ipso*-I substitution mechanism.[46–48] Similarities can be drawn between this *homolytic* mechanism and that of recently identified concerted *nucleophilic* aromatic substitutions, where a lone pair assists the elimination of bromide in a concerted fashion.[49,50] The resulting triplet radical pair ^{3}**B** is expected to undergo spontaneous ISC, as one of the unpaired electrons is fully localized on a heavy iodine

Figure 3. Scope of the reaction

Variation of (A) the nucleophilic coupling partner (NuY) and (B) the substrate. Reaction conditions (unless otherwise stated): **10** or corresponding substrate (0.3 mmol, 1.0 equiv), NuY (0.9 mmol, 3.0 equiv), solvent(s) (v/v) (0.05 M) (TosMIC [3.0 equiv] and MeCN–H_2O [9:1] for all reactions in B), room temperature (r.t.), 2 × Kessil PR160L 427 nm lamps, 18 h. [a]5.0 equiv NuY. [b]1.5 equiv NuY. [c]6 h reaction time. [d]90 min reaction time. [e]This compound was isolated and characterized without chromatographic purification owing to its instability on silica and alumina gels; the reported yield was measured for a 0.1 mmol-scale reaction by quantitative ^{1}H NMR spectroscopy against dimethyl terephthalate. [f]2 h reaction time. [g]3 h reaction time. [h]21 h reaction time. [i]Yield based on recovered starting material.

Please cite this article in press as: Lockhart et al., A radical–polar crossover approach to complex nitrogen heterocycles via the triplet state, Chem (2026), https://doi.org/10.1016/j.chempr.2025.102904

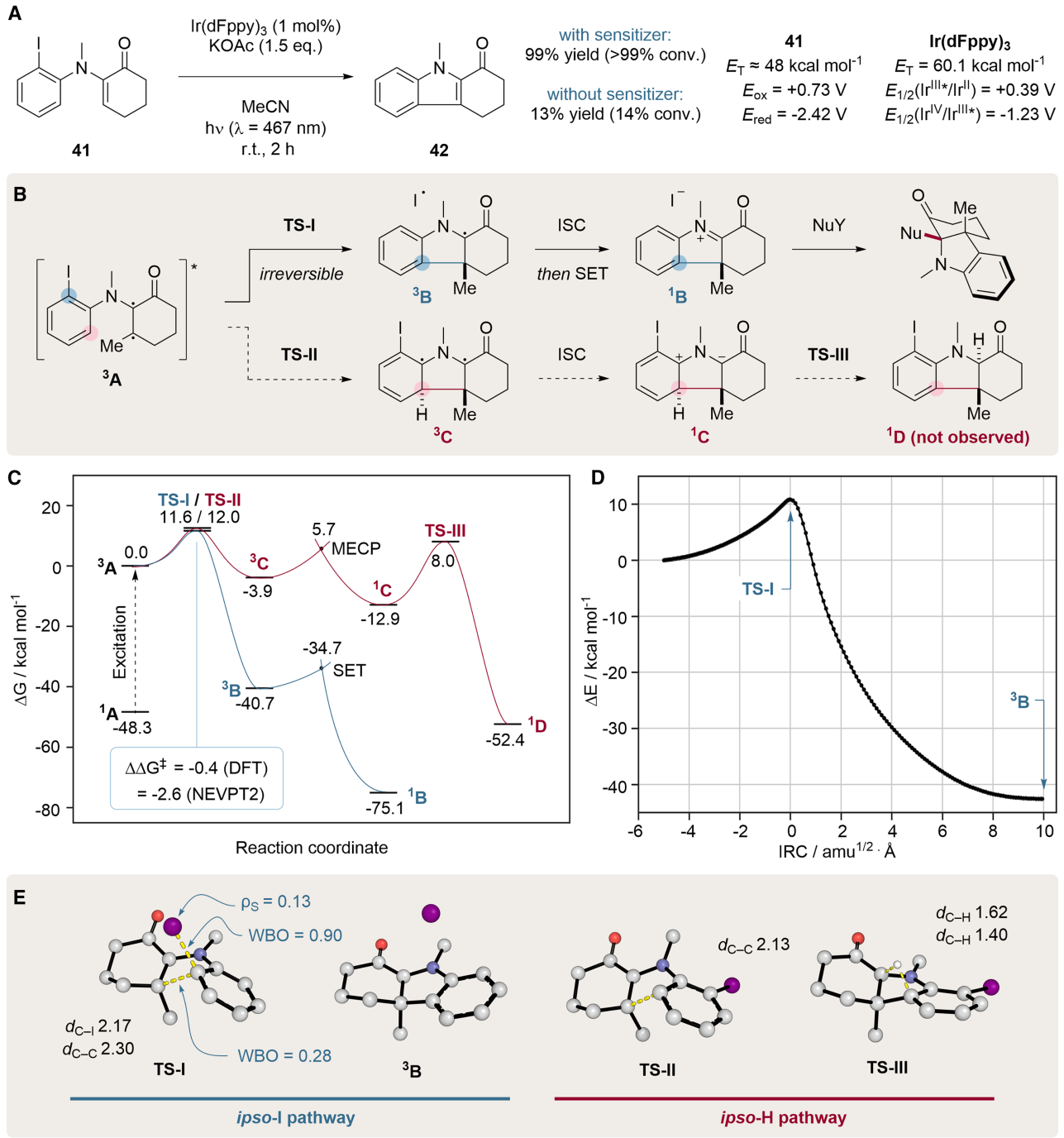


Figure 4. Experimental and computational mechanistic investigations

(A) A sensitization experiment is consistent with the reaction proceeding via the triplet state. Conversions and yields were measured by quantitative ^{1}H NMR spectroscopy against dimethyl terephthalate; redox potentials are relative to Fc^{+}/Fc.

(B) Proposed reaction mechanism, in which an irreversible *ipso*-I cyclization step is selectivity-determining.

(C) Potential energy surfaces for the *ipso*-H and *ipso*-I cyclization pathways available to intermediate **^{3}A**, computed at the M06-2X-D3/def2-QZVPP(SMD=MeCN)//M06-2X-D3/def2-TZVP(SMD=MeCN) level.

(D) IRC computed for **TS-I**.

(E) Computed structures of transition states **TS-I–III** and triplet intermediate **^{3}B**; distances, d, in Å are indicated by dotted lines.

MECP, minimum energy crossing point; amu, atomic mass units; WBO, Wiberg bond order; ρ_S, natural spin density.

Please cite this article in press as: Lockhart et al., A radical–polar crossover approach to complex nitrogen heterocycles via the triplet state, Chem (2026), https://doi.org/10.1016/j.chempr.2025.102904

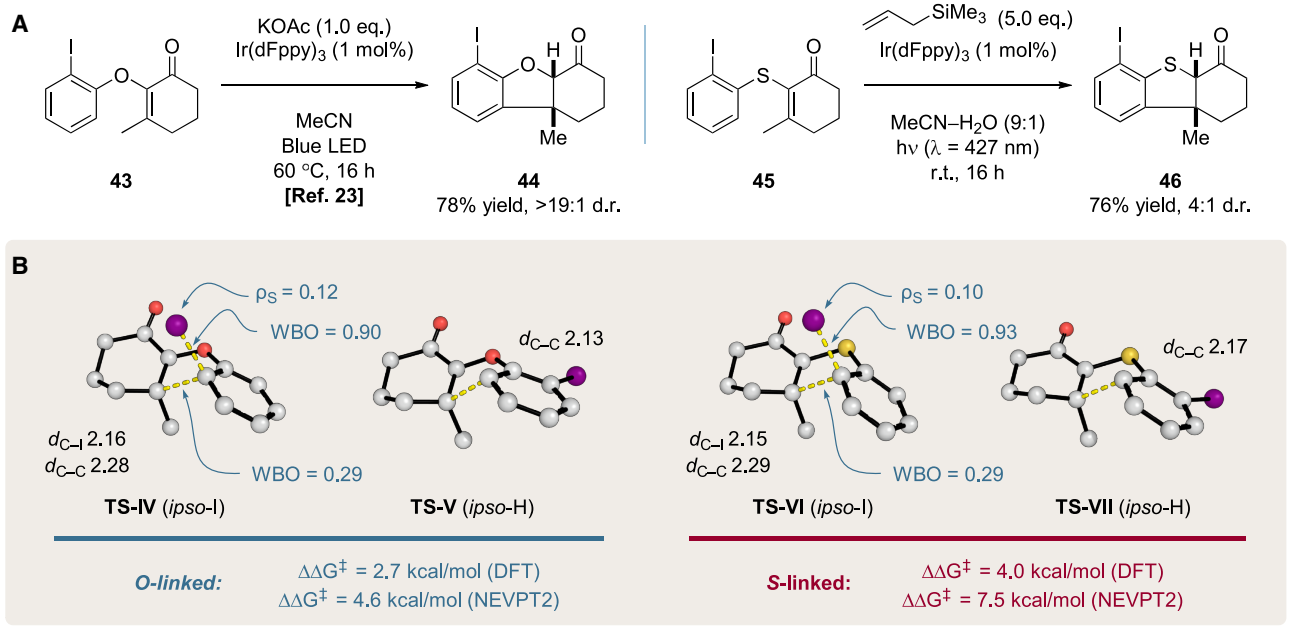


Figure 5. Experimental and computational studies to probe the regioselectivity of analogous photochemical cyclizations of oxygen- and sulfur-linked enones

(A) Both *O*- and *S*-linked substrates give *ipso*-H rather than *ipso*-I cyclization products when irradiated in the presence of an iridium sensitizer.

(B) Transition structures **TS-IV-VII** computed at the M06-2X-D3/def2-QZVPP(SMD=MeCN)//M06-2X-D3/def2-TZVP(SMD=MeCN) level. In both cases, the *ipso*-H transition state is lower in energy.

atom. The putative singlet radical pair could then readily participate in an outer-sphere SET event ($\Delta G^{\ddagger}$ = 6.0 kcal mol^{-1}) to form the experimentally observed iminium iodide product, ^{1}**B**; alternatively, SET could be viewed as an inner-sphere process occurring when there is still a significant degree of bonding between the iodine atom and the rest of the molecule (see Section S4.4.1). In contrast, regioisomeric cyclization via **TS-II** to form triplet diradical ^{3}**C**—a pathway that could account for the formation of trace side-products in some reactions but that otherwise is not observed experimentally—was found to be only mildly exergonic (−3.9 kcal mol^{-1}). This intermediate could undergo ISC to ground-state zwitterion ^{1}**C**, passing through a relatively high minimum energy crossing point of 9.6 kcal mol^{-1}, affording product ^{1}**D** via an intramolecular hydrogen transfer (**TS-III**, $\Delta G^{\ddagger}$ = 20.9 kcal mol^{-1}).

Motivated by these emerging computational insights, which suggest that delocalization within the $\sigma^{*}_{C–I}$ may be responsible for the energetic lowering of **TS-I**, we decided to investigate the electronic influence of the linking heteroatom. Experimentally, both the *O*-linked[23] and *S*-linked analogs **43** and **45** were found to selectively undergo *ipso*-H cyclization upon sensitized irradiation, affording compounds **44** and **46** in high yields, with no discernible formation of attendant RPC products, even in the presence of allyltrimethylsilane to report on possible cation generation via an *ipso*-I pathway (Figure 5A). Computational analysis using both DFT and NEVPT2:CASSCF theoretical frameworks on these heterocyclic systems was found to accurately reproduce experimental observations (Figure 5B). In contrast to *N*-alkyl-linked systems, *O*-linked and *S*-linked systems exhibited high selectivity toward *ipso*-H cyclization, with computed energy differences of 4.6 and 7.5 kcal mol^{-1}, respectively. Further NBO analysis of the *ipso*-I cyclization transition structures (**TS-I**, **TS-IV**, and **TS-VI**) revealed that they were of similar lateness, as indicated by their corresponding WBO of 0.28–0.29 for the forming C–C bond and 0.90–0.93 for the breaking C–I bond. However, their corresponding C–I σ* NBO showed distinct electron occupancies of 0.105, 0.088, and 0.073, respectively. This suggests delocalization from the linking heteroatom into the $\sigma^{*}_{C–I}$ orbital during C–C bond formation, leading to greater energetic stabilization for nitrogen-linked systems than for those linked by oxygen and sulfur. Further supporting this proposal is the reduced, yet still moderate, *ipso*-I selectivity observed for an *N*-carbamoyl-linked substrate when compared with *N*-alkyl-linked substrates (see Sections S2.25 and S4.7). Taken together, these findings offer a compelling framework for designing new types of homolytic aromatic or vinylic substitution reactions, where site selectivity (leading to RPC) can be influenced by stereoelectronic effects.

One implication of a diradical cyclization mechanism is that leaving groups other than iodine should also be viable; moreover, radical addition to the arene would represent the stereodetermining step of any asymmetric variant. Reactions involving the loss of sulfur-centered radicals are well-studied,[51–55] particularly in the context of Smiles-type rearrangements.[56–59] An elegant example of this class of reaction was recently reported by the Nevado group,[60] who showed that the addition of radicals generated under photoredox catalysis to enantioenriched *N*-arylsulfinyl acrylamides initiates a stereospecific radical sulfinyl Smiles rearrangement.[61–63] Inspired by these precedents, we theorized that the successful use of an *S*-chiral leaving group

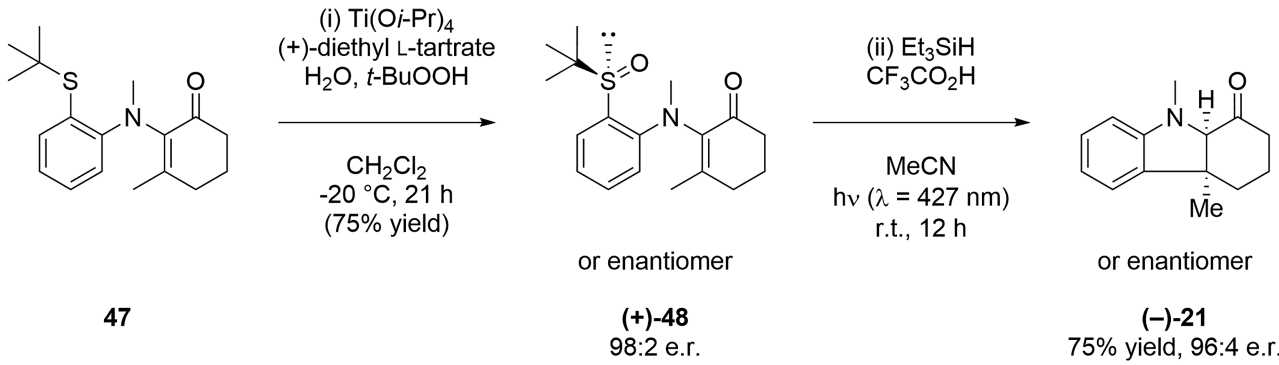


Figure 6. Enantioselective visible-light-mediated cyclization with loss of a sulfur-based leaving group

Reaction conditions: (i) substrate **47** (1.0 equiv), Ti(O*i*-Pr)$_4$ (1.0 equiv), (+)-diethyl L-tartrate (2.0 equiv), H_2O (1.0 equiv), *t*-BuOOH (2.0 equiv), CH_2Cl_2 ([**47**] = 0.1 M), −20°C, 21 h. (ii) Substrate **(+)-48** (0.1 mmol), Et_3SiH (0.5 mmol), CF_3CO_2H (0.3 mmol), Kessil PR160L 427 nm lamp, MeCN ([**(+)-48**] = 0.05 M), r.t., 12 h. E.r. determined by chiral stationary phase high-performance liquid chromatography. Sulfoxide **(+)-48** and *cis*-fused indoline **(–)-21** are enantioenriched compounds whose absolute configurations are unknown.[64]

in our system would serve as additional evidence in support of the *ipso*-substitution mechanism (the suitability of other halogen and sulfur-based leaving groups is discussed in Sections S2.23 and S2.24). Thus, we synthesized an enantioenriched *N*-aryl enaminone substrate, **(+)-48**, bearing an *ortho*-sulfinyl substituent in 75% yield and 98:2 enantiomeric ratio (e.r.) from the corresponding sulfide, **47**, under Kagan oxidation conditions (Figure 6).[65] Pleasingly, when irradiated in the presence of triethylsilane and trifluoroacetic acid in acetonitrile solution, this compound underwent eliminative photocyclization with transfer of chirality from sulfur to carbon, delivering the expected iminium reduction product, **(–)-21**, in 75% yield and 96:4 e.r.

In conclusion, we have discovered that incorporating an *ortho*-iodine substituent is an effective strategy for transitioning from diradical to ionic reactivity during photocyclizations of the *N*-aryl enaminone substrate class. Quantum calculations in conjunction with experimental mechanistic investigations identify an irreversible *ipso*-I substitution process in the triplet state as the central step of this complexity-generating cascade. The availability of this pathway enables the course of the photocyclization to be strategically redirected from isomerization (via singlet zwitterion/diradical intermediates) to RPC. ISC and SET within the radical pair resulting from *ipso*-substitution lead to the formation of an iminium iodide salt as the primary photoproduct of the reaction, which can be intercepted thermally by a variety of two-electron nucleophiles. The intermediacy of an alkene triplet diradical (as opposed to an aryl radical) circumvents the need for a photolabile bond to achieve regioselective cyclization, permitting control over the absolute stereochemistry of the C(sp^3)-rich indoline products through the use of an *ortho*-sulfinyl group in place of iodine. We anticipate that the reactivity described herein will inspire the development of other triplet-state reactions incorporating RPC.

METHODS

Synthetic procedures, characterization data, and details of computational studies are contained in the supplemental information.

RESOURCE AVAILABILITY

Lead contact

Requests for further information and resources should be directed to and will be fulfilled by the lead contact, Martin Smith (martin.smith@chem.ox.ac.uk).

Materials availability

Chemicals were obtained from commercial suppliers or prepared as indicated in the supplemental information.

Data and code availability

All relevant datasets generated within this study are available in the supplemental information. Single-crystal X-ray diffraction data have been deposited in the Cambridge Crystallographic Data Centre: CCDC 2243732 (**29**), 2243733 (**24**), and CCDC 2330002 (**41**) contain the crystallographic data for this paper.

ACKNOWLEDGMENTS

The EPSRC has provided financial support for studentships (to Z.L. and M.V.P.) via the Centre for Doctoral Training in Synthesis for Biology and Medicine (EP/L015838/1). R.S.P. acknowledges support from the NSF (CHE-1955876) and computational resources from the RMACC Summit supercomputer supported by the National Science Foundation (ACI-1532235 and ACI-1532236), the University of Colorado Boulder, Colorado State University, and the Extreme Science and Engineering Discovery Environment (XSEDE) through allocation TG-CHE180056. We are grateful to Owen Smith and Madeleine J. Hindson for assistance with X-ray crystallography and to Kathryn G. Leslie for help with photophysical studies. A CC-BY license is applied to the author-accepted manuscript arising from this submission, in accordance with EPSRC's open access conditions.

AUTHOR CONTRIBUTIONS

Z.L., M.V.P., J.V.A.-R., R.S.P., and M.D.S. conceived and designed the study; Z.L., J.A., and S.C. performed the synthetic and mechanistic experiments and analyzed data for all compounds; M.V.P., J.V.A.-R., and R.S.P. performed the computational study; Z.L., M.V.P., J.V.A.-R., R.S.P., and M.D.S. co-wrote the paper.

DECLARATION OF INTERESTS

The authors declare no competing interests.

Please cite this article in press as: Lockhart et al., A radical–polar crossover approach to complex nitrogen heterocycles via the triplet state, Chem (2026), https://doi.org/10.1016/j.chempr.2025.102904

SUPPLEMENTAL INFORMATION

Supplemental information can be found online at https://doi.org/10.1016/j.chempr.2025.102904.

Received: October 10, 2024
Revised: July 18, 2025
Accepted: December 8, 2025

REFERENCES

1. Lampard, C., Murphy, J.A., and Lewis, N. (1993). Tetrathiafulvene as a Catalyst for Radical–Polar Crossover Reactions. J. Chem. Soc., Chem. Commun., 295–297. https://doi.org/10.1039/C39930000295.
2. Wiles, R.J., and Molander, G.A. (2020). Photoredox-Mediated Net-Neutral Radical/Polar Crossover Reactions. Isr. J. Chem. *60*, 281–293. https://doi.org/10.1002/ijch.201900166.
3. Sharma, S., Singh, J., and Sharma, A. (2021). Visible Light Assisted Radical-Polar/Polar-Radical Crossover Reactions in Organic Synthesis. Adv. Synth. Catal. *363*, 3146–3169. https://doi.org/10.1002/adsc.202100205.
4. Pitzer, L., Schwarz, J.L., and Glorius, F. (2019). Reductive radical-polar crossover: traditional electrophiles in modern radical reactions. Chem. Sci. *10*, 8285–8291. https://doi.org/10.1039/C9SC03359A.
5. Donabauer, K., and König, B. (2021). Strategies for the Photocatalytic Generation of Carbanion Equivalents for Reductant-Free C–C Bond Formations. Acc. Chem. Res. *54*, 242–252. https://doi.org/10.1021/acs.accounts.0c00620.
6. Shu, C., Mega, R.S., Andreassen, B.J., Noble, A., and Aggarwal, V.K. (2018). Synthesis of Functionalized Cyclopropanes from Carboxylic Acids by a Radical Addition–Polar Cyclization Cascade. Angew. Chem. Int. Ed. Engl. *57*, 15430–15434. https://doi.org/10.1002/anie.201808598.
7. Milligan, J.A., Phelan, J.P., Polites, V.C., Kelly, C.B., and Molander, G.A. (2018). Radical/Polar Annulation Reactions (RPARs) Enable the Modular Construction of Cyclopropanes. Org. Lett. *20*, 6840–6844. https://doi.org/10.1021/acs.orglett.8b02968.
8. Wei, X.-J., Yang, D.-T., Wang, L., Song, T., Wu, L.-Z., and Liu, Q. (2013). A Novel Intermolecular Synthesis of γ-Lactones via Visible-Light Photoredox Catalysis. Org. Lett. *15*, 6054–6057. https://doi.org/10.1021/ol402954t.
9. Margrey, K.A., and Nicewicz, D.A. (2016). A General Approach to Catalytic Alkene Anti-Markovnikov Hydrofunctionalization Reactions via Acridinium Photoredox Catalysis. Acc. Chem. Res. *49*, 1997–2006. https://doi.org/10.1021/acs.accounts.6b00304.
10. Reed, N.L., Lutovsky, G.A., and Yoon, T.P. (2021). Copper-Mediated Radical–Polar Crossover Enables Photocatalytic Oxidative Functionalization of Sterically Bulky Alkenes. J. Am. Chem. Soc. *143*, 6065–6070. https://doi.org/10.1021/jacs.1c02747.
11. Kischkewitz, M., Okamoto, K., Mück-Lichtenfeld, C., and Studer, A. (2017). Radical-polar crossover reactions of vinylboron ate complexes. Science *355*, 936–938. https://doi.org/10.1126/science.aal3803.
12. Murray, P.R.D., Leibler, I.N.-M., Hell, S.M., Villalona, E., Doyle, A.G., and Knowles, R.R. (2022). Radical Redox Annulations: A General Light-Driven Method for the Synthesis of Saturated Heterocycles. ACS Catal. *12*, 13732–13740. https://doi.org/10.1021/acscatal.2c04316.
13. Prusinowski, A.F., Twumasi, R.K., Wappes, E.A., and Nagib, D.A. (2020). Vicinal, Double C–H Functionalization of Alcohols via an Imidate Radical-Polar Crossover Cascade. J. Am. Chem. Soc. *142*, 5429–5438. https://doi.org/10.1021/jacs.0c01318.
14. Trudel, V., Tien, C.-H., Trofimova, A., and Yudin, A.K. (2021). Interrupted reactions in chemical synthesis. Nat. Rev. Chem. *5*, 604–623. https://doi.org/10.1038/s41570-021-00304-2.
15. Naito, T., Tada, Y., Nishiguchi, Y., and Ninomiya, I. (1985). Photocyclisation of Enamides. Part 23. Reductive Photocyclisation of Enamides. J. Chem. Soc., Perkin Trans. *1*, 487–491. https://doi.org/10.1039/P19850000487.
16. Gramain, J.-C., Troin, Y., and Vallée-Goyet, D. (1991). Photocyclisation de *N*-aroylenamines derivees d'acides carboxyliques heteroaromatiques. Syntheses de spirocyclohexyl piperidines accolees a un heterocycle. Tetrahedron *47*, 7301–7308. https://doi.org/10.1016/S0040-4020(01)89732-5.
17. Schultz, A.G. (1983). Photochemical Six-Electron Heterocyclization Reactions. Acc. Chem. Res. *16*, 210–218. https://doi.org/10.1021/ar00090a005.
18. Schultz, A.G., Yee, Y.K., and Berger, M.H. (1977). Total Synthesis of *dl*-Lycoramine. J. Am. Chem. Soc. *99*, 8065–8067. https://doi.org/10.1021/ja00466a057.
19. Wolff, T. (1978). Flash Photolytic Studies on the Photochemical Formation of Five-Membered Sulfur Heterocycles. J. Am. Chem. Soc. *100*, 6157–6159. https://doi.org/10.1021/ja00487a032.
20. Wolff, T. (1981). Flash Photolytic Studies on the Photoconversion of Aryl Vinyl Ethers to Dihydrofurans. J. Org. Chem. *46*, 978–983. https://doi.org/10.1021/jo00318a025.
21. Edtmüller, V., Pöthig, A., and Bach, T. (2017). Enantioselective photocyclisation reactions of 2-aryloxycyclohex-2-enones mediated by a chiral copper-bisoxazoline complex. Tetrahedron *73*, 5038–5047. https://doi.org/10.1016/j.tet.2017.05.005.
22. Dutta, S., Erchinger, J.E., Strieth-Kalthoff, F., Kleinmans, R., and Glorius, F. (2024). Energy transfer photocatalysis: exciting modes of reactivity. Chem. Soc. Rev. *53*, 1068–1089. https://doi.org/10.1039/D3CS00190C.
23. Münster, N., Parker, N.A., van Dijk, L., Paton, R.S., and Smith, M.D. (2017). Visible Light Photocatalysis of 6π Heterocyclization. Angew. Chem. Int. Ed. Engl. *56*, 9468–9472. https://doi.org/10.1002/anie.201705333.
24. Beckwith, A.L.J., Easton, C.J., and Serelis, A.K. (1980). Some Guidelines for Radical Reactions. J. Chem. Soc., Chem. Commun. *482–483*, 482. https://doi.org/10.1039/C39800000482.
25. Traynham, J.G. (1979). Ipso Substitution in Free-Radical Aromatic Substitution Reactions. Chem. Rev. *79*, 323–330. https://doi.org/10.1021/cr60320a002.
26. Tiecco, M. (1980). Radical Ipso Attack and Ipso Substitution in Aromatic Compounds. Acc. Chem. Res. *13*, 51–57. https://doi.org/10.1021/ar50146a004.
27. Ayitou, A.J.-L., Ugrinov, A., and Sivaguru, J. (2009). 6π-Photocyclization of *O*-*tert*-butylacrylanilides. N-substitution dictates the regiochemistry of cyclization. Photochem. Photobiol. Sci. *8*, 751–754. https://doi.org/10.1039/b903861b.
28. Cava, M.P., Stern, P., and Wakisaka, K. (1973). An improved photochemical aporphine synthesis. Tetrahedron *29*, 2245–2249. https://doi.org/10.1016/S0040-4020(01)93344-7.
29. Daigle, M., Miao, D., Lucotti, A., Tommasini, M., and Morin, J.-F. (2017). Helically Coiled Graphene Nanoribbons. Angew. Chem. Int. Ed. Engl. *56*, 6213–6217. https://doi.org/10.1002/anie.201611834.
30. Stuyver, T., Chen, B., Zeng, T., Geerlings, P., De Proft, F., and Hoffmann, R. (2019). Do Diradicals Behave Like Radicals? Chem. Rev. *119*, 11291–11351. https://doi.org/10.1021/acs.chemrev.9b00260.
31. Rohrbach, S., Shah, R.S., Tuttle, T., and Murphy, J.A. (2019). Neutral Organic Super Electron Donors Made Catalytic. Angew. Chem. Int. Ed. Engl. *58*, 11454–11458. https://doi.org/10.1002/anie.201905814.
32. Popescu, M.V., Mekereeya, A., Alegre-Requena, J.V., Paton, R.S., and Smith, M.D. (2020). Visible-Light-Mediated Heterocycle Functionalization via Geometrically Interrupted [2+2] Cycloaddition. Angew. Chem. Int. Ed. Engl. *59*, 23020–23024. https://doi.org/10.1002/anie.202009704.
33. Petasis, N.A., and Akritopoulou, I. (1993). The boronic acid Mannich reaction: A new method for the synthesis of geometrically pure allylamines. Tetrahedron Lett. *34*, 583–586. https://doi.org/10.1016/S0040-4039(00)61625-8.
34. Carrera, D.E. (2017). The acid promoted Petasis reaction of organotrifluoroborates with imines and enamines. Chem. Commun. *53*, 11185–11188. https://doi.org/10.1039/C7CC04397J.

Please cite this article in press as: Lockhart et al., A radical–polar crossover approach to complex nitrogen heterocycles via the triplet state, Chem (2026), https://doi.org/10.1016/j.chempr.2025.102904

35. Morita, Y., Hesse, M., and Schmid, H. (1968). Über das alkaloid Eripin aus Hunteria umbellate. Mitteilung über Alkaloide [1]. Helv. Chim. Acta *51*, 1438–1443. https://doi.org/10.1002/hlca.19680510627.

36. Modha, S.G., Pöthig, A., Dreuw, A., and Bach, T. (2019). [6π] Photocyclization to cis-Hexahydrocarbazol-4-ones: Substrate Modification, Mechanism, and Scope. J. Org. Chem. *84*, 1139–1153. https://doi.org/10.1021/acs.joc.8b03144.

37. Poplata, S., Bauer, A., Storch, G., and Bach, T. (2019). Intramolecular [2+2] Photocycloaddition of Cyclic Enones: Selectivity Control by Lewis Acids and Mechanistic Implications. Chemistry *25*, 8135–8148. https://doi.org/10.1002/chem.201901304.

38. Peschel, M.T., Kabaciński, P., Schwinger, D.P., Thyrhaug, E., Cerullo, G., Bach, T., Hauer, J., and de Vivie-Riedle, R. (2021). Activation of 2-Cyclohexenone by BF_3 Coordination: Mechanistic Insights from Theory and Experiment. Angew. Chem. Int. Ed. Engl. *60*, 10155–10163. https://doi.org/10.1002/anie.202016653.

39. El-Sayed, M.A. (1968). The Triplet State: Its Radiative and Nonradiative Properties. Acc. Chem. Res. *1*, 8–16. https://doi.org/10.1021/ar50001a002.

40. Schalk, O., Schuurman, M.S., Wu, G., Lang, P., Mucke, M., Feifel, R., and Stolow, A. (2014). Internal Conversion versus Intersystem Crossing: What Drives the Gas Phase Dynamics of Cyclic α,β-Enones? J. Phys. Chem. A *118*, 2279–2287. https://doi.org/10.1021/jp4124937.

41. Singh, A., Teegardin, K., Kelly, M., Prasad, K.S., Krishnan, S., and Weaver, J.D. (2015). Facile synthesis and complete characterization of homoleptic and heteroleptic cyclometalated Iridium(III) complexes for photocatalysis. J. Organomet. Chem. *776*, 51–59. https://doi.org/10.1016/j.jorganchem.2014.10.037.

42. Schuster, D.I., Lem, G., and Kaprinidis, N.A. (1993). New Insights into an Old Mechanism: [2 + 2] Photocycloaddition of Enones to Alkenes. Chem. Rev. *93*, 3–22. https://doi.org/10.1021/cr00017a001.

43. Poplata, S., Tröster, A., Zou, Y.-Q., and Bach, T. (2016). Recent Advances in the Synthesis of Cyclobutanes by Olefin [2 + 2] Photocycloaddition Reactions. Chem. Rev. *116*, 9748–9815. https://doi.org/10.1021/acs.chemrev.5b00723.

44. Grewer, C., and Brauer, H.-D. (1994). Mechanism of the Triplet-State Quenching by Molecular Oxygen in Solution. J. Phys. Chem. *98*, 4230–4235. https://doi.org/10.1021/j100067a006.

45. Turro, N.J., Ramamurthy, V., and Scaiano, J.C. (2010). Is Evidence for Oxygen Quenching of a Reaction Good Evidence for Triplet Involvement? In Modern Molecular Photochemistry of Organic Molecules (University Science Books), pp. 1039–1040.

46. Motherwell, W.B., and Pennell, A.M.K. (1991). A Novel Route to Biaryls *via* Intramolecular Free Radical *ipso* Substitution Reactions. J. Chem. Soc., Chem. Commun. *877–879*, 877. https://doi.org/10.1039/C39910000877.

47. Sandfort, F., Knecht, T., Pinkert, T., Daniliuc, C.G., and Glorius, F. (2020). Site-Selective Thiolation of (Multi)halogenated Heteroarenes. J. Am. Chem. Soc. *142*, 6913–6919. https://doi.org/10.1021/jacs.0c01630.

48. Prier, C.K., and MacMillan, D.W.C. (2014). Amine α-heteroarylation *via* photoredox catalysis: a homolytic aromatic substitution pathway. Chem. Sci. *5*, 4173–4178. https://doi.org/10.1039/C4SC02155J.

49. Kwan, E.E., Zeng, Y., Besser, H.A., and Jacobsen, E.N. (2018). Concerted nucleophilic aromatic substitutions. Nat. Chem. *10*, 917–923. https://doi.org/10.1038/s41557-018-0079-7.

50. Rohrbach, S., Smith, A.J., Pang, J.H., Poole, D.L., Tuttle, T., Chiba, S., and Murphy, J.A. (2019). Concerted Nucleophilic Aromatic Substitution Reactions. Angew. Chem. Int. Ed. Engl. *58*, 16368–16388. https://doi.org/10.1002/anie.201902216.

51. Fiorentino, M., Testaferri, L., Tiecco, M., and Troisi, L. (1977). Homolytic Aromatic *Ipso* Substitutions in Benzothiazoles by the Nucleophilic 1-Adamantyl Radical. Chem. Commun. *316–317*, 316. https://doi.org/10.1039/C39770000316.

52. Köhler, J.J., and Speckamp, W.N. (1977). Intramolecular radical reactions in α-halomethyl substituted piperidine sulfonamides by. Tetrahedron Lett. *18*, 631–634. https://doi.org/10.1016/S0040-4039(01)92711-X.

53. Chu, X.-Q., Ge, D., Cui, Y.-Y., Shen, Z.-L., and Li, C.-J. (2021). Desulfonylation via Radical Process: Recent Developments in Organic Synthesis. Chem. Rev. *121*, 12548–12680. https://doi.org/10.1021/acs.chemrev.1c00084.

54. Feigenbaum, A., Pete, J.P., and Scholler, D. (1984). Photochemical Reactivity of α-Sulfonyloxy Enones: An Easy Method for Arylation of 1,2-Diketones. J. Org. Chem. *49*, 2355–2360. https://doi.org/10.1021/jo00187a011.

55. Motherwell, W.B., Pennell, A.M.K., and Ujjainwalla, F. (1992). Tri-n-butylstannyl Radical Induced Rearrangement of Homopropargyl (But-3-ynyl) Arenesulfonates: A Route to Novel 4-Aryl-5,6-dihydro-1,2-oxathiin 2,2-Dioxides. Chem. Commun., 1067–1068. https://doi.org/10.1039/C39920001067.

56. Loven, R., and Speckamp, W.N. (1972). A novel 1,4-arylradical rearrangement. Tetrahedron Lett. *13*, 1567–1570. https://doi.org/10.1016/S0040-4039(01)84687-6.

57. Whalley, D.M., and Greaney, M.F. (2022). Recent Advances in the Smiles Rearrangement: New Opportunities for Arylation. Synthesis *54*, 1908–1918. https://doi.org/10.1055/a-1710-6289.

58. Radhoff, N., and Studer, A. (2022). 1,4-Aryl migration in ketene-derived enolates by a polar-radical-crossover cascade. Nat. Commun. *13*, 3083. https://doi.org/10.1038/s41467-022-30817-3.

59. Zhen, G., Zeng, G., Jiang, K., Wang, F., Cao, X., and Yin, B. (2023). Visible-Light-Induced Diradical-Mediated *ipso*-Cyclization towards Double Dearomative [2+2]-Cycloaddition or Smiles-Type Rearrangement. Chemistry *29*, e202203217. https://doi.org/10.1002/chem.202203217.

60. Hervieu, C., Kirillova, M.S., Suárez, T., Müller, M., Merino, E., and Nevado, C. (2021). Asymmetric, visible light-mediated radical sulfinyl-Smiles rearrangement to access all-carbon quaternary stereocentres. Nat. Chem. *13*, 327–334. https://doi.org/10.1038/s41557-021-00668-4.

61. Hervieu, C., Kirillova, M.S., Hu, Y., Cuesta-Galisteo, S., Merino, E., and Nevado, C. (2024). Chiral arylsulfinylamides as reagents for visible light-mediated asymmetric alkene aminoarylations. Nat. Chem. *16*, 607–614. https://doi.org/10.1038/s41557-023-01414-8.

62. Noten, E.A., Ng, C.H., Wolesensky, R.M., and Stephenson, C.R.J. (2024). A general alkene aminoarylation enabled by N-centred radical reactivity of sulfinamides. Nat. Chem. *16*, 599–606. https://doi.org/10.1038/s41557-023-01404-w.

63. Zhang, Z., Wang, X., Sivaguru, P., and Wang, Z. (2022). Exploring the synthetic application of sulfinyl radicals. Org. Chem. Front. *9*, 6063–6076. https://doi.org/10.1039/D2QO01403C.

64. Favre, H.A., and Powell, W.H. (2013). Specification of Configuration and Conformation. In Nomenclature of Organic Chemistry (Royal Society of Chemistry), pp. 1156–1292. https://doi.org/10.1039/9781849733069-01156.

65. Pitchen, P., Dunach, E., Deshmukh, M.N., and Kagan, H.B. (1984). An Efficient Asymmetric Oxidation of Sulfides to Sulfoxides. J. Am. Chem. Soc. *106*, 8188–8193. https://doi.org/10.1021/ja00338a030.

Chem, Volume *12*

Supplemental information

A radical–polar crossover approach to complex nitrogen heterocycles via the triplet state

Zachariah Lockhart, Mihai V. Popescu, Juan V. Alegre-Requena, Jay Ahuja, Shaokang Chai, Robert S. Paton, and Martin D. Smith

Supplemental Methods

S1. General information

S2. Synthetic procedures and characterization data

S2.1. Synthesis and photochemical reactivity of 5-methyl substrate **1**

S2.2. Synthesis and photochemical reactivity of *N*-allyl substate **4**

S2.3. Synthesis of β-methyl substrate **10**

S2.4. Synthesis of **28**, a substrate bearing a tethered carbamate group

S2.5. Synthesis of β-ethyl substrate **S13**

S2.6. Synthesis of β-piperidinyl substrate **S17**

S2.7. Synthesis of *N*-allyl substrate **S20**

S2.8. Synthesis of *N*-benzyl substrate **S24**

S2.9. Synthesis of 5-chloro substrate **S28**

S2.10. Synthesis of cyclopentenone substrate **S30**

S2.11. Synthesis of 3-methyl substrate **S34**

S2.12. Synthesis of *para*-nitro and *para*-*N*-acetyl substrates **S35** and **S36**

S2.13. Synthesis of *para*-bromo substrate **S37**

S2.14. Synthesis of *para*-iodo substrate **S38**

S2.15. Photochemical reactivity of β-methyl substrate **10** in the presence of various nucleophiles (nucleophile scope)

S2.16. Photochemical reactivity of **28**, a substrate bearing a tethered carbamate group

S2.17. Photochemical reactivity of alternative *N*-aryl enaminone substrates in the presence of TosMIC (substrate scope)

S2.18. Synthesis and photochemical reactivity of β-hydrogen, *ortho*-iodinated cyclohexenone substrate **41**

S2.19. Synthesis and photochemical reactivity of β-hydrogen, *ortho*-iodinated cyclopentenone substrate **S43**

S2.20. Synthesis and photochemical reactivity of β-hydrogen, *ortho*-unsubstituted substrate **S45**

S2.21. Synthesis and photochemical reactivity of an *S*-linked analogue

S2.22. Synthesis and photochemical reactivity of **(±)-** and **(+)-48**, substrates bearing an *ortho*-sulfinyl group

S2.23. Synthesis and photochemical reactivity of substrates bearing alternative sulfur-based leaving groups

S2.24. Synthesis and photochemical reactivity of substrates bearing alternative halogen leaving groups

S2.25. Synthesis and photochemical reactivity of an *N*-carbamoyl-linked analogue

S3. Experimental mechanistic studies

S3.1. Synthesis, characterization and reactivity of the putative cationic intermediate

S3.2. Evidence for the involvement of an excited triplet state

S3.3. Evidence against the formation of an aryl radical

S3.4. Quantum yield studies

S3.5. Measurement of ^{13}C kinetic isotope effects (KIEs) at natural abundance[S39]

S4. Computational details

S4.1. General information

S4.2. DFT benchmarking

S4.3. Validation of Minimum Energy Crossing Points (MECPs)

S4.4. Formation of ^{1}**B** from ^{3}**B**

S4.5. Comparison of Mulliken spin densities for ^{3}**A** and ^{2}**A**

S4.6. Three-dimensional structures pertaining to computed reaction pathways available to intermediate ^{3}**A**

S4.7. Comparison of *N*, *O* and *S* linking atoms

S4.8. Modelling the asymmetric variant

S4.9. Alternative halogen leaving groups

S4.10. Adiabatic triplet energies of various substrates

S5. Reaction optimization data

S6. Supplemental references

Data S1 – UV–vis spectra

Data S2 – HPLC traces

Data S3 – NMR spectra

Data S4 – Crystal data and structural refinement

Supplemental Methods

S1. General information

Compound names and atom numbers

Systematic names for all compounds were generated in ChemDraw Professional (version 22); the atom-numbering scheme used for NMR assignment is *arbitrary* and does not follow any particular convention.

Solvents, reagents and light sources

Anhydrous acetonitrile, tetrahydrofuran and 1,4-dioxane were obtained using an MBraun SPS-5 solvent purifier. Water was purified using a PURELAB Chorus 1 Complete system. Other solvents and reagents were used directly as received from commercial suppliers or prepared according to literature procedures as specified. Kessil® PR160L 427 nm or PR160 467 nm LED lamps were used for all preparative-scale photoreactions.

Chromatography

Flash column chromatography was performed on Geduran Si 60 for column chromatography (40-63 μm particle size) or Millipore Aluminium oxide 90 standardized for column chromotographic adsorption analysis according to Brockmann (basic, activity stage I).

Thin-layer chromatography was performed on Supelco TLC Silica gel 60 F_{254} or Alugram Alox N / UV_{254} pre-coated (0.2 mm) aluminium plates. Visualization was achieved under ultraviolet (UV) light (λ_{max} = 254 nm) or by staining with aqueous potassium permanganate or ethanolic vanillin solutions.

Chiral high-performance liquid chromatography (HPLC) was performed on a Dionex Ultimate 3000 system comprising a Dionex LPG-3400SD pump, WPS-3000SL autosampler, TCC-3000SD column compartment fitted with the appropriate Daicel Chiralpak column (dimensions: 0.46 cm ø x 25 cm) and corresponding guard column (0.4 cm ø × 1 cm), and a DAD-3000 diode array detector. Reverse-phase HPLC was performed using an Agilent InfinityLab Poroshell 120 EC-C18 column (dimensions: 0.3 cm ø x 10 cm) on an otherwise identical system. Wavelengths (λ) are reported in nm, retention times (τ_R) in minutes (min), temperatures (T) in °C, and solvent flow rates in mL min^{-1}.

Nuclear magnetic resonance spectroscopy

Unless otherwise stated, nuclear magnetic resonance (NMR) spectra were acquired at 298 K on Bruker Avance spectrometers and referenced to residual non-deuterated solvent signals. Mnova (version 14) or TopSpin (version 4) was used for processing and viewing NMR data. Chemical shifts (δ) are quoted in parts per million (ppm) and coupling constants (*J*) in Hertz (Hz). ^{1}H NMR spectra are reported as follows: δ / ppm (number of protons, multiplicity, coupling constant *J* = / Hz [where appropriate], atom assignment). Multiplicity is abbreviated as follows: s = singlet, br = broad, d = doublet, t = triplet, q =

quartet, m = multiplet. Where signals are not fully resolved but two-dimensional experiments unambiguously identify the regions of multiplet corresponding to particular hydrogens, this is indicated with a subscript denoting the portion of the multiplet. For example, $H3_{RHS}$ would indicate that the right-hand side of the multiplet corresponds to H3. ^{13}C NMR spectra are reported as follows: δ / ppm (atom assignment). Two-dimensional (e.g. COSY, HSQC, HMBC and NOESY) experiments were used to assign ^{1}H and ^{13}C NMR spectra for all novel compounds. Where ^{1}H signals overlap, the number of protons quoted for a given spectral range was determined through multiplicity-edited HSQC analysis; similarly, coincident ^{13}C signals were identified by HSQC and HMBC correlations.

Infrared spectroscopy

Fourier transform infrared (FTIR) spectra were recorded as thin films on a Tensor 27 FTIR spectrometer equipped with a diamond attenuated total reflectance (ATR) absorption module. Only selected maximum absorbances (ν_{max}) of the most intense peaks are reported (cm^{-1}).

High-resolution mass spectrometry

High-resolution mass spectrometry (HRMS) was performed on Bruker MicroTOF or Waters Micromass GCT / BioAccord instruments under electrospray ionization (ESI) or atmospheric-pressure chemical ionization (APCI) conditions.

Melting points

Melting points (MP) were determined using a Reichert melting point apparatus and are uncorrected.

Polarimetry

Optical rotations were measured at the sodium D-line (589 nm) using a SCHMIDT+HAENSCH UniPol 2020 polarimeter containing a cell of path length, *l*, 1 dm at 25 °C. Specific rotations are reported in degrees for concentrations (*c*) in g 100 mL^{-1}; the calculation thus includes a correction factor of 100. Reported values are the average of eight readings.

Absorption and emission spectroscopy

Absorption spectra were acquired at 298 K using an Agilent Cary 60 ultraviolet–visible (UV–vis) spectrophotometer. Emission spectra were acquired at 298 K using an Edinburgh Instruments FS5 spectrofluorometer equipped with a xenon arc lamp (providing an excitation range of 230–1000 nm), a thermostatic sample holder (SC-20) and an R13456 PMT detector (200–950 nm spectral coverage, Hamamatsu), operating Fluoracle® software.

Crystallography

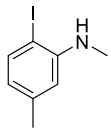
Single-crystal X-ray diffraction studies were conducted by Owen A. Smith on a (Rigaku) Oxford Diffraction/Agilent Supernovae A diffractometer (Cu-K_α radiation, λ = 1.54184 Å) equipped with a graphite monochromator, within the Department of Chemistry at the University of Oxford. Samples

were mounted in perfluoropolyether oil and cooled to 150 K during the data collection process by a Crysostream[S1] N_2 open-flow cooling device. The raw frame data was integrated and reduced using CrysalisPro. CRYSTALS[S2,S3] was used to obtain an *ab initio* solution using SuperFlip[S4] embedded within CRYSTALS and for structure refinement. CCDC 2243732 (**29**), 2243733 (**24**) and CCDC 2330002 (**41**) contain the supplementary crystallographic data for this paper.

S2. Synthetic procedures and characterization data

S2.1. Synthesis and photochemical reactivity of 5-methyl substrate **1**

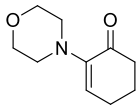
2-Iodo-*N*,5-dimethylaniline, **S1**



n-Butyllithium in hexanes (7.0 mL, 1.6 M, 11 mmol, 1.1 eq.) was added over 30 min *via* syringe pump to a stirred, -78 °C solution of 2-iodo-5-methylaniline (2.33 g, 10.0 mmol, 1.0 eq.) in anhydrous tetrahydrofuran (20 mL, 0.5 M) under an argon atmosphere. Methyl iodide (0.68 mL, 1.6 g, 11 mmol, 1.1 eq.) was added in one portion after complete addition of the organometallic reagent. After a further 5 min at -78 °C, the acetone–dry ice bath was replaced with a tepid water bath, and the reaction mixture was allowed to warm to room temperature over a period of 2 h. Ammonium chloride solution (sat. aq., 20 mL) was added, followed by diethyl ether (20 mL). The layers were separated, and the aqueous phase was extracted with additional diethyl ether (2 x 20 mL). The combined organic extracts were washed with brine (40 mL), dried over anhydrous magnesium sulfate, filtered and concentrated *in vacuo*. The crude residue was purified by flash column chromatography (silica gel, 10% dichloromethane in pentane) to afford **S1** (1.37 g, 5.54 mmol, 55%) as an off-white solid. The spectral data matched that previously reported in the literature.[S5]

^{1}H NMR (400 MHz, $CDCl_3$) δ = 7.52 (1H, d, *J* = 7.9), 6.40 (1H, d, *J* = 2.0), 6.31 (1H, dd, *J* = 8.0, 2.0), 4.16 (1H, br s), 2.89 (3H, s), 2.30 (3H, s).

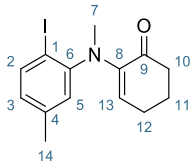
2-Morpholinocyclohex-2-en-1-one, **S2**



This compound was prepared according to a literature procedure.[S6] A mixture of cyclohexane-1,2-dione (2.24 g, 20.0 mmol, 1.0 eq.) and morpholine (2.2 mL, 2.2 g, 25 mmol, 1.3 eq.) in toluene (50 mL, 0.4 M) were heated to reflux under Dean–Stark conditions for 12 h. After cooling to room temperature, the orange liquid thus obtained was decanted from the viscous brown oil coating the bottom of the flask and concentrated *in vacuo*. The crude residue was purified by flash column chromatography (silica gel, 50% ethyl acetate in pentane) to afford **S2** (3.04 g, 1.68 mmol, 84%) as a pale-yellow solid. The spectral data matched that previously reported in the literature.[S7]

^{1}H NMR (400 MHz, $CDCl_3$) δ = 5.99 (1H, t, *J* = 4.6), 3.84–3.74 (4H, m), 2.85–2.77 (4H, m), 2.51–2.37 (4H, m), 2.00–1.88 (2H, m).

2-((2-Iodo-5-methylphenyl)(methyl)amino)cyclohex-2-en-1-one, **1**



This compound was prepared by analogy to a literature procedure.[S8] Aniline **S1** (618 mg, 2.50 mmol, 1.0 eq.), morpholine enamine **S2** (453 mg, 2.50 mmol, 1.0 eq.) and *para*-toluenesulfonic acid monohydrate (476 mg, 2.50 mmol, 1.0 eq.) were heated to 50 °C in toluene (12.5 mL, 0.2 M) for 3 h. The reaction was cooled to room temperature and diluted with ethyl acetate (25 mL). The solution was washed with sodium hydrogencarbonate (sat. aq., 3 x 12.5 mL) followed by brine (25 mL). The organic layer was dried over anhydrous sodium sulfate, filtered and concentrated *in vacuo*. The crude residue was purified by flash column chromatography on alumina gel (gradient elution from 5 to 10% ethyl acetate in pentane) to afford **1** (379 mg, 1.11 mmol, 44%) as a viscous yellow oil, which turned over slowly upon storage at -18 °C to a buff solid.

^{1}H NMR (400 MHz, $CDCl_3$) δ = 7.68 (1H, d, *J* = 8.0, H2), 6.77 (1H, dd, *J* = 2.1, 0.8, H5), 6.62 (1H, ddd, *J* = 8.1, 2.1, 0.8, H3), 6.01 (1H, t, *J* = 4.6, H13), 2.91 (3H, s, H7), 2.51–2.40 (4H, m, $H10_{LHS}$ & $H12_{RHS}$), 2.25 (3H, s, H14), 2.07–1.96 (2H, m, H11).

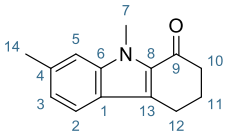
^{13}C NMR (101 MHz, $CDCl_3$) δ = 195.6 (C9), 151.6 (C6), 145.3 (C8), 139.9 (C2), 139.1 (C4), 128.9 (C13), 127.0 (C3), 124.6 (C5), 93.9 (C1), 40.6 (C7), 39.7 (C10), 25.7 (C12), 23.0 (C11), 21.1 (C14).

FTIR (neat) ν/cm^{-1} = 2942, 1686, 1612, 1468, 1366, 1306, 1188, 1110, 1055, 1015, 806.

HRMS (ESI) *m/z* calcd. for $C_{14}H_{17}ONI$ $[M+H]^+$: 342.0349; found: 342.0349.

MP 56–58 °C.

7,9-Dimethyl-2,3,4,9-tetrahydro-1*H*-carbazol-1-one, **2**



Enaminone **1** (102.4 mg, 0.300 mmol, 1.0 eq.), *fac*-Ir(dFppy)$_3$ (2.3 mg, 3.0 μmol, 1 mol%) and potassium acetate (44.2 mg, 0.450 mmol, 1.5 eq.) were charged to a Schlenk tube equipped with a magnetic stir bar. The vessel was sealed with a septum and then evacuated and back-filled with argon three times. Argon-sparged acetonitrile (6.0 mL, 0.05 M) was added *via* syringe. The reaction mixture was stirred under constant irradiation with a single Kessil PR160 467 nm LED lamp (positioned *ca.* 3 cm from the flask and directed toward it) for 2 h, with cooling to ambient temperature being achieved using a strong jet of nitrogen gas directed at the flask. The reaction mixture was concentrated *in vacuo*,

and the crude residue was purified by flash column chromatography (silica gel, 10% ethyl acetate in pentane) to afford indole **2** (60.2 mg, 0.282 mmol, 94%) as an off-white solid.

^{1}H NMR (400 MHz, $CDCl_3$) δ = 7.53 (1H, d, *J* = 8.2, H2), 7.12 (1H, app. s, H5), 6.98 (1H, dd, *J* = 8.2, 1.4, H3), 4.04 (3H, s, H7), 2.99 (2H, t, *J* = 6.1, H12), 2.63 (2H, dd, *J* = 7.1, 5.7, H10), 2.51 (3H, s, H14), 2.20 (2H, quint., *J* = 6.3, H11).

^{13}C NMR (101 MHz, $CDCl_3$) δ = 192.1 (C9), 140.3 (C6), 137.2 (C4), 130.3 (C8), 129.5 (C13), 122.8 (C1), 122.3 (C3), 121.1 (C2), 110.0 (C5), 40.0 (C10), 31.6 (C7), 24.9 (C11), 22.5 (C14), 22.0 (C12).

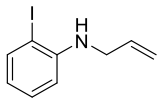
FTIR (neat) ν/cm^{-1} = 2942, 1656, 1622, 1532, 1475, 1259, 1181, 1080, 940, 800, 733.

HRMS (ESI) *m/z* calcd. for $C_{14}H_{16}NO$ $[M+H]^+$: 214.1226; found: 214.1224.

MP 62–63 °C.

S2.2. Synthesis and photochemical reactivity of *N*-allyl substate **4**

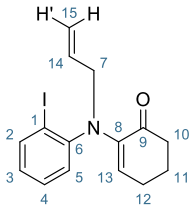
N-Allyl-2-iodoaniline, **S3**



To a stirred mixture of 2-iodoaniline (4.38 g, 20.0 mmol, 1.0 eq.) and potassium carbonate (3.04 g, 22.0 mmol, 1.1 eq.) in *N*,*N*-dimethylformamide (40 mL, 0.5 M) was added allyl bromide (1.9 mL, 2.7 g, 22 mmol, 1.1 eq.) in one portion at room temperature. After 18 h, the reaction mixture was diluted with ethyl acetate (40 mL) and washed sequentially with water (3 x 40 mL) and brine (40 mL). The combined aqueous extracts were back-extracted with ethyl acetate (40 mL); the resulting organic layer was washed sequentially with water (3 x 40 mL) and brine (40 mL). The combined organic extracts were dried over anhydrous sodium sulfate, filtered and concentrated *in vacuo*. The crude residue was purified by flash column chromatography (silica gel, 5 to 10% dichloromethane in pentane) to afford **S3** (2.52 g, 9.72 mmol, 49%) as a colourless oil. The spectral data matched that previously reported in the literature.[S9]

^{1}H NMR (400 MHz, $CDCl_3$) δ = 7.68 (1H, dd, *J* = 7.8, 1.5), 7.21 (1H, ddd, *J* = 8.5, 7.3, 1.5), 6.57 (1H, dd, *J* = 8.2, 1.5), 6.46 (1H, td, *J* = 7.5, 1.5), 5.97 (1H, ddt, *J* = 17.2, 10.3, 5.1), 5.31 (1H, dq, *J* = 17.2, 1.7), 5.22 (1H, dq, *J* = 10.3, 1.5), 4.45–4.23 (1H, br m, NH), 3.84 (2H, tt, *J* = 5.5, 1.7).

2-(Allyl(2-iodophenyl)amino)cyclohex-2-en-1-one, **4**



This compound was prepared by analogy to a literature procedure.[S8] Aniline **S3** (1.52 g, 5.87 mmol, 1.0 eq.), morpholine enamine **S2** (2.13 g, 11.7 mmol, 2.0 eq.) and *para*-toluenesulfonic acid monohydrate (2.23 g, 11.7 mmol, 1.0 eq.) were heated to 50 °C in toluene (14.5 mL, 0.4 M) for 3 h. The reaction was cooled to room temperature and diluted with ethyl acetate (30 mL). The solution was washed with sodium hydrogencarbonate (sat. aq., 3 x 15 mL) followed by brine (30 mL). The organic layer was dried over anhydrous sodium sulfate, filtered and concentrated *in vacuo*. The crude residue was purified by flash column chromatography on alumina gel (eluent: 5% ethyl acetate in pentane) to afford **4** (940 mg, 2.66 mmol, 45%) as a viscous yellow oil.

^{1}H NMR (400 MHz, $CDCl_3$) δ = 7.83 (1H, dd, *J* = 7.9, 1.5, H2), 7.24 (1H, ddd, *J* = 7.9, 7.2, 1.4, H4), 7.04 (1H, dd, *J* = 8.0, 1.6, H5), 6.78 (1H, ddd, *J* = 7.8, 7.3, 1.6, H3), 5.99 (1H, t, *J* = 4.6, H13), 5.91 (1H, ddt, *J* = 17.3, 10.3, 5.8, H14), 5.16 (1H, dq, *J* = 17.3, 1.6, H15), 5.11 (1H, dq, *J* = 10.3, 1.5, H15'),

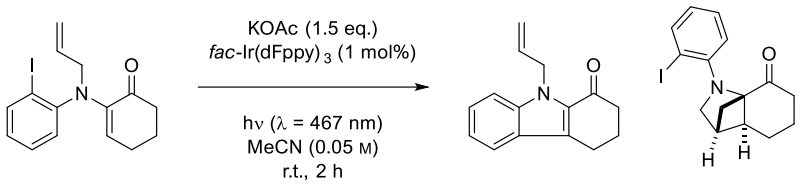
4.01 (2H, dt, *J* = 5.9, 1.6, H7), 2.49–2.43 (2H, m, H10), 2.43–2.36 (2H, m, H12), 2.05–1.94 (2H, m, H11).

^{13}C NMR (101 MHz, $CDCl_3$) δ = 195.8 (C9), 150.3 (C6), 143.3 (C8), 140.4 (C2), 135.2 (C14), 131.2 (C13), 128.7 (C4), 125.8 (C3), 125.4 (C5), 117.3 (C15), 98.7 (C1), 54.8 (C7), 39.7 (C10), 25.7 (C12), 22.9 (C11).

FTIR (neat) ν/cm^{-1} = 2937, 1684, 1466, 1193, 1155, 1113, 1016, 919, 891, 763, 732.

HRMS (ESI) *m/z* calcd. for $C_{15}H_{17}INO$ $[M+H]^+$: 354.0349; found: 354.0347.

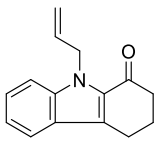
Photocyclization of **4**



4 **5** 86% yield **6** 10% yield

Enaminone **4** (106.0 mg, 0.300 mmol, 1.0 eq.), *fac*-Ir(dFppy)$_3$ (2.3 mg, 3.0 μmol, 1 mol%) and potassium acetate (44.2 mg, 0.450 mmol, 1.5 eq.) were charged to a Schlenk tube equipped with a magnetic stir bar. The vessel was sealed with a septum and then evacuated and back-filled with argon three times. Argon-sparged acetonitrile (6.0 mL, 0.05 M) was added *via* syringe. The reaction mixture was stirred under constant irradiation with a single Kessil PR160 467 nm LED lamp (positioned *ca.* 3 cm from the flask and directed toward it) for 2 h, with cooling to ambient temperature being achieved using a strong jet of nitrogen gas directed at the flask. The reaction mixture was concentrated *in vacuo*, and the crude residue was purified by flash column chromatography (silica gel, gradient elution from 5 to 25% ethyl acetate in pentane) to afford indole **5** (57.9 mg, 0.257 mmol, 86%) as a viscous colourless oil, alongside bridged cyclobutane **6** (10.6 mg, 0.0300 mmol, 10%) as an off-white solid.

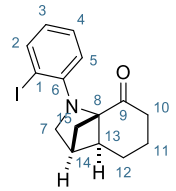
9-Allyl-2,3,4,9-tetrahydro-1H-carbazol-1-one, **5**



The spectral data matched that previously reported in the literature.[S10]

^{1}H (400 MHz, $CDCl_3$) δ = 7.67 (1H, dt, *J* = 8.0, 1.0), 7.43–7.30 (2H, m), 7.16 (1H, ddd, *J* = 8.0, 6.6, 1.3), 5.99 (1H, ddt, *J* = 17.1, 10.3, 5.2), 5.23 (2H, dt, *J* = 5.2, 1.7), 5.09 (1H, dq, *J* = 10.3, 1.5), 4.95 (1H, dq, *J* = 17.1, 1.7), 3.04 (2H, t, *J* = 6.1), 2.65 (2H, dd, *J* = 7.2, 5.7), 2.23 (2H, quint, *J* = 6.3).

rac-1-(2-Iodophenyl)hexahydro-3,7a-methanoindol-7(1*H*)-one, **6**



Broad signals on the ^{1}H NMR spectrum of compound **6** in DMSO-d_6 solution at 298 K suggested the presence of two slowly interconverting conformers. Signal coalescence was observed upon heating to 368 K; however, the sample quickly degraded (reverting to *N*-aryl enaminone **4**) at this temperature, precluding the compound's full characterization. The two conformers were therefore individually characterized at 253 K in CD_2Cl_2 solution; the ^{1}H and ^{13}C NMR data for both are provided below.

Major rotamer:

^{1}H NMR (500 MHz, CD_2Cl_2, 253 K) δ* = 7.82–7.78 (1H, m, H2), 7.17–7.11 (1H, m, H4), 6.70–6.64 (1H, m, H3), 6.45 (1H, dd, *J* = 8.2, 1.5, H5), 4.29 (1H, d, *J* = 8.0, H7), 3.03 (1H, dd, *J* = 8.5, 2.8, H15), 2.73 (1H, d, *J* = 2.8, H14), 2.66–2.61 (1H, m, H7'), 2.64–2.56 (1H, m, H10), 2.53–2.47 (1H, m, H13), 2.28 (1H, dtd, *J* = 12.8, 3.2, 1.3, H10'), 2.21–2.15 (1H, m, H12), 2.07–1.94 (3H, m, H11, H11' & H15'), 1.81–1.70 (1H, m, H12').

^{13}C NMR (126 MHz, CD_2Cl_2, 253 K) δ = 205.1 (C9), 152.7 (C6), 140.4 (C2), 127.4 (C4), 123.4 (C3), 120.6 (C5), 92.1 (C1), 75.2 (C8), 61.6 (C7), 58.1 (C13), 41.6 (C14), 40.9 (C10), 38.1 (C15), 29.1 (C12), 24.9 (C11).

Minor rotamer:

^{1}H NMR (500 MHz, CD_2Cl_2, 253 K) δ = 7.84–7.80 (1H, m, H2), 7.17–7.11 (1H, m, H4), 6.70–6.64 (1H, m, H3), 6.24 (1H, dd, *J* = 8.1, 1.5, H5), 4.42 (1H, dd, *J* = 7.8, 1.1, H7), 2.94 (1H, dt, *J* = 7.8, 2.8, H15), 2.75 (1H, d, *J* = 3.3, H14), 2.66–2.61 (1H, m, H7'), 2.50–2.44 (1H, m, H13), 2.51–2.42 (2H, m, H10 & H10'), 2.19–2.11 (2H, m, H11 & H12), 2.07–1.94 (2H, m, H11' & H15'), 1.94–1.83 (1H, m, H12').

^{13}C NMR (126 MHz, CD_2Cl_2, 253 K) δ = 204.3 (C9), 151.4 (C6), 140.9 (C2), 127.7 (C4), 123.6 (C3), 119.7 (C5), 92.8 (C1), 74.1 (C8), 61.5 (C7), 49.8 (C13), 43.2 (C15), 41.1 (C14), 39.8 (C10), 25.1 (C12), 24.6 (C11).

* Where signals of the two rotamers overlapped, the chemical shifts and number of protons quoted for a given spectral range were determined through multiplicity-edited HSQC analysis; integration of clearly resolved signals within MestReNova indicates an approximate molar ratio of 3:2 between the two rotamers.

The observation of nuclear Overhauser effect (nOe) correlations by 2D NOESY corresponding to H5↔H13 in the minor conformer and H5↔H15’ in the major conformer is consistent with this structure.

FTIR (neat) ν/cm^{-1} = 2944, 1706, 1578, 1465, 1433, 1294, 1104, 1012, 947, 872, 753.

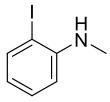
HRMS (ESI) *m/z* calcd. for $C_{15}H_{17}INO$ $[M+H]^+$: 354.0349; found: 354.0345.

MP 136–137 °C.

S2.3. Synthesis of β-methyl substrate **10**

A strategy devised by Schultz and co-workers was employed to prepare substrates containing β-substituents other than hydrogen.[S11]

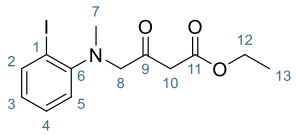
2-Iodo-*N*-methylaniline, **S4**



n-Butyllithium in hexanes (8.8 mL, 2.5 M, 22 mmol, 1.1 eq.) was added over 30 min *via* syringe pump to a stirred, -78 °C solution of 2-iodoaniline (4.38 g, 20.0 mmol, 1.0 eq.) in anhydrous tetrahydrofuran (40 mL, 0.5 M) under an argon atmosphere. Methyl iodide (1.4 mL, 3.2 g, 22 mmol, 1.1 eq.) was added in one portion after complete addition of the organometallic reagent. After a further 5 min at -78 °C, the acetone–dry ice bath was replaced with a tepid water bath, and the reaction mixture was allowed to warm to room temperature over a period of 2 h. Ammonium chloride solution (sat. aq., 40 mL) was added, followed by diethyl ether (40 mL). The layers were separated, and the aqueous phase was extracted with additional diethyl ether (2 x 40 mL). The combined organic extracts were washed with brine (80 mL), dried over anhydrous magnesium sulfate, filtered and concentrated *in vacuo*. The crude residue was purified by flash column chromatography (silica gel, 10% dichloromethane in pentane) to afford **S4** (3.26 g, 14.0 mmol, 70%) as a pale-yellow oil. The spectral data matched that previously reported in the literature.[S12]

^{1}H NMR (400 MHz, $CDCl_3$) δ = 7.67 (1H, dt, *J* = 7.8, 1.4), 7.30–7.21 (1H, m), 6.57 (1H, dd, *J* = 8.2, 1.5), 6.51–6.42 (1H, m), 4.21 (1H, br s), 2.89 (3H, d, *J* = 5.1).

Ethyl 4-((2-iodophenyl)(methyl)amino)-3-oxobutanoate, **S5**



This compound was prepared by analogy to a literature procedure.[S13] To a stirred mixture of **S4** (2.43 g, 10.4 mmol, 1.0 eq.), sodium hydrogencarbonate (1.75 g, 20.8 mmol, 2.0 eq.) and sodium iodide (3.13 g, 20.9 mmol, 2.0 eq.) in acetonitrile (21 mL, 0.5 M) at room temperature was added ethyl 4-chloroacetoacetate (95% w/w, 3.0 mL, 21 mmol, 2.0 eq.) in one portion. The reaction mixture was heated to 75 °C for 18 h with stirring. After this time, the reaction mixture was allowed to cool to room temperature before adding triethylamine (4.4 mL, 3.2 g, 32 mmol, 3.0 eq.) in one portion and stirring for a further 30 min. The reaction mixture was concentrated *in vacuo*, and the crude residue thus obtained was dissolved in ethyl acetate (40 mL) and washed successively with sodium thiosulfate (sat. aq., 20 mL) and water (20 mL). The aqueous washings were extracted with ethyl acetate (2 x 40 mL), and the combined organic extracts were subjected to a final wash with brine (60 mL), dried over

anhydrous sodium sulfate, filtered and concentrated *in vacuo*. The crude residue was purified twice by flash column chromatography (silica gel, 5% ethyl acetate in pentane; then, silica gel, dichloromethane) to afford **S5** (1.44 g, 3.99 mmol, 38%) as a viscous pale-yellow oil.

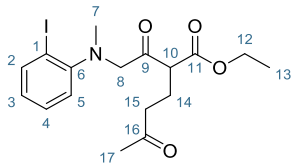
^{1}H NMR (400 MHz, $CDCl_3$) δ = 7.84 (1H, dd, *J* = 7.9, 1.5, H2), 7.31 (1H, ddd, *J* = 8.0, 7.3, 1.5, H4), 7.14 (1H, dd, *J* = 8.0, 1.6, H5), 6.81 (1H, ddd, *J* = 7.8, 7.3, 1.6, H3), 4.17 (2H, q, *J* = 7.1, H12), 3.90 (2H, s, H8), 3.65 (2H, s, H10), 2.79 (3H, s, H7), 1.25 (3H, t, *J* = 7.1, H13).

^{13}C NMR (101 MHz, $CDCl_3$) δ = 202.0 (C9), 167.5 (C11), 153.0 (C6), 140.3 (C2), 129.4 (C4), 126.1 (C3), 122.6 (C5), 97.4 (C1), 66.0 (C8), 61.5 (C12), 46.6 (C10), 43.2 (C7), 14.2 (C13).

FTIR (neat) ν/cm^{-1} = 2984, 1746, 1721, 1472, 1315, 1228, 1182, 1032, 1015, 950, 760.

HRMS (ESI) *m/z* calcd. for $C_{13}H_{16}O_3NINa$ $[M+Na]^+$: 384.00671; found: 384.00665.

Ethyl 2-(*N*-(2-iodophenyl)-*N*-methylglycyl)-5-oxohexanoate, **S6**



Aminoketone **S5** (2.34 g, 6.48 mmol, 1.0 eq.) was dissolved in dichloromethane (13 mL, 0.5 M). Potassium carbonate (895 mg, 6.48 mmol, 1.0 eq.) was added in one portion followed by freshly distilled methyl vinyl ketone (0.54 mL, 0.46 g, 6.5 mmol, 1.0 eq.). The reaction mixture was stirred for 24 h at room temperature before being concentrated *in vacuo*. The crude residue was purified by flash column chromatography (silica gel, gradient elution from 2 to 5% ethyl acetate in dichloromethane) to afford **S6** (1.93 g, 4.48 mmol, 69%) as a viscous orange-yellow oil.

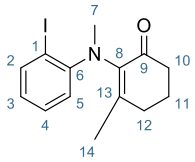
^{1}H NMR (400 MHz, $CDCl_3$) δ = 7.82 (1H, dd, *J* = 7.9, 1.5, H2), 7.34–7.25 (1H, m, H4), 7.15 (1H, dd, *J* = 8.0, 1.5, H5), 6.78 (1H, td, *J* = 7.6, 1.5, H3), 4.13 (2H, q, *J* = 7.1, H12), 4.02 (1H, d, *J* = 17.5, H8), 3.96 (1H, d, *J* = 17.5, H8'), 3.84 (1H, t, *J* = 7.0, H10), 2.81 (3H, s, H7), 2.44 (2H, app. td, *J* = 7.1, 1.5, H15), 2.11–2.00 (2H, m, H14), 2.08 (3H, s, H17), 1.20 (3H, t, *J* = 7.1, H13).

^{13}C NMR (101 MHz, $CDCl_3$) δ = 207.6 (C16), 203.4 (C9), 169.3 (C11), 153.0 (C6), 140.3 (C2), 129.2 (C4), 125.9 (C3), 122.7 (C5), 97.1 (C1), 65.2 (C8), 61.6 (C12), 53.8 (C10), 42.8 (C7), 40.7 (C15), 23.0 (C17), 21.7 (C14), 14.2 (C13).

FTIR (neat) ν/cm^{-1} = 2982, 1744, 1716, 1580, 1472, 1369, 1182, 1162, 1015, 858, 760.

HRMS (ESI) *m/z* calcd. for $C_{17}H_{22}O_4NINa$ $[M+Na]^+$: 454.04857; found: 454.04777.

2-((2-Iodophenyl)(methyl)amino)-3-methylcyclohex-2-en-1-one, **10**



Sodium methoxide (30 wt% in methanol, 0.81 mL, 0.24 g, 4.4 mmol, 1.1 eq.) was added in one portion to a stirred, argon-sparged solution of diketone **S6** (1.70 g, 3.94 mmol, 1.0 eq.) in methanol (40 mL, 0.1 M) at room temperature. The reaction mixture was stirred at this temperature for a further 2 h before adding a solution of lithium hydroxide monohydrate (165 mg, 3.93 mmol, 1.0 eq.) in water (20 mL) and heating to 75 °C. After 10 min, the reaction mixture was cooled to room temperature and acidified to *ca.* pH 2 with HCl (1 M aq., *ca.* 20 mL). The reaction mixture was heated to 75 °C for a further 30 min before cooling to room temperature, adding water (40 mL) and extracting with ethyl acetate (3 x 40 mL). The combined organic extracts were washed with brine (80 mL), dried over anhydrous sodium sulfate, filtered and concentrated *in vacuo*. The crude residue was purified by flash column chromatography (silica gel, gradient elution from 20 to 30% diethyl ether in pentane) to afford **10** (896 mg, 2.63 mmol, 67%) as a pale-yellow solid.

^{1}H NMR (400 MHz, $CDCl_3$) δ = 7.72 (1H, dd, *J* = 7.8, 1.6, H2), 7.31–7.22 (1H, m, H4), 7.03 (1H, dd, *J* = 8.2, 1.5, H5), 6.57 (1H, ddd, *J* = 7.8, 7.2, 1.5, H3), 3.05 (3H, s, H7), 2.53–2.41 (4H, m, $H10_{LHS}$ & $H12_{RHS}$), 2.09–1.98 (2H, m, H11), 1.76 (3H, t, *J* = 1.0, H14).

^{13}C NMR (101 MHz, $CDCl_3$) δ = 196.5 (C9), 154.7 (C13), 151.7 (C6), 141.2 (C2), 140.6 (C8), 128.8 (C4), 122.3 (C3), 120.0 (C5), 87.5 (C1), 40.6 (C7), 38.7 (C10), 32.9 (C12), 21.9 (C11), 21.4 (C14).

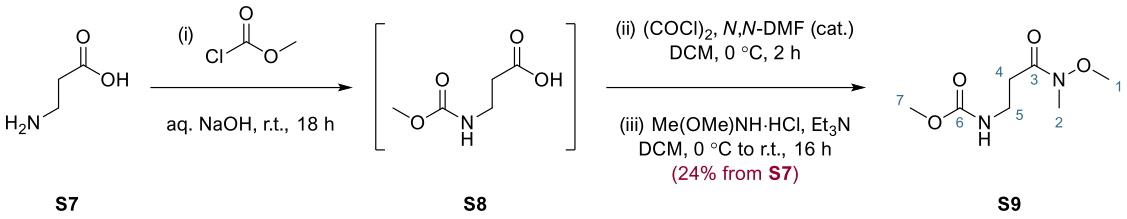
FTIR (neat) ν/cm^{-1} = 2946, 1674, 1580, 1472, 1317, 1207, 1115, 1060, 1008, 928, 753.

HRMS (ESI) *m/z* calcd. for $C_{14}H_{16}ONINa$ $[M+Na]^+$: 364.01688; found: 364.01705.

MP 50–51°C.

S2.4. Synthesis of **28**, a substrate bearing a tethered carbamate group

Methyl (3-(methoxy(methyl)amino)-3-oxopropyl)carbamate, **S9**



To a stirred, 0 °C solution of β-alanine (**S7**) (2.67 g, 30.0 mmol, 1.0 eq.) in aqueous sodium hydroxide (1 M, 30 mL) were simultaneously added methyl chloroformate (2.3 mL, 2.8 g, 30 mmol, 1.0 eq.) and sodium hydroxide (2 M aq., 15 mL). The reaction mixture was allowed to warm to room temperature over 18 h. Hydrochloric acid (1 M aq., 50 mL) was added slowly with ice-bath cooling, and the resulting aqueous mixture was extracted with ethyl acetate (3 x 50 mL). The combined organic extracts were washed with brine (75 mL), dried over anhydrous sodium sulfate, filtered and concentrated *in vacuo*, affording 2.73 g (18.6 mmol assuming a purity of 100%) of **S8** (presumed) as a viscous pale-yellow oil (this material was used directly in next step without characterization or chromatographic purification). The crude residue was dissolved in dichloromethane (19 mL). Oxalyl chloride (1.8 mL, 2.7 g, 21 mmol) was added in one portion, and the solution was cooled to 0 °C. Two drops of *N*,*N*-dimethylformamide were added by glass dropping pipette to the reaction mixture with stirring; effervescence was immediately observed. The reaction mixture was stirred for a further 2 h with ice-bath cooling before being concentrated *in vacuo*. The resulting material was re-dissolved in dichloromethane (19 mL). *N*,*O*-Dimethylhydroxylamine hydrochloride (1.99 g, 20.4 mmol) was added in one portion, and the solution was cooled to 0 °C. Triethylamine (5.8 mL, 4.2 g, 42 mmol) was added dropwise *via* syringe over 5 min; the addition was accompanied by the formation of dense fumes and a white precipitate (additional dichloromethane was necessary to mobilize the slurry that formed). The reaction mixture was allowed to warm to room temperature over 16 h before being diluted with dichloromethane (20 mL) and washed successively with water (20 mL), hydrochloric acid (1 M aq., 20 mL), sodium hydrogencarbonate (sat. aq., 20 mL) and brine (20 mL). The organic layer was dried over anhydrous sodium sulfate, filtered and concentrated *in vacuo*. The crude residue was purified by flash column chromatography (silica gel, 50% ethyl acetate in dichloromethane) to afford **S9** (1.37 g, 7.20 mmol, 24% over three steps from **S7**) as a pale-yellow oil.

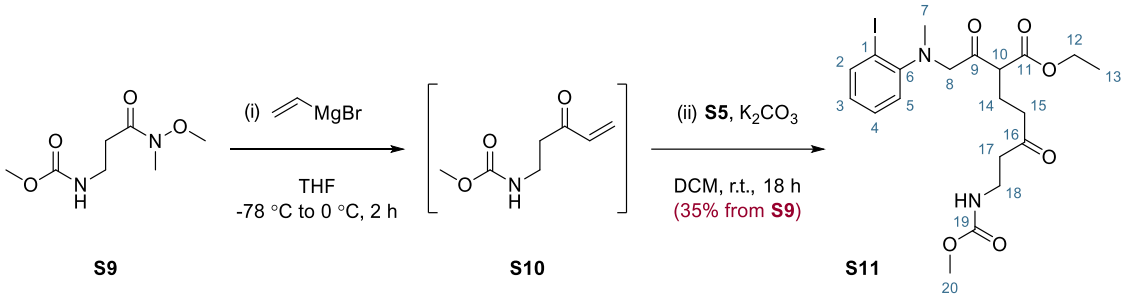
^{1}H NMR (400 MHz, $CDCl_3$) δ = 5.42 (1H, br s, NH), 3.65 (3H, s, H1), 3.62 (3H, s, H7), 3.44 (2H, q, *J* = 6.0, H5), 3.15 (3H, s, H2), 2.63 (2H, br t, *J* = 5.8, H4).

^{13}C NMR (101 MHz, $CDCl_3$) δ = 173.1 (C3), 157.2 (C6), 61.3 (C1), 52.0 (C7), 36.4 (C5), 32.3 (C4), 32.1 (C2).

FTIR (neat) ν/cm^{-1} = 3337 (br), 1706, 1648, 1533, 1446, 1390, 1267, 1193, 1150, 1010.

HRMS (ESI) *m/z* calcd. for $C_7H_{15}N_2O_4$ $[M+H]^+$: 191.1026; found: 191.1025.

Ethyl 2-(*N*-(2-iodophenyl)-*N*-methylglycyl)-7-((methoxycarbonyl)amino)-5-oxoheptanoate, **S11**



To a -78 °C solution of Weinreb amide **S9** (1.34 g, 7.05 mmol, 1.0 eq.) in anhydrous THF (35 mL, 0.2 M) under an argon atmosphere was added a solution of vinylmagnesium bromide (1.0 M in THF, 21 mL, 21 mmol, 3.0 eq.) dropwise *via* syringe pump over 15 min, with stirring. After complete addition of the Grignard reagent, the dry ice–acetone bath was replaced with an ice–water bath, and the reaction mixture was allowed to warm to 0 °C over 2 h. The reaction mixture was added dropwise to hydrochloric acid (1 M aq., 50 mL) with ice-bath cooling. The resulting mixture was transferred to a separating funnel using diethyl ether (50 mL). After thorough mixing, the layers were separated, and the aqueous phase was extracted with additional diethyl ether (2 x 25 mL). The combined organic extracts were washed with brine (50 mL), dried over anhydrous magnesium sulfate, filtered and concentrated *in vacuo*, affording 917 mg (5.83 mmol assuming a purity of 100%) of presumably vinyl ketone **S10** as an orange oil (owing to its propensity to polymerize, this material was used directly in next step without characterization or further purification). The crude residue and aminoketone **S5** (1.99 g, 5.51 mmol) were immediately dissolved in dichloromethane (12 mL). Potassium carbonate (762 mg, 5.51 mmoL) was added in one portion, and the resulting mixture was stirred for 18 h at room temperature before being concentrated *in vacuo*. The crude residue was purified by flash column chromatography (silica gel, 5 to 10% ethyl acetate in dichloromethane) to afford **S11** (1.29 g, 2.49 mmol, 35% from **S9** over two steps) as a viscous yellow oil.

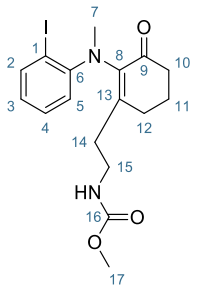
^{1}H NMR (400 MHz, $CDCl_3$) δ = 7.81 (1H, dd, *J* = 7.9, 1.4, H2), 7.32–7.26 (1H, m, H4), 7.14 (1H, dd, *J* = 8.0, 1.5, H5), 6.78 (1H, td, *J* = 7.6, 1.5, H3), 5.16 (1H, br s, NH), 4.12 (2H, q, *J* = 7.1, H12), 4.00 (1H, d, *J* = 17.4, H8), 3.94 (1H, d, *J* = 17.4, H8'), 3.85 (1H, t, *J* = 6.9, H10), 3.62 (3H, s, H20), 3.35 (2H, q, *J* = 5.8, H18), 2.80 (3H, s, H7), 2.57 (2H, t, *J* = 5.7, H17), 2.40 (2H, app. td, *J* = 7.2, 2.8, H15), 2.13–1.97 (2H, m, H14), 1.19 (3H, t, *J* = 7.1, H13).

^{13}C NMR (101 MHz, $CDCl_3$) δ = 208.9 (C16), 203.5 (C9), 169.3 (C11), 157.1 (C19), 152.9 (C6), 140.3 (C2), 129.3 (C4), 125.9 (C3), 122.7 (C5), 97.2 (C1), 65.1 (C8), 61.6 (C12), 53.7 (C10), 52.1 (C20), 43.0 (C7), 42.5 (C17), 40.0 (C15), 35.7 (C18), 21.5 (C14), 14.1 (C13).

FTIR (neat) ν/cm^{-1} = 3390 (br), 2945, 1709, 1579, 1471, 1250, 1190, 1097, 1015, 1015, 761.

HRMS (ESI) *m/z* calcd. for C20H27IN2O6 $[M+H]^+$: 519.0987; found: 519.0978.

Methyl (2-(2-((2-iodophenyl)(methyl)amino)-3-oxocyclohex-1-en-1-yl)ethyl)carbamate, **28**



A solution of diketone **S11** (1.11 g, 2.14 mmol, 1.0 eq.) in *tert*-butanol (21 mL, 0.1 M) was sparged with argon for 15 min before adding potassium *tert*-butoxide (264 mg, 2.35 mmol, 1.1 eq.) in one portion under an argon atmosphere (the solution was gently heated using a tepid water bath during the sparging process to prevent freezing of the solvent). The reaction mixture was heated to reflux with stirring for 75 min. The reaction mixture was cooled to room temperature and quenched by the addition of ammonium chloride (sat. aq., 40 mL). The resulting mixture was transferred to a separating funnel using water (40 mL) and diethyl ether (40 mL). After thorough mixing, the layers were separated, and the aqueous phase was extracted with additional diethyl ether (2 x 40 mL). The combined organic extracts were washed with brine (80 mL), dried over anhydrous magnesium sulfate, filtered and concentrated *in vacuo*. The crude residue was purified by flash column chromatography (silica gel, 25 to 50% ethyl acetate in pentane) to afford **28** (441 mg, 1.03 mmol, 48%) as an extremely viscous yellow-brown oil.

^{1}H NMR (600 MHz, $CDCl_3$) δ = 7.72 (1H, dd, *J* = 7.8, 1.5, H2), 7. 20 (1H, ddd, *J* = 8.7, 7.2, 1.6, H4), 6.96 (1H, dd, *J* = 8.2, 1.5, H5), 6.60 (1H, ddd, *J* = 7.8, 7.2, 1.5, H3), 4.73–4.48 (1H, br m, NH), 3.59 (3H, s, H17), 3.12 (2H, q, *J* = 6.7, H15), 3.05 (3H, s, H7), 2.53–2.48 (2H, m, H10), 2.45 (2H, t, *J* = 6.1, H12), 2.35 (2H, t, *J* = 7.3, H14), 2.01 (2H, quint, *J* = 6.1, H11).

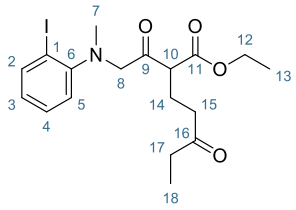
^{13}C NMR (151 MHz, $CDCl_3$) δ = 197.2 (C9), 156.9 (C16), 155.5 (C13), 152.3 (C6), 142.2 (C8), 141.1 (C2), 129.1 (C4), 123.3 (C3), 121.7 (C5), 89.7 (C1), 52.1 (C17), 41.3 (C7), 39.0 (C10), 38.1 (C15), 34.7 (C14), 30.4 (C12), 21.9 (C11).

FTIR (neat) ν/cm^{-1} = 3333 (br), 2945, 1717, 1672, 1579, 1532, 1472, 1434, 1258, 1010, 755.

HRMS (ESI) *m/z* calcd. for $C_{17}H_{21}IN_2O_3$ $[M+H]^+$: 429.0670; found: 429.0665.

S2.5. Synthesis of β-ethyl substrate **S13**

Ethyl 2-(*N*-(2-iodophenyl)-*N*-methylglycyl)-5-oxoheptanoate, **S12**



Aminoketone **S5** (1.56 g, 4.32 mmol, 1.0 eq.) was dissolved in dichloromethane (8.6 mL, 0.5 M). Potassium carbonate (598 mg, 4.33 mmol, 1.0 eq.) was added in one portion followed by freshly distilled ethyl vinyl ketone (0.43 mL, 0.37 g, 4.4 mmol, 1.0 eq.). The reaction mixture was stirred for 21 h at room temperature before being concentrated *in vacuo*. The crude residue was purified by flash column chromatography (silica gel, 10 to 20% ethyl acetate in pentane) to afford **S12** (1.44 g, 3.23 mmol, 75%) as a viscous pale-yellow oil.

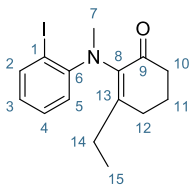
^{1}H NMR (400 MHz, $CDCl_3$) δ = 7.79 (1H, dd, *J* = 7.9, 1.5, H2), 7.31–7.24 (1H, m, H4), 7.13 (1H, dd, *J* = 8.1, 1.6, H5), 6.76 (1H, td, *J* = 7.6, 1.6, H3), 4.11 (2H, q, *J* = 7.1, H12), 4.01 (1H, d, *J* = 17.6, H8), 3.95 (1H, d, *J* = 17.5, H8'), 3.82 (1H, t, *J* = 7.0, H10), 2.79 (3H, s, H7), 2.43–2.36 (2H, m, H15), 2.34 (2H, q, *J* = 7.3, H17), 2.12–1.98 (2H, m, H14), 1.18 (3H, t, *J* = 7.1, H13), 0.99 (3H, t, *J* = 7.3, H18).

^{13}C NMR (101 MHz, $CDCl_3$) δ = 210.3 (C16), 203.3 (C9), 169.3 (C11), 152.9 (C6), 140.2 (C2), 129.2 (C4), 125.8 (C3), 122.7 (C5), 97.0 (C1), 65.1 (C8), 61.5 (C12), 53.9 (C10), 42.7 (C7), 39.2 (C15), 35.9 (C17), 21.8 (C14), 14.1 (C13), 7.8 (C18).

FTIR (neat) ν/cm^{-1} = 2940, 1743, 1716, 1471, 1368, 1186, 1115, 1015, 760, 724, 641.

HRMS (ESI) *m/z* calcd. for $C_{18}H_{25}O_4NI$ $[M+H]^+$: 446.0823; found: 446.0821.

3-Ethyl-2-((2-iodophenyl)(methyl)amino)cyclohex-2-en-1-one, **S13**



A solution of diketone **S12** (737 mg, 1.66 mmol, 1.0 eq.) in *tert*-butanol (17 mL, 0.1 M) was sparged with argon for 15 min before adding potassium *tert*-butoxide (204 mg, 1.82 mmol, 1.1 eq.) in one portion under an argon atmosphere (the solution was gently heated using a tepid water bath during the sparging process to prevent freezing of the solvent). The reaction mixture was heated to reflux with stirring for 1 h. The reaction mixture was cooled to room temperature and quenched by the addition of ammonium chloride (sat. aq., 40 mL). The resulting mixture was transferred to a separating funnel using water (40 mL) and diethyl ether (40 mL). After thorough mixing, the layers were separated, and the

aqueous phase was extracted with additional diethyl ether (2 x 40 mL). The combined organic extracts were washed with brine (80 mL), dried over anhydrous magnesium sulfate, filtered and concentrated *in vacuo*. The crude residue was purified twice by flash column chromatography (silica gel, gradient elution from 10 to 20% diethyl ether in pentane; then, silica gel, dichloromethane) to afford **S13** (265 mg, 0.746 mmol, 45%) as a yellow solid.

^{1}H NMR (400 MHz, $CDCl_3$) δ = 7.72 (1H, dd, *J* = 7.8, 1.6, H2), 7.24 (1H, ddd, *J* = 8.1, 7.2, 1.6, H4), 7.01 (1H, dd, *J* = 8.2, 1.6, H5), 6.57 (1H, ddd, *J* = 7.8, 7.2, 1.5, H3), 3.07 (3H, s, H7), 2.55–2.47 (2H, m, H10), 2.44 (2H, t, *J* = 6.1, H12), 2.21 (2H, q, *J* = 7.6, H14), 2.10–1.99 (2H, m, H11), 0.85 (3H, t, *J* = 7.6, H15).

^{13}C NMR (101 MHz, $CDCl_3$) δ = 197.1 (C9), 159.9 (C13), 152.2 (C6), 141.2 (C2), 140.3 (C8), 128.8 (C4), 122.5 (C3), 120.5 (C5), 88.3 (C1), 41.3 (C7), 39.0 (C10), 29.9 (C12), 27.4 (C14), 22.0 (C11), 10.5 (C15).

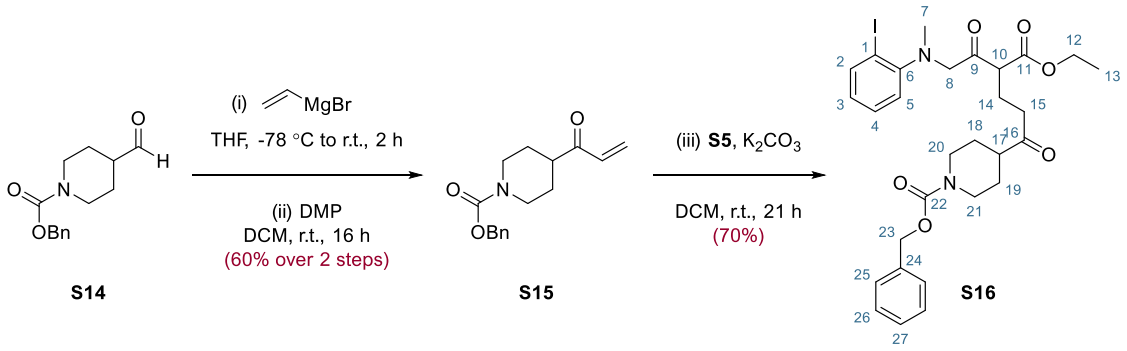
FTIR (neat) ν/cm^{-1} = 2935, 1673, 1579, 1471, 1293, 1202, 1114, 1057, 1008, 922, 753.

HRMS (ESI) *m/z* calcd. for $C_{15}H_{18}INO$ $[M+H]^+$: 356.0506; found: 356.0498.

MP 42–44 °C.

S2.6. Synthesis of β-piperidinyl substrate **S17**

Benzyl 4-(4-(ethoxycarbonyl)-6-((2-iodophenyl)(methyl)amino)-5-oxohexanoyl)piperidine-1-carboxylate, **S16**



To a -78 °C solution of 1-((benzyloxy)methyl)piperidine-4-carbaldehyde (**S14**) (2.47 g, 9.99 mmol, 1.0 eq.) in anhydrous tetrahydrofuran (20 mL, 0.5 M) under an argon atmosphere was added vinylmagnesium bromide (1.0 M in tetrahydrofuran solution, 12 mL, 12 mmol, 1.2 eq.) dropwise *via* syringe pump over 15 min, with stirring. After complete addition of the Grignard reagent, the reaction mixture was allowed to warm to room temperature over 2 h. The reaction mixture was diluted with diethyl ether (20 mL) and quenched by the sequential addition of ammonium chloride (sat. aq., 20 mL) and water (10 mL). The layers were separated, and the aqueous phase was extracted with additional diethyl ether (2 x 20 mL). The combined organic extracts were dried over anhydrous magnesium sulfate, filtered and concentrated *in vacuo*. The crude residue was dissolved in dichloromethane (40 mL) and cooled to 0 °C using an ice–water bath. Dess–Martin periodinane (4.67 g, 11.0 mmol) was added in one portion, and the resulting mixture was stirred for 15 min at 0 °C. The reaction mixture was allowed to warm to room temperature over 16 h. The reaction mixture was quenched by the addition of sodium thiosulfate (sat. aq., 20 mL) and sodium hydrogencarbonate (sat. aq., 20 mL). The layers were separated, and the organic phase was washed with additional portions of sodium hydrogen carbonate (sat. aq., 2 x 20 mL) followed by brine (20 mL). The organic layer was dried over anhydrous magnesium sulfate, filtered and concentrated *in vacuo*. The crude residue was purified by flash column chromatography (silica gel, 25% ethyl acetate in pentane) to afford vinyl ketone **S15** (1.64 g, 6.00 mmol, 60% from **S14** over two steps) as a viscous colourless oil. A sample of this compound retained for analysis underwent polymerization on the timescale of minutes–hours, despite being stored in the dark at -18 °C, precluding its full characterization; however, the following ^{1}H and ^{13}C NMR spectroscopic data, obtained immediately after the compound's isolation, supports its tentative assignment as the structure shown.

^{1}H NMR (400 MHz, $CDCl_3$) δ = 7.40–7.28 (5H, m), 6.45 (1H, dd, *J*, 17.4, 10.5), 6.29 (1H, dd, *J* = 17.4, 1.4), 5.81 (1H, dd, *J* = 10.5, 1.4), 5.13 (2H, s), 4.30–4.08 (2H, br m), 2.92 (2H, br t, *J* = 12.6), 2.78 (1H. tt, *J* = 11.1, 3.8), 1.92–1.72 (2H, br m), 1.68–1.56 (2H, m).

^{13}C NMR (101 MHz, $CDCl_3$) δ = 201.4, 155.3, 136.9, 134.4, 128.8, 128.6, 128.1, 128.0, 67.3, 45.9, 43.5, 27.6.

Vinyl ketone **S15** (1.31 g, 4.79 mmol, 1.00 eq.) was dissolved in dichloromethane (5 mL) immediately after its purification and isolation in the preceding step. Potassium carbonate (692 mg, 5.00 mmol, 1.05 eq.) was added in one portion followed by aminoketone **S5** (1.81 g, 5.01 mmol, 1.05 eq.) as a solution in dichloromethane (5 mL). The reaction mixture was stirred for 21 h at room temperature before being concentrated *in vacuo*. The crude residue was purified by flash column chromatography (silica gel, 30% ethyl acetate in pentane) to afford **S16** (2.14 g, 3.37 mmol, 70%) as a viscous yellow oil.

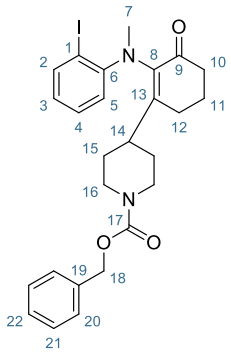
^{1}H NMR (600 MHz, $CDCl_3$) δ = 7.73 (1H, dd, *J* = 7.9, 1.4, H2), 7.30–7.18 (6H, m, $H25_{LHS}$, $H26_{LHS}$, $H27_{RHS}$ & $H4_{RHS}$), 7.07 (1H, dd, *J* = 8.0, 1.4, H5), 6.70 (1H, td, *J* = 7.7, 1.4, H3), 5.03 (2H, s, H23), 4.20–3.97 (4H, m, H12 & two of the four protons represented by H20/H21), 3.93 (1H, d, *J* = 17.4, H8), 3.88 (1H, d, *J* = 17.3, H8'), 3.78 (1H, t, *J* = 6.9, H10), 2.89–2.63 (2H, m, two of the four protons represented by H20/H21), 2.73 (3H, s, H7), 2.44–2.28 (3H, m, $H15_{LHS}$ & $H17_{RHS}$), 2.05–1.92 (2H, m, H14), 1.88–1.52 (2H, m, two of the four protons represented by H18/H19), 1.45–1.35 (2H, m, two of the four protons represented by H18/H19), 1.12 (3H, t, *J* = 7.1, H13).

^{13}C NMR (151 MHz, $CDCl_3$) δ = 210.7 (C16), 203.4 (C9), 169.2 (C11), 155.1 (C22), 152.8 (C6), 140.2 (C2), 136.8 (C24), 129.2 (C4), 128.5 (C25 or C26), 128.0 (C27), 127.9 (C25 or C26), 125.8 (C3), 122.7 (C5), 97.1 (C1), 67.1 (C23), 65.0 (C8), 61.5 (C12), 53.6 (C10), 48.2 (C17), 43.4(0) & 43.3(9) (C20 & C21), 42.8 (C7), 37.5 (C15), 27.4(0) & 27.3(9) (C18 & C19), 21.6 (C14), 14.1 (C13).

FTIR (neat) ν/cm^{-1} = 2944, 1743, 1699, 1471, 1434, 1279, 1226, 1132, 1015, 912, 731.

HRMS (ESI) *m/z* calcd. for $C_{29}H_{36}O_6N_2I$ $[M+H]^+$: 635.1613; found: 635.1611.

Benzyl 4-(2-((2-iodophenyl)(methyl)amino)-3-oxocyclohex-1-en-1-yl)piperidine-1-carboxylate, **S17**



A solution of diketone **S16** (1.70 g, 2.68 mmol, 1.0 eq.) in *tert*-butanol (27 mL, 0.1 M) was sparged with argon for 15 min before adding potassium *tert*-butoxide (601 mg, 5.36 mmol, 2.0 eq.) in one portion

under an argon atmosphere (the solution was gently heated using a tepid water bath during the sparging process to prevent freezing of the solvent). The reaction mixture was heated to reflux with stirring for 2 h. The reaction mixture was cooled to room temperature and quenched by the addition of ammonium chloride (sat. aq., 50 mL). The resulting mixture was transferred to a separating funnel using water (50 mL) and diethyl ether (50 mL). After thorough mixing, the layers were separated, and the aqueous phase was extracted with additional diethyl ether (2 x 50 mL). The combined organic extracts were washed with brine (100 mL), dried over anhydrous magnesium sulfate, filtered and concentrated *in vacuo*. The crude residue was purified twice by flash column chromatography (silica gel, gradient elution from 20 to 100% diethyl ether in pentane; then, silica gel, 5% ethyl acetate in dichloromethane) to afford **S17** (460 mg, 0.845 mmol, 32%) as a yellow foam solid.

^{1}H NMR (400 MHz, DMSO-d_6) δ = 7.71 (1H, dd, *J* = 7.8, 1.6, H2), 7.39–7.22 (6H, m, $H20_{LHS}$, $H21_{LHS}$, $H22_{LHS}$ & $H4_{RHS}$), 7.01 (1H, dd, *J* = 8.2, 1.5, H5), 6.61 (1H, td, *J* = 7.5, 1.5, H3), 5.03 (2H, s, H18), 3.96 (2H, br d, *J* = 13.0, H16), 2.99 (3H, s, H7), 2.84 (1H, tt, *J* = 12.1, 3.3, H14), 2.54 (2H, br s, H16'), 2.47–2.39 (2H, m, H10), 2.34–2.26 (2H, m, H12), 1.93 (2H, quint, *J* = 6.1, H11), 1.31 (2H, qd, *J* = 12.4, 4.0, H15), 1.19–1.05 (2H, br m, H15').

^{13}C NMR (101 MHz, DMSO-d_6) δ = 196.1 (C9), 159.2 (C13), 154.2 (C17), 152.1 (C6), 140.7 (C2), 139.6 (C8), 136.9 (C19), 128.8 (C4), 128.4 (C20 or C21), 127.8 (C22), 127.5 (C20 or C21), 122.5 (C3), 120.8 (C5), 88.6 (C1), 66.1 (C18), 43.5 (C16), 41.0 (C7), 38.9 (C14), 38.4 (C10), 27.6 (C15), 25.6 (C12), 21.5 (C11).

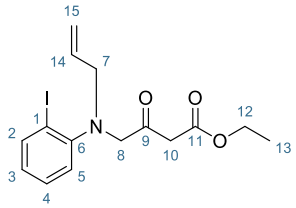
FTIR (neat) ν/cm^{-1} = 2944, 1697, 1678, 1471, 1433, 1229, 1205, 1120, 1010, 755, 698.

HRMS (ESI) *m/z* calcd. for $C_{26}H_{29}IN_2O_3$ $[M+H]^+$: 545.1296; found: 545.1307.

MP 44–46 °C (ambiguous phase transition owing to foam nature of solid).

S2.7. Synthesis of *N*-allyl substrate **S20**

Ethyl 4-(allyl(2-iodophenyl)amino)-3-oxobutanoate, **S18**



This compound was prepared by analogy to a literature procedure.[S13] To a stirred mixture of **S3** (2.35 g, 9.07 mmol, 1.0 eq.), sodium hydrogencarbonate (1.52 g, 18.1 mmol, 2.0 eq.) and sodium iodide (2.72 g, 18.1 mmol, 2.0 eq.) in acetonitrile (18 mL, 0.5 M) at room temperature was added ethyl 4-chloroacetoacetate (95% w/w, 2.6 mL, 18 mmol, 2.0 eq.) in one portion. The reaction mixture was heated to 75 °C for 18 h with stirring. After this time, the reaction mixture was allowed to cool to room temperature before adding triethylamine (3.8 mL, 2.8 g, 2.7 mmol, 3.0 eq.) in one portion and stirring for a further 30 min. The reaction mixture was concentrated *in vacuo*, and the crude residue thus obtained was dissolved in ethyl acetate (40 mL) and washed successively with sodium thiosulfate (sat. aq., 20 mL) and water (20 mL). The aqueous washings were extracted with ethyl acetate (2 x 40 mL), and the combined organic extracts were subjected to a final wash with brine (60 mL), dried over anhydrous sodium sulfate, filtered and concentrated *in vacuo*. The crude residue was purified by flash column chromatography (silica gel, gradient elution from 2 to 10% ethyl acetate in pentane) to afford **S18** (874 mg, 2.26 mmol, 25%) as a viscous yellow oil.

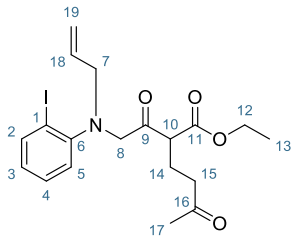
^{1}H NMR (400 MHz, $CDCl_3$) δ = 7.85 (1H, dd, *J* = 7.9, 1.5, H2), 7.29 (1H, ddd, *J* = 7.9, 7.3, 1.5, H4), 7.13 (1H, dd, *J* = 8.0, 1.6, H5), 6.82 (1H, ddd, *J* = 7.9, 7.3, 1.6, H3), 5.90 (1H, ddt, *J* = 16.8, 10.1, 6.6, H14), 5.27–5.16 (2H, m, H15), 4.14 (2H, q, *J* = 7.1, H12), 3.96 (2H, s, H8), 3.68 (2H, dt, *J* = 6.5, 1.3, H7), 3.52 (2H, s, H10), 1.23 (3H, t, *J* = 7.2, H13).

^{13}C NMR (101 MHz, $CDCl_3$) δ = 202.5 (C9), 167.4 (C11), 151.2 (C6), 140.4 (C2), 133.9 (C14), 129.2 (C4), 126.4 (C3), 124.3 (C5), 119.5 (C15), 98.9 (C1), 61.9 (C8), 61.4 (C12), 58.5 (C7), 46.7 (C10), 14.2 (C13).

FTIR (neat) ν/cm^{-1} = 2984, 1744, 1720, 1469, 1315, 1220, 1033, 1014, 928, 761, 724.

HRMS (ESI) *m/z* calcd. for $C_{15}H_{19}O_3NI$ $[M+H]^+$: 388.0404; found: 388.0401.

Ethyl 2-(*N*-allyl-*N*-(2-iodophenyl)glycyl)-5-oxohexanoate, **S19**



Aminoketone **S18** (874 mg, 2.26 mmol, 1.0 eq.) was dissolved in dichloromethane (4.5 mL, 0.5 M). Potassium carbonate (312 mg, 2.26 mmol, 1.0 eq.) was added in one portion followed by freshly distilled methyl vinyl ketone (0.19 mL, 0.16 g, 2.3 mmol, 1.0 eq.). The reaction mixture was stirred for 21 h at room temperature before being concentrated *in vacuo*. The crude residue was purified by flash column chromatography (silica gel, gradient elution from 1.25 to 5% ethyl acetate in dichloromethane) to afford **S19** (891 mg, 1.95 mmol, 86%) as a viscous orange-yellow oil.

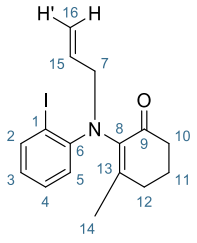
^{1}H NMR (400 MHz, $CDCl_3$) δ = 7.84 (1H, dd, *J* = 7.9, 1.5, H2), 7.32–7.23 (1H, m, H4), 7.15 (1H, dd, *J* = 8.0, 1.6, H5), 6.80 (1H, td, *J* = 7.6, 1.6, H3), 5.90 (1H, ddt, *J* = 16.7, 10.1, 6.5, H18), 5.27–5.15 (2H, m, H19), 4.09 (2H, q, *J* = 7.1, H12), 4.05 (2H, app. s, H8), 3.82–3.73 (2H, m, $H10_{LHS}$ & $H7_{RHS}$), 3.66 (1H, ddt, *J* = 14.4, 6.7, 1.3, H7'), 2.29 (2H, t, *J* = 7.3, H15), 2.04 (3H, s, H17), 2.06–1.91 (2H, m, H14), 1.17 (3H, t, *J* = 7.1, H13).

^{13}C NMR (101 MHz, $CDCl_3$) δ = 207.5 (C16), 204.3 (C9), 169.2 (C11), 151.2 (C6), 140.3 (C2), 134.3 (C18), 129.0 (C4), 126.2 (C3), 124.6 (C5), 119.2 (C19), 98.8 (C1), 61.5 (C12), 61.0 (C8), 58.1 (C7), 53.6 (C10), 40.6 (C15), 29.9 (C17), 21.5 (C14), 14.1 (C13).

FTIR (neat) ν/cm^{-1} = 2981, 1743, 1716, 1469, 1368, 1212, 1161, 1014, 931, 762, 723.

HRMS (ESI) *m/z* calcd. for $C_{19}H_{24}O_4NINa$ $[M+Na]^+$: 480.0642; found: 480.0636.

2-(Allyl(2-iodophenyl)amino)-3-methylcyclohex-2-en-1-one, **S20**



Sodium methoxide (30 wt% in methanol, 0.40 mL, 0.12 g, 2.2 mmol, 1.1 eq.) was added in one portion to a stirred, argon-sparged solution of diketone **S19** (901 mg, 1.97 mmol, 1.0 eq.) in methanol (20 mL, 0.1 M) at room temperature. The reaction mixture was stirred at this temperature for a further 2 h before adding a solution of lithium hydroxide monohydrate (83 mg, 2.0 mmol, 1.0 eq.) in water (10 mL) and heating to 75 °C. After 10 min, the reaction mixture was cooled to room temperature and acidified to

ca. pH 2 with HCl (1 M aq., *ca.* 10 mL). The reaction mixture was heated to 75 °C for a further 30 min before cooling to room temperature, adding water (20 mL) and extracting with ethyl acetate (3 x 20 mL). The combined organic extracts were washed with brine (40 mL), dried over anhydrous sodium sulfate, filtered and concentrated *in vacuo*. The crude residue was purified by flash column chromatography (silica gel, gradient elution from 10 to 20% diethyl ether in pentane) to afford **S20** (511 mg, 1.39 mmol, 71%) as a pale-yellow solid.

^{1}H NMR (400 MHz, $CDCl_3$) δ = 7.75 (1H, dd, *J* = 7.9, 1.6, H2), 7.20 (1H, ddd, *J* = 8.2, 7.2, 1.6, H4), 7.03 (1H, dd, *J* = 8.2, 1.6, H5), 6.61 (1H, ddd, *J* = 7.8, 7.2, 1.5, H3), 5.95 (1H, ddt, *J* = 17.3, 10.2, 6.2, H15), 5.14 (1H, dq, *J* = 17.2, 1.7, H16), 5.08 (1H, dq, *J* = 10.2, 1.4, H16'), 4.13 (2H, dt, *J* = 6.2, 1.5, H7), 2.52–2.40 (4H, m, $H10_{LHS}$ & $H12_{RHS}$), 2.05–1.94 (2H, m, H11), 1.78 (3H, t, *J* = 0.9, H14)

^{13}C NMR (101 MHz, $CDCl_3$) δ = 197.1 (C9), 155.8 (C13), 150.9 (C6), 141.0 (C2), 139.4 (C8), 135.7 (C15), 128.8 (C4), 123.5 (C3), 123.3 (C5), 117.5 (C16), 91.4 (C1), 55.1 (C7), 39.0 (C10), 33.0 (C12), 22.0 (C11), 21.7 (C14).

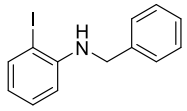
FTIR (neat) ν/cm^{-1} = 2926, 1672, 1579, 1469, 1432, 1193, 1170, 1011, 925, 758, 732.

HRMS (ESI) *m/z* calcd. for $C_{16}H_{19}INO$ $[M+H]^+$: 368.0506; found: 368.0500.

MP 65–66 °C

S2.8. Synthesis of *N*-benzyl substrate **S24**

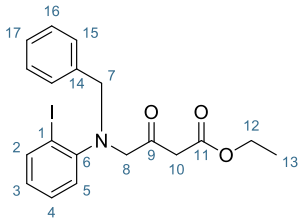
N-benzyl-2-iodoaniline, **S21**



This compound was prepared according to a literature procedure.[S14] Sodium cyanoborohydride (754 mg, 12.0 mmol, 1.2 eq.) was added in portions to a stirred mixture of 2-iodoaniline (2.19 g, 10.0 mmol, 1.0 eq.), benzaldehyde (1.2 mL, 1.3 g, 12 mmol, 1.2 eq.) and zinc chloride (1.64 g, 12.0 mmol, 1.2 eq.) in methanol (50 mL, 0.2 M) at room temperature. A condenser was attached to the flask, and the reaction mixture was heated to reflux. After 2 h, the reaction mixture was cooled to room temperature and quenched by the addition of sodium hydroxide (1 M aq., 50 mL). The resulting mixture was transferred to a separating funnel using water (25 mL) and diethyl ether (50 mL). After thorough mixing, the layers were separated, and the aqueous phase was extracted with additional diethyl ether (2 x 25 mL). The combined organic extracts were washed with brine (50 mL), dried over anhydrous magnesium sulfate, filtered and concentrated *in vacuo*. The crude residue was purified by flash column chromatography (silica gel, 10% pentane in dichloromethane) to afford **S21** (2.71 g, 8.77 mmol, 88%) as a yellow oil. The spectral data matched that previously reported in the literature.[S12]

^{1}H NMR (400 MHz, $CDCl_3$) δ = 7.71 (1H, dd, *J* = 7.8, 1.5), 7.44–7.27 (5H, m), 7.22–7.14 (1H, m), 6.57 (1H, dd, *J* = 8.2, 1.5), 6.48 (1H, ddd, *J* = 7.8, 7.3, 1.5), 4.66 (1H, br t, *J* = 5.6), 4.43 (2H, d, *J* = 5.6).

Ethyl 4-(benzyl(2-iodophenyl)amino)-3-oxobutanoate, **S22**



This compound was prepared by analogy to a literature procedure.[S13] To a stirred mixture of **S21** (4.31 g, 13.9 mmol, 1.0 eq.), sodium hydrogencarbonate (2.34 g, 27.9 mmol, 2.0 eq.) and sodium iodide (4.18 g, 27.9 mmol, 2.0 eq.) in acetonitrile (28 mL, 0.5 M) at room temperature was added ethyl 4-chloroacetoacetate (95% w/w, 4.0 mL, 28 mmol, 2.0 eq.) in one portion. The reaction mixture was heated to 75 °C for 18 h with stirring. After this time, the reaction mixture was allowed to cool to room temperature, bezfore adding triethylamine (5.8 mL, 4.2 g, 42 mmol, 3.0 eq.) in one portion and stirring for a further 30 min. The reaction mixture was concentrated *in vacuo*, and the crude residue thus obtained was dissolved in ethyl acetate (60 mL) and washed successively with sodium thiosulfate (sat. aq., 30 mL) and water (30 mL). The aqueous washings were extracted with ethyl acetate (2 x 60 mL),

and the combined organic extracts were subjected to a final wash with brine (90 mL), dried over anhydrous sodium sulfate, filtered and concentrated *in vacuo*. The crude residue was purified twice by flash column chromatography (silica gel, 10% ethyl acetate in pentane; then, silica gel, dichloromethane) to afford **S22** (1.74 g, 3.98 mmol, 29%) as a viscous yellow oil.

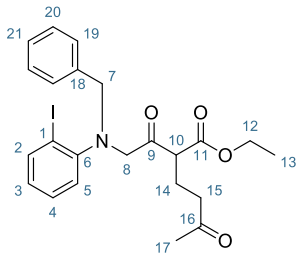
^{1}H NMR (400 MHz, $CDCl_3$) δ = 7.87 (1H, dd, *J* = 7.9, 1.5, H2), 7.41–7.21 (6H, m, H4, H15, H16 & H17), 7.17 (1H, dd, *J* = 8.1, 1.6, H5), 6.82 (1H, td, *J* = 7.5, 1.6, H3), 4.30 (2H, s, H7), 4.11 (2H, q, *J* = 7.1, H12), 3.91 (2H, s, H8), 3.43 (2H, s, H10), 1.19 (3H, t, *J* = 7.1, H13).

^{13}C NMR (101 MHz, $CDCl_3$) δ = 201.9 (C9), 167.1 (C11), 151.1 (C6), 140.3 (C2), 136.9 (C14), 129.3 (C15), 129.1 (C4), 128.5 (C16), 127.8 (C17), 126.5 (C3), 125.1 (C5), 98.6 (C1), 61.7 (C8), 61.4 (C12), 58.8 (C7), 46.8 (C10), 14.2 (C13).

FTIR (neat) ν/cm^{-1} = 2984, 1746, 1721, 1469, 1314, 1031, 1014, 763, 738, 721, 700.

HRMS (ESI) *m/z* calcd. for $C_{19}H_{21}O_3NI$ $[M+H]^+$: 438.0561; found: 438.0561.

Ethyl 2-(*N*-benzyl-*N*-(2-iodophenyl)glycyl)-5-oxohexanoate, **S23**



Aminoketone **S22** (1.13 g, 2.58 mmol, 1.0 eq.) was dissolved in dichloromethane (5.2 mL, 0.5 M). Potassium carbonate (357 mg, 2.58 mmol, 1.0 eq.) was added in one portion followed by freshly distilled methyl vinyl ketone (0.22 mL, 0.19 g, 2.6 mmol, 1.0 eq.). The reaction mixture was stirred for 21 h at room temperature before being concentrated *in vacuo*. The crude residue was purified by flash column chromatography (silica gel, 5% ethyl acetate in dichloromethane) to afford **S23** (1.04 g, 2.05 mmol, 79%) as a viscous pale-yellow oil.

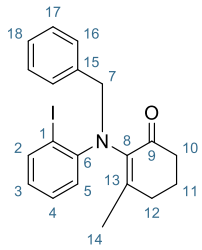
^{1}H NMR (400 MHz, $CDCl_3$) δ = 7.86 (1H, dd, *J* = 7.9, 1.4, H2), 7.44–7.36 (2H, m, H19), 7.35–7.20 (5H, m, H4, $H5_{RHS}$, H20 & H21), 6.81 (1H, ddd, *J* = 7.8, 7.0, 1.8, H3), 4.40 (1H, d, *J* = 13.9, H7), 4.30 (1H, d, *J* = 13.9, H7'), 4.08–3.98 (3H, m, H8 & H12), 3.94 (1H, d, *J* = 17.9, H8'), 3.67 (1H, t, *J* = 7.1, H10), 2.26 (2H, t, *J* = 7.3, H15), 2.03 (3H, s, H17), 2.03–1.84 (2H, m, H14), 1.10 (3H, t, *J* = 7.1, H13).

^{13}C NMR (101 MHz, $CDCl_3$) δ = 207.5 (C16), 204.1 (C9), 169.0 (C11), 151.2 (C6), 140.2 (C2), 137.3 (C18), 129.2 (C19), 129.0 (C4), 128.5 (C20), 127.7 (C21), 126.3 (C3), 125.4 (C5), 98.6 (C1), 61.5 (C12), 60.8 (C8), 58.4 (C7), 53.9 (C10), 40.5 (C15), 29.9 (C17), 21.6 (C14), 14.1 (C13).

FTIR (neat) ν/cm^{-1} = 2937, 1743, 1716, 1469, 1369, 1206, 1160, 1015, 763, 721, 699.

HRMS (ESI) *m/z* calcd. for $C_{23}H_{27}O_4NI$ $[M+H]^+$: 508.0979; found: 508.0986.

2-(Benzyl(2-iodophenyl)amino)-3-methylcyclohex-2-en-1-one, **S24**



Sodium methoxide (30 wt% in methanol, 0.75 mL, 0.22 g, 4.0 mmol, 1.1 eq.) was added in one portion to a stirred, argon-sparged solution of diketone **S23** (1.85 g, 3.65 mmol, 1.0 eq.) in methanol (36 mL, 0.1 M) at room temperature. The reaction mixture was stirred at this temperature for a further 2 h before adding a solution of lithium hydroxide monohydrate (153 mg, 3.65 mmol, 1.0 eq.) in water (18 mL) and heating to 75 °C. After 10 min, the reaction mixture was cooled to room temperature and acidified to *ca.* pH 2 with HCl (1 M aq., *ca.* 18 mL). The reaction mixture was heated to 75 °C for a further 30 min before cooling to room temperature, adding water (40 mL) and extracting with ethyl acetate (3 x 40 mL). The combined organic extracts were washed with brine (80 mL), dried over anhydrous sodium sulfate, filtered and concentrated *in vacuo*. The crude residue was purified by flash column chromatography (silica gel, gradient elution from 10 to 20% diethyl ether in pentane) to afford **S24** (586 mg, 1.40 mmol, 39%) as a viscous yellow oil.

^{1}H NMR (400 MHz, $CDCl_3$) δ = 7.78 (1H, dd, *J* = 7.9, 1.5, H2), 7.47–7.40 (2H, m, H16), 7.30–7.22 (2H, m, H17). 7.22–7.12 (2H, m, $H18_{LHS}$ & $H4_{RHS}$), 7.07 (1H, dd, *J* = 8.2, 1.6, H5), 6.63 (1H, ddd, *J* = 7.9, 7.1, 1.6, H3), 4.73 (2H, s, H7), 2.38–2.28 (4H, m, $H12_{LHS}$ & $H10_{RHS}$), 1.93–1.83 (2H, m, H11), 1.81 (3H, t, *J* = 1.0, H14).

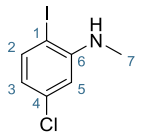
^{13}C NMR (101 MHz, $CDCl_3$) δ = 197.6 (C9), 155.5 (C13), 150.5 (C6), 140.9 (C2), 140.1 (C8), 138.5 (C15), 128.9 (C4), 128.6 (C16), 128.2 (C17), 127.0 (C18), 124.6 (C5), 124.1 (C3), 92.9 (C1), 55.9 (C7), 39.0 (C10), 33.0 (C12), 22.0 (C11), 21.5 (C14).

FTIR (neat) ν/cm^{-1} = 2928, 1673, 1579, 1465, 1432, 1165, 1011, 928, 760, 726, 698.

HRMS (ESI) *m/z* calcd. for $C_{20}H_{20}ONINa$ $[M+Na]^+$: 440.0482; found: 440.0480.

S2.9. Synthesis of 5-chloro substrate **S28**

5-Chloro-2-iodo-*N*-methylaniline, **S25**



n-Butyllithium in hexanes (8.8 mL, 2.5 M, 22 mmol, 1 eq.) was added over 30 min *via* syringe pump to a stirred, -78 °C solution of 5-chloro-2-iodoaniline (5.07 g, 20.0 mmol, 1.0 eq.) in anhydrous tetrahydrofuran (40 mL, 0.5 M) under an argon atmosphere. Methyl iodide (1.4 mL, 3.2 g, 22 mmol, 1.1 eq.) was added in one portion after complete addition of the organometallic reagent. After a further 5 min at -78 °C, the acetone–dry ice bath was replaced with a tepid water bath, and the reaction mixture was allowed to warm to room temperature over a period of 2 h. Ammonium chloride solution (sat. aq., 40 mL) was added, followed by diethyl ether (40 mL). The layers were separated, and the aqueous phase was extracted with additional diethyl ether (2 x 40 mL). The combined organic extracts were washed with brine (80 mL), dried over anhydrous magnesium sulfate, filtered and concentrated *in vacuo*. The crude residue was purified by flash column chromatography (silica gel, gradient elution from 5 to 10% dichloromethane in pentane) to afford **S25** (2.38 g, 8.90 mmol, 44%) as a yellow oil.

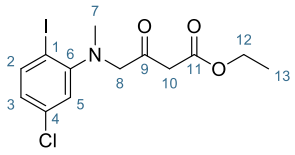
^{1}H NMR (400 MHz, $CDCl_3$) δ = 7.53 (1H, d, *J* = 8.3, H2), 6.51 (1H, d, *J* = 2.3, H5), 6.45 (1H, dd, *J* = 8.3, 2.4, H3), 4.28 (1H, br s, NH), 2.88 (3H, d, *J* = 5.1, H7).

^{13}C NMR (101 MHz, $CDCl_3$) δ = 149.2 (C6), 139.4 (C2), 135.8 (C4), 118.4 (C3), 110.0 (C5), 82.0 (C1), 31.0 (C7).

FTIR (neat) ν/cm^{-1} = 3405 (br), 2980, 1584, 1506, 1399, 1284, 1094, 1003, 880, 830, 783.

HRMS (APCI) *m/z* calcd. for C_7H_8NClI $[M+H]^+$: 267.9384; found: 267.9385.

Ethyl 4-((5-chloro-2-iodophenyl)(methyl)amino)-3-oxobutanoate, **S26**



This compound was prepared by analogy to a literature procedure.[S13] To a stirred mixture of **S25** (1.75 g, 6.54 mmol, 1.0 eq.), sodium hydrogencarbonate (1.10 g, 13.1 mmol, 2.0 eq.) and sodium iodide (1.96 g, 13.1 mmol, 2.0 eq.) in acetonitrile (13 mL, 0.5 M) at 75 °C was added ethyl 4-chloroacetoacetate (95% w/w, 1.9 mL, 13 mmol, 2.0 eq.) over 30 min *via* syringe pump. After heating for a further 12 h, the reaction mixture was concentrated *in vacuo*, and the crude residue thus obtained was dissolved in ethyl acetate (30 mL) and washed successively with sodium thiosulfate (sat. aq., 15 mL) and water (15 mL). The aqueous washings were extracted with ethyl acetate (2 x 30 mL),

and the combined organic extracts were subjected to a final wash with brine (45 mL), dried over anhydrous sodium sulfate, filtered and concentrated *in vacuo*. The crude residue was purified by flash column chromatography (silica gel, gradient elution 10 to 20% diethyl ether in pentane) to afford **S26** (670 mg, 1.69 mmol, 26%) as a viscous yellow oil.

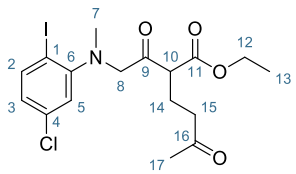
^{1}H NMR (400 MHz, $CDCl_3$) δ = 7.73 (1H, d, *J* = 8.4, H2), 7.12 (1H, d, *J* = 2.4, H5), 6.80 (1H, dd, *J* = 8.4, 2.4, H3), 4.18 (2H, q, *J* = 7.1, H12), 3.94 (2H, s, H8), 3.59 (2H, s, H10), 2.81 (3H, s, H7), 1.26 (3H, t, *J* = 7.1, H13).

^{13}C NMR (101 MHz, $CDCl_3$) δ = 201.0 (C9), 167.2 (C11), 154.2 (C6), 140.9 (C2), 135.3 (C4), 126.0 (C3), 123.2 (C5), 93.8 (C1), 65.5 (C8), 61.6 (C12), 46.6 (C10), 42.7 (C7), 14.2 (C13).

FTIR (neat) ν/cm^{-1} = 2985, 1745, 1721, 1457, 1315, 1228, 1185, 1098, 1032, 1016, 805.

HRMS (ESI) *m/z* calcd. for $C_{13}H_{16}ClINO_3$ $[M+H]^+$: 395.9858; found: 395.9857.

Ethyl 2-(*N*-(5-chloro-2-iodophenyl)-*N*-methylglycyl)-5-oxohexanoate, **S27**



Aminoketone **S26** (1.03 g, 2.60 mmol, 1.0 eq.) was dissolved in dichloromethane (5.2 mL, 0.5 M). Potassium carbonate (360 mg, 2.60 mmol, 1.0 eq.) was added in one portion followed by freshly distilled methyl vinyl ketone (0.22 mL, 0.18 g, 2.6 mmol, 1.0 eq.). The reaction mixture was stirred for 24 h at room temperature before being concentrated *in vacuo*. The crude residue was purified by flash column chromatography (silica gel, 20% ethyl acetate in pentane) to afford **S27** (807 mg, 1.73 mmol, 67%) as a viscous yellow oil.

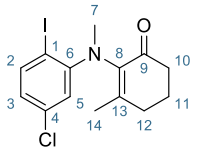
^{1}H NMR (400 MHz, $CDCl_3$) δ = 7.70 (1H, d, *J* = 8.4, H2), 7.12 (1H, d, *J* = 2.4, H5), 6.78 (1H, dd, *J* = 8.4, 2.4, H3), 4.14 (2H, q, *J* = 7.1, H12), 4.07 (1H, d, *J* = 18.0, H8), 3.99 (1H, d, *J* = 18.0, H8'), 3.73 (1H, t, *J* = 7.0, H10), 2.83 (3H, s, H7), 2.47 (2H, t, *J* = 7.1, H15), 2.13–2.02 (2H, m, H14), 2.10 (3H, s, H17), 1.22 (3H, t, *J* = 7.1, H13).

^{13}C NMR (101 MHz, $CDCl_3$) δ = 207.6 (C16), 202.6 (C9), 169.2 (C11), 154.2 (C6), 140.9 (C2), 135.1 (C4), 125.7 (C3), 123.2 (C5), 93.4 (C1), 64.7 (C8), 61.7 (C12), 54.1 (C10), 42.3 (C7), 40.6 (C15), 30.0 (C17), 21.7 (C14), 14.2 (C13).

FTIR (neat) ν/cm^{-1} = 2941, 1744, 1716, 1571, 1457, 1368, 1187, 1161, 1099, 1014, 805.

HRMS (ESI) *m/z* calcd. for $C_{17}H_{22}O_4NClI$ $[M+H]^+$: 466.0277; found: 466.0277.

2-((5-Chloro-2-iodophenyl)(methyl)amino)-3-methylcyclohex-2-en-1-one, **S28**



Sodium methoxide (30 wt% in methanol, 0.33 mL, 0.096 g, 1.8 mmol, 1.1 eq.) was added in one portion to a stirred, argon-sparged solution of diketone **S27** (749 mg, 1.61 mmol, 1.0 eq.) in methanol (16 mL, 0.1 M) at room temperature. The reaction mixture was stirred at this temperature for a further 2 h before adding a solution of lithium hydroxide monohydrate (68 mg, 1.6 mmol, 1.0 eq.) in water (8 mL) and heating to 75 °C. After 10 min, the reaction mixture was cooled to room temperature and acidified to *ca.* pH 2 with HCl (1 M aq., *ca.* 8 mL). The reaction mixture was heated to 75 °C for a further 30 min before cooling to room temperature, adding water (20 mL) and extracting with ethyl acetate (3 x 20 mL). The combined organic extracts were washed with brine (40 mL), dried over anhydrous sodium sulfate, filtered and concentrated *in vacuo*. The crude residue was purified three times by flash column chromatography (silica gel, 20% diethyl ether in pentane; then, silica gel, dichloromethane; then, silica gel, 20% tetrahydrofuran in pentane) to afford **S28** (253 mg, 0.674 mmol, 42%) as a pale-yellow solid.

^{1}H NMR (400 MHz, $CDCl_3$) δ = 7.60 (1H, d, *J* = 8.4, H2), 6.97 (1H, d, *J* = 2.4, H5), 6.56 (1H, dd, *J* = 8.4, 2.4, H3), 3.03 (3H, s, H7), 2.53–2.42 (4H, m, $H10_{LHS}$ & $H12_{RHS}$), 2.09–1.98 (2H, m, H11), 1.79 (3H, t, *J* = 0.9, H14).

^{13}C NMR (101 MHz, $CDCl_3$) δ = 196.0 (C9), 155.4 (C13), 152.8 (C6), 142.0 (C2), 140.1 (C8), 135.0 (C4), 122.2 (C3), 119.7 (C5), 83.6 (C1), 40.8 (C7), 38.5 (C10), 32.9 (C12), 21.8 (C11), 21.5 (C14).

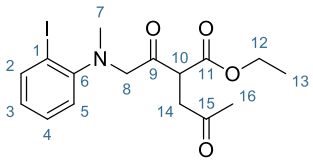
FTIR (neat) ν/cm^{-1} = 2947, 1675, 1570, 1467, 1393, 1373, 1203, 1109, 1005, 930, 792.

HRMS (ESI) *m/z* calcd. for $C_{14}H_{16}ONClI$ $[M+H]^+$: 375.9960; found: 375.9961.

MP 81–83 °C.

S2.10. Synthesis of cyclopentenone substrate **S30**

Ethyl 2-(*N*-(2-iodophenyl)-*N*-methylglycyl)-4-oxopentanoate, **S29**



To a stirred mixture of **S5** (1.85 g, 5.12 mmol, 1.0 eq.), sodium hydrogencarbonate (863 mg, 10.3 mmol, 2.0 eq.) and sodium iodide (1.54 g, 10.3 mmol, 2.0 eq.) in acetonitrile (25 mL, 0.2 M) at room temperature was added chloroacetone (0.82 mL, 0.95 g, 10 mmol, 2.0 eq.) in one portion. The reaction mixture was heated to 75 °C for 18 h with stirring. After this time, the reaction mixture was allowed to cool to room temperature before being diluted with water (25 mL). The resulting mixture was extracted with diethyl ether (3 x 25 mL), and the combined organic extracts were concentrated *in vacuo*. The crude residue was purified by flash column chromatography (silica gel, dichloromethane) to afford **S29** (652 mg, 1.56 mmol, 31%) as a pale-yellow oil.

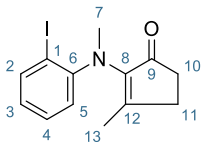
^{1}H NMR (400 MHz, $CDCl_3$) δ = 7.82 (1H, dd, *J* = 7.9, 1.5, H2), 7.34–7.26 (2H, m, H4), 7.18 (1H, dd, *J* = 8.0, 1.6, H5), 6.82–6.74 (1H, m, H3), 4.30–4.05 (5H, m, H8, H10 & H12), 3.16 (1H, dd, *J* = 18.5, 8.8, H14), 3.00 (1H, dd, *J* = 18.5, 5.2, H14'), 2.87 (3H, s, H7), 2.18 (3H, s, H16), 1.16 (3H, t, *J* = 7.1, H13).

^{13}C NMR (101 MHz, $CDCl_3$) δ = 205.7 (C9), 203.0 (C15), 168.7 (C11), 153.2 (C6), 140.3 (C2), 129.2 (C4), 125.7 (C3), 123.0 (C5), 96.9 (C1), 65.7 (C8), 62.0 (C12), 50.1 (C10), 42.6 (C7), 41.8 (C14), 29.8 (C16), 14.1 (C13).

FTIR (neat) ν/cm^{-1} = 2988, 1746, 1719, 1472, 1445, 1428, 1399, 1366, 1350, 1268, 1234, 1187, 1161, 1132, 1016, 758, 743.

HRMS (APCI) *m/z* calcd. for $C_{16}H_{21}INO_4$ $[M+H]^+$: 418.0510; found: 418.0509.

2-((2-Iodophenyl)(methyl)amino)-3-methylcyclopent-2-en-1-one, **S30**



Sodium methoxide (30 wt% in methanol, 0.32 mL, 0.093 g, 1.7 mmol, 1.1 eq.) was added in one portion to a stirred, argon-sparged solution of diketone **S29** (656 mg, 1.57 mmol, 1.0 eq.) in methanol (16 mL, 0.1 M) at room temperature. The reaction mixture was stirred at this temperature for a further 2 h before adding a solution of lithium hydroxide monohydrate (65.9 mg, 1.57 mmol, 1.0 eq.) in water (8 mL) and heating to 75 °C. After 10 min, the reaction mixture was cooled to room temperature and acidified to

ca. pH 2 with HCl (1 M aq., *ca.* 8 mL). The reaction mixture was heated to 75 °C for a further 30 min before cooling to room temperature, adding water (20 mL) and extracting with dichloromethane (3 x 20 mL). The combined organic extracts were washed with brine (40 mL), dried over anhydrous sodium sulfate, filtered and concentrated *in vacuo*. The crude residue was purified by flash column chromatography on neutral alumina gel (gradient elution from 20 to 40% ethyl acetate in pentane) to afford **S30** (201 mg, 0.614 mmol, 39%) as a pale-yellow solid.

^{1}H NMR (400 MHz, $CDCl_3$) δ = 7.78 (1H, dd, *J* = 7.9, 1.5, H2), 7.30 (1H, ddd, *J* = 8.0, 7.2, 1.5, H4), 7.13 (1H, dd, *J* = 8.1, 1.5, H5), 6.70 (1H, ddd, *J* = 7.8, 7.2, 1.5, H3), 3.23 (3H, s, H7), 2.53–2.47 (2H, m, H10), 2.46–2.40 (2H, m, H11), 1.50–1.47 (3H, m, H13).

^{13}C NMR (101 MHz, $CDCl_3$) δ = 206.3 (C9), 160.0 (C12), 150.8 (C6), 143.9 (C8), 140.7 (C2), 129.0 (C4), 124.0 (C3), 121.9 (C5), 92.5 (C1), 39.1 (C7), 33.7 (C11), 29.5 (C10), 17.4 (C13).

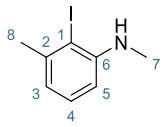
FTIR (neat) ν/cm^{-1} = 2864, 2805, 1696, 1632, 1579, 1469, 1291, 1210, 1157, 1108, 1054, 1024, 1012, 746.

HRMS (APCI) *m/z* calcd. for $C_{13}H_{15}INO$ $[M+H]^+$: 328.0193; found: 328.0194.

MP 47–53 °C.

S2.11. Synthesis of 3-methyl substrate **S34**

2-Iodo-*N*,3-dimethylaniline, **S31**



2-Iodo-3-nitrotoluene (5.00 g, 19.0 mmol, 1.0 eq.) was dissolved in a 2:1 (v/v) mixture of ethanol (64 mL) and glacial acetic acid (32 mL) (0.2 M). Iron powder (10.6 g, 190 mmol, 10 eq.) was added slowly in portions at room temperature with stirring before heating the mixture to 60 °C for 2 h. After this time, the reaction mixture was cooled to room temperature and added slowly by dropping funnel to a mixture of sodium hydrogencarbonate (50 g) in water (500 mL) with vigorous stirring. The neutralized reaction mixture was extracted with ethyl acetate (3 x 100 mL). The combined organic extracts were washed with brine (150 mL), dried over anhydrous sodium sulfate, filtered and concentrated *in vacuo*. The crude residue was dissolved in anhydrous tetrahydrofuran (38 mL, 0.5 M) under an argon atmosphere, and the resulting solution was cooled to −78 °C in an acetone–dry ice bath and stirred magnetically. *N*-Butyllithium in hexanes (8.2 mL, 2.5 M in hexanes, 21 mmol) was added dropwise *via* syringe pump over 30 min to the reaction mixture. Methyl iodide (1.3 mL, 3.0 g, 21 mmol) was added in one portion after complete addition of the organometallic reagent. After a further 5 min at −78 °C, the acetone–dry ice bath was replaced with a tepid water bath, and the reaction mixture was allowed to warm to room temperature over 2 h. Ammonium chloride solution (sat. aq., 40 mL) was added, followed by diethyl ether (40 mL). The layers were separated, and the aqueous phase was extracted with additional diethyl ether (2 x 40 mL). The combined organic extracts were washed with brine (80 mL), dried over anhydrous magnesium sulfate, filtered and concentrated *in vacuo*. The crude residue was purified by flash column chromatography (silica gel, 1% diethyl ether in pentane) to afford **S31** (4.10 g, 16.6 mmol, 87% over two steps) as a colourless oil.

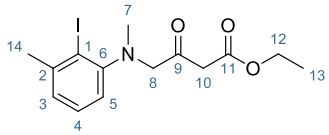
^{1}H NMR (400 MHz, $CDCl_3$) δ = 7.13 (1H, t, *J* = 7.7, H4), 6.68–6.61 (1H, m, H3), 6.43–6.36 (1H, m, H5), 4.39 (1H, br s, NH), 2.90 (3H, d, *J* = 5.0, H7), 2.44 (3H, s, H8).

^{13}C NMR (101 MHz, $CDCl_3$) δ = 148.6 (C6), 142.3 (C2), 128.9 (C4), 118.7 (C3), 107.4 (C5), 92.6 (C1), 31.4 (C7), 29.7 (C8).

FTIR (neat) ν/cm^{-1} =3407 (br), 2904, 2818, 1587, 1503, 1468, 1319, 1281, 1159, 1002, 764, 703.

HRMS (ESI) *m/z* calcd. For $C_8H_{11}IN$ $[M+H]^+$: 247.9931; found: 247.9929.

Ethyl 4-((2-iodo-3-methylphenyl)(methyl)amino)-3-oxobutanoate, **S32**



This compound was prepared by analogy to a literature procedure.[S13] To a stirred mixture of **S31** (3.97 g, 16.1 mmol, 1.0 eq.), sodium hydrogencarbonate (2.70 g, 32.1 mmol, 2.0 eq.) and sodium iodide (4.82 g, 32.2 mmol, 2.0 eq.) in acetonitrile (32 mL, 0.5 M) at room temperature was added ethyl 4-chloroacetoacetate (95% w/w, 4.6 mL, 32 mmol, 2.0 eq.) in one portion. The reaction mixture was heated to 75 °C for 18 h with stirring. After this time, the reaction mixture was allowed to cool to room temperature before adding triethylamine (6.7 mL, 4.9 g, 48 mmol, 3.0 eq.) in one portion and stirring for a further 30 min. The reaction mixture was concentrated *in vacuo*, and the crude residue thus obtained was dissolved in ethyl acetate (60 mL) and washed successively with sodium thiosulfate (sat. aq., 30 mL) and water (30 mL). The aqueous washings were extracted with ethyl acetate (2 x 60 mL), and the combined organic extracts were subjected to a final wash with brine (90 mL), dried over anhydrous sodium sulfate, filtered and concentrated *in vacuo*. The crude residue was purified twice by flash column chromatography (silica gel, 5% ethyl acetate in pentane; then, silica gel, dichloromethane) to afford **S32** (2.47 g, 6.58 mmol, 41%) as a viscous yellow oil.

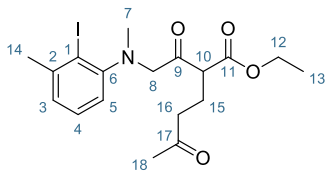
^{1}H NMR (400 MHz, $CDCl_3$) δ = 7.18 (1H, t, *J* = 7.7, H4), 7.05–6.98 (1H, m, H3), 6.98–6.90 (1H, m, H5), 4.17 (2H, q, *J* = 7.2, H12), 3.85 (2H, s, H8), 3.69 (2H, s, H10), 2.75 (3H, s, H7), 2.49 (3H, s, H14), 1.25 (3H, t, *J* = 7.1, H13).

^{13}C NMR (101 MHz, $CDCl_3$) δ = 202.2 (C9), 167.6 (C11), 153.7 (C6), 143.8 (C2), 128.7 (C4), 126.3 (C3), 119.8 (C5), 105.6 (C1), 66.5 (C8), 61.4 (C12), 46.6 (C10), 43.8 (C7), 30.0 (C14), 14.2 (C13).

FTIR (neat) ν/cm^{-1} = 2981, 1746, 1721, 1464, 1315, 1227, 1183, 1030, 1013, 785, 720.

HRMS (ESI) *m/z* calcd. For $C_{14}H_{19}INO_3$ $[M+H]^+$: 376.0404; found: 376.0396.

Ethyl 2-(*N*-(2-iodo-3-methylphenyl)-*N*-methylglycyl)-5-oxohexanoate, **S33**



Aminoketone **S32** (2.35 g, 6.26 mmol, 1.0 eq.) was dissolved in dichloromethane (12.5 mL, 0.5 M). Potassium carbonate (866 mg, 6.27 mmol, 1.0 eq.) was added in one portion followed by freshly distilled methyl vinyl ketone (0.52 mL, 0.44 g, 6.2 mmol, 1.0 eq.). The reaction mixture was stirred for 21 h at room temperature before being concentrated *in vacuo*. The crude residue was purified by flash

column chromatography (silica gel, 20 to 30% ethyl acetate in pentane) to afford **S33** (2.45 g, 5.50 mmol, 88%) as a viscous yellow oil.

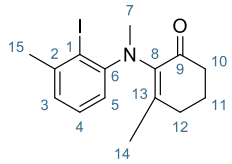
^{1}H NMR (400 MHz, $CDCl_3$) δ = 7.17 (1H, t, *J* = 7.7, H4), 7.00 (1H, ddd, *J* = 7.5, 1.5, 0.7, H3), 6.95 (1H, dd, *J* = 7.9, 1.6, H5), 4.13 (2H, q, *J* = 7.1, H12), 4.00–3.86 (3H, m, H8 & H10), 2.77 (3H, s, H7), 2.47 (3H, s, H14), 2.43 (2H, app. td, *J* = 7.0, 1.5, H16), 2.12–2.00 (2H, m, H15), 2.08 (3H, s, H18), 1.20 (3H, t, *J* = 7.1, H13).

^{13}C NMR (101 MHz, $CDCl_3$) δ = 207.6 (C17), 203.7 (C9), 169.4 (C11), 153.6 (C6), 143.7 (C2), 128.6 (C4), 126.0 (C3), 119.9 (C5), 105.5 (C1), 65.7 (C8), 61.5 (C12), 53.7 (C10), 43.4 (C7), 40.7 (C16), 30.0(1) & 29.9(6) (C14 & C18), 21.8 (C15), 14.1 (C13).

FTIR (neat) ν/cm^{-1} = 2980, 1744, 1717, 1464, 1369, 1161, 1098, 1013, 860, 787, 720.

HRMS (ESI) *m/z* calcd. For $C_{18}H_{25}INO_4$ $[M+H]^+$: 446.0823; found: 446.0814.

2-((2-Iodo-3-methylphenyl)(methyl)amino)-3-methylcyclohex-2-en-1-one, **S34**



Sodium methoxide (30 wt% in methanol, 1.06 mL, 0.308 g, 5.70 mmol, 1.1 eq.) was added in one portion to a stirred, argon-sparged solution of diketone **S33** (2.31 g, 5.19 mmol, 1.0 eq.) in methanol (52 mL, 0.1 M) at room temperature. The reaction mixture was stirred at this temperature for a further 2 h before adding a solution of lithium hydroxide monohydrate (239 mg, 5.70 mmol, 1.1 eq.) in water (26 mL) and heating to 75 °C. After 10 min, the reaction mixture was cooled to room temperature and acidified to *ca.* pH 2 with HCl (1 M aq., *ca.* 26 mL). The reaction mixture was heated to 75 °C for a further 30 min before cooling to room temperature, adding water (50 mL) and extracting with ethyl acetate (3 x 50 mL). The combined organic extracts were washed with brine (100 mL), dried over anhydrous sodium sulfate, filtered and concentrated *in vacuo*. The crude residue was purified by flash column chromatography (silica gel, 20% diethyl ether in pentane) to afford **S34** (1.13 g, 3.18 mmol, 61%) as a cream-coloured solid.

^{1}H NMR (400 MHz, $CDCl_3$) δ = 7.13 (1H, dd, *J* = 8.1, 7.3, H4), 6.87 (1H, dd, *J* = 8.2, 1.6, H5), 6.84 (1H, ddd, *J* = 7.3, 1.6, 0.7, H3), 3.08 (3H, s, H7), 2.51–2.39 (4H, m, $H10_{LHS}$ & $H12_{RHS}$), 2.43 (3H, s, H15), 2.06–1.95 (2H, m, H11), 1.76 (3H, t, *J* = 0.9, H14).

^{13}C NMR (101 MHz, $CDCl_3$) δ = 196.8 (C9), 154.1 (C13), 152.8 (C6), 143.2 (C2), 141.2 (C8), 128.2 (C4), 122.9 (C3), 118.9 (C5), 97.3 (C1), 41.2 (C7), 39.0 (C10), 33.1 (C12), 30.7 (C15), 22.0 (C11), 21.5 (C14).

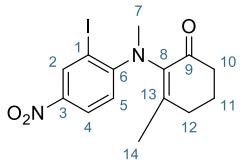
FTIR (neat) ν/cm^{-1} = 2947, 1675, 1575, 1462, 1290, 1199, 1079, 1007, 937, 777, 731.

HRMS (ESI) *m/z* calcd. For $C_{15}H_{19}INO$ $[M+H]^+$: 356.0506; found: 356.0503.

MP 90–92 °C.

S2.12. Synthesis of *para*-nitro and *para*-*N*-acetyl substrates **S35** and **S36**

2-((2-Iodo-4-nitrophenyl)(methyl)amino)-3-methylcyclohex-2-en-1-one, **S35**



Copper(II) nitrate trihydrate (483 mg, 2.00 mmol, 1.0 eq.) was added in one portion to **10** (682 mg, 2.00 mmol, 1.0 eq.) dissolved in a 1:1 (v/v) mixture of acetic anhydride (2.0 mL) and glacial acetic acid (2.0 mL) (0.5 M) at room temperature. After sonicating for 2 min, the reaction mixture was stirred at room temperature for 1 h before being added dropwise to a mixture of sodium hydrogencarbonate (*ca.* 6 g) in water (100 mL) with vigorous stirring. The resulting mixture was transferred to a separating funnel using ethyl acetate (50 mL) and a small volume of water. After thorough mixing, the layers were separated, and the aqueous phase was extracted with additional ethyl acetate (2 x 50 mL). The combined organic extracts were washed with brine (75 mL), dried over anhydrous sodium sulfate, filtered and concentrated *in vacuo* (residual acetic anhydride was azeotropically removed with toluene). The crude residue was purified by flash column chromatography (silica gel, 1% ethyl acetate in dichloromethane) to afford **S35** (220 mg, 0.570 mmol, 28%) as an extremely viscous orange-brown oil, which turned over slowly upon storage at -18 °C to an orange solid.

^{1}H NMR (400 MHz, $CDCl_3$) δ = 8.61 (1H, d, *J* = 2.7, H2), 8.15 (1H, dd, *J* = 9.2, 2.7, H4), 6.95 (1H, d, *J* = 9.2, H5), 3.11 (3H, s, H7), 2.52 (4H, app. t, *J* = 6.4, H10 & H12), 2.13–2.02 (2H, m, H11), 1.82 (3H, s, H14).

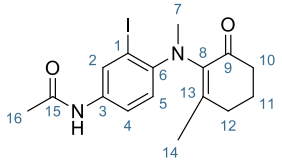
^{13}C NMR (101 MHz, $CDCl_3$) δ = 195.0 (C9), 156.8 & 156.7 (C6 & C13), 140.4 (C3), 139.6 (C8), 138.0 (C2), 124.9 (C4), 116.4 (C5), 80.8 (C1), 41.5 (C7), 37.9 (C10), 32.6 (C12), 21.7 (C11 & C14, coincident).

FTIR (neat) ν/cm^{-1} = 2944, 1674, 1576, 1498, 1320, 1307, 1264, 1208, 1114, 748, 727.

HRMS (APCI) *m/z* calcd. For $C_{14}H_{16}O_3N_2I$ $[M+H]^+$: 387.0200; found: 387.0200.

MP 85–87 °C.

N-(3-Iodo-4-(methyl(2-methyl-6-oxocyclohex-1-en-1-yl)amino)phenyl)acetamide, **S36**



Nitro compound **S35** (182 mg, 0.471 mmol, 1.0 eq.) was dissolved in a 2:1 (v/v) mixture of ethanol (3.2 mL) and glacial acetic acid (1.6 mL) (0.1 M). Iron powder (263 mg, 4.71 mmol, 10 eq.) was added slowly in portions at room temperature with stirring before heating the mixture to 60 °C for 2 h. After this time, the reaction mixture was cooled to room temperature and added slowly by dropping funnel to a mixture of sodium hydrogencarbonate (*ca.* 3 g) in water (50 mL) with vigorous stirring. The neutralized reaction mixture was extracted with ethyl acetate (3 x 50 mL). The combined organic extracts were washed with brine (75 mL), dried over anhydrous sodium sulfate, filtered and concentrated *in vacuo*. The crude residue was dissolved in dichloromethane (4.8 mL) along with acetic anhydride (0.13 mL, 0.14 g, 1.4 mmol). The reaction mixture mixture was stirred at room temperature for 2 h before being concentrated *in vacuo*. The crude residue was purified by flash column chromatography (silica gel, 25% ethyl acetate in dichloromethane) to afford **S36** (104 mg, 0.261 mmol, 55% over two steps from **S33**) as a light brown foam solid.

^{1}H NMR (400 MHz, $CDCl_3$) δ = 7.84 (1H, d, *J* = 2.5, H2), 7.62 (1H, br s, NH), 7.38 (1H, dd, *J* = 8.8, 2.5, H4), 6.93 (1H, d, *J* = 8.8, H5), 3.02 (3H, s, H7), 2.52–2.39 (4H, m, $H10_{LHS}$ & $H12_{RHS}$), 2.09 (3H, s, H16), 2.07–1.97 (2H, m, H11), 1.77 (3H, s, H14).

^{13}C NMR (101 MHz, $CDCl_3$) δ = 196.9 (C9), 168.4 (C15), 155.2 (C13), 148.4 (C6), 140.6 (C8), 132.6 (C2), 132.3 (C3), 121.2 (C4), 120.0 (C5), 87.4 (C1), 40.8 (C7), 38.8 (C10), 33.0 (C12), 24.4 (C16), 21.9 (C11), 21.6 (C14).

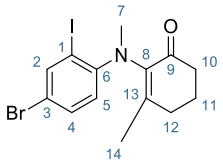
FTIR (neat) ν/cm^{-1} = 3307 (br), 2947, 1664, 1592, 1520, 1487, 1384, 1310, 1290, 1117, 731.

HRMS (ESI) *m/z* calcd. For $C_{16}H_{19}O_2N_2Ina$ $[M+Na]^+$: 421.0383; found: 421.0378.

MP 64–68 °C (ambiguous phase transition owing to foam nature of solid).

S2.13. Synthesis of *para*-bromo substrate **S37**

2-((4-Bromo-2-iodophenyl)(methyl)amino)-3-methylcyclohex-2-en-1-one, **S37**



N-Bromosuccinimide (187 mg, 1.05 mmol, 1.05 eq.) was added in one portion to a stirred solution of **10** (341 mg, 0.999 mmol, 1.0 eq.) in acetonitrile (10 mL, 0.1 M) at room temperature. The reaction mixture was stirred for 1 h at this temperature before charging additional *N*-bromosuccinimide (18 mg, 0.10 mmol, 0.1 eq.). After stirring for a further 3 h, the reaction mixture was concentrated *in vacuo*, and the crude residue thus obtained was dissolved in ethyl acetate (10 mL) and washed with sodium hydrogencarbonate (sat. aq., 2 x 5 mL) and brine (5 mL). The organic layer was dried over anhydrous sodium sulfate, filtered and concentrated *in vacuo*. The crude residue was purified by flash column chromatography (silica gel, gradient elution from 30 to 40% diethyl ether in pentane) to afford **S37** (189 mg, 0.450 mmol, 45%) as a pale-yellow solid.

^{1}H NMR (400 MHz, $CDCl_3$) δ = 7.82 (1H, d, *J* = 2.3, H2), 7.35 (1H, dd, *J* = 8.7, 2.4, H4), 6.89 (1H, d, *J* = 8.8, H5), 3.02 (3H, s, H7), 2.51–2.42 (4H, m, $H10_{LHS}$ & $H12_{RHS}$), 2.08–1.97 (2H, m, H11), 1.80 (3H, t, *J* = 0.9, H14).

^{13}C NMR (101 MHz, $CDCl_3$) δ = 196.2 (C9), 155.4 (C13), 151.1 (C6), 142.7 (C2), 140.3 (C8), 131.6 (C4), 120.9 (C5), 113.2 (C3), 87.3 (C1), 40.8 (C7), 38.6 (C10), 32.9 (C12), 21.9 (C11), 21.6 (C14).

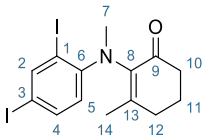
FTIR (neat) ν/cm^{-1} = 2947, 1674, 1468, 1375, 1290, 1203, 1118, 1018, 913, 802, 743.

HRMS (ESI) *m/z* calcd. For $C_{14}H_{16}ON^{79}BrI$ ($C_{14}H_{16}ON^{81}BrI$) $[M+H]^+$: 419.9454 (421.9434); found: 419.9454 (421.9432).

MP 87–88 °C

S2.14. Synthesis of *para*-iodo substrate **S38**

2-((2,4-Diiodophenyl)(methyl)amino)-3-methylcyclohex-2-en-1-one, **S38**



To a solution of **10** (341 mg, 0.999 mmol, 1.0 eq.) in dichloromethane (5 mL, 0.2 M) at room temperature was added iodine (279 mg, 1.10 mmol, 1.1 eq.) and silver sulfate (343 mg, 1.10 mmol, 1.1 eq.) with vigorous stirring. After 3 h, the reaction mixture was filtered through celite, and the filtrate was concentrated *in vacuo*. The crude residue was purified by flash column chromatography (silica gel, 25% diethyl ether in pentane) to afford **S38** (292 mg, 0.668 mmol, 63%) as a pale-yellow solid.

^{1}H NMR (600 MHz, $CDCl_3$) δ = 7.99 (1H, d, *J* = 2.1, H2), 7.51 (1H, dd, *J* = 8.7, 2.1, H4), 6.77 (1H, d, *J* = 8.6, H5), 3.01 (3H, s, H7), 2.50–2.43 (4H, m, $H10_{LHS}$ & $H12_{RHS}$), 2.02 (2H, quint, H11), 1.79 (3H, s, H14).

^{13}C NMR (151 MHz, $CDCl_3$) δ = 196.1 (C9), 155.4 (C13), 151.7 (C6), 148.3 (C2), 140.2 (C8), 137.5 (C4), 121.5 (C5), 87.9 & 83.3 (C1 & C3), 40.7 (C7), 38.6 (C10), 32.9 (C12), 21.9 (C11), 21.6 (C14).

FTIR (neat) ν/cm^{-1} = 2945, 1673, 1563, 1465, 1375, 1290, 1202, 1118, 1013, 807, 730.

HRMS (ESI) *m/z* calcd. For $C_{14}H_{15}NINa$ $[M+Na]^+$: 489.9135; found: 489.9135.

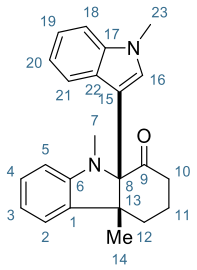
MP 89–90 °C.

S2.15. Photochemical reactivity of β-methyl substrate **10** in the presence of various nucleophiles (nucleophile scope)

General Procedure A

Enaminone **10** (102.4 mg, 0.300 mmol, 1.0 eq.) and (if non-volatile) the appropriate nucleophile (3.0 eq., unless otherwise stated) and/or basic additive were charged to a Schlenk tube equipped with a magnetic stir bar. The vessel was sealed with a septum, and the flask was evacuated and back-filled with argon three times. Solvent(s) and nucleophile (if volatile), both argon-sparged, were added *via* syringe. The reaction mixture was stirred under constant irradiation with two Kessil PR160L 427 nm LED lamps (each positioned *ca.* 3 cm from the flask and directed toward it) for the specified time, with cooling to ambient temperature being achieved using a strong jet of nitrogen gas directed at the flask. Triethylamine (2.0 mL) was added to the reaction mixture at the end of the irradiation period, and the resulting mixture was concentrated *in vacuo*. The crude residue was purified by flash column chromatography to afford the corresponding indoline product.

rac-4a,9-Dimethyl-9a-(1-methyl-1*H*-indol-3-yl)-2,3,4,4a,9,9a-hexahydro-1*H*-carbazol-1-one, **13**



This compound was prepared from **10** (102.4 mg, 0.300 mmol, 1.0 eq.) according to General Procedure A. Irradiation was performed in the presence of 1-methylindole (112 μL, 118 mg, 0.897 mmol, 3.0 eq.) in a 9:1 (v/v) mixture of acetonitrile (5.4 mL) and hexafluoroisopropanol (0.6 mL) (0.05 M) over a period of 18 h. Flash column chromatography on alumina gel (gradient elution from 5 to 25% dichloromethane in pentane) yielded **13** (83.9 mg, 0.244 mmol, 81%) as a peach-coloured solid.

^{1}H NMR (400 MHz, DMSO-d_6) δ = 7.43–7.38 (1H, m, H18), 7.36 (1H, d, J = 8.1, H21), 7.31 (1H, s, H16), 7.16–7.06 (2H, m, $H19_{LHS}$ & $H4_{RHS}$), 6.99 (1H, dd, J = 7.2, 1.3, H2), 6.95 (1H, ddd, J = 8.1, 7.0, 1.1, H20), 6.67 (1H, td, J = 7.4, 1.0, H3), 6.51 (1H, d, J = 7.7, H5), 3.78 (3H, s, H23), 2.79–2.66 (1H, m, H10), 2.72 (3H, s, H7), 2.39–2.27 (1H, m, H10'), 2.09–1.98 (1H, m, H12), 1.93–1.74 (2H, m, $H11_{LHS}$ & $H12'_{RHS}$), 1.68–1.51 (1H, m, H11'), 0.84 (3H, s, H14).

^{13}C NMR (101 MHz, DMSO-d_6) δ = 212.0* (C9), 150.2 (C6), 136.6 (C17), 133.8 (C1), 129.3 (C16), 127.9 (C4), 127.5 (C22), 121.6 (C2 & C21, coincident), 121.0 (C19), 119.1 (C20), 117.3 (C3), 109.7

* Identified through HMBC correlations.

(C18), 108.8 (C15), 105.6 (C5), 81.9 (C8), 52.7 (C13), 39.7 (C10), 32.5 (C23), 32.1 (C12), 31.8 (C7), 27.1 (C14), 20.0 (C11).

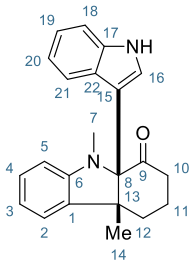
The observation of a transient nuclear Overhauser effect (nOe) by 1D NOESY for H21 upon selective inversion of H14 is consistent with the formation of the *cis*-diastereomer shown.

FTIR (neat) ν/cm^{-1} = 2938, 1707, 1604, 1488, 1371, 1305, 1020, 911, 739.

HRMS (ESI) *m/z* calcd. For $C_{23}H_{25}N_2O$ $[M+H]^+$: 345.1961; found: 345.1954.

MP 163–165 °C.

rac-9a-(1*H*-Indol-3-yl)-4a,9-dimethyl-2,3,4,4a,9,9a-hexahydro-1*H*-carbazol-1-one, **14**



This compound was prepared from **10** (102.4 mg, 0.300 mmol, 1.0 eq.) according to General Procedure A. Irradiation was performed in the presence of indole (105.4 mg, 0.900 mmol, 3.0 eq.) in a 9:1 (v/v) mixture of acetonitrile (5.4 mL) and hexafluoroisopropanol (0.6 mL) (0.05 M) over a period of 18 h. Flash column chromatography on alumina gel (gradient elution from 20 to 100% dichloromethane in pentane) yielded **14** (82.6 mg, 0.250 mmol, 83%) as an off-white solid.

^{1}H NMR (400 MHz, DMSO-d_6) δ = 11.20 (1H, s, NH), 7.38 (1H, dt, *J* = 8.1, 0.9, H18), 7.33 (1H, d, *J* = 8.1, H21), 7.27–7.21 (1H, m, H16), 7.10 (1H, td, *J* = 7.7, 1.3, H4), 7.05 (1H, ddd, *J* = 8.1, 7.0, 1.2, H19), 6.99 (1H, dd, *J* = 7.2, 1.3, H2), 6.91 (1H, ddd, *J* = 8.1, 6.9, 1.1, H20), 6.66 (1H, td, *J* = 7.4, 1.0, H3), 6.51 (1H, d, *J* = 7.7, H5), 2.81–2.60 (1H, m, H10), 2.72 (3H, m, H7), 2.38–2.27 (1H, m, H10'), 2.10–1.96 (1H, m, H12), 1.93–1.75 (2H, m, H11$_{LHS}$ & H12'$_{RHS}$), 1.69–1.52 (1H, m, H11'), 0.84 (3H, s, H14).

^{13}C NMR (101 MHz, DMSO-d_6) δ = 212.2 (C9), 150.2 (C6), 136.2 (C17), 134.0 (C1), 127.9 (C4), 127.1 (C22), 125.0 (C16), 121.6 (C2), 121.4 (C21), 120.8 (C19), 118.9 (C20), 117.2 (C3), 111.5 (C18), 109.7 (C15), 105.5 (C5), 81.9 (C8), 52.7 (C13), 39.6 (C10), 32.3 (C12), 31.7 (C7), 27.0 (C14), 19.9 (C11).

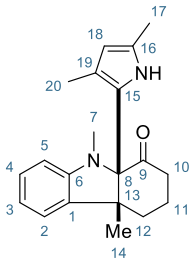
The observation of nuclear Overhauser effect (nOe) correlations by 2D NOESY corresponding to H14↔H21 is consistent with the formation of the *cis*-diastereomer shown.

FTIR (neat) ν/cm^{-1} = 3406 (br), 2981, 1701, 1604, 1489, 1457, 1421, 1305, 1021, 912, 743.

HRMS (ESI) *m/z* calcd. For $C_{22}H_{23}ON_2$ $[M+H]^+$: 331.1805; found: 331.1802.

MP 189–191 °C.

rac-9a-(3,5-Dimethyl-1*H*-pyrrol-2-yl)-4a,9-dimethyl-2,3,4,4a,9,9a-hexahydro-1*H*-carbazol-1-one, **15**



This compound was prepared from **10** (102.4 mg, 0.300 mmol, 1.0 eq.) according to General Procedure A, except that the reaction mixture was degassed by three freeze–pump–thaw cycles prior to irradiation. Irradiation was performed in the presence of 2,4-dimethylpyrrole (93 μL, 86 mg, 0.90 mmol, 3.0 eq.) in a 9:1 (v/v) mixture of acetonitrile (5.4 mL) and water (0.6 mL) (0.05 M) over a period of 18 h. Flash column chromatography on alumina gel (gradient elution from 25 to 50% dichloromethane in pentane) yielded **15** (63.0 mg, 0.204 mmol, 68%) as an extremely viscous brown oil.

^{1}H NMR (400 MHz, DMSO-d_6) δ = 9.78 (1H, s, NH), 7.08 (1H, td, *J* = 7.6, 1.3, H4), 6.99 (1H, dd, *J* = 7.2, 1.3, H2), 6.66 (1H, td, *J* = 7.4, 1.0, H3), 6.46 (1H, d, *J* = 7.7, H5), 5.48 (1H, d, *J* = 2.8, H18), 2.55 (3H, s, H7), 2.30 (1H, ddd, *J* = 16.6, 8.5, 6.0, H10), 2.11–1.89 (2H, m, H10'$_{LHS}$ & H12$_{RHS}$), 2.10 (3H, s, H17), 1.86–1.67 (2H, m, H12'$_{LHS}$ & H11$_{RHS}$), 1.76 (3H, s, H20), 1.61–1.45 (1H, m, H11'), 0.76 (3H, s, H14).

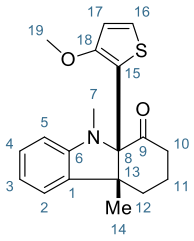
^{13}C NMR (101 MHz, DMSO-d_6) δ = 206.3 (C9), 149.5 (C6), 134.5 (C1), 127.8 (C4), 125.0 (C16), 121.9 (C2), 120.5 (C15 or C19), 117.4 (C3), 115.2 (C15 or C19), 108.6 (C18), 105.7 (C5), 80.6 (C8), 52.4 (C13), 36.1 (C10), 32.5 (C12), 30.3 (C7), 26.9 (C14), 18.3 (C11), 12.8 (C20), 12.6 (C17).

The observation of nuclear Overhauser effect (nOe) correlations by 2D NOESY corresponding to H14↔NH and H14↔H20 is consistent with the formation of the *cis*-diastereomer shown.

FTIR (neat) ν/cm^{-1} = 3396 (br), 2923, 2861, 1699, 1603, 1490, 1449, 1306, 1209, 1022, 788, 741.

HRMS (ESI) *m/z* calcd. For $C_{20}H_{25}N_2O$ $[M+H]^+$: 309.1961; found: 309.1958.

rac-9a-(3-Methoxythiophen-2-yl)-4a,9-dimethyl-2,3,4,4a,9,9a-hexahydro-1*H*-carbazol-1-one, **16**



This compound was prepared from **10** (102.4 mg, 0.300 mmol, 1.0 eq.) according to General Procedure A. Irradiation was performed in the presence of 3-methoxythiophene (0.15 mL, 0.17 g, 1.5 mmol, 5.0 eq.) in a 9:1 (v/v) mixture of acetonitrile (5.4 mL) and hexafluoroisopropanol (0.6 mL) (0.05 M) over a period of 18 h. Flash column chromatography on alumina gel (eluent: 25% dichloromethane in pentane) yielded **16** (42.8 mg, 0.131 mmol, 44%) as a pale pink solid.

^{1}H NMR (400 MHz, DMSO-d_6) δ = 7.34 (1H, dd, J = 5.5, 0.8, H16), 7.09 (1H, td, J = 7.6, 1.2, H4), 7.05–6.99 (2H, m, H17$_{LHS}$ & H2$_{RHS}$), 6.72 (1H, td, J = 7.4, 1.0, H3), 6.51 (1H, d, J = 7.8, H5), 3.67 (3H, s, H19), 2.66 (3H, s, H7), 2.40 (1H, ddd, J = 16.9, 8.3, 6.9, H10), 2.09 (1H, ddd, J = 16.9, 8.9, 5.5, H10'), 2.03–1.93 (2H, m, H12 & H12'), 1.83–1.68 (1H, m, H11), 1.52 (1H, m, H11'), 0.91 (3H, s, H14).

^{13}C NMR (101 MHz, DMSO-d_6) δ = 205.3 (C9), 154.0 (C18), 149.4 (C6), 134.5 (C1), 127.9 (C4), 123.0 (C16), 121.9 (C2), 119.5 (C15), 118.4 (C3), 117.7 (C17), 106.5 (C5), 80.1 (C8), 58.2 (C19), 52.0 (C13), 36.5 (C10), 32.4 (C12), 31.6 (C7), 26.7 (C14), 18.3 (C11).

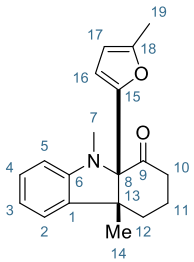
The observation of nuclear Overhauser effect (nOe) correlations by 2D NOESY corresponding to H14↔H19 is consistent with the formation of the *cis*-diastereomer shown.

FTIR (neat) ν/cm^{-1} = 2935, 2852, 2813, 1710, 1603, 1555, 1487, 1381, 1304, 1239, 1063, 1022, 742.

HRMS (ESI) *m/z* calcd. For $C_{19}H_{22}O_2NS$ $[M+H]^+$: 328.1366; found: 328.1367.

MP 78–80 °C.

rac-4a,9-Dimethyl-9a-(5-methylfuran-2-yl)-2,3,4,4a,9,9a-hexahydro-1*H*-carbazol-1-one, **17**



This compound was prepared from **10** (102.4 mg, 0.300 mmol, 1.0 eq.) according to General Procedure A. Irradiation was performed in the presence of 2-methylfuran (82 μL, 75 mg, 0.91 mmol, 3.0 eq.) in a 9:1 (v/v) mixture of acetonitrile (5.4 mL) and hexafluoroisopropanol (0.6 mL) (0.05 M) over a period of 18 h. Flash column chromatography on alumina gel (gradient elution from 2 to 10% diethyl ether in pentane yielded **17** (51.9 mg, 0.176 mmol, 59%) as a pale-yellow solid.

^{1}H NMR (400 MHz, DMSO-d_6) δ = 7.07 (1H, td, J = 7.6, 1.3, H4), 6.98 (1H, dd, J = 7.3, 1.3, H2), 6.66 (1H, td, J = 7.4, 1.0, H3), 6.48 (1H, d, J = 7.8, H5), 6.27 (1H, d, J = 3.2, H16), 6.13–6.06 (1H, m, H17), 2.81 (3H, s, H7), 2.75–2.62 (1H, m, H10), 2.34–2.23 (1H, m, H10'), 2.25 (3H, s, H19), 2.20–2.09 (1H, m, H12), 1.93–1.77 (2H, m, $H11_{LHS}$ & $H12'_{RHS}$), 1.60–1.44 (1H, m, H11'), 0.89 (3H, s, H14).

^{13}C NMR (101 MHz, DMSO-d_6) δ = 211.2 (C9), 151.5 (C18), 150.0 (C6), 147.9 (C15), 132.9 (C1), 127.9 (C4), 121.2 (C2), 117.7 (C3), 110.8 (C16), 106.3 (C17), 105.9 (C5), 81.5 (C8), 53.0 (C13), 39.9 (C10), 32.3 (C12), 31.8 (C7), 26.1 (C14), 20.5 (C11), 13.3 (C19).

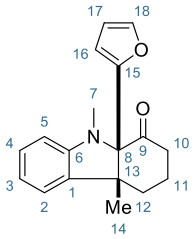
The observation of a transient nuclear Overhauser effect (nOe) by 1D NOESY for H16 upon selective inversion of H14 is consistent with the formation of the *cis*-diastereomer shown.

FTIR (neat) ν/cm^{-1} = 2925, 1718, 1606, 1486, 1457, 1363, 1304, 1120, 1022, 786, 740.

HRMS (ESI) *m/z* calcd. For $C_{19}H_{22}O_2N$ $[M+H]^+$: 296.1645; found: 296.1647.

MP 71–73 °C.

rac-9a-(Furan-2-yl)-4a,9-dimethyl-2,3,4,4a,9,9a-hexahydro-1*H*-carbazol-1-one, **18**



This compound was prepared from **10** (102.4 mg, 0.300 mmol, 1.0 eq.) according to General Procedure A, except that the reaction mixture was degassed by three freeze–pump–thaw cycles prior to irradiation. Irradiation was performed in the presence of potassium 2-furantrifluoroborate[S15] (156.6 mg, 0.900 mmol, 3.0 eq.) in a 3:1 (v/v) mixture of acetonitrile (4.5 mL) and water (1.5 mL) (0.05 M) over a period of 18 h. Flash column chromatography on silica gel (gradient elution from 2 to 5% ethyl acetate in pentane) yielded **18** (46.1 mg, 0.164 mmol, 55%) as a peach-coloured solid.

^{1}H NMR (400 MHz, DMSO-d_6) δ = 7.69 (1H, dd, J = 1.8, 0.8, H18), 7.08 (1H, td, J = 7.6, 1.3, H4), 6.99 (1H, dd, J = 7.3, 1.2, H2), 6.67 (1H, td, J = 7.4, 1.0, H3), 6.55–6.47 (2H, m, $H5_{LHS}$ & $H17_{RHS}$), 6.44 (1H, dd, J = 3.3, 0.8, H16), 2.78 (3H, s, H7), 2.66 (1H, ddd, J = 15.1, 10.9, 6.7, H10), 2.34 (1H,

dddd, J = 15.2, 5.5, 3.9, 1.6, H10'), 2.17–2.06 (1H, m, H12), 1.92–1.74 (2H, m, H11$_{LHS}$ & H12'$_{RHS}$), 1.63–1.48 (1H, m, H11'), 0.87 (3H, s, H14).

^{13}C NMR (101 MHz, DMSO-d_6) δ = 210.6 (C9), 150.1 & 150.0 (C6 & C15), 142.9 (C18), 133.2 (C1), 128.0 (C4), 121.3 (C2), 117.8 (C3), 110.3 (C17), 110.1 (C16), 106.0 (C5), 81.3 (C8), 53.2 (C13), 39.6 (C10), 32.9 (C12), 31.8 (C7), 25.7 (C14), 20.2 (C11).

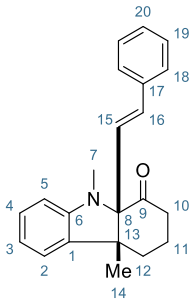
The observation of nuclear Overhauser effect (nOe) correlations by 2D NOESY corresponding to H14↔H16 is consistent with the formation of the *cis*-diastereomer shown.

FTIR (neat) ν/cm^{-1} = 2929, 1716, 1605, 1485, 1363, 1304, 1207, 1153, 1020, 858, 739.

HRMS (ESI) *m/z* calcd. For $C_{18}H_{20}O_2N$ $[M+H]^+$: 282.1489; found: 282.1488.

MP 79–81 °C.

rac-4a,9-Dimethyl-9a-(I-styryl)-2,3,4,4a,9,9a-hexahydro-1*H*-carbazol-1-one, **19**



This compound was prepared from **10** (102.4 mg, 0.300 mmol, 1.0 eq.) according to General Procedure A, except that the reaction mixture was degassed by three freeze–pump–thaw cycles prior to irradiation. Irradiation was performed in the presence of potassium *trans*-styryltrifluoroborate (94.5 mg, 0.450 mmol, 1.5 eq.) in a 3:1 (v/v) mixture of acetonitrile (4.5 mL) and water (1.5 mL) (0.05 M) over a period of 18 h. Flash column chromatography on silica gel (gradient elution from 2.5 to 5% ethyl acetate in pentane) yielded **19** (62.5 mg, 0.197 mmol, 66%) as a viscous yellow oil.

^{1}H NMR (400 MHz, DMSO-d_6) δ = 7.59–7.52 (2H, m, H18), 7.42–7.32 (2H, m, H19), 7.31–7.25 (1H, m, H20), 7.06 (1H, td, J = 7.6, 1.3, H4), 6.96 (1H, dd, J = 7.3, 1.3, H2), 6.64 (1H, td, J = 7.4, 1.0, H3), 6.51[*] (2H, app. s, H15 & H16), 6.48 (1H, dd, J = 7.8, 0.8, H5), 2.87 (3H, s, H7), 2.78–2.63 (1H, m, H10), 2.25–2.09 (2H, m, H10'$_{LHS}$ & H12$_{RHS}$), 1.90–1.78 (2H, m, H11$_{LHS}$ & H12'$_{RHS}$), 1.59–1.41 (1H, m, H11'), 1.12 (3H, s, H14).

[*] While splitting was not observed under these conditions, it is assumed that H15 and H16 are indeed spin-coupled; the singlet appearance of this signal is likely the result of a pronounced roofing effect between two near-isochronous doublets.

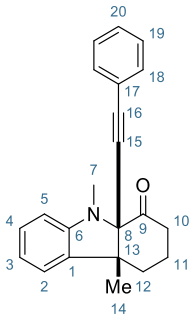
^{13}C NMR (101 MHz, DMSO-d_6) δ = 214.3 (C9), 150.5 (C6), 136.2 (C17), 133.5 (C16), 133.2 (C1), 128.6 (C19), 128.0 (C20), 127.9 (C4), 126.6 (C18), 123.9 (C15), 121.0 (C2), 117.3 (C3), 105.8 (C5), 83.7 (C8), 53.7 (C13), 39.6 (C10), 32.4 (C12), 31.6 (C7), 25.9 (C14), 21.5 (C11).

The observation of nuclear Overhauser effect (nOe) correlations by 2D NOESY corresponding to H14↔H15/16 (signals coincident) is consistent with the formation of the *cis*-diastereomer shown.

FTIR (neat) ν/cm^{-1} = 2959, 1715, 1606, 1486, 1368, 1306, 1125, 976, 913, 742, 694.

HRMS (ESI) *m/z* calcd. for $C_{22}H_{24}ON$ $[M+H]^+$: 318.1852; found: 318.1852.

rac-4a,9-Dimethyl-9a-(phenylethynyl)-2,3,4,4a,9,9a-hexahydro-1*H*-carbazol-1-one, **20**



This compound was prepared from **10** (102.4 mg, 0.300 mmol, 1.0 eq.) according to General Procedure A, except that the reaction mixture was degassed by three freeze–pump–thaw cycles prior to irradiation. Irradiation was performed in the presence of potassium (2-phenylethynyl)trifluoroborate[S16] (93.6 mg, 0.450 mmol, 1.5 eq.) in a 3:1 (v/v) mixture of acetonitrile (4.5 mL) and water (1.5 mL) (0.05 M) over a period of 18 h. Flash column chromatography on silica gel (eluent: 5% ethyl acetate in pentane) yielded **20** (49.7 mg, 0.158 mmol, 53%) as a viscous orange oil.

^{1}H NMR (400 MHz, DMSO-d_6) δ = 7.51–7.45 (2H, m, H18), 7.44–7.35 (3H, m, H19 & H20), 7.09 (1H, td, *J* = 7.6, 1.3, H4), 7.07–7.01 (1H, m, H2), 6.70 (1H, td, *J* = 7.4, 1.0, H3), 6.55 (1H, d, *J* = 7.5, H5), 2.90 (3H, s, H7), 2.68–2.56 (1H, m, H10), 2.38 (1H, ddd, *J* = 14.6, 5.7, 4.2, H10'), 2.07 (1H, ddt, *J* = 12.5, 5.9, 2.0, H12), 1.93–1.80 (2H, m, H11$_{LHS}$ & H12'$_{RHS}$), 1.59 (1H, m, H11'), 1.40 (3H, s, H14).

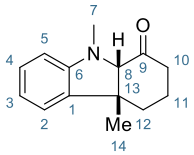
^{13}C NMR (101 MHz, DMSO-d_6) δ = 208.1 (C9), 149.4 (C6), 133.9 (C1), 131.6 (C18), 129.1 (C20), 128.7 (C19), 128.1 (C4), 121.5 (C17), 121.2 (C2), 118.3 (C3), 107.1 (C5), 89.6 (C16), 83.3 (C15), 79.6 (C8), 53.7 (C13), 37.7 (C10), 33.6 (C12), 31.3 (C7), 24.7 (C14), 21.4 (C11).

The observation of nuclear Overhauser effect (nOe) correlations by 2D NOESY corresponding to H14↔H18 is consistent with the formation of the *cis*-diastereomer shown.

FTIR (neat) ν/cm^{-1} = 2927, 2868, 2814, 1726, 1607, 1484, 1449, 1306, 1118, 1021, 756, 741, 691.

HRMS (ESI) *m/z* calcd. for $C_{22}H_{22}ON$ $[M+H]^+$: 316.1696; found: 316.1696.

rac-4a,9-Dimethyl-2,3,4,4a,9,9a-hexahydro-1*H*-carbazol-1-one, **21**



This compound was prepared from **10** (102.4 mg, 0.300 mmol, 1.0 eq.) according to General Procedure A, except that the reaction mixture (excluding nucleophile) was degassed by three freeze–pump–thaw cycles prior to irradiation (the nucleophile was deoxygenated separately by sparging with argon before being added to the degassed reaction mixture). Irradiation was performed in the presence of triethylsilane (0.14 mL, 0.10 g, 0.88 mmol, 2.9 eq.) in a 9:1 (v/v) mixture of acetonitrile (5.4 mL) and water (0.6 mL) (0.05 M) over a period of 6 h. Flash column chromatography on silica gel (gradient elution from 2.5 to 5% ethyl acetate in pentane) yielded **21** (51.8 mg, 0.241 mmol, 80%) as a viscous colourless oil. ^{1}H and ^{13}C NMR spectroscopic data for this compound in $CDCl_3$ have been reported elsewhere.[S24]

^{1}H NMR (400 MHz, DMSO-d_6) δ = 7.08 (1H, td, J = 7.6, 1.3, H4), 7.04 (1H, dd, J = 7.3, 1.3, H2), 6.72 (1H, td, J = 7.4, 1.0, H3), 6.60 (1H, d, J = 7.8, H5), 3.12 (1H, d, J = 1.1, H8), 2.65 (3H, s, H7), 2.58–2.48 (1H, m, H10), 2.31–2.20 (1H, m, H10'), 1.79–1.66 (3H, m, $H11_{LHS}$, $H11'_{LHS}$ & $H12_{RHS}$), 1.66–1.54 (1H, m, H12'), 1.32 (3H, s, H14).

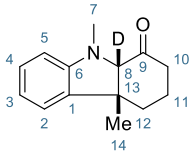
^{13}C NMR (101 MHz, DMSO-d_6) δ = 210.9 (C9), 151.0 (C6), 137.3 (C1), 127.7 (C4), 121.2 (C2), 118.6 (C3), 108.0 (C5), 81.0 (C8), 48.2 (C13), 37.7 (C10), 35.5 (C12), 34.7 (C7), 24.5 (C14), 20.7 (C11).

The observation of nuclear Overhauser effect (nOe) correlations by 2D NOESY corresponding to H8↔H14 is consistent with the formation of the *cis*-diastereomer shown.

FTIR (neat) ν/cm^{-1} = 2957, 1713, 1605, 1483, 1453, 1309, 1259, 1140, 1022, 977, 743.

HRMS (ESI) *m/z* calcd. for $C_{14}H_{18}NO$ $[M+H]^+$: 216.1383; found: 216.1382.

rac-4a,9-Dimethyl-2,3,4,4a,9,9a-hexahydro-1*H*-carbazol-1-one-9a-*d*, **22**



This compound was prepared from **10** (102.4 mg, 0.300 mmol, 1.0 eq.) according to General Procedure A, except that the reaction mixture (excluding nucleophile) was degassed by three freeze–pump–thaw cycles prior to irradiation (the nucleophile was added after this process *without* argon-sparging). Irradiation was performed in the presence of triethyl(silane-*d*) (0.14 mL, 0.10 g, 0.88 mmol, 2.9 eq.) in a 9:1 (v/v) mixture of acetonitrile (5.4 mL) and water (0.6 mL) (0.05 M) over a period of 6 h. Flash

column chromatography on silica gel (gradient elution from 2.5 to 5% ethyl acetate in pentane) yielded **22** (51.4 mg, 0.238 mmol, 79%, >99% D[*]) as a viscous pale-yellow oil.

^{1}H NMR (400 MHz, DMSO-d_6) δ = 7.08 (1H, td, J = 7.6, 1.3, H4), 7.04 (1H, dd, J = 7.3, 1.2, H2), 6.72 (1H, td, J = 7.4, 1.0, H3), 6.60 (1H, d, J = 7.8, H5), 2.65 (3H, s, H7), 2.59–2.49 (1H, m, H10), 2.31–2.19 (1H, m, H10'), 1.78–1.65 (3H, m, H11$_{LHS}$, H11'$_{LHS}$ & H12$_{RHS}$), 1.65–1.55 (1H, m, H12'), 1.32 (3H, s, H14).

^{2}H NMR (92 MHz, DMSO-h_6) δ[†] = 3.06 (s).

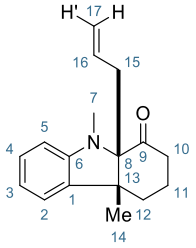
^{13}C NMR (101 MHz, DMSO-d_6) δ = 210.9 (C9), 151.1 (C6), 137.3 (C1), 127.7 (C4), 121.2 (C2), 118.6 (C3), 108.0 (C5), 80.5 (1:1:1 t, $^{1}J_{CD}$ = 21.5, C8), 48.1 (C13), 37.7 (C10), 35.5 (C12), 34.6 (C7), 24.4 (C14), 20.7 (C11).

The stereochemistry of this compound was assigned by analogy to that of its non-deuterated analogue, **21**.

FTIR (neat) ν/cm^{-1} = 2956, 2868, 2803, 1709, 1605, 1481, 1453, 1349, 1302, 1126, 1021, 932, 743.

HRMS (ESI) *m/z* calcd. for $C_{14}{}^{1}H_{17}{}^{2}HNO$ $[M+H]^+$: 217.1446; found: 217.1443.

rac-9a-Allyl-4a,9-dimethyl-2,3,4,4a,9,9a-hexahydro-1*H*-carbazol-1-one, **23**



This compound was prepared from **10** (102.4 mg, 0.300 mmol, 1.0 eq.) according to General Procedure A. Irradiation was performed in the presence of allyltrimethylsilane (0.14 mL, 0.10 g, 0.88 mmol, 2.9 eq.) in a 9:1 (v/v) mixture of acetonitrile (5.4 mL) and hexafluoroisopropanol (0.6 mL) (0.05 M) over a period of 18 h. Flash column chromatography on silica gel (eluent: 2% ethyl acetate in pentane) yielded **23** (61.5 mg, 0.241 mmol, 80%) as a light brown oil.

^{1}H NMR (400 MHz, DMSO-d_6) δ = 7.01 (1H, td, J = 7.6, 1.3, H4), 6.92 (1H, dd, J = 7.3, 1.3, H2), 6.59 (1H, td, J = 7.4, 1.0, H3), 6.38 (1H, d, J = 7.7, H5), 5.62 (1H, ddt, J = 17.2, 10.2, 7.1, H16), 5.16 (1H, dq, J = 16.9, 1.7, H17), 4.98 (1H, dq, J = 10.0, 1.5, H17'), 2.82 (3H, s, H7), 2.77 (1H, ddt, J = 15.5,

[*] Deuterium incorporation was estimated by HRMS; no signal corresponding to H8 was observed by ^{1}H NMR spectroscopy.
[†] The ^{2}H NMR spectrum was referenced to the triplet corresponding to DMSO-d_1 observed at natural abundance; a deuterium chemical shift of 2.50 ppm was assumed for this signal.

7.0, 1.6, H15), 2.56 (1H, ddt, *J* = 15.5, 7.2, 1.4, H15'), 2.32 (1H, ddd, *J* = 14.5, 11.1, 6.2, H10), 2.21 (1H, dddd, *J* = 14.4, 5.4, 3.7, 1.4, H10'), 2.00–1.90 (1H, m, H12), 1.81–1.65 (2H, m, H12'$_{LHS}$ & H11$_{RHS}$), 1.58–1.42 (1H, m, H11'), 1.19 (3H, s, H14).

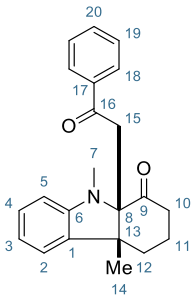
^{13}C NMR (101 MHz, DMSO-d_6) δ = 213.9 (C9), 150.7 (C6), 134.3 (C16), 134.0 (C1), 127.8 (C4), 120.6 (C2), 118.1 (C17), 117.1 (C3), 105.0 (C5), 79.6 (C8), 51.7 (C13), 39.2 (C10), 34.1 (C12), 33.4 (C15), 30.5 (C7), 23.1 (C14), 20.8 (C11).

The observation of nuclear Overhauser effect (nOe) correlations by 2D NOESY corresponding to H14↔H15, H14↔H15' and H14↔H16 is consistent with the formation of the *cis*-diastereomer shown.

FTIR (neat) ν/cm^{-1} = 2937, 1706, 1605, 1488, 1370, 1305, 1120, 1021, 916, 871, 739.

HRMS (ESI) *m/z* calcd. for $C_{17}H_{22}NO$ $[M+H]^+$: 256.1696; found: 256.1692.

rac-4a,9-Dimethyl-9a-(2-oxo-2-phenylethyl)-2,3,4,4a,9,9a-hexahydro-1*H*-carbazol-1-one, **24**





CCDC 2243733

This compound was prepared from **10** (102.4 mg, 0.300 mmol, 1.0 eq.) according to General Procedure A, except that the reaction mixture was degassed by three freeze–pump–thaw cycles prior to irradiation. Irradiation was performed in the presence of 1-phenyl-1-trimethylsilyloxyethylene[S17] (173 mg, 0.899 mmol, 3.0 eq.) and sodium trifluoroacetate (40.8 mg, 0.300 mmol, 1.0 eq.) in nitromethane solution (6.0 mL, 0.05 M) over a period of 18 h. Instead of adding triethylamine at the end of the irradiation period, the reaction mixture was diluted with methanol (6.0 mL) and stirred for 30 min at room temperature before concentrating *in vacuo*. Flash column chromatography on silica gel (gradient elution from 50 to 100% dichloromethane in pentane) yielded **24** (56.7 mg, 0.170 mmol, 57%) as a pale green solid. Diffraction-quality crystals were grown by vapour diffusion of cyclohexane into a solution of the product in tetrahydrofuran followed by slow evaporation of the resulting mixture.

^{1}H NMR (400 MHz, DMSO-d_6) δ = 8.09–7.98 (2H, m, H18), 7.71–7.61 (1H, m, H20), 7.59–7.49 (2H, m, H19), 7.03 (1H, td, *J* = 7.6, 1.3, H4), 6.96 (1H, dd, *J* = 7.3, 1.3, H2), 6.62 (1H, td, *J* = 7.4, 1.0, H3), 6.47–6.34 (1H, m, H5), 3.89 (1H, d, *J* = 18.4, H15), 3.70 (1H, d, *J* = 18.4, H15'), 2.64 (3H, s, H7), 2.52–2.40 (1H, m, H10), 2.19 (1H, dt, *J* = 15.1, 5.6, H10'), 2.07–1.90 (2H, m, H12 & H12'), 1.89–1.76 (1H, m, H11), 1.53–1.37 (1H, m, H11'), 1.18 (3H, s, H14).

^{13}C NMR (101 MHz, DMSO-d_6) δ = 207.6 (C9), 198.6 (C16), 149.9 (C6), 136.2 (C17), 134.4 (C1), 133.5 (C20), 128.8 (C19), 128.1 (C18), 127.7 (C4), 121.2 (C2), 117.3 (C3), 105.9 (C5), 77.7 (C8), 51.2 (C13), 39.2 (C15), 37.4 (C10), 33.2 (C12), 29.6 (C7), 25.0 (C14), 20.7 (C11).

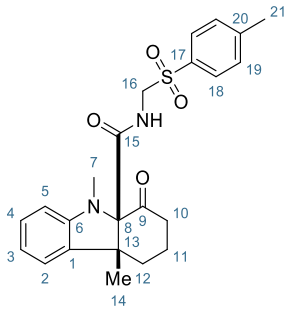
The stereochemistry of this compound was confirmed through single-crystal X-ray diffraction (CCDC 2243733). The observation of nuclear Overhauser effect (nOe) correlations by 2D NOESY corresponding to H14↔H15 and H14↔H15' is also consistent with the formation of the *cis*-diastereomer shown.

FTIR (neat) ν/cm^{-1} = 2941, 1699, 1684, 1602, 1488, 1449, 1348, 1307, 1217, 1021, 742.

HRMS (ESI) *m/z* calcd. for $C_{22}H_{24}O_2N$ $[M+H]^+$: 334.1802; found: 334.1801.

MP 93–95 °C.

rac-4b,9-Dimethyl-8-oxo-*N*-(tosylmethyl)-4b,5,6,7,8,9-hexahydro-8a*H*-carbazole-8a-carboxamide, **25**



This compound was prepared from **10** (102.4 mg, 0.300 mmol, 1.0 eq.) according to General Procedure A, except that the reaction mixture was degassed by three freeze–pump–thaw cycles prior to irradiation. Irradiation was performed in the presence of *para*-toluenesulfonylmethyl isocyanide (TosMIC) (175.7 mg, 0.900 mmol, 3.0 eq.) in a 9:1 (v/v) mixture of acetonitrile (5.4 mL) and water (0.6 mL) (0.05 M) over a period of 18 h. Flash column chromatography on silica gel (gradient elution from 20 to 30% ethyl acetate in pentane) yielded **25** (94.1 mg, 0.221 mmol, 74%) as an off-white solid.

^{1}H NMR (400 MHz, $CDCl_3$) δ = 7.83–7.74 (2H, m, H18), 7.47 (1H, t, *J* = 6.9, NH), 7.35 (2H, d, *J* = 8.1, H19), 7.16 (1H, td, *J* = 7.6, 1.3, H4), 6.90 (1H, dd, *J* = 7.4, 1.3, H2), 6.81 (1H, td, *J* = 7.4, 1.0, H3), 6.54 (1H, d, *J* = 7.8, H5), 4.91 (1H, dd, *J* = 14.1, 7.5, H16), 4.59 (1H, dd, *J* = 14.1, 6.1, H16'), 3.00 (3H, s, H7), 2.60 (1H, ddd, *J* = 15.5, 11.2, 7.2, H10), 2.44 (3H, s, H21), 2.17 (1H, dddd, *J* = 15.5, 6.2, 3.6, 1.3, H10'), 2.07 (1H, dtd, *J* = 14.3, 3.8, 1.4, H12), 1.93 (1H, ddd, *J* = 14.3, 13.0, 4.1, H12'), 1.85–1.72 (1H, m, H11), 1.62–1.47 (1H, m, H11'), 1.08 (3H, s, H14).

^{13}C NMR (101 MHz, $CDCl_3$) δ = 209.7 (C9), 168.6 (C15), 150.0 (C6), 145.7 (C20), 134.2 (C17), 132.7 (C1), 130.2 (C19), 128.8 (C18), 128.7 (C4), 121.4 (C2), 120.0 (C3), 108.1 (C5), 85.3 (C8), 60.0 (C16), 52.6 (C13), 40.1 (C10), 34.5 (C7), 32.3 (C12), 27.2 (C14), 21.8 (C21), 20.1 (C11).

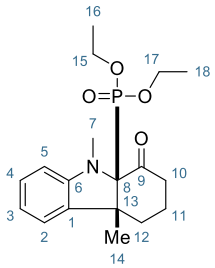
The observation of nuclear Overhauser effect (nOe) correlations by 2D NOESY corresponding to H14↔NH and H14↔H18 (weak) is consistent with the formation of the *cis*-diastereomer shown.

FTIR (neat) ν/cm^{-1} = 3341, 2934, 1716, 1677, 1482, 1322, 1290, 1145, 1086, 745, 668.

HRMS (ESI) *m/z* calcd. for $C_{23}H_{27}O_4N_2S$ $[M+H]^+$: 427.1686; found: 427.1684.

MP 148–150 °C.

Diethyl (4b,9-dimethyl-8-oxo-4b,5,6,7,8,9-hexahydro-8a*H*-carbazol-8a-yl)phosphonate (racemate), **26**



This compound was prepared from **10** (102.4 mg, 0.300 mmol, 1.0 eq.) according to General Procedure A, except that the reaction mixture was degassed by three freeze–pump–thaw cycles prior to irradiation. Irradiation was performed in the presence of diethylphosphite (116 μL, 124 mg, 0.900 mmol, 3.0 eq.) in a 9:1 (v/v) mixture of acetonitrile (5.4 mL) and water (0.6 mL) (0.05 M) over a period of 18 h. Flash column chromatography on silica gel (eluent: 50% ethyl acetate in pentane) yielded **26** (60.0 mg, 0.171 mmol, 57%) as a viscous yellow oil.

^{1}H NMR (400 MHz, DMSO-d_6) δ = 7.03 (1H, td, *J* = 7.6, 1.3, H4), 6.92 (1H, dd, *J* = 7.3, 1.3, H2), 6.62 (1H, td, *J* = 7.4, 1.0, H3), 6.46 (1H, d, *J* = 7.8, H5), 4.25–4.05 (4H, m, H15, H15', H17 & H17'), 3.08 (3H, s, H7), 2.81–2.69 (1H, m, H10), 2.34–2.10 (3H, m, $H12_{LHS}$, $H12'_{LHS}$ & $H10'_{RHS}$), 1.99–1.87 (1H, m, H11), 1.43–1.31* (1H, m, H11'), 1.32–1.22* (6H, m, H16 & H18), 1.30* (3H, s, H14).

^{13}C NMR (101 MHz, DMSO-d_6) δ = 210.6 (d, $^2J_{CP}$ = 9.6, C9), 150.3 (d, $^3J_{CP}$ = 13.0, C6), 131.9 (d, $^3J_{CP}$ 14.1, C1), 127.9 (C4), 120.3 (C2), 117.6 (C3), 106.0 (C5), 84.7 (d, $^1J_{CP}$ = 153.7, C8), 62.4 (d, $^2J_{CP}$ = 7.2, C15 or C17), 62.3 (d, $^2J_{CP}$ = 7.5, C15 or C17), 54.7 (d, $^2J_{CP}$ = 1.8, C13), 40.1 (C10), 33.0 (C7), 30.9

* Multiplicity-edited HSQC analysis confirmed the total number of protons within this complex multiplet as 10, and provided the precise spectral ranges for the protons in question.

(C12), 27.2 (d, $^{3}J_{CP}$ = 5.4, C14), 22.8 (C11), 16.2* (d, $^{3}J_{CP}$ ≈ 6, C16 or C18), 16.1* (d, $^{3}J_{CP}$ ≈ 6, C16 or C18).

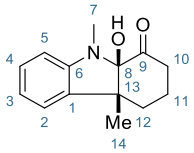
^{31}P NMR (162 MHz, DMSO-d_6) δ = 26.7 (minor), 19.4 (major).

The observation of transient nuclear Overhauser effect (nOe) enhancements by 1D NOESY for H15/H15'/H17/H17' (signals coincident) upon selective inversion of H14 is consistent with the formation of the *cis*-fused heterocycle shown as the major diastereomer. This compound was formed and isolated as the major component of a mixture containing a compound with near-identical NMR spectroscopic features, assumed to be the corresponding *trans*-isomer, in a molar ratio between 20:1 and 19:1 (estimated from relative integrations of ^{31}P resonances). Screening reactions performed during reaction optimization (see Section S5) revealed a strong dependence of the ratio of these two products on solvent polarity; the *trans*-fused iminium trapping product was not observed for any nucleophile other than diethylphosphite.

FTIR (neat) ν/cm^{-1} = 2935, 1719, 1605, 1484, 1458, 1304, 1245, 1048, 1022, 965, 742.

HRMS (ESI) *m/z* calcd. for $C_{18}H_{27}NO_4P$ $[M+H]^+$: 352.1672; found: 352.1665.

rac-9a-Hydroxy-4a,9-dimethyl-2,3,4,4a,9,9a-hexahydro-1*H*-carbazol-1-one, **11**



This compound was prepared from **10** (102.4 mg, 0.300 mmol, 1.0 eq.) according to General Procedure A, except that the reaction mixture was degassed by three freeze–pump–thaw cycles prior to irradiation; also, no triethylamine was added at the end of the reaction. Irradiation was performed in the presence of potassium acetate (44.2 mg, 0.450 mmol, 1.5 eq.) in a 9:1 (v/v) mixture of acetonitrile (5.4 mL) and water (0.6 mL) (0.05 M) over a period of 90 min. Flash column chromatography on silica gel (gradient elution from 5 to 10% ethyl acetate in pentane) yielded **11** (61.6 mg, 0.266 mmol, 89%) as an off-white solid.

^{1}H NMR (500 MHz, CD_3CN) δ† = 7.14 (1H, td, *J* = 7.6, 1.3, H4), 7.06 (1H, dd, *J* = 7.3, 1.3, H2), 6.79 (1H, td, *J* = 7.4, 1.0, H3), 6.57 (1H, d, *J* = 7.8, H5), 4.51 (1H, s, OH), 2.77–2.66 (1H, m, H10), 2.54

* Overlap of these signals makes accurate determination of their *J* values difficult; approximate values are thus reported.

† The use of a relatively short relaxation delay (D1) of 1 second led to lower-than-expected integration values for the aromatic protons of this compound. Importantly, however, multiplicity-edited HSQC analysis confirmed the number of nuclei in each chemical environment.

(3H, s, H7), 2.47–2.39 (1H, m, H10'), 1.86–1.66 (4H, m, $H11_{LHS}$, $H11'_{LHS}$, $H12_{RHS}$ & $H12'_{RHS}$), 1.27 (3H, s, H14).

^{13}C NMR (126 MHz, CD_3CN) δ = 211.1 (C9), 150.5 (C6), 138.1 (C1), 128.7 (C4), 122.0 (C2), 119.8 (C3), 108.5 (C5), 98.1 (C8), 54.1 (C13), 40.0 (C12), 38.1 (C10), 28.7 (C7), 21.9 (C11), 18.1 (C14).

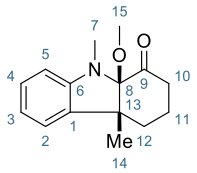
The observation of nuclear Overhauser effect (nOe) correlations by 2D NOESY corresponding to H14↔OH is consistent with the formation of the *cis*-diastereomer shown.

FTIR (neat) ν/cm^{-1} = 3485, 2944, 1711, 1607, 1479, 1275, 1124, 1106, 1070, 1007, 735.

HRMS (ESI) *m/z* calcd. for $C_{14}H_{18}NO_2$ $[M+H]^+$: 232.1332; found: 232.1329; *m/z* calcd. for $C_{14}H_{17}NO_2Na$ $[M+Na]^+$: 254.1152; found: 254.1148.

MP not determined; sample decomposed upon heating at some temperature below 100 °C.

rac-9a-Methoxy-4a,9-dimethyl-2,3,4,4a,9,9a-hexahydro-1*H*-carbazol-1-one, **27**



This compound was isolated and characterized without chromatographic purification owing to its instability on silica and alumina gels. Enaminone **10** (34.1 mg, 0.0999 mmol, 1.0 eq.) and potassium phosphate (31.8 mg, 0.150 mmol, 1.5 eq.) were charged to a flame-dried Schlenk tube equipped with a magnetic stir bar. The vessel was sealed with a septum, and the flask was evacuated and back-filled with argon three times. Anhydrous acetonitrile (1.8 mL; obtained from the solvent purification system described above) and methanol (0.2 mL; dried over 3 Å molecular sieves and filtered through a 0.2 μm PTFE syringe filter prior to use) (0.05 M), both argon-sparged, were added *via* syringe. The reaction mixture was stirred under constant irradiation with a single Kessil PR160L 427 nm LED lamp (positioned *ca.* 3 cm from the flask and directed toward it) for 2 h, with cooling to ambient temperature being achieved using a strong jet of nitrogen gas directed at the flask, after which time the reaction mixture was concentrated *in vacuo*. The analytical data below were collected using a $CDCl_3$ solution of the resulting material, which contained predominantly indoline **27** alongside trace unknown side-products. A near-identical experiment was performed in parallel, differing only in that dimethyl terephthalate was added to the reaction mixture at the end of the irradiation period as a solution in acetonitrile (25.0 mM, 1.0 mL, 0.25 mmol, 0.25 eq.). The resulting mixture was concentrated *in vacuo*, and the crude residue was dissolved in $CDCl_3$ for analysis by quantitative ^1H NMR spectroscopy. The NMR yield of indoline **27** measured against dimethyl terephthalate for this reaction was 77%.

^{1}H NMR (400 MHz, $CDCl_3$) δ = 7.18 (1H, td, *J* = 7.6, 1.2, H4), 7.00 (1H, dd, *J* = 7.3, 1.3, H2), 6.80 (1H, td, *J* = 7.4, 1.0, H3), 6.49 (1 H, d, *J* = 7.7, H5), 2.98 (3H, s, H15), 2.81 (3H, s, H7), 2.57–2.39 (2H, m, H10 & H10'), 1.73–1.60* (4H, m, $H12_{LHS}$, $H12'_{LHS}$, $H11_{RHS}$ & $H11'_{RHS}$), 1.42 (3H, s, H14).

^{13}C NMR (101 MHz, $CDCl_3$) δ = 206.9 (C9), 149.4 (C6), 135.7 (C1), 128.4 (C4), 120.7 (C2), 118.9 (C3), 104.8 (C5), 100.1 (C8), 53.0(0) & 52.9(6) (C13 & C15), 41.4 (C12), 38.9 (C10), 29.3 (C7), 19.5 (C11), 18.9 (C14).

The observation of nuclear Overhauser effect (nOe) correlations by 2D NOESY corresponding to H14↔H15 is consistent with the formation of the *cis*-diastereomer shown.

FTIR (neat) ν/cm^{-1} = 2946, 2834, 1723, 1606, 1490, 1372, 1307, 1085, 1016, 929, 866, 741.

HRMS (ESI) *m/z* calcd. for $C_{15}H_{20}NO_2$ $[M+H]^+$: 246.1489; found: 246.1478; *m/z* calcd. for $C_{14}H_{19}NO_2Na$ $[M+Na]^+$: 268.1308; found: 268.1296.

Unsuccessful nucleophiles

Several nucleophiles that failed to deliver trapping products upon irradiation with enaminone **10** in acetonitrile-based solvent systems are presented in Figure S1.

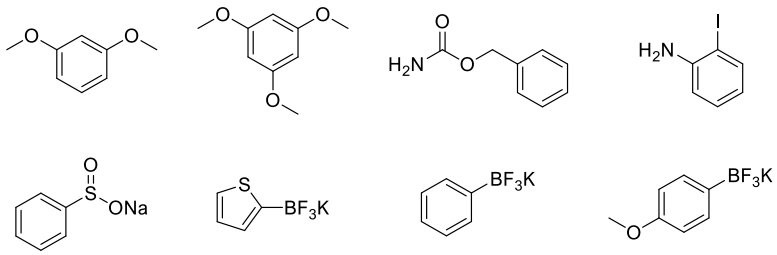
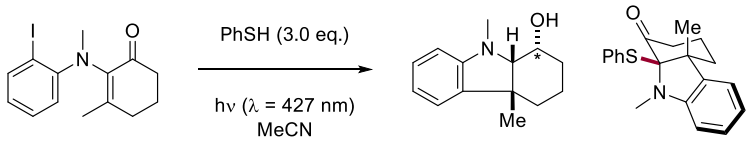


Figure S1. Nucleophiles that failed to deliver the expected nucleophilic trapping product in the radical−polar crossover reaction of β-methyl substrate **10** under typical irradiation conditions.

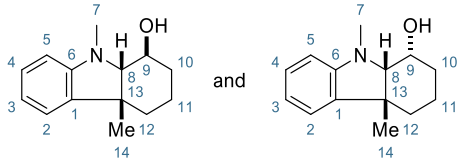
While the expected nucleophilic trapping product (**S40**) was not formed when **10** was irradiated in the presence of thiophenol, an alternative compound of interest, indoline **S39**, was generated in a yield of 58% as a 1.3:1 mixture of diastereomers, differing only in the configuration at C9 (Scheme S1). This product is thought to have formed *via* single-electron transfer within an iminium thiolate charge-transfer complex.

* Overlap with the water signal led to over-integration of this multiplet. Multiplicity-edited HSQC analysis confirmed the total number of protons as 4 within this spectral range.



Scheme S1. Irradiating **10** in the presence of thiophenol resulted in the formation of indoline **S39** as a mixture of diastereomers; the expected nucleophilic trapping product, **S40**, was not observed.

rac-4a,9-Dimethyl-2,3,4,4a,9,9a-hexahydro-1*H*-carbazol-1-ol, **S39**



Enaminone **10** (34.1 mg, 0.0999 mmol, 1.0 eq.) and thiophenol (31 µL, 33 mg, 0.30 mmol, 3.0 eq.) were dissolved in acetonitrile (2.0 mL, 0.05 M) in a Schlenk tube equipped with a magnetic stir bar. The vessel was sealed with a septum, and the reaction mixture was degassed by three freeze–pump–thaw cycles. The reaction mixture was stirred under constant irradiation with a single Kessil PR160L 427 nm LED lamp (positioned *ca.* 3 cm from the flask and directed toward it) for 18 h, with cooling to ambient temperature being achieved using a strong jet of nitrogen gas directed at the flask. Triethylamine (0.7 mL) was added to the reaction mixture at the end of the irradiation period, and the resulting mixture was concentrated *in vacuo*. The crude residue was purified by flash column chromatography (silica gel, dichloromethane) to afford **S39** (12.5 mg, 0.0575 mmol, 58%, 1.3:1.0 d.r.) as a colourless oil.

Major:

^{1}H NMR (600 MHz, $CDCl_3$) δ* = 7.14–7.10 (1H, m, H4), 6.99–6.95 (1H, m, H2), 6.77–6.73 (1H, m, H3), 6.60 (1H, d, *J* = 7.8, H5), 4.10–4.05 (1H, m, H9), 3.07 (1H, d, *J* = 3.9, H8), 2.94 (3H, s, H7), 1.93–1.86 (1H, m, H10), 1.70–1.60 (2H, m, H10'$_{LHS}$ & H11$_{RHS}$), 1.56–1.47 (2H, m, H12$_{LHS}$ & H11'$_{RHS}$), 1.46–1.40 (1H, m, H12'), 1.34 (3H, s, H14).

^{13}C NMR (151 MHz, $CDCl_3$) δ = 152.4 (C6), 139.2(2) (C1), 127.6 (C4), 121.1 (C2), 118.7 (C3), 108.6 (C5), 76.4 (C8), 69.3 (C9), 43.9 (C13), 37.1 (C7), 34.1 (C12), 27.7 (C10), 24.7 (C14), 18.8 (C11).

Minor:

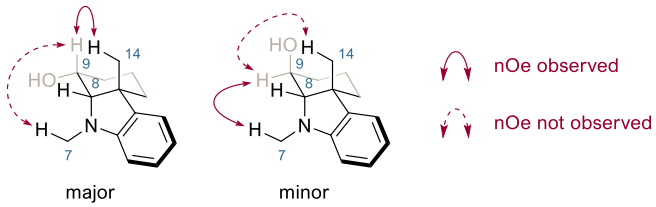
^{1}H NMR (600 MHz, $CDCl_3$) δ = 7.12–7.08 (1H, m, H4), 6.99–6.95 (1H, m, H2), 6.75–6.70 (1H, m, H3), 6.53 (1H, d, *J* = 7.8, H5), 4.10–4.05 (1H, m, H9), 2.89 (1H, d, *J* = 4.0, H8), 2.84 (3H, s, H7),

* Chemical shift ranges and integrations reported for diastereotopic methylene signals were obtained indirectly using multiplicity-edited HSQC and HMBC data.

1.81–1.72 (2H, m, $H10_{LHS}$ & $H11_{RHS}$), 1.63–1.51 (3H, m, $H12_{LHS}$, $H10'_{LHS}$ & $H12'_{RHS}$), 1.42 (3H, s, H14), 1.35–1.29 (1H, m, H11').

^{13}C NMR (151 MHz, $CDCl_3$) δ = 151.2 (C6), 139.2(4) (C1), 127.5 (C4), 120.9 (C2), 118.4 (C3), 108.1 (C5), 77.9 (C8), 68.4 (C9), 43.0 (C13), 35.4 (C12), 35.1 (C7), 30.2 (C10), 25.7 (C14), 16.9 (C11).

The observation of strong nuclear Overhauser effect (nOe) correlations corresponding to H8↔H14 in both diastereomers, H9↔H14 in the major diastereomer only, and H7↔H9 in the minor diasteromer only is indicative of the relative stereochemistry depicted for each isomer.

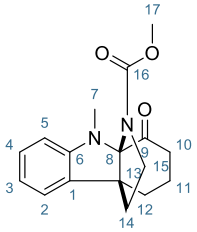


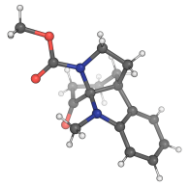
FTIR (neat) ν/cm^{-1} = 3390 (br), 2931, 2861, 2805, 1605, 1483, 1457, 1300, 1251, 1133, 1056, 1022, 741.

HRMS (ESI) *m/z* calcd. for $C_{14}H_{20}ON$ $[M+H]^+$: 218.1539; found: 218.1539.

S2.16. Photochemical reactivity of **28**, a substrate bearing a tethered carbamate group

Methyl 9-methyl-8-oxo-5,6,7,8-tetrahydro-9*H*-8a,4b-(epiminoethano)carbazole-10-carboxylate (racemate), **29**





CCDC 2243732

N-Aryl enaminone **28** (128.5 mg, 0.300 mmol, 1.0 eq.) was dissolved in a 9:1 (v/v) mixture of acetonitrile (5.4 mL) and water (0.6 mL) (0.05 M) in a Schlenk tube equipped with a magnetic stir bar. The vessel was sealed with a septum, and the reaction mixture was degassed by three freeze–pump–thaw cycles. The reaction mixture was stirred under constant irradiation with two Kessil PR160L 427 nm LED lamps (each positioned *ca.* 3 cm from the flask and directed toward it) for 3 h, with cooling to ambient temperature being achieved using a strong jet of nitrogen gas directed at the flask. Triethylamine (2.0 mL) was added to the reaction mixture at the end of the irradiation period, and the resulting mixture was concentrated *in vacuo*. The crude residue was purified by flash column chromatography on alumina gel (eluent: 20% ethyl acetate in pentane) to afford **29** (79.6 mg, 0.265 mmol, 88%) as a peach-coloured solid. Diffraction-quality crystals were grown by vapour diffusion of *n*-hexane into a solution of the product in dichloromethane.

^{1}H NMR (600 MHz, CD_2Cl_2, 298 K) δ = 7.13 (1H, td, *J* = 7.7, 1.3, H4), 6.95 (1H, dd, *J* = 7.2, 1.3, H2), 6.66 (1H, t, *J* = 7.4, H3), 6.40 (1H, d, *J* = 7.8, H5), 3.89–3.82* (1H, br m, H15), 3.70* (3H, br s, H17), 3.47 (1H, ddd, *J* = 10.8, 8.4, 5.6, H15'), 2.99* (3H, br s, H7), 2.48 (1H, ddd, *J* = 13.5, 10.1, 6.6, H14), 2.31 (1H, dddd, *J* = 13.5, 5.7, 4.4, 1.1, H14'), 2.12 (1H, ddd, *J* = 12.6, 8.4, 6.9, H14), 2.08–1.92 (3H, m, H11, H12 & H14'), 1.79 (1H, ddd, *J* = 14.2, 11.0, 3.6, H12'), 1.74–1.63 (1H, m, H11').

Cooling of the CD_2Cl_2 solution to 253 K (spectra below) resulted in resolution of the broad ^{1}H resonances (marked above with an asterisk, *) into two clear sets of signals, each of which presumably corresponds to different rotational states about the carbamate C–N bond; the two conformers were present in a *ca.* 72:28 ratio at this temperature. As a result of slow chemical exchange at room temperature, it was necessary to collect ^{13}C NMR data for this compound at low temperature.

^{13}C NMR (151 MHz, CD_2Cl_2, 253 K) δ = 207.4 ($C9_B$), 207.2 ($C9_A$), 155.7 ($C16_A$), 154.8 ($C16_B$), 149.7 ($C6_B$), 149.6 ($C6_A$), 130.4 ($C1_B$), 130.3 ($C1_A$), 128.9 ($C4_A$ & $C4_B$, coincident), 121.1(3) ($C2_B$), 121.1(0) ($C2_A$), 117.3 ($C3_B$), 117.0 ($C3_A$), 105.6 ($C5_B$), 105.5 ($C5_A$), 95.1 ($C8_A$), 94.6 ($C8_B$), 64.6 ($C13_B$), 62.8 ($C13_A$), 52.9 ($C17_A$), 52.5 ($C17_B$), 47.6 ($C15_B$), 47.0 ($C15_A$), 38.2 ($C14_A$), 37.8 ($C10_A$), 37.5 ($C10_B$), 36.9 ($C14_B$), 31.3 ($C7_A$), 30.9(0) ($C7_B$), 30.8(5) ($C12_B$), 30.3 ($C12_A$), 24.0 ($C11_A$), 23.8 ($C11_B$). (Here,

the subscript ‘A’ denotes signals corresponding to the major component of the rotameric mixture, while ‘B’ denotes resonances of the minor component.)

The structure of this compound was confirmed through single-crystal X-ray diffraction (CCDC 2243732).

FTIR (neat) ν/cm^{-1} = 2947, 1729, 1703, 1610, 1487, 1446, 1369, 1198, 1073, 1017, 745.

HRMS (ESI) *m/z* calcd. for $C_{17}H_{21}N_2O_3$ $[M+H]^+$: 301.1547; found: 301.1544.

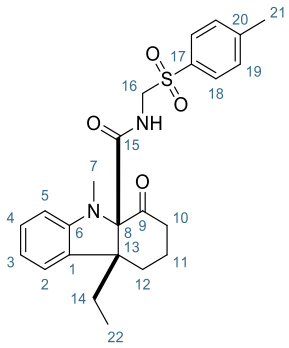
MP 110–112 °C.

S2.17. Photochemical reactivity of alternative *N*-aryl enaminone substrates in the presence of TosMIC (substrate scope)

General Procedure B

The appropriate enaminone substrate (0.300 mmol, 1.0 eq.) and *para*-toluenesulfonylmethyl isocyanide (TosMIC) (175.7 mg, 0.900 mmol, 3.0 eq.) were dissolved in a 9:1 (v/v) mixture of acetonitrile (5.4 mL) and water (0.6 mL) (0.05 M) in a Schlenk tube equipped with a magnetic stir bar. The vessel was sealed with a septum, and the reaction mixture was degassed by three freeze–pump–thaw cycles. The reaction mixture was stirred under constant irradiation with two Kessil PR160L 427 nm LED lamps (each positioned *ca.* 3 cm from the flask and directed toward it) for 18 h, with cooling to ambient temperature being achieved using a strong jet of nitrogen gas directed at the flask. Triethylamine (2.0 mL) was added to the reaction mixture at the end of the irradiation period, and the resulting mixture was concentrated *in vacuo*. The crude residue was purified by flash column chromatography to afford the corresponding indoline product.

rac-4b-ethyl-9-methyl-8-oxo-*N*-(tosylmethyl)-4b,5,6,7,8,9-hexahydro-8a*H*-carbazole-8a-carboxamide, **30**



This compound was prepared from **S13** (106.6 mg, 0.300 mmol, 1.0 eq.) and *para*-toluenesulfonylmethyl isocyanide (TosMIC) (175.7 mg, 0.900 mmol, 3.0 eq.) according to General Procedure B. Flash column chromatography on silica gel (eluent: 25% ethyl acetate in pentane) yielded **30** (85.1 mg, 0.193 mmol, 64%) as a white solid.

^{1}H NMR (400 MHz, $CDCl_3$) δ = 7.82–7.76 (2H, m, H18), 7.42 (1H, t, *J* = 6.9, NH), 7.39–7.30 (2H, m, H19), 7.17 (1H, td, *J* = 7.6, 1.4, H4), 6.88 (1H, dd, *J* = 7.3, 1.3, H2), 6.79 (1H, t, *J* = 7.4, H3), 6.56 (1H, d, *J* = 7.8, H5), 4.95 (1H, dd, *J* = 14.2, 7.6, H16), 4.58 (1H, dd, *J* = 14.2, 6.0, H16'), 3.09 (3H, s, H7), 2.69 (1H, ddd, *J* = 14.7, 12.2, 6.5, H10), 2.44 (3H, s, H21), 2.31–2.21 (1H, m, H12), 2.12 (1H, dddd, *J* = 14.6, 5.1, 3.3, 1.5, H10'), 1.90–1.70 (2H, m, $H11_{LHS}$ & $H12'_{RHS}$), 1.57–1.43 (2H, m, H11' & H14), 1.33–1.19 (1H, m, H14'), 0.72 (3H, t, *J* = 7.4, H22).

^{13}C NMR (101 MHz, $CDCl_3$) δ = 210.4 (C9), 168.5 (C15), 150.6 (C6), 145.7 (C20), 134.2 (C17), 130.2 (C19), 129.5 (C1), 128.8 (C18), 128.7 (C4), 123.3 (C2), 119.2 (C3), 108.5 (C5), 87.0 (C8), 60.0 (C16), 56.3 (C13), 40.7 (C10), 35.5 (C7), 30.2 (C14), 27.2 (C12), 21.8 (C21), 20.6 (C11), 8.4 (C22).

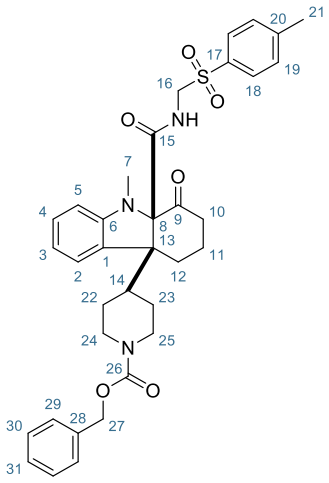
The observation of nuclear Overhauser effect (nOe) correlations by 2D NOESY corresponding to H14↔NH, H14'↔NH (weak), H14↔H18 (weak) and H14'↔H18 (weak) is consistent with the formation of the *cis*-diastereomer shown.

FTIR (neat) ν/cm^{-1} = 3351 (br), 2942, 1716, 1677, 1603, 1481, 1322, 1145, 1085, 913, 736.

HRMS (ESI) *m/z* calcd. for $C_{24}H_{29}N_2O_4S$ $[M+H]^+$: 441.1843; found: 441.1847.

MP 78–80 °C

Benzyl 4-(9-methyl-1-oxo-9a-((tosylmethyl)carbamoyl)-1,2,3,4,9,9a-hexahydro-4a*H*-carbazol-4a-yl)piperidine-1-carboxylate (racemate), **31**



This compound was prepared from **S17** (163.3 mg, 0.300 mmol, 1.0 eq.) and *para*-toluenesulfonylmethyl isocyanide (TosMIC) (175.7 mg, 0.900 mmol, 3.0 eq.) according to General Procedure B. Flash column chromatography on silica gel (eluent: 10% ethyl acetate in dichloromethane) yielded **31** (78.7 mg, 0.125 mmol, 42%) as a green solid.

^{1}H NMR (400 MHz, $CDCl_3$) δ = 7.85–7.76 (2H, m, H18), 7.66–7.42 (1H, br m, NH), 7.40–7.23* (7H, m, $H19_{LHS}$ & H29 to H31), 7.18 (1H, ddd, *J* = 7.7, 6.5, 2.2, H4), 6.87–6.75 (2H, m, $H2_{LHS}$ & $H3_{RHS}$), 6.57 (1H, d, *J* = 7.8, H4), 5.16–4.95 (3H, m, $H16_{LHS}$ & $H27_{RHS}$), 4.40–4.31 (1H, m, H16'), 4.26–3.82 (2H, m, two of the four protons represented by H24/H25), 3.05 (3H, s, H7), 2.71–2.47 (3H, m, $H10_{RHS}$ & two of the four protons represented by H24/H25), 2.44 (3H, s, H21), 2.24–2.13 (1H, m, H12), 2.08–1.91 (2H, m, $H10'_{LHS}$ & $H12'_{RHS}$), 1.91–1.76 (2H, m, $H11_{LHS}$ & $H14_{RHS}$), 1.76–1.60 (1H, m, one of the

* Overlap with the residual non-deuterated chloroform signal led to over-integration of this multiplet. Multiplicity-edited HSQC analysis confirmed the number of protons as 7 within this spectral range.

four protons represented by H22/H23), 1.59–1.43 (2H, m, H11'$_{LHS}$ & one of the four protons represented by H22/H23), 1.38–1.15 (1H, m, one of the four protons represented by H22/H23), 0.96–0.56 (1H, m, one of the four protons represented by H22/H23).

^{13}C NMR (101 MHz, $CDCl_3$) δ = 209.1 (C9), 168.9 (C15), 155.0 (C26), 151.1 (C6), 145.8 (C20), 136.9 (C28), 134.2 (C17), 130.3 (C19), 129.0 (C4), 128.9 (C1), 128.7 (C18), 128.5 (C29 or C30), 128.0 (C31), 127.9 (C29 or C30), 123.6 (C2), 119.7 (C3), 108.8 (C5), 86.8 (C8), 67.0 (C27), 60.1 (C16), 58.8 (C13), 44.4 & 44.1 (C24 & C25), 42.2 (C14), 39.3 (C10), 35.4 (C7), 28.9 & 27.5 (C22 & C23), 26.4 (C12), 21.9 (C21), 19.8 (C11).

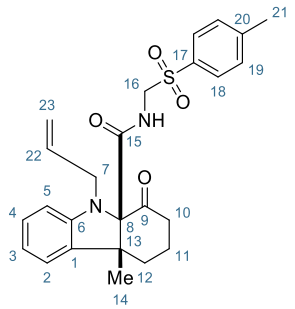
The observation of nuclear Overhauser effect (nOe) correlations by 2D NOESY corresponding to H14↔NH is consistent with the formation of the *cis*-diastereomer shown; cross-peaks at (7.54 ppm, 1.48 ppm) and (1.48 ppm, 7.54 ppm) on the 2D NOESY spectrum, indicative of a through-space interaction between NH and one of the four protons represented by H22/H23, also support this assignment.

FTIR (neat) ν/cm^{-1} = 3349 (br), 2946, 1682, 1480, 1322, 1285, 1244, 1145, 1086, 912, 733.

HRMS (ESI) *m/z* calcd. for $C_{35}H_{40}O_6N_3S$ $[M+H]^+$: 630.2632; found: 630.2629.

MP not determined; sample underwent an unclear phase transition / decomposed upon heating at *ca.* 100 °C.

rac-9-Allyl-4b-methyl-8-oxo-*N*-(tosylmethyl)-4b,5,6,7,8,9-hexahydro-8a*H*-carbazole-8a-carboxamide, **32**



This compound was prepared from **S20** (110.2 mg, 0.300 mmol, 1.0 eq.) and *para*-toluenesulfonylmethyl isocyanide (TosMIC) (175.7 mg, 0.900 mmol, 3.0 eq.) according to General Procedure B. Flash column chromatography on silica gel (eluent: 25% ethyl acetate in pentane) yielded **32** (57.4 mg, 0.127 mmol, 42%) as a white solid, alongside an impure mixture of compounds containing **S41**; the latter material was subjected to preparatory thin-layer chromatography on silica gel (eluent: 25% ethyl acetate in pentane), affording pure **S41** (6.2 mg, 0.017 mmol, 6%) as a white solid.

^{1}H NMR (400 MHz, $CDCl_3$) δ = 7.80–7.72 (2H, m, H18), 7.43 (1H, t, *J* = 6.8, NH), 7.33 (2H, d, *J* = 8.0, H19), 7.10 (1H, td, *J* = 7.6, 1.2, H4), 6.90 (1H, dd, *J* = 7.3, 1.3, H2), 6.80 (1H, td, *J* = 7.4, 1.0, H3), 6.48 (1H, d, *J* = 7.8, H5), 6.08 (1H, ddt, *J* = 17.6, 10.6, 3.6, H22), 5.28–5.15 (2H, m, H23 & H23'), 4.74 (1H, dd, *J* = 14.1, 6.7, H16), 4.66 (1H, dd, *J* = 14.1, 6.8, H16'), 4.18–4.01 (2H, m, H7 & H7'), 2.88 (1H, td, *J* = 13.6, 6.2, H10), 2.43 (3H, s, H21), 2.28–2.19 (1H, m, H10'), 2.19–2.11 (1H, m, H12), 2.06 (1H, td, *J* = 13.7, 3.9, H12'), 1.92–1.80 (1H, m, H11), 1.55 (1H, qt, *J* = 13.3, 4.2, H11'), 1.13 (3H, s, H14).

^{13}C NMR (101 MHz, $CDCl_3$) δ = 210.9 (C9), 168.3 (C15), 149.1 (C6), 145.6 (C20), 135.9 (C22), 134.2 (C17), 132.1 (C1), 130.2 (C19), 128.8 (C18), 128.5 (C4), 121.1 (C2), 120.0 (C3), 115.1 (C23), 109.0 (C5), 87.5 (C8), 60.0 (C16), 54.0 (C13), 51.2 (C7), 41.1 (C10), 31.2 (C12), 27.2 (C14), 21.8 (C21), 21.6 (C11).

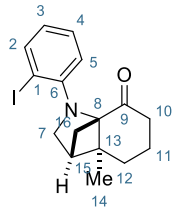
The observation of nuclear Overhauser effect (nOe) correlations by 2D NOESY corresponding to H14↔NH and H14↔H18 is consistent with the formation of the *cis*-diastereomer shown.

FTIR (neat) ν/cm^{-1} = 3382 (br), 2933, 1716, 1680, 1504, 1480, 1326, 1146, 1086, 915, 736.

HRMS (ESI) *m/z* calcd. for $C_{25}H_{29}N_2O_4S$ $[M+H]^+$: 453.1843; found: 453.1844.

MP 58–62 °C (unclear phase transition owing to foam nature of solid).

rac-1-(2-Iodophenyl)-3a-methylhexahydro-3,7a-methanoindol-7(1*H*)-one, **S41**



Isolated from the photoreaction of **S20**, as described above.

^{1}H NMR (400 MHz, $CDCl_3$) δ = 7.80 (1H, dd, *J* = 7.9, 1.5, H2), 7.17–7.08 (1H, m, H4), 6.66 (1H, td, *J* = 7.5, 1.4, H3), 6.44 (1H, d, *J* = 8.1, H5), 4.29 (1H, d, *J* = 8.3, H7), 3.08–3.00 (1H, m, H16), 2.68 (1H, ddd, *J* = 14.3, 12.9, 5.6, H10), 2.62–2.55 (2H, m, $H15_{LHS}$ & $H7'_{RHS}$), 2.45–2.27 (2H, m, $H12_{LHS}$ & $H10'_{RHS}$), 2.25–2.13 (1H, m, H11), 2.12–1.97 (1H, m, H11'), 1.96 (1H, d, *J* = 8.0, H16'), 1.84–1.74 (1H, m, H12'), 1.17 (3H, s, H14).

^{13}C NMR (101 MHz, $CDCl_3$) δ = 204.1 (C9), 152.1 (C6), 140.4 (C2), 127.5 (C4), 123.5 (C3), 120.6 (C5), 93.3 (C1), 76.9 (C8), 59.5 (C13), 58.1 (C7), 43.8 (C15), 40.9 (C10), 38.2 (C16), 31.5 (C12), 27.5 (C11), 16.6 (C14).

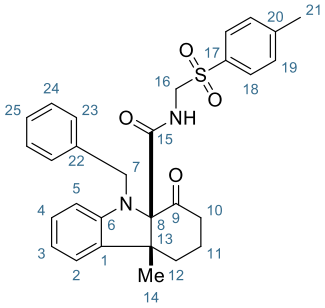
The stereochemistry of this compound was assigned by analogy to that of **6** above.

FTIR (neat) ν/cm^{-1} = 2956, 1704, 1579, 1469, 1433, 1299, 1038, 754, 648.

HRMS (ESI) *m/z* calcd. for $C_{16}H_{19}INO$ $[M+H]^+$: 368.0506; found: 368.0502.

MP 148–150 °C.

rac-9-Benzyl-4b-methyl-8-oxo-*N*-(tosylmethyl)-4b,5,6,7,8,9-hexahydro-8a*H*-carbazole-8a-carboxamide, **33**



This compound was prepared from **S24** (125.2 mg, 0.300 mmol, 1.0 eq.) and *para*-toluenesulfonylmethyl isocyanide (TosMIC) (175.7 mg, 0.900 mmol, 3.0 eq.) according to General Procedure B. Flash column chromatography on silica gel (gradient elution from 5 to 25% ethyl acetate in pentane) yielded **33** (79.2 mg, 0.158 mmol, 53%) as an off-white solid.

^{1}H NMR (400 MHz, $CDCl_3$) δ = 7.65–7.57 (2H, m, H18), 7.39–7.23* (7H, m, $H24_{LHS}$, $H19_{RHS}$, $H23_{RHS}$ & $H25_{RHS}$), 7.17 (1H, t, *J* = 6.7, NH), 7.04 (1H, td, *J* = 7.7, 1.3, H4), 6.96 (1H, dd, *J* = 7.4, 1.3, H2), 6.83 (1H, td, *J* = 7.4, 1.0, H3), 6.32 (1H, d, *J* = 7.8, H5), 4.69 (2H, s, H7), 4.67 (1H, dd, *J* = 14.1, 7.2, H16), 4.38 (1H, dd, *J* = 14.1, 6.2, H16'), 2.94 (1H, td, *J* = 13.8, 6.3, H10), 2.45 (3H, s, H21), 2.37–2.26 (1H, m, H10'), 2.25–2.16 (1H, m, H12), 2.10 (1H, td, *J* = 13.7, 3.8, H12'), 1.98–1.85 (1H, m, H11), 1.63 (1H, qt, *J* = 13.2, 4.3, H11'), 1.26 (3H, s, H14).

^{13}C NMR (101 MHz, $CDCl_3$) δ = 211.1 (C9), 168.3 (C15), 149.4 (C6), 145.4 (C20), 138.8 (C22), 134.2 (C17), 132.5 (C1), 130.1 (C19), 129.4 (C24), 128.7 (C18), 128.5 (C4), 127.4 (C25), 125.6 (C23), 121.2 (C2), 120.3 (C3), 109.3 (C5), 87.6 (C8), 59.9 (C16), 54.2 (C13), 52.4 (C7), 41.3 (C10), 31.7 (C12), 27.2 (C14), 21.8 (C21), 21.5 (C11).

The observation of nuclear Overhauser effect (nOe) correlations by 2D NOESY corresponding to H14↔NH and H14↔H18 (weak) is consistent with the formation of the *cis*-diastereomer shown.

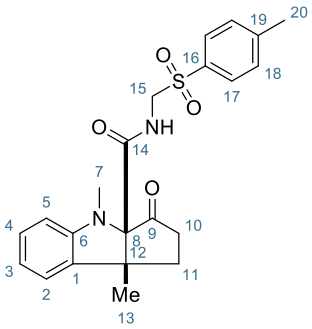
FTIR (neat) ν/cm^{-1} = 3395 (br), 2935, 1716, 1681, 1601, 1479, 1326, 1145, 1086, 912, 733.

* Overlap with the residual non-deuterated chloroform signal led to over-integration of this multiplet. Multiplicity-edited HSQC analysis confirmed the number of protons as 7 within this spectral range.

HRMS (ESI) *m/z* calcd. for $C_{29}H_{31}N_2O_4S$ $[M+H]^+$: 503.1999; found: 503.1999.

MP 68–72 °C (unclear phase transition owing to foam nature of solid).

rac-4,8b-Dimethyl-3-oxo-*N*-(tosylmethyl)-2,3,4,8b-tetrahydrocyclopenta[b]indole-3a(1*H*)-carboxamide, **34**



This compound was prepared from **S30** (98.2 mg, 0.300 mmol, 1.0 eq.) and *para*-toluenesulfonylmethyl isocyanide (TosMIC) (175.7 mg, 0.900 mmol, 3.0 eq.) according to General Procedure B. Flash column chromatography on silica gel (30% ethyl acetate in pentane) yielded **34** (70.1 mg, 0.170 mmol, 57%) as a pale-yellow solid.

^{1}H NMR (400 MHz, $CDCl_3$) δ = 7.83–7.76 (2H, m, H17), 7.46 (1H, t, *J* = 6.9, NH), 7.41–7.34 (2H, m, H18), 7.19 (1H, td, *J* = 7.7, 1.3, H4), 7.04 (1H, dd, *J* = 7.4, 1.3, H2), 6.87 (1H, td, *J* = 7.4, 1.0, H3), 6.55 (1H, d, *J* = 7.9, H5), 4.88 (1H, dd, *J* = 14.2, 7.5, H15''), 4.61 (1H, dd, *J* = 14.2, 6.3, H15'), 2.91 (3H, s, H7), 2.46 (3H, s, H20), 2.40 (1H, ddd, *J* = 18.3, 7.5, 1.1, H10'), 2.29–2.19 (1H, m, H10''), 2.10–1.98 (1H, m, H11'), 1.75 (1H, ddd, *J* = 18.1, 13.0, 8.9, H11'), 1.17 (3H, s, H13).

^{13}C NMR ($CDCl_3$, 101 MHz) δ = 212.3 (C9), 169.2 (C14), 149.8 (C6), 145.8 (C19), 134.1 (C1), 133.5 (C16), 130.2 (C18), 129.1 (C4), 128.8 (C17), 122.5 (C2), 121.0 (C3), 108.9 (C5), 82.6 (C8), 59.8 (C15), 55.6 (C12), 39.2 (C10), 33.8 (C11), 33.2 (C7), 24.3 (C13), 21.9 (C20).

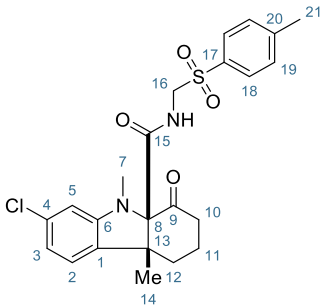
The observation of nuclear Overhauser effect (nOe) correlations by 2D NOESY corresponding to H13↔NH is consistent with the formation of the *cis*-diastereomer shown.

FTIR (neat) ν/cm^{-1} = 3356 (br), 2926, 2856, 1747, 1677, 1599, 1507, 1482, 1323, 1143, 1116, 1085, 1022, 992, 961, 910, 814, 734.

HRMS (APCI) *m/z* calcd. for $C_{22}H_{25}N_2O_4S$ $[M+H]^+$: 413.1530; found: 413.1532.

MP 49–60 °C.

rac-2-Chloro-4b,9-dimethyl-8-oxo-*N*-(tosylmethyl)-4b,5,6,7,8,9-hexahydro-8a*H*-carbazole-8a-carboxamide, **35**



This compound was prepared from **S28** (112.7 mg, 0.300 mmol, 1.0 eq.) and *para*-toluenesulfonylmethyl isocyanide (TosMIC) (175.7 mg, 0.900 mmol, 3.0 eq.) according to General Procedure B. Flash column chromatography on silica gel (gradient elution from 20 to 40% ethyl acetate in pentane) yielded **35** (86.4 mg, 0.187 mmol, 62%) as an off-white solid.

^{1}H NMR (400 MHz, $CDCl_3$) δ = 7.80–7.74 (2H, m, H18), 7.48 (1H, t, *J* = 6.9, NH), 7.38–7.29 (2H, m, H19), 6.83–6.72 (2H, m, $H2_{LHS}$ & $H3_{RHS}$), 6.48 (1H, d, *J* = 1.6, H5), 4.87 (1H, dd, *J* = 14.1, 7.3, H16), 4.62 (1H, dd, *J* = 14.1, 6.3, H16'), 2.97 (3H, s, H7), 2.64 (1H, ddd, *J* = 15.4, 11.6, 7.0, H10), 2.44 (3H, s, H21), 2.23 (1H, dddd, *J* = 15.4, 5.9, 3.3, 1.4, H10'), 2.02 (1H, dtd, *J* = 14.4, 3.8, 1.5, H12), 1.91 (1H, ddd, *J* = 14.4, 13.0, 3.9, H12'), 1.85–1.74 (1H, m, H11), 1.61–1.46 (1H, m, H11'), 1.07 (3H, s, H14).

^{13}C NMR (101 MHz, $CDCl_3$) δ = 209.7 (C9), 168.0 (C15), 151.3 (C6), 145.8 (C20), 134.3 (C4), 134.1 (C17), 131.4 (C1), 130.2 (C19), 128.8 (C18), 122.2 (C2), 119.6 (C3), 108.4 (C5), 85.5 (C8), 60.0 (C16), 52.6 (C13), 40.2 (C10), 34.4 (C7), 32.5 (C12), 27.1 (C14), 21.8 (C21), 20.3 (C11).

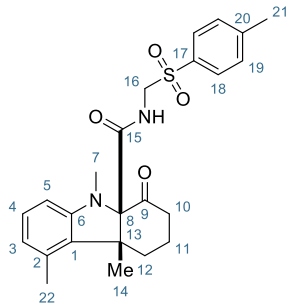
The observation of nuclear Overhauser effect (nOe) correlations by 2D NOESY corresponding to H14↔NH and H14↔H18 (weak) is consistent with the formation of the *cis*-diastereomer shown.

FTIR (neat) ν/cm^{-1} = 3340 (br), 2936, 1716, 1678, 1481, 1289, 1145, 1085, 902, 813, 732.

HRMS (ESI) *m/z* calcd. for $C_{23}H_{26}O_4N_2ClS$ $[M+H]^+$: 461.1296; found: 461.1296.

MP not determined; sample underwent an unclear phase transition between *ca.* 80–90 °C.

rac-4,4b,9-Trimethyl-8-oxo-*N*-(tosylmethyl)-4b,5,6,7,8,9-hexahydro-8a*H*-carbazole-8a-carboxamide, **36**



This compound was prepared from **S34** (106.6 mg, 0.300 mmol, 1.0 eq.) according to General Procedure B. Flash column chromatography on silica gel (gradient elution from 20 to 40% ethyl acetate in pentane) yielded **36** (76.4 mg, 0.173 mmol, 58%) as an off-white solid.

^{1}H NMR (400 MHz, $CDCl_3$) δ = 7.84–7.76 (2H, m, H18), 7.48 (1H, t, *J* = 6.9, NH), 7.39–7.33 (2H, m, H19), 7.06 (1H, t, *J* = 7.7, H4), 6.57 (1H, d, *J* = 7.6, H5), 6.42 (1H, d, *J* = 7.8, H3), 4.92 (1H, dd, *J* = 14.2, 7.5, H16), 4.61 (1H, dd, *J* = 14.1, 6.1, H16'), 2.89 (3H, s, H7), 2.50 (1H, dt, *J* = 16.2, 8.3, H10), 2.45 (3H, s, H21), 2.35–2.25 (1H, m, H12), 2.27 (3H, s, H22), 2.06 (1H, ddd, *J* = 15.6, 8.0, 4.4, H10'), 1.96 (1H, ddd, *J* = 14.7, 13.4, 4.6, H12'), 1.84 (1H, m, H11), 1.65–1.51 (1H, m, H11'), 1.13 (3H, s, H14).

^{13}C NMR (101 MHz, $CDCl_3$) δ = 208.7 (C9), 168.6 (C15), 150.3 (C6), 145.7 (C20), 134.3 (C17), 133.3 (C2), 130.2 (C19), 129.3 (C1), 128.8 (C18), 128.6 (C4), 123.4 (C5), 106.5 (C3), 85.5 (C8), 60.0 (C16), 53.5 (C13), 39.0 (C10), 34.4 (C7), 31.5 (C12), 24.1 (C14), 21.9 (C21), 19.8 (C11), 18.5 (C22).

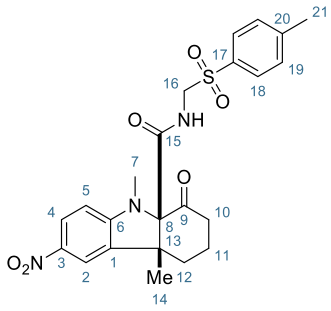
The observation of nuclear Overhauser effect (nOe) correlations by 2D NOESY corresponding to H14↔NH and H14↔H18 (weak) is consistent with the formation of the *cis*-diastereomer shown.

FTIR (neat) ν/cm^{-1} = 3352 (br), 2959, 1715, 1677, 1503, 1470, 1323, 1291, 1144, 913, 734.

HRMS (ESI) *m/z* calcd. for $C_{24}H_{29}N_2O_4S$ $[M+H]^+$: 441.1843; found: 441.1838.

MP 64–68 °C (unclear phase transition owing to foam nature of solid).

rac-4b,9-Dimethyl-3-nitro-8-oxo-*N*-(tosylmethyl)-4b,5,6,7,8,9-hexahydro-8a*H*-carbazole-8a-carboxamide, **37**



This compound was prepared from **S35** (115.9 mg, 0.300 mmol, 1.0 eq.) according to General Procedure B, except with a larger quantity of TosMIC (292.9 mg, 1.50 mmol, 5.0 eq.) and a longer irradiation time of 21 h. Flash column chromatography on silica gel (gradient elution from 0 to 5% ethyl acetate in dichloromethane) yielded **37** (41.5 mg, 0.0880 mmol, 29%, 64% based on recovered starting material) as a yellow solid, alongside unreacted **S35** (63.0 mg, 0.163 mmol) as an extremely viscous orange-brown oil.

^{1}H NMR (400 MHz, DMSO-d_6) δ = 9.11 (1H, t, J = 6.5, NH), 8.08 (1H, dd, J = 8.8, 2.3, H4), 7.88 (1H, d, J = 2.3, H2), 7.79–7.72 (2H, m, H18), 7.48–7.40 (2H, m, H19), 6.63 (1H, d, J = 8.9, H5), 4.84 (1H, dd, J = 14.1, 6.8, H16), 4.62 (1H, dd, J = 14.1, 6.3, H16'), 2.94 (3H, s, H7), 2.67 (1H, ddd, J = 15.3, 11.7, 6.2, H10), 2.40 (3H, s, H21), 2.30–2.16 (2H, m, H10' & H12), 1.91–1.79 (2H, m, H11 & H12'), 1.44–1.26 (1H, m, H11'), 1.17 (3H, s, H14).

^{13}C NMR (101 MHz, DMSO-d_6) δ = 208.2 (C9), 167.0 (C15), 155.4 (C6), 144.7 (C20), 138.9 (C3), 135.1 (C17), 134.0 (C1), 129.7 (C19), 128.5 (C18), 126.7 (C4), 117.7 (C2), 105.5 (C5), 85.2 (C8), 60.5 (C16), 51.4 (C13), 39.9 (C10), 33.4 (C7), 32.5 (C12), 26.5 (C14), 21.1 (C21), 19.8 (C11).

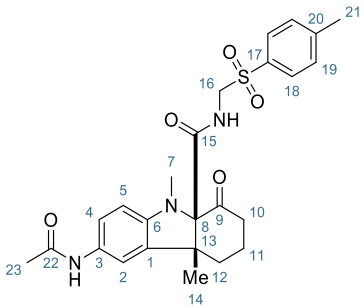
The observation of nuclear Overhauser effect (nOe) correlations by 2D NOESY corresponding to H14↔NH and H14↔H18 (weak) is consistent with the formation of the *cis*-diastereomer shown.

FTIR (neat) ν/cm^{-1} = 3331 (br), 2927, 1681, 1604, 1498, 1379, 1145, 1121, 1086, 1059, 735.

HRMS (ESI) *m/z* calcd. for $C_{23}H_{25}O_6N_3NaS$ $[M+Na]^+$: 494.1356; found: 494.1359.

MP not determined; sample decomposed upon heating at some temperature above 150 °C.

rac-3-Acetamido-4b,9-dimethyl-8-oxo-*N*-(tosylmethyl)-4b,5,6,7,8,9-hexahydro-8a*H*-carbazole-8a-carboxamide, **38**



This compound was prepared from **S36** (119.5 mg, 0.300 mmol, 1.0 eq.) and *para*-toluenesulfonylmethyl isocyanide (TosMIC) (175.7 mg, 0.900 mmol, 3.0 eq.) according to General Procedure B. Flash column chromatography on silica gel (gradient elution from 25 to 50% ethyl acetate in dichloromethane) yielded **38** (100.2 mg, 0.207 mmol, 69%) as a buff solid.

^{1}H NMR (400 MHz, DMSO-d_6) δ = 9.63 (1H, s, R–NH–$COCH_3$), 8.95 (1H, t, J = 6.7, R–NH–$SO_2C_6H_4CH_3$), 7.77–7.69 (2H, m, H18), 7.48–7.40 (2H, m, H19), 7.24 (1H, dd, J = 8.3, 2.1, H4), 7.18 (1H, d, J = 2.0, H2), 6.42 (1H, d, J = 8.4, H5), 4.84 (1H, dd, J = 14.0, 7.0, H16), 4.56 (1H, dd, J = 14.0, 6.3, H16'), 2.86 (3H, s, H7), 2.65 (1H, ddd, J = 14.6, 12.1, 6.3, H10), 2.40 (3H, s, H21), 2.16–1.99 (2H, m, H10'$_{LHS}$ & H12$_{RHS}$), 1.96 (3H, s, H23), 1.91–1.74 (2H, m, H12'$_{LHS}$ & H11$_{RHS}$), 1.45–1.27 (1H, m, H11'), 1.07 (3H, s, H14).

^{13}C NMR (101 MHz, DMSO-d_6) δ = 210.4 (C9), 168.3 (C15), 167.4 (C22), 145.8 (C6), 144.5 (C20), 135.3 (C17), 132.2 (C1), 131.2 (C3), 129.7 (C19), 128.4 (C18), 119.6 (C4), 113.7 (C2), 106.4 (C5), 85.1 (C8), 60.6 (C16), 52.0 (C13), 40.5 (C10), 33.9 (C7), 31.6 (C12), 26.9 (C14), 23.7 (C23), 21.1 (C21), 20.1 (C11).

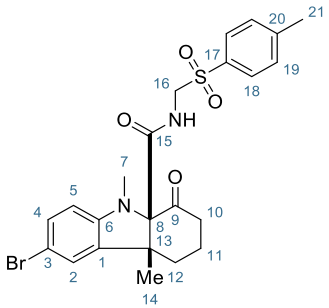
The observation of nuclear Overhauser effect (nOe) correlations by 2D NOESY corresponding to H14↔NH and H14↔H18 is consistent with the formation of the *cis*-diastereomer shown.

FTIR (neat) ν/cm^{-1} = 3352 (br), 2934, 1714, 1667, 1553, 1487, 1301, 1144, 1085, 812, 756.

HRMS (ESI) *m/z* calcd. for $C_{25}H_{30}N_3O_5S$ $[M+H]^+$: 484.1901; found: 484.1898.

MP 104–106 °C.

rac-3-Bromo-4b,9-dimethyl-8-oxo-*N*-(tosylmethyl)-4b,5,6,7,8,9-hexahydro-8a*H*-carbazole-8a-carboxamide, **39**



This compound was prepared from **S37** (126.0 mg, 0.300 mmol, 1.0 eq.) and *para*-toluenesulfonylmethyl isocyanide (TosMIC) (175.7 mg, 0.900 mmol, 3.0 eq.) according to General Procedure B. Flash column chromatography on silica gel (gradient elution from 20 to 40% ethyl acetate in pentane) yielded **39** (119.7 mg, 0.237 mmol, 79%) as a pale-yellow solid.

^{1}H NMR (400 MHz, $CDCl_3$) δ = 7.82–7.71 (2H, m, H18), 7.47 (1H, t, *J* = 6.8, NH), 7.38–7.33 (2H, m, H19), 7.23 (1H, dd, *J* = 8.3, 2.0, H4), 6.97 (1H, d, *J* = 2.0, H2), 6.39 (1H, d, *J* = 8.3, H5), 4.88 (1H, dd, *J* = 14.1, 7.4, H16), 4.61 (1H, dd, *J* = 14.1, 6.3, H16'), 2.98 (3H, s, H7), 2.63 (1H, ddd, *J* = 15.4, 11.6, 7.0, H10), 2.44 (3H, s, H21), 2.22 (1H, dddd, *J* = 15.4, 6.0, 3.4, 1.3, H10'), 2.02 (1H, dtd, *J* = 14.4, 3.9, 1.5, H12), 1.91 (1H, ddd, *J* = 14.4, 12.9, 3.9, H12'), 1.86–1.74 (1H, m, H11), 1.62–1.47 (1H, m, H11'), 1.07 (3H, s, H14).

^{13}C NMR (101 MHz, $CDCl_3$) δ = 209.6 (C9), 168.0 (C15), 149.2 (C6), 145.8 (C20), 135.1 (C1), 134.1 (C17), 131.4 (C4), 130.2 (C19), 128.8 (C18), 124.5 (C2), 111.8 (C3), 109.5 (C5), 85.4 (C8), 60.0 (C16), 52.9 (C13), 40.2 (C10), 34.5 (C7), 32.4 (C12), 27.1 (C14), 21.9 (C21), 20.3 (C11).

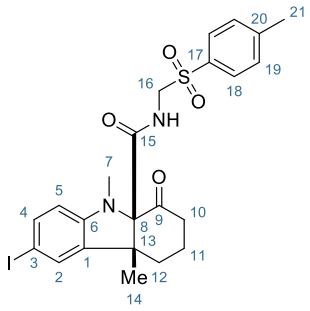
The observation of nuclear Overhauser effect (nOe) correlations by 2D NOESY corresponding to H14↔NH and H14↔H18 (weak) is consistent with the formation of the *cis*-diastereomer shown.

FTIR (neat) ν/cm^{-1} = 3343 (br), 2934, 1715, 1678, 1478, 1322, 1145, 1085, 912, 809, 732.

HRMS (ESI) *m/z* calcd. for $C_{23}H_{26}O_4N_2{}^{79}BrS$ ($C_{23}H_{26}O_4N_2{}^{81}BrS$) $[M+H]^+$: 505.0791 (507.0771); found:505.0791 (507.0770).

MP not determined; sample decomposed upon heating at some temperature above 150 °C.

rac-3-Iodo-4b,9-dimethyl-8-oxo-*N*-(tosylmethyl)-4b,5,6,7,8,9-hexahydro-8a*H*-carbazole-8a-carboxamide, **40**



This compound was prepared from **S38** (140.1 mg, 0.300 mmol, 1.0 eq.) and *para*-toluenesulfonylmethyl isocyanide (TosMIC) (175.7 mg, 0.900 mmol, 3.0 eq.) according to General Procedure B. Flash column chromatography on silica gel (eluent: 25% ethyl acetate in pentane) yielded **40** (118.5 mg, 0.215 mmol, 72%) as an off-white solid.

^{1}H NMR (400 MHz, DMSO-d_6) δ = 8.98 (1H, t, *J* = 6.6, NH), 7.78–7.70 (2H, m, H18), 7.47–7.40 (2H, m, H19), 7.37 (1H, dd, *J* = 8.1, 1.8, H4), 7.28 (1H, d, *J* = 1.8, H2), 6.35 (1H, d, *J* = 8.2, H5), 4.83 (1H, dd, *J* = 14.0, 6.9, H16), 4.56 (1H, dd, *J* = 14.0, 6.2, H16'), 2.85 (3H, s, H7), 2.66 (1H, ddd, *J* = 15.0, 12.2, 6.3, H10), 2.40 (3H, s, H21), 2.21–2.09 (2H, m, H12$_{LHS}$ & H10'$_{RHS}$), 1.90–1.71 (2H, m, H11$_{LHS}$ & H12'$_{RHS}$), 1.40–1.25 (1H, m, H11'), 1.08 (3H, s, H14).

^{13}C NMR (101 MHz, DMSO-d_6) δ = 209.8 (C9), 167.7 (C15), 149.6 (C6), 144.5 (C20), 136.5 (C4), 135.5 & 135.3 (C1 & C17), 129.7 (C19), 129.4 (C2), 128.4 (C18), 109.2 (C5), 84.9 (C8), 79.5 (C3), 60.6 (C16), 52.1 (C13), 40.3 (C10), 33.6 (C7), 31.6 (C12), 26.7 (C14), 21.1 (C21), 20.2 (C11).

The observation of nuclear Overhauser effect (nOe) correlations by 2D NOESY corresponding to H14↔NH and H14↔H18 (weak) is consistent with the formation of the *cis*-diastereomer shown.

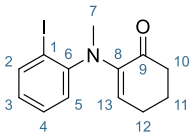
FTIR (neat) ν/cm^{-1} = 3347 (br), 2936, 1716, 1680, 1478, 1323, 1146, 1086, 913, 811, 736.

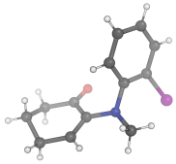
HRMS (ESI) *m/z* calcd. for $C_{23}H_{26}IN_2O_4S$ $[M+H]^+$: 553.0653; found: 553.0641.

MP not determined; sample decomposed upon heating at some temperature above 150 °C.

S2.18. Synthesis and photochemical reactivity of β-hydrogen, *ortho*-iodinated cyclohexenone substrate **41**

2-((2-Iodophenyl)(methyl)amino)cyclohex-2-en-1-one, **41**





CCDC 2330002

This compound was prepared by analogy to a literature procedure.[S8] Aniline **S4** (466 mg, 2.00 mmol, 1.0 eq.), morpholine enamine **S2** (362 mg, 2.00 mmol, 1.0 eq.) and *para*-toluenesulfonic acid monohydrate (380 mg, 2.00 mmol, 1.0 eq.) were heated to 50 °C in toluene (10 mL, 0.2 M) for 3 h. The reaction was cooled to room temperature and diluted with ethyl acetate (20 mL). The solution was washed with sodium hydrogencarbonate (sat. aq., 3 x 10 mL) followed by brine (20 mL). The organic layer was dried over anhydrous sodium sulfate, filtered and concentrated *in vacuo*. The crude residue was purified by flash column chromatography on alumina gel (eluent: 5% ethyl acetate in pentane) to afford **41** (286 mg, 0.875 mmol, 44%) as a cream-coloured solid. Diffraction-quality crystals were grown by vapour diffusion of *n*-hexane into a solution of the product in dichloromethane.

^{1}H NMR (400 MHz, $CDCl_3$) δ = 7.87–7.80 (1H, m, H2), 7.29–7.20 (1H, m, H4), 6.97 (1H, dd, *J* = 7.9, 1.5, H5), 6.83–6.75 (1H, m, H3), 6.03 (1H, t, *J* = 4.6, H13), 2.93 (3H, s, H7), 2.50–2.39 (4H, m, $H10_{LHS}$ & $H12_{RHS}$), 2.01 (2H, quint, *J* = 6.2, H11).

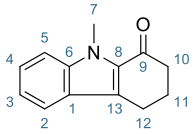
^{13}C NMR (101 MHz, $CDCl_3$) δ = 195.5 (C9), 151.8 (C6), 145.2 (C8), 140.3 (C2), 129.0(1) & 128.9(7) (C4 & C13), 125.9 (C3), 123.7 (C5), 98.0 (C1), 40.6 (C7), 39.7 (C10), 25.7 (C12), 23.0 (C11).

FTIR (neat) ν/cm^{-1} = 2944, 1686, 1468, 1304, 1209, 1113, 1055, 1016, 904, 762, 727.

HRMS (ESI) *m/z* calcd. for $C_{13}H_{15}INO$ $[M+H]^+$: 328.0193; found: 328.0188.

MP 99–100 °C.

9-Methyl-2,3,4,9-tetrahydro-1*H*-carbazol-1-one, **42**



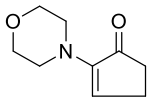
Enaminone **41** (98.2 mg, 0.300 mmol, 1.0 eq.) and potassium acetate (44.2 mg, 0.450 mmol, 1.5 eq.) were dissolved in a 9:1 (v/v) mixture of acetonitrile (5.4 mL) and water (0.6 mL) (0.05 M) in a Schlenk tube equipped with a magnetic stir bar. The vessel was sealed with a septum, and the reaction mixture was degassed by three freeze–pump–thaw cycles. The reaction mixture was stirred under constant

irradiation with two Kessil PR160L 427 nm LED lamps (each positioned *ca.* 3 cm from the flask and directed toward it) for 2 h, with cooling to ambient temperature being achieved using a strong jet of nitrogen gas directed at the flask. The reaction mixture was concentrated *in vacuo*, and the crude residue was purified by flash column chromatography (silica gel, 10% ethyl acetate in pentane) to afford indole **42** (55.3 mg, 0.278 mmol, 92%) as an off-white solid. The spectral data matched that previously reported in the literature.[S18]

^{1}H NMR (400 MHz, $CDCl_3$) δ = 7.66 (1H, dt, *J* = 8.1, 1.0), 7.41 (1H, ddd, *J* = 8.0, 6.7, 1.1), 7.35 (1H, dt, *J* = 8.6, 1.0), 7.15 (1H, ddd, *J* = 8.0, 6.8, 1.1), 4.08 (3H, s), 3.02 (2H, t, *J* = 6.1), 2.65 (2H, dd, *J* = 7.2, 5.7), 2.22 (2H, quint, *J* = 6.2).

S2.19. Synthesis and photochemical reactivity of β-hydrogen, *ortho*-iodinated cyclopentenone substrate **S43**

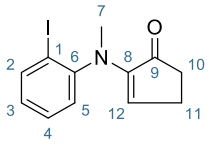
2-Morpholinocyclopent-2-en-1-one, **S42**



This compound was prepared by analogy to a literature procedure.[S6] A mixture of cyclohexane-1,2-dione (981 mg, 10.0 mmol, 1.0 eq.) and morpholine (1.1 mL, 1.1 g, 13 mmol, 1.3 eq.) in toluene (25 mL, 0.4 M) were heated to reflux under Dean–Stark conditions for 12 h. After cooling to room temperature, the orange liquid thus obtained was decanted from the viscous brown oil coating the bottom of the flask and concentrated *in vacuo*. The crude residue was purified by flash column chromatography (silica gel, 50% ethyl acetate in pentane) to afford **S42** (370 mg, 2.21 mmol, 21%) as a brown solid. The spectral data matched that previously reported in the literature.[S7]

^{1}H NMR (400 MHz, $CDCl_3$) δ = 6.37 (1H, t, *J* = 2.7), 3.91–3.66 (4H, m), 3.20–2.95 (4H, m), 2.59–2.46 (2H, m), 2.46–2.34 (2H, m).

2-((2-Iodophenyl)(methyl)amino)cyclopent-2-en-1-one, **S43**



This compound was prepared by analogy to a literature procedure.[S8] Aniline **S4** (350 mg, 1.50 mmol, 1.0 eq.), morpholine enamine **S42** (251 mg, 1.50 mmol, 1.0 eq.) and *para*-toluenesulfonic acid monohydrate (285 mg, 1.50 mmol, 1.0 eq.) were heated to 50 °C in toluene (15 mL, 0.1 M) for 3 h. The reaction was cooled to room temperature and diluted with ethyl acetate (25 mL). The solution was washed with sodium hydrogencarbonate (sat. aq., 3 x 12.5 mL) followed by brine (25 mL). The organic layer was dried over anhydrous sodium sulfate, filtered and concentrated *in vacuo*. The crude residue was purified by flash column chromatography (silica gel, 10% diethyl ether in pentane) to afford **S43** (273 mg, 0.872 mmol, 58%) as a brown solid.

^{1}H NMR (400 MHz, $CDCl_3$) δ = 7.86 (1H, dd, *J* = 7.9, 1.5, H2), 7.36–7.26 (1H, ddd, *J* = 7.9, 7.3, 1.5, H4), 7.03 (1H, dd, *J* = 7.9, 1.6, H5), 6.90 (1H, ddd, *J* = 7.9, 7.3, 1.6, H3), 6.26 (1H, t, *J* = 3.2, H12), 3.09 (3H, s, H7), 2.59–2.49 (2H, m, H11), 2.48–2.39 (2H, m, H10).

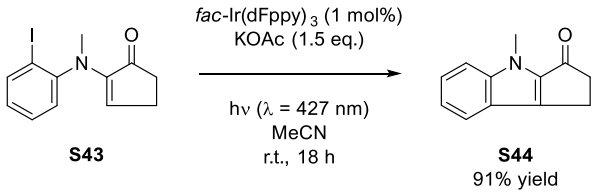
^{13}C NMR ($CDCl_3$, 101 MHz) δ = 203.2 (C9), 149.7 (C6), 148.3 (C8), 139.8 (C2), 132.2 (C12), 129.1 (C4), 127.4 (C3), 126.2 (C5), 98.7 (C1), 40.5 (C7), 35.0 (C10), 23.3 (C11).

FTIR (neat) ν/cm^{-1} = 1701, 1611, 1576, 1506, 1322, 1260, 1043, 1029, 790, 727.

HRMS (APCI) *m/z* calcd. for $C_{12}H_{13}INO$ $[M+H]^+$: 314.0036; found: 314.0038.

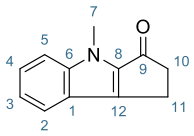
MP 69–70 °C.

Photocyclization of cyclopentenone **S43**



Enaminone **S43** (31.3 mg, 0.100 mmol, 1.0 eq.), *fac*-Ir(dFppy)$_3$ (0.8 mg, 1 μmol, 1 mol%) and potassium acetate (14.7 mg, 0.150 mmol, 1.5 eq.) were charged to a Schlenk tube equipped with a magnetic stir bar. The vial was sealed with a septum and then evacuated and back-filled with argon three times. Argon-sparged acetonitrile (2.0 mL, 0.05 M) was added *via* syringe, and the reaction mixture was sparged with argon for a further 15 min. The reaction mixture was stirred under constant irradiation with a single Kessil PR160L 427 nm LED lamp (positioned *ca.* 3 cm from the vial and directed toward it) for 18 h, with cooling to ambient temperature being achieved by submerging the vial in cold water contained in a water-jacketed vessel. The reaction mixture was concentrated *in vacuo*, and the crude residue thus obtained was purified by flash column chromatography (silica gel, 20% ethyl acetate in pentane) to afford indole **S44** (16.9 mg, 0.0912 mmol, 91%) as an off-white solid.

4-Methyl-1,4-dihydrocyclopenta[b]indol-3(2H)-one, **S44**



^{1}H NMR (400 MHz, $CDCl_3$) δ = 7.69 (1H, dt, *J* = 8.1, 1.0, H2), 7.42 (1H, ddd, *J* = 8.1, 6.8, 1.2, H4), 7.36 (1H, dt, *J* = 8.5, 1.0, H5), 7.18 (1H, ddd, *J* = 8.0, 6.8, 1.1, H3), 3.91 (3H, s, H7), 3.09–3.02 (2H, m, H10), 3.01–2.94 (2H, m, H11).

^{13}C NMR (101 MHz, $CDCl_3$) δ = 194.9 (C9), 145.0(7) & 145.0(0) (C12 & C6), 139.0 (C8), 126.9 (C4), 123.2 (C1), 121.9 (C2), 120.3 (C3), 111.1 (C5), 41.6 (C11), 31.1 (C7), 19.7 (C10).

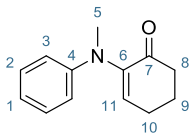
FTIR (neat) ν/cm^{-1} = 2923, 2854, 1670, 1485, 1445, 1405, 1378, 1348, 1260, 1235, 1201, 1132, 1097, 1041, 1023, 884, 809, 743.

HRMS (APCI) *m/z* calcd. for $C_{12}H_{12}NO$ $[M+H]^+$: 186.0913; found: 186.0908.

MP 114–116 °C.

S2.20. Synthesis and photochemical reactivity of β-hydrogen, *ortho*-unsubstituted substrate **S45**

2-(Methyl(phenyl)amino)cyclohex-2-en-1-one, **S45**



This compound was prepared by analogy to a literature procedure.[S8] *N*-Methylaniline (0.27 mL, 0.27 g, 2.5 mmol, 1.0 eq.), morpholine enamine **S2** (453 mg, 2.50 mmol, 1.0 eq.) and *para*-toluenesulfonic acid monohydrate (476 mg, 2.50 mmol, 1.0 eq.) were heated to 50 °C in toluene (12.5 mL, 0.2 M) for 3 h. The reaction was cooled to room temperature and diluted with ethyl acetate (25 mL). The solution was washed with sodium hydrogencarbonate (sat. aq., 3 x 12.5 mL) followed by brine (25 mL). The organic layer was dried over anhydrous sodium sulfate, filtered and concentrated *in vacuo*. The crude residue was purified by flash column chromatography on alumina gel (gradient elution from 5 to 10% ethyl acetate in pentane) to afford **S45** (232 mg, 1.15 mmol, 46%) as a viscous yellow oil.

^{1}H NMR (400 MHz, $CDCl_3$) δ = 7.24–7.14 (2H, m, H2), 6.83–6.66 (4H, m, $H1_{LHS}$, $H11_{LHS}$ & $H3_{RHS}$), 3.07 (3H, s, H5), 2.60–2.48 (4H, m, $H8_{LHS}$ & $H10_{RHS}$), 2.14–2.03 (2H, m, H9).

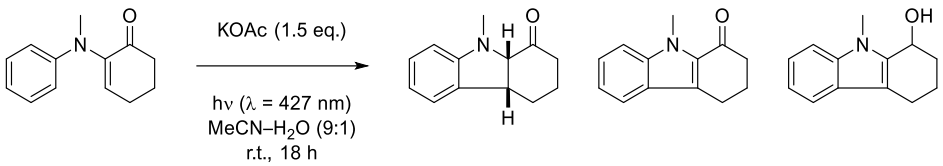
^{13}C NMR (101 MHz, $CDCl_3$) δ = 196.6 (C7), 149.1 & 144.8 (C4 & C6), 143.2 (C11), 129.0 (C2), 118.5 (C1), 114.9 (C3), 39.6 (C5), 39.5 (C8), 26.1 (C10), 23.0 (C9).

FTIR (neat) ν/cm^{-1} = 2945, 1685, 1598, 1500, 1326, 1215, 1110, 903, 750, 693, 640.

HRMS (ESI) *m/z* calcd. for $C_{13}H_{16}NO$ $[M+H]^+$: 202.1226; found: 202.1223.

Photocyclization of **S45**

The irradiation of this substrate with UV light in ethanolic solution has previously been reported by Pete and co-workers.[S19]



Analytical-scale reaction:

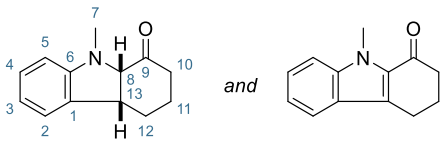
Enaminone **S45** (20.1 mg, 0.0999 mmol, 1.0 eq.) and potassium acetate (14.7 mg, 0.150 mmol, 1.5 eq.) were dissolved in a 9:1 (v/v) mixture of acetonitrile (1.8 mL) and water (0.2 mL) (0.05 M) in a Schlenk tube equipped with a magnetic stir bar. The vessel was sealed with a septum, and the reaction mixture was degassed by three freeze–pump–thaw cycles. The reaction mixture was stirred under constant

irradiation with a single Kessil PR160L 427 nm LED lamp (positioned *ca.* 3 cm from the flask and directed toward it) for 18 h, with cooling to ambient temperature being achieved using a strong jet of nitrogen gas directed at the flask. Dimethyl terephthalate was added at the end of the irradiation period as a solution in acetonitrile (25.0 mM, 1.0 mL, 0.25 mmol, 0.25 eq.). The resulting mixture was concentrated *in vacuo*, and the crude residue was dissolved in $CDCl_3$ for analysis by quantitative ^1H NMR spectroscopy. The NMR yields of indoline **S46**, indole **42** and indole **S47** measured against dimethyl terephthalate were 21%, 45% and 13%, respectively.

Preparative-scale reaction:

Enaminone **S45** (60.4 mg, 0.300 mmol, 1.0 eq.) and potassium acetate (44.2 mg, 0.450 mmol, 1.5 eq.) were dissolved in a 9:1 (v/v) mixture of acetonitrile (5.4 mL) and water (0.6 mL) (0.05 M) in a Schlenk tube equipped with a magnetic stir bar. The vessel was sealed with a septum, and the reaction mixture was degassed by three freeze–pump–thaw cycles. The reaction mixture was stirred under constant irradiation with two Kessil PR160L 427 nm LED lamps (each positioned *ca.* 3 cm from the flask and directed toward it) for 18 h, with cooling to ambient temperature being achieved using a strong jet of nitrogen gas directed at the flask. The reaction mixture was concentrated *in vacuo*, and the crude residue was purified by flash column chromatography (silica gel, gradient elution 5 to 20% ethyl acetate in pentane) to afford a *ca.* 2:3 mixture (estimated from relative integrations of ^1H resonances) of indoline **S46** and indole **42** (25.9 mg, corresponding to isolated yields of *ca.* 17% and 26%, respectively), alongside an impure sample of indole **S47**; the latter material was subjected to further flash column chromatographic purification (silica gel, dichloromethane), affording pure **S47** (6.5 mg, 0.032 mmol, 11%) as a white solid.

rac-9-Methyl-2,3,4,4a,9,9a-hexahydro-1*H*-carbazol-1-one, **S46**, *and* 9-methyl-2,3,4,9-tetrahydro-1*H*-carbazol-1-one, **42**



S46 **42**

Indoline **S46** was characterized as a mixture with **42**. ^1H and ^{13}C NMR data corresponding to the former compound are reported below; the NMR spectral data of **42** matched that reported above.

^1H NMR (400 MHz, $CDCl_3$) δ = 7.19–7.12 (1H, m, H4), 7.11–7.05 (1H, m, H2), 6.82–6.73 (1H, m, H3), 6.57 (1H, d, *J* = 7.9, H5), 3.58 (1H, td, *J* = 8.2, 5.7, H13), 3.48 (1H, d, *J* = 8.4, H8), 2.74 (3H, s, H7), 2.66–2.55 (1H, m, H10), 2.47–2.36 (1H, m, H10'), 2.03–1.87 (2H, m, $H11_{LHS}$ & $H12_{RHS}$), 1.82–1.58 (2H, m, $H11'_{LHS}$ & $H12'_{RHS}$).

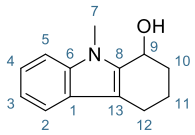
^{13}C NMR (101 MHz, $CDCl_3$) δ = 211.3 (C9), 152.0 (C6), 133.2 (C1), 128.2 (C4), 123.4 (C2), 119.1 (C3), 108.5 (C5), 74.2 (C8), 44.4 (C13), 38.7 (C10), 35.1 (C7), 29.3 (C12), 22.4 (C11).

The observation of a transient (negative) nOe enhancement by 1D NOESY for H13 upon selective inversion of H8 suggests the formation of the *cis*-diastereomer shown.

FTIR (neat) ν/cm^{-1} = 2941, 2862, 1711, 1657, 1607, 1482, 1314, 1251, 1123, 934, 827, 743.

HRMS (ESI) *m/z* calcd. for $C_{13}H_{14}NO$ $[M+H]^+$: 200.1070; found: 200.1070; *m/z* calcd. for $C_{13}H_{16}NO$ $[M+H]^+$: 202.1226; found: 202.1224.

9-Methyl-2,3,4,9-tetrahydro-1*H*-carbazol-1-ol, **S47**



^{1}H NMR (400 MHz, $CDCl_3$) δ = 7.53 (1H, app. d, *J* = 7.9, H2), 7.31 (1H, app. d, *J* = 8.2, H5), 7.28–7.20 (1H, m, H4), 7.10 (1H, ddd, *J* = 8.0, 6.9, 1.1, H3), 4.95 (1H, dt, *J* = 7.7, 3.6, H9), 3.78 (3H, s, H7), 2.87 (1H, dt, *J* = 15.8, 4.2, H12), 2.68–2.56 (1H, m, H12'), 2.18–2.08 (1H, m, H10), 2.08–1.86 (3H, m, H10'$_{LHS}$, H11$_{RHS}$ & H11'$_{RHS}$), 1.67 (1H, br d, *J* = 8.1, OH).

^{13}C NMR (101 MHz, $CDCl_3$) δ = 137.5 (C6), 135.7 (C8), 126.4 (C1), 122.3 (C4), 119.1 & 119.0 (C2 & C3), 112.1 (C13), 109.2 (C5), 62.1 (C9), 33.4 (C10), 29.6 (C7), 21.3 (C12), 18.7 (C11).

FTIR (neat) ν/cm^{-1} = 3323 (br), 2934, 2838, 1471, 1378, 1247, 1195, 1154, 1068, 995, 926, 738.

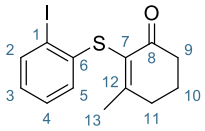
HRMS (ESI) *m/z* calcd. for $C_{13}H_{16}NO$ $[M+H]^+$: 202.1226; found: 202.1226.

MP 94–96 °C.

S2.21. Synthesis and photochemical reactivity of an *S*-linked analogue

See Section S4.7 for a discussion of these results.

2-((2-Iodophenyl)thio)-3-methylcyclohex-2-en-1-one, **45**



This compound was prepared by analogy to a literature procedure.[S24] 6-Methyl-7-oxabicyclo[4.1.0]heptan-2-one[S25] (253 mg, 2.01 mmol, 1.0 eq.), 2-iodobenzenethiol[S26] (608 mg, 2.58 mmol, 1.3 eq.) and potassium carbonate (276 mg, 2.00 mmol, 1.0 eq.) were charged to a two-necked round-bottomed flask equipped with a condenser and magnetic stir bar. The flask was evacuated and back-filled with argon three times before adding argon-sparged dry acetonitrile (8 mL, 0.2 M) to the vessel. The reaction mixture was heated to reflux with stirring. After 18 h, the reaction mixture was poured into a solution of sodium hydroxide (1 M aq., 20 mL). The aqueous phase was extracted with diethyl ether (3 x 10 mL). The combined organic extracts were washed with brine (15 mL), dried over magnesium sulfate and concentrated *in vacuo*. The crude residue was purified by flash column chromatography (silica gel, 20% ethyl acetate in pentane) to afford **45** (424 mg, 1.23 mmol, 61%) as an off-white solid.

^{1}H NMR (400 MHz, $CDCl_3$) δ = 7.75 (1H, dd, *J* = 7.8, 1.2, H2), 7.16 (1H, td, *J* = 7.8, 1.3, H3), 6.82–6.72 (2H, m, H4 & H5), 2.66–2.54 (4H, m, H9 & H11), 2.24 (3H, s, H13), 2.14–2.02 (2H, m, H10).

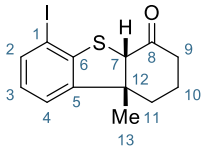
^{13}C NMR (101 MHz, $CDCl_3$) δ = 194.1 (C8), 170.6 (C12), 141.5 (C6), 139.6 (C2), 130.3 (C7), 128.5 (C4), 126.4 (C5), 126.4 (C3), 96.9 (C1), 38.4 (C9), 34.5 (C11), 24.7 (C13), 21.9 (C10).

FTIR (neat) ν/cm^{-1} = 3047, 2950, 1669, 1583, 1438, 1421, 1360, 1320, 1271, 1191, 1037, 1010, 778.

HRMS (APCI) *m/z* calcd. for $C_{13}H_{13}IOS$ $[M+H]^+$: 344.9805; found: 344.9805.

MP 92–94 °C.

rac-6-Iodo-9b-methyl-2,3,4a,9b-tetrahydrodibenzo[b,d]thiophen-4(1*H*)-one, **46**



Enone **45** (34.4 mg, 0.0999 mmol, 1.0 eq.) and *fac*-Ir(dFppy)$_3$ (0.8 mg, 1 μmol, 1 mol%) were charged to a Schlenk tube equipped with a magnetic stir bar. The vessel was sealed with a septum, and the flask was evacuated and back-filled with argon three times. Acetonitrile (1.8 mL), water (0.2 mL) and allyltrimethylsilane (79 μL, 57 mg, 0.50 mol, 5.0 eq.), all argon-sparged, were added *via*

(micro)syringe. The reaction mixture was stirred under constant irradiation with a single Kessil PR160L 427 nm LED lamp (positioned *ca.* 3 cm from the flask and directed toward it) for 16 h, with cooling to ambient temperature being achieved by submerging the flask in cold water contained in a water-jacketed vessel. After the irradiation period, the reaction mixture was concentrated *in vacuo*, and the crude residue thus obtained was purified by flash column chromatography (silica gel, 20% diethyl ether in pentane) to afford **46** (26.3 mg, 0.0764 mmol, 76%, *ca.* 4:1 d.r.) as an off-white solid.

Dihydrobenzothiophene **46** was characterized as a mixture of diastereomers; spectral data corresponding to the major (*cis*) diastereomer are reported below.

^{1}H NMR (400 MHz, $CDCl_3$) δ = 7.53 (1H, dd, *J* = 7.8, 1.1, H2), 7.01 (1H, dd, *J* = 7.6, 1.1, H4), 6.83 (1H, t, *J* = 7.7, H3), 3.98–3.92 (1H, m, H7), 2.86–2.74 (1H, m, H9), 2.36 (1H, app. dtt, *J* = 15.4, 5.4, 1.2, H9'), 2.17 (1H, ddd, *J* = 13.8, 8.3, 5.3, H11), 1.95–1.79 (2H, m, H10), 1.68–1.55 (1H, m, H11'), 1.44 (3H, s, H13)

^{13}C NMR ($CDCl_3$, 101 MHz) δ = 207.5 (C8), 146.5 (C6), 137.2 (C2), 127.03 (C5), 126.7 (C3), 122.2 (C4), 88.8 (C1), 63.1 (C7), 56.5 (C12), 37.5 (C9), 34.7 (C11), 26.1 (C13), 21.1 (C10).

The observation of nuclear Overhauser effect (nOe) correlations by 2D NOESY corresponding to H7↔H13 is consistent with the formation of the major diastereomer with *cis*-stereochemistry as shown.

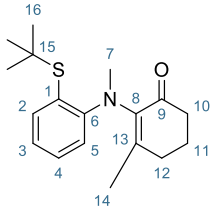
FTIR (neat) ν/cm^{-1} = 2958, 2924, 2852, 1704, 1462, 1405, 1348, 1073, 1040, 807, 776, 721.

HRMS (APCI) *m/z* calcd. for $C_{13}H_{13}IOSNa$ $[M+Na]^+$: 366.9624; found: 366.9610.

MP 79–82 °C.

S2.22. Synthesis and photochemical reactivity of **(±)-** and **(+)-48**, substrates bearing an *ortho*-sulfinyl group

2-((2-(*tert*-Butylthio)phenyl)(methyl)amino)-3-methylcyclohex-2-en-1-one, **47**



This compound was prepared by analogy to a literature procedure.[S20] Aryl iodide **10** (341 mg, 0.999 mmol, 1.0 eq.), $Pd_2(dba)_3$ (22.9 mg, 25.0 µmol, 2.5 mol%) and Xantphos (28.9 mg, 49.9 µmol, 5.0 mol%) were added to a microwave vial equipped with a magnetic stir bar. The vial was sealed with a septum cap, and evacuated and back-filled with argon three times. Argon-sparged anhydrous 1,4-dioxane (2.0 mL, 0.5 M) was added to the vial *via* syringe, followed by *N*,*N*-diisopropylethylamine (0.35 mL, 0.26 g, 2.0 mmol, 2.0 eq.) and 2-methyl-2-propanethiol (0.15 mL, 0.12 g, 1.3 mmol, 1.3 eq.). The reaction mixture was heated to 110 °C for 18 h with continuous stirring. After this time, the reaction mixture was allowed to cool to room temperature before being concentrated *in vacuo*. The crude residue was purified twice by flash column chromatography (silica gel, 75% dichloromethane in pentane; then, silica gel, 5 to 10% ethyl acetate in pentane) to afford **47** (140 mg, 0.461 mmol, 46%) as a viscous yellow oil.

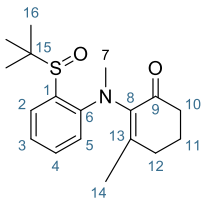
^{1}H NMR (600 MHz, $CDCl_3$) δ = 7.36 (1H, dd, *J* = 7.6, 1.7, H2), 7.30–7.25 (1H, m, H4), 6.98 (1H, dd, *J* = 8.3, 1.3, H5), 6.76 (1H, td, *J* = 7.4, 1.3, H3), 3.02 (3H, s, H7), 2.51 (2H, t, *J* = 6.7, H10), 2.33 (2H, t, *J* = 6.1, H12), 2.03 (2H, quint, *J* = 6.2, H11), 1.44 (3H, s, H14), 1.13 (9H, s, H16).

^{13}C NMR (151 MHz, $CDCl_3$) δ = 196.3 (C9), 155.1 (C6), 149.1 (C13), 143.7 (C8), 140.1 (C2), 130.0 (C4), 121.1 (C1), 118.9 (C3), 116.3 (C5), 47.4 (C15), 39.2 (C10), 39.1 (C7), 32.9 (C12), 30.4 (C16), 21.8 (C11), 20.3 (C14).

FTIR (neat) ν/cm^{-1} = 2924, 2854, 1682, 1583, 1473, 1378, 1323, 1213, 1168, 1122, 930, 757.

HRMS (ESI) *m/z* calcd. for $C_{18}H_{26}NOS$ $[M+H]^+$: 304.1730; found: 304.1728.

(±)-2-((2-(*tert*-Butylsulfinyl)phenyl)(methyl)amino)-3-methylcyclohex-2-en-1-one, **(±)-48**



rac

Thioether **47** (47.0 mg, 0.155 mmol, 1.0 eq.) was dissolved in ethanol (1.6 mL, 0.1 M) in a 7 mL vial equipped with a magnetic stir bar. Sodium tungstate dihydrate (10.2 mg, 0.0309 mmol, 0.2 eq.) was added in one portion to the solution, followed by hydrogen peroxide solution (34.5–36.5% w/w aq., 68 µL, 0.78 mmol, 5.0 eq.) in one portion *via* micropipette, and the vial was sealed with a screw cap. The reaction mixture was heated to 50 °C for 4.5 h with continuous stirring. After this time, the reaction mixture was concentrated *in vacuo*, and the crude residue was purified by flash column chromatography (silica gel, 50% ethyl acetate in dichloromethane) to afford racemic sulfoxide **(±)-48** (45.8 mg, 0.143 mmol, 93%) as a white solid. This material was used as a racemic standard for chiral HPLC analyses of enantioenriched material (see below).

^{1}H NMR (400 MHz, $CDCl_3$) δ = 7.70 (1H, dd, *J* = 7.8, 1.7, H2), 7.43–7.34 (1H, m, H4), 7.04 (1H, dd, *J* = 8.3, 1.1, H5), 7.00 (1H, ddd, *J* = 8.1, 7.3, 1.1, H3), 2.98 (3H, s, H7), 2.62–2.52 (1H, m, H10), 2.52–2.31 (3H, m, $H10_{LHS}$, $H12_{RHS}$ & $H12'_{RHS}$), 2.18–1.90 (2H, m, H11 & H11'), 1.52 (3H, s, H14), 1.07 (9H, s, H16).

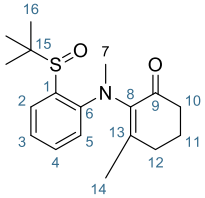
^{13}C NMR (101 MHz, $CDCl_3$) δ = 196.6 (C9), 154.0 (C13), 150.3 (C6), 142.5 (C8), 132.1 (C4), 129.0 (C1), 127.2 (C2), 120.0 (C3), 117.6 (C5), 57.7 (C15), 39.1 (C10), 38.6 (C7), 33.5 (C12), 22.7 (C16), 21.5 (C11), 20.6 (C14).

FTIR (neat) ν/cm^{-1} = 2945, 1676, 1587, 1475, 1292, 1175, 1118, 1046, 1027, 930, 763.

HRMS (ESI) m/z calcd. for $C_{18}H_{25}No_2SNa$ $[M+Na]^+$: 342.1498; found: 342.1499.

MP 109–110 °C.

(+)-2-((2-(*tert*-Butylsulfinyl)phenyl)(methyl)amino)-3-methylcyclohex-2-en-1-one, **(+)-48**



ent

This compound was prepared by analogy to a literature procedure.[S21] Dichloromethane (1.5 mL) was added under an argon atmosphere to (+)-diethyl L-tartrate (190 mg, 0.921 mmol, 2.0 eq.) in a septum-sealed 10 mL microwave vial equipped with a magnetic stir bar. The resulting solution was sparged with argon for 2 min before adding titanium isopropoxide (0.14 mL, 0.13 g, 0.47 mmol, 1.0 eq.) and water (8.3 µL, 8.3 mg, 0.46 mmol, 1.0 eq.) sequentially *via* syringe under continuous and vigorous stirring. The resulting mixture was sparged with argon for an additional 2 min. An argon-sparged solution of thioether **47** (140 mg, 0.461 mmol, 1.0 eq.) in dichloromethane (3.0 mL) was added to the mixture *via* syringe. The vial was cooled to -20 °C using a Polar Bear Plus Crystal.

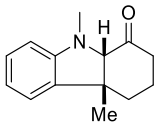
Tert-Butyl hydroperoxide (0.18 mL, 5.0–6.0 M in decane, *ca.* 0.90 mmol, *ca.* 2.0 eq.) was added *via* syringe, and the resulting mixture was vigorously stirred at -20 °C for 21 h. After this time, water (83 μL, 4.6 mmol, 10 eq.) was added *via* syringe to the reaction mixture. Stirring was continued for 10 min at -20 °C before allowing the quenched reaction mixture to warm to room temperature over 20 min. The reaction mixture was diluted with dichloromethane and filtered through a short plug of basic alumina (*ca.* 5 g). The filtrate (*ca.* 50 mL in volume) was washed successively with sodium hydroxide solution (1 M aq., 3 x 25 mL) and brine (50 mL) before being dried over anhydrous magnesium sulfate, filtered and concentrated *in vacuo*. The crude residue was purified by flash column chromatography (silica gel, 50% ethyl acetate in dichloromethane) to afford enantioenriched sulfoxide (+)-**48** (110 mg, 0.344 mmol, 75%, 98:2 e.r.) as a white solid.

The spectral data of this compound matched that of the racemate reported above.

Chiral HPLC: (Chiralpak IG-3, 40% EtOH, 60% hexane, 1.0 mL min^{-1}, λ = 210 nm); τ_R (minor) = 6.6 min, τ_R (major) = 8.0 min; e.r. 98:2.

$[\alpha]_D^{25}$ +318° (*c* = 1.0, $CDCl_3$).

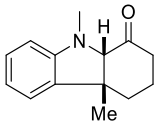
(±)-4a,9-Dimethyl-2,3,4,4a,9,9a-hexahydro-1*H*-carbazol-1-one, **(±)-21**, *from* **(±)-48**



rac

Racemic *ortho*-sulfinyl substrate **(±)-48** (31.9 mg, 0.0999 mmol, 1.0 eq.) was charged to a Schlenk tube equipped with a magnetic stir bar. The vessel was sealed with a septum and then evacuated and back-filled with argon three times. Acetonitrile (2.0 mL, 0.05 M), triethylsilane (80 μL, 58 mg, 0.50 mmol, 5.0 eq.) and trifluoroacetic acid (23 μL, 34 mg, 0.30 mmol, 3.0 eq.), all argon-sparged, were added successively *via* (micro)syringe. The reaction mixture was stirred under constant irradiation with a single Kessil PR160L 427 nm LED lamp (positioned *ca.* 3 cm from the flask and directed toward it) for 12 h, with cooling to ambient temperature being achieved using a strong jet of nitrogen gas directed at the flask. Triethylamine (0.7 mL) was added to the reaction mixture at the end of the irradiation period, and the resulting mixture was concentrated *in vacuo*. The crude residue was purified by flash column chromatography (silica gel, 5% ethyl acetate in pentane) to afford racemic **(±)-21** (15.5 mg, 0.0720 mmol, 72%) as a viscous colourless oil. This material (whose spectral data matched that reported for the same compound above) was used as a racemic standard for chiral HPLC analyses of enantioenriched material (see below).

(–)-4a,9-Dimethyl-2,3,4,4a,9,9a-hexahydro-1*H*-carbazol-1-one, **(–)-21**, *from* **(+)-48**



ent

Enantioenriched *ortho*-sulfinyl substrate **(+)-48** (31.9 mg, 0.0999 mmol, 1.0 eq.) was charged to a Schlenk tube equipped with a magnetic stir bar. The vessel was sealed with a septum and then evacuated and back-filled with argon three times. Acetonitrile (2.0 mL, 0.05 M), triethylsilane (80 μL, 58 mg, 0.50 mmol, 5.0 eq.) and trifluoroacetic acid (23 μL, 34 mg, 0.30 mmol, 3.0 eq.), all argon-sparged, were added successively *via* (micro)syringe. The reaction mixture was stirred under constant irradiation with a single Kessil PR160L 427 nm LED lamp (positioned *ca.* 3 cm from the flask and directed toward it) for 12 h, with cooling to ambient temperature being achieved using a strong jet of nitrogen gas directed at the flask. Triethylamine (0.7 mL) was added to the reaction mixture at the end of the irradiation period, and the resulting mixture was concentrated *in vacuo*. The crude residue was purified by flash column chromatography (silica gel, 5% ethyl acetate in pentane) to afford enantioenriched **(–)-21** (16.1 mg, 0.0748 mmol, 75%) as a viscous colourless oil.

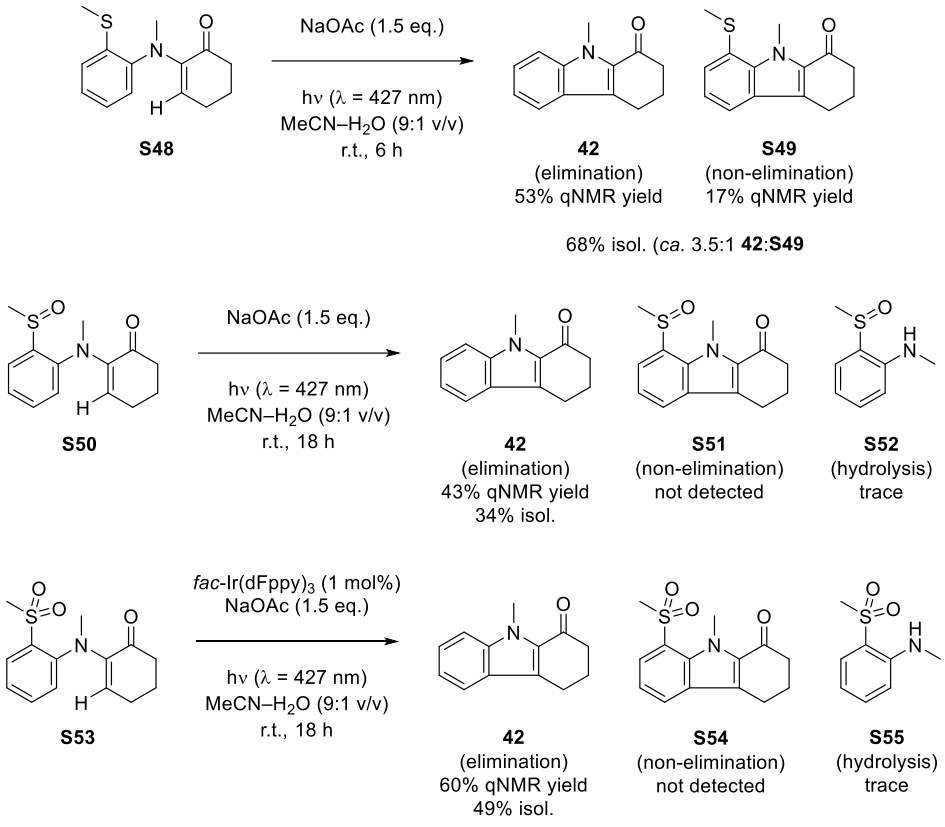
The spectral data of this compound matched that of the racemate reported above.

Chiral HPLC: (Chiralpak IA, 10% dichloromethane, 90% hexane, 1.0 mL min^{-1}, λ = 249 nm); τ_R (minor) = 7.7 min, τ_R (major) = 8.46 min; e.r. 96:4.

$[\alpha]_D^{25}$ -153° (*c* = 1.0, $CDCl_3$).

S2.23. Synthesis and photochemical reactivity of substrates bearing alternative sulfur-based leaving groups

In addition to exploring the photochemical reactivity of *ortho*-sulfinyl substrate **48**, we have shown that enaminones **S48**, **S50** and **S53** bearing *ortho*-sulfanyl, -sulfinyl and -sulfonyl substituents undergo predominantly or exclusively eliminative photocyclization upon (sensitized) irradiation in acetonitrile solution (Scheme S2).

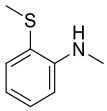


Scheme S2. Summary of results for substrates bearing sulfur-based leaving groups at different oxidation states. Yields were measured by quantitative ^{1}H NMR (qNMR) spectroscopy against dibromomethane (0.50 eq.) or refer to isolated (isol.) material as specified.

In the presence of sodium acetate, this process yields **42**, in which the *ortho*-substituent has been lost, as the sole (non-trace) photocyclization product when SOMe or SO_2Me leaving groups are used (i.e., for substrates **S50** and **S53**, respectively). In the reaction of *ortho*-SMe-substituted substrate **S48** (i.e., when X = SMe), the same product, **42**, was formed in major quantities alongside a minor 'non-elimination' product, **S49**. (The only other identifiable components of the crude photolysates of **S50** and **S53** were anilines **S52** and **S55**, respectively, presumably arising from hydrolysis of the starting material; **S51** or **S54** were not observed.)

Full experimental details are summarized in the section to follow.

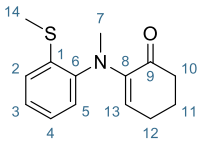
N-Methyl-2-(methylthio)aniline, **S56**



n-Butyllithium in hexanes (14 mL, 1.6 M, 22 mmol, 1.1 eq.) was added over 30 min *via* syringe pump to a stirred, -78 °C solution of 2-(methylthio)aniline (2.78 g, 20.0 mmol, 1.0 eq.) in anhydrous tetrahydrofuran (40 mL, 0.5 M) under an argon atmosphere. The resulting slurry was stirred at -78 °C for 5 min before adding methyl iodide (1.37 mL, 22.0 mmol, 1.1 eq.) dropwise by syringe. After a further 5 min at -78 °C, the acetone–dry ice bath was replaced with a tepid water bath, and the reaction mixture was allowed to warm to room temperature over a period of 2 h. Ammonium chloride solution (sat. aq., 40 mL) was added, followed by diethyl ether (40 mL). The layers were separated, and the aqueous phase was extracted with additional diethyl ether (2 x 40 mL). The combined organic extracts were washed with brine (80 mL), dried over anhydrous magnesium sulfate, filtered and concentrated *in vacuo*. The crude residue was purified by flash column chromatography (silica gel, 10% dichloromethane in pentane) to afford **S56** (2.23 g, 14.6 mmol, 73%) as a yellow oil. The spectral data matched that previously reported in the literature.[S22]

^{1}H NMR (400 MHz, $CDCl_3$) δ = 7.41 (1H, dd, *J* = 7.6, 1.6), 7.23 (1H, ddd, *J* = 8.1, 7.4, 1.6), 6.68 (1H, td, *J* = 7.5, 1.3), 6.63 (1H, dd, *J* = 8.1, 1.3), 5.00 (1H, br s), 2.91 (3H, s), 2.34 (3H, s).

2-(Methyl(2-(methylthio)phenyl)amino)cyclohex-2-en-1-one, **S48**



This compound was prepared by analogy to a literature procedure.[S8] Aniline **S56** (583 mg, 3.80 mmol, 1.0 eq.), morpholine enamine **S2** (1.03 g, 5.71 mmol, 1.5 eq.) and *para*-toluenesulfonic acid monohydrate (1.09 g, 5.73 mmol, 1.5 eq.) were heated to 50 °C in toluene (20 mL, 0.2 M) for 3 h. The reaction was cooled to room temperature and diluted with ethyl acetate (25 mL). The solution was washed with sodium hydrogencarbonate (sat. aq., 3 x 20 mL) followed by brine (40 mL). The organic layer was dried over anhydrous sodium sulfate, filtered and concentrated *in vacuo*. The crude residue was purified by flash column chromatography (alumina gel, 10% diethyl ether in pentane) to afford **S48** (508 mg, 2.05 mmol, 54%) as an off-white solid.

^{1}H NMR (400 MHz, $CDCl_3$) δ = 7.18–7.14 (1H, m, H2), 7.10–7.01 (2H, m, $H3_{LHS}$ & $H4_{RHS}$), 6.92–6.86 (1H, m, H5), 6.03 (1H, t, *J* = 4.6, H13), 2.94 (3H, s, H7), 2.51–2.39 (4H, m, $H10_{LHS}$ & $H12_{RHS}$), 2.42 (3H, s, H14), 2.03–1.96 (2H, m, H11).

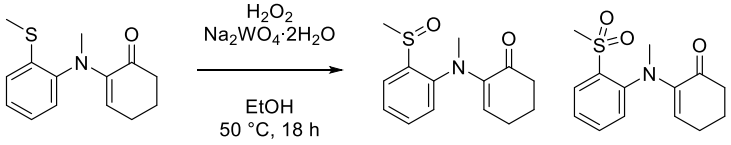
^{13}C NMR (101 MHz, $CDCl_3$) δ = 195.5 (C9), 147.5 (C6), 145.2 (C8), 134.8 (C1), 128.7 (C13), 125.9 (C2), 125.1 (C4), 124.7 (C3), 122.2 (C5), 39.8 (C10), 39.7 (C7), 25.7 (C12), 23.1 (C11), 15.3 (C14).

FTIR (neat) ν/cm^{-1} = 2919, 1686, 1473, 1438, 1303, 1111, 1069, 760, 735.

HRMS (ESI) *m/z* calcd. for $C_{14}H_{18}NOS$ $[M+H]^+$: 248.1104; found: 248.1104.

MP 89–91 °C.

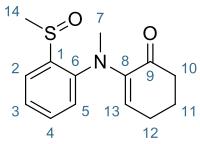
Oxidation of aryl sulfide **S48**



S48 **S50** 31% yield **S53** 36% yield

Hydrogen peroxide (34.5% w/w aq., 1.3 mL, 0.51 g, 15 mmol, 10 eq.) was added in portions to a mixture of aryl sulfide **S48** (379 mg, 1.53 mmol, 1.0 eq.) and sodium tungstate dihydrate (50.5 mg, 0.153 mmol, 0.1 eq.) in ethanol (15 mL, 0.1 M) at room temperature. The reaction mixture was heated to 50 °C for 18 h with continuous stirring. After this time, the reaction mixture was allowed to cool to room temperature, before adding water (15 mL) and removing ethanol and other volatiles *in vacuo*. The resulting aqueous mixture was extracted with ethyl acetate (3 x 15 mL). The combined organic extracts were washed with brine (30 mL), dried over anhydrous sodium sulfate, filtered and concentrated *in vacuo.* The crude residue was purified by flash column chromatography (silica gel, 25% ethyl acetate in pentane) to afford sulfoxide **S50** (124 mg, 0.471 mmol, 31%) as a yellow oil, alongside sulfone **S53** (153 mg, 0.548 mmol, 36%) as a white solid.

2-(Methyl(2-(methylsulfinyl)phenyl)amino)cyclohex-2-en-1-one, **S50**



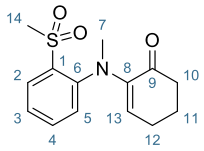
^{1}H NMR (400 MHz, $CDCl_3$) δ = 7.95–7.92 (1H, m, H2), 7.40–7.28 (2H, m, $H4_{LHS}$ & $H3_{RHS}$), 6.91 (1H, dd, *J* = 7.4, 1.5, H5), 6.22 (1H, t, *J* = 4.6, H13), 2.94 (3H, s, H7), 2.88 (3H, s, H14), 2.51–2.40 (4H, m, $H12_{LHS}$ & $H10_{RHS}$), 2.08–1.93 (2H, m, H11).

^{13}C NMR (101 MHz, $CDCl_3$) δ = 195.7 (C9), 147.0 (C6), 145.3 (C8), 140.0 (C1), 131.7 (C13), 131.5 (C4), 125.6 (C3), 124.7 (C2), 122.2 (C5), 42.1 (C14), 41.1 (C7), 39.6 (C10), 25.8 (C12), 22.9 (C11).

FTIR (neat) ν/cm^{-1} = 2922, 2869, 1682, 1586, 1473, 1296, 1111, 1068, 1027, 770.

HRMS (ESI) *m/z* calcd. for $C_{14}H_{18}NO_2S$ $[M+H]^+$: 264.1053; found: 264.1054.

2-(Methyl(2-(methylsulfonyl)phenyl)amino)cyclohex-2-en-1-one, **S53**



^{1}H NMR (400 MHz, $CDCl_3$) δ = 8.10 (1H, dd, *J* = 7.9, 1.6, H2), 7.46 (1H, td, *J* = 7.7, 1.7, H4), 7.31 (1H, td, *J* = 7.6, 1.2, H3), 6.98 (1H, dd, *J* = 7.9, 1.2, H5), 6.25 (1H, t, *J* = 4.6, H13), 3.30 (3H, s, H14), 2.98 (3H, s, H7), 2.56–2.49 (2H, m, H12), 2.45–2.35 (2H, m, H10), 2.04–1.97 (2H, m, H11).

^{13}C NMR (101 MHz, $CDCl_3$) δ = 195.7 (C9), 150.3 (C6), 145.2 (C8), 136.0 (C1), 134.3 (C4), 130.5 (C2), 128.4 (C13), 125.8 (C3), 125.1 (C5), 43.0 (C7 & C14, coincident), 39.7 (C10), 25.7 (C12), 23.0 (C11).

FTIR (neat) ν/cm^{-1} = 2930, 1681, 1475, 1300, 1148, 1063, 961, 771, 737.

HRMS (ESI) *m/z* calcd. for $C_{14}H_{18}NO_3S$ $[M+H]^+$: 280.1002; found: 280.1002.

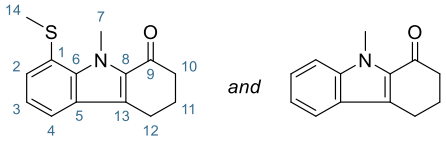
MP 94–96 °C.

Photocyclization of aryl sulfide **S48**

See above for scheme and discussion

Aryl sulfide **S48** (24.7 mg, 0.999 mmol, 1.0 eq.) and sodium acetate (12.3 mg, 0.150 mmol, 1.5 eq.) were charged to a Schlenk tube equipped with a magnetic stir bar. The vessel was sealed with a septum and then evacuated and back-filled with argon three times. Acetonitrile (1.8 mL) and water (0.2 mL) (0.05 M) were added *via* syringe, and the resulting mixture was degassed by three freeze–pump–thaw cycles. The reaction mixture was stirred under constant irradiation with a single Kessil PR160L 427 nm LED lamp (positioned *ca.* 3 cm from the flask and directed toward it) for 6 h, with cooling to ambient temperature being achieved using a strong jet of nitrogen gas directed at the flask. The resulting mixture was concentrated *in vacuo*. Dibromomethane (3.5 μL, 8.7 mg, 50 μmol, 0.5 eq.) was added to the crude residue before dissolving in $CDCl_3$ for analysis by quantitative ^{1}H NMR spectroscopy, which indicated NMR yields for indoles **42** and **S49** of 53% and 17%, respectively. The crude residue was purified by flash column chromatography (silica gel, 10% diethyl ether in pentane) to afford a *ca.* 3.5:1 mixture (estimated from relative integrations of ^{1}H resonances) of **42** and **S49** (14.3 mg, corresponding to isolated yields of *ca.* 53% and 15%, respectively) as a colourless oil.

9-Methyl-8-(methylthio)-2,3,4,9-tetrahydro-1H-carbazol-1-one, **S49**, *and* 9-methyl-2,3,4,9-tetrahydro-1*H*-carbazol-1-one, **42**



S49 **42**

Indole **S49** was characterized as a mixture with **42**. ^{1}H and ^{13}C NMR data corresponding to the former compound are reported below; the NMR spectral data of **42** matched that reported above.

^{1}H NMR (600 MHz, $CDCl_3$) δ = 7.50 (1H, dd, *J* = 8.0, 1.1, H4), 7.31 (1H, dd, *J* = 7.4, 1.1, H2), 7.10–7.05 (1H, m, H3), 4.56 (3H, s, H7), 2.99 (2H, t, *J* = 6.1, H12), 2.65 (2H, dd, *J* = 7.3, 5.7, H10), 2.51 (3H, s, H14), 2.27–2.16 (2H, m, H11).

^{13}C NMR (151 MHz, $CDCl_3$) δ = 192.3 (C9), 138.1 (C6), 131.2 (C8), 129.3 (C13), 129.0 (C2), 126.3 (C5), 122.2 (C1), 120.6 (C3), 119.8 (C4), 40.6 (C10), 34.8 (C7), 24.7 (C11), 22.0 (C12), 19.0 (C14).

HRMS (ESI) *m/z* calcd. for $C_{14}H_{16}NOS$ $[M+H]^+$: 246.0947; found: 246.0949.

Photocyclization of aryl sulfoxide **S50**

See above for scheme and discussion

Aryl sulfoxide **S50** (26.3 mg, 0.999 mmol, 1.0 eq.) and sodium acetate (12.3 mg, 0.150 mmol, 1.5 eq.) were charged to a Schlenk tube equipped with a magnetic stir bar. The vessel was sealed with a septum and then evacuated and back-filled with argon three times. Acetonitrile (1.8 mL) and water (0.2 mL) (0.05 M) were added *via* syringe, and the resulting mixture was degassed by three freeze–pump–thaw cycles. The reaction mixture was stirred under constant irradiation with a single Kessil PR160L 427 nm LED lamp (positioned *ca.* 3 cm from the flask and directed toward it) for 18 h, with cooling to ambient temperature being achieved using a strong jet of nitrogen gas directed at the flask. The resulting mixture was concentrated *in vacuo*. Dibromomethane (3.5 μL, 8.7 mg, 50 μmol, 0.5 eq.) was added to the crude residue before dissolving in $CDCl_3$ for analysis by quantitative ^{1}H NMR spectroscopy, which indicated an NMR yield for indole **42** of 43%. The crude residue was purified by flash column chromatography (silica gel, 10% diethyl ether in pentane) to afford **42** (6.8 mg, 0.034 mmol, 34%) as a pale-yellow solid, whose spectral data matched that reported above for this compound.

Photocyclization of aryl sulfone **S53**

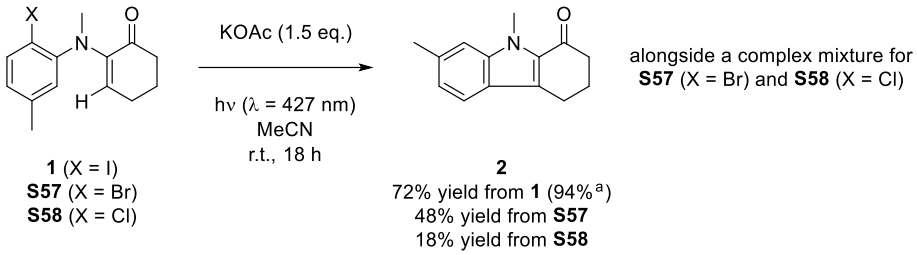
See above for scheme and discussion

Aryl sulfoxide **S53** (27.9 mg, 0.10 mmol, 1.0 eq.), *fac*-Ir(dFppy)$_3$ (0.8 mg, 1 μmol, 1 mol%) and sodium acetate (12.3 mg, 0.15 mmol, 1.5 eq.) were charged to a Schlenk tube equipped with a magnetic stir bar. The vessel was sealed with a septum and then evacuated and back-filled with argon three times.

Acetonitrile (1.8 mL) and water (0.2 mL) (0.05 M) were added *via* syringe, and the resulting mixture was degassed by three freeze–pump–thaw cycles. The reaction mixture was stirred under constant irradiation with a single Kessil PR160L 427 nm LED lamp (positioned *ca.* 3 cm from the flask and directed toward it) for 18 h, with cooling to ambient temperature being achieved using a strong jet of nitrogen gas directed at the flask. The resulting mixture was concentrated *in vacuo*. Dibromomethane (3.5 μL, 8.7 mg, 50 μmol, 0.5 eq.) was added to the crude residue before dissolving in $CDCl_3$ for analysis by quantitative ^1H NMR spectroscopy, which indicated an NMR yield for indole **42** of 60%. The crude residue was purified by flash column chromatography (silica gel, 10% diethyl ether in pentane) to afford indole **42** (9.8 mg, 49 μmol, 49%) as a pale-yellow solid, whose spectral data matched that reported above for this compound.

S2.24. Synthesis and photochemical reactivity of substrates bearing alternative halogen leaving groups

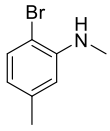
To assess the photocyclization efficiency of substrates containing different *ortho*-halogen substituents, substrates **1**, **S57** and **S58** (all containing an aromatic methyl group to probe the regiochemical course of the reaction) were separately irradiated with 427 nm light in acetonitrile solution in the presence of potassium acetate (Scheme S3).



Scheme S3. Halogen leaving group study. Yields were measured by quantitative ^{1}H NMR spectroscopy against dimethyl terephthalate for 0.1 mmol-scale photoreactions. [a] Isolated yield from a 0.3 mmol reaction performed in the presence of *fac*-Ir(dFppy)$_3$ and 467 nm light for 2 h under otherwise identical conditions.

Within this compound series and under these reaction conditions, the yield of the eliminative photocyclization product, indole **2**, appears to correlate inversely with the strength of the carbon–halogen bond present in the starting material. Thus, chloro substrate **S58** gave **2** in a low yield of 18%, alongside a complex mixture of side-products that could not be cleanly resolved.* Indole **2** was formed in a larger yield of 48% from bromo substrate **S57**, albeit still alongside considerable amounts of (unidentified) side-products. Finally, the parent iodine-containing compound, **1**, cyclized with minimal side-product formation to **2** in 72% yield under these conditions. In the absence of characterization data for the reaction side-products, it is not possible to draw firm conclusions about regioselectivity or other aspects of the reaction mechanism from these results. Nevertheless, the preliminary data reported here appear to suggest that alternative reaction pathways (e.g. *ipso*-H cyclization) begin to at least compete with, if not outcompete, *ipso*-X cyclization in the triplet state when the iodine substituent in **1** is replaced with bromine or chlorine atoms. See Section S4.9 for further discussion of these results.

2-Bromo-*N*,5-dimethylaniline, **S59**

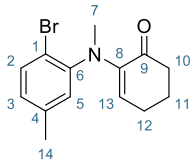


* Repeating the photocyclization of chloro substrate **S58** in the presence of *fac*-Ir(dFppy)$_3$ in either MeCN or MeCN–H_2O (9:1 v/v) led to extremely complex product mixtures containing only trace quantities of indole **2**. The photocatalytic generation of chlorine radicals (which are known to be extremely reactive toward C–H bonds) from KCl, one of the presumed by-products of *ipso*-Cl photocyclization in the presence of KOAc, could account for the intractable product distributions obtained when **S58** was irradiated in the presence of a photocatalyst.

A solution of *n*-butyllithium in hexanes (7.0 mL, 1.6 M, 11 mmol, 1.1 eq.) was added over 30 min *via* syringe pump to a stirred, -78 °C solution of 2-bromo-5-methylaniline (1.86 g, 10.0 mmol, 1.0 eq.) in anhydrous tetrahydrofuran (20 mL, 0.5 M) under an argon atmosphere. Methyl iodide (0.68 mL, 11 mmol, 1.1 eq.) was added in one portion after complete addition of the organometallic reagent. After a further 5 min at -78 °C, the acetone–dry ice bath was replaced with a tepid water bath, and the reaction mixture was allowed to warm to room temperature over a period of 2 h. Ammonium chloride solution (sat. aq., 20 mL) was added, followed by diethyl ether (20 mL). The layers were separated, and the aqueous phase was extracted with additional diethyl ether (2 x 20 mL). The combined organic extracts were washed with brine (40 mL), dried over anhydrous magnesium sulfate, filtered and concentrated *in vacuo*. The crude residue was purified by flash column chromatography (silica gel, 10% dichloromethane in pentane) to afford **S59** (1.05 g, 5.25 mmol, 52%) as a pale-yellow oil. The spectral data matched that previously reported in the literature.[S23]

^{1}H NMR (400 MHz, $CDCl_3$) δ = 7.29 (1H, d, *J* = 7.9), 6.45 (1H, d, *J* = 2.0), 6.41 (1H, dd, *J* = 7.9, 2.0), 4.29 (1H, br s), 2.89 (3H, s), 2.30 (3H, s).

2-((2-Bromo-5-methylphenyl)(methyl)amino)cyclohex-2-en-1-one, **S57**



Aniline **S59** (500 mg, 2.50 mmol, 1.0 eq.), morpholine enamine **S2** (453 mg, 2.50 mmol, 1.0 eq.) and *para*-toluenesulfonic acid monohydrate (476 mg, 2.50 mmol, 1.0 eq.) were heated to 50 °C in toluene (12.5 mL, 0.2 M) for 3 h. The reaction was cooled to room temperature and diluted with ethyl acetate (25 mL). The solution was washed with sodium hydrogencarbonate (sat. aq., 3 x 12.5 mL), followed by brine (25 mL). The organic layer was dried over anhydrous sodium sulfate, filtered and concentrated *in vacuo*. The crude residue was purified by flash column chromatography on alumina gel (gradient elution from 5 to 10% ethyl acetate in pentane) to afford **S57** (337 mg, 1.15 mmol, 46%) as a viscous yellow oil, which turned over to a pale-yellow solid upon storage at -18 °C.

^{1}H NMR (400 MHz, $CDCl_3$) δ = 7.39 (1H, d, *J* = 8.0, H2), 6.79 (1H, dd, *J* = 2.0, 0.8, H5), 6.76–6.70 (1H, m, H3), 6.05 (1H, t, *J* = 4.6, H13), 2.95 (3H, s, H7), 2.52–2.40 (4H, m, $H10_{LHS}$ & $H12_{RHS}$), 2.25 (3H, s, H14), 2.06–1.96 (2H, m, H11).

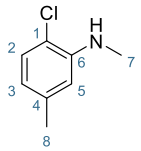
^{13}C NMR (101 MHz, $CDCl_3$) δ = 195.6 (C9), 148.3 (C6), 145.2 (C8), 138.0 (C4), 133.5 (C2), 129.6 (C13), 126.1 (C3), 124.8 (C5), 116.8 (C1), 40.2 (C7), 39.6 (C10), 25.7 (C12), 23.1 (C11), 21.1 (C14).

FTIR (neat) ν/cm^{-1} = 2943, 2867, 2829, 1687, 1480, 1309, 1215, 1162, 1111, 1056, 1027, 936, 805.

HRMS (ESI) *m/z* calcd. for $C_{14}H_{17}ON^{79}Br$ ($C_{14}H_{17}ON^{81}Br$) $[M+H]^+$: 294.0488 (296.0466); found: 294.0488 (296.0468).

MP 48–50 °C.

2-Chloro-*N*,5-dimethylaniline, **S60**



A solution of *n*-butyllithium in hexanes (7.0 mL, 1.6 M, 11 mmol, 1.1 eq.) was added over 30 min *via* syringe pump to a stirred, -78 °C solution of 2-iodo-5-methylaniline (1.42 g, 10.0 mmol, 1.0 eq.) in anhydrous tetrahydrofuran (20 mL, 0.5 M) under an argon atmosphere. Methyl iodide (0.68 mL, 11 mmol, 1.1 eq.) was added in one portion after complete addition of the organometallic reagent. After a further 5 min at -78 °C, the acetone–dry ice bath was replaced with a tepid water bath, and the reaction mixture was allowed to warm to room temperature over a period of 2 h. Ammonium chloride solution (sat. aq., 20 mL) was added, followed by diethyl ether (20 mL). The layers were separated, and the aqueous phase was extracted with additional diethyl ether (2 x 20 mL). The combined organic extracts were washed with brine (40 mL), dried over anhydrous magnesium sulfate, filtered and concentrated *in vacuo*. The crude residue was purified by flash column chromatography (silica gel, 10% dichloromethane in pentane) to afford **S60** (880 mg, 5.65 mmol, 56%) as a pale-yellow oil.

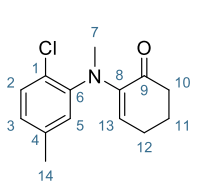
^{1}H NMR (400 MHz, $CDCl_3$) δ = 7.18–7.09 (1H, m, H2), 6.53–6.42 (2H, m, $H5_{LHS}$ & $H3_{RHS}$), 4.29 (1H, br s, NH), 2.90 (3H, d, *J* = 5.2, H7), 2.32 (3H, s, H8).

^{13}C NMR (101 MHz, $CDCl_3$) δ = 144.8 (C6), 137.9 (C4), 128.7 (C2), 117.9 (C3), 116.3 (C1), 111.6 (C5), 30.5 (C7), 21.6 (C8).

FTIR (neat) ν/cm^{-1} = 3433 (br), 2918, 1603, 1515, 1409, 1310, 1187, 1082, 1039, 841, 791.

HRMS (ESI) *m/z* calcd. for $C_8H_{11}ClN$ $[M+H]^+$: 156.0575; found: 156.0573.

2-((2-Chloro-5-methylphenyl)(methyl)amino)cyclohex-2-en-1-one, **S58**



Aniline **S60** (389 mg, 2.50 mmol, 1.0 eq.), morpholine enamine **S2** (453 mg, 2.50 mmol, 1.0 eq.) and *para*-toluenesulfonic acid monohydrate (476 mg, 2.50 mmol, 1.0 eq.) were heated to 50 °C in toluene (12.5 mL, 0.2 M) for 3 h. The reaction was cooled to room temperature and diluted with ethyl acetate

(25 mL). The solution was washed with sodium hydrogencarbonate (sat. aq., 3 x 12.5 mL), followed by brine (25 mL). The organic layer was dried over anhydrous sodium sulfate, filtered and concentrated *in vacuo*. The crude residue was purified by flash column chromatography on alumina gel (gradient elution from 5 to 10% ethyl acetate in pentane) to afford **S58** (256 mg, 1.03 mmol, 41%) as a viscous pale-green oil, which turned over to a pale green solid upon storage at -18 °C.

^{1}H NMR (400 MHz, $CDCl_3$) δ = 7.23–7.16 (1H, m, H2), 6.83–6.75 (2H, m, H3 & H5), 6.08 (1H, t, *J* = 4.6, H13), 2.96 (3H, s, H7), 2.52–2.40 (4H, m, $H10_{LHS}$ & $H12_{RHS}$), 2.27 (3H, s, H14), 2.06–1.95 (2H, m, H11).

^{13}C NMR (101 MHz, $CDCl_3$) δ = 195.6 (C9), 146.8 (C6), 145.2 (C8), 137.3 (C4), 130.3 (C2), 129.8 (C13), 126.2 (C1), 125.4 & 124.3 (C3 & C5), 40.0 (C7), 39.6 (C10), 25.7 (C12), 23.1 (C11), 21.1 (C14).

FTIR (neat) ν/cm^{-1} = 2947, 2864, 2830, 1686, 1485, 1311, 1216, 1114, 1062, 1040, 938, 865, 807.

HRMS (ESI) *m/z* calcd. for $C_{14}H_{17}ONCl$ $[M+H]^+$: 250.0993; found: 250.0993.

MP 48–49 °C.

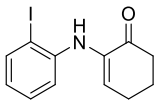
General procedure for 0.1 mmol-scale photocyclization of substrates **1**, **S57** and **S58** in the absence of photocatalyst

Enaminone **1**, **S57** or **S58** (34.1 mg, 29.4 mg or 25.0 mg, respectively, 0.10 mmol, 1.0 eq.) and potassium acetate (14.7 mg, 0.15 mmol, 1.5 eq.) were charged to a Schlenk tube equipped with a magnetic stir bar. The vessel was sealed with a septum and then evacuated and back-filled with argon three times. Acetonitrile (2.0 mL, 0.05 M) was added *via* syringe, and the resulting mixture was degassed by three freeze–pump–thaw cycles. The reaction mixture was stirred under constant irradiation with a single Kessil PR160L 427 nm LED lamp (positioned *ca.* 3 cm from the flask and directed toward it) for 18 h, with cooling to ambient temperature being achieved using a strong jet of nitrogen gas directed at the flask. Dimethyl terephthalate was added at the end of the irradiation period as a solution in acetonitrile (25.0 mM, 1.0 mL, 0.25 mmol, 0.25 eq.). The resulting mixture was concentrated *in vacuo*, and the crude residue was dissolved in $CDCl_3$ for analysis by quantitative ^{1}H NMR spectroscopy. The NMR yields of indole **2** from **1**, **S57** and **S58**, measured against dimethyl terephthalate, were 72%, 48% and 18%, respectively.

S2.25. Synthesis and photochemical reactivity of an *N*-carbamoyl-linked analogue

See Section S4.7 for a discussion of these results.

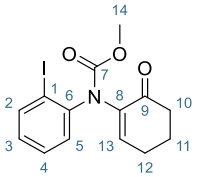
2-((2-Iodophenyl)amino)cyclohex-2-en-1-one, **S61**



This compound was prepared according to a literature procedure.[S8] 2-Iodoaniline (2.19 g, 10.0 mmol, 1.0 eq.), morpholine enamine **S2** (1.81 g, 9.99 mmol, 1.0 eq.) and *para*-toluenesulfonic acid monohydrate (1.90 g, 9.99 mmol, 1.0 eq.) were heated to 50 °C in toluene (50 mL, 0.2 M) for 3 h. The reaction was cooled to room temperature and diluted with ethyl acetate (100 mL). The solution was washed with sodium hydrogencarbonate (sat. aq., 3 x 50 mL) followed by brine (100 mL). The organic layer was dried over anhydrous sodium sulfate, filtered and concentrated *in vacuo*. The crude residue was purified by flash column chromatography (silica gel, 5 to 10% diethyl ether in pentane) to afford **S61** (2.82 g, 9.00 mmol, 90%) as a white solid. The spectral data matched that previously reported in the literature.[S8]

^{1}H NMR (400 MHz, CDCl3) δ = 7.79 (1H, dd, *J* = 7.9, 1.2), 7.33–7.13* (2H, m), 6.64 (1H, ddd, *J* = 8.0, 6.8, 2.0), 6.56 (1H, br s), 6.36 (1H, t, *J* = 4.7), 2.63–2.54 (2H, m), 2.46 (2H, q, *J* = 5.8), 2.04 (2H, quint., *J* = 6.1).

Methyl (2-iodophenyl)(6-oxocyclohex-1-en-1-yl)carbamate, **S62**



This compound was prepared by analogy to a literature procedure.[S27] *n*-Butyllithium in hexanes (0.88 mL, 2.48 M, 2.2 mmol, 1.1 eq.) was added dropwise over 10 min to a stirred, -78 °C solution of hexamethyldisilazane (0.46 mL, 0.35 g, 2.2 mmol, 1.1 eq.) in anhydrous tetrahydrofuran (5.0 mL) under an argon atmosphere. After warming to room temperature, the resulting solution was transferred to a stirred, -78 °C solution of **S61** (627 mg, 2.00 mmol, 1.0 eq.) and methyl cyanoformate (0.63 mL, 0.68 g, 7.9 mmol, 4.0 eq.) in anhydrous tetrahydrofuran (5 mL) over 1 h *via* syringe pump. After stirring for a further 15 min at this temperature, the reaction mixture was quenched by the addition of ammonium chloride (sat. aq., 5 mL). The resulting mixture was allowed to warm to room temperature and diluted with ethyl acetate (10 mL). The layers were separated, and the aqueous phase was extracted with additional ethyl acetate (3 x 10 mL). The combined organic extracts were washed with brine

* Overlap with the residual non-deuterated chloroform signal led to over-integration of this multiplet; the integral of 2 was obtained through multiplicity-edited HSQC analysis.

(10 mL), dried over anhydrous sodium sulfate, filtered and concentrated in vacuo. The crude residue was purified by flash column chromatography (silica gel, 20% to 40% ethyl acetate in pentane) to afford **S62** (211 mg, 0.568 mmol, 28%) as a white solid.

^{1}H NMR (400 MHz, $CDCl_3$) δ = 7.89–7.82 (1H, m, H2), 7.37–7.28 (2H, m, H4 & H5), 7.18 (1H, t, *J* = 4.3, H13), 6.98 (1H, ddd, *J* = 7.9, 6.7, 2.3, H3), 3.71 (3H, s, H14), 2.83–2.25 (4H, m, H10 & H12), 2.25–1.80 (2H, m, H13).

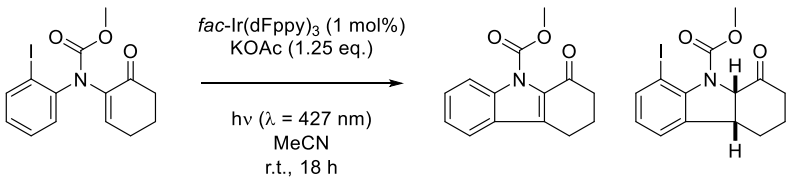
^{13}C NMR (101 MHz, $CDCl_3$) δ = 194.8 (C9), 154.6 (C7), 146.2 (C13), 145.2 (C6), 140.4 (C8), 139.7 (C2), 129.8 (C5), 129.2 (C3), 128.9 (C4), 100.3 (C1), 53.6 (C14), 38.5 (C10), 25.9 (C12), 22.6 (C11).

FTIR (neat) ν/cm^{-1} = 1723, 1689, 1469, 1439, 1329, 1240, 1201, 1119, 1067, 1037, 745, 711.

HRMS (APCI) *m/z* calcd. for $C_{14}H_{15}INO_3$ $[M+H]^+$: 372.0091; found: 372.0091.

MP 104–108 °C.

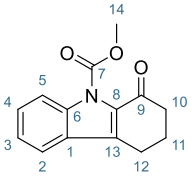
Photocyclization of enaminone **S62**



S62 | **S63** 58% yield | **S64** 13% yield

Enaminone **S62** (74.2 mg, 0.200 mmol, 1.0 eq.), *fac*-Ir(dFppy)$_3$ (1.5 mg, 2.0 μmol, 1 mol%) and potassium acetate (24.5 mg, 0.250 mmol, 1.25 eq.) were charged to a 10 mL microwave vial equipped with a magnetic stir bar. The vial was sealed with an aluminium cap and then evacuated and back-filled with argon three times. Argon-sparged acetonitrile (4.0 mL, 0.05 M) was added *via* syringe, and the reaction mixture was sparged with argon for a further 15 min. The reaction mixture was stirred under constant irradiation with a single Kessil PR160L 427 nm LED lamp (positioned *ca.* 3 cm from the flask and directed toward it) for 18 h, with cooling to ambient temperature being achieved by submerging the flask in cold water contained in a water-jacketed vessel. After the irradiation period, the reaction mixture was concentrated *in vacuo*, and the crude residue thus obtained was purified by flash column chromatography (silica gel, 20% ethyl acetate in pentane) to afford indole **S63** (28.2 mg, 0.116 mmol, 58%) and indoline **S64** (9.5 mg, 0.026 mmol, 13%), both as yellow solids.

Methyl 1-oxo-1,2,3,4-tetrahydro-9*H*-carbazole-9-carboxylate, **S63**



^{1}H NMR (400 MHz, CD_2Cl_2) δ = 8.01 (1H, dt, *J* = 8.5, 0.9, H2), 7.65 (1H, ddd, *J* = 7.9, 1.3, 0.8, H5), 7.50 (1H, ddd, *J* = 8.5, 7.2, 1.3, H4), 7.31 (1H, ddd, *J* = 8.0, 7.2, 1.0, H3), 3.99 (3H, s, H14), 2.97 (2H, t, *J* = 6.1, H10), 2.68–2.61 (2H, m, H12), 2.30–2.20 (2H, m, H11).

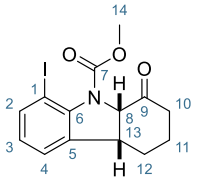
^{13}C NMR (CD_2Cl_2, 101 MHz) δ = 187.8 (C9), 151.7 (C7), 138.8 (C6), 137.7 (C8), 132.4 (C13), 128.8 (C4), 126.9 (C1), 123.2 (C3), 121.2 (C5), 114.6 (C2), 54.1 (C14), 39.2 (C12), 23.8 (C11), 21.7 (C10).

FTIR (neat) ν/cm^{-1} = 2953, 1742, 1674, 1607, 1552, 1440, 1366, 1226, 1137, 961, 750.

HRMS (APCI) *m/z* calcd. for $C_{14}H_{14}NO_3$ $[M+H]^+$: 244.0968; found: 244.0968.

MP 62–68 °C.

rac-Methyl 8-iodo-1-oxo-1,2,3,4,4a,9a-hexahydro-9*H*-carbazole-9-carboxylate, **S64**



^{1}H NMR (400 MHz, $CDCl_3$) δ = 7.66 (1H, dt, *J* = 8.0, 1.1, H2), 7.04 (1H, dt, *J* = 7.4, 1.3, H4), 6.79 (1H, t, *J* = 7.7, H3), 5.05 (1H, d, *J* = 8.5, H8), 4.23–4.15 (1H, m, H13), 3.84 (3H, s, H14), 2.48–2.33 (2H, m, H10), 2.28–2.16 (2H, m, H12), 2.03–1.91 (1H, m, H11), 1.64–1.47[*] (1H, m, H11').

^{13}C NMR (101 MHz, $CDCl_3$) δ = 205.9 (C9), 154.1 (C7), 146.2 (C6), 139.3 (C2), 136.7 (C5), 126.6 (C3), 122.2 (C4), 85.6 (C1), 71.6 (C8), 53.2 (C14), 45.7 (C13), 40.5 (C10), 25.0 (C12), 21.9 (C11).

The observation of nuclear Overhauser effect (nOe) correlations by 2D NOESY corresponding to H8↔H13 is consistent with the formation of the *cis*-diastereomer shown.

FTIR (neat) ν/cm^{-1} = 2951, 1722, 1444, 1375, 1332, 1284, 1246, 1197, 1098, 913, 735.

HRMS (APCI) *m/z* calcd. for $C_{14}H_{15}INO_3$ $[M+H]^+$: 372.0091; found: 372.0089.

MP 44–50 °C.

[*] Overlap with the water signal led to over-integration of this multiplet; the integral of 1 was obtained through multiplicity-edited HSQC analysis.

S3. Experimental mechanistic studies

S3.1. Synthesis, characterization and reactivity of the putative cationic intermediate

The putative iminium ion intermediate in the photochemical reaction of *N*-aryl enaminone **10** was formally generated with a trifluoroacetate counterion by treating a solution of hemiaminal **11** (23.3 mg, 0.101 mmol, 1.0 eq.) in CD_3CN (0.6 mL) with trifluoroacetic acid (39 µL, 58 mg, 0.51 mmol, 5.1 eq.) at room temperature (Figure S2A). ^{1}H NMR spectra recorded at time intervals, *t*, after the addition of acid revealed quantitative conversion of the starting material to a new compound within 60 min; this compound was characterized fully by ^{1}H and ^{13}C spectroscopy as enol species **12** (Figure S2B). (^{1}H resonances observed transiently at *t* = 15 min may correspond to the keto tautomer of the iminium salt; however, the short lifetime of this species precluded its full characterization.)

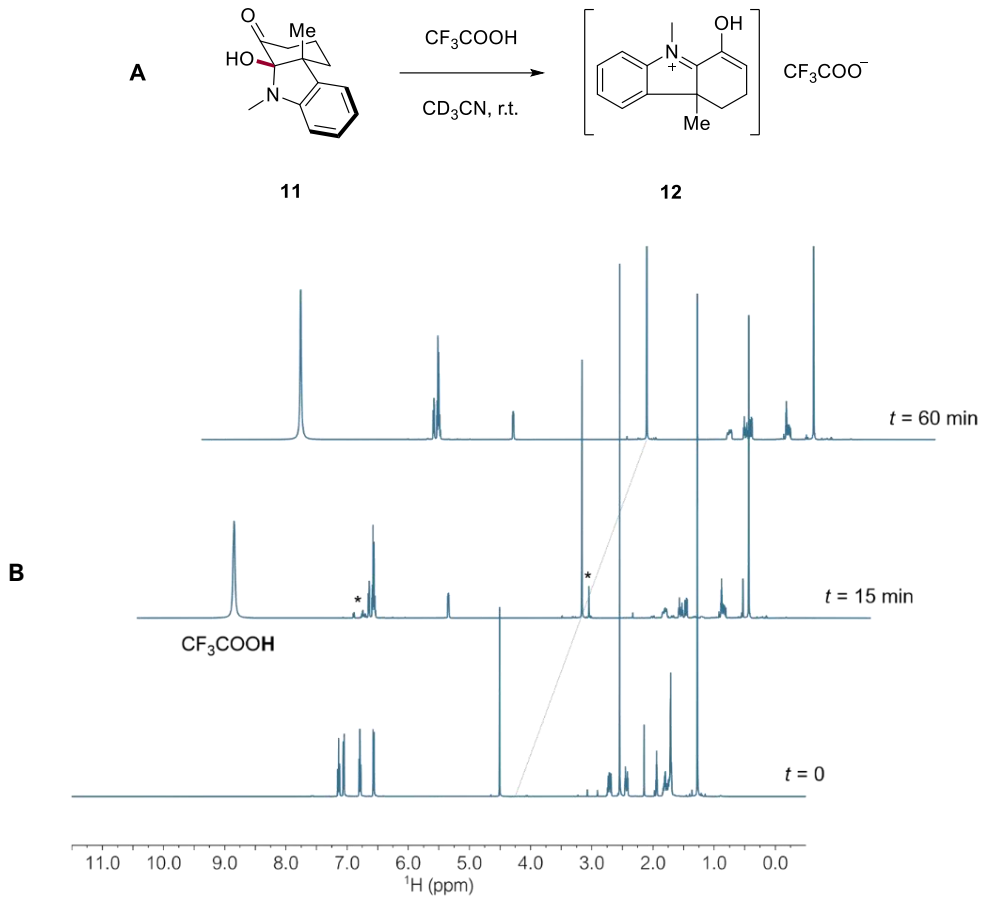


Figure S2. Treating hemiaminal **11** with trifluoroacetic acid yields an iminium salt. **(A)** Reaction scheme. **(B)** Stacked ^{1}H NMR spectra showing the conversion of hemiaminal **11** to enol iminium trifluoroacetate **12** in CD_3CN at time intervals, *t*, after addition of trifluoroacetic acid. A grey line has been added to assist the reader in distinguishing signals around 4.25 ppm. Signals marked with an asterisk (*) on the spectrum recorded at *t* = 15 min may correspond to the keto tautomer of the iminium trifluoroacetate salt, potentially observed fleetingly under these conditions prior to chemical equilibration.

To confirm that the proposed iminium trapping event occurs *via* a non-photochemical mechanism, the above solution of iminium trifluoroacetate **12** was treated with triethylsilane (48 µL, 35 mg, 0.30 mmol,

3.0 eq.) in the dark and analysed at regular intervals by ^{1}H NMR spectroscopy (Figures S3 and S4). This resulted in the slow accumulation of the expected iminium reduction product, **21**, demonstrating the viability of a *thermal* iminium trapping event in the photochemical reaction of *N*-aryl enaminone **10** in the presence of triethylsilane and other two-electron nucleophiles.

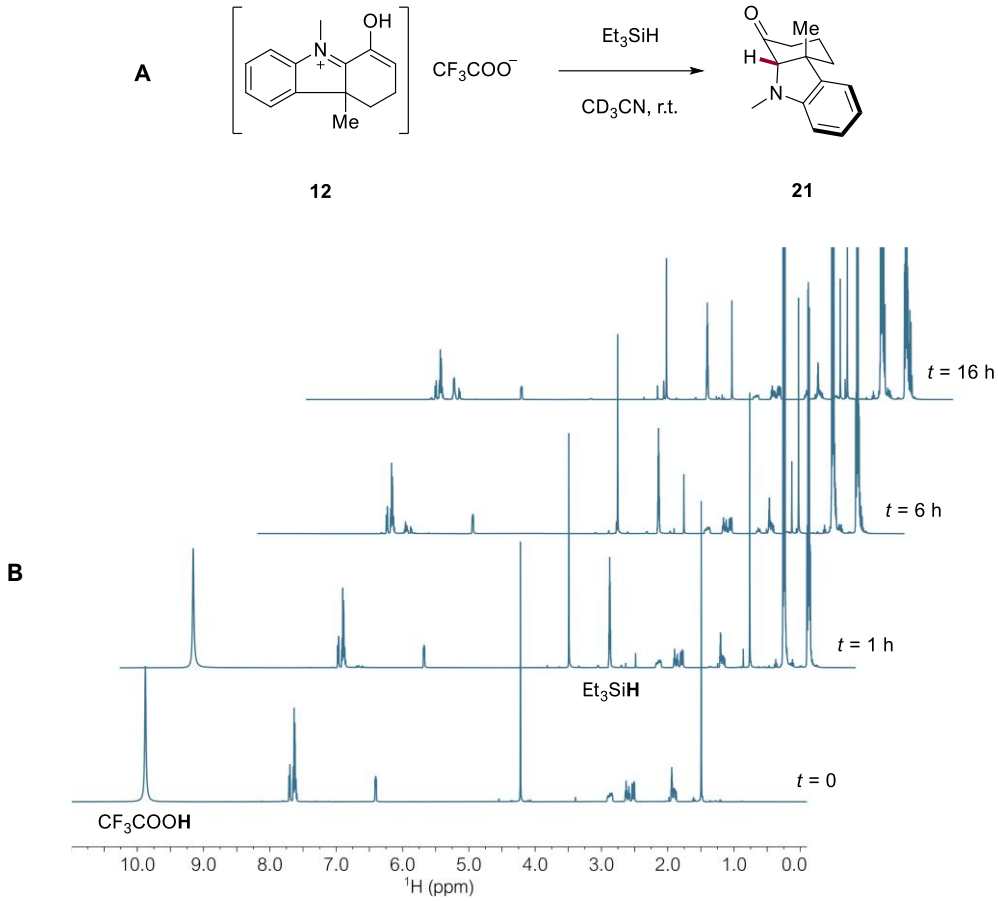


Figure S3. Treating iminium salt **12** with triethylsilane yields indoline **21**. **(A)** Reaction scheme. **(B)** Stacked ^{1}H NMR spectra of enol iminium trifluoroacetate **12**, formed by treating hemiaminal **11** with trifluoroacetic acid in CD_3CN, at time intervals, *t*, after addition of triethylsilane.

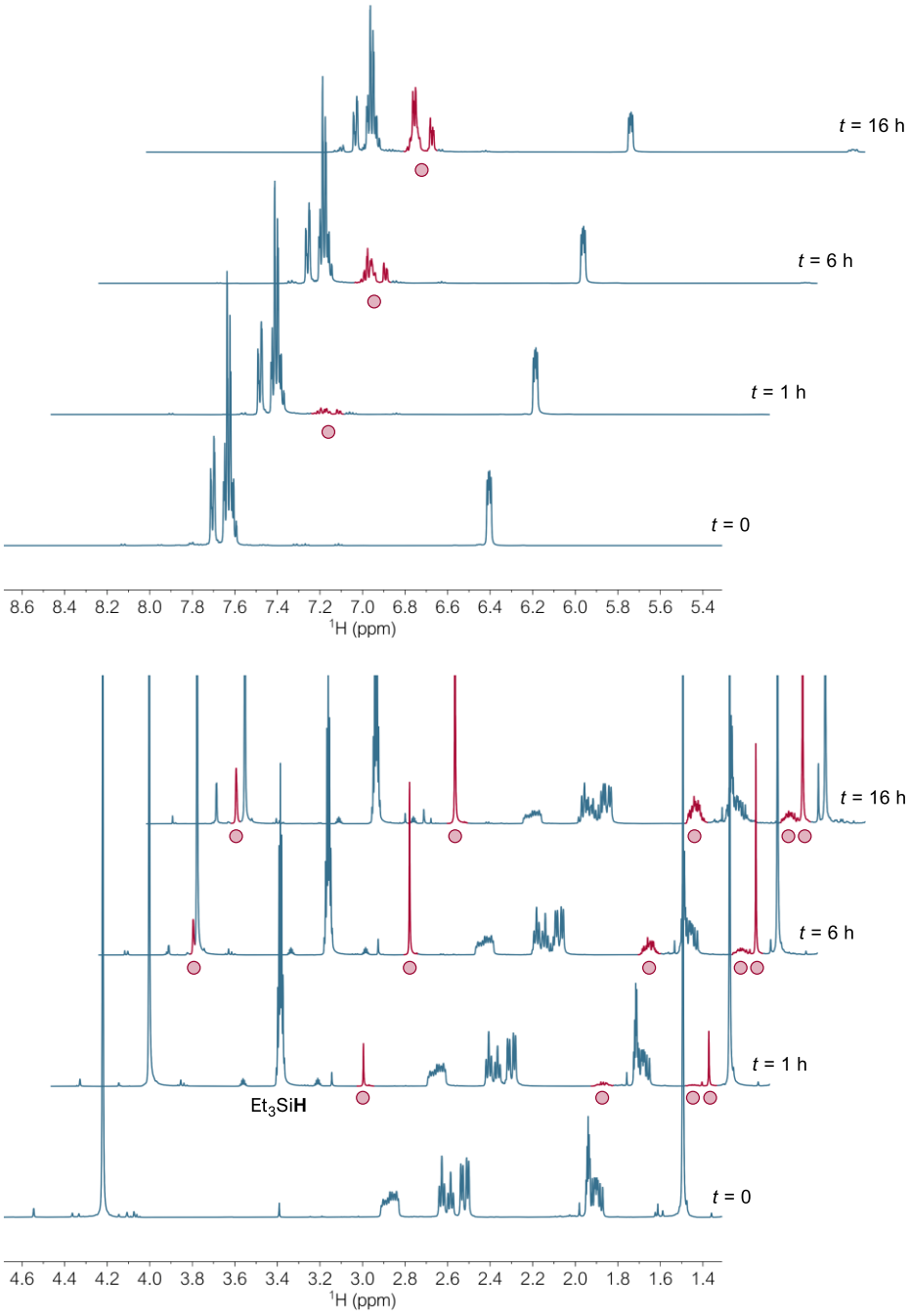
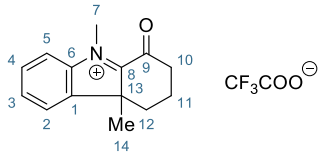


Figure S4. Expanded views of stacked ^{1}H NMR spectra of enol iminium trifluoroacetate **12** in CD_3CN at time intervals, *t*, after addition of triethylsilane. Signals corresponding to indoline **21** are highlighted in red and marked with a red circle.

4a,9-Dimethyl-1-oxo-2,3,4,4a-tetrahydro-1*H*-carbazol-9-ium 2,2,2-trifluoroacetate, **12**



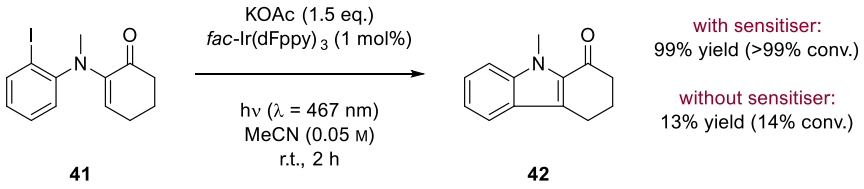
^{1}H NMR (500 MHz, CD_3CN) δ = 7.73–7.67 (1H, m, H5), 7.67–7.57 (3H, m, H2, H3 & H4), 6.40 (1H, dd, *J* = 6.1, 3.3, H10), 4.22 (3H, s, H7), 2.93–2.81 (1H, m, H11), 2.61 (1H, dtd, *J* = 20.8, 6.0, 1.3, H11'), 2.52 (1H, ddt, *J* = 13.5, 5.1, 0.9, H12), 1.94–1.85 (1H, m, H12'), 1.49 (3H, s, H14).

^{13}C NMR (126 MHz, CD_3CN) δ 180.3 (C8), 159.4 (q, $^{2}J_{CF}$ = 39.7, $CF_3\underline{C}OO^-$), 144.3 (C6), 142.8 (C9), 142.0 (C1), 131.5 (C10), 130.9 (C3), 130.5 (C2 or C4), 124.2 (C2 or C4), 116.3 (q, $^{1}J_{CF}$ = 286.4, $\underline{C}F_3COO^-$), 116.2 (C5), 53.9 (C13), 37.1 (C7), 31.9 (C12), 24.1 (C11), 22.5 (C14).

S3.2. Evidence for the involvement of an excited triplet state

S3.2.1. Triplet sensitization

A rate acceleration was observed when the photocyclization of **41** was performed in the presence of *fac*-Ir(dFppy)$_3$ (Scheme S4). Full conversion of the starting material and a 99% NMR yield of **42** was obtained after 2 h in the presence of 1 mol% of the iridium sensitizer. In its absence, a conversion of only 14% was observed after the same reaction time.



Scheme S4. Photocyclization of **41** in the presence and absence of an iridium photocatalyst. Yields and conversions were measured by quantitative ^{1}H NMR spectroscopy against dimethyl terephthalate.

Experimental procedure

Enaminone **41** (32.7 mg, 0.100 mmol, 1.0 eq.), *fac*-Ir(dFppy)$_3$ (0.8 mg, 1 μmol, 1 mol%) and potassium acetate (14.7 mg, 0.150 mmol, 1.5 eq.) were charged to a Schlenk tube equipped with a magnetic stir bar. The vessel was sealed with a septum and then evacuated and back-filled with argon three times. Argon-sparged acetonitrile (2.0 mL, 0.05 M) was added *via* syringe. The reaction mixture was stirred under constant irradiation with a single Kessil PR160 467 nm LED lamp (positioned *ca.* 3 cm from the flask and directed toward it) for 2 h, with cooling to ambient temperature being achieved using a strong jet of nitrogen gas directed at the flask. Dimethyl terephthalate was added at the end of the irradiation period as a solution in acetonitrile (25.0 mM, 1.0 mL, 0.25 mmol, 0.25 eq.). The resulting mixture was concentrated *in vacuo*, and the crude residue was dissolved in $CDCl_3$ for analysis by quantitative ^{1}H NMR spectroscopy. The NMR yield of indole **42** measured against dimethyl terephthalate was 99% (full conversion of **41**). A near-identical experiment was performed in parallel, differing only in that *fac*-Ir(dFppy)$_3$ was excluded; the NMR yield of indole **42** measured against dimethyl terephthalate for this reaction was 13% (14% conversion of **41**).

S3.2.2. Stern–Volmer luminescence quenching of *fac*-Ir(dFppy)$_3$ by **41**

To confirm that an interaction occurs between substrate **41** and the excited photocatalyst under the catalysed reaction conditions, Stern–Volmer constants were obtained for the quenching of *fac*-Ir(dFppy)$_3$ in acetonitrile by substrate **41** and tetra-*n*-butylammonium acetate.*

Into a 1-cm quartz cuvette was placed 2.5 mL of a 5 μM solution of *fac*-Ir(dFppy)$_3$ in anhydrous acetonitrile. The cuvette was sealed with a rubber septum, and the solution was gently sparged with argon for 10 min. An emission spectrum (excitation wavelength = 420 nm) was measured between 430 and 650 nm. An argon-sparged solution of substrate **41** (5 mM) in anhydrous acetonitrile was added to the above photocatalyst solution in 5 μL portions. Emission spectra were recorded after each addition (Figure S5). This procedure was repeated using tetra-*n*-butylammonium acetate (dried prior to use by heating to 100 °C under high vacuum for 16 h) in place of **41** as the quencher (Figure S6).

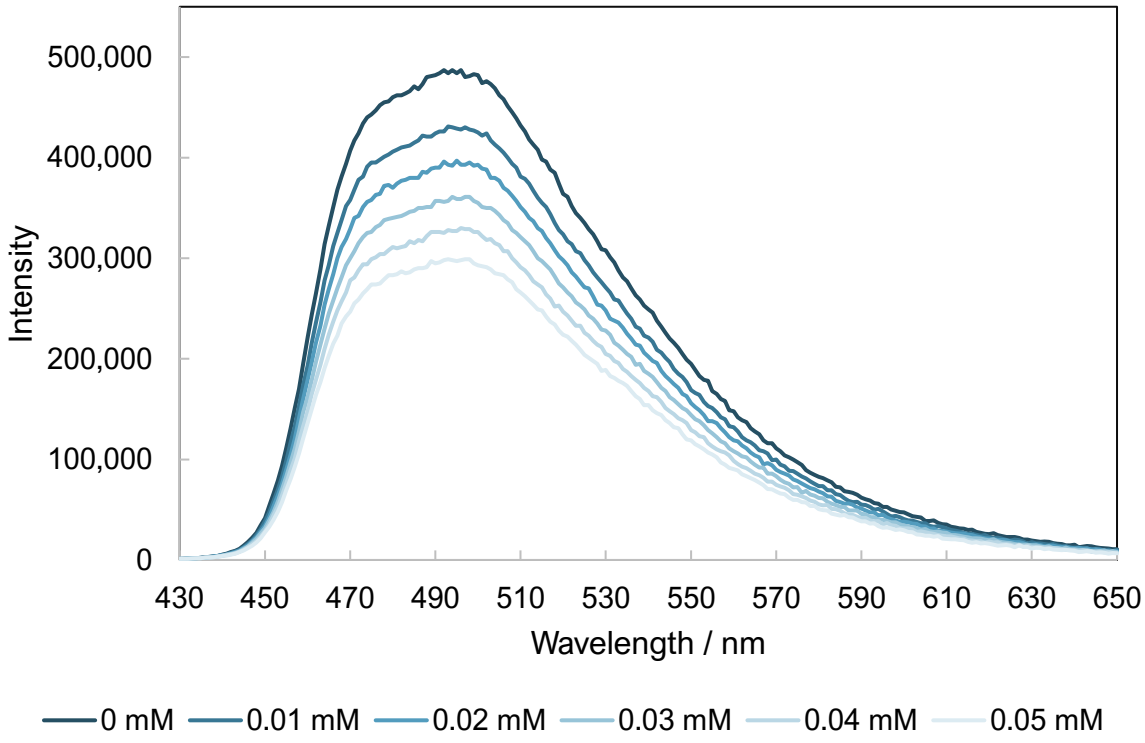


Figure S5. Emission spectra recorded for a degassed 5 μM acetonitrile solution of *fac*-Ir(dFppy)$_3$ in the presence of different concentrations of substrate **41**. Excitation wavelength = 420 nm.

* Tetra-*n*-butylammonium acetate was used instead of potassium acetate, owing to the former salt's higher solubility in acetonitrile.

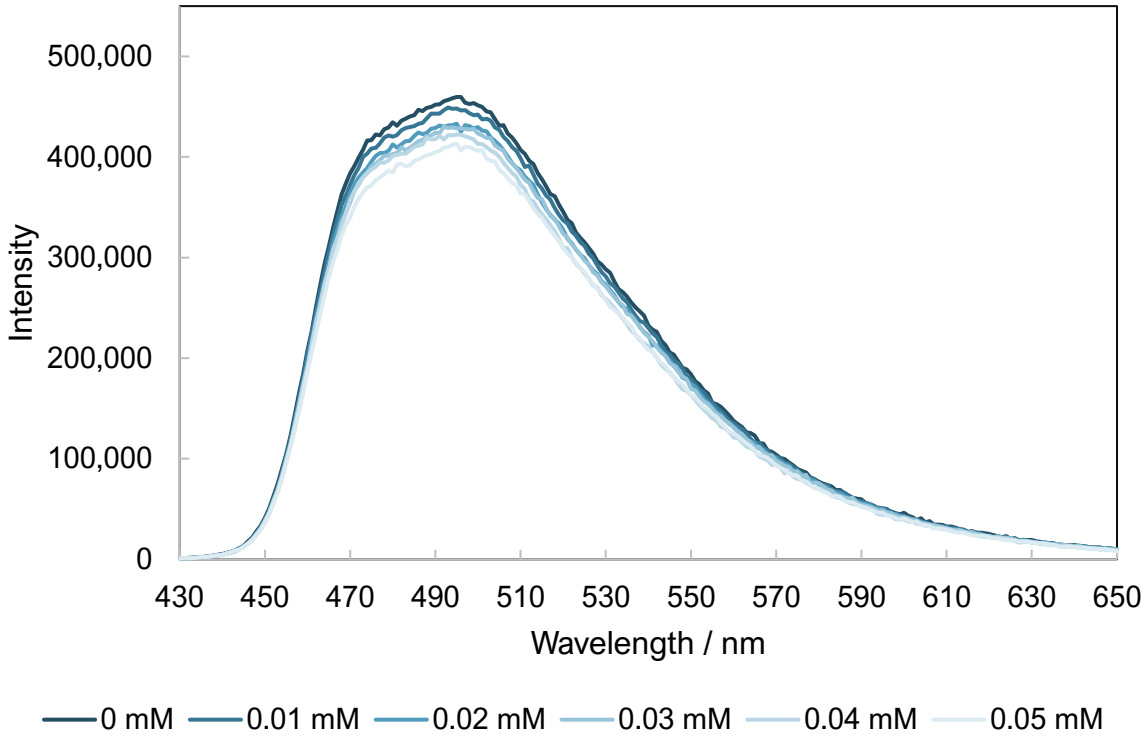


Figure S6. Emission spectra recorded for a degassed 5 μM acetonitirile solution of *fac*-[Ir(dFppy)$_3$] in the presence of different concentrations of tetra-*n*-butylammonium acetate, (*n*-Bu)$_4$NOAc. Excitation wavelength = 420 nm.

For substrate **41**, a linear plot of I_0/I vs. concentration of quencher, [Q], was obtained (Figure S7, closed/solid dots). From the slope of this line, the Stern–Volmer constant, K_{SV}, for **41** was calculated as 1.2 x 10^4 M^{-1} according to the equation:

$$\frac{I_0}{I} = 1 + K_{SV}[Q]$$

In the same manner, the Stern–Volmer constant, K_{SV}, for tetra-*n*-butylammonium acetate (Figure S7, open dots) was calculated as 2.1 x 10^3 M^{-1}.

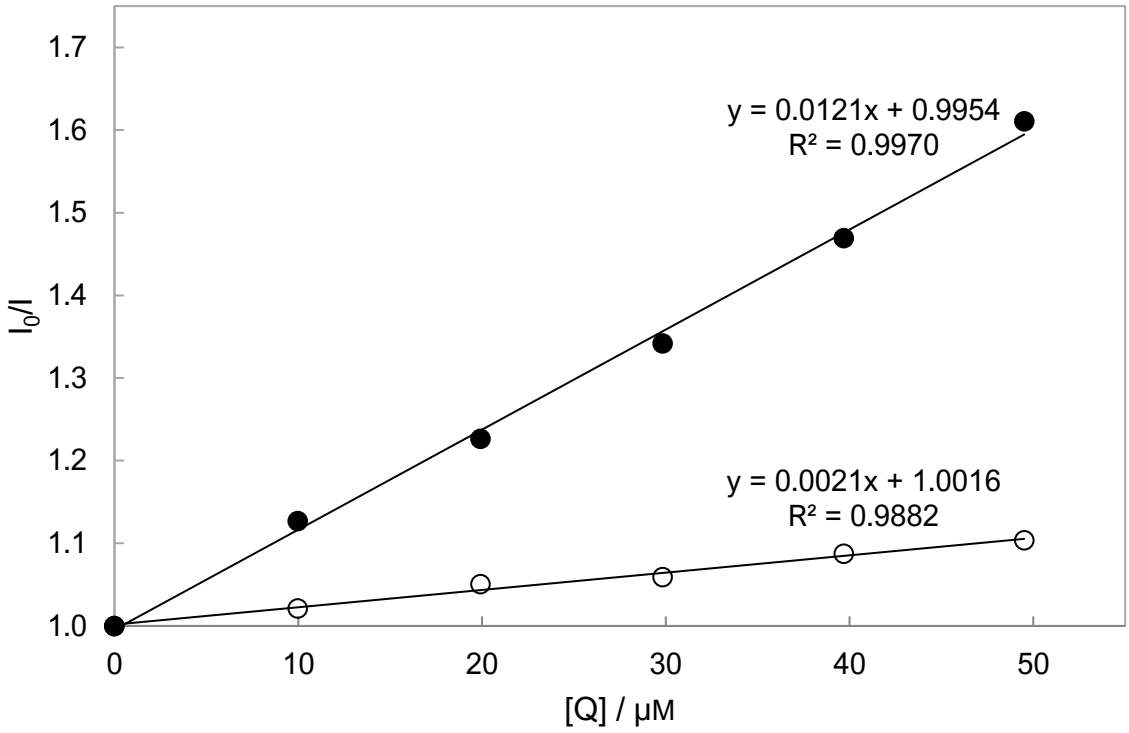


Figure S7. Stern–Volmer plot for the luminescence quenching of *fac*-Ir(dFppy)$_3$ in the presence of quencher, Q, in acetonitrile solution, where Q is substrate **41** (●) or (*n*-Bu)$_4$NOAc (○). I_0 is the intensity of emission in the absence of quencher; I is the same quantity in the presence of different concentrations of Q.

S3.2.3. Voltammetry

To examine the feasibility of a photoredox-catalysed pathway occurring in the presence of *fac*-Ir(dFppy)$_3$, the ground-state reduction and oxidation potentials of substrate **41** were measured in acetonitrile by square-wave voltammetry. A PalmSens EmStat3 potentiostat, equipped with a glassy carbon working electrode, Pt wire (0.5 mm diameter) counter electrode and leak-free Ag/AgCl (3.4 M KCl) reference electrode, was used for these measurements. Square-wave voltammograms were acquired with a 5 mV step potential, 100 mV modulation amplitude and 5 Hz frequency, and internally referenced to the Fc^+/Fc couple; an argon-sparged solution of tetra-*n*-butylammonium hexafluorophosphate in acetonitrile (0.1 M, 5 mL) was used as the supporting electrolyte. The half-wave oxidation and reduction potentials of **41** in acetonitrile were measured as +0.73 V and –2.42 V, respectively, *vs.* Fc^+/Fc (Figure S8).

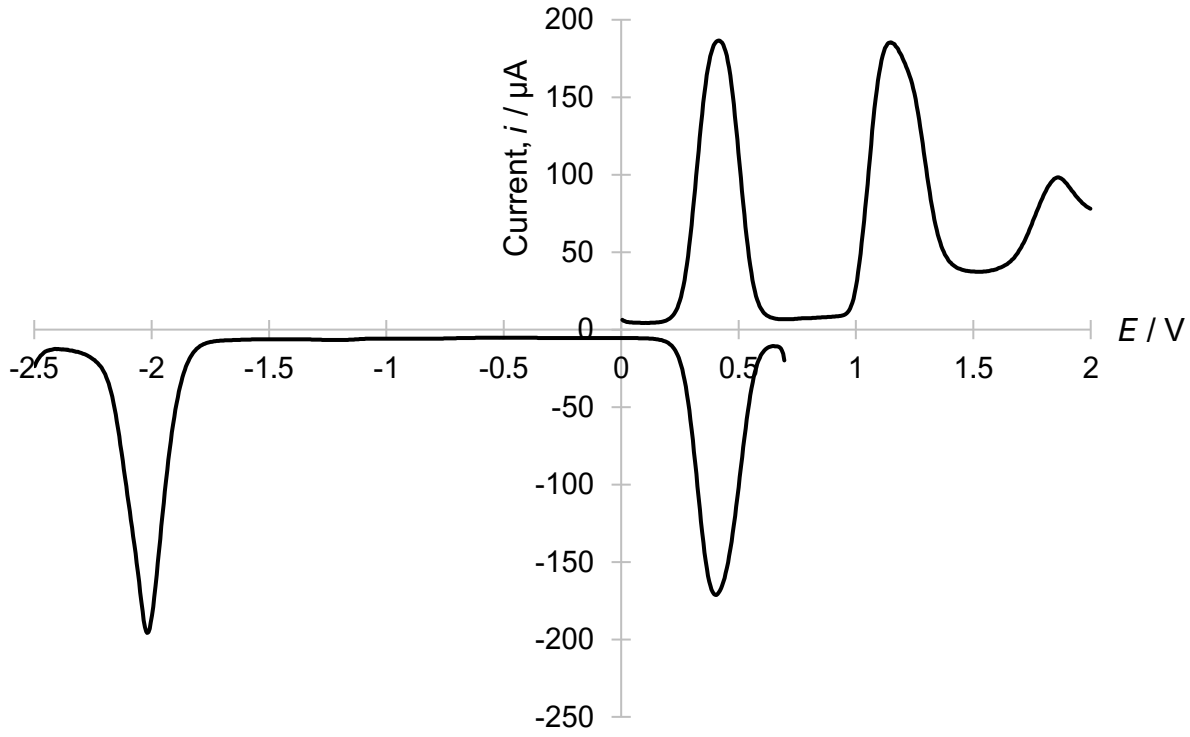
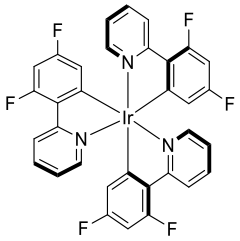


Figure S8. Square-wave voltammogram of substrate **41** in acetonitrile, internally referenced to Fc^+/Fc.

S3.2.4. Discussion of triplet sensitization and related studies

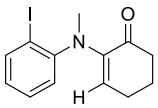
The substantial rate acceleration observed in the presence of *fac*-Ir(dFppy)$_3$ shows that the reaction can occur efficiently from the triplet state. Emission spectroscopy confirms that the triplet metal-to-ligand charge transfer (^{3}MLCT) state of *fac*-Ir(dFppy)$_3$ is efficiently quenched by substrate **41**, with a Stern–Volmer constant, K_{SV}, of 1.2 x 10^4 M^{-1}. In contrast, (*n*-Bu)$_4$NOAc is a relatively inefficient quencher (K_{SV} = 2.1 x 10^3 M^{-1}). As a result, the rate acceleration observed in the presence of *fac*-Ir(dFppy)$_3$ for the photocyclization of **41** likely arises from an interaction between the substrate and excited photocatalyst, rather than an interaction between the acetate base and excited photocatalyst. The photocatalyst *fac*-Ir(dFppy)$_3$ is not sufficiently oxidising or reducing in the excited state to activate substrate **41** by single-electron transfer, whose half-wave oxidation and reduction potentials were measured as +0.73 V and –2.42 V, respectively, *vs.* Fc^+/Fc. In contrast, the triplet-state energy (E_T) of this photocatalyst (E_T = 60.1 kcal mol^{-1})[S29] is substantially higher than that of **41** (E_T = 48.1 kcal mol^{-1}) (Figure S9). It is likely, therefore, that quenching of the excited photocatalyst by substrate **41** occurs by a triplet energy transfer mechanism.



$$E_{1/2}\left(\mathrm{Ir}^{\mathrm{III}*}/\mathrm{Ir}^{\mathrm{II}}\right) = +0.39\ \mathrm{V}\ vs.\ \mathrm{Fc}^+/\mathrm{Fc}$$

$$E_{1/2}\left(\mathrm{Ir}^{\mathrm{IV}}/\mathrm{Ir}^{\mathrm{III}*}\right) = -1.23\ \mathrm{V}\ vs.\ \mathrm{Fc}^+/\mathrm{Fc}$$

$$E_{\mathrm{T}} = 60.1\ \mathrm{kcal/mol}\ (lit.)$$



$$E_{ox} = +0.73\ \mathrm{V}\ vs.\ \mathrm{Fc}^+/\mathrm{Fc}$$

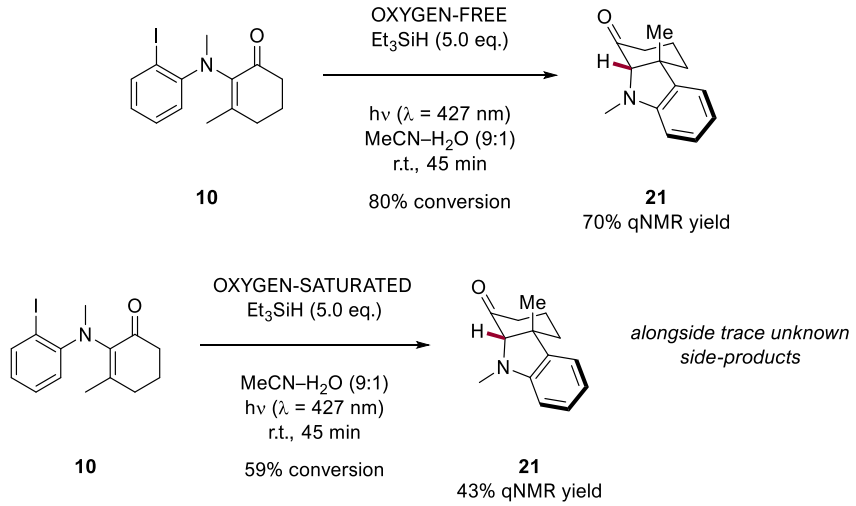
$$E_{red} = -2.42\ \mathrm{V}\ vs.\ \mathrm{Fc}^+/\mathrm{Fc}$$

$$E_{\mathrm{T}} = 48.1\ k\mathrm{cal/mol}\ (calc.)$$

Figure S9. Summary of electrochemical and photophysical properties of *fac*-Ir(dFppy)$_3$ (reported by Weaver and co-workers[S29]) and substrate **41**. All experimental values were obtained in acetonitrile solution.

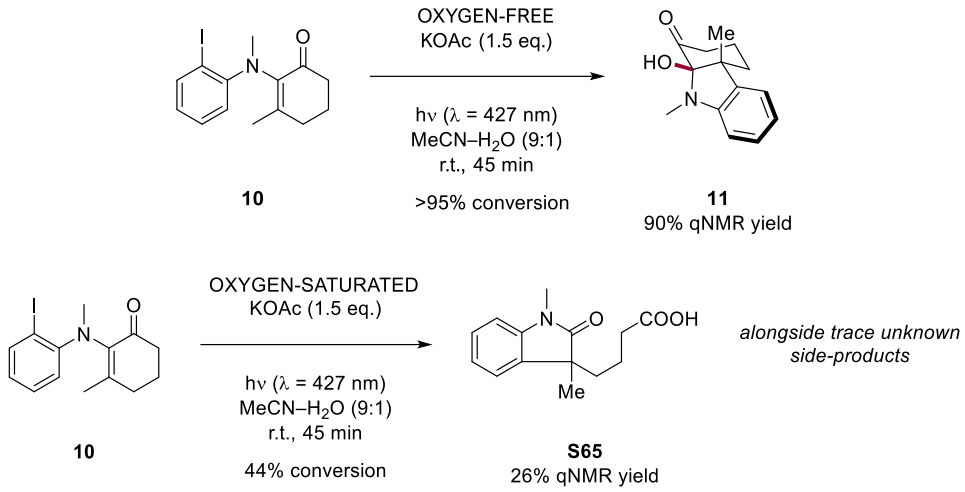
S3.2.5. Oxygen quenching

Attempts to probe the formation of a triplet state in the *absence* of photosensitizer using known triplet quenchers were hampered by the low triplet energies of the substrates, calculated for substrate **10** as 48.3 kcal mol^{-1}. Compounds that might be expected to quench this triplet state (that is, compounds with triplet energies lower than 48 kcal mol^{-1}) either absorbed in the same range of wavelengths as the substrate and/or were insoluble in the polar aprotic reaction medium; both effects would effectively shield the substrate from the incident light, leading to a reduced reaction rate regardless of the state multiplicity of the reaction. Nevertheless, it was possible observe a lower rate of reaction (alongside the formation of oxidative degradation products) in the presence of oxygen for β-methyl substrate **10** under two sets of conditions. In the presence of triethylsilane, irradiation of **10** in a rigorously degassed acetonitrile–water mixture gave 80% conversion of starting material and a 70% yield of indoline **21**, both measured by quantitative ^{1}H NMR spectroscopy (qNMR) against dimethyl terephthalate, after an irradiation period of 45 min (Scheme S5). In contrast, whenever the reaction was repeated with oxygen-sparging of the medium prior to irradiation, the same product was obtained in a diminished yield of 43% alongside trace unknown side-products and a larger recovery of starting material (59% conversion).



Scheme S5. Photochemical reaction of β-methyl substrate **10** in the presence of triethylsilane with and without oxygen-sparging of the reaction medium prior to irradiation.

Irradiating **10** in the presence of potassium acetate likewise gave markedly different results depending on the oxygen content of the reaction mixture. When rigorously degassed, the expected hemiaminal product, **11**, was obtained in a qNMR yield of 90% with no starting material recovery after an irradiation period of 45 min (Scheme S6); while, in contrast, when saturated with oxygen, a ring-opened oxidation product, **S65**, derived from hemiaminal **11** (not observed) was formed (26% qNMR yield), again alongside trace unknown side-products and a substantial amount of starting material (44% conversion).



Scheme S6. Photochemical reaction of β-methyl substrate **10** in the presence of potassium acetate with and without oxygen-sparging prior to irradiation.

While oxygen is known to quench both singlet and triplet excited states, it has been postulated[S30] that states of sufficiently long lifetime as to observe fluorescence are required to observe any substantial rate decrease upon oxygen sparging for reactions mediated by an excited singlet state. Thus, the absence of fluorescence at room temperature upon exciting a degassed 100 μM acetonitrile solution of **10** at 350 nm (the approximate position of longest-wavelength absorption band of the molecule) in the spectrofluorometer described above suggests that the lower rates of reaction for **10** in the presence of oxygen arise from quenching of a reactive triplet state.

Experimental procedures

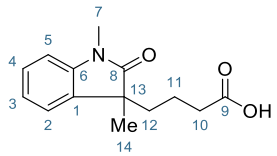
Reactions in the presence of triethylsilane:

Enaminone **10** (34.1 mg, 0.0999 mmol, 1.0 eq.) was dissolved in a 9:1 (v/v) mixture of acetonitrile (1.8 mL) and water (0.2 mL) (0.05 M) in a Schlenk tube equipped with a magnetic stir bar. The vessel was sealed with a septum, and the reaction mixture was degassed by three freeze–pump–thaw cycles. Argon-sparged triethylsilane (80 μL, 58 mg, 0.50 mol, 5.0 eq.) was added *via* syringe. The reaction mixture was stirred under constant irradiation with a single Kessil PR160L 427 nm LED lamp (positioned *ca.* 3 cm from the flask and directed toward it) for 45 min, with cooling to ambient temperature being achieved using a strong jet of nitrogen gas directed at the flask. Dimethyl terephthalate was added at the end of the irradiation period as a solution in acetonitrile (25.0 mM, 1.0 mL, 0.25 mmol, 0.25 eq.). The resulting mixture was concentrated *in vacuo*, and the crude residue was dissolved in $CDCl_3$ for analysis by quantitative ^1H NMR spectroscopy. The NMR yield of indoline **21** measured against dimethyl terephthalate was 90%; the conversion of **10** was 70%. A near-identical experiment was performed in parallel, differing only in that the reaction mixture was sparged with oxygen prior to irradiation. Analysis of the crude product of this reaction as above by quantitative ^1H NMR spectroscopy revealed the formation of indoline **21** in a yield of 43% measured against dimethyl terephthalate, alongside several trace unknown side-products; the conversion of **10** was 59%.

Reactions in the presence of potassium acetate:

Enaminone **10** (34.1 mg, 0.0999 mmol, 1.0 eq.) and potassium acetate (14.7 mg, 0.150 mmol, 1.5 eq.) were dissolved in a 9:1 (v/v) mixture of acetonitrile (1.8 mL) and water (0.2 mL) (0.05 M) in a Schlenk tube equipped with a magnetic stir bar. The vessel was sealed with a septum, and the reaction mixture was degassed by three freeze–pump–thaw cycles. The reaction mixture was stirred under constant irradiation with a single Kessil PR160L 427 nm LED lamp (positioned *ca.* 3 cm from the flask and directed toward it) for 45 min, with cooling to ambient temperature being achieved using a strong jet of nitrogen gas directed at the flask. Dimethyl terephthalate was added at the end of the irradiation period as a solution in acetonitrile (25.0 mM, 1.0 mL, 0.25 mmol, 0.25 eq.). The resulting mixture was concentrated *in vacuo*, and the crude residue was dissolved in $CDCl_3$ for analysis by quantitative ^{1}H NMR spectroscopy. The NMR yield of hemiaminal **11** measured against dimethyl terephthalate was 90%; the conversion of **10** was >99%. A near-identical experiment was performed in parallel, differing only in that the reaction mixture was sparged with oxygen prior to irradiation. Analysis of the crude product of this reaction as above by quantitative ^{1}H NMR spectroscopy revealed the formation of oxindole **S65** in a yield of 26% measured against dimethyl terephthalate, alongside several trace unknown side-products; the conversion of **10** was 44%. Flash column chromatography on silica gel (gradient elution from 2.5 to 5% ethanol in chloroform) provided an analytical sample of the major product.

4-(1,3-Dimethyl-2-oxoindolin-3-yl)butanoic acid, **S65**



^{1}H NMR (400 MHz, $CDCl_3$) δ = 7.30–7.24 (1H, m, H4), 7.17 (1H, dd, *J* = 7.3, 1.3, H2), 7.07 (1H, td, *J* = 7.5, 1.0, H3), 6.84 (1H, dd, *J* = 7.8, 0.8, H5), 3.22 (3H, s, H7), 2.27–2.17 (2H, m, H10 & H10'), 1.93 (1H, ddd, *J* = 13.4, 11.9, 4.9, H12), 1.80 (1H, ddd, *J* = 13.4, 12.0, 4.7, H12'), 1.35 (3H, s, H14), 1.35–1.17 (2H, m, H11 & H11').

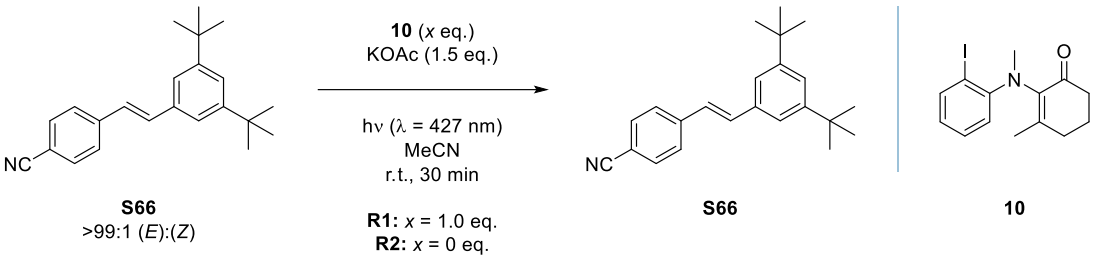
^{13}C NMR (101 MHz, $CDCl_3$) δ = 180.6 (C8), 177.8 (C9), 143.3 (C6), 133.7 (C1), 128.0 (C4), 122.8 (C3), 122.7 (C2), 108.2 (C5), 48.4 (C13), 37.7 (C12), 33.8 (C10), 26.3 (C7), 24.0 (C14), 19.9 (C11).

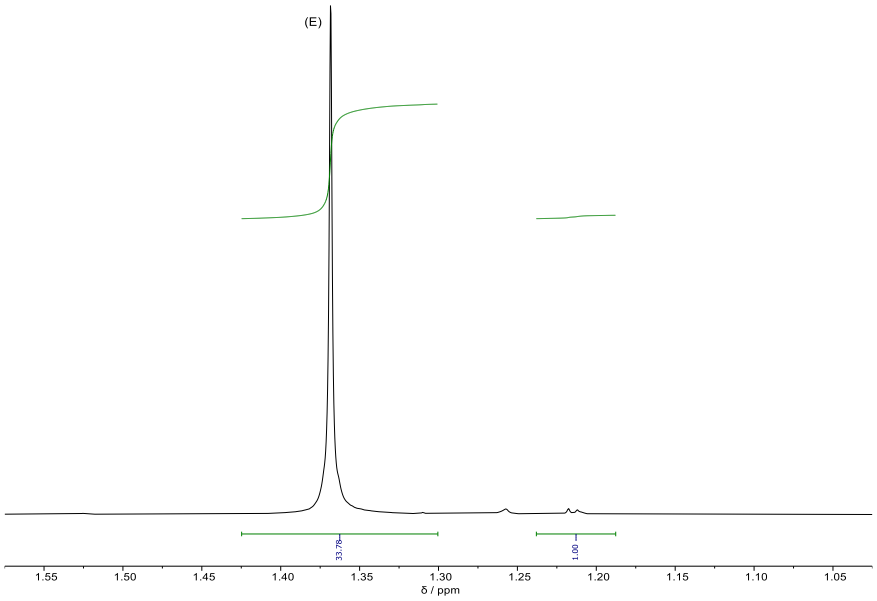
FTIR (neat) ν/cm^{-1} = 3055 (br), 1707 (br), 1612, 1470, 1378, 1179, 1126, 1019, 909, 734.

HRMS (ESI) *m/z* calcd. for $C_{14}H_{17}O_3NNa$ $[M+Na]^+$: 270.11006; found: 270.11013.

S3.2.6. Possible triplet quenching by a stilbene derivative

An attempt was also made to use a stilbene derivative, **S66**, to report on triplet-state formation upon the direct excitation of β-methyl substrate **10**. It was hypothesized that, if the triplet state of the latter compound was populated during its photochemical reaction, it might sensitize the isomerization of co-added (*E*)-**S66** (which, by analogy to related compounds,[S31] is thought to have a triplet energy of *ca.* 47 kcal mol^{-1}) to (*Z*)-**S66**. While the (*E*)-stilbene derivative did absorb very weakly in the same region as the enaminone substrate, a small change in (*E*):(*Z*) ratio could be qualitatively observed when **S66** was irradiated with 427 nm light for 30 min in the presence of enaminone **10** that was not observed in the absence of the latter compound (see Figures S10 and S11 in the following pages). This effect, albeit minor, is suggestive of a triplet state being populated upon direct irradiation of enaminone **10** in the absence of a sensitizer.





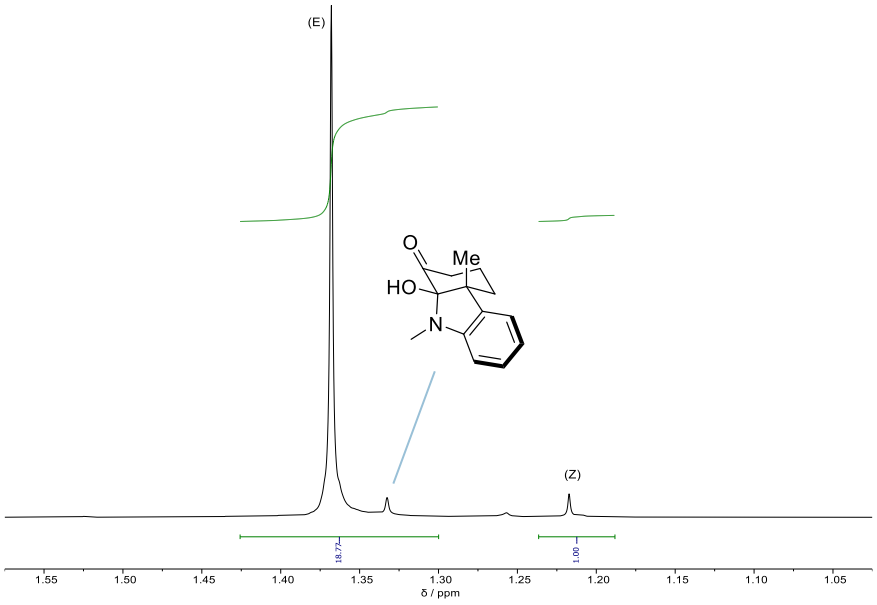


Figure S10. Irradiation of (*E*)-**S66** in the presence of 1.0 equivalent of β-methyl substrate **10** led to a small degree of alkene isomerization, which did not occur in the absence of **10**; this can be seen in the truncated ^{1}H NMR spectra displayed above (acquired at 400 MHz in $CDCl_3$) for the crude product mixtures obtained from reactions **R1** (top) and **R2** (bottom).

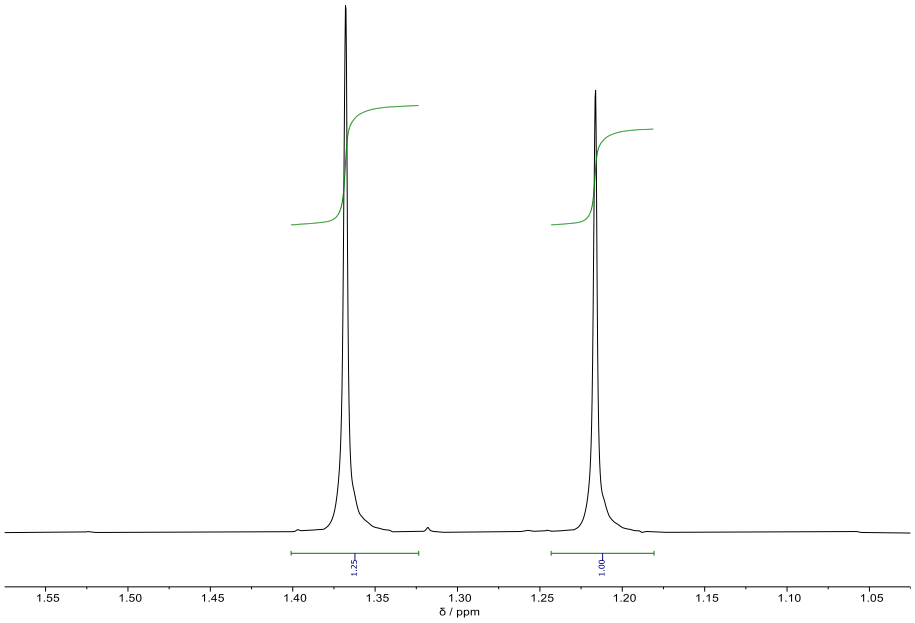
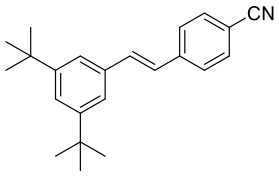


Figure S11. Reference ^{1}H NMR spectrum acquired at 400 MHz in $CDCl_3$ of a diastereomerically impure (*ca.* 1.25:1 d.r.) sample of **S66**, isolated during the synthesis of (*E*)-**S66** (see below for details); the ^{1}H resonances at 1.37 ppm and 1.22 ppm correspond to –C(C$\underline{H}_3$)$_3$ in the (*E*) and (*Z*) diastereoisomers, respectively.

(*E*)-4-(3,5-Di-*tert*-butylstyryl)benzonitrile, **S66**



This compound was prepared according to a modified literature procedure.[S32] Aqueous sodium hydroxide (1.0 M, 3.0 mL, 3.0 mmol, 1.5 eq.) was added in one portion to a stirred, room-temperature solution of (3,5-di-*tert*-butylbenzyl)triphenylphosphonium bromide (1.36 g, 2.49 mmol, 1.25 eq.) in dichloromethane (10 mL, 0.2 M) followed by 4-formylbenzonitrile (262 mg, 2.00 mmol, 1.0 eq.), also in one portion. After stirring for 1 h, the reaction mixture was diluted with dichloromethane (20 mL) and washed once with water (10 mL). The layers were separated, and the aqueous phase was extracted with additional dichloromethane (10 mL). The combined organic extracts were dried over anhydrous magnesium sulfate, filtered and concentrated *in vacuo*. The crude residue was purified by flash column chromatography (silica gel, 5% ethyl acetate in pentane) to afford **S66** (*ca.* 630 mg, (*E*):(*Z*) ≈ 1.25:1) as a viscous colourless oil, which was dissolved together with iodine (50 mg) in *n*-hexane (20 mL) and heated to reflux for 12 h. Ethyl acetate (20 mL) was added after cooling to room temperature to dissolve the solids that had formed during the reaction. The resulting solution was washed successively with sodium thiosulfate (sat. aq., 2 x 10 mL) and brine (20 mL) before being dried over anhydrous sodium sulfate, filtered and concentrated *in vacuo* to afford (*E*)-**S66** (496 mg, 1.56 mmol, 78% over two steps) as an off-white solid. The spectral data matched that previously reported in the literature.[S32]

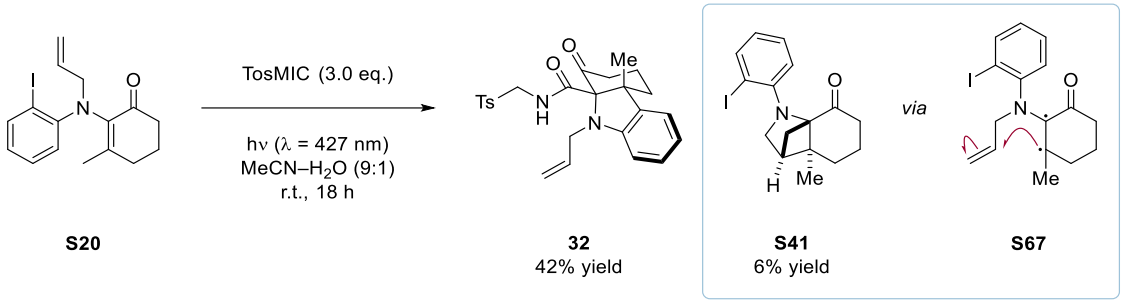
^{1}H NMR (400 MHz, $CDCl_3$) δ = 7.67–7.56 (4H, m), 7.42 (1H, t, *J* = 1.7), 7.39 (2H, d, *J* = 1.7), 7.27 (1H, d, *J* = 16.3), 7.09 (1H, d, *J* = 16.3), 1.38 (18H, s).

Experimental procedure for stilbene irradiations

Stilbene (*E*)-**S66** (31.7 mg, 0.0998 mmol, 1.0 eq.), enaminone **10** (34.1 mg, 0.0999 mmol, 1.0 eq.), potassium acetate (14.7 mg, 0.150 mmol, 1.5 eq.) and acetonitrile (2.0 mL, 0.05 M) were charged to a Schlenk tube equipped with a magnetic stir bar. The vessel was sealed with a septum, and the reaction mixture was degassed by three freeze–pump–thaw cycles. The reaction mixture was stirred under constant irradiation with a single Kessil PR160L 427 nm LED lamp (positioned *ca.* 3 cm from the flask and directed toward it) for 30 min, with cooling to ambient temperature being achieved using a strong jet of nitrogen gas directed at the flask. The resulting mixture was concentrated *in vacuo*, and the crude residue was dissolved in $CDCl_3$ for analysis by quantitative ^{1}H NMR spectroscopy. A near-identical experiment was performed in parallel, differing only in that enaminone **10** was excluded.

S3.2.7. Side-product formation in the photoreaction of *N*-allyl substrate **S20**

The formation of **S41**, an intramolecular [2+2]-photocycloadduct, in 6% yield as a side-product in the radical–polar crossover reaction to form **32** (performed in the absence of sensitizer) is indicative of triplet-state formation *via* intersystem crossing upon the direct excitation of **S20** and related compounds (Scheme S7; see above for experimental procedure and characterization data).

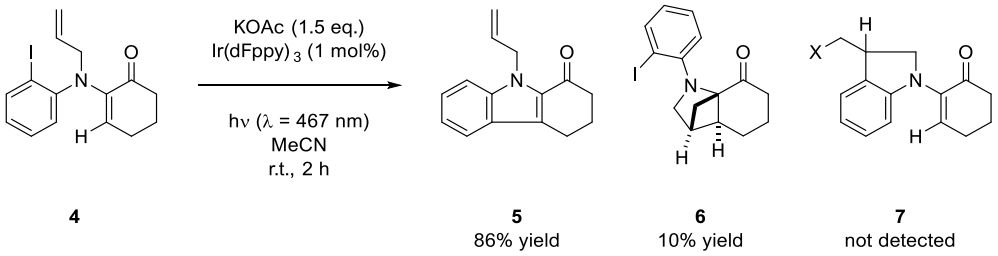


Scheme S7. A [2+2]-cycloaddition competes with radical–polar crossover in the unsensitized photoreaction of *N*-allyl substrate **S20**, suggesting a common triplet diradical intermediate (**S67**) to both pathways.

S3.3. Evidence against the formation of an aryl radical

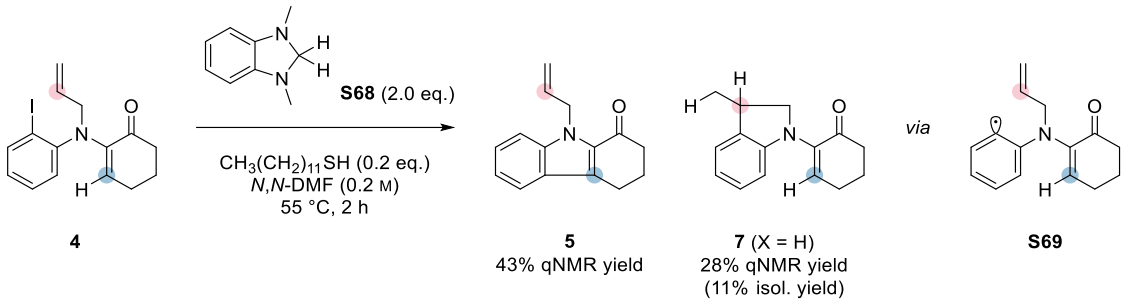
S3.3.1. Radical clock study

When irradiated in acetonitrile solution using a 467 nm LED lamp in the presence of potassium acetate and *fac*-Ir(dFppy)$_3$ at room temperature for 2 h, **4** underwent efficient photocyclization to give indole **5** in 86% yield alongside a single side-product, **6**, in 10% yield (Scheme S8; see above for experimental procedure and characterization data). No other products could be identified by analysis of the crude product mixture by either ^{1}H NMR spectroscopy or thin-layer chromatography. As outlined in the manuscript, the absence of **7** (X = H or I), or any other products that might be expected to form as a result of an aryl radical 5-*exo*-*trig* cyclization, suggests that homolysis of the C–I bond to form an aryl radical does *not* occur upon photochemical activation of *N*-allyl substrate **4**. Together with the absence of aryl radical 5-*exo*-*trig* products, the formation of [2+2]-cycloadduct **6** (in which the carbon–iodine bond present in the starting material has been preserved) as the sole side-product of the sensitized photoreaction of **4** suggests that the triplet state formed by energy transfer between the excited photocatalyst and substrate is *not* dissociative but instead displays diradical reactivity.



Scheme S8. The photochemical reaction of *N*-allyl substrate **4** undermines a mechanism involving the cyclization of an aryl radical. X = H or I.

To conclusively rule out the possibility of an aryl radical being formed *via* a competing dissociative reaction channel in the excited state, we subjected *N*-allyl substrate **4** to conditions reported by Murphy and co-workers for the thermal generation of aryl radicals from aryl halides (Scheme S9).[S33] These conditions gave a mixture of cyclization products: indole **5**, which ostensibly arises from 5-*endo*-*trig* cyclization of the putative aryl radical followed by oxidation *in situ*, and indoline **7** (X = H), which corresponds to a reductive aryl radical 5-*exo*-*trig* cyclization product, in 43% and 28% yields, respectively, measured by quantitative ^{1}H NMR spectroscopy against dimethyl terephalate. This result demonstrates that 5-*exo*-*trig* cyclization is a viable reaction pathway available to aryl radical **S69**. Thus, the failure to observe 5-*exo*-*trig* cyclization products related to **7** in the *photochemical* reaction of *N*-allyl substrate **4** is likely a result of the same aryl radical intermediate not forming under these conditions, rather than the cyclization mode itself being unfeasible.

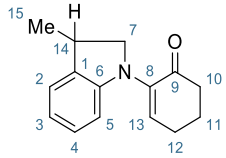


Scheme S9. Treating *N*-allyl substrate **4** with a neutral organic super electron donor (**S68**) gave a mixture of products ostensibly arising from 5-*endo*- (**5**) and 5-*exo*-*trig* (**7**, X = H) cyclization of aryl radical **S69**.

Experimental procedure

This reaction was performed under conditions reported by Murphy and co-workers;[S33] the dihydrobenzimidazole reagent, **S68**, was synthesized according to a literature procedure and stored under argon at -18 °C prior to use.[S34] The following compounds were charged sequentially to a 7 mL glass vial equipped with magnetic stir bar: *N*-allyl substrate **4** (106.0 mg, 0.300 mmol, 1.0 eq.), dihydrobenzimidazole **S68** (88.9 mg, 0.600, 2.0 eq.) as a solution in *N*,*N*-dimethylformamide (1.5 mL, 0.2 M), and 1-dodecanethiol (14.5 µL, 12.3 mg, 0.0605 mmol, 0.2 eq). The vial was kept open to air whilst the reaction mixture was heated to 55 °C with stirring. After 2 h, the reaction mixture was poured onto brine (50 mL); the resulting aqueous mixture was extracted with ethyl acetate (3 x 10 mL). The combined organic extracts were dried over anhydrous sodium sulfate before adding dimethyl terephthalate as a solution in acetonitrile (25.0 mM, 3.0 mL, 0.75 mmol, 0.25 eq.), concentrating *in vacuo*, and dissolving the resulting crude residue in $CDCl_3$ for analysis by quantitative ^1H NMR spectroscopy. The NMR yields of indole **5** and indoline **7** (X = H) measured against dimethyl terephthalate were 43% and 28%, respectively. Flash column chromatographic purification of the crude product mixture on silica gel (eluent: 5% ethyl acetate in pentane) furnished impure samples of **5** and **7** (X = H). The former sample was contaminated with the NMR internal standard dimethyl terephthalate but otherwise possessed identical spectral data to that obtained previously for this compound (see above); subsequent attempts to resolve the two components of this mixture by flash column chromatography were unsuccessful. The latter sample containing **7** (X = H) was successfully purified by flash column chromatography on alumina gel (eluent: 5% ethyl acetate in pentane) to afford **7** (X = H) (7.5 mg, 32 µmol, 11%) as a viscous orange oil. This sample contained a minor (less than *ca.* 5%) impurity, which appears to be structurally related to the starting material, **4**, but whose exact identity is unknown; multiple subsequent chromatographic purification attempts to remove this contaminant were unsuccessful.

2-(3-Methylindolin-1-yl)cyclohex-2-en-1-one, **7** (X = H)



^{1}H NMR (400 MHz, $CDCl_3$) δ = 7.10–7.05 (1H, m, H2), 7.04–6.96 (1H, m, H4), 6.74–6.67 (2H, m, H3 & H13), 6.46–6.33 (1H, m, H5), 3.83 (1H, t, *J* = 8.7, H7), 3.47–3.33 (1H, m, H14), 3.27 (1H, t, *J* = 8.6, H7'), 2.62–2.54 (2H, m, H10), 2.54–2.46 (2H, m, H12), 2.10–2.02 (2H, m, H11), 1.33 (3H, d, *J* = 6.8, H15).

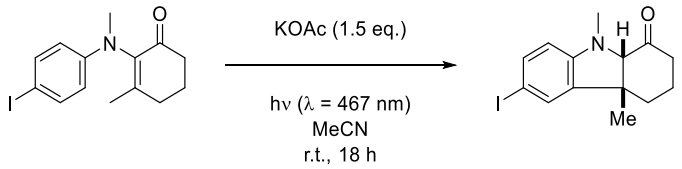
^{13}C NMR (101 MHz, $CDCl_3$) δ = 196.1 (C9), 148.5 (C6), 141.1 (C8), 135.8 (C1), 134.6 (C13), 127.1 (C4), 123.5 (C2), 118.7 (C3), 109.7 (C5), 61.1 (C7), 39.5 (C10), 35.3 (C14), 25.7 (C12), 23.1 (C11), 19.0 (C15).

FTIR (neat) ν/cm^{-1} = 2957, 2925, 2867, 1685, 1602, 1484, 1459, 1265, 1231, 1156, 1119, 914, 745.

HRMS (ESI) *m/z* calcd. for $C_{15}H_{18}NO$ $[M+H]^+$: 228.1383; found: 228.1383.

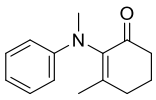
S3.3.2. Synthesis and photochemical reactivity of an 'iodo-displaced' substrate

An additional result that can be interpreted as refuting an aryl radical-based mechanism is the clean isomerization (a known triplet process[S24]) of *N*-aryl enaminone **S70** to *cis*-indoline **S71** in 77% yield under photochemical activation (Scheme S10); no other non-trace products could be identified in the crude product mixture of this reaction by ^{1}H NMR spectroscopy. This result demonstrates that mere substitution of the aromatic ring with an iodine substituent is not sufficient to divert the photochemical path of excited-state *N*-aryl enaminones from isomerization; rather, C–I bond rupture only occurs when the leaving group is situated at an aromatic carbon available to attack by the putative diradical intermediate. The finding also points away from alternative mechanisms involving the formation of charge-transfer complexes, which might in this case have been expected to give rise to *des*-iodo derivatives of either the starting material or product.



Scheme S10. *para*-Iodinated substrate **S70** undergoes isomerization rather than radical–polar crossover.

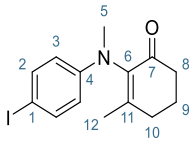
3-Methyl-2-(methyl(phenyl)amino)cyclohex-2-en-1-one, **S72**



This compound was prepared according to a literature procedure.[S24] 6-Methyl-7-oxabicyclo[4.1.0]heptan-2-one[S25] (631 mg, 5.00 mmol, 1.0 eq.) and *N*-methylaniline (0.65 mL, 0.64 g, 6.0 mmol, 1.2 eq.) in a two-necked round-bottomed flask equipped with a condenser and magnetic stir bar were dissolved in a 3:1 (v/v) mixture of methanol (9 mL) and water (3 mL) (*ca.* 0.4 M). The resulting mixture was sparged with argon for 15 min before being heated to reflux with stirring. After 21 h, the reaction mixture was poured into water (20 mL) and extracted with diethyl ether (3 x 10 mL). The combined organic extracts were washed with brine (15 mL), dried over anhydrous magnesium sulfate, filtered and concentrated *in vacuo*. The crude residue was purified by flash column chromatography (silica gel, 30% diethyl ether in pentane) to afford **S72** (369 mg, 1.71 mmol, 34%) as a viscous yellow-brown oil. The spectral data matched that previously reported in the literature.[S24]

^{1}H NMR (200 MHz, $CDCl_3$) δ = 7.25–7.07 (2H, m), 6.82–6.62 (1H, m), 6.59–6.44 (2H, m), 3.02 (3H, s), 2.62–2.43 (4H, m), 2.24–1.95 (2H, m), 1.88 (3H, s).

2-((4-Iodophenyl)(methyl)amino)-3-methylcyclohex-2-en-1-one, **S70**



To a solution of enaminone **S72** (365 mg, 1.70 mmol, 1.0 eq.) in dichloromethane (10 mL, *ca.* 0.2 M) at room temperature was added iodine (473 mg, 1.86 mmol, 1.1 eq.) and silver sulfate (581 mg, 1.86 mmol, 1.1 eq.) with vigorous stirring. After 3 h, the reaction mixture was filtered through celite, and the filtrate was concentrated *in vacuo*. The crude residue was purified by flash column chromatography (silica gel, 75% dichloromethane in pentane) to afford **S70** (155 mg, 0.453 mmol, 27%) as a viscous green oil.

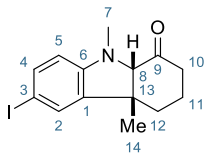
^{1}H NMR (400 MHz, $CDCl_3$) δ = 7.44–7.35 (2H, m, H2), 6.36–6.27 (2H, m, H3), 2.98 (3H, s, H5), 2.58–2.46 (4H, m, $H10_{LHS}$ & $H8_{RHS}$), 2.05 (2H, quint, *J* = 6.2, H9), 1.86 (3H, t, *J* = 0.9).

^{13}C NMR (101 MHz, $CDCl_3$) δ = 195.7 (C7), 159.0 (C11), 148.1 (C4), 139.4 (C6), 137.7 (C2), 114.2 (C3), 77.9 (C1), 38.8 (C8), 38.0 (C5), 32.3 (C10), 22.1 (C9), 20.2 (C12).

FTIR (neat) ν/cm^{-1} = 2940, 1673, 1587, 1489, 1354, 1342, 1290, 1226, 1117, 925, 808.

HRMS (ESI) *m/z* calcd. for $C_{14}H_{17}ONI$ $[M+H]^+$: 342.0349; found: 342.0348.

rac-6-Iodo-4a,9-dimethyl-2,3,4,4a,9,9a-hexahydro-1*H*-carbazol-1-one, **S71**



Enaminone **S70** (34.1 mg, 0.0999 mmol, 1.0 eq.) and potassium acetate (14.7 mg, 0.150 mmol, 1.5 eq.) were dissolved in acetonitrile (2.0 mL, 0.05 M) in a Schlenk tube equipped with a magnetic stir bar. The vessel was sealed with a septum, and the reaction mixture was degassed by three freeze–pump–thaw cycles. The reaction mixture was stirred under constant irradiation with a single Kessil PR160 467 nm LED lamp (positioned *ca.* 3 cm from the flask and directed toward it) for 18 h, with cooling to ambient temperature being achieved using a strong jet of nitrogen gas directed at the flask. The reaction mixture was concentrated *in vacuo*, and the crude residue was purified by flash column chromatography (silica gel, gradient elution from 5 to 10% ethyl acetate in pentane) to afford indoline **S71** (26.3 mg, 0.0771 mmol, 77%) as a viscous colourless oil.

^{1}H NMR (400 MHz, $CDCl_3$) δ = 7.41 (1H, dd, *J* = 8.2, 1.8, H4), 7.23 (1H, d, *J* = 1.8, H2), 6.33 (1H, d, *J* = 8.2, H5), 3.17 (1H, s, H8), 2.68 (3H, s, H7), 2.69–2.57 (1H, m, H10), 2.32 (1H, dt, *J* = 15.5, 5.7, H10’), 1.94–1.70 (3H, m, H11, H11’ & H12), 1.64–1.54 (1H, m, H12’), 1.36 (3H, s, H14).

^{13}C NMR (101 MHz, $CDCl_3$) δ = 211.1 (C9), 151.3 (C6), 140.4 (C1), 136.8 (C4), 130.4 (C2), 110.5 (C5), 81.5 (C8), 80.1 (C3), 48.7 (C13), 38.0 (C10), 36.3 (C12), 34.8 (C7), 24.7 (C14), 21.1 (C11).

The observation of nuclear Overhauser effect (nOe) correlations by 2D NOESY corresponding to H8↔H14 is consistent with the formation of the *cis*-diastereomer shown.

FTIR (neat) ν/cm^{-1} = 2957, 1713, 1595, 1477, 1453, 1257, 1231, 1069, 908, 805, 734.

HRMS (ESI) *m/z* calcd. for $C_{14}H_{17}INO$ $[M+H]^+$: 342.0349; found: 342.0345.

S3.4. Quantum yield studies

A Thorlabs M405L4 405 nm (1000 mW min.) mounted LED equipped with a liquid light guide was used for quantum yield measurements. The photon flux of this light source was determined by ferrioxalate actinometry, as described below. An Agilent Cary 60 UV-vis spectrophotometer was used for all absorption measurements.

S3.4.1. Chemical actinometry[S35]

A 0.0060 M solution of potassium ferrioxalate was prepared by dissolving 147.4 mg (0.300 mmol) of $K_3[Fe(C_2O_4)_3]\cdot 3H_2O$ in 50 mL of 0.05 M aqueous H_2SO_4 and stored in the dark. The absorbance of this solution at 405 nm (the irradiation wavelength) was measured as 1.13 a.u. (Figure S12).

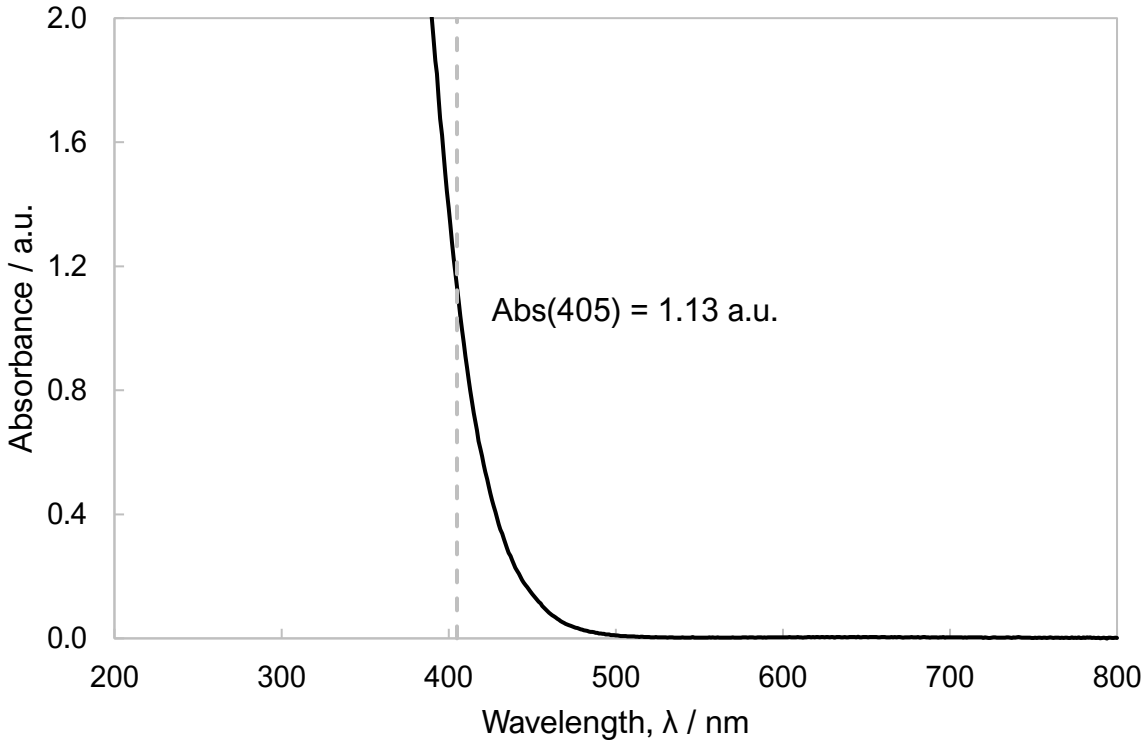


Figure S12. UV–vis absorption profile of the potassium ferrioxalate solution used for chemical actinometry.

Three 3.0 mL samples of the above ferrioxalate solution were placed in quartz cuvettes and irradiated with stirring for 8.0 s. An identical control sample was kept in the dark. After irradiation, 0.30 mL aliquots of each sample were transferred to vials containing 1.35 mL of a buffered, 0.1% solution of 1,10-phenanthroline (prepared by dissolving 100.0 mg of 1,10-phenanthroline and 13.56 g of sodium acetate in 100 mL of 0.5 M aqueous H_2SO_4) and 1.35 mL of distilled water. The resulting solutions were stored in the dark for 1 h before being analysed by UV–vis spectroscopy (Figure S13). The irradiation conditions were selected to ensure that (i) the conversion of ferrioxalate did not exceed 15% and (ii) the absorbances of the final $[Fe(phen)_3]^{2+}$ solutions were within the range 0.5–1.0.

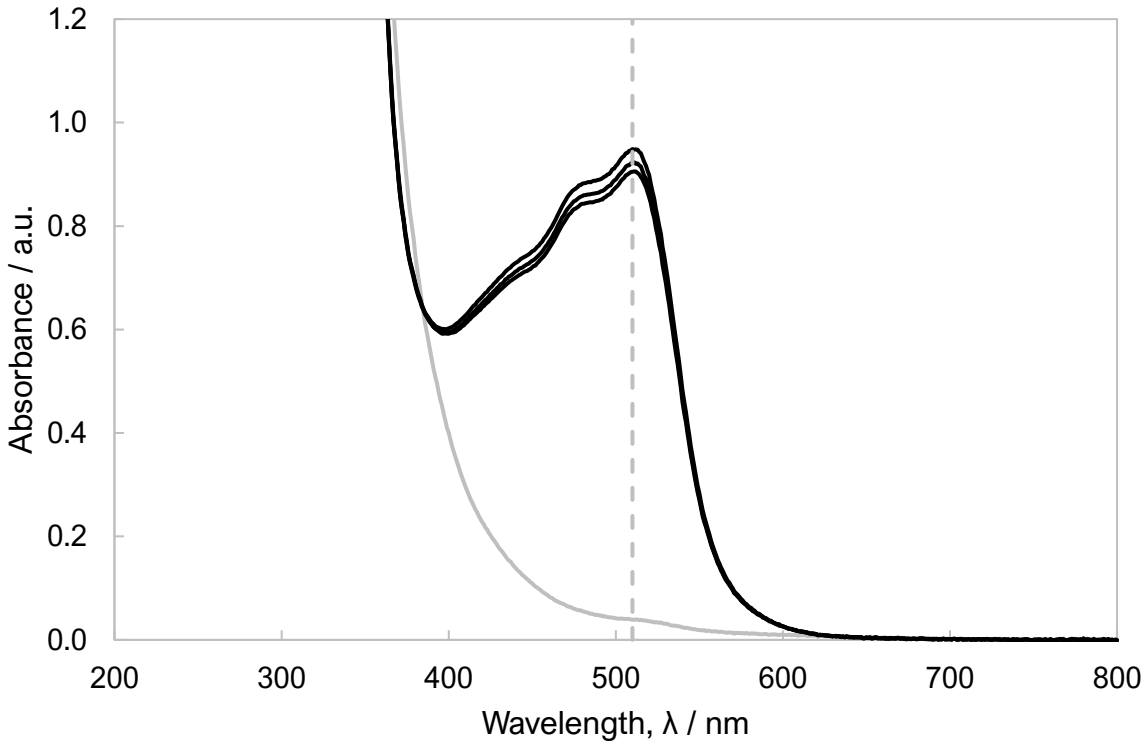


Figure S13. UV–vis absorption profiles of three samples of ferrioxalate solution after irradiation and complexation with 1,10-phenanthroline (black traces) and one control sample (grey trace).

The quantum yield of reaction, Φ_R, for the photoreduction of the ferrioxalate anion (Scheme S11) was determined by Alegria *et al.* to be 1.14 at 405 nm.[S36]

$$[Fe(C_2O_4)_3]^{3-} \xrightarrow{h\nu} [Fe(C_2O_4)_2]^{2-} + 2\ CO_2$$

Scheme S11. Photoreduction of the ferrioxalate anion.

The photon flux, f, of the 405 nm LED was calculated using the following equation:

$$f = \frac{n(Fe^{2+})}{\Phi_R t(1 - 10^{-A})}$$

where $n(Fe^{2+})$ is the number of moles of Fe^{2+} formed during the irradiation period, Φ_R is the quantum yield for ferrioxalate photoreduction at the irradiation wavelength (1.14 at 405 nm), t is the irradiation time in s (8.0 s), A is the absorbance of the 0.0060 M ferrioxalate solution at the irradiation wavelength (1.13 a.u. at 405 nm).

The amount in mol of Fe^{2+} formed during the irradiation period, $n(Fe^{2+})$, was calculated for each sample using the following equation:

$$n(Fe^{2+}) = \frac{V_1 V_3 \Delta A_{510}}{V_2 \varepsilon_{510} l}$$

where V_1 is the volume of ferrioxalate solution placed in the cuvette prior to irradiation in L, V_2 is the volume of the aliquot taken for complexation in L, V_3 is the final volume of the complexation solution in L, ΔA_{510} is the difference in absorbance between the irradiated and dark samples at 510 nm after complexation with 1,10-phenanthroline, ε_{510} is the molar attenuation coefficient of $[Fe(phen)_3]^{2+}$ at 510 nm (11,100 $L \cdot mol^{-1} \cdot cm^{-1}$), and l is the optical path length, in cm, of the cuvette.

The values of $n(Fe^{2+})$ and f calculated for each sample are presented in Table S1.

Table S1. Summary of results of ferrioxalate actinometry.

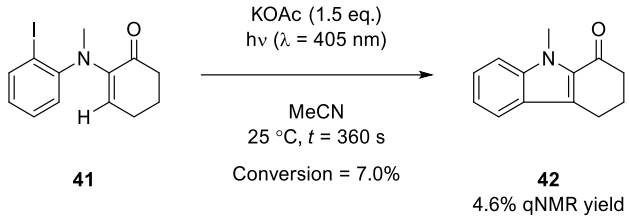
Sample	A_{510} / a.u.	ΔA_{510} / a.u.	$n(Fe^{2+})$ / mol	f / einsteins·s^{-1}
Dark	0.039	0	-	-
Sample 1	0.949	0.910	2.46 x 10^{-6}	2.91 x 10^{-7}
Sample 2	0.905	0.866	2.34 x 10^{-6}	2.77 x 10^{-7}
Sample 3	0.923	0.884	2.39 x 10^{-6}	2.83 x 10^{-7}
		AVERAGE	2.40 x 10^{-6}	2.84 x 10^{-7}

An average value of 2.84 x 10^{-7} einsteins·s^{-1} was obtained for the photon flux, f, of the 405 nm LED.

S3.4.2. Determination of the quantum yield of reaction for β-hydrogen, *ortho*-iodinated substrate **41**

Experimental procedure

Substrate **41** (49.1 mg, 0.150 mmol, 1.0 eq.) and potassium acetate (22.1 mg, 0.225 mmol, 1.5 eq.) were charged to a 1 cm quartz cuvette equipped with a magnetic stir bar followed by argon-sparged acetonitrile (3.0 mL, 0.05 M). The resulting mixture was gently sparged with argon for 5 min before sealing the cuvette with a rubber septum under an argon atmosphere. The reaction mixture was irradiated with continuous stirring using the calibrated light source for 360 s at 25 °C inside the sample chamber of an Agilent Cary 60 spectrophotometer equipped with a Peltier temperature control accessory. After irradiation, the reaction mixture was transferred to a round-bottomed flask containing dimethyl terephthalate (7.3 mg, 0.038 mmol, 0.25 eq.) and concentrated *in vacuo*. The crude residue was dissolved in $CDCl_3$ for analysis by quantitative ^1H NMR spectroscopy. The NMR yield of **42** measured against dimethyl terephthalate was 4.6%. The conversion of starting material was measured to be 7.0% (Scheme S12).



Scheme S12. Product distribution obtained from the photocyclization of *ortho*-iodinated substrate **41** after irradiation for 360 s using the calibrated light source.

Calculation

The quantum yield was determined using the following equation:

$$\Phi_R = \frac{moles\ of\ product\ formed}{ft(1-10^{-A})}$$

where f is the photon flux of the light source, in einsteins·s^{-1}, determined by ferrioxalate actinometry, t is the irradiation time in s, A is the absorbance of a 0.05 M solution of the substrate in acetonitrile and $(1-10^{-A})$ is the fraction of light absorbed by the substrate.

The absorbance at 405 nm of a 50 mM acetonitrile solution of **41** was measured to be 0.341 a.u. (Figure S14). The irradiation time was chosen to ensure that the conversion of **41** did not exceed 15%.

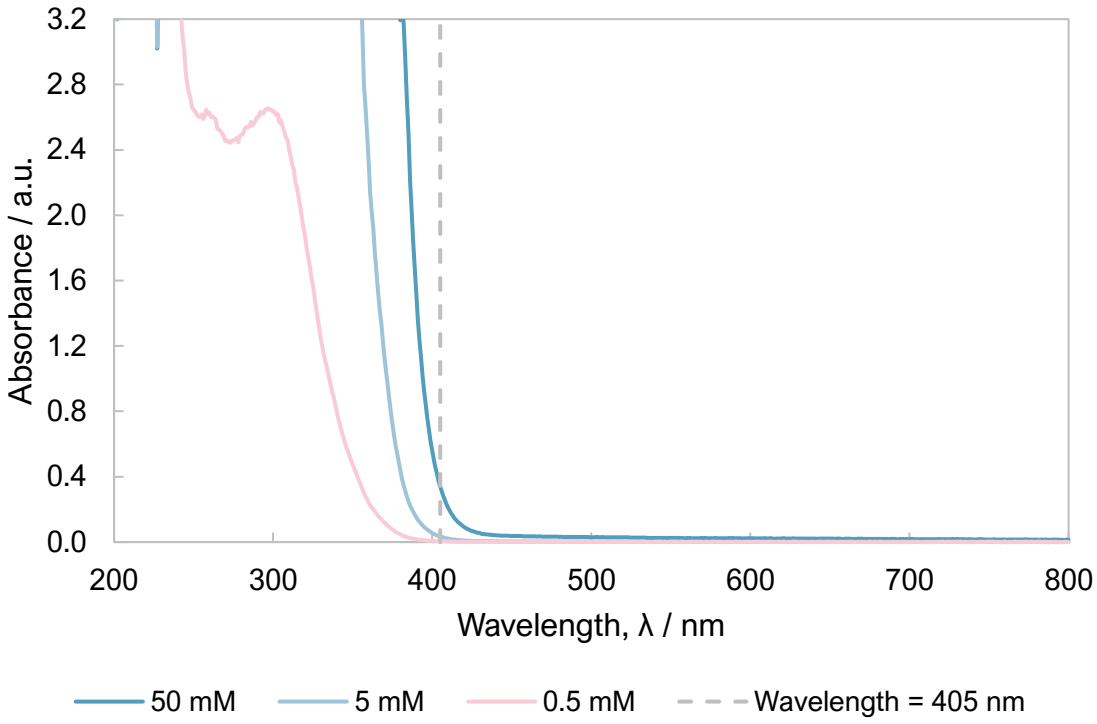
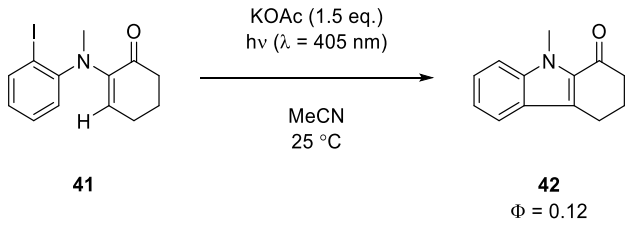


Figure S14. UV–vis absorption profiles of *ortho*-iodinated substrate **41** at different concentrations in acetonitrile.

The quantum yield of **42** at 405 nm was calculated as 0.12 (Scheme S13).



41 **42**
Φ = 0.12

Scheme S13. Photocyclization of *ortho*-iodinated substrate **41** with fractional quantum yield of reaction.

The calculation of the quantum yield of **42** at 405 nm is provided below:

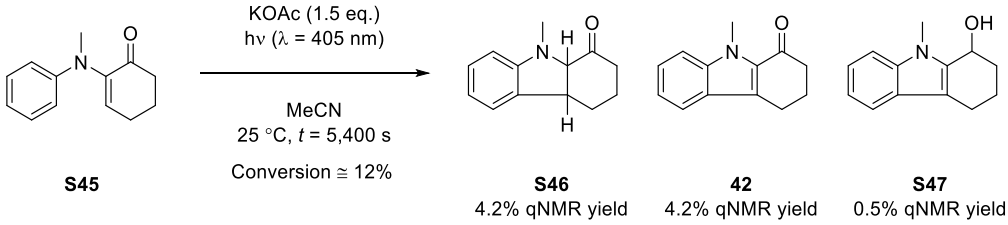
$$\Phi_R = \frac{moles\ of\ product\ formed}{ft(1-10^{-A})}$$

$$= \frac{0.046 \times 1.50 \times 10^{-4}\ mol}{2.84 \times 10^{-7}\ mol\ s^{-1} \times 360\ s \times (1-10^{-0.341})} = 0.12$$

S3.4.3. Determination of the quantum yield of reaction for β-hydrogen, *ortho*-unsubstituted substrate **S45**

Experimental procedure

Substrate **S45** (30.2 mg, 0.150 mmol, 1.0 eq.) and potassium acetate (22.1 mg, 0.225 mmol, 1.5 eq.) were charged to a 1 cm quartz cuvette equipped with a magnetic stir bar followed by argon-sparged acetonitrile (3.0 mL, 0.05 M). The resulting mixture was gently sparged with argon for 5 min before sealing the cuvette with a rubber septum under an argon atmosphere. The reaction mixture was irradiated with continuous stirring using the calibrated light source for 5,400 s at 25 °C inside the sample chamber of an Agilent Cary 60 spectrophotometer equipped with a Peltier temperature control accessory. After irradiation, the reaction mixture was transferred to a round-bottomed flask containing dimethyl terephthalate (7.3 mg, 0.038 mmol, 0.25 eq.) and concentrated *in vacuo*. The crude residue was dissolved in $CDCl_3$ for analysis by quantitative ^{1}H NMR spectroscopy. The NMR yields of **S46**, **42** and **S47** measured against dimethyl terephthalate were 4.2, 4.2 and 0.5%, respectively. The conversion of starting material was estimated to be *ca.* 12% (signal overlap prevented accurate integration of ^{1}H resonances corresponding to the starting material) (Scheme S14).



Scheme S14. Product distribution obtained from the photocyclization of *ortho*-unsubstituted substrate **S45** after irradiation for 5,400 s using the calibrated light source.

Calculation

The quantum yields of each product were determined using the following equation:

$$\Phi_R = \frac{moles\ of\ product\ formed}{ft(1-10^{-A})}$$

where f is the photon flux of the light source, in einsteins·s^{-1}, determined by ferrioxalate actinometry, t is the irradiation time in s, A is the absorbance of a 0.05 M solution of the substrate in acetonitrile and $(1-10^{-A})$ is the fraction of light absorbed by the substrate.

The absorbance at 405 nm of a 50 mM acetonitrile solution of **S45** was measured to be in excess of 2 arbitrary units (Figure S15), meaning that virtually all incident light is absorbed by the analyte under the irradiation conditions, i.e. $(1-10^{-A}) \cong 1$. The irradiation time was chosen to ensure that the conversion of **S45** did not exceed 15%.

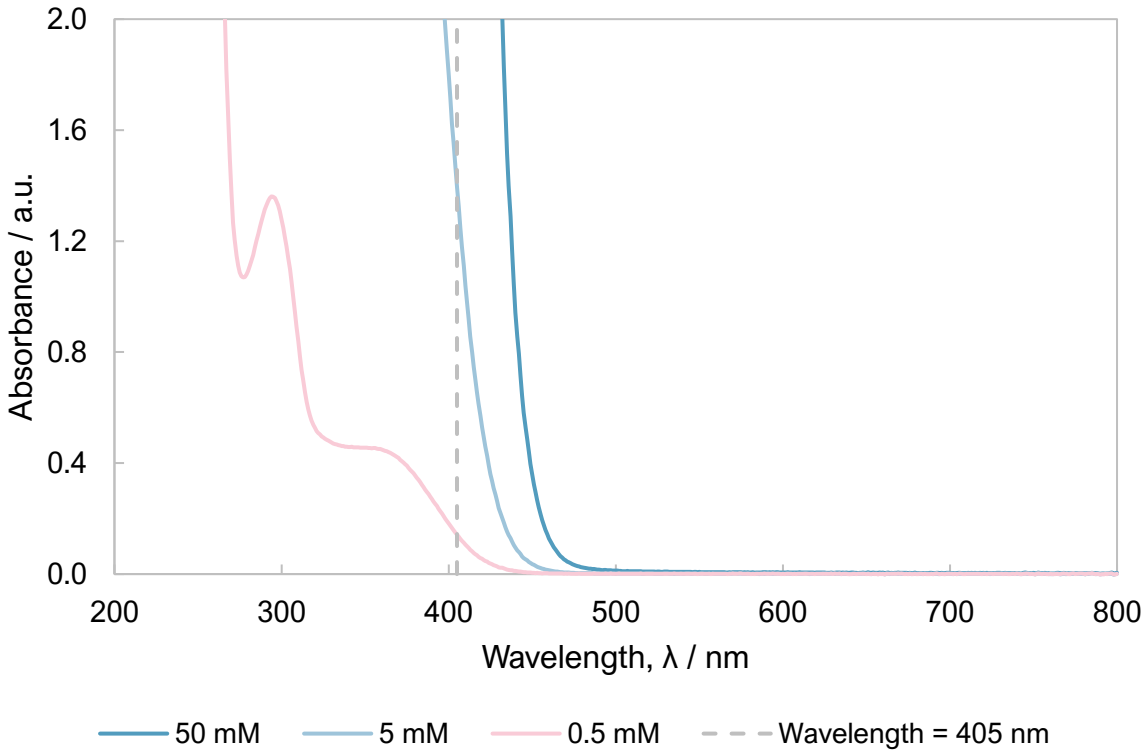
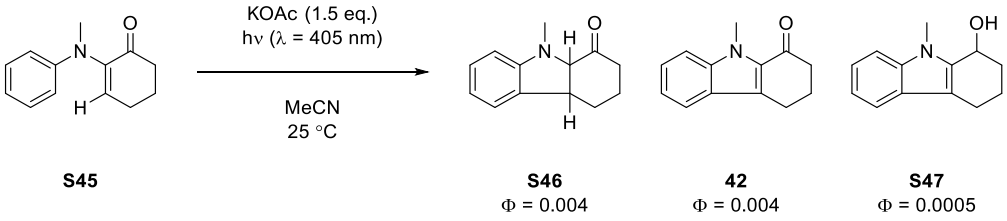


Figure S15. UV–vis absorption profiles of *ortho*-unsubstituted substrate **S45** at different concentrations in acetonitrile.

The quantum yields of **S46**, **42** and **S47** at 405 nm were calculated as 0.004, 0.004 and 0.0005, respectively (Scheme S15).



Scheme S15. Photocyclization of *ortho*-unsubstituted substrate **S45** with fractional quantum yields of reaction.

The calculation of the quantum yield of **S46** at 405 nm is provided below as an example.

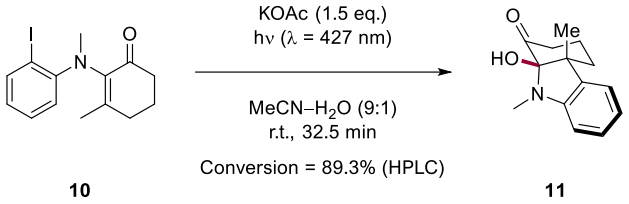
$$\Phi_R = \frac{moles\ of\ product\ formed}{ft(1-10^{-A})}$$

$$= \frac{0.042 \times 1.50 \times 10^{-4}\ mol}{2.84 \times 10^{-7}\ mol\ s^{-1} \times 5{,}400\ s \times (1-10^{-2})} = 0.004$$

S3.4.4. Discussion

Experiments conducted to determine the quantum yield of photocyclization for **41** and its non-iodinated analogue **S45** revealed a 14-fold increase in reaction efficiency upon introducing an *ortho*-iodine substituent. This difference could reflect a more efficient intersystem crossing event leading to the reactive triplet state in the presence of an iodine atom (the heavy atom effect) or the emergence of a competing mechanism for recycling the starting material (either in the ground[S37] or triplet excited state) in the absence of an irreversible *ipso*-I cyclization pathway. The moderate quantum yield of photocyclization of 0.12 measured for substrate **41** in the absence of photocatalyst suggests that a long-lived radical chain process does not constitute the dominant reaction pathway under these conditions.[S38]

S3.5. Measurement of ^{13}C kinetic isotope effects (KIEs) at natural abundance[S39]



S3.5.1. Procedure for high-conversion photoreaction of **10** and NMR sample preparation

Enaminone **10** (341 mg, 1.00 mmol, 1.0 eq.) and potassium acetate (147 mg, 1.50 mmol, 1.5 eq.) were charged to a Schlenk tube equipped with a magnetic stir bar. The reaction vessel was sealed with a septum and evacuated and back-filled with argon three times. The contents of the flask were dissolved in a mixture of acetonitrile and water (20 mL, 9:1 v/v, 0.05 M) that had been previously degassed by three freeze–pump–thaw cycles. The reaction mixture was stirred under constant irradiation with a single Kessil PR160L 427 nm LED lamp (positioned *ca.* 3 cm from the flask and directed toward it), with cooling to ambient temperature being achieved using a strong jet of nitrogen gas directed at the flask. Irradiation was stopped periodically and aliquots of the reaction mixture were taken for reverse-phase HPLC analysis (see below for calibration plots and further details): after an irradiation time of 32.5 min, the conversion of **10** and yield of **11** were measured as 89.3% and 86.1%, respectively, against 1,3,5-trimethoxybenzene. The reaction mixture was concentrated *in vacuo*, and the resulting crude residue was purified twice by flash column chromatography (silica gel, gradient elution from 5 to 10% ethyl acetate in pentane; then, silica gel, dichloromethane) to afford 34.8 mg of impure starting material; additional purification by flash column chromatography on alumina gel (gradient elution from 5 to 10% ethyl acetate in pentane) yielded analytically pure **10** (29.0 mg, corresponding to a recovery yield of *ca.* 9%[*]), which was dissolved in DMSO-d_6 (0.45 mL) for analysis by quantitative ^{13}C NMR spectroscopy. A 'standard' NMR sample was prepared by dissolving 34.8 mg of unfractionated starting material (that is, material from the same batch as that used for the photoreaction above, but which had not been itself subjected to the photochemical reaction conditions) in DMSO-d_6 (0.45 mL) and analysed under the same NMR conditions as the fractionated material (see below for full details of spectral acquisition and processing).

S3.5.2. Calibration of HPLC instrument for quantitative analysis

Calibration plots for starting material and product were obtained by reverse-phase HPLC analysis of stock solutions containing a fixed concentration of 1,3,5-trimethoxybenzene (1.0 mM) alongside **10** and **11** in concentrations ranging from 0.05 to 1.0 mM in acetonitrile (Figure S16). HPLC: (InfinityLab Poroshell 120 EC-C18, gradient elution from 5 (t = 0) to 40 (t = 0.25 min) to 90% (t = 9.00 min)

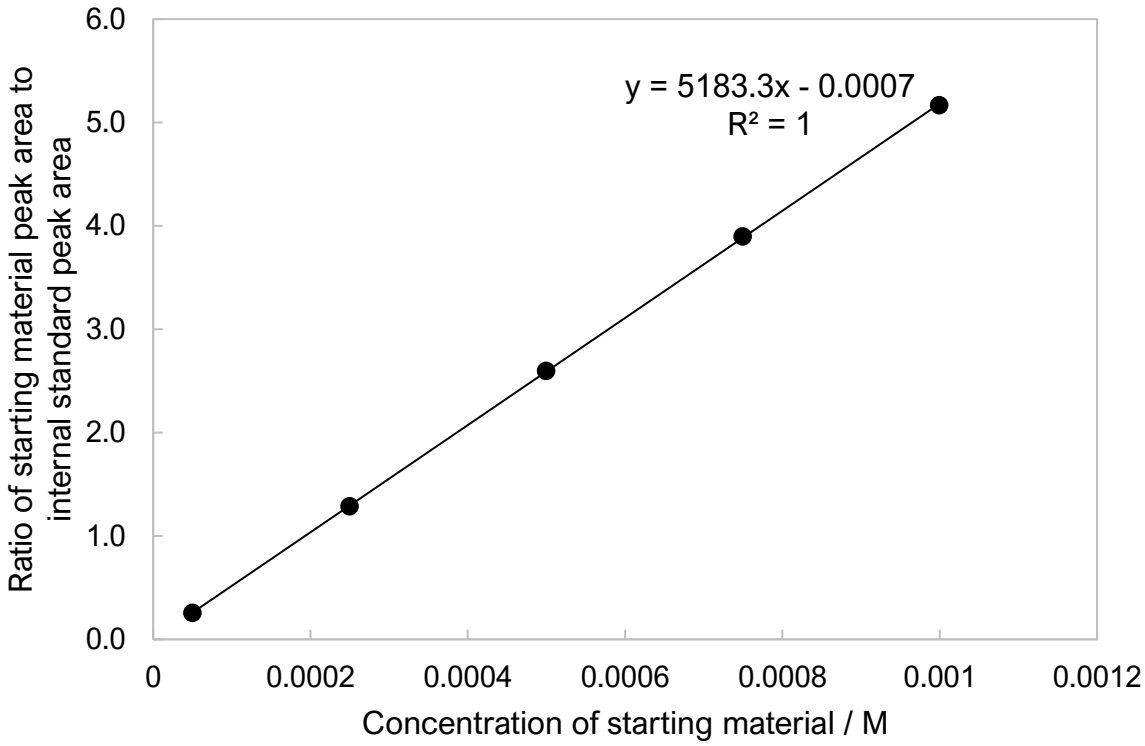
[*] Material losses upon transfer in DMSO-d_6 solution prior to the final chromatographic purification step account, at least in part, for the recovery yield of starting material being lower than the 10.7% value measured by HPLC.

acetonitrile in water, 0.4 mL min^{-1}, T = 40 °C, λ = 242 nm); τ_R (internal standard) = 6.61 min, τ_R (product) = 7.60 min, τ_R (starting material) = 8.95 min.

Samples of the reaction mixture were prepared for HPLC analysis as follows. A 0.2 mL aliquot of the reaction mixture (reaction concentration: 50 mM) was taken using a 1.0 mL gastight syringe and added to a 10 mL volumetric flask containing 1.0 mL of a 10 mM acetonitrile solution of 1,3,5-trimethoxybenzene. The final volume of the solution was adjusted to 10 mL using acetonitrile, and analysed directly by HPLC according to the instrument method described above. (Final concentration of 1,3,5-trimethoxybenzene = 1.0 mM; theoretical maximum concentration of analyte [i.e., starting material or product] = 1.0 mM.) Conversion and yield data obtained in this way are presented in Table S2 for the high-conversion, 1 mmol-scale photochemical reaction of **10** described above.

Table S2. Time-course conversion and yield data for a high-conversion, 1 mmol-scale photochemical reaction of **10** obtained by reverse-phase HPLC analysis of the reaction mixture.

Aliquot	Reaction time / min	Starting material peak area / internal standard peak area	Conversion of starting material / %	Product peak area / internal standard peak area	Yield of product / %
1	27.5	0.90743	82.5	2.79431	79.5
2	32.5	0.55249	89.3	3.02623	86.1



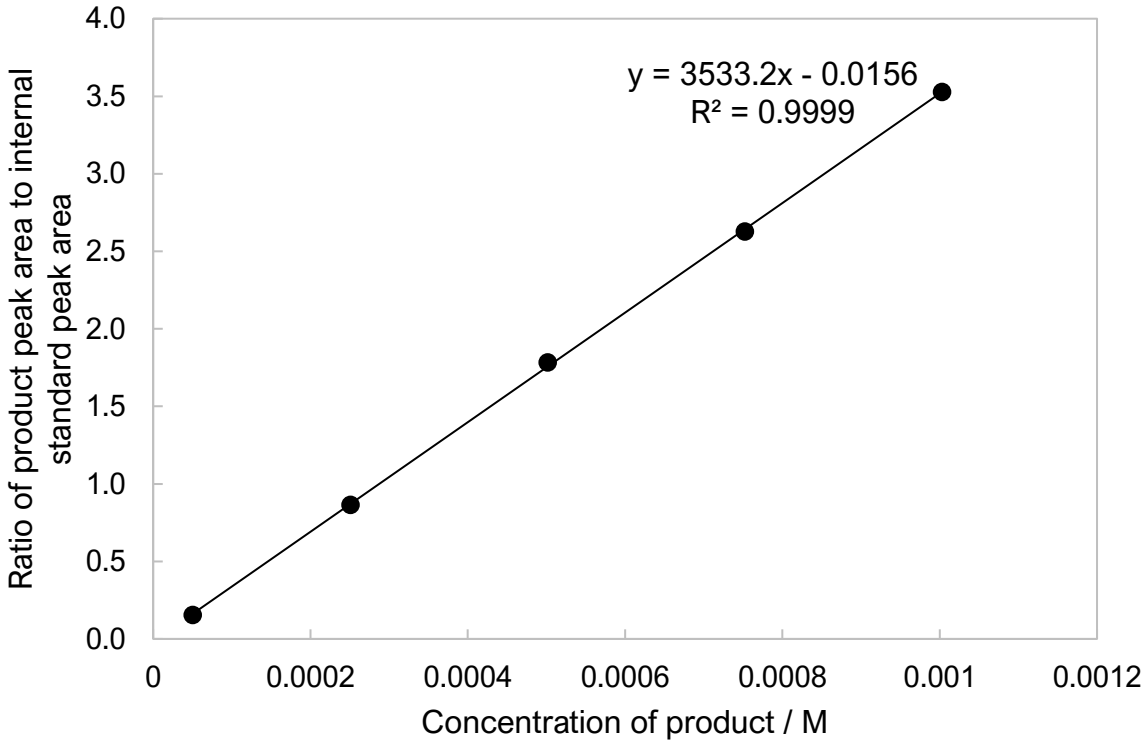


Figure S16. HPLC calibration plots for starting material and product.

S3.5.3. Spectral acquisition and processing

Quantitative ^{13}C spectra were acquired in triplicate for both the fractionated and unfractionated samples of starting material at 150.92 MHz on a two-channel Bruker AVIII HD 600 spectrometer equipped with a dedicated 5 mm BB-F/^{1}H Prodigy N_2 cryoprobe, with inverse-gated decoupling (WALTZ-16) and a 90° pulse angle. 512 scans were collected in each experiment, with a relaxation delay of 40 s between pulses. (Longitudinal relaxation, T_1, rates were determined by the inversion-recovery method; the largest T_1 value was measured as 5.8 s.) 65,536 data points were collected for each free induction decay (FID); Fourier transform was performed after zero-filling to 1,048,576 points and applying an exponential multiply (EM) window function with line-broadening of 1.0 Hz. The spectra were manually phased before applying an automatic fifth-order polynomial baseline correction. Integrals were measured across a ±15 Hz region centred on each ^{13}C resonance. Peak integrals obtained across three NMR experiments for the fractionated and unfractionated samples of starting material are summarized in **Tables S3** and **S4**, respectively. (The peak integral of C11 was set to a value of 100 in each spectrum; all NMR data were processed within TopSpin.)

Table S3. ^{13}C integrations of fractionated starting material ('Sample').

Carbon	Spectrum 1	Spectrum 2	Spectrum 3	Mean, IntSample	Standard, deviation, ΔIntSample
9	100.02	100.0178	99.6191	99.88563	0.18847
13	100.683	101.4565	100.8986	101.01270	0.32592
6	98.8187	98.9748	99.4667	99.08673	0.27613
2	98.3434	100.1907	98.7541	99.09607	0.79197
8	97.4085	97.6995	97.387	97.49833	0.14252
4	99.36	100.5302	99.2467	99.71230	0.58019
3	98.3826	98.7288	97.876	98.32913	0.35020
5	99.9195	100.8145	100.4939	100.40930	0.37025
1	104.4437	105.6502	104.1324	104.74210	0.65458
7	100.7269	100.1074	99.5986	100.14430	0.46136
10	99.009	100.0778	99.9495	99.67877	0.47648
12	98.6101	98.6623	99.227	98.83313	0.27932
11	100	100	100	100.00000	0.00000
14	100.6442	101.4602	100.569	100.89113	0.40356

Table S4. ^{13}C integrations of unfractionated starting material ('Standard').

Carbon	Spectrum 1	Spectrum 2	Spectrum 3	Mean, IntStandard	Standard, deviation, ΔIntStandard
9	99.5945	98.5165	98.6651	98.92537	0.47702
13	100.1709	100.3107	100.3332	100.27160	0.07180
6	100.0999	99.3911	99.5586	99.68320	0.30248
2	99.5083	97.9123	99.5152	98.97860	0.75399
8	96.9525	96.9607	97.7754	97.22953	0.38600
4	100.8249	99.9011	100.6887	100.47157	0.40720
3	99.4712	98.9464	98.4515	98.95637	0.41635
5	101.0133	100.4006	100.5768	100.66357	0.25755
1	102.749	100.6106	101.7447	101.70143	0.87353
7	98.3125	98.1294	98.2952	98.24570	0.08254
10	101.0797	99.8887	100.9318	100.63340	0.53003
12	99.3137	98.3771	99.3468	99.01253	0.44952
11	100	100	100	100	0
14	103.2152	101.0224	101.2193	101.81897	0.99055

S3.5.4. Calculation of ^{13}C KIE values

^{13}C KIEs were calculated for each ^{13}C resonance using the following equation

$$KIE = \frac{\ln(1-F)}{\ln\left[\frac{R}{R_0}(1-F)\right]}$$

where F corresponds to fractional conversion of starting material measured by HPLC and R/R_0 is the signal's mean integration, obtained across three identical NMR experiments, in the recovered sample of starting material (i.e. 'IntSample') divided by its corresponding value in the unfractionated material (i.e. 'IntStandard'). The error in this quantity, $\Delta(R/R_0)$, was calculated according to the following equation

$$\Delta\left(\frac{R}{R_0}\right) = \frac{R}{R_0}\sqrt{\left(\frac{\Delta IntSample}{IntSample}\right)^2 + \left(\frac{\Delta IntStandard}{IntStandard}\right)^2}$$

The errors associated with the KIE measurements were calculated using the following equations

$$\Delta KIE = KIE\sqrt{\left(\frac{\Delta KIE_R}{KIE}\right)^2 + \left(\frac{\Delta KIE_F}{KIE}\right)^2}$$

$$\Delta KIE_R = \frac{-\ln(1-F)}{\frac{R}{R_0}\ln^2\left[\frac{R}{R_0}(1-F)\right]}\Delta\left(\frac{R}{R_0}\right)$$

$$\Delta KIE_F = \frac{-\ln\frac{R}{R_0}}{(1-F)\ln^2\left[\frac{R}{R_0}(1-F)\right]}\Delta F$$

where ΔKIE_R and ΔKIE_F are the uncertainties in calculated KIEs due to $\Delta(R/R_0)$ and ΔF, respectively. The error in the HPLC measurement of fractional conversion, ΔF, was assumed to be 0.01 (that is, 1.0%).

R/R_0 and ^{13}C KIE values are presented with their associated errors for all ^{13}C starting material resonances in Tables S5 and S6, respectively. These data are further summarized in Table S7.

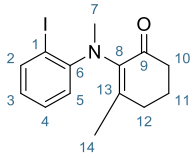
Table S5. R/R_0 values and their associated errors for all starting material ^{13}C resonances.

Carbon	IntSample	IntStandard	R/R_0	$\Delta(R/R_0)$
9	99.88563333	98.92536667	1.009706981	0.005228
13	101.0127	100.2716	1.007390926	0.003329
6	99.08673333	99.6832	0.994016377	0.004095
2	99.09606667	98.9786	1.001186789	0.011054
8	97.49833333	97.22953333	1.002764592	0.004242
4	99.7123	100.4715667	0.99244297	0.007037
3	98.32913333	98.95636667	0.993661516	0.005477
5	100.4093	100.6635667	0.997474094	0.004477
1	104.7421	101.7014333	1.029897973	0.01094
7	100.1443	98.2457	1.019325019	0.004773
10	99.67876667	100.6334	0.990513753	0.007045
12	98.83313333	99.01253333	0.998188108	0.005338
11	100	100	1	0
14	100.8911333	101.8189667	0.990887421	0.010423

Table S6. Calculated ^{13}C KIE values and their associated errors for all starting material ^{13}C resonances.

Carbon	KIE	ΔKIE_R	ΔKIE_F	ΔKIE
9	1.004336110	0.002334326	-0.000182369	0.002341439
13	1.003301922	0.001486888	-0.000138730	0.001493346
6	0.997324901	0.001831470	0.000111724	0.001834875
2	1.000530374	0.004939716	-0.000022222	0.004939766
8	1.001235390	0.001895418	-0.000051798	0.001896126
4	0.996621190	0.003147769	0.000141015	0.003150926
3	0.997166199	0.002449703	0.000118334	0.002452560
5	0.998870953	0.002001308	0.000047227	0.002001865
1	1.013342012	0.004874841	-0.000566173	0.004907609
7	1.008628284	0.002129221	-0.000364441	0.002160185
10	0.995758175	0.003151967	0.000176880	0.003156927
12	0.999190139	0.002386222	0.000033887	0.002386463
11	1	0	0.00000000	0
14	0.995925346	0.004662892	0.000169937	0.004665988

Table S7. Summary of ^{13}C KIE results.



Carbon	^{13}C KIE (expt.)	^{13}C KIE (calc. for **TS-I**)	^{13}C KIE (calc. for **TS-II**)
9	1.004(2)	0.998	0.998
13	1.003(1)	1.009	1.019
6	0.997(2)	1.002	1.002
2	1.001(5)	1.007	1.006
8	1.001(2)	1.000	0.998
4	0.997(3)	1.004	1.007
3	0.997(2)	1.004	1.004
5	0.999(2)	1.004	1.043
1	**1.013(5)**	**1.051**	**1.004**
7	-[a]	1.000	1.000
10	0.996(3)	1.000	1.000
12	0.999(2)	1.000	0.999
11	1.000 (assumed)	1.001	1.000
14	0.996(5)	0.999	0.998

[a] Not determined; overlap with DMSO solvent signal led to over-estimation of this integral.

Theoretical KIEs were calculated at the M06-2X-D3/Def2-TZVP(SMD=MeCN) level of theory using the Kinisot python package.[S40]

S4. Computational details

S4.1. General information

The hybrid meta-GGA M06-2X[S41] density functional in conjunction with Ahlrichs's triple-ζ Def2-TZVP[S42,S43] basis set were used together with Grimme's zero-damped D3 correction[S44] to optimize all stationary point structures. To these optimized structures, single-point energy corrections (M06-2X-D3/Def2-QZVPP) were applied. *AQME* was used to generate inputs of single-point energy calculations for closed-shell singlets and triplets using their optimization outputs.[S45] For both optimization and single point calculations the integral equation formalism variant of the polarizable continuum model (IEF-PCM), with the SMD solvation model was applied to account for solvent effects (solvent=acetonitrile).[S46] *Gaussian 16* version C.01 was employed for all density functional theory (DFT) calculations, using an "ultrafine" pruned (99,590) grid for numerical integration of the exchange-correlation functional and its derivatives.[S47] ORCA 5.0.4[S48] was employed in the calculation of single-point energy corrections using n-electron valence state perturbation theory (NEVPT2).[S49-S51] Conformation search was performed manually. Minimum energy crossing points were located using *MECPro*.[S52] Population analysis was performed using *NBO 6.0* interfaced with *Gaussian*.[S53] Molecular graphics were generated using *PyMol*.[S54] Vibrational frequency calculations were performed to verify that stationary points were either minima or first-order saddle points on the potential energy surface (PES), and to generate vibrational data used in *GoodVibes*.[S55] Intrinsic reaction coordinate (IRC) calculations were performed to ensure that the transition structures connected to their corresponding starting and final geometries.[S56] The computed thermochemistry data were corrected following Grimme's quasi-harmonic (QHA)[S57] model for entropy with a frequency cut-off value of 100.0 cm^{-1} using the *GoodVibes* program at 298.15 K (25˚C), unless otherwise stated. Also, *GoodVibes* applied (i) 1 M standard concentration corrections to all individual calculations to account for reactions in solution (i.e. change in standard concentration from 1 atm to 1 M)[S58] and (ii) multi-conformational corrections (G_{conf}) to all final Boltzmann weighted G to include the entropic stabilization created by multiple accessible low-lying conformers.[S59] G values of all the energy profiles correspond to the Boltzmann weighted G of all the conformers found in each step. Boltzmann weighted G (G_{av}) were calculated with *GoodVibes* as:

$$G_{av} = \sum_i G_i \times p_i \tag{1}$$

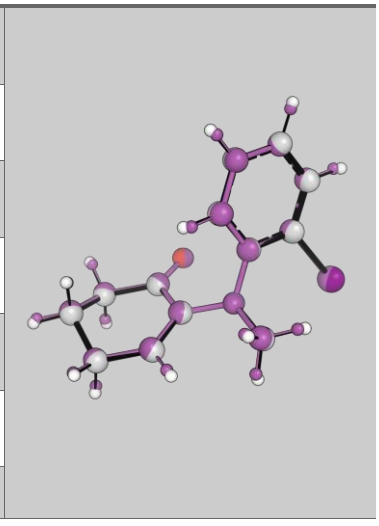
where G_i is the relative Gibbs free energy of the corresponding conformers of a certain reaction step and pi is the probability of each conformer calculated as:

$$p_i = \frac{e^{\frac{-G_i}{RT}}}{\sum_i \left(e^{\frac{-G_i}{RT}}\right)} \tag{2}$$

S4.2. DFT benchmarking

As the C–I bond in the starting material is broken during the reaction, we postulated that an accurate description of C–I bond lengths was essential, and so we began our investigation by identifying the best DFT level of theory to describe the geometry of the starting materials. A single-crystal X-ray structure of **41** served as a benchmark against which computed bond lengths and angles were compared. Different types of functionals were chosen for this investigation: GGA (B97-D3(BJ)[S60]), hybrid-GGA (B3LYP-D3(BJ) [S61-S64]), and hybrid-meta-GGA (M06-2X-D3), as well as range-separated functionals (ωB97X-D,[S65] CAM-B3LYP-D3(BJ),[S66] LC-ωHPBE[S67-70]), in conjunction with the Def2-TZVP basis set. The benchmarking results are reported in Table S8. Out of the six functionals explored, M06-2X-D3, ωB97XD and CAM-B3LYP-D3(BJ) gave the best description of the key C–I bond (showing <0.1% variation), with deviations in the main structural bond lengths (C–C, C–O and C–N) also being minimal (<1.1%), while all other dihedral and bond angles proved to be in excellent agreement with the experimental structure.

Table S8. Relevant bond lengths obtained experimentally and computationally for **41**, together with superimposed chemical structure (grey – M06-2X-D3; purple – X-ray). Variations between experiment and computation are presented in brackets

Functional	$C-I$	$C=O$	$C=C$	$C1-N$	$C2-N$	$C3-N$	Superimposed Structures
M06-2X-D3	2.092 (0.0%)	1.212 (0.4%)	1.344 (0.4%)	1.405 (0.9%)	1.425 (0.2%)	1.457 (0.4%)	
B3LYP-D3(BJ)	2.113 (1.1%)	1.219 (0.2%)	1.350 (0.9%)	1.404 (1.0%)	1.424 (0.3%)	1.459 (0.3%)	
ωB97XD	2.094 (0.1%)	1.213 (0.3%)	1.344 (0.4%)	1.404 (1.0%)	1.424 (0.3%)	1.454 (0.6%)	
CAM-B3LYP-D3(BJ)	2.094 (0.1%)	1.213 (0.3%)	1.341 (0.2%)	1.402 (1.1%)	1.422 (0.4%)	1.453 (0.7%)	
LC-ωHPBE	2.072 (0.9%)	1.212 (0.4%)	1.337 (0.1%)	1.402 (1.1%)	1.421 (0.5%)	1.449 (1.0%)	
B97-D3(BJ)	2.127 (1.7%)	1.227 (0.8%)	1.360 (1.6%)	1.406 (0.8%)	1.426 (0.1%)	1.464 (0.1%)	
Experiment	2.091(4)	1.217(5)	1.338(5)	1.418(5)	1.428(5)	1.463(5)	

We proceeded to investigate the variation of G as a function of DFT theory level, opting to measure changes in selectivity between *ipso*-I and *ipso*-H cyclization (proceeding *via* **TS-I** and **TS-II**, respectively) from intermediate ^{3}**A** (Table S9). Values of $\Delta\Delta G^{\ddagger}$ ranging from -7.1 to 2.4 kcal mol^{-1} were obtained from this analysis, with most DFT levels of theory predicting lower energies for **TS-I**. While the geometry of **TS-II** did not change significantly with respect to the level of theory, the C–I bond length in **TS-I** showed substantial variation. Plotting the difference in G against the computed bond lengths obtained during the structural benchmarking (Figure S17) revealed a good Pearson correlation of R^2=0.97, suggesting that the variation in predicted selectivity arises from inaccuracies in modelling

the C–I bond length. As expected, the three functionals that performed best during the structural benchmarking (M06-2X-D3, ωB97XD and CAM-B3LYP-D3(BJ)) also displayed very similar selectivity values, ranging from -0.4 to -0.7 kcal mol^{-1}. Out of the three best-performing functionals, M06-2X-D3 was chosen to compute the potential energy surface (PES) of the transformation in question, as it has been previously used to study a similar system lacking the *ortho*-iodine substituent.[S24] Furthermore, the M06-2X functional has been used extensively in the investigation of triplet-state reactivity and has been shown to accurately describe radicals.[S71,S72] For the purposes of this study, the reaction PES was computed at the M06-2X-D3/Def2-QZVPP(SMD=MeCN)//M06-2X-D3/Def2-TZVP(SMD=MeCN) level of theory.

Table S9. Level of theory benchmarking for transition states **TS-I** and **TS-II**.

Functional[a]	$\Delta\Delta G^{\ddagger}$ / $kcal \cdot mol^{-1}$	**C–I / Å**
M06-2X-D3	-0.4	2.174
ωB97X-D	-0.7	2.164
B3LYP-D3(BJ)	-3.9	2.229
LC-ωHPBE	2.4	2.119
B97-D3(BJ)	-7.1	2.254
CAM-B3LYP-D3(BJ)	-0.4	2.171
NEVPT2:CASSCF(10,10)[b]	-2.6	N/A

[a]Using Def2-TZVP basis set in conjunction SMD=MeCN solvation model. [b]Calculation was performed as a single point using geometries obtained at the M06-2X-D3/Def2-TZVP(SMD=MeCN) level of theory.

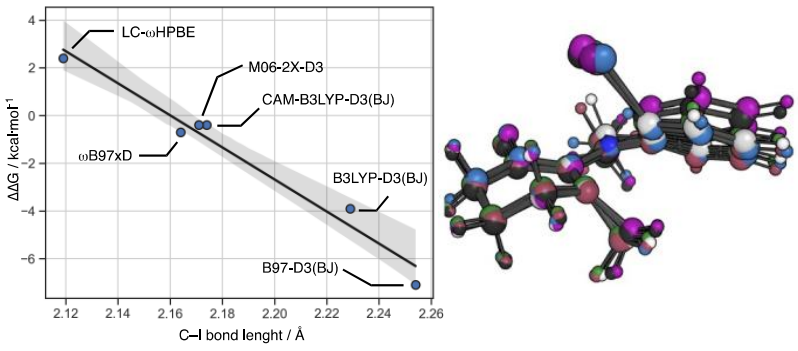


Figure S17. Plot of selectivity free energy ΔΔG *vs.* C–I bond length at various levels of theory (left); optimized transition state **TS-I** at various levels of theory (right).

We performed additional NEVPT2:CASSCF(10,10)/Def2-TZVP(SMD=MeCN)//M06-2X-D3/Def2-TZVP(SMD=MeCN) calculations, which indicated a selectivity of -2.6 kcal mol^{-1}, further corroborating that the reaction is selective for **TS-I**. An example input file used in the NEVPT2 calculations can be found in Table S10. Representations of the molecular orbitals included in the active space are shown in Figures S18 and S19; the orbitals observed in these representations are analogous in **TS-I** and **TS-II** (Table S11).

Table S10. Example ORCA input file used for NEVPT2:CASSCF calculations.

```
! NEVPT2 def2-TZVP
%maxcore 4000
%pal nprocs 16
end
%CPCM SMD TRUE
    SMDSOLVENT "ACETONITRILE"
END
%casscf
            nel 10
            norb 10
            mult 1
            PTMethod SC_NEVPT2
            MaxIter 2000
            switchstep SuperCI
            orbstep DIIS
end
* xyz 0 1
MOLECULAR COORDINATES
*
```

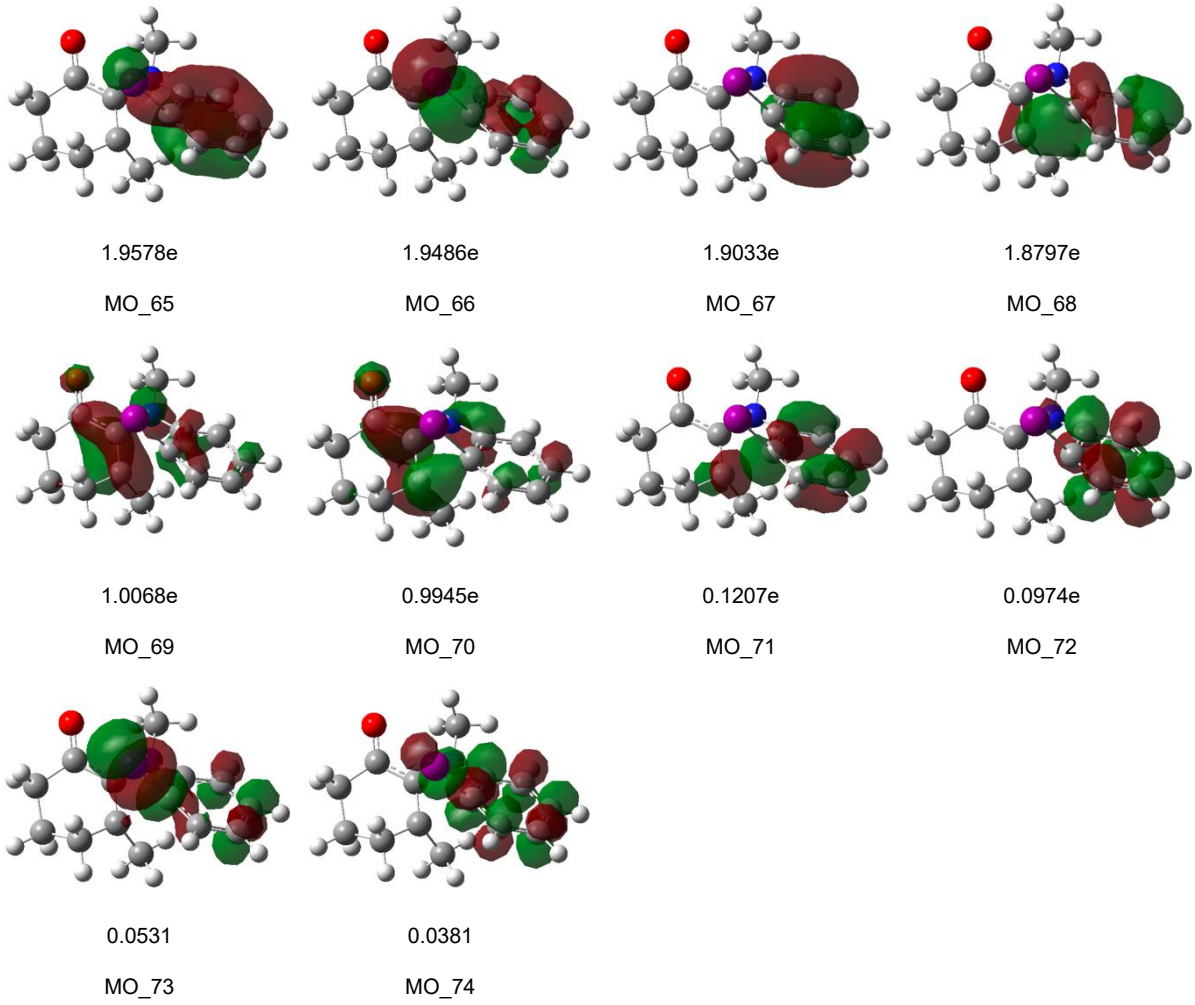


Figure S18. Molecular orbitals for structure **TS-I** obtained with the NEVPT2:CASSCF(10,10)/Def2-TZVP(SMD=MeCN) method, visualized using an isovalue of 0.04 together with their corresponding electron occupancy.

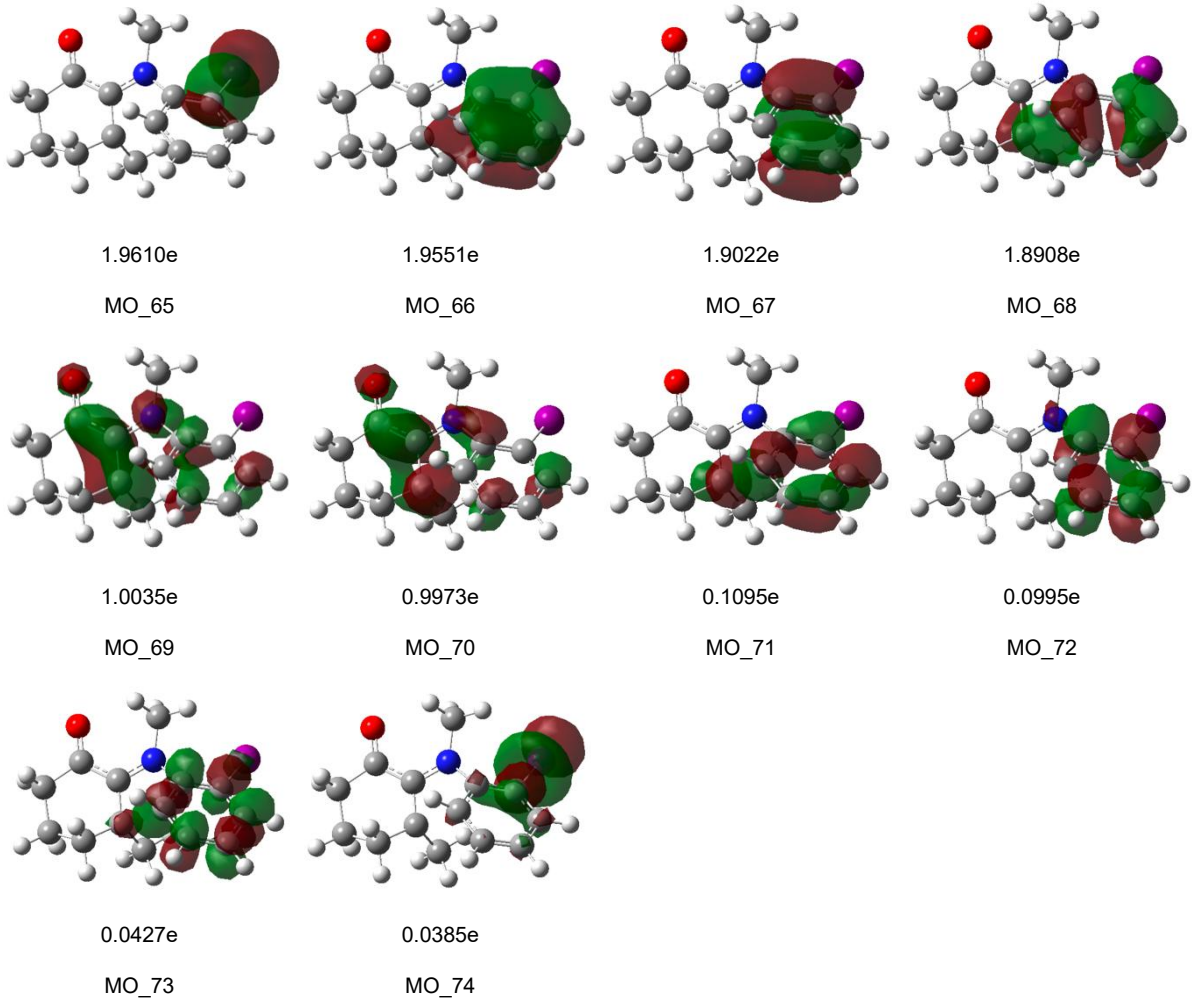


Figure S19. Molecular orbitals for structure **TS-II** obtained with the NEVPT2:CASSCF(10,10)/Def2-TZVP(SMD=MeCN) method, visualized using an isovalue of 0.04 together with their corresponding electron occupancy.

Table S11. Active space orbital correlation between **TS-I** and **TS-II**.

TS-I	**TS-II**	**TS-I**	**TS-II**
MO-65	MO-66	MO-70	MO-70
MO-66	MO-65	MO-71	MO-71
MO-67	MO-67	MO-72	MO-72
MO-68	MO-68	MO-73	MO-74
MO-69	MO-69	MO-74	MO-73

S4.3. Validation of Minimum Energy Crossing Points (MECPs)

We performed single-point energy calculations at the MECP geometry obtained with *MECPro* in T_1 and S_0 (as singlet diradical) states with the optimization level of theory (M06-2X-D3/Def2-TZVP). G values were estimated using projected frequencies obtained from *Gaussian 16*. During this analysis, we discovered that the singlet diradical species **C_MECP** contained a considerable amount of spin contamination ($<S^2> = 0.30$ after spin annihilation). This result prompted us to determine whether the MECP geometries obtained with *MECPro* were reliable enough. A thorough validation process was carried out on the lowest DFT energy conformer (**C_b_MECP**) using multiconfigurational methods, such as the complete active space self-consistent field (CASSCF) including the N-Electron Valence State Perturbation Theory (NEVPT2). In this analysis, we tested multiple basis sets (Def2-SVP and Def2-TZVP) and CAS sizes ((8,8), (10,10) and (12,12)). As seen in Table S12, all the multiconfigurational methods led to small energy differences between the T_1 and S_0 states (0.2–0.4 kcal mol^{-1}). These low energy differences suggest that the geometries obtained with *MECPro* using DFT protocols are reliable for use in this study. In this analysis, the choice of active space size and basis set did not influence greatly the results. The shape of the orbitals included in the active space are identical for T_1 and S_0 calculations (Figures S20 and S21; Table S13).

Table S12. Energy of S_0 and T_1 states, occupancy and $\Delta E(T_1\text{-}S_0)$ of different NEVPT2:CASSCF methods.

Entry	System	CAS	Basis set	Energy (a.u.)		Active space occupancy (e)		$\Delta E(T_1\text{-}S_0)$ (kcal mol^{-1})
				S_0	T_1	S_0	T_1	
1	C_b_MECP	8,8	Def2-SVP	-967.166523	-967.166760	[1.9886, 1.9368, 1.8942, 1.0489, 0.9507, 0.1060, 0.0633, 0.0114]	[1.9886, 1.9375, 1.8962, 1.0013, 0.9983, 0.1040, 0.0627, 0.0114]	0.2
2	C_b_MECP	8,8	Def2-TZVP	-968.724833	-968.725135	[1.9864, 1.9379, 1.8962, 1.0432, 0.9565, 0.1040, 0.0622, 0.0136]	[1.9863, 1.9385, 1.8983, 1.0012, 0.9985, 0.1020, 0.0616, 0.0137]	0.2
3	C_b_MECP	10,10	Def2-TZVP	-968.727251	-968.727818	[1.9856, 1.9819, 1.9367, 1.8940, 1.0829, 0.9169, 0.1057, 0.0636, 0.0164, 0.0162]	[1.9856, 1.9819, 1.9368, 1.8937, 1.0011, 0.9986, 0.1061, 0.0636, 0.0164, 0.0162]	0.4
4	C_b_MECP	12,12	Def2-TZVP	-968.721514	-968.722033	[1.9805, 1,9798, 1.9361,	[1.9805, 1.9798, 1.9598, 1.9363, 1.8932, 1.0012,	0.3

	1.8936, 1.0875, 1.0875, 0.9125, 0.1065, 0.0653, 0.0441, 0.0171, 0.0170]	0.9988, 0.1070, 0.0652, 0.0441, 0.0171, 0.0170]

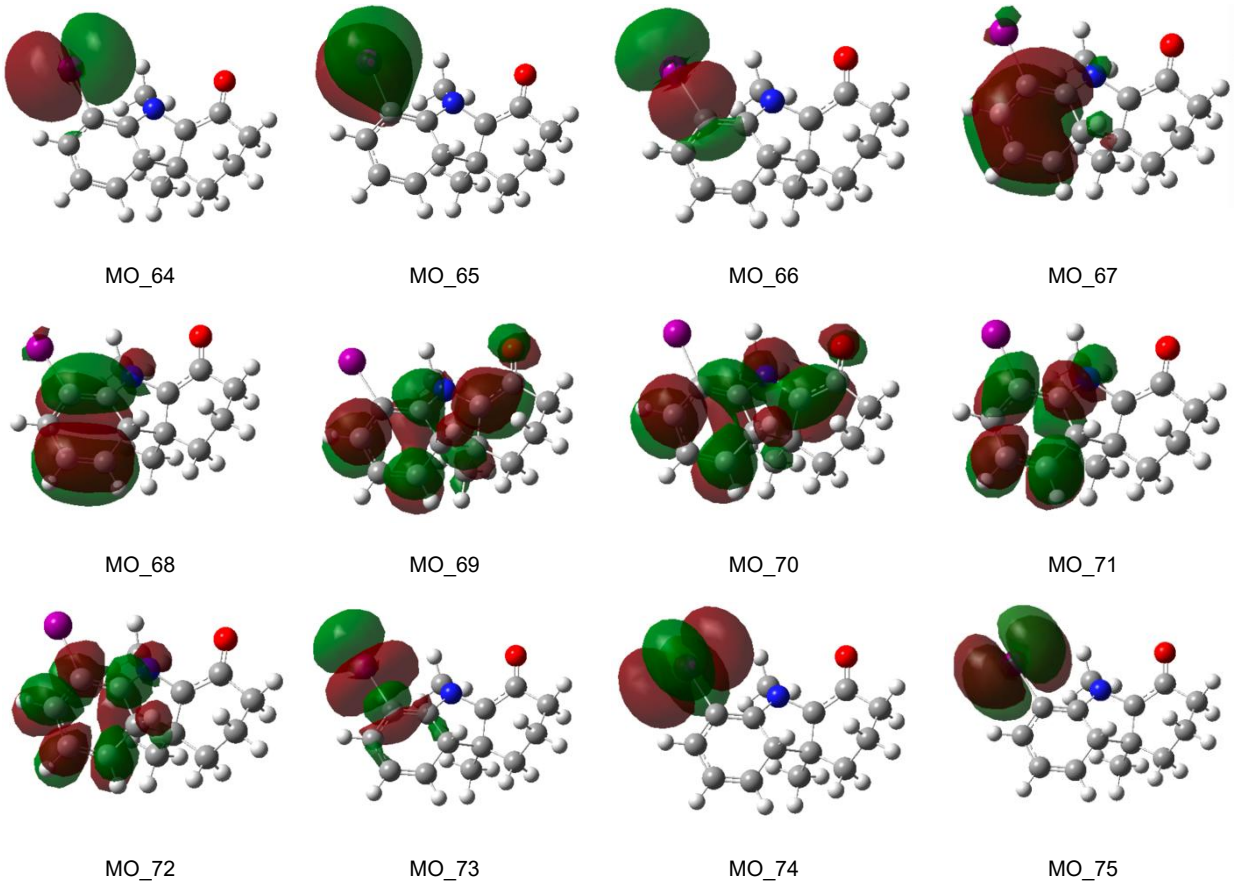


Figure S20. Molecular orbitals for structure **C_b_MECP** obtained with the NEVPT2:CASSCF(12,12)/Def2-TZVP method, visualized using an isovalue of 0.04 in the T_1 state.

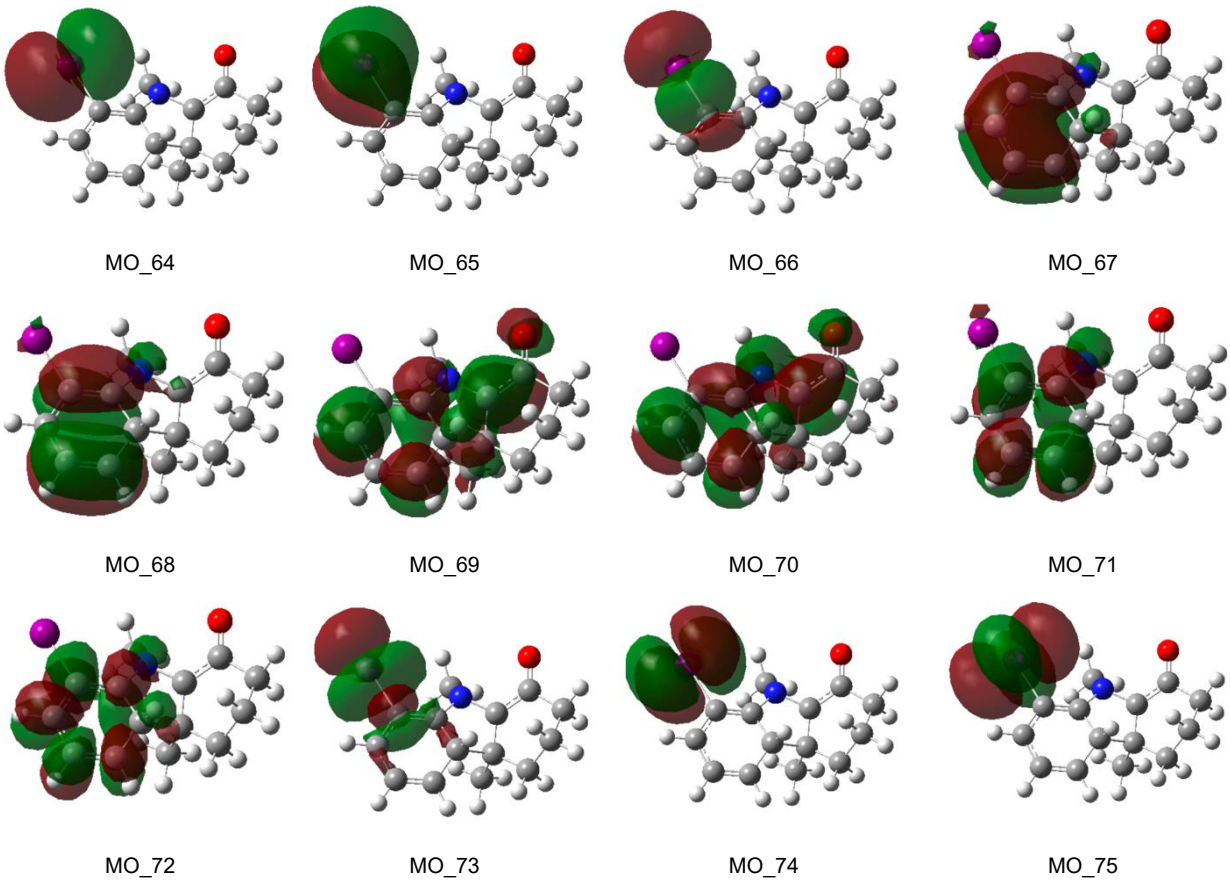


Figure S21. Molecular orbitals for structure **C_b_MECP** obtained with the NEVPT2:CASSCF(12,12)/Def2-TZVP method, visualized using an isovalue of 0.04 in the S_0 state.

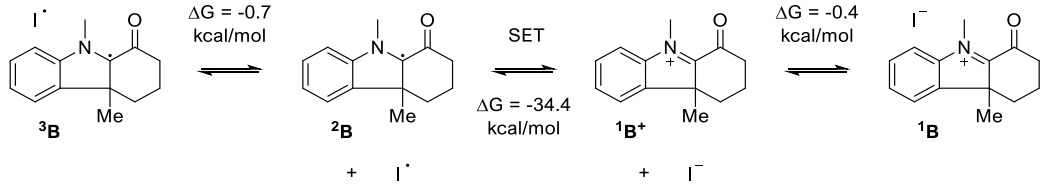
Table S13. Active space orbital correlation between T_1 and S_0 states of **C_b_MECP**.

T1	S0	T1	S0
MO-64	MO-64	MO-70	MO-70
MO-65	MO-65	MO-71	MO-71
MO-66	MO-66	MO-72	MO-72
MO-67	MO-67	MO-73	MO-74
MO-68	MO-68	MO-74	MO-75
MO-69	MO-69	MO-75	MO-74

S4.4. Formation of ^{1}**B** from ^{3}**B**

Upon cyclization of intermediate ^{3}**A** to ^{3}**B**, the formation of the final product ^{1}**B** must occur *via* a series of intersystem crossing and electron transfer events. As intermediate ^{3}**B** is effectively a pair of doublets with one of the unpaired electrons localized on an iodine atom, it is expected that intersystem crossing is highly facile due to the associated large spin-orbit coupling constants. As such intermediate ^{3}**B** is

expected to spontaneously intersystem cross to its corresponding open-shell singlet form, which can then undergo outer-sphere electron transfer to form iminium ion $^{1}\mathbf{B}^{+}$. To estimate the barrier for the outer-sphere electron transfer process, we applied the Marcus–Hush[S73-S80] theory for electron transfer, between the infinitely separated substrate radical (referred to here as $^{2}\mathbf{B}$) and iodine radical (Scheme S16).



Scheme S16. SET from iodine radical to $^{2}\mathbf{B}$.

In this method, DFT calculations (M06-2X-D3/Def2-QZVPP(SMD=MeCN)) are employed to measure λ_i (inner reorganization energies) and λ_0 (solvent reorganization energy). The total λ values ($\lambda_i + \lambda_0$) are obtained with single point energy calculations (instead of Gibbs free energy) of the reagents into the geometries of the products in non-equilibrium solvent phase. In order to generate meaningful results about solvent reorganization, the calculations when changing electronic states require the NonEq=write (original state) and NonEq=read (final state) keywords in *Gaussian 16* to store and read the solvent cages (using Link 1 jobs). For example, in the SET:

$$^{2}\mathbf{B} + \mathbf{I}^{\cdot} \rightarrow {}^{1}\mathbf{B}^{+} + \mathbf{I}^{-}$$

λ_1 (λ in the forward direction of the SET) is obtained through four single-point energy calculations:

Initial substrates before SET

(1) $^{2}\mathbf{B}$ in its geometry with normal SMD solvation, with multiplicity = 2 and charge = 0

(2) $\mathbf{I}\cdot$ in its geometry with normal SMD solvation, with multiplicity = 2 and charge = 0

Initial substrates after SET

(3) $^{2}\mathbf{B}$ in the geometry of $^{1}\mathbf{B}^{+}$, with multiplicity = 2 and charge = 0 and SMD using NonEq=Read (applying multiplicity = 1 and charge = 1 for the initial NonEq=Write)

(4) $\mathbf{I}^{\cdot}$ in the geometry of $\mathbf{I}^{-}$, with multiplicity = 2 and charge = 0 and SMD using NonEq=Read (applying multiplicity = 1 and charge = -1 for the initial NonEq=Write)

and applying the following formula:

$$\lambda = \big(E(3) - E(1)\big) + \big((E(4) - E(2)\big) \qquad (3)$$

where the difference in energy between (3) and (1) correspond to the distortion of the **^{2}B** compound and the difference between (4) and (2) relates to the solvent distortion created by the iodine atom when accepting an electron. The energy parabolas might not have the same curvature in the two directions of the SET. For this reason, we also calculated λ_2 (backward direction) with equation (3) using the following four single-point energy calculations:

Products before SET

(1) **^{1}B$^+$** in its geometry with normal SMD solvation, with multiplicity = 1 and charge = 1

(2) **I$^-$** in its geometry with normal SMD solvation, with multiplicity = 1 and charge = -1

Products after SET

(3) **^{1}B$^+$** in the geometry of **^{2}B**, with multiplicity = 1, charge = 1 and SMD using NonEq=Read (applying multiplicity = 2 and charge = 0 for the initial NonEq=Write)

(4) **I$^-$** in the geometry of **I$^\cdot$**, with multiplicity = 1, charge = -1 and SMD using NonEq=Read (applying multiplicity = 2 and charge = 0 for the initial NonEq=Write)

After calculating λ_1 and λ_2 with equation (3) (Table S14), the averaged λ values were calculated as suggested previously[S81] using equation (4):

Table S14. Computed energies in Hartree for **^{2}B** and **^{1}B$^+$** in their corresponding oxidation states as well as their vertical oxidized/reduced energies.

Charge	Structure + Solvation Sphere			
	^{2}B	**^{1}B$^+$**	I$^\cdot$	I$^-$
0	-673.122995	-673.061310	-297.615013	-297.550422
+/-1	-672.921505	-672.978507	-297.753657	-297.817704

$$\lambda_1 = (-673.061310 + 673.122995) + (-297.550422 + 297.615013)$$

$$\lambda_1 = 0.126276\ Hartee = 79.2\ kcal \cdot mol^{-1}$$

$$\lambda_2 = (-672.921505 + 672.978507) + (-297.753657 + 297.817704)$$

$$\lambda_2 = 0.121049\ Hartee = 76.0\ kcal \cdot mol^{-1}$$

$$\lambda = \sqrt{\lambda_1 \cdot \lambda_2} \qquad (4)$$

$$\lambda = \sqrt{79.2 \cdot 76.0}\ = 77.6\ kcal \cdot mol^{-1}$$

Then, the $\Delta G_{SET}^{\ddagger}$ barrier was obtained following equation (5):

$$\Delta G_{SET}^{\ddagger} = \frac{(\Delta G + \lambda)^2}{4\lambda} \quad (5)$$

$$\Delta G_{SET}^{\ddagger} = \frac{(-34.4 + 77.6)^2}{4 \cdot 77.6} = 6.0\ kcal \cdot mol^{-1}$$

The low activation energy found suggests that single-electron transfer occurs rapidly.

We have also localized a minimum energy crossing point connecting structures **^{3}B** and **^{1}B** (closed-shell singlet) computed at the M06-2X-D3/Def2-QZVPP(SMD=MeCN)//M06-2X-D3/Def2-TZVP(SMD=MeCN) level of theory, which was found to be ΔG = 5.4 kcal·mol^{-1} (**B_MECP**) (Figure S22), suggesting that intersystem crossing is a facile process.

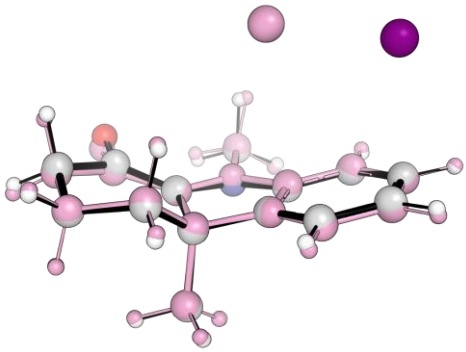


Figure S22. Overlayed structures of the computed **B_MECP** (grey) and its corresponding **^{3}B** minimum (pink).

S4.4.1. Possibility of an inner-sphere electron transfer event leading to ^{1}B

As outlined in the manuscript, this SET event could alternatively be viewed as an *inner-sphere* process occurring when there is still a significant degree of bonding between the iodine atom and the rest of the molecule. We envision two scenarios where this could occur.

The first scenario involves a concerted ISC event *during* the breaking of the C–I bond. Single-point energy calculations on the S_0 surface along the IRC of **TS-I** reveal that the closed-shell S_0 and the open-shell T_1 surfaces intersect multiple times as **TS-I** is crossed (Figure S23A). This low energy separation between the two electronic surfaces suggests a viable pathway for ISC along the reaction coordinate, leading directly to the formation of **^{1}B**. As this process would involve SET while substantial bonding between the iodine atom and the rest of the molecule, it could be interpreted as an inner-sphere process.

We also explored the possibility of an inner-sphere SET process occurring upon the formation of intermediate **^{3}B**. Similar to our previous proposal, after ISC generates a radical pair, rather than undergoing an outer-sphere electron transfer, the two radical fragments could recombine to re-form the C–I bond. The resulting α-iodoamine could then undergo E1 elimination to form **^{1}B**. The required intermediate, however, is highly unstable and does not exist as a minimum on the S_0 potential energy

surface. This is supported by a relaxed C–I bond scan starting from **^{1}B**, which indicates the absence of a shallow intermediate even at a bond distance of 1.8 Å (Figure S23B). As such, we believe that this scenario is highly unlikely.

It is important to note that the ISC event, which is a prerequisite for electron transfer – whether through an inner- or outer-sphere mechanism – is fundamentally probabilistic. As a result, it is difficult to unequivocally state which mechanism is most likely, and it is possible both mechanisms could operate simultaneously.

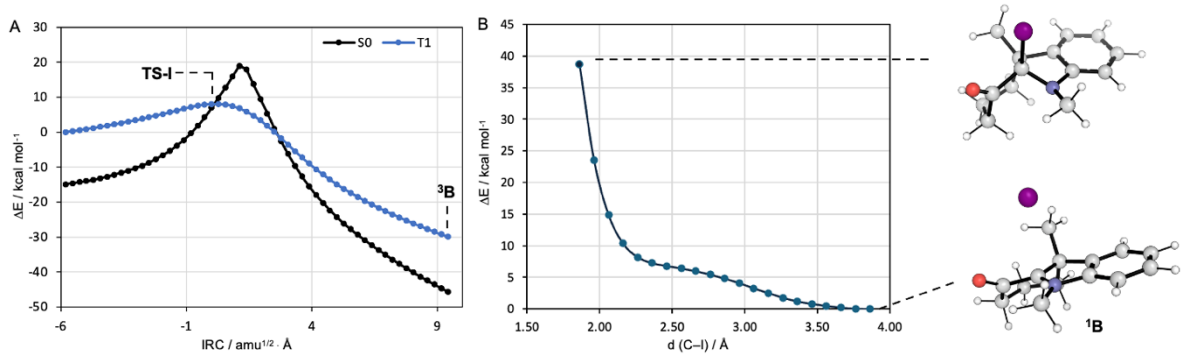


Figure S23. Computational studies indicate that an inner-sphere electron transfer event is plausible. **(A)** Single-point energy calculations performed on the S_0 surface (black) along the IRC of **TS-I** at the M06-2X-D3/def2-TZVP(SMD=MeCN) level of theory. **(B)** Relaxed C–I bond distance scan on the S_0 surface starting from intermediate **^{1}B** at the M06-2X-D3/def2-SVP(SMD=MeCN) level of theory.

S4.5. Comparison of Mulliken spin densities for ^{3}**A** and ^{2}**A**

We also explored whether the photochemical reaction of β-methyl substrate **10** (or **A**, as we have denoted it when describing our computational studies) could be initiated through single-electron oxidation. While we have already provided substantial evidence supporting the involvement of an alkene triplet diradical, the results of these Mulliken spin density calculations are noteworthy in that they demonstrate that an alternative mechanism proceeding *via* the corresponding radical cation is unfeasible even if such an intermediate were to hypothetically form (that is, not merely because this specific substrate class does not undergo single-electron oxidation under specific reaction conditions). This stems from the spin density of ^{2}**A** being delocalized almost exclusively across the nitrogen and the aromatic ring, resulting in negligible radical character on the enone (Figure S24). In effect, the hypothetical species resulting from single-electron oxidation of **A** is an *amine* radical cation, not an alkene radical cation. In contrast, the corresponding compound in its first excited triplet state, ^{3}**A**, has spin density localized on the β-carbon of the enone – it is this specific (nucleophilic) carbon-centred radical that undergoes the key homolytic aromatic substitution step leading to radical–polar crossover.

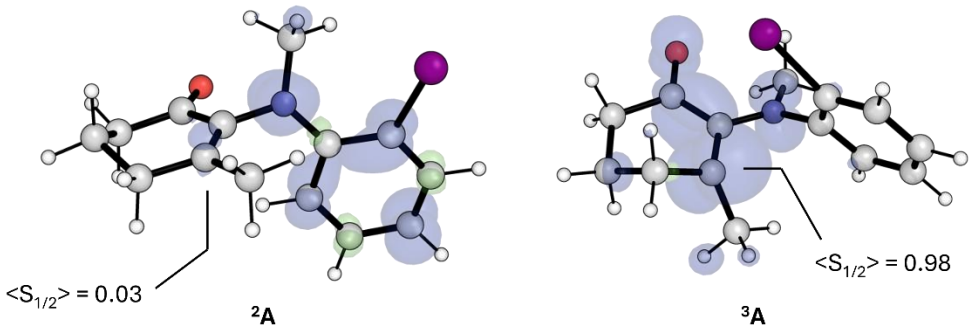
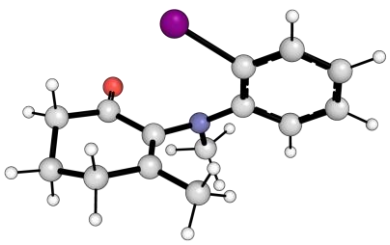
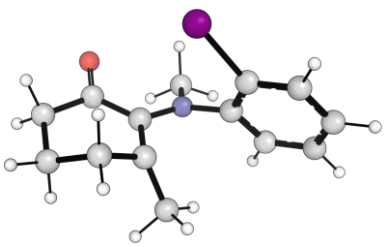


Figure S24. Mulliken spin densities computed at the M06-2X-D3/def2-QZVPP(SMD=MeCN)//M06-2X-D3/def2-TZVPP(SMD=MeCN) level of theory for the radical cation (^{2}**A**) and triplet diradical (^{3}**A**). Spin density plots were generated using an isovalue of 0.005 with α-spin = blue and β-spin = green.

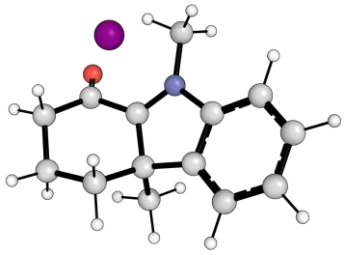
S4.6. Three-dimensional structures pertaining to computed reaction pathways available to intermediate **^{3}A**



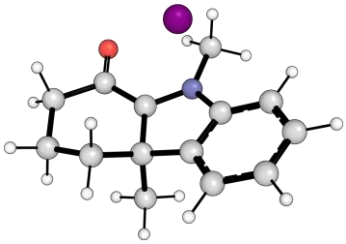
1A



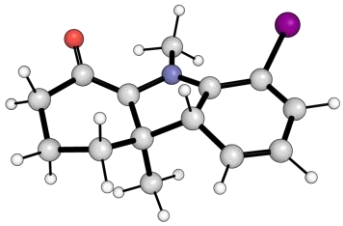
3A



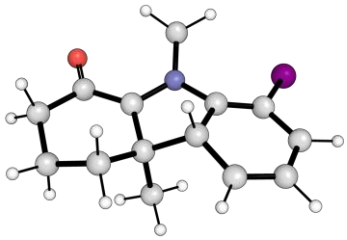
1B



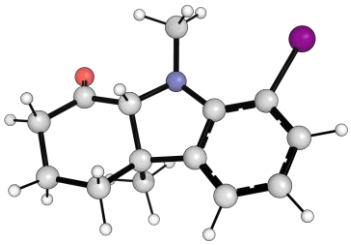
3B



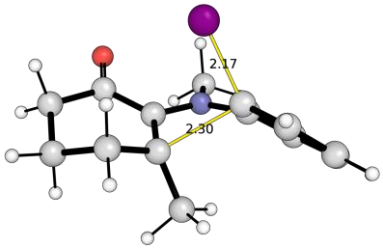
1C



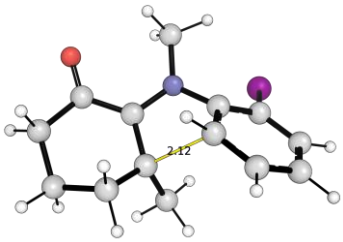
3C



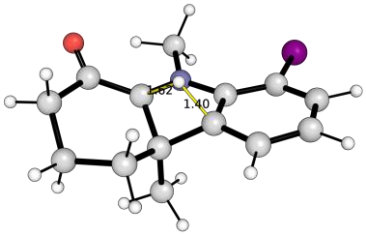
1D



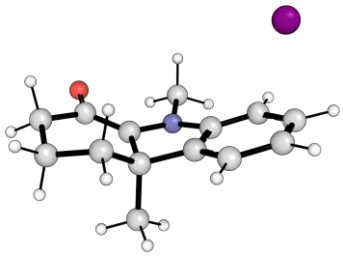
TS-I



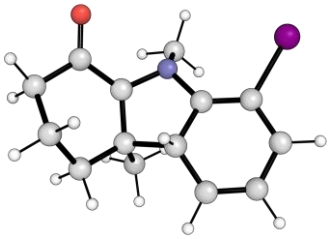
TS-II



TS-III



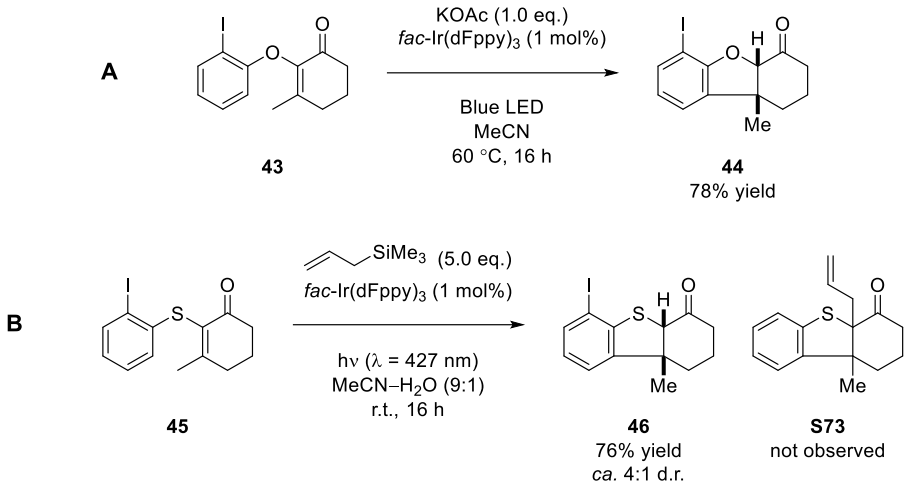
B_MECP



C_MECP

S4.7. Comparison of *N*, *O* and *S* linking atoms

We have previously shown that sensitized irradiation of 2-aryloxycyclohexenones bearing *ortho*-halogen substituents (e.g. *ortho*-iodinated substrate **43**) leads to high-yielding isomerization reactions, without side-product formation (Scheme S17A).[S24] This contrasts with the reactivity observed in this study for *N*-(2-iodoaryl) enaminones, such as **10**, which undergo eliminative photocyclization. To explore the photochemical behaviour of analogous *S*-linked substrates, we synthesized **45** containing an *ortho*-iodine substituent, as described above. Irradiation of this compound in the presence of *fac*-Ir(dFppy)$_3$ and allyltrimethylsilane in aqueous acetonitrile led to the formation of isomerization product **46** in 76% yield and *ca.* 4:1 d.r. (Scheme S17B). While some trace, unidentified side-products were present in the crude photolysate, no allylated products indicating the formation of cationic intermediates *via* a radical–polar crossover mechanism, such as **S73**, were observed; that is, the only non-trace product, **46**, arose from an isomerization (*ipso*-H cyclization) pathway.



Scheme S17. *O*- and *S*-linked substrates exhibit photochemical behaviour that is distinct from their *N*-linked analogues. **(A)** Previously reported isomerization of a 2-aryloxycyclohexenone substrate, **43**, bearing an *ortho*-iodo substituent.[S24] **(B)** Related sulfur-linked substrates also undergo isomerization in the triplet state, illustrated by the formation of **46** as the major product upon sensitized irradiation of **45**.

Computational analysis performed at the NEVPT2:CASSCF(10,10)/Def2-TZVP(SMD=MeCN)//M06-2X-D3/Def2-TZVP(SMD=MeCN) level of theory for these heterocyclic systems was found to accurately reproduce experimental observations. In contrast to *N*-alkyl-linked systems, *O*-linked and *S*-linked systems exhibited high selectivity toward *ipso*-H cyclization, with computed energy differences of 4.6 and 7.5 kcal/mol, respectively (Figure S25).

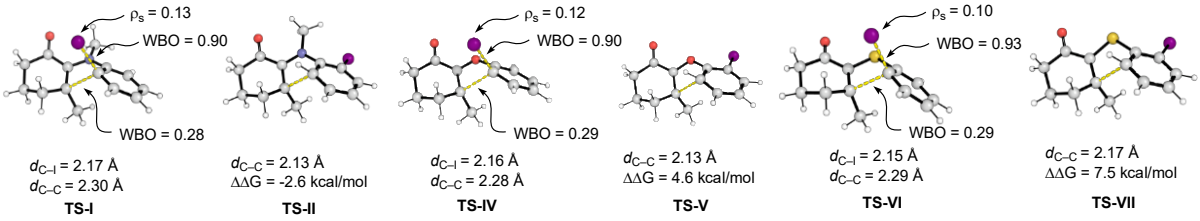


Figure S25. Comparison of *N*-linked (**TS-I** and **TS-II**), *O*-linked (**TS-IV** and **TS-V**), and *S*-linked (**TS-VI** and **TS-VII**) cyclization transition states (*ipso*-I and *ipso*-H) computed at the NEVPT2:CASSCF(10,10)/Def2-TZVP(SMD=MeCN)//M06-2X-D3/Def2-TZVP(SMD=MeCN) level of theory, including bond distances, Wiberg bond orders (WBO) and NBO spin densities.

Further NBO analysis of the *ipso*-I cyclization transition structures (**TS-I**, **TS-IV** and **TS-VI**) performed at the M06-2X-D3/Def2-QZVPP(SMD=MeCN) revealed that they were of a similar lateness, as indicated by their corresponding Wiberg bond orders (WBO) of 0.28-0.29 for the forming C–C bond and 0.90-0.93 for the breaking C–I bond. However, their corresponding C–I σ* Natural Bond Orbitals showed distinct electron occupancies of 0.105, 0.088, and 0.073, respectively. This is suggestive of delocalization from the linking heteroatom into the C–I σ* orbital during C–C bond formation, leading to greater energetic stabilization for *N*-alkyl-linked systems than for those linked by oxygen and sulfur. This phenomenon aligns with the linking atom's ability to delocalize into the aromatic π-system, thereby increasing its electron density. (An overlay of *ipso*-I and *ipso*-H transition structures is provided in Figure S26.)

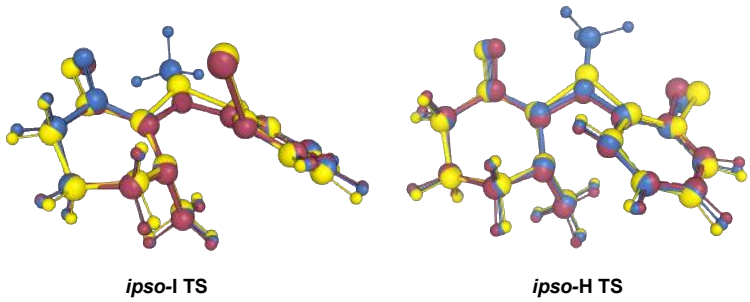
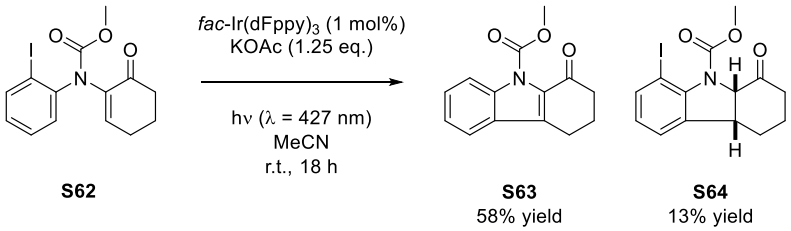


Figure S26. Overlay of transition structures for *ipso*-I cyclization (left) and *ipso*-H cyclization (right) for *N*-alkyl-linked (blue), *O*-linked (red) and *S*-linked (yellow) systems.

As described above, an *N*-carbamoyl-linked substrate **S62** cyclized with lower (albeit still moderately high) *ipso*-I selectivity relative to *N*-alkyl-linked substrates (Scheme S18). This finding further supports

our hypothesis that the linking heteroatom's capacity to donate into the C–I σ* orbital during C–C bond formation is a key determinant of selectivity.



Scheme S18. Irradiation of an *N*-carbamoyl-linked substrate (**S62**) gave a mixture of *ipso*-I (**S63**) and *ipso*-H (**S64**) cyclization products, enriched in the former.

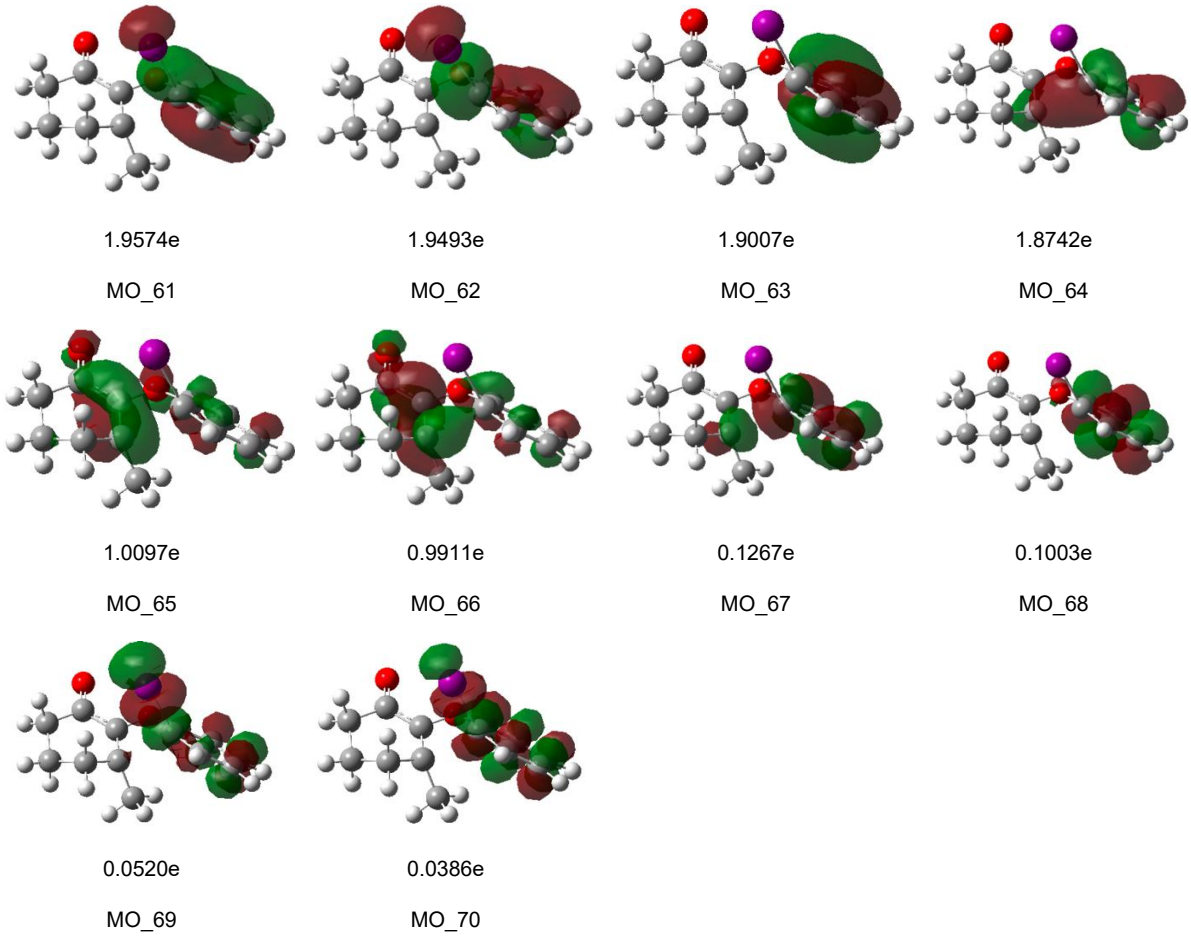


Figure S27. Molecular orbitals for structure **TS-IV** obtained with the NEVPT2:CASSCF(10,10)/Def2-TZVP(SMD=MeCN) method, visualized using an isovalue of 0.04 together with their corresponding electron occupancy.

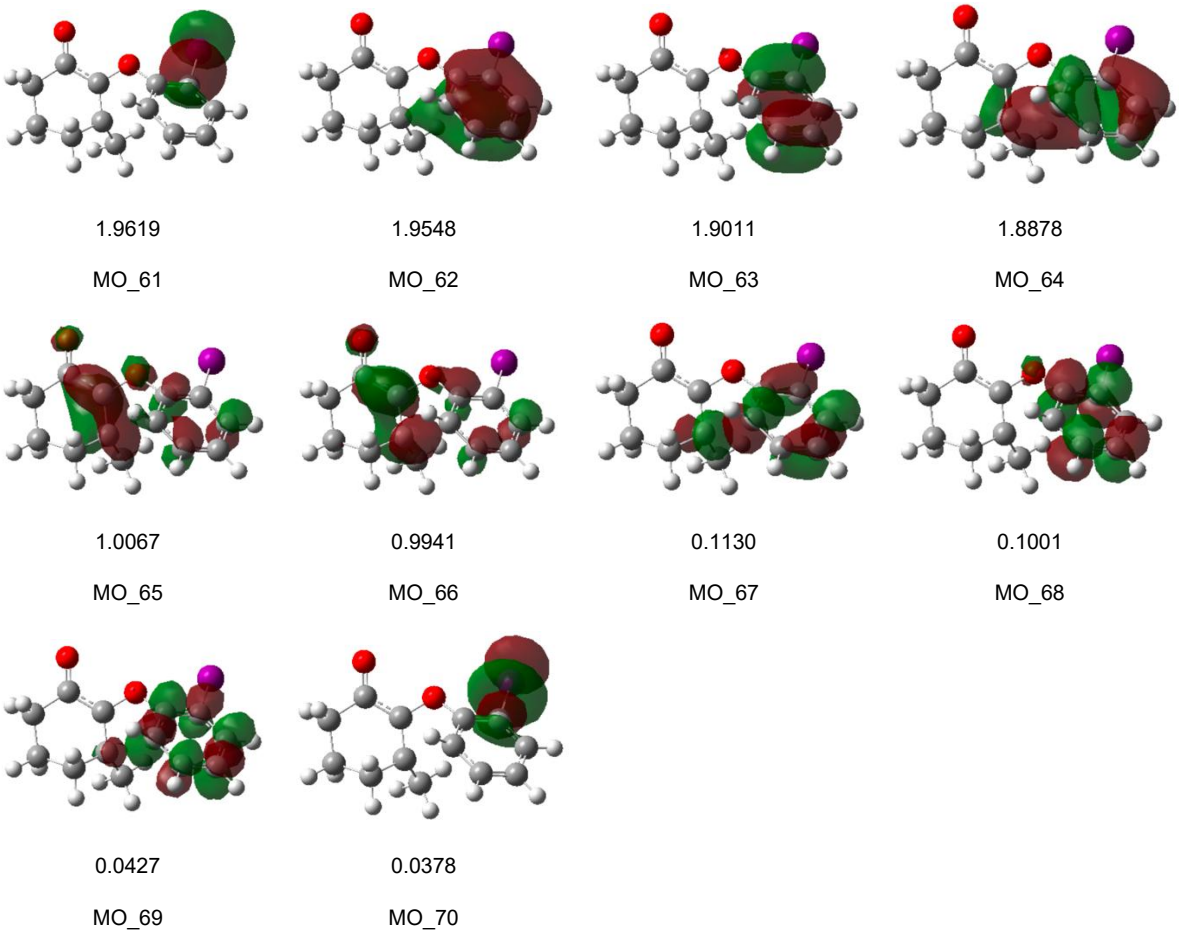


Figure S28. Molecular orbitals for structure **TS-V** obtained with the NEVPT2:CASSCF(10,10)/Def2-TZVP(SMD=MeCN) method, visualized using an isovalue of 0.04 together with their corresponding electron occupancy.

Table S15. Active space orbital correlation between **TS-IV** and **TS-V**.

TS-IV	**TS-V**
MO-61	MO-62
MO-62	MO-61
MO-63	MO-63
MO-64	MO-64
MO-65	MO-65
MO-66	MO-66
MO-67	MO-67
MO-68	MO-68
MO-69	MO-70
MO-70	MO-69

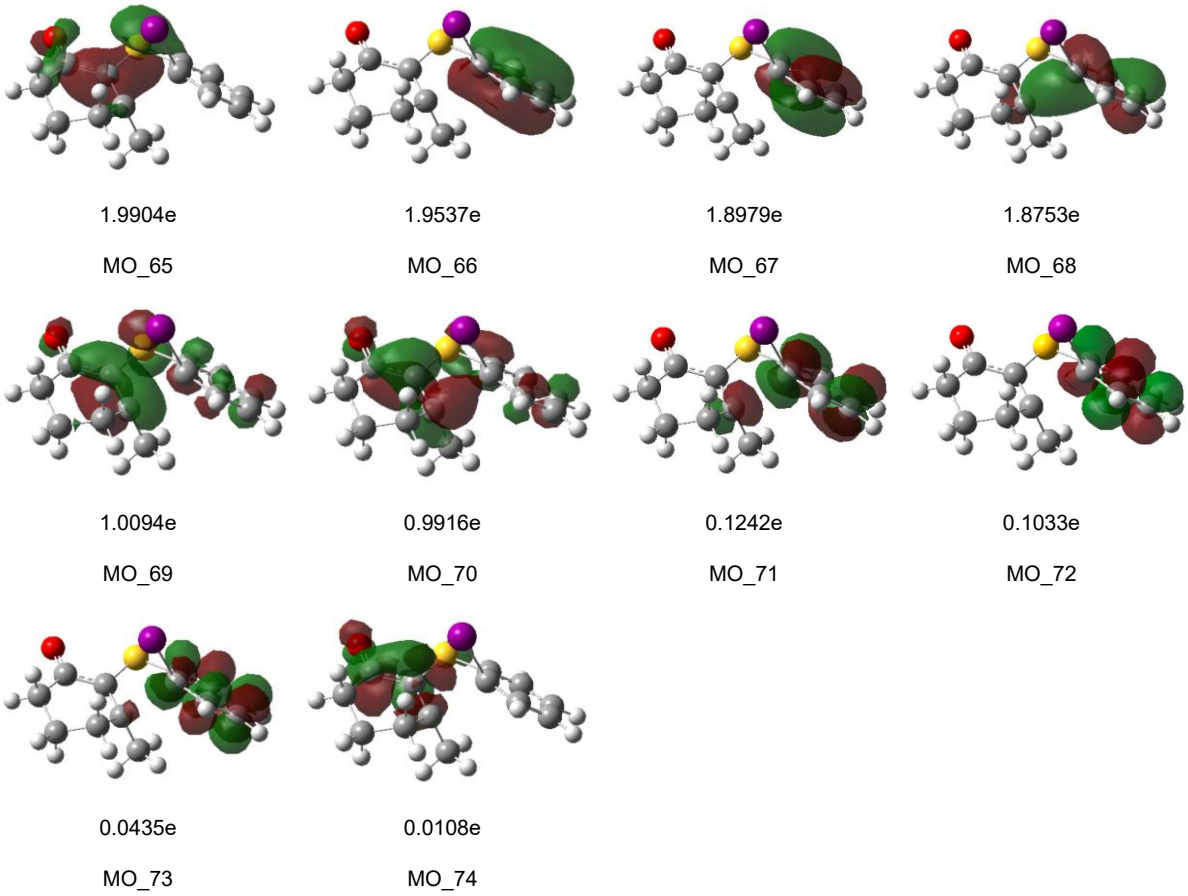


Figure S29. Molecular orbitals for structure **TS-VI** obtained with the NEVPT2:CASSCF(10,10)/Def2-TZVP(SMD=MeCN) method, visualized using an isovalue of 0.04 together with their corresponding electron occupancy.

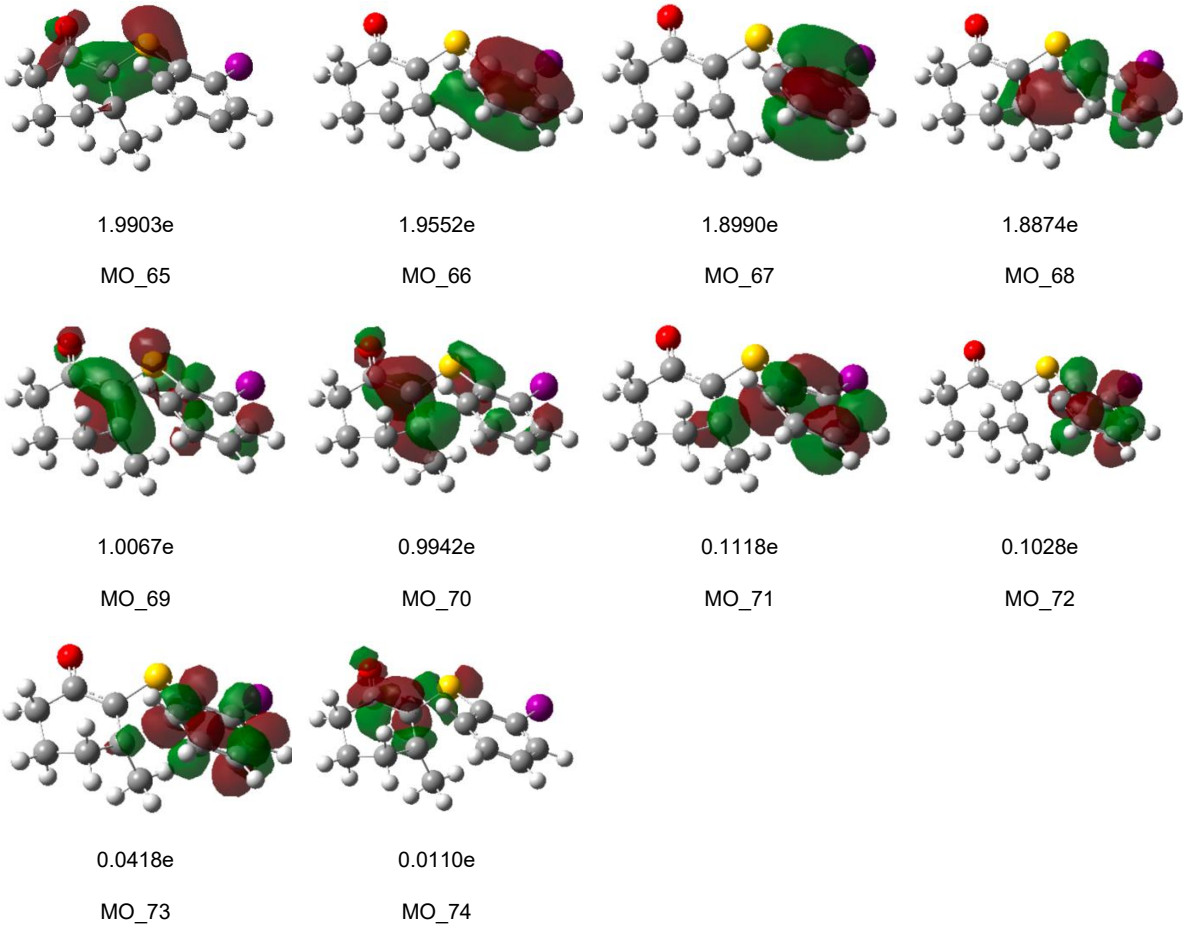


Figure S30. Molecular orbitals for structure **TS-VII** obtained with the NEVPT2:CASSCF(10,10)/Def2-TZVP(SMD=MeCN) method, visualized using an isovalue of 0.04 together with their corresponding electron occupancy.

Table S16. Active space orbital correlation between **TS-VI** and **TS-VII**.

TS-VI	**TS-VII**
MO-65	MO-65
MO-66	MO-66
MO-67	MO-67
MO-68	MO-68
MO-69	MO-69
MO-70	MO-70
MO-71	MO-71
MO-72	MO-72
MO-73	MO-73
MO-74	MO-74

S4.8. Modelling the asymmetric variant

Computational investigations were conducted at the M06-2X-D3/Def2-QZVPP(SMD=MeCN)//M06-2X-D3/Def2-TZVP(SMD=MeCN) level to further rationalize the observed regio- and enantioselectivity of the photocyclization of *ortho*-sulfinyl-substituted substrate **48** (Figure S31). These investigations revealed behaviour similar to the *ortho*-iodinated system. Specifically, cyclization at the *ortho*-position bearing the leaving group was computed to be favoured by 2.6 kcal/mol, which is consistent with the >19:1 regioselectivity observed experimentally. Furthermore, assuming (*R*)-stereochemistry at the sulfur atom, the computed chirality transfer step was found to be 2.8 kcal/mol in favour of forming the (*R*)-configured quaternary carbon stereocentre (a predicted 98% enantiospecificity). This prediction is consistent with the experimentally observed enantiomeric ratio of 96:4 measured for the product (taking into account the initial enantiomeric ratio of 98:2 measured for the starting material).

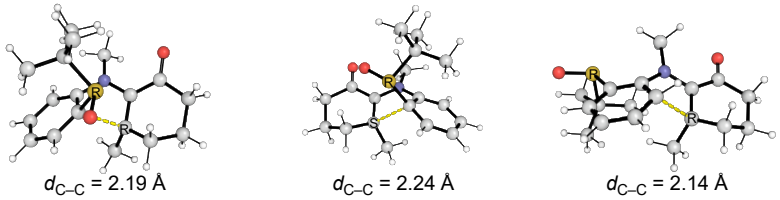


Figure S31. Computed diastereo- and regioselectivities for the photocyclization of substrate **48** computed at the M06-2X-D3/Def2-QZVPP(SMD=MeCN)//M06-2X-D3/Def2-TZVP(SMD=MeCN) level of theory.

S4.9. Alternative halogen leaving groups

The effect of the changing the halogen ('X') leaving group on the regiochemical course of the reaction was also investigated computationally, again at the M06-2X-D3/Def2-QZVPP(SMD=MeCN)//M06-2X-D3/Def2-TZVP(SMD=MeCN) level, which indicated that *ipso*-X selectivity decreases with increasing C–X bond strength, consistent with experimental observations (see Section S2.24). Further NBO analysis performed on the *ipso*-X cyclization transition structures reflects this trend: the NBO spin density on the halogen atom decreases from 0.13 e- in **TS-I** to 0.05 e- in **TS-I_Cl**, while the Wiberg bond order (WBO) of the breaking C–X bond increases from 0.90 to 0.98, respectively (Figure S32).

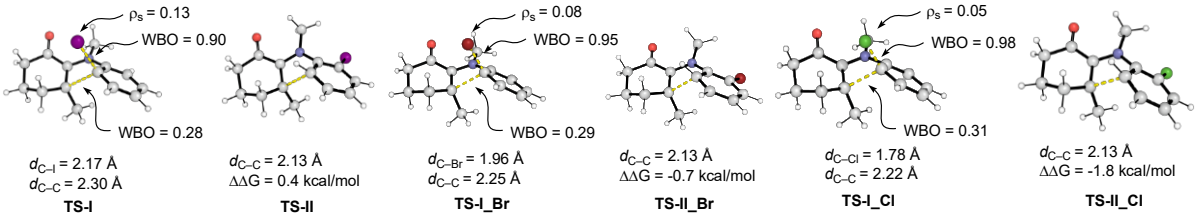
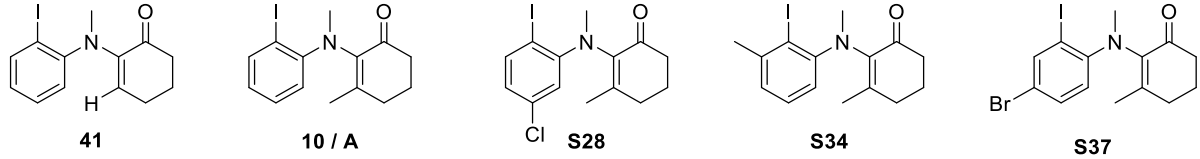


Figure S32. Comparison of photocyclization transition structures with iodine (**TS-I** and **TS-II**, left), bromine (**TS-I_Br** and **TS-II_Br**, middle), and chlorine (**TS-I_Cl** and **TS-II_Cl**, right) leaving groups, computed at the M06-2X-D3/Def2-QZVPP(SMD=MeCN)//M06-2X-D3/Def2-TZVP(SMD=MeCN) level of theory, including bond distances, Wiberg bond orders (WBO) and NBO spin densities.

S4.10. Adiabatic triplet energies of various substrates



41 TE = 48.1 kcal/mol

10 / A TE = 48.3 kcal/mol

S28 TE = 49.3 kcal/mol

S34 TE = 47.5 kcal/mol

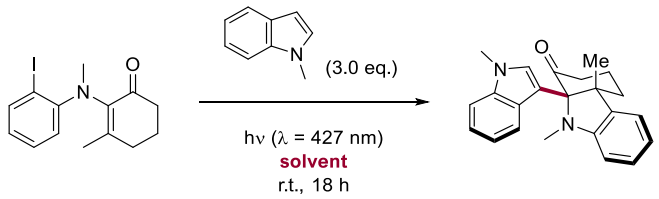
S37 TE = 49.2 kcal/mol

Figure S33. Computed adiabatic triplet energies (TE) for substrates **41**, **10**, **S28**, **S34** and **S37** at the M06-2X-D3/Def2-QZVPP//M06-2X-D3/Def2-TZVP level of theory.

S5. Reaction optimization data

Initial reaction optimization experiments were conducted with *fac*-Ir(dFppy)$_3$. However, it was quickly observed that when the HI by-product is not buffered – as in the case of β-substituted substrates irradiated in the presence of nucleophiles and without base – the reaction mixtures become coloured. This results in an insignificant difference in rate between reactions conducted (without base) in the presence and absence of a photosensitizer.

Table S17. Screening of conditions for the photocyclization of β-methyl substrate **10** in the presence of 1-methylindole.



10 **13**

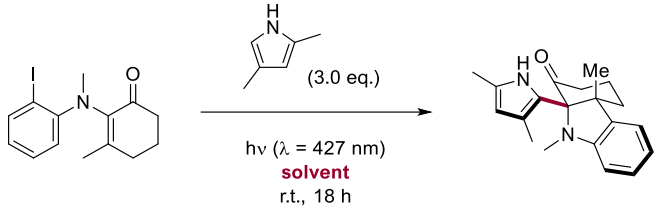
Entry	Solvent	Conversion[a] / %	Yield of **13** / %
1[b]	MeCN–TFE (9:1)	87	70
2[b]	MeCN–MeOH (9:1)	94	80
3[b]	MeCN–H_2O (9:1)	86	75
4[b,c]	MeCN–AcOH (9:1)	93	76

[a] Conversions and yields were measured by quantitative ^{1}H NMR spectroscopy against dimethyl terephthalate (0.25 eq.) unless otherwise stated.
[b] Reaction conditions (unless otherwise stated): **10** (0.1 mmol), 1-methylindole (0.3 mmol), solvent(s) (0.05 M), 1 x Kessil PR160L 427 nm LED lamp, r.t., Ar, 18 h; the end-of-reaction mixture was concentrated *in vacuo* after adding Et_3N (0.7 mL) in one portion.
[c] The end-of-reaction mixture was concentrated *in vacuo* without quenching the HI by-product.

5[b]	MeCN–HFIP (9:1)	>95%	85
6[b,c]	MeCN–HFIP (9:1)	>95%	84
7[d]	MeCN–HFIP (9:1)	-[e]	81[f]

[d] Reaction conditions: **10** (0.3 mmol), 1-methylindole (0.9 mmol), solvent(s) (0.05 M), 2 x Kessil PR160L 427 nm LED lamps, r.t., Ar, 18 h; the end-of-reaction mixture was concentrated *in vacuo* after adding Et_3N (2.0 mL) in one portion.
[e] Not determined.
[f] Isolated yield after flash column chromatography on alumina gel.

Table S18. Screening of conditions for the photocyclization of β-methyl substrate **10** in the presence of 2,4-dimethyl-1*H*-pyrrole.

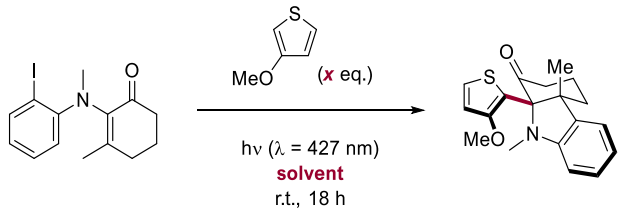


10 **15**

Entry	Solvent	Conversion[a] / %	Yield of **15** / %
1[b]	MeCN–HFIP (9:1)	>95	65
2[b]	MeCN–H_2O (9:1)	>95	69
3[b]	MeCN–TFE (9:1)	>95	61
4[c]	MeCN–H_2O (9:1)	-[d]	68[e]

[a] Conversions and yields were measured by quantitative ^{1}H NMR spectroscopy against dimethyl terephthalate (0.25 eq.) unless otherwise stated.
[b] Reaction conditions: **10** (0.1 mmol), 2,4-dimethyl-1*H*-pyrrole (0.3 mmol), solvent(s) (0.05 M), 1 x Kessil PR160L 427 nm LED lamp, r.t., Ar, 18 h; the end-of-reaction mixture was concentrated in vacuo after adding Et_3N (0.7 mL) in one portion.
[c] Reaction conditions: **10** (0.3 mmol), 2,4-dimethyl-1*H*-pyrrole (0.9 mmol), MeCN–H_2O (9:1) (0.05 M), 2 x Kessil PR160L 427 nm LED lamps, r.t., Ar, 18 h; the end-of-reaction mixture was concentrated in vacuo after adding Et_3N (2.0 mL) in one portion.
[d] Not determined.
[e] Isolated yield after flash column chromatography on alumina gel.

Table S19. Screening of conditions for the photocyclization of β-methyl substrate **10** in the presence of 3-methoxythiophene.

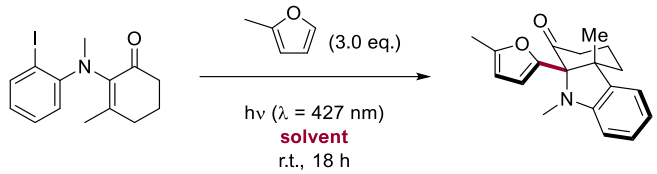


10 **16**

Entry	Solvent	*x* / eq.	Conversion[a] / %	Yield of **16** / %
1[b]	MeCN	3.0	72	30
2[b]	MeCN–H_2O (9:1)	3.0	>95	28
3[b]	MeCN–TFE (9:1)	3.0	92	34
4[b]	MeCN–HFIP (9:1)	3.0	92	35
5[b]	MeCN–HFIP (9:1)	5.0	89	44
6[c]	MeCN–HFIP (9:1)	5.0	-[d]	44[e]

[a] Conversions and yields were measured by quantitative ^{1}H NMR spectroscopy against dimethyl terephthalate (0.25 eq.) unless otherwise stated.
[b] Reaction conditions: **10** (0.1 mmol), 3-methoxythiophene (0.3 or 0.5 mmol), solvent(s) (0.05 M), 1 x Kessil PR160L 427 nm LED lamp, r.t., Ar, 18 h; the end-of-reaction mixture was concentrated *in vacuo* after adding Et_3N (0.7 mL) in one portion.
[c] Reaction conditions: **10** (0.3 mmol), 3-methoxythiophene (1.5 mmol), MeCN–HFIP (9:1) (0.05 M), 2 x Kessil PR160L 427 nm LED lamps, r.t., Ar, 18 h; the end-of-reaction mixture was concentrated *in vacuo* after adding Et_3N (2.0 mL) in one portion.
[d] Not determined.
[e] Isolated yield after flash column chromatography on alumina gel.

Table S20. Screening of conditions for the photocyclization of β-methyl substrate **10** in the presence of 2-methylfuran.

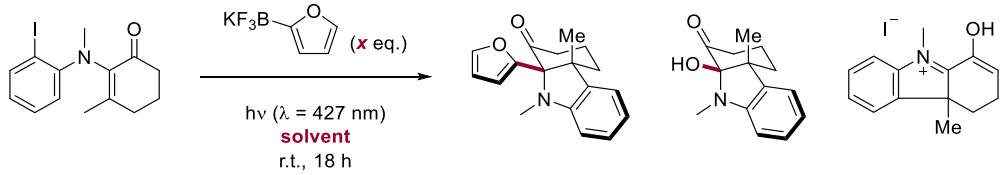


10 **17**

Entry	Solvent	Conversion[a] / %	Yield of **17** / %
1[b]	MeCN	75	40
2[b]	MeCN–H_2O (9:1)	>95	39
3[b]	MeCN–TFE (9:1)	86	52
4[b]	MeCN–HFIP (9:1)	91	56
5[c]	MeCN–HFIP (9:1)	-[d]	59[e]

[a] Conversions and yields were measured by quantitative ^{1}H NMR spectroscopy against dimethyl terephthalate (0.25 eq.) unless otherwise stated.
[b] Reaction conditions: **10** (0.1 mmol), 2-methylfuran (0.3 mmol), solvent(s) (0.05 M), 1 x Kessil PR160L 427 nm LED lamp, r.t., Ar, 18 h; the end-of-reaction mixture was concentrated *in vacuo* after adding Et_3N (0.7 mL) in one portion.
[c] Reaction conditions: **10** (0.3 mmol), 2-methylfuran (0.9 mmol), MeCN–HFIP (9:1) (0.05 M), 2 x Kessil PR160L 427 nm LED lamps, r.t., Ar, 18 h; the end-of-reaction mixture was concentrated *in vacuo* after adding Et_3N (2.0 mL) in one portion.
[d] Not determined.
[e] Isolated yield after flash column chromatography on alumina gel.

Table S21. Screening of conditions for the photocyclization of β-methyl substrate **10** in the presence of potassium furan-2-trifluoroborate.



10 **18** **11** **S74**

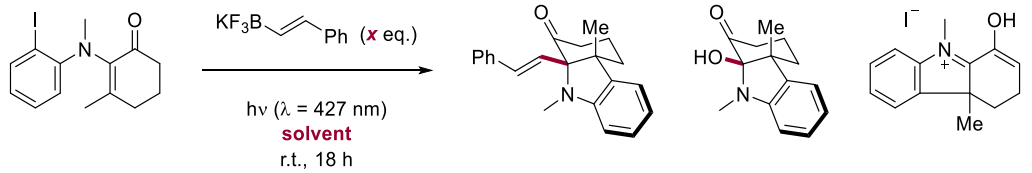
Entry	Solvent	*x* / eq.	Conversion[a] / %	Yield of **18** / %	Yield of hemiaminal **11** / %	Yield of **S74** / %
1[b]	MeCN	3.0	>95	31	n.d.[c]	n.d.
2[b]	$MeNO_2$	3.0	>95	40	n.d.	n.d.
3[b,d]	$MeNO_2$	3.0	>95	40	n.d.	n.d.
4[b]	MeCN–MeOH (9:1)	3.0	>95	44	7	n.d.
5[b]	MeCN–TFE (9:1)	3.0	>95	35	n.d.	n.d.

[a] Conversions and yields were measured by quantitative ^{1}H NMR spectroscopy against dimethyl terephthalate (0.25 eq.) unless otherwise stated.
[b] Reaction conditions (unless otherwise stated): **10** (0.1 mmol), potassium furan-2-trifluoroborate (0.15, 0.3 or 0.5 mmol), solvent(s) (0.05 M), 1 x Kessil PR160L 427 nm LED lamp, r.t., Ar, 18 h; the end-of-reaction mixture was concentrated *in vacuo* after adding Et_3N (0.7 mL) in one portion.
[c] Not detected.
[d] Reaction performed in the presence of CF_3COONa (1.0 eq.).

6[b]	MeCN–HFIP (9:1)	3.0	>95	*ca.* 30–40[e]	trace	n.d.
7[b]	MeCN–H_2O (9:1)	3.0	>95	59	10	trace
8[b]	MeCN–H_2O (9:1)	5.0	>95	38	12	trace
9[b]	MeCN–H_2O (9:1)	1.5	>95	52	17	trace
10[b,f]	MeCN–H_2O (9:1)	1.5	>95	53	14	trace
11[b]	MeCN–H_2O (19:1)	1.5	>95	44	19	trace
12[b]	MeCN–H_2O (3:1)	1.5	>95	45	11	15
13[b]	MeCN–H_2O (3:1)	3.0	>95	64	16	6
14[b]	MeCN–H_2O (1:1)	1.5	>95	35	10	21
15[b]	MeCN–H_2O (1:1)	3.0	>95	51	trace	8
16[g]	MeCN–H_2O (3:1)	3.0	-[h]	55[i]	-	-

[e] Signal overlap made accurate integration of ^{1}H resonances corresponding to this compound impossible.
[f] Reaction concentration, [**10**] = 0.1 M.
[g] Reaction conditions: **10** (0.3 mmol), potassium furan-2-trifluoroborate (0.9 mmol), MeCN–H_2O (3:1) (0.05 M), 2 x Kessil PR160L 427 nm LED lamps, r.t., Ar, 18 h; the end-of-reaction mixture was concentrated *in vacuo* after adding Et_3N (2.0 mL) in one portion.
[h] Not determined.
[i] Isolated yield after flash column chromatography on silica gel.

Table S22. Screening of conditions for the photocyclization of β-methyl substrate **10** in the presence of potassium *trans*-styryltrifluoroborate.



10 **19** **11** **S74**

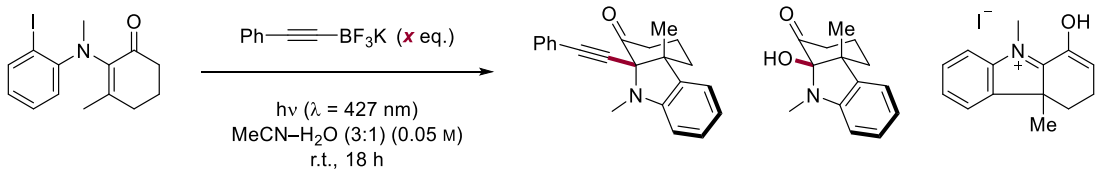
Entry	Solvent	*x* / eq.	Conversion[a] / %	Yield of **19** / %	Yield of hemiaminal **11** / %	Yield of **S74** / %
1[b]	MeCN–H_2O (9:1)	1.5	>95	53	trace	n.d.[c]
2[b]	MeCN–H_2O (3:1)	1.5	>95	67	n.d.	n.d.
3[b]	MeCN–H_2O (1:1)	1.5	>95	<50[d]	n.d.	n.d.
4[b]	MeCN–H_2O (3:1)	2.0	>95	44	38	n.d.
5[b]	MeCN–H_2O (3:1)	3.0	>95	n.d.	77	n.d.

[a] Conversions and yields were measured by quantitative 1H NMR spectroscopy against dimethyl terephthalate (0.25 eq.) unless otherwise stated.
[b] Reaction conditions: **10** (0.1 mmol), potassium *trans*-styryltrifluoroborate (0.15, 0.2 or 0.3 mmol), solvent(s) (0.05 M), 1 x Kessil PR160L 427 nm LED lamp, r.t., Ar, 18 h; the end-of-reaction mixture was concentrated *in vacuo* after adding Et_3N (0.7 mL) in one portion.
[c] Not detected.
[d] Signal overlap made accurate integration of ^1H resonances corresponding to this compound impossible; the quoted value represents an upper bound estimate.

6[e]	MeCN–H_2O (3:1)	1.5	-[f]	66[g]	-	-

[e] Reaction conditions: **10** (0.3 mmol), potassium *trans*-styryltrifluoroborate (0.45 mmol), MeCN–H_2O (3:1) (0.05 M), 2 x Kessil PR160L 427 nm LED lamp, r.t., Ar, 18 h; the end-of-reaction mixture was concentrated *in vacuo* after adding Et_3N (2.0 mL) in one portion.
[f] Not determined.
[g] Isolated yield after flash column chromatography on silica gel.

Table S23. Screening of conditions for the photocyclization of β-methyl substrate **10** in the presence of potassium (phenylethynyl)trifluoroborate.

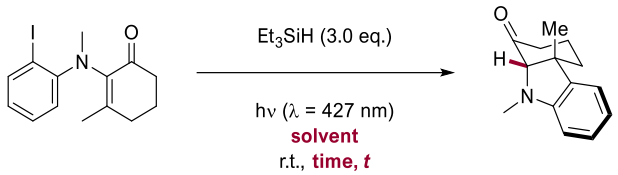


10 **20** **11** **S74**

Entry	Solvent	*x* / eq.	Conversion[a] / %	Yield of **20** / %	Yield of hemiaminal **11** / %	Yield of **S74** / %
1[b]	MeCN–H_2O (3:1)	1.5	90	51	n.d.[c]	n.d.
2[b]	MeCN–H_2O (3:1)	3.0	90	51	n.d.	n.d.
3[d]	MeCN–H_2O (3:1)	1.5	-[e]	53[f]	-	-

[a] Conversions and yields were measured by quantitative ^{1}H NMR spectroscopy against dimethyl terephthalate (0.25 eq.) unless otherwise stated.
[b] Reaction conditions: **10** (0.1 mmol), potassium (phenylethynyl)trifluoroborate (0.15 or 0.3 mmol), solvent(s) (0.05 M), 1 x Kessil PR160L 427 nm LED lamp, r.t., Ar, 18 h; the end-of-reaction mixture was concentrated *in vacuo* after adding Et_3N (0.7 mL) in one portion.
[c] Not detected.
[d] Reaction conditions: **10** (0.3 mmol), potassium (phenylethynyl)trifluoroborate (0.45 mmol), MeCN–H_2O (3:1) (0.05 M), 2 x Kessil PR160L 427 nm LED lamps, r.t., Ar, 18 h; the end-of-reaction mixture was concentrated *in vacuo* after adding Et_3N (2.0 mL) in one portion.
[e] Not determined.
[f] Isolated yield after flash column chromatography on silica gel.

Table S24. Screening of conditions for the photocyclization of β-methyl substrate **10** in the presence of triethylsilane.

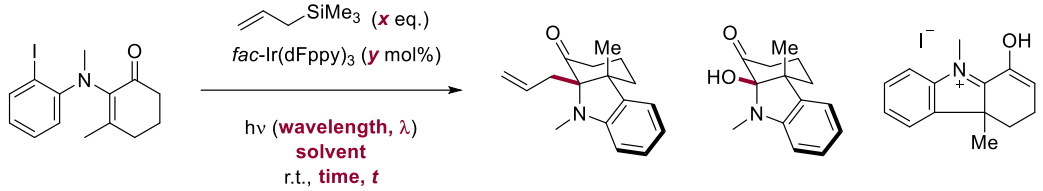


10 **21**

Entry	Solvent	*t* / h	Conversion[a] / %	Yield of **21** / %
1[b]	MeCN–HFIP (9:1)	3	>95	84
2[b]	MeCN–TFE (9:1)	3	>95	84[b]
3[b]	MeCN–H_2O (9:1)	3	>95	87[b]
4[c]	MeCN–H_2O (9:1)	6	-[d]	80[e]

[a] Conversions and yields were measured by quantitative ^{1}H NMR spectroscopy against dimethyl terephthalate (0.25 eq.) unless otherwise stated.
[b] Reaction conditions: **10** (0.1 mmol), triethylsilane (0.3 mmol), solvent(s) (0.05 M), 1 x Kessil PR160L 427 nm LED lamp, r.t., 3 h; the end-of-reaction mixture was concentrated *in vacuo* after adding Et_3N (0.7 mL) in one portion.
[c] Reaction conditions: **10** (0.3 mmol), triethylsilane (0.9 mmol), MeCN–H_2O (9:1) (0.05 M), 2 x Kessil PR160L 427 nm LED lamps, r.t., 6 h; the end-of-reaction mixture was concentrated *in vacuo* after adding Et_3N (2.0 mL) in one portion.
[d] Not determined.
[e] Isolated yield after flash column chromatography on silica gel.

Table S25. Screening of conditions for the photocyclization of β-methyl substrate **10** in the presence of allyltrimethylsilane.



Entry	*x* / eq.	*y* / mol%	λ / nm	Solvent	*t* / h	Conversion[a] / %	Yield of **23** / %
1[b]	3.0	1	440	MeCN	3	68	50
2[b]	3.0	1	440	DMF	3	>95	64
3[b]	3.0	1	440	DMSO-d_6	3	>95	trace[c]
4[b]	3.0	1	440	MeOH	3	94	34
5[b]	3.0	1	440	DMF–H_2O (9:1)	3	>95	n.d.[d,e]
6[b]	3.0	1	440	MeCN–H_2O (9:1)	3	94	70

[a] Conversions and yields were measured by quantitative ^{1}H NMR (qNMR) spectroscopy against dimethyl terephthalate (0.25 eq.) unless otherwise stated.
[b] Reaction conditions (unless otherwise stated): **10** (0.1 mmol), allyltrimethylsilane (0.3 or 0.5 mmol), *fac*-Ir(dFppy)$_3$ (0 or 1 μmol), solvent(s) (0.05 M), 1 x Kessil PR160L (or PR160) 440 or 427 nm LED lamp, r.t., Ar, 18 h; the end-of-reaction mixture was concentrated *in vacuo* without quenching the HI by-product.
[c] Hemiaminal **11** was formed as the major product in a qNMR yield of 54%.
[d] Not detected.
[e] Hemiaminal **11** and iminium iodide **S74** were obtained as the major products of this reaction.

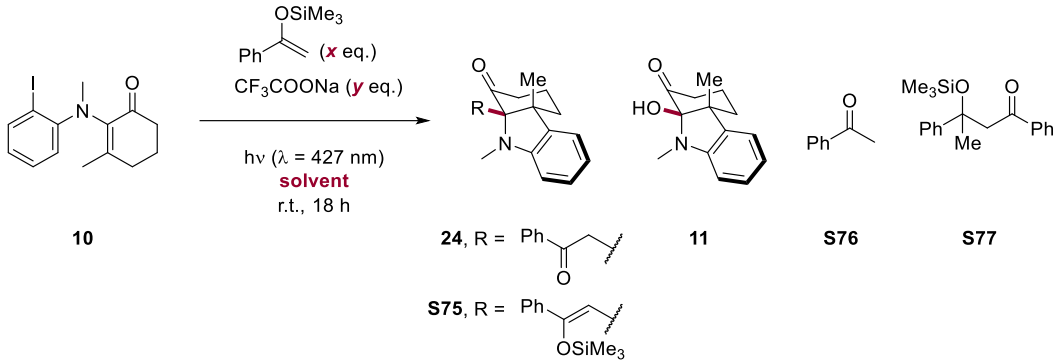
7[b]	3.0	1	440	MeCN–MeOH	3	92	69
8[b,f]	3.0	0	440	MeCN	6	48	33
9[b,f]	3.0	0	440	Me_2CO	6	53	19
10[b,f]	3.0	0	440	DCM	6	54	22
11[b,f]	3.0	0	440	DCM–MeOH (9:1)	6	69	45
12[b,f]	3.0	0	440	EtOAc	6	56	8
13[b,f]	3.0	0	440	MeCN–H_2O (9:1)	6	>95	62
14[b,f]	3.0	0	440	MeCN–MeOH (9:1)	6	76	59
15[b,f]	5.0	0	440	MeCN–MeOH (9:1)	16	>95	63
16[b,f]	5.0	0	440	MeCN–TFE (9:1)	16	86	71

[f] The end-of-reaction mixture was concentrated *in vacuo* after adding Et_3N (0.7 mL) in one portion.

17[b,f]	5.0	0	427	MeCN–TFE (9:1)	6	95	85
18[b,f]	5.0	0	427	MeCN–HFIP (9:1)	6	>95	78
19[b,f]	3.0	0	427	MeCN–TFE (9:1)	16	>95	80
20[g]	3.0	0	427	MeCN–TFE (9:1)	18	-[h]	69%[i]
21[g]	3.0	0	427	MeCN–HFIP (9:1)	18	-[h]	80%[i]

[g] Reaction conditions: **10** (0.3 mmol), allyltrimethylsilane (0.9 mmol), solvent(s) (0.05 M), 2 x Kessil PR160L 427 nm LED lamps, r.t., 18 h; the end-of-reaction mixture was concentrated *in vacuo* after adding Et_3N (2.0 mL) in one portion.
[h] Not determined.
[i] Isolated yield after flash column chromatography on silica gel.

Table S26. Screening of conditions for the photocyclization of β-methyl substrate **10** in the presence of 1-phenyl-1-trimethylsiloxyethylene.



Entry	*x* / eq.	Additive (*y* / eq.)	Solvent	Conversion / %	Yield of **24** (yield of **S75**[a]) / %	Yield of hemiaminal **11** / %	Yield of acetophenone, **S76** / %
1[b,c]	3.0	none	MeCN	82	n.d.[d] (n.d.)	trace	n.d.[e]
2[b,c]	3.0	none	MeCN–HFIP (9:1)	>95	n.d. (n.d.)	-[f]	98

[a] The ^{1}H NMR data of this compound has been assigned tentatively by analogy to that of the desired product **24**.
[b] Reaction conditions (unless otherwise stated): **10** (0.1 mmol), 1-phenyl-1-trimethylsiloxyethylene (0.3 or 0.5 mmol), additive (0 or 0.3 mmol), solvent(s) (0.05 M), 1 x Kessil PR160L 427 nm LED lamp, r.t., Ar, 18 h; the end-of-reaction mixture was concentrated *in vacuo* after adding Et_3N (0.7 mL) in one portion.
[c] Conversions and yields were measured by quantitative ^{1}H NMR (qNMR) spectroscopy against 1,3,5-trimethoxybenzene (0.33 eq.).
[d] Not detected.
[e] The Mukaiyama aldol product **S77** derived from acetophenone was formed in a qNMR yield of 50%.
[f] A complex mixture of products was obtained in which hemiaminal **11** was present in major amounts; signal overlap made accurate integration of ^{1}H resonances corresponding to this compound impossible.

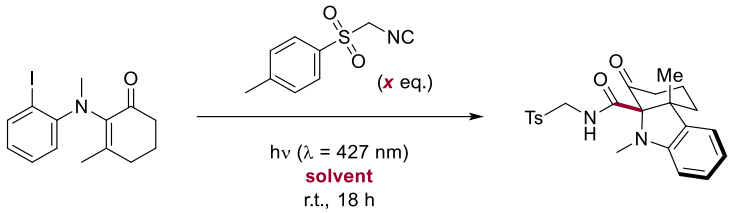
3[b,c]	3.0	none	MeCN–TFE (9:1)	81	n.d. (n.d.)	45	108
4[b,c]	3.0	none	MeCN–H_2O (9:1)	>95	n.d. (n.d.)	55	-[g]
5[b,c]	3.0	none	DMF	85	n.d. (n.d.)	trace	49
6[b,h]	3.0	CF_3COONa (1.0)	MeCN	94	26 (7)	trace	32
7[b,h]	5.0	CF_3COONa (1.0)	MeCN	94	10 (27)	trace	7
8[b,h,i]	3.0	CF_3COONa (1.0)	MeCN	93	29 (n.d.)	n.d.	184
9[b,h,i]	3.0	CF_3COONa (1.0)	MeCN–HFIP (9:1)	91	19 (n.d.)	n.d.	123
10[b,h,i]	3.0	CF_3COONa (1.0)	DMF	94	15 (n.d.)	n.d.	46

[g] Acetophenone (**S76**) was formed in relatively large quantities; ^{1}H resonances corresponding to this compound, however, could not be accurately integrated within TopSpin.
[h] Conversions and yields were measured by quantitative ^{1}H NMR spectroscopy against dimethyl terephthalate (0.25 eq.).
[i] The end-of-reaction mixture was concentrated *in vacuo* after adding MeOH (2.0 mL) and stirring at r.t. for 30 min.

11[b,h,i]	3.0	CF_3COONa (1.0)	$MeNO_2$	93	49 (n.d.)	n.d.	74
12[b,h,i]	5.0	CF_3COONa (1.0)	$MeNO_2$	95	49 (n.d.)	n.d.	265
13[j]	3.0	CF_3COONa (1.0)	$MeNO_2$	-[k]	57[l]	-	-

[j] Reaction conditions: **10** (0.3 mmol), 1-phenyl-1-trimethylsiloxyethylene (0.9 mmol), CF_3COONa (0.3 mmol), $MeNO_2$ (0.05 M), 2 x Kessil PR160L 427 nm LED lamp, r.t., Ar, 18 h; the end-of-reaction mixture was concentrated *in vacuo* after adding MeOH (6.0 mL) and stirring at r.t. for 30 min.
[k] Not determined.
[l] Isolated yield after flash column chromatography on silica gel.

Table S27. Screening of conditions for the photocyclization of β-methyl substrate **10** in the presence of *para*-toluenesulfonylmethyl isocyanide.

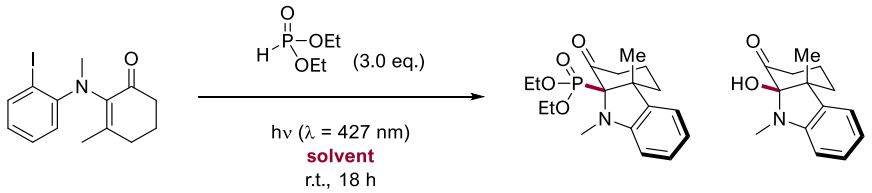


10 **25**

Entry	Solvent	*x* / eq.	Conversion[a] / %	Yield of **25** / %
1[b]	MeCN	3.0	77	25
2[b]	MeCN–HFIP (9:1)	3.0	88	33
3[b]	MeCN–H_2O (9:1)	5.0	>95	58
4[b]	MeCN–H_2O (19:1)	3.0	83	33
5[b]	MeCN–H_2O (9:1)	3.0	>95	56
6[c]	MeCN–H_2O (9:1)	3.0	-[d]	74%[e]

[a] Conversions and yields were measured by quantitative 1H NMR spectroscopy against dimethyl terephthalate (0.25 eq.) unless otherwise stated.
[b] Reaction conditions: **10** (0.1 mmol), *para*-toluenesulfonylmethyl isocyanide (0.3 mmol), solvent(s) (0.05 M), 1 x Kessil PR160L 427 nm LED lamp, r.t., Ar, 18 h; the end-of-reaction mixture was concentrated *in vacuo* after adding Et_3N (0.7 mL) in one portion.
[c] Reaction conditions: **10** (0.3 mmol), *para*-toluenesulfonylmethyl isocyanide (0.9 mmol), MeCN–H_2O (9:1) (0.05 M), 2 x Kessil PR160L 427 nm LED lamps, r.t., Ar, 18 h; the end-of-reaction mixture was concentrated *in vacuo* after adding Et_3N (2.0 mL) in one portion.
[d] Not determined.
[e] Isolated yield after flash column chromatography on silica gel.

Table S28. Screening of conditions for the photocyclization of β-methyl substrate **10** in the presence of diethyl phosphonate.



10 **26** **11**

Entry	Solvent	Conversion[a] / %	Yield of **26** / %	Diastereomeric ratio (d.r.) of **26**	Yield of hemiaminal **11** / %
1[b]	MeCN	>95	40	1.0 : 2.1	26
2[b]	MeCN–TFE (9:1)	>95	48	1.0 : 1.4	20
3[b]	MeCN–HFIP (9:1)	>95	49	1.0 : 2.1	16
4[b]	MeCN–H_2O (9:1)	>95	53	>19.0 : 1.0	19
5[b]	MeCN–H_2O (3:1)	>95	31	>19.0 : 1.0	30
6[b]	MeCN–H_2O (19:1)	>95	75	4.0 : 1.0	7

[a] Conversions and yields were measured by quantitative ^{1}H NMR spectroscopy against dimethyl terephthalate (0.25 eq.) unless otherwise stated.
[b] Reaction conditions: **10** (0.1 mmol), diethyl phosphonate (0.3 mmol), solvent(s) (0.05 M), 1 x Kessil PR160L 427 nm LED lamp, r.t., Ar, 18 h; the end-of-reaction mixture was concentrated *in vacuo* after adding Et_3N (0.7 mL) in one portion.

7[c]	MeCN–H_2O (9:1)	-[d]	57[e]	>19.0 : 1.0	-

[c] Reaction conditions: **10** (0.3 mmol), diethyl phosphonate (0.9 mmol), MeCN–H_2O (9:1) (0.05 M), 2 x Kessil PR160L 427 nm LED lamp, r.t., Ar, 18 h; the end-of-reaction mixture was concentrated *in vacuo* after adding Et_3N (0.7 mL) in one portion.
[d] Not determined.
[e] Isolated yield after flash column chromatography on silica gel.

S6. Supplemental references

[S1]. Cosier, J., and Glazer, A. M. (1986). A nitrogen-gas-stream cryostat for general X-ray diffraction studies. J. Appl. Cryst. *19*, 105–107. https://doi.org/10.1107/S0021889886089835.

[S2]. Parois, P., Cooper, R. I., and Thompson, A. L. (2015). Crystal structures of increasingly large molecules: meeting the challenges with CRYSTALS software. Chem. Cent. J. *9*, 30. https://doi.org/10.1186/s13065-015-0105-4.

[S3]. Cooper, R. I., Thompson, A. L., and Watkin, D. J. (2010). CRYSTALS enhancements: dealing with hydrogen atoms in refinement. J. Appl. Cryst. *43*, 1100–1107. https://doi.org/10.1107/S0021889810025598.

[S4]. Palatinus, L., and Chapuis, G. (2007). SUPERFLIP - a computer program for the solution of crystal structures by charge flipping in arbitrary dimensions. J. Appl. Cryst. *40*, 786–790. https://doi.org/10.1107/S0021889807029238.

[S5]. Wei, Z., Jing, X., Yang, Y., Yuan, J., Liu, M., He, C., and Duan, C. (2023). A Platinum(II)-Based Molecular Cage with Aggregation-Induced Emission for Enzymatic Photocyclization of Alkynylaniline. Angew. Chem. Int. Ed. *62*, e202214577. https://doi.org/10.1002/anie.202214577.

[S6]. Ohashi, M., Takahashi, T., Inoue, S., and Sato, K. (1975). The Mannich Reaction of Alicyclic α-Diketones. A Novel Synthesis of 2-Hydroxy-3-methyl-2-cyclohexen-1-one. Bull. Chem. Soc. Jpn. *48*, 1892–1896. https://doi.org/10.1246/bcsj.48.1892.

[S7]. Li, Y., Zhang, R., Bi, X., and Fu, J. (2018). Multifunctionalization of Unactivated Cyclic Ketones via Synergistic Catalysis of Copper and Diarylamine: Access to Cyclic α-Enaminone. Org. Lett. *20*, 1207–1211. https://doi.org/10.1021/acs.orglett.8b00125.

[S8]. Shi, H., Guo, T., Zhang-Negrerie, D., Du, Y., and Zhao, K. (2014). Synthesis of substituted tetrahydron-1H-carbazol-1-one and analogs via PhI(OCOCF3)2-mediated oxidative C–C bond formation. Tetrahedron *70*, 2753–2760. https://doi.org/10.1016/j.tet.2014.02.083.

[S9]. Laursen, S. R., Jensen, M. T., Lindhardt, A. T., Jacobsen, M. F., and Skrydstrup, T. (2016). A Palladium-Catalyzed Double Carbonylation Approach to Isatins from 2-Iodoanilines. Eur. J. Org. Chem. *2016*, 1881–1885. https://doi.org/10.1002/ejoc.201600143.

[S10]. Kotha, S., Saifuddin, M., and Aswar, V. R. (2016). A diversity-oriented approach to indolocarbazoles via Fischer indolization and olefin metathesis: total synthesis of tjipanazole D and I. Org. Biomol. Chem. *14*, 9868–9873. https://doi.org/10.1039/c6ob01679k.

[S11]. Schultz, A. G., and Chiu, I.-C. (1978). Heteroatom directed photoarylation; an approach to the synthesis of Aspidosperma alkaloids. J. Chem. Soc., Chem. Commun. 29. https://doi.org/10.1039/c39780000029.

[S12]. Zhou, P.-X., Zhou, Z.-Z., Chen, Z.-S., Ye, Y.-Y., Zhao, L.-B., Yang, Y.-F., Xia, X.-F., Luo, J.-Y., and Liang, Y.-M. (2013). Palladium-catalyzed insertion of α-diazocarbonyl compounds for the synthesis of cyclic amino esters. Chem. Commun. *49*, 561–563. https://doi.org/10.1039/C2CC37464A.

[S13]. Zhang, Y., and Silverman, R. B. (2012). Direct Amination of γ-Halo-β-ketoesters with Anilines. J. Org. Chem. *77*, 3462–3467. https://doi.org/10.1021/jo300239e.

[S14]. Lizos, D. E., and Murphy, J. A. (2003). Concise synthesis of (±)-horsfiline and (±)-coerulescine by tandem cyclisation of iodoaryl alkenyl azides. Org. Biomol. Chem. *1*, 117–122. https://doi.org/10.1039/b208114h.

[S15]. Molander, G. A., Canturk, B., and Kennedy, L. E. (2009). Scope of the Suzuki-Miyaura Cross-Coupling Reactions of Potassium Heteroaryltrifluoroborates. J. Org. Chem. *74*, 973–980. https://doi.org/10.1021/jo802590b.

[S16]. Borrel, J., and Waser, J. (2022). Tosyloxybenziodoxolone: A Platform for Performing the Umpolung of Alkynes in One-Pot Transformations. Org. Lett. *24*, 142–146. https://doi.org/10.1021/acs.orglett.1c03771.

[S17]. Khan, I., Reed-Berendt, B. G., Melen, R. L., and Morrill, L. C. (2018). FLP-Catalyzed Transfer Hydrogenation of Silyl Enol Ethers. Angew. Chem. Int. Ed. *57*, 12356–12359. https://doi.org/10.1002/anie.201808800.

[S18]. Popp, T. A., and Bracher, F. (2015). N-Methylation of Aromatic Amines and N-Heterocycles under Acidic Conditions with the TTT (1,3,5-Trioxane–Triethylsilane–Trifluoroacetic Acid) System. Synthesis *47*, 3333–3338. https://doi.org/10.1055/S-0034-1381049.

[S19]. Arnould, J. C., Cossy, J., and Pete, J. P. (1980). Reactivite photochimique des α-aminoenones: reactions de cyclisation et nouveau type de reaction dans les α-sulfonamido-cyclohexenones. Tetrahedron *36*, 1585–1592. https://doi.org/10.1016/S0040-4020(01)83126-4.

[S20]. Itoh, T., and Mase, T. (2004). A General Palladium-Catalyzed Coupling of Aryl Bromides/Triflates and Thiols. Org. Lett. *6*, 4587–4590. https://doi.org/10.1021/ol047996t.

[S21]. Pitchen, P., Dunach, E., Deshmukh, M. N., and Kagan, H. B. (1984). An Efficient Asymmetric Oxidation of Sulfides to Sulfoxides. J. Am. Chem. Soc. *106*, 8188–8193. https://doi.org/10.1021/ja00338a030.

[S22]. Guo, Y.-Q., Chen, F., Deng, C.-L., and Zhang, X.-G. (2021). Iodine-promoted ring-opening methylation of benzothiazoles with dimethyl sulfite. Chem. Commun. *57*, 1923–1926. https://doi.org/10.1039/D0CC08096A.

[S23]. Miyakoshi, T., Niggli, N. E., and Baudoin, O. (2022). Remote Construction of N-Heterocycles via 1,4-Palladium Shift-Mediated Double C−H Activation. Angew. Chem. Int. Ed. *61*, e202116101. https://doi.org/10.1002/anie.202116101.

[S24]. Münster, N., Parker, N. A., van Dijk, L., Paton, R. S., and Smith, M. D. (2017). Visible Light Photocatalysis of 6π Heterocyclization. Angew. Chem. Int. Ed. 56, 9468–9472. https://doi.org/10.1002/anie.201705333.

[S25]. Yates, P., and Langford, G. E. (1981). Synthesis of some bicyclo[2.2.2]oct-5-en-2-ones and bicyclo[2.2.2]octan-2-ones. Rearrangements accompanying oxidative decarboxylation with lead tetraacetate. Can. J. Chem. *59*, 344–355. https://doi.org/10.1139/v81-054.

[S26]. Duhail, T., Zhu, M., Rombault, C., Dagousset, G., Messaoudi, S., Magnier, E., and Anselmi, E. (2022). Dual Photocatalysis for the Straightforward Coupling of Thiosugars and Arylsulfoximines: Towards Unprecedented Cyclic Heteroatomic Structures. Eur. J. Org. Chem. *2022*, e202200173. https://doi.org/10.1002/ejoc.202200173.

[S27]. Dounay, A. B., Humphreys, P. G., Overman, L. E. and Wrobleski, A. D. (2008). Total Synthesis of the Strychnos Alkaloid (+)-Minfiensine: Tandem Enantioselective Intramolecular Heck−Iminium Ion Cyclization. J. Am. Chem. Soc. *130*, 5368–5377 https://doi.org/10.1021/ja800163v.

[S28]. Pavlishchuk, V. V., and Addison, A. W. (2000). Conversion constants for redox potentials measured versus different reference electrodes in acetonitrile solutions at 25°C. Inorg. Chim. Acta *298*, 97–102. https://doi.org/10.1016/S0020-1693(99)00407-7.

[S29]. Singh, A., Teegardin, K., Kelly, M., Prasad, K. S., Krishnan, S., and Weaver, J. D. (2015). Facile synthesis and complete characterization of homoleptic and heteroleptic cyclometalated Iridium(III) complexes for photocatalysis. J. Organomet. Chem. *776*, 51–59. https://doi.org/10.1016/j.jorganchem.2014.10.037.

[S30]. Turro, N. J., Ramamurthy, V., and Scaiano, J. (2010). Is Evidence for Oxygen Quenching of a Reaction Good Evidence for Triplet Involvement? In Modern Molecular Photochemistry of Organic Molecules, University Science Books, pp. 1039–1040.

[S31]. Görner, H. (1989). Phosphorescence of trans-Stilbene, Stilbene Derivatives, and Stilbene-like Molecules at 77 K. J. Phys. Chem. *93*, 1826–1832. https://doi.org/10.1021/j100342a027.

[S32]. Schenk, R., Gregorius, H., Meerholz, K., Heinze, J., and Müllen, K. (1991). Novel Oligo(phenylenevinylenes): Models for the Charging of Extended π Chains. J. Am. Chem. Soc. *113*, 2634–2647. https://doi.org/10.1021/ja00007a042.

[S33]. Rohrbach, S., Shah, R. S., Tuttle, T., and Murphy, J. A. (2019). Neutral Organic Super Electron Donors Made Catalytic. Angew. Chem. Int. Ed. *58*, 11454–11458. https://doi.org/10.1002/anie.201905814.

[S34]. Lim, C.-H., Ilic, S., Alherz, A., Worrell, B. T., Bacon, S. S., Hynes, J. T., Glusac, K. D., and Musgrave, C. B. (2019). Benzimidazoles as Metal-Free and Recyclable Hydrides for CO2 Reduction to Formate. J. Am. Chem. Soc. *141*, 272–280. https://doi.org/10.1021/jacs.8b09653.

[S35]. Kuhn, H. J., Braslavsky, S. E., and Schmidt, R. (1989). Chemical actinometry. Pure Appl. Chem. *61*, 187–210. https://doi.org/10.1351/pac198961020187.

[S36]. Alegria, A. E., Krishna, C. M., Elespuru, R. K., and Riesz, P. (1989). An ESR study of the visible light photochemistry of gilvocarcin V. Photochem. Photobiol. *49*, 257–265. https://doi.org/10.1111/j.1751-1097.1989.tb04104.x.

[S37]. Wolff, T., and Waffenschmidt, R. (1980). Studies on the Reaction Mechanism of the Photocyclization of N-Aryl Enamines. Dependence of Quantum Yields on Back and Side Reactions. J. Am. Chem. Soc. *102*, 6098–6102. https://doi.org/10.1021/ja00539a021.

[S38]. Cismesia, M. A., and Yoon, T. P. (2015). Characterizing chain processes in visible light photoredox catalysis. Chem. Sci. *6*, 5426–5434. https://doi.org/10.1039/C5SC02185E.

[S39]. Singleton, D. A., and Thomas, A. A. (1995). High-Precision Simultaneous Determination of Multiple Small Kinetic Isotope Effects at Natural Abundance. J. Am. Chem. Soc. *117*, 9357–9358. https://doi.org/10.1021/ja00141a030.

[S40]. Paton, R. S. (2022). Kinisot: v2.0.1. Zenodo. https://doi.org/10.5281/zenodo.595243.

[S41]. Zhao, Y., and Truhlar, D. G. (2008). The M06 suite of density functionals for main group thermochemistry, thermochemical kinetics, noncovalent interactions, excited states, and transition elements: two new functionals and systematic testing of four M06-class functionals and 12 other functionals. Theor. Chem. Acc. *120*, 215–241. https://doi.org/10.1007/s00214-007-0310-x.

[S42]. Weigend, F., and Ahlrichs, R. (2005). Balanced basis sets of split valence, triple zeta valence and quadruple zeta valence quality for H to Rn: Design and assessment of accuracy. Phys. Chem. Chem. Phys. *7*, 3297–3305. https://doi.org/10.1039/b508541a.

[S43]. Weigend, F. (2006). Accurate Coulomb-fitting basis sets for H to Rn. Phys. Chem. Chem. Phys. *8*, 1057–1065. https://doi.org/10.1039/b515623h.

[S44]. Grimme, S., Antony, J., Ehrlich, S., and Krieg, H. (2010). A consistent and accurate ab initio parametrization of density functional dispersion correction (DFT-D) for the 94 elements H-Pu. J. Chem. Phys. *132*, 154104. https://doi.org/10.1063/1.3382344.

[S45]. Alegre-Requena, J. V., Sowndarya S. V., S., Pérez-Soto, R., Alturaifi, T. M., and Paton, R. S. (2023). AQME: Automated quantum mechanical environments for researchers and educators. WIREs Comput. Mol. Sci. *13*, e1663. https://doi.org/10.1002/wcms.1663.

[S46]. Marenich, A. V., Cramer, C. J., and Truhlar, D. G. (2009). Universal Solvation Model Based on Solute Electron Density and on a Continuum Model of the Solvent Defined by the Bulk Dielectric Constant and Atomic Surface Tensions. J. Phys. Chem. B *113*, 6378–6396. https://doi.org/10.1021/jp810292n.

[S47]. Frisch, M. J., Trucks, G. W., Schlegel, H. B., Scuseria, G. E., Robb, M. A., Cheeseman, J. R., Scalmani, G., Barone, V., Petersson, G. A., Nakatsuji, H., et al. (2016). Gaussian 16, Revision C.01.

[S48]. Neese, F. (2012). The ORCA program system. WIREs Comput. Mol. Sci. *2*, 73–78. https://doi.org/10.1002/wcms.81.

[S49]. Havenith, R. W. A., Taylor, P. R., Angeli, C., Cimiraglia, R., and Ruud, K. (2004). Calibration of the n-electron valence state perturbation theory approach. J. Chem. Phys. *120*, 4619–4625. https://doi.org/10.1063/1.1645243.

[S50]. Angeli, C., Cimiraglia, R., Evangelisti, S., Leininger, T., and Malrieu, J.-P. (2001). Introduction of n-electron valence states for multireference perturbation theory. J. Chem. Phys. *114*, 10252–10264. https://doi.org/10.1063/1.1361246.

[S51]. Angeli, C., Cimiraglia, R., and Malrieu, J.-P. (2001). N-electron valence state perturbation theory: a fast implementation of the strongly contracted variant. Chem. Phys. Lett. *350*, 297–305. https://doi.org/10.1016/S0009-2614(01)01303-3.

[S52]. Snyder, J. D., Hamill, L.-A., Faleumu, K. E. and Ess, D. H. (2019). MECPro Version 1.0.5: Minimum Energy Crossing Program.

[S53]. Glendening, E. D., Landis, C. R., and Weinhold, F. (2013). NBO 6.0: Natural Bond Orbital Analysis Program. J. Comput. Chem. *34*, 1429–1437. https://doi.org/10.1002/jcc.23266.

[S54]. The PyMOL Molecular Graphics System, Version 2.0.7.

[S55]. Luchini, G., Alegre-Requena, J. V., Funes-Ardoiz, I., and Paton, R. S. (2020). GoodVibes: automated thermochemistry for heterogeneous computational chemistry data. F1000Research *9*, 291. https://doi.org/10.12688/f1000research.22758.1.

[S56]. Fukui, K. (1981). The Path of Chemical Reactions – The IRC Approach. (1981). Acc. Chem. Res. *14*, 363–368. https://doi.org/10.1021/ar00072a001.

[S57]. Grimme, S. (2012). Supramolecular Binding Thermodynamics by Dispersion-Corrected Density Functional Theory. Chem. Eur. J. *18*, 9955–9964. https://doi.org/10.1002/chem.201200497.

[S58]. Bryantsev, V. S., Diallo, M. S., and Goddard III, W. A. (2008). Calculation of Solvation Free Energies of Charged Solutes Using Mixed Cluster/Continuum Models. J. Phys. Chem. B *112*, 9709–9719. https://doi.org/10.1021/jp802665d.

[S59]. Plata, R. E., and Singleton, D. A. (2015). A Case Study of the Mechanism of Alcohol-Mediated Morita Baylis–Hillman Reactions. The Importance of Experimental Observations. J. Am. Chem. Soc. *137*, 3811–3826. https://doi.org/10.1021/ja5111392.

[S60]. Grimme, S. (2006). Semiempirical GGA-Type Density Functional Constructed with a Long-Range Dispersion Correction. J. Comput. Chem. *27*, 1787–1799. https://doi.org/10.1002/jcc.20495.

[S61]. Becke, A. D. (1993). Density-functional thermochemistry. III. The role of exact exchange. J. Chem. Phys. *98*, 5648–5652. https://doi.org/10.1063/1.464913.

[S62]. Stephens, P. J., Devlin, F. J., Chabalowski, C. F., and Frisch, M. J. (1994). Ab Initio Calculation of Vibrational Absorption and Circular Dichroism Spectra Using Density Functional Force Fields. J. Phys. Chem. *98*, 11623–11627. https://doi.org/10.1021/j100096a001.

[S63]. Vosko, S. H., Wilk, L., and Nusair, M. (1980). Accurate spin-dependent electron liquid correlation energies for local spin density calculations: a critical analysis. Can. J. Phys. *58*, 1200–1211. https://doi.org/10.1139/p80-159.

[S64]. Lee, C., Yang, W., and Parr, R. G. (1988). Development of the Colle-Salvetti correlation-energy formula into a functional of the electron density. Phys. Rev. B *37*, 785–789. https://doi.org/10.1103/PhysRevB.37.785.

[S65]. Chai, J.-D., and Head-Gordon, M. (2008). Long-range corrected hybrid density functionals with damped atom–atom dispersion corrections. Phys. Chem. Chem. Phys. *10*, 6615–6620. https://doi.org/10.1039/b810189b.

[S66]. Yanai, T., Tew, D. P., and Handy, N. C. (2004). A new hybrid exchange–correlation functional using the Coulomb-attenuating method (CAM-B3LYP). Chem. Phys. Lett. 393, 51–57. https://doi.org/10.1016/j.cplett.2004.06.011.

[S67]. Vydrov, O. A., Scuseria, G. E., and Perdew, J. P. (2007). Tests of functionals for systems with fractional electron number. J. Chem. Phys. *126*, 154109. https://doi.org/10.1063/1.2723119.

[S68]. Vydrov, O. A., and Scuseria, G. E. (2006). Assessment of a long-range corrected hybrid functional. J. Chem. Phys. *125*, 234109. https://doi.org/10.1063/1.2409292.

[S69]. Vydrov, O. A., Heyd, J., Krukau, A. V., and Scuseria, G. E. (2006). Importance of short-range versus long-range Hartree-Fock exchange for the performance of hybrid density functionals. J. Chem. Phys. *125*, 074106. https://doi.org/10.1063/1.2244560

[S70]. Henderson, T. M., Izmaylov, A. F., Scalmani, G., and Scuseria, G. E. (2009). Can short-range hybrids describe long-range-dependent properties? J. Chem. Phys. *131*, 044108. https://doi.org/10.1063/1.3185673.

[S71]. St. John, P. C., Guan, Y., Kim, Y., Kim, S., and Paton, R. S. (2020). Prediction of organic homolytic bond dissociation enthalpies at near chemical accuracy with sub-second computational cost. Nat. Commun. *11*, 2328. https://doi.org/10.1038/s41467-020-16706-7.

[S72]. Zhao, Y., and Truhlar, D. G. (2008). How Well Can New-Generation Density Functionals Describe the Energetics of Bond-Dissociation Reactions Producing Radicals? J. Phys. Chem. A *112*, 1095–1099. https://doi.org/10.1021/jp7109127.

[S73]. Marcus, R. A. (1957). On the Theory of Oxidation-Reduction Reactions Involving Electron Transfer. III. Applications to Data on the Rates of Organic Redox Reactions. J. Chem. Phys. *26*, 872–877. https://doi.org/10.1063/1.1743424.

[S74]. Marcus, R. A. (1957). On the Theory of Oxidation-Reduction Reactions Involving Electron Transfer. II. Applications to Data on the Rates of Isotopic Exchange Reactions. J. Chem. Phys. *26*, 867–871. https://doi.org/10.1063/1.1743423.

[S75]. Marcus, R. A. (1963). ON THE THEORY OF OXIDATION–REDUCTION REACTIONS INVOLVING ELECTRON TRANSFER. V. COMPARISON AND PROPERTIES OF ELECTROCHEMICAL AND CHEMICAL RATE CONSTANTS. J. Phys. Chem. *67*, 853–857. https://doi.org/10.1021/j100798a033.

[S76]. Marcus, R. A. (1965). On the Theory of Electron-Transfer Reactions. VI. Unified Treatment for Homogeneous and Electrode Reactions. J. Chem. Phys. *43*, 679–701. https://doi.org/10.1063/1.1696792.

[S77]. Marcus, R. A. (1964). Chemical and Electrochemical Electron-Transfer Theory. Annu. Rev. Phys. Chem. *15*, 155–196. https://doi.org/10.1146/annurev.pc.15.100164.001103.

[S78]. Marcus, R. A., and Sutin, N. (1985). Electron transfers in chemistry and biology. Biochim. Biophys. Acta, Rev. Bioenerg. *811*, 265–322. https://doi.org/10.1016/0304-4173(85)90014-X.

[S79]. Hush, N. S. (1958). Adiabatic Rate Processes at Electrodes. I. Energy-Charge Relationships. J. Chem. Phys. *28*, 962–972. https://doi.org/10.1063/1.1744305.

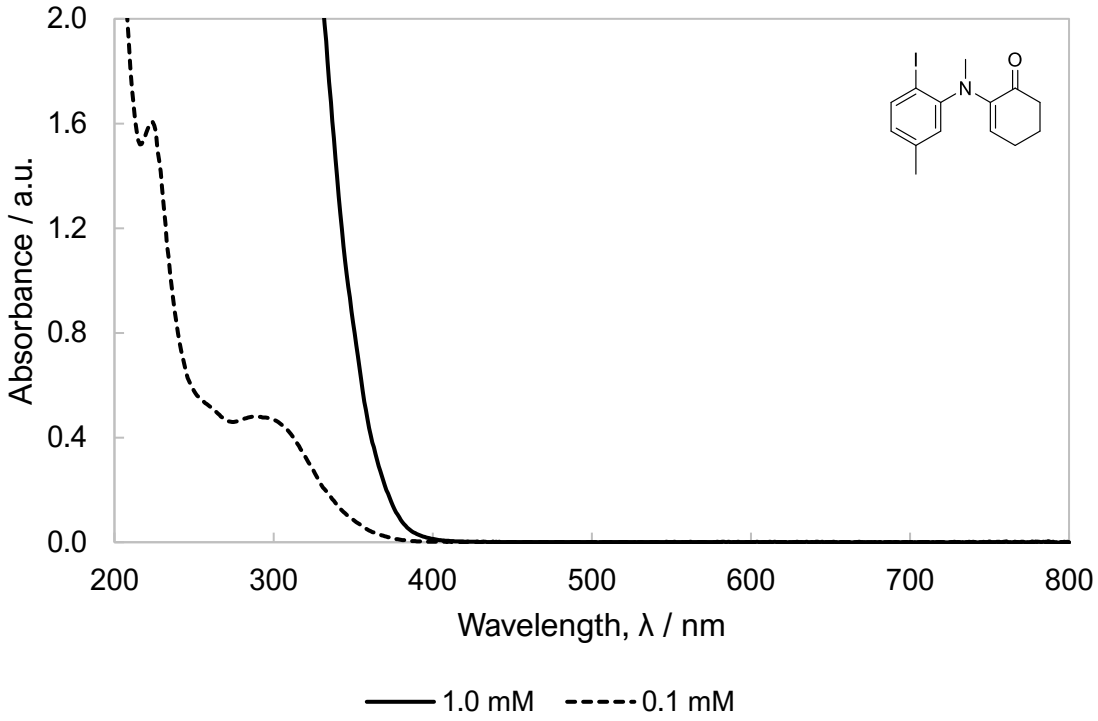
[S80]. Hush, N. S. (1999). Electron transfer in retrospect and prospect 1: Adiabatic electrode processes. J. Electroanal. Chem. *470*, 170–195. https://doi.org/10.1016/S0022-0728(99)00168-0.

[S81]. López-Estrada, O., Laguna, H. G., Barrueta-Flores, C., and Amador-Bedolla, C. (2018). Reassessment of the Four-Point Approach to the Electron-Transfer Marcus–Hush Theory. ACS Omega *3*, 2130–2140. https://doi.org/10.1021/acsomega.7b01425.

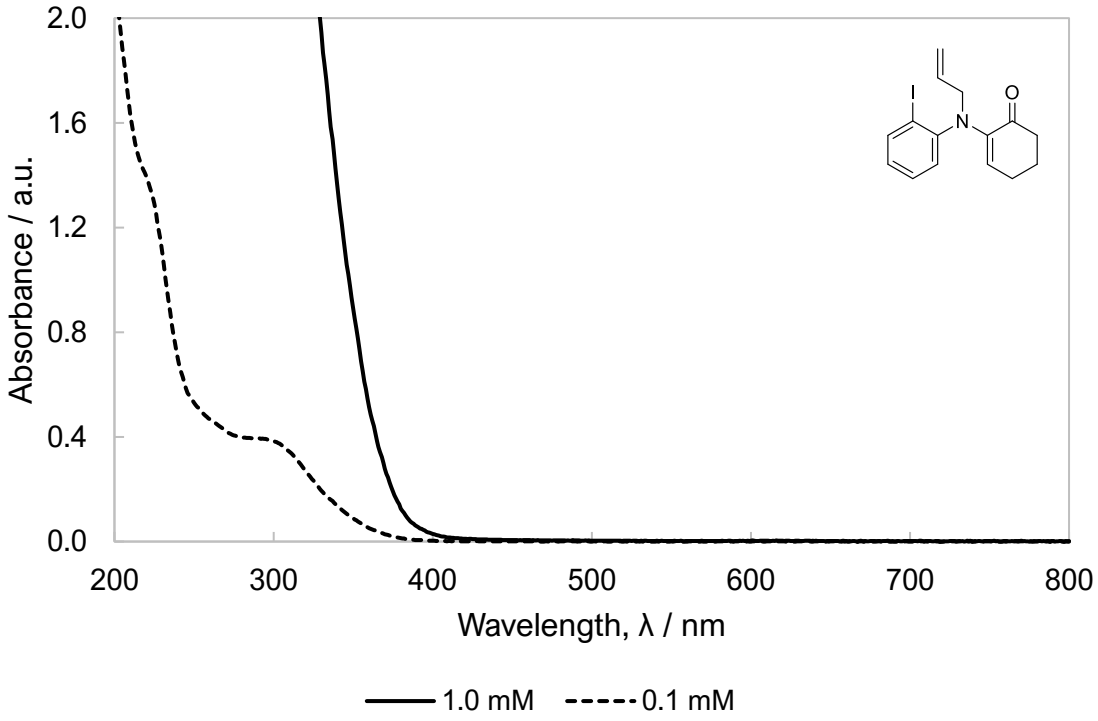
Data S1 – UV–vis spectra

All spectra were acquired in acetonitrile solution at the concentrations indicated.

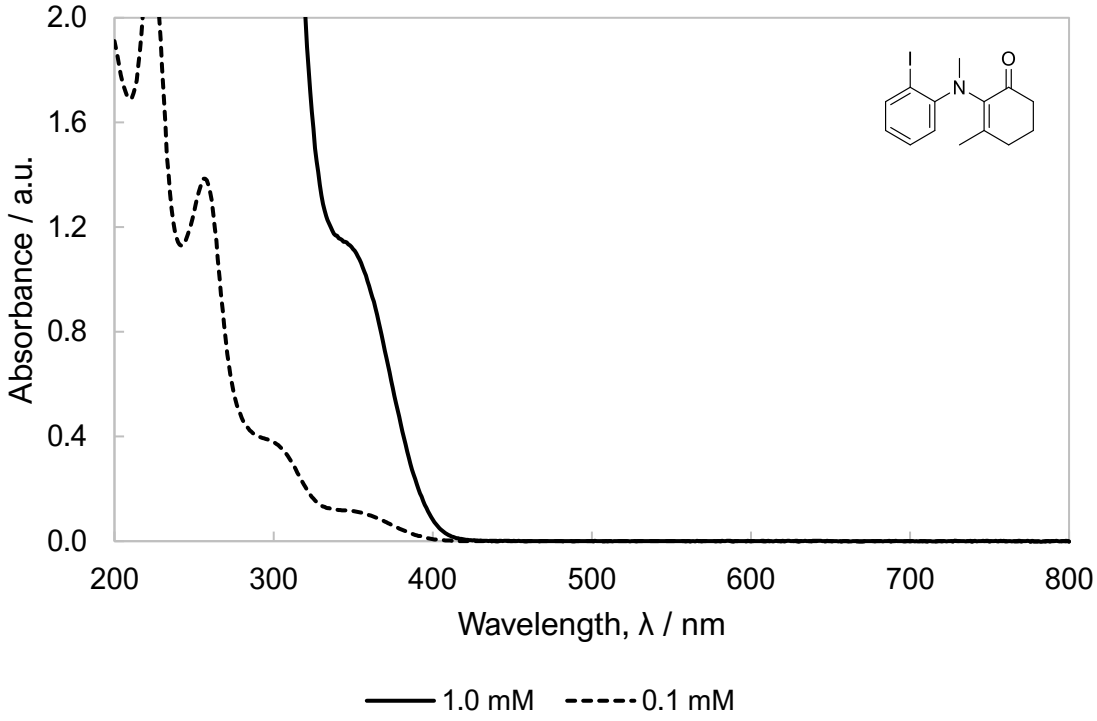
2-((2-Iodo-5-methylphenyl)(methyl)amino)cyclohex-2-en-1-one, **1**



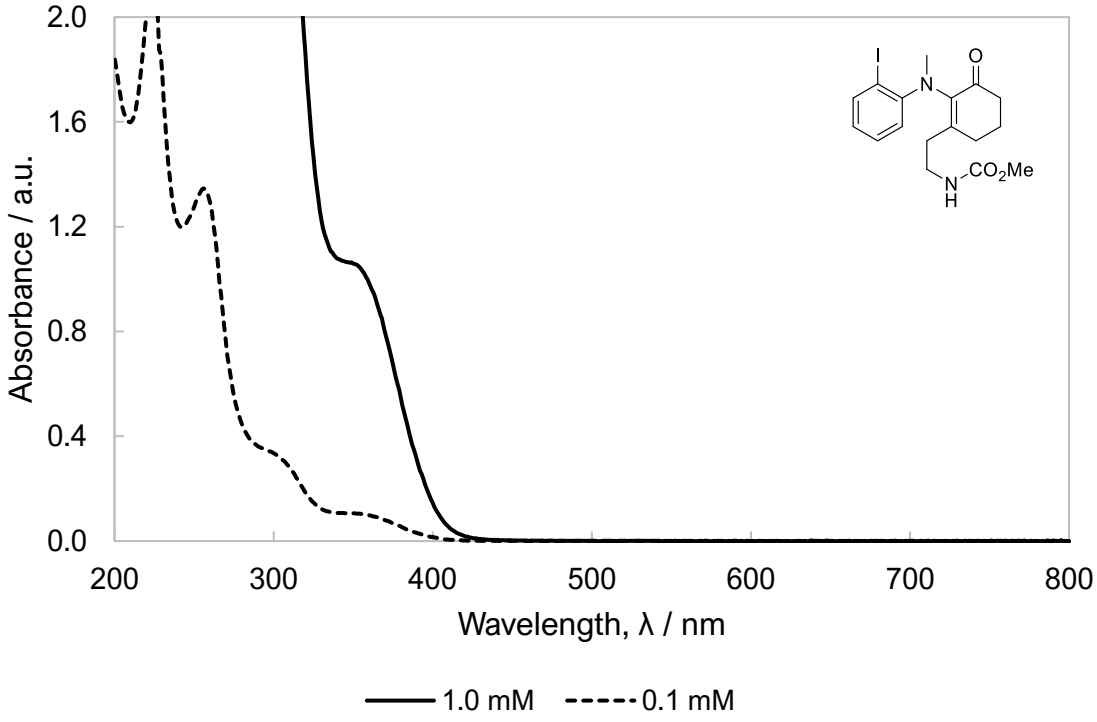
2-(Allyl(2-iodophenyl)amino)cyclohex-2-en-1-one, **4**



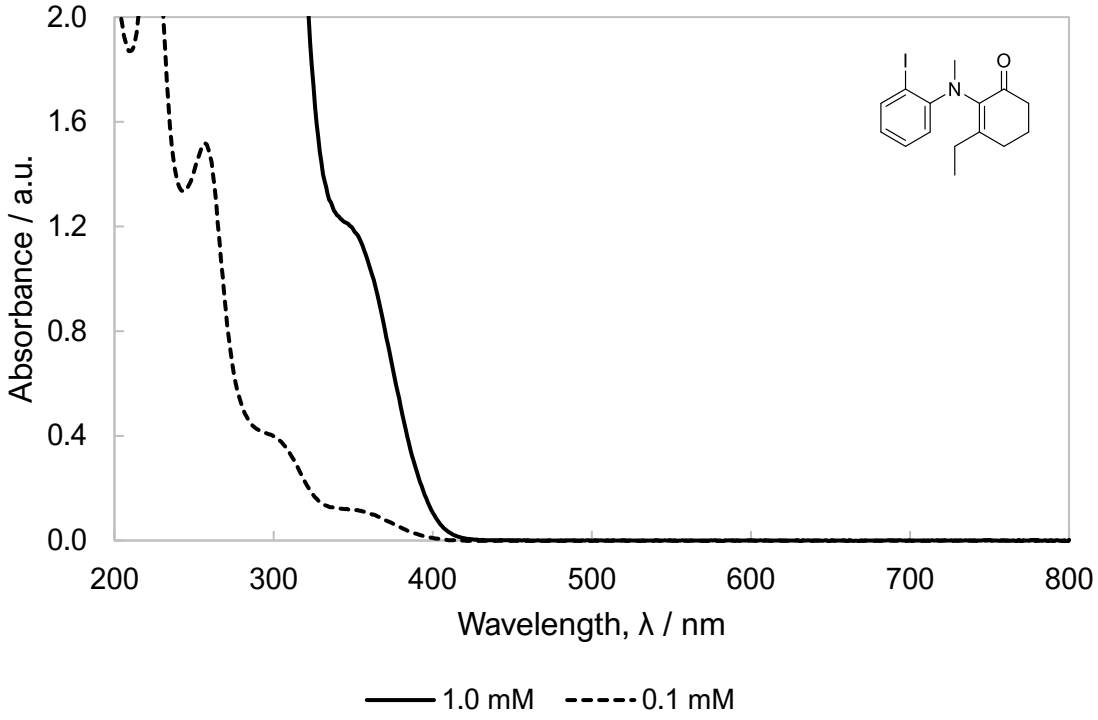
2-((2-Iodophenyl)(methyl)amino)-3-methylcyclohex-2-en-1-one, **10**



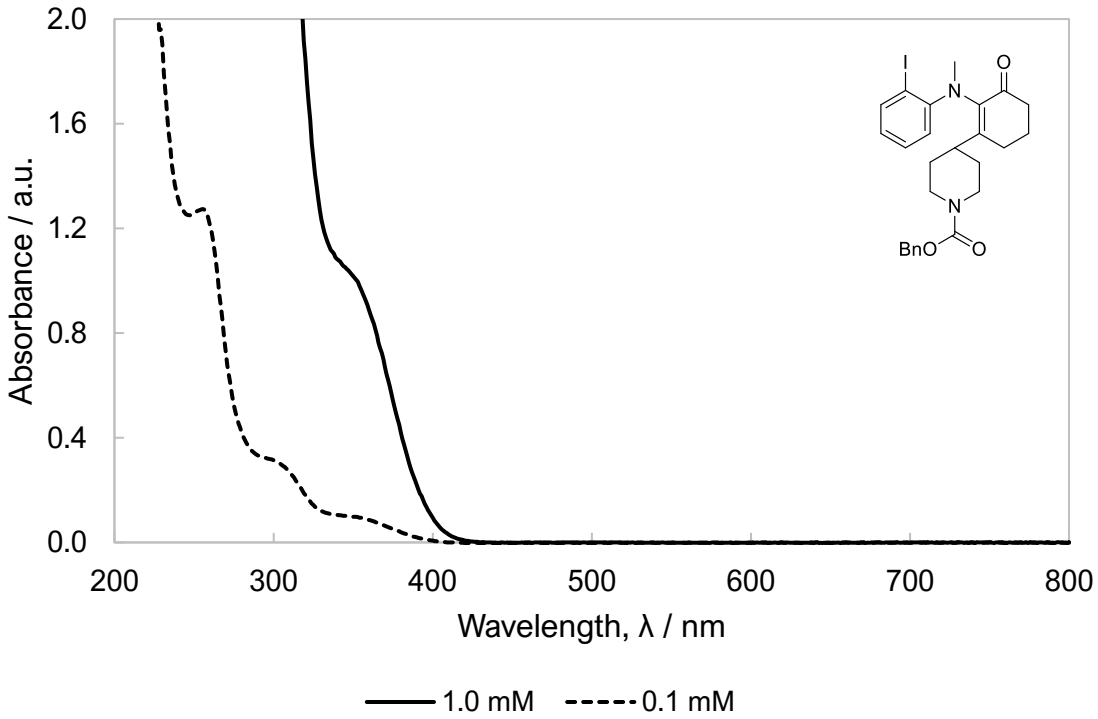
Methyl (2-(2-((2-iodophenyl)(methyl)amino)-3-oxocyclohex-1-en-1-yl)ethyl)carbamate, **28**



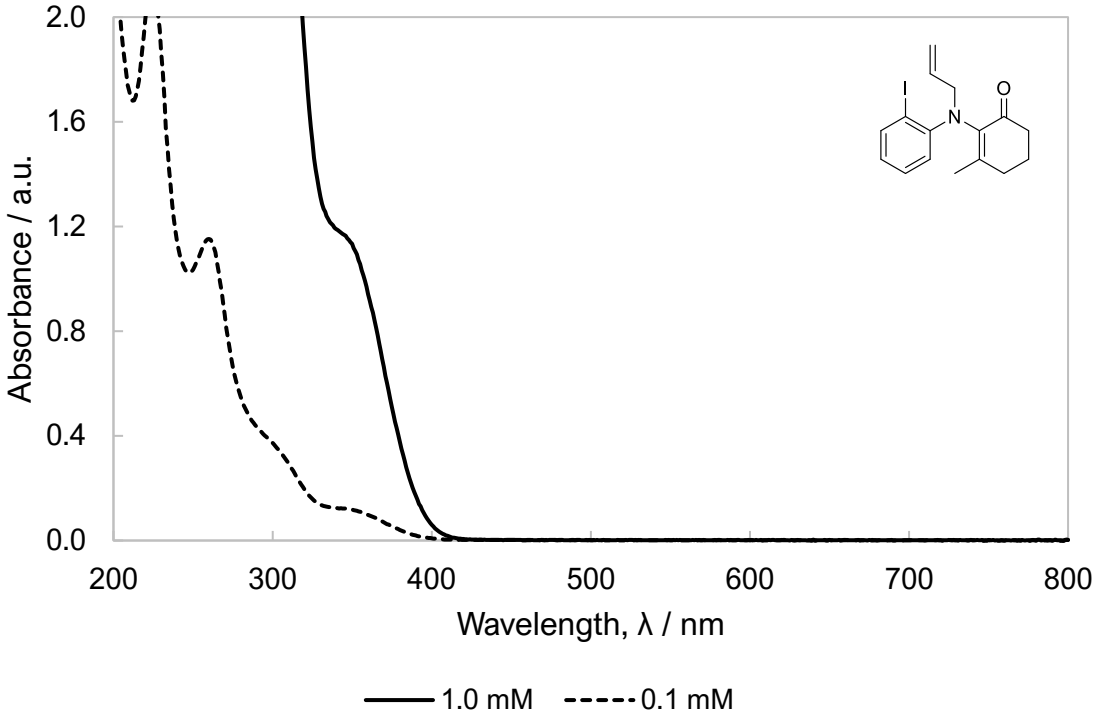
3-Ethyl-2-((2-iodophenyl)(methyl)amino)cyclohex-2-en-1-one, **S13**



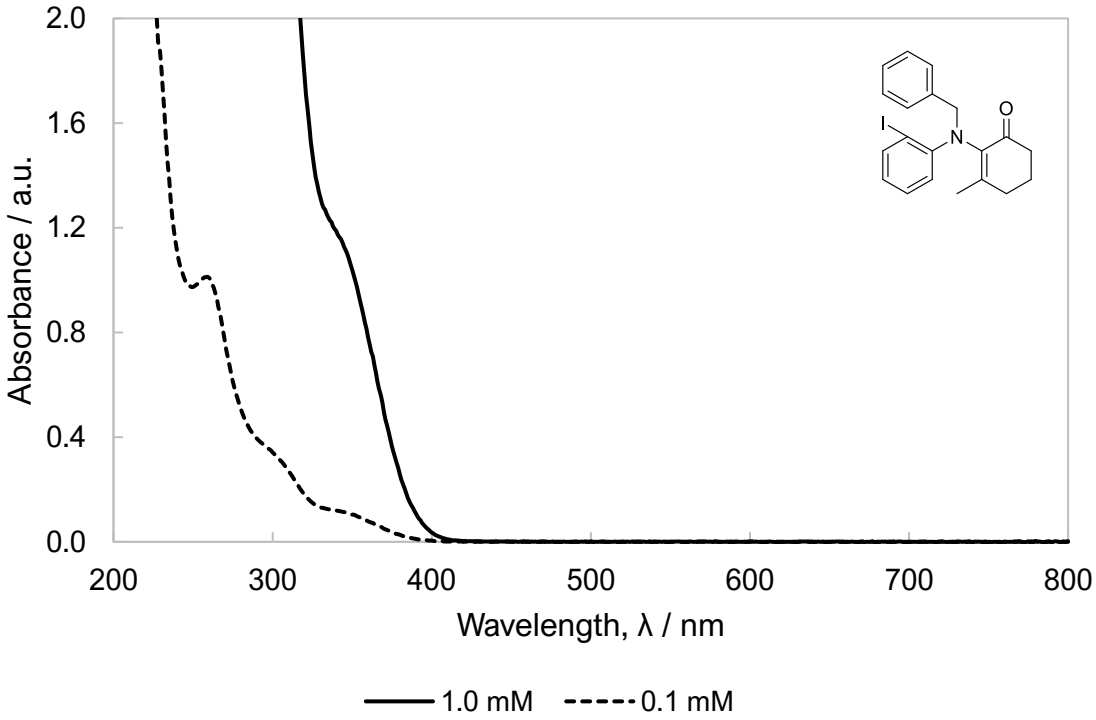
Benzyl 4-(2-((2-iodophenyl)(methyl)amino)-3-oxocyclohex-1-en-1-yl)piperidine-1-carboxylate, **S17**



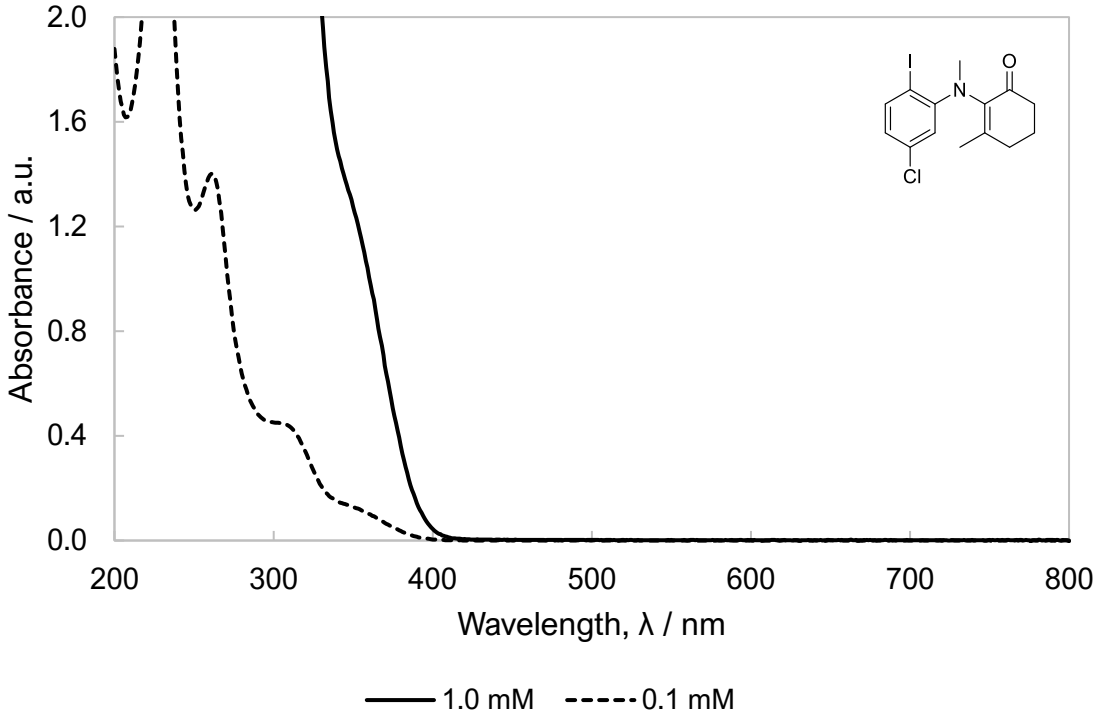
2-(Allyl(2-iodophenyl)amino)-3-methylcyclohex-2-en-1-one, **S20**



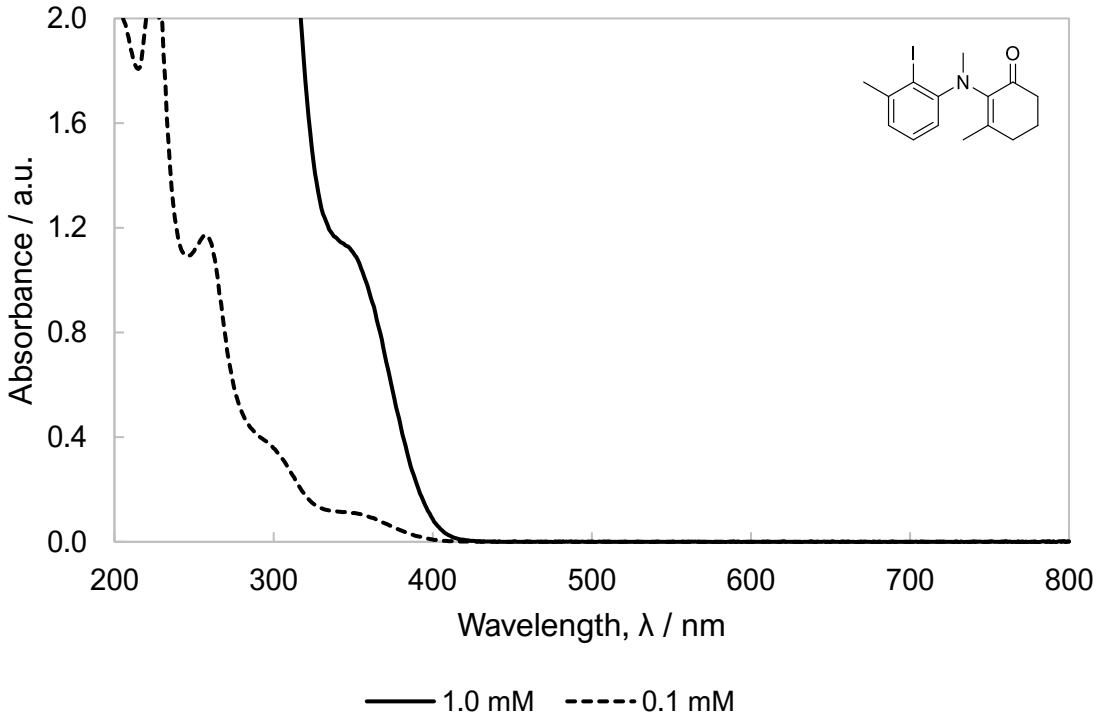
2-(Benzyl(2-iodophenyl)amino)-3-methylcyclohex-2-en-1-one, **S24**



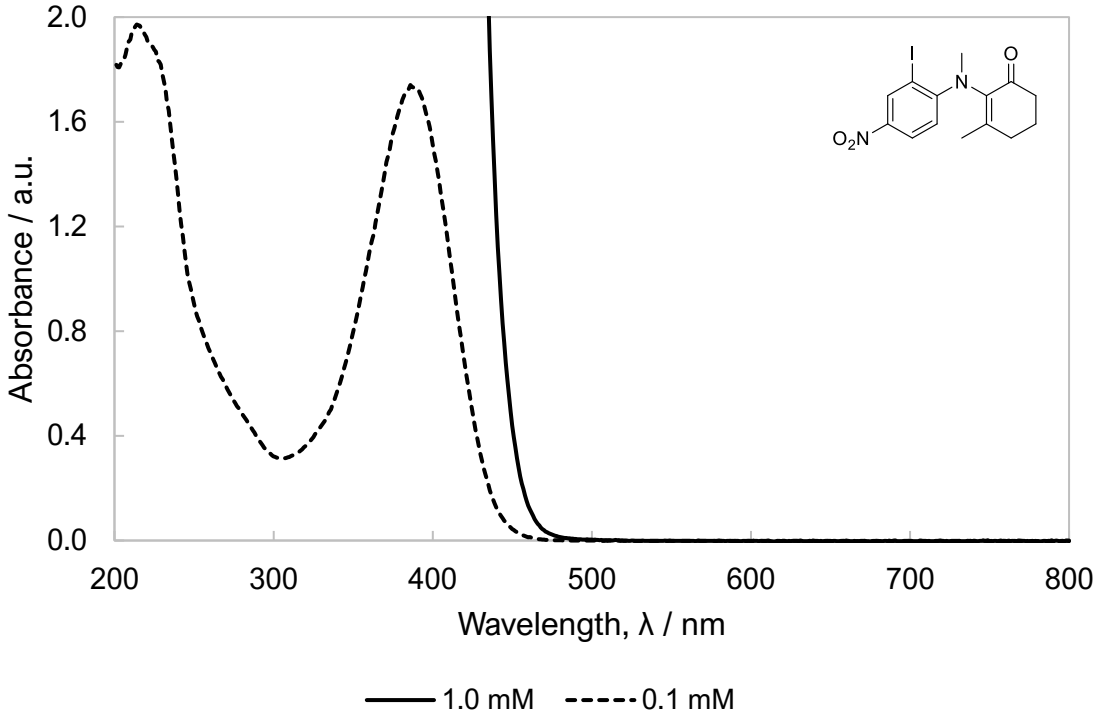
2-((5-Chloro-2-iodophenyl)(methyl)amino)-3-methylcyclohex-2-en-1-one, **S28**



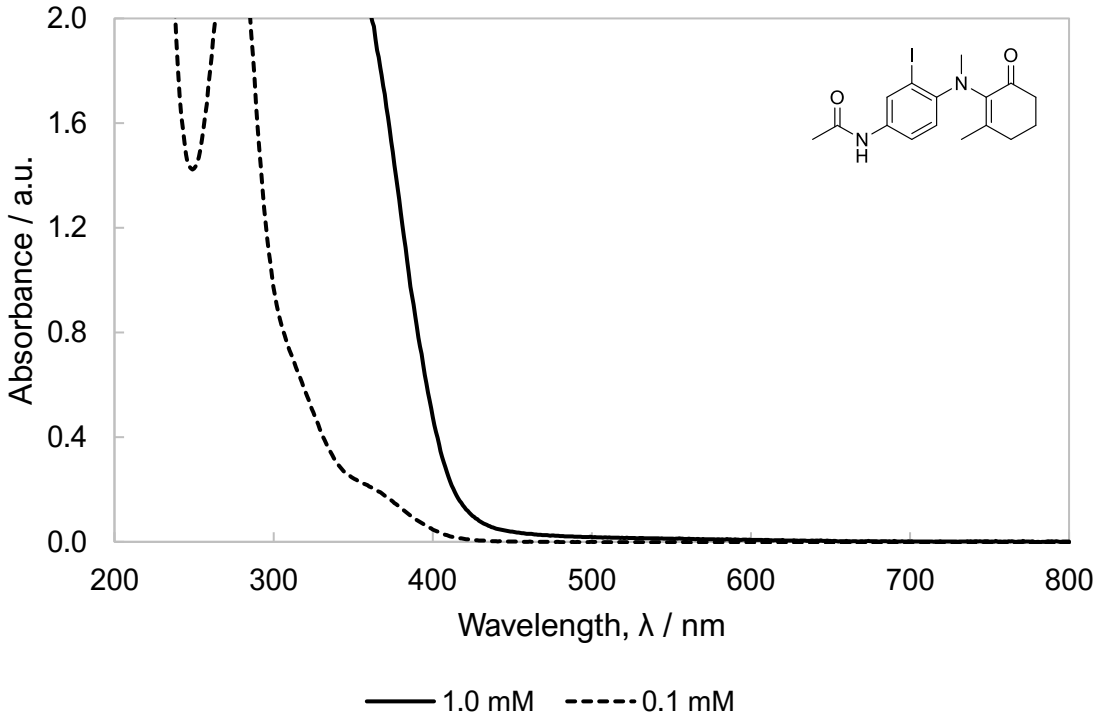
2-((2-Iodo-3-methylphenyl)(methyl)amino)-3-methylcyclohex-2-en-1-one, **S34**



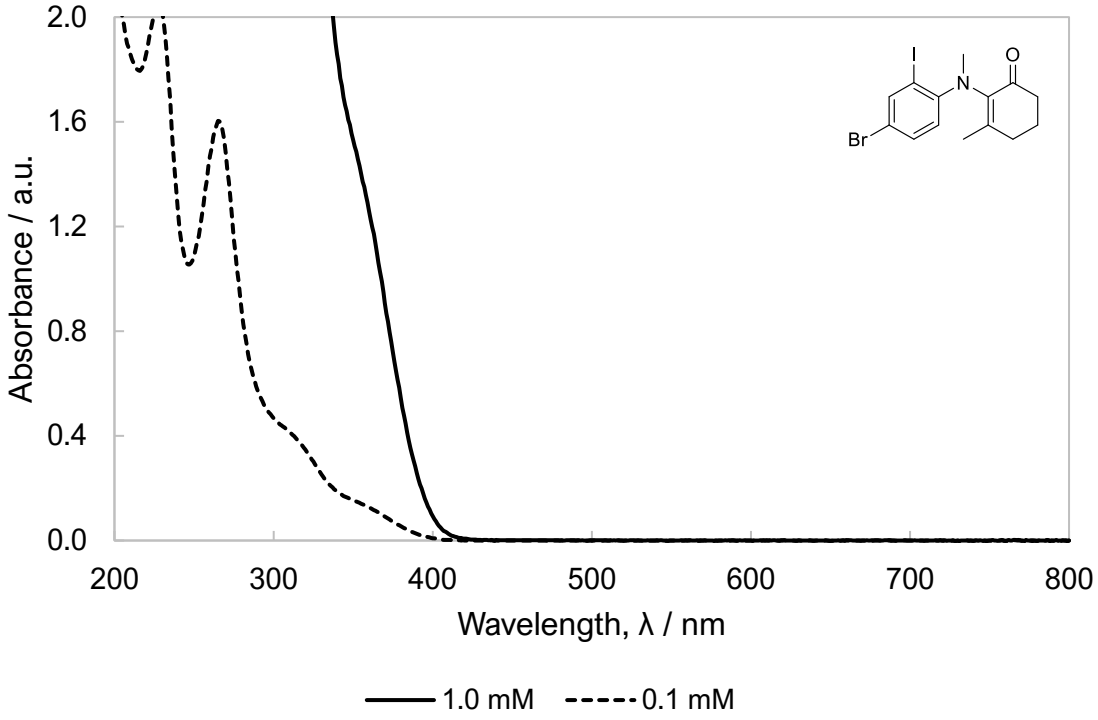
2-((2-Iodo-4-nitrophenyl)(methyl)amino)-3-methylcyclohex-2-en-1-one, **S35**



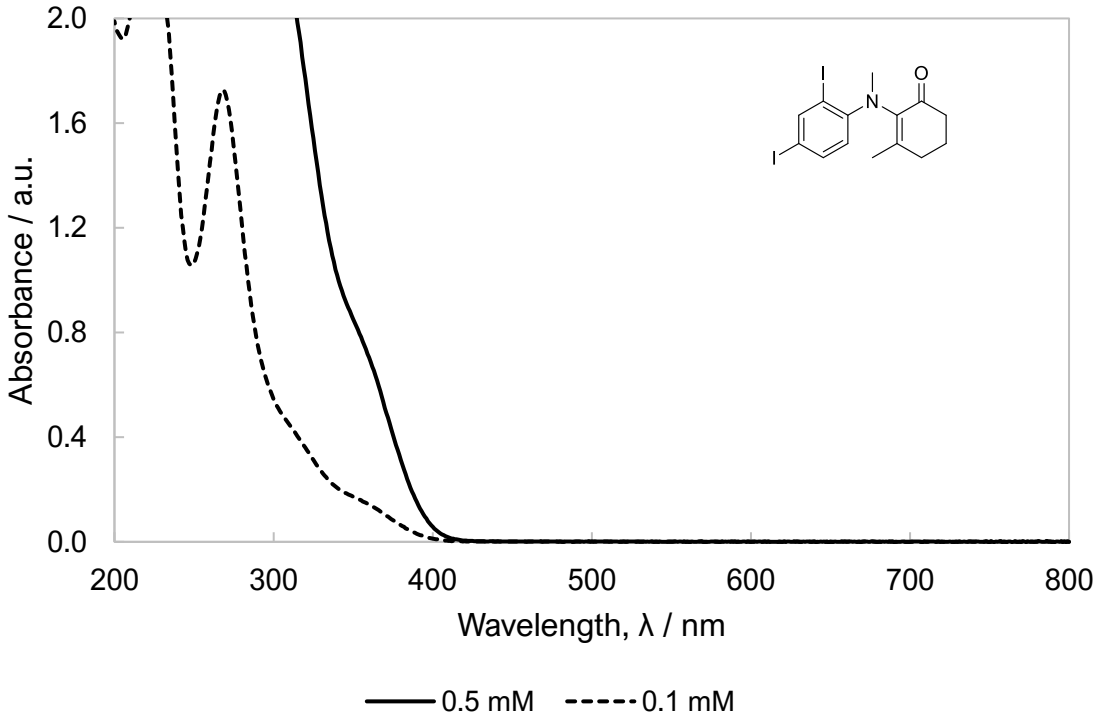
N-(3-Iodo-4-(methyl(2-methyl-6-oxocyclohex-1-en-1-yl)amino)phenyl)acetamide, **S36**



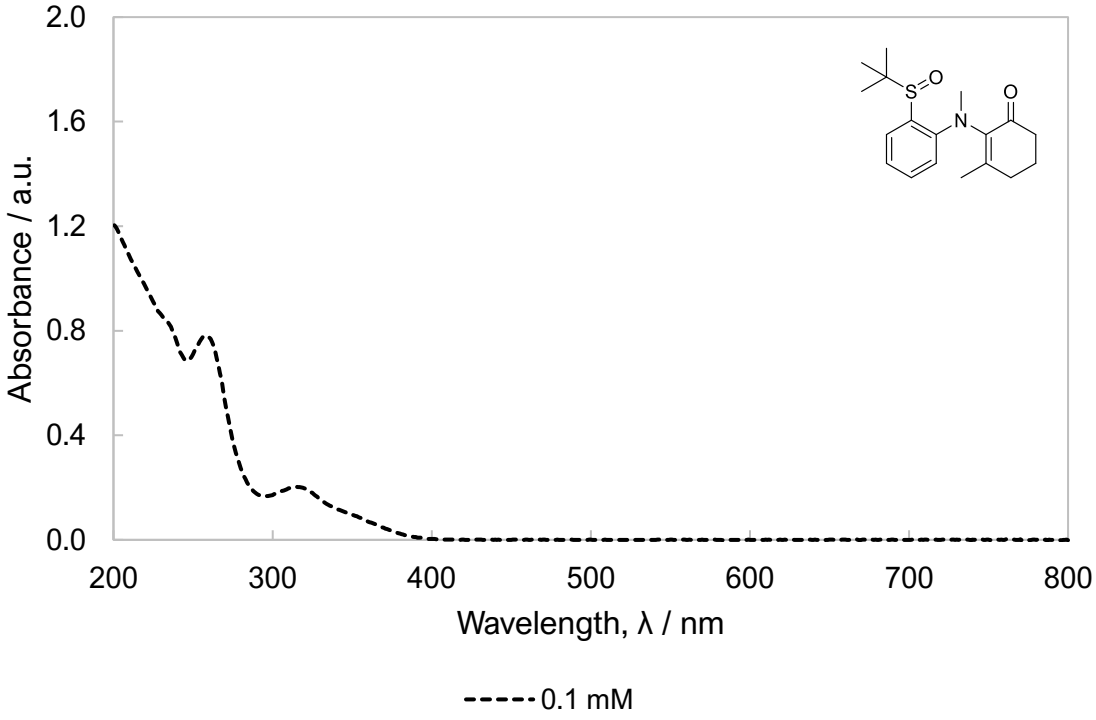
2-((4-Bromo-2-iodophenyl)(methyl)amino)-3-methylcyclohex-2-en-1-one, **S37**



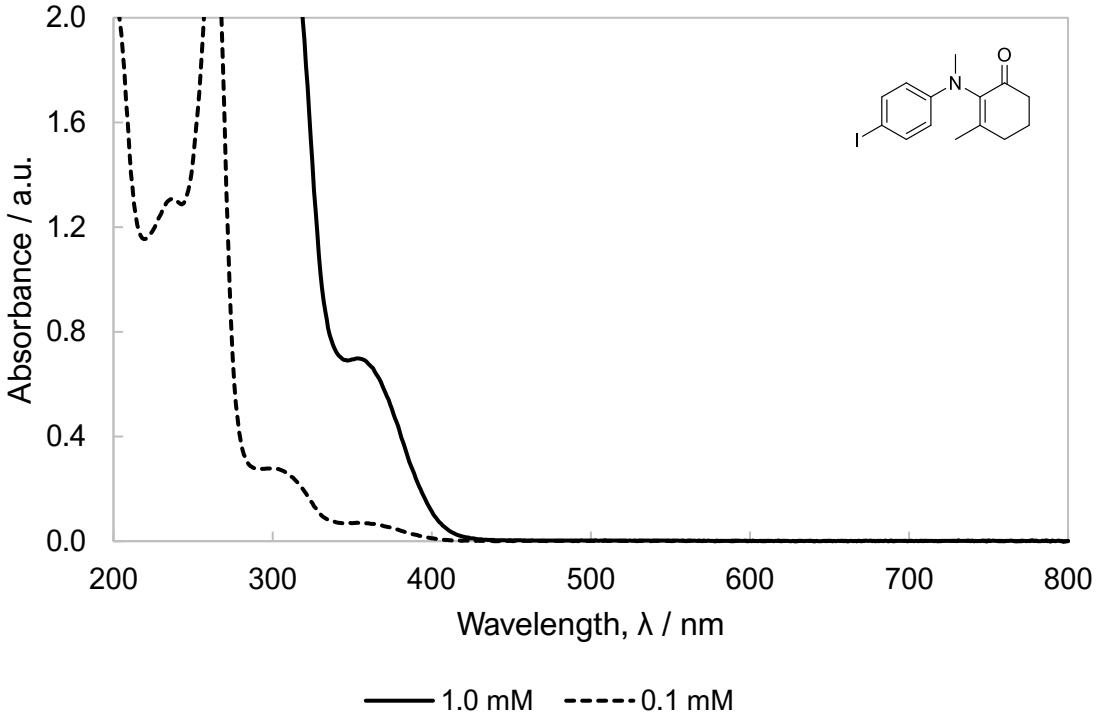
2-((2,4-Diiodophenyl)(methyl)amino)-3-methylcyclohex-2-en-1-one, **S38**



(±)-2-((2-(*tert*-Butylsulfinyl)phenyl)(methyl)amino)-3-methylcyclohex-2-en-1-one, **(±)-48**



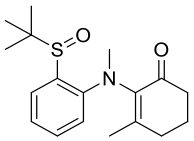
2-((4-Iodophenyl)(methyl)amino)-3-methylcyclohex-2-en-1-one, **S70**



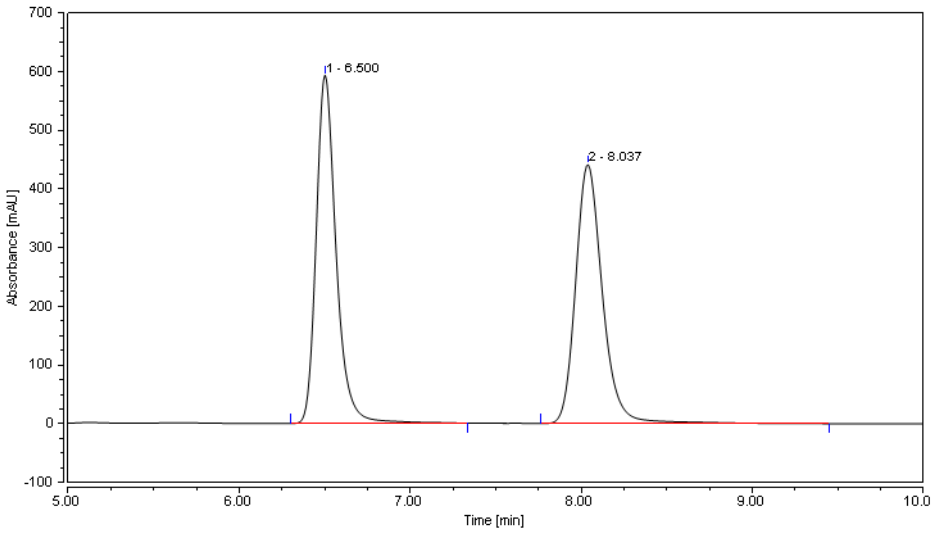
Data S2 – HPLC traces

2-((2-(*tert*-Butylsulfinyl)phenyl)(methyl)amino)-3-methylcyclohex-2-en-1-one, **48**

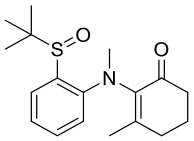
Chiral HPLC: (Chiralpak IG-3, 40% ethanol, 60% hexane, 1.0 mL min^{-1}, λ = 210 nm); τ_R (minor) = 6.6 min, τ_R (major) = 8.0 min.



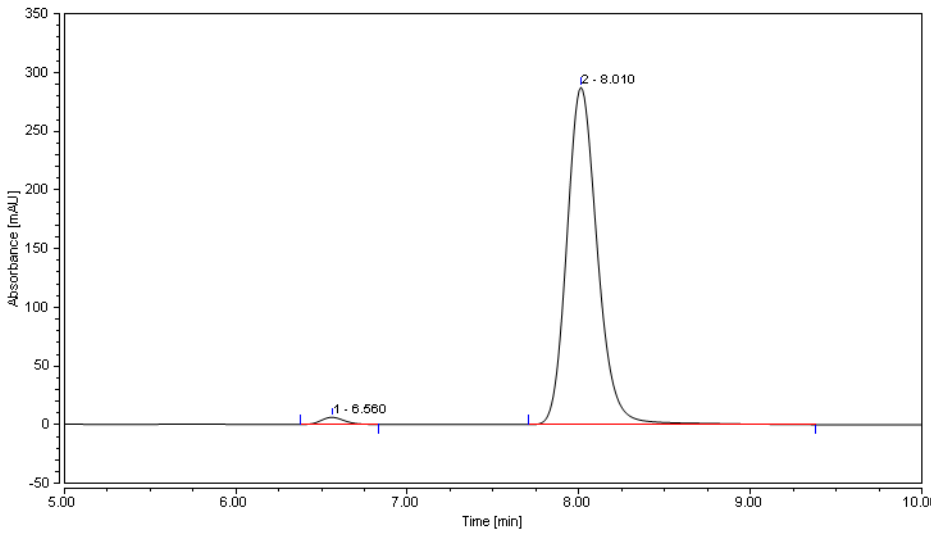
(±)-48
rac



Peak	Retention time / min	Area / mAU*min	Height / mAU	Relative area / %
1	6.500	80.233	592.866	49.96
2	8.037	80.369	441.396	50.04
Total		160.602	1034.262	100.00



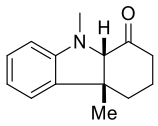
(+)-48
ent



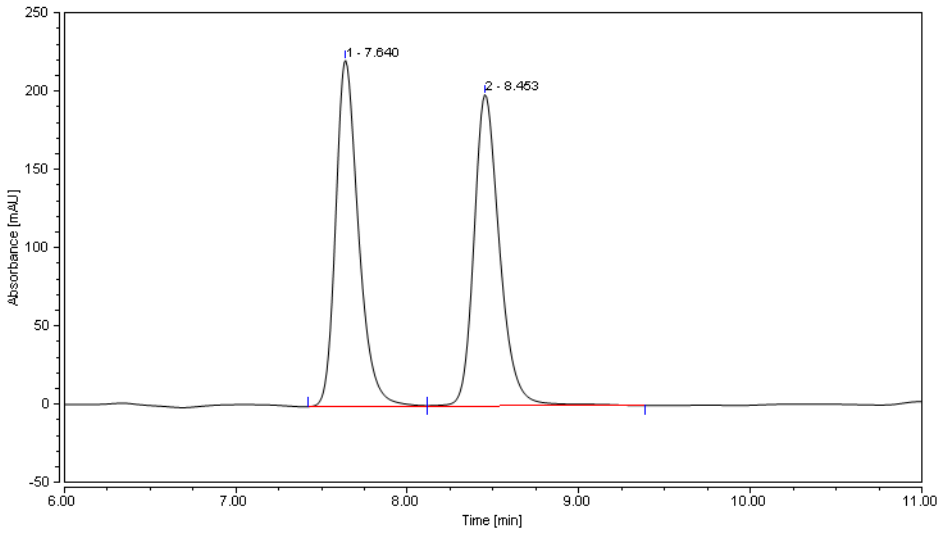
Peak	Retention Time (min)	Area (mAU*min)	Height (mAU)	Relative Area (%)
1	6.560	0.946	6.106	1.57
2	8.010	59.290	287.268	98.43
Total		60.236	293.375	100.00

4a,9-Dimethyl-2,3,4,4a,9,9a-hexahydro-1*H*-carbazol-1-one, **21**

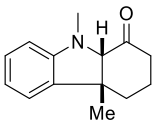
Chiral HPLC: (Chiralpak IA, 10% dichloromethane, 90% hexane, 1.0 mL min^{-1}, λ = 249 nm); τ_R (minor) = 7.7 min, τ_R (major) = 8.5 min.



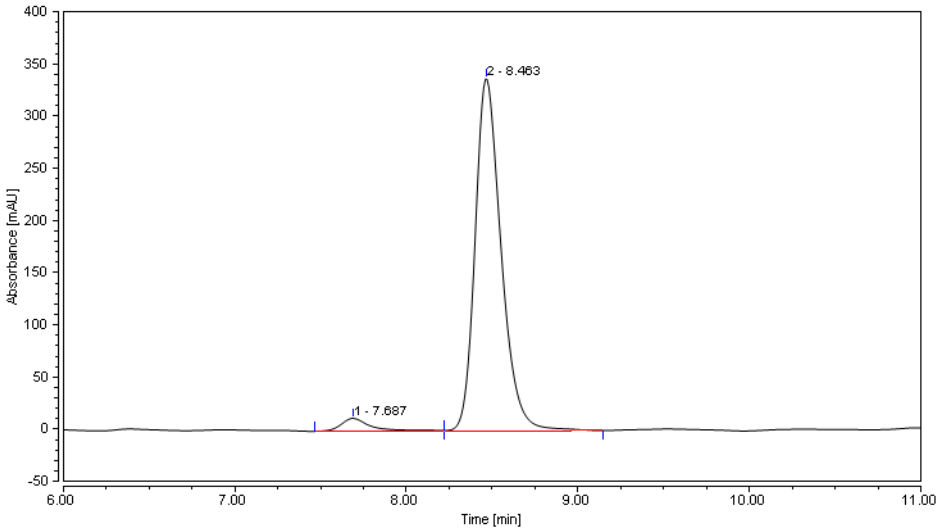
(±)-21
rac



Peak	Retention Time (min)	Area (mAU*min)	Height (mAU)	Relative Area (%)
1	7.640	34.151	221.177	49.66
2	8.453	34.616	199.116	50.34
Total		68.766	420.293	100.00



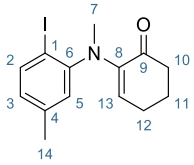
(–)-21
ent

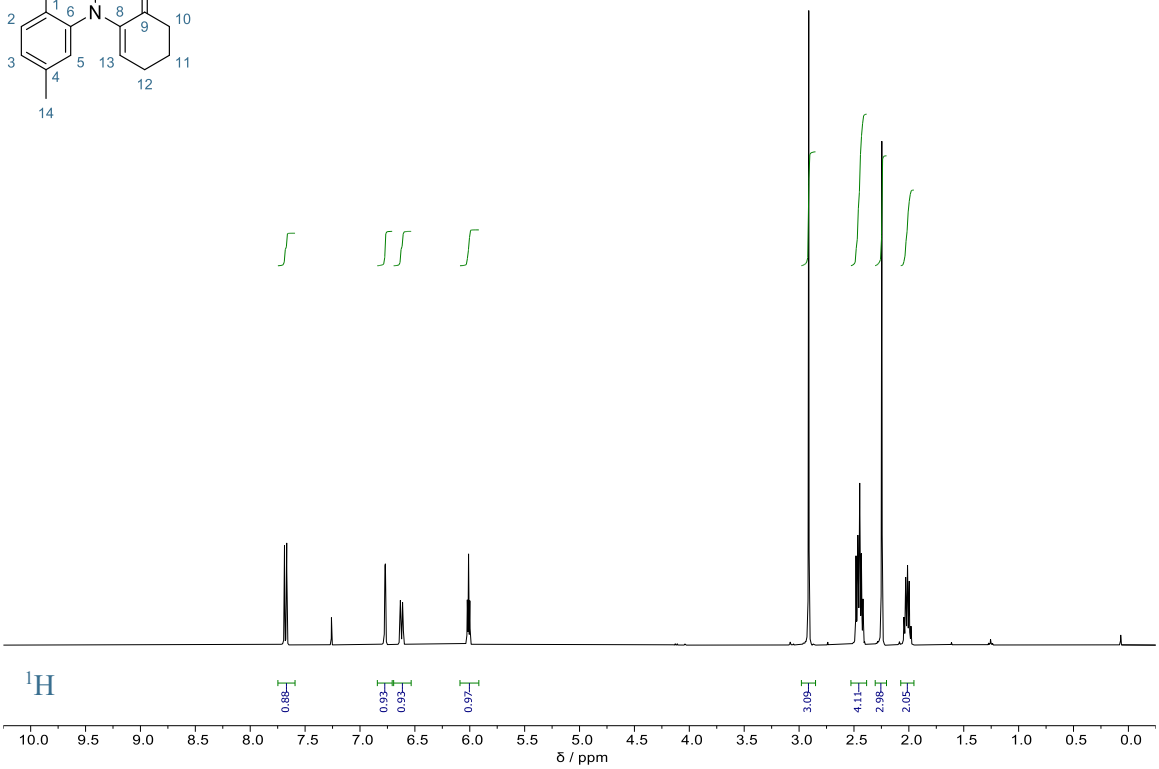


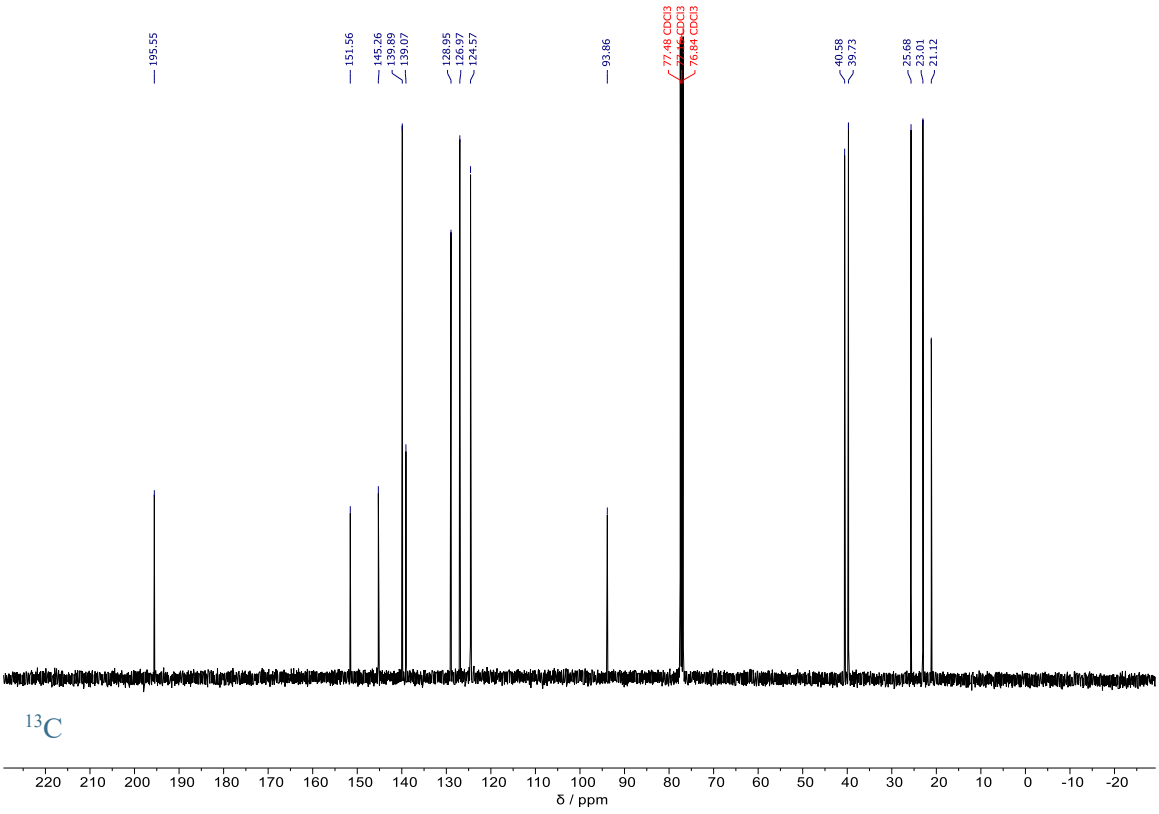
Peak	Retention Time (min)	Area (mAU*min)	Height (mAU)	Relative Area (%)
1	7.687	2.507	12.328	4.05
2	8.463	59.339	337.906	95.95
Total		61.846	350.324	100.00

Data S3 – NMR spectra

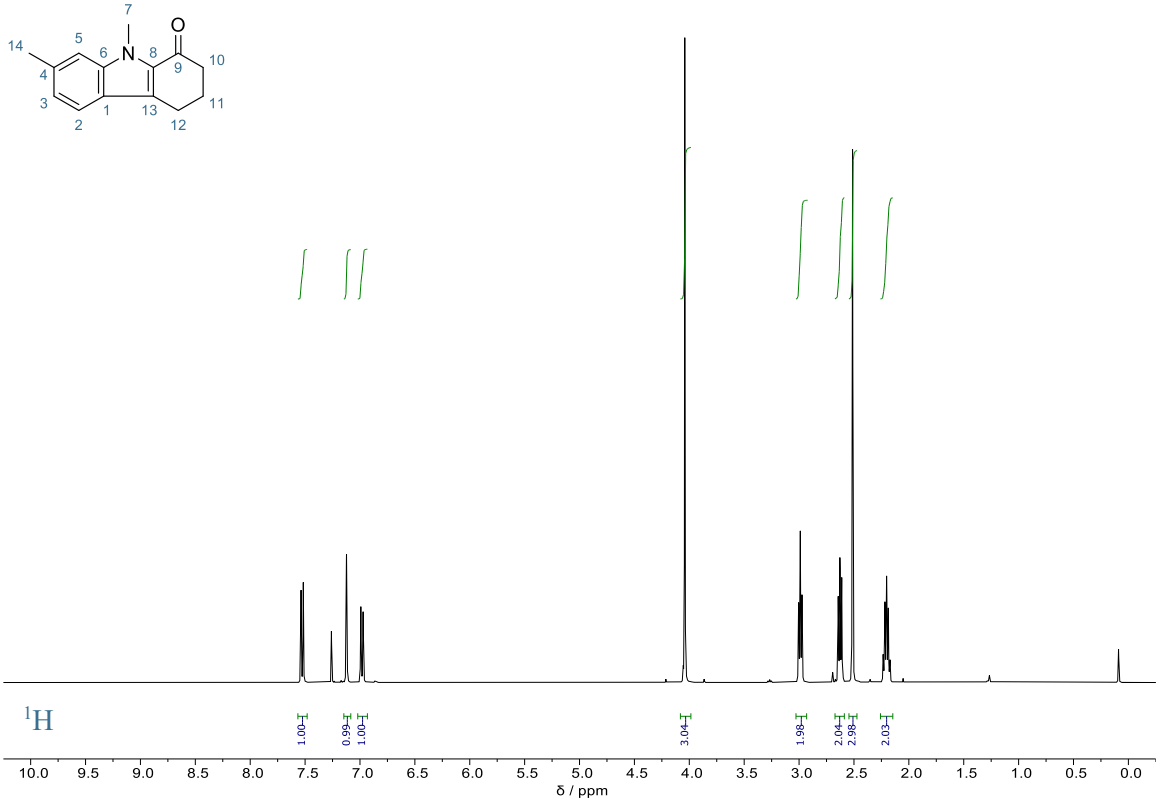
2-((2-Iodo-5-methylphenyl)(methyl)amino)cyclohex-2-en-1-one, **1**

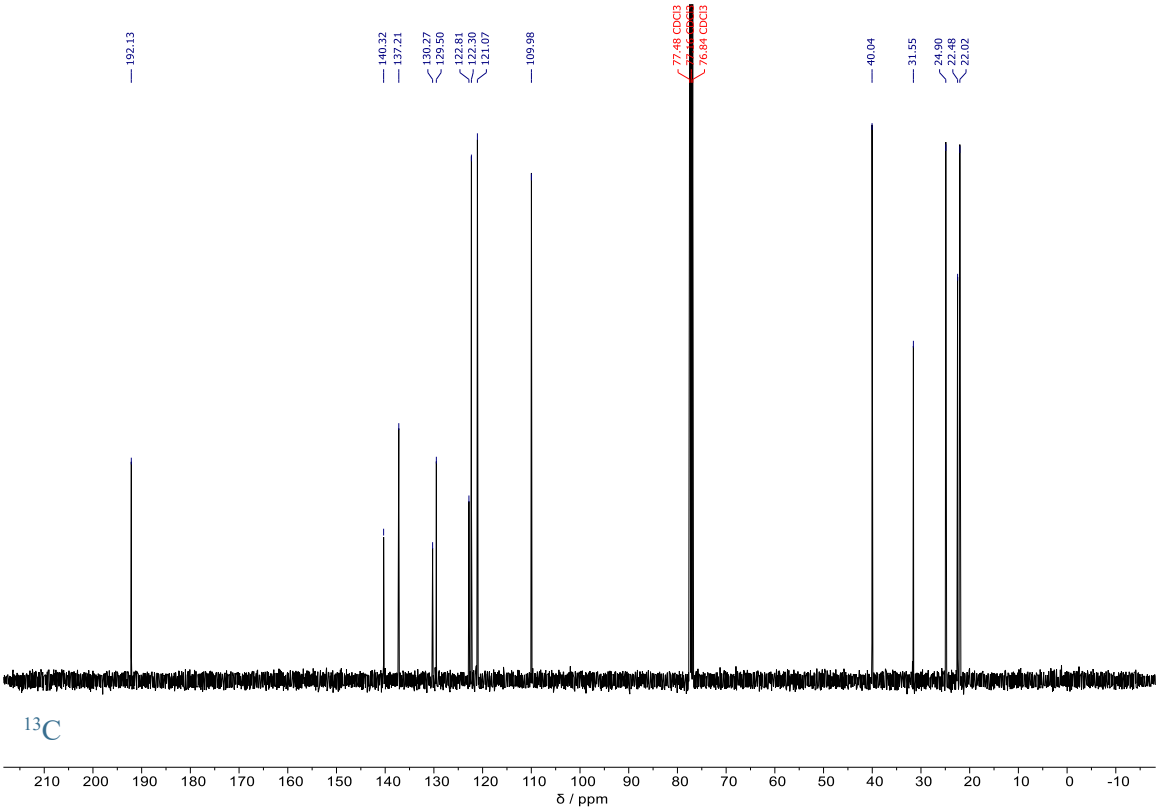




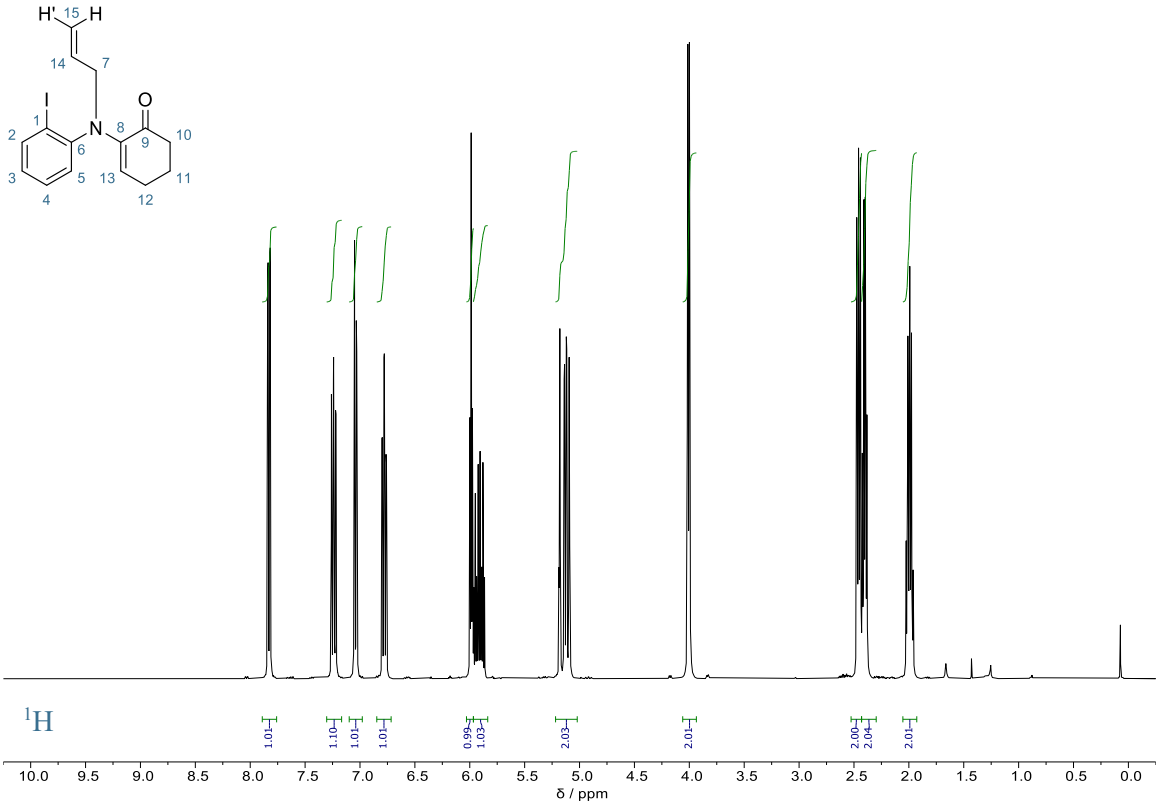


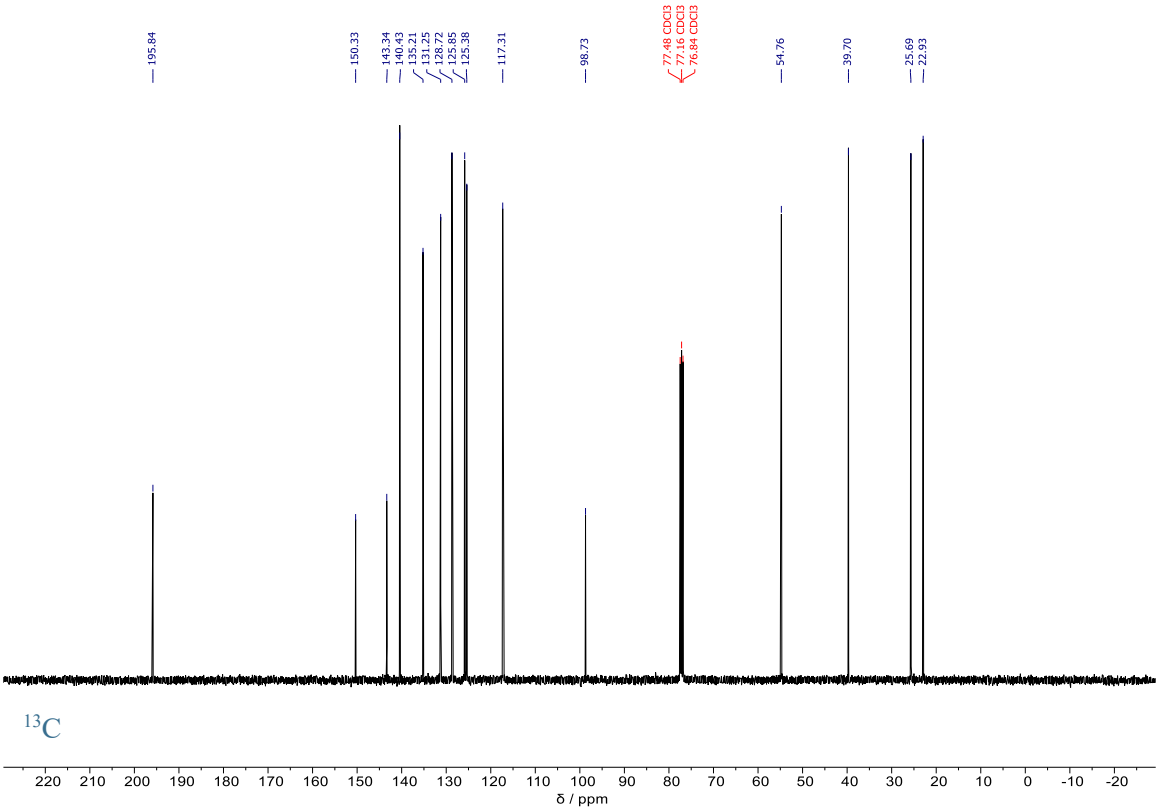
7,9-Dimethyl-2,3,4,9-tetrahydro-1*H*-carbazol-1-one, **2**



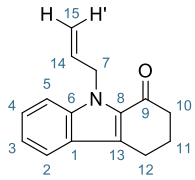


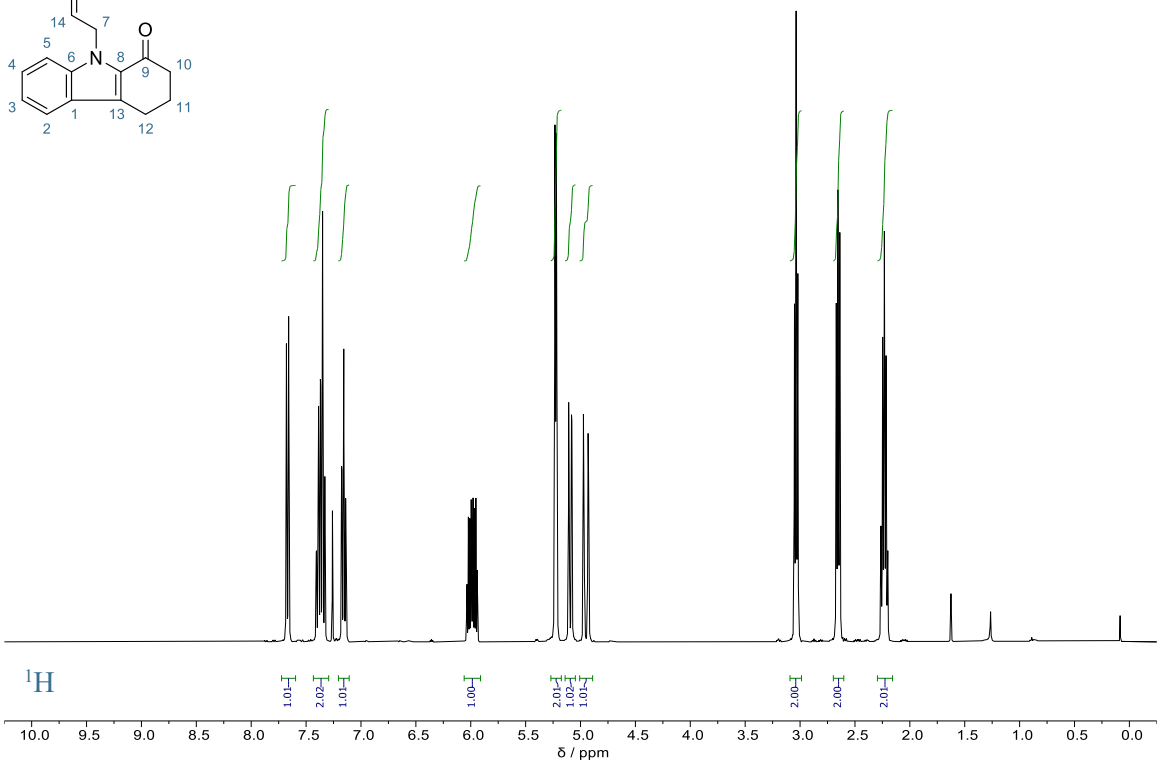
2-(Allyl(2-iodophenyl)amino)cyclohex-2-en-1-one, **4**

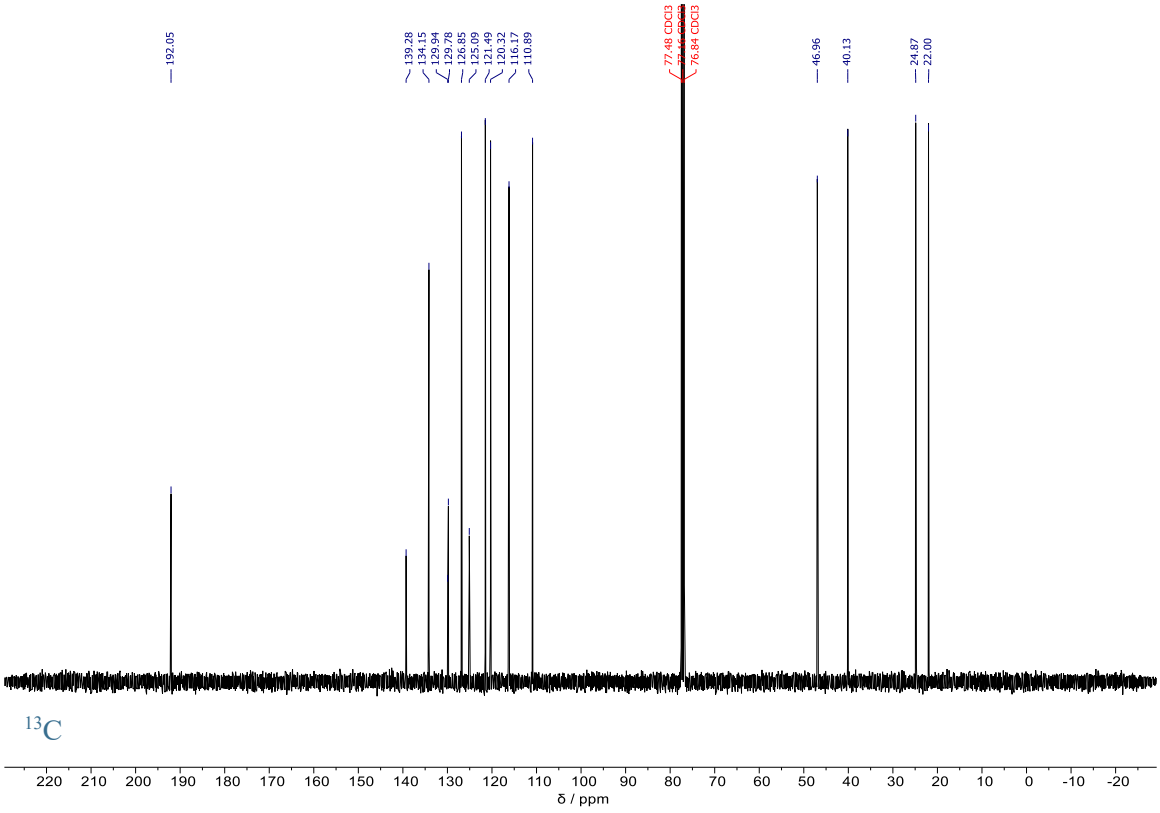




9-Allyl-2,3,4,9-tetrahydro-1H-carbazol-1-one, **5**

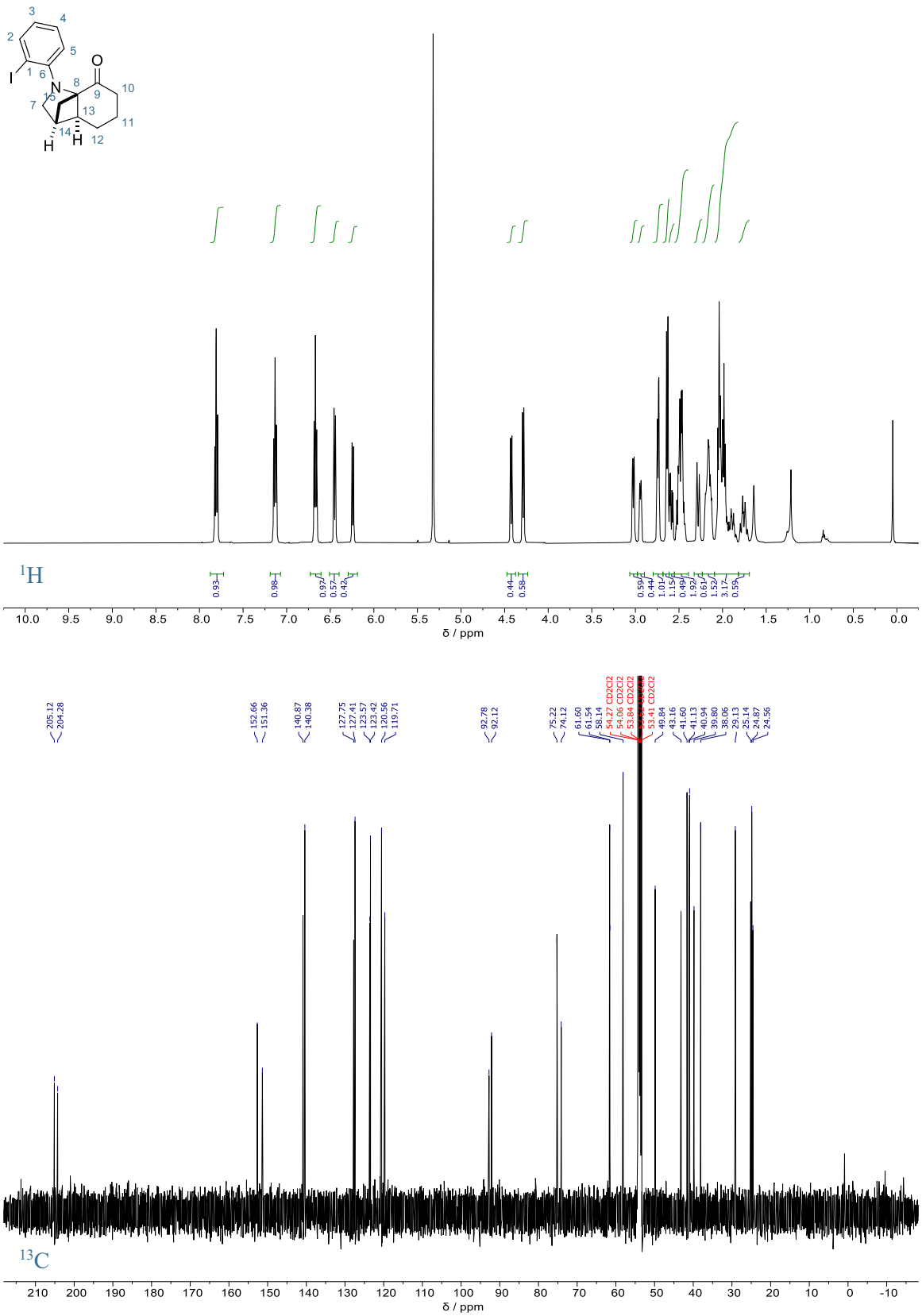




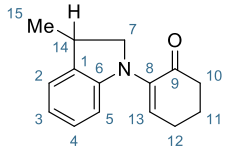


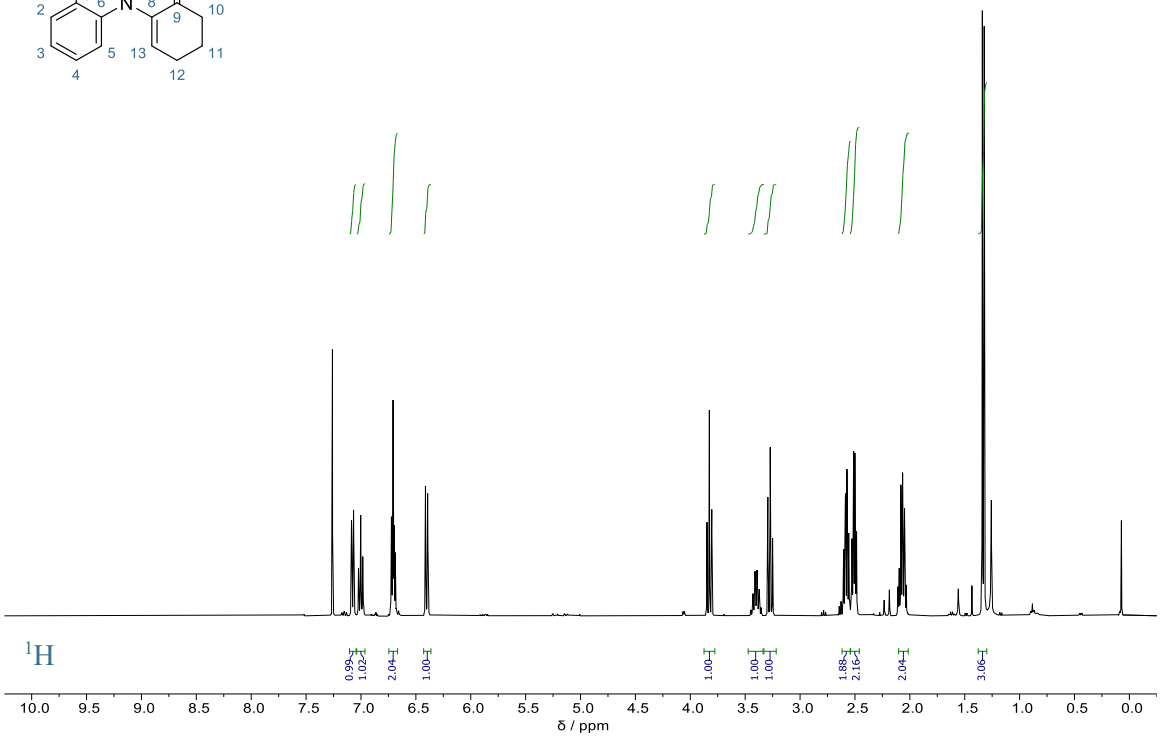
rac-1-(2-Iodophenyl)hexahydro-3,7a-methanoindol-7(1*H*)-one, **6**

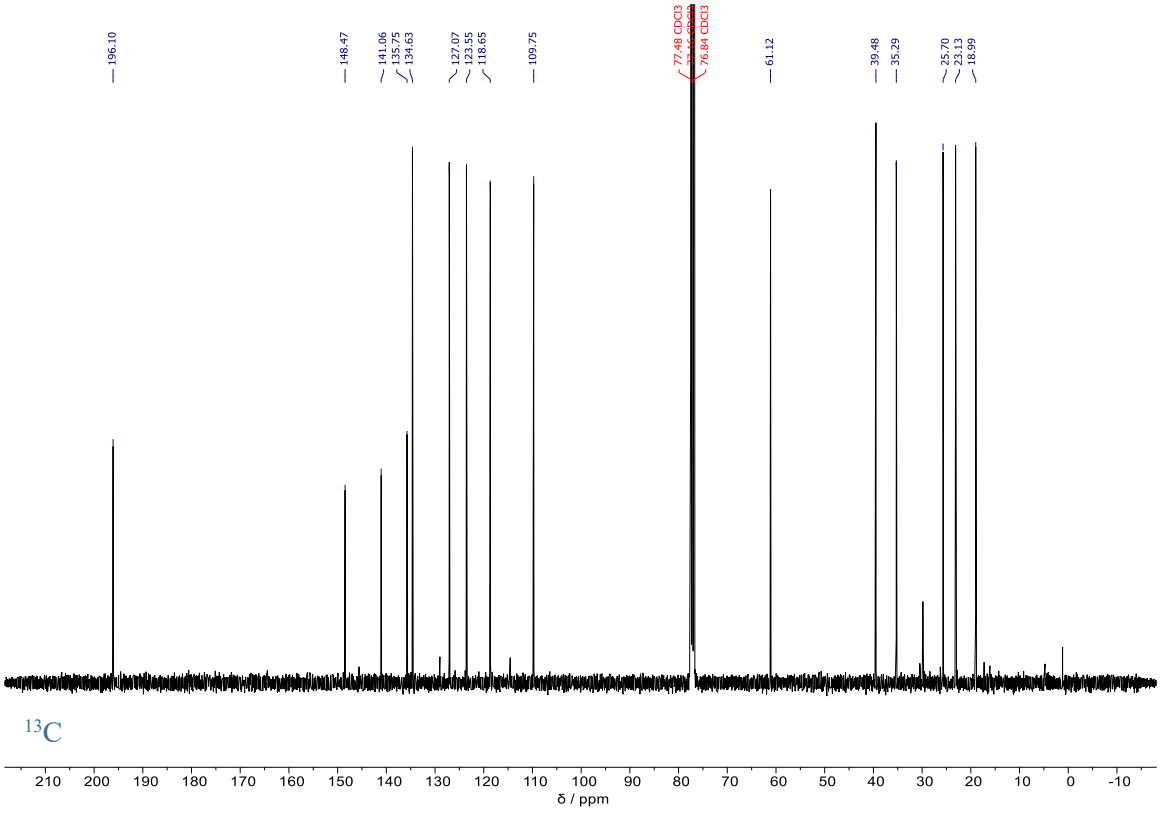
(^{1}H and ^{13}C in CD_2Cl_2 at 253 K)



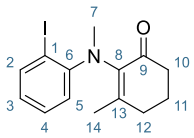
2-(3-Methylindolin-1-yl)cyclohex-2-en-1-one, **7** (X = H)

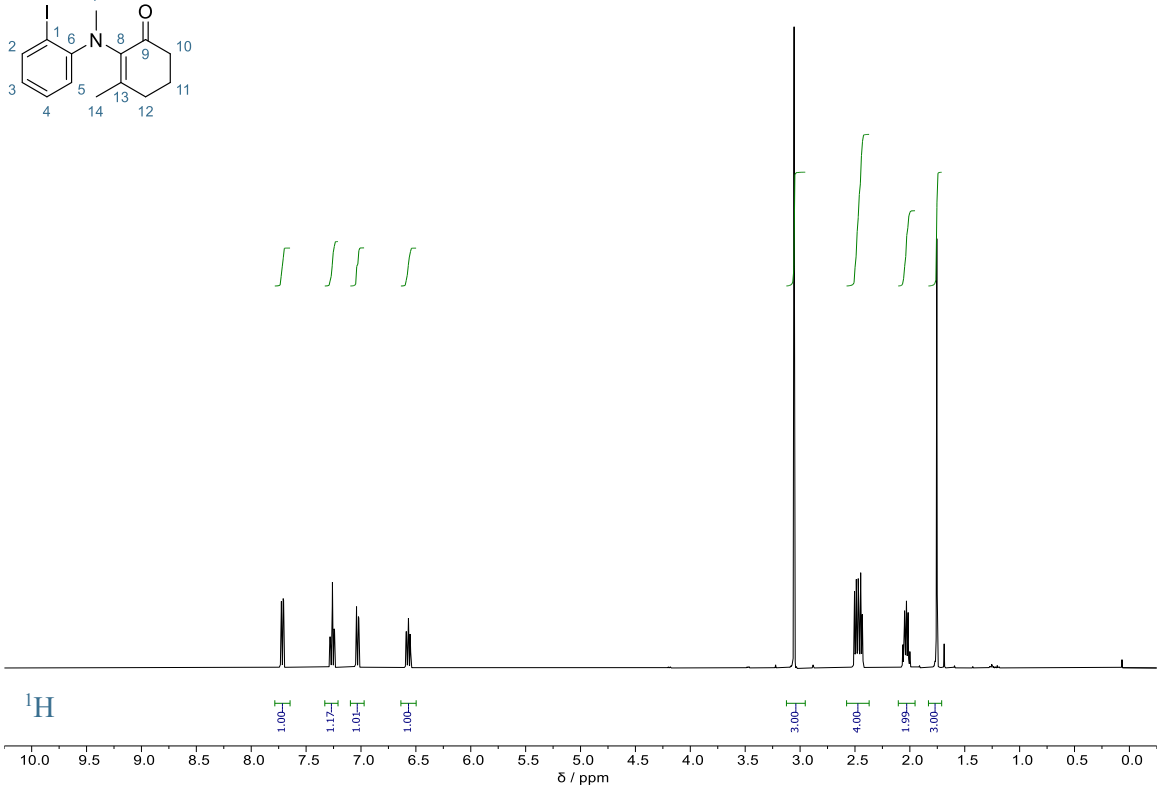


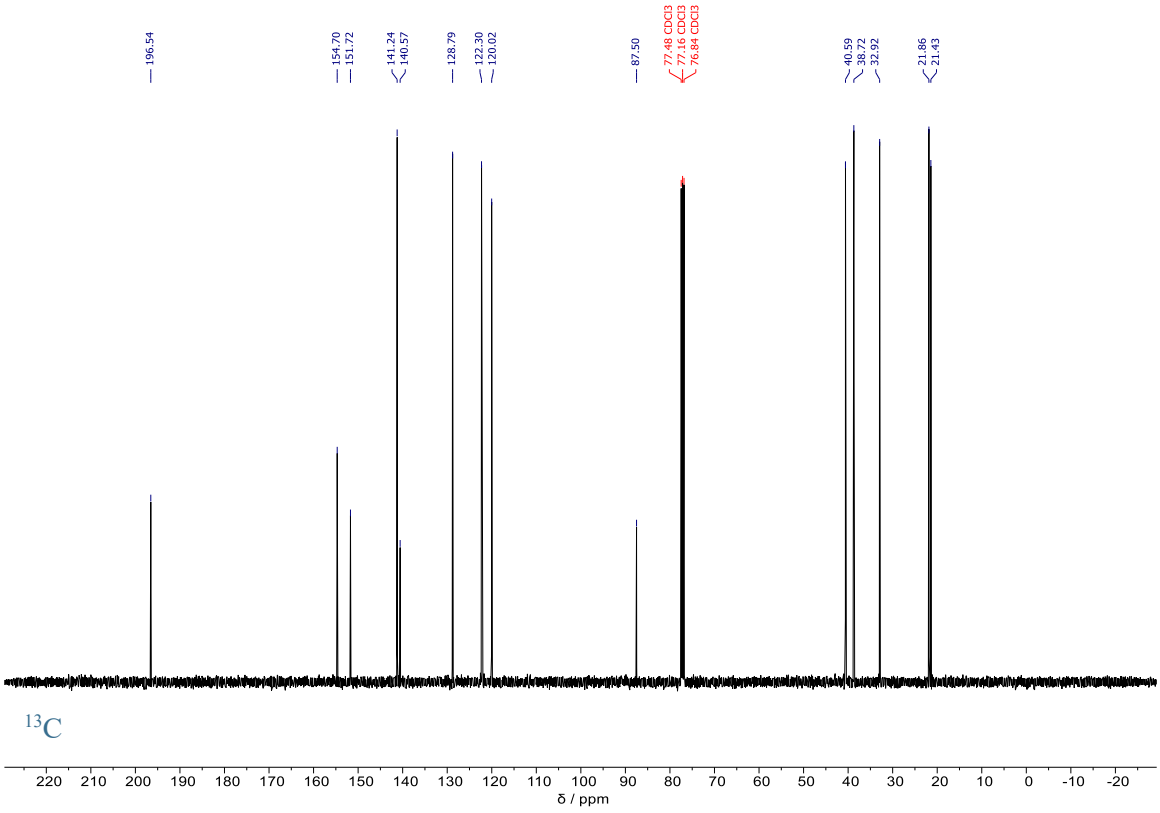




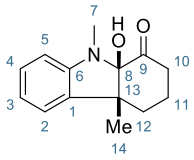
2-((2-Iodophenyl)(methyl)amino)-3-methylcyclohex-2-en-1-one, **10**

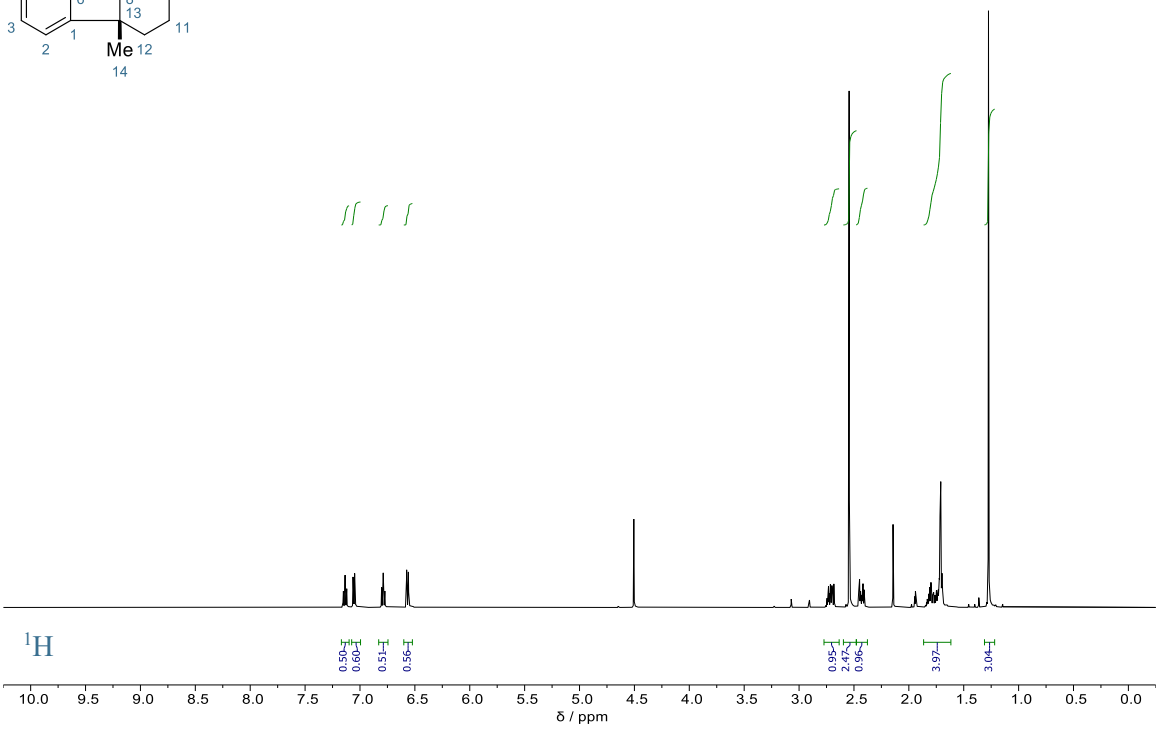


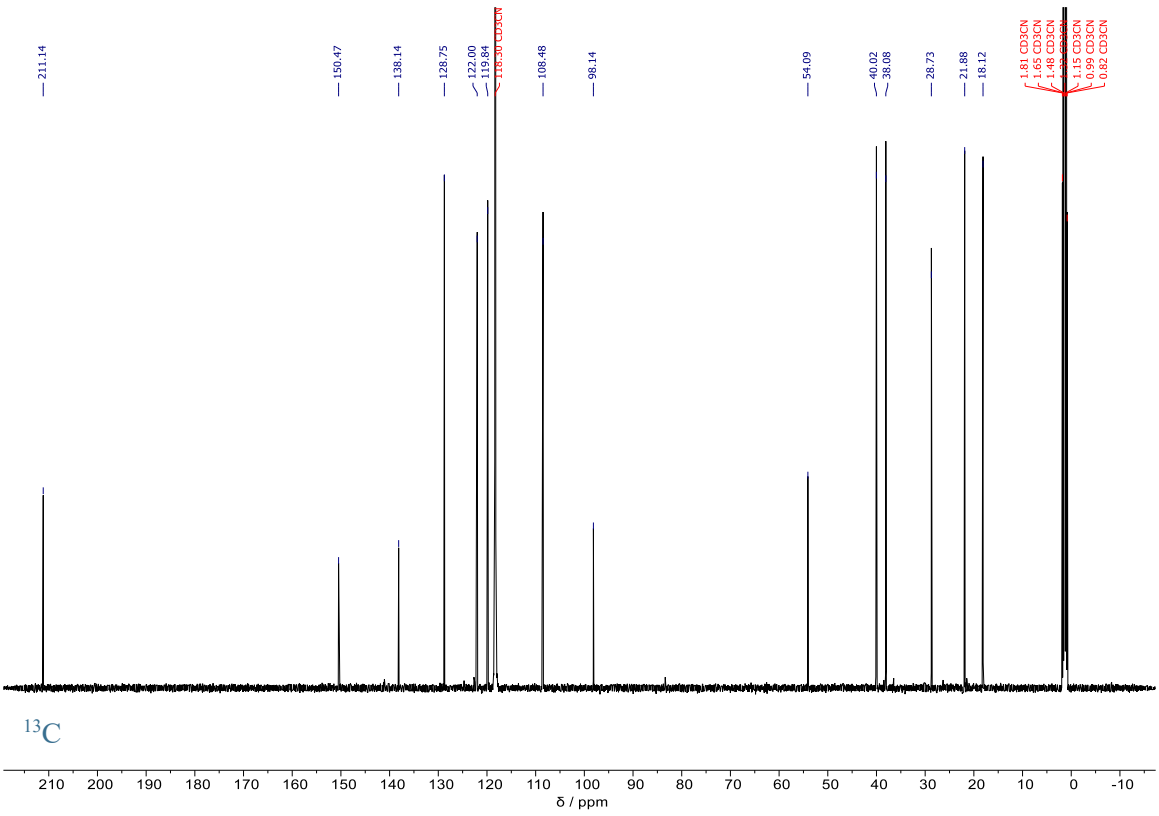




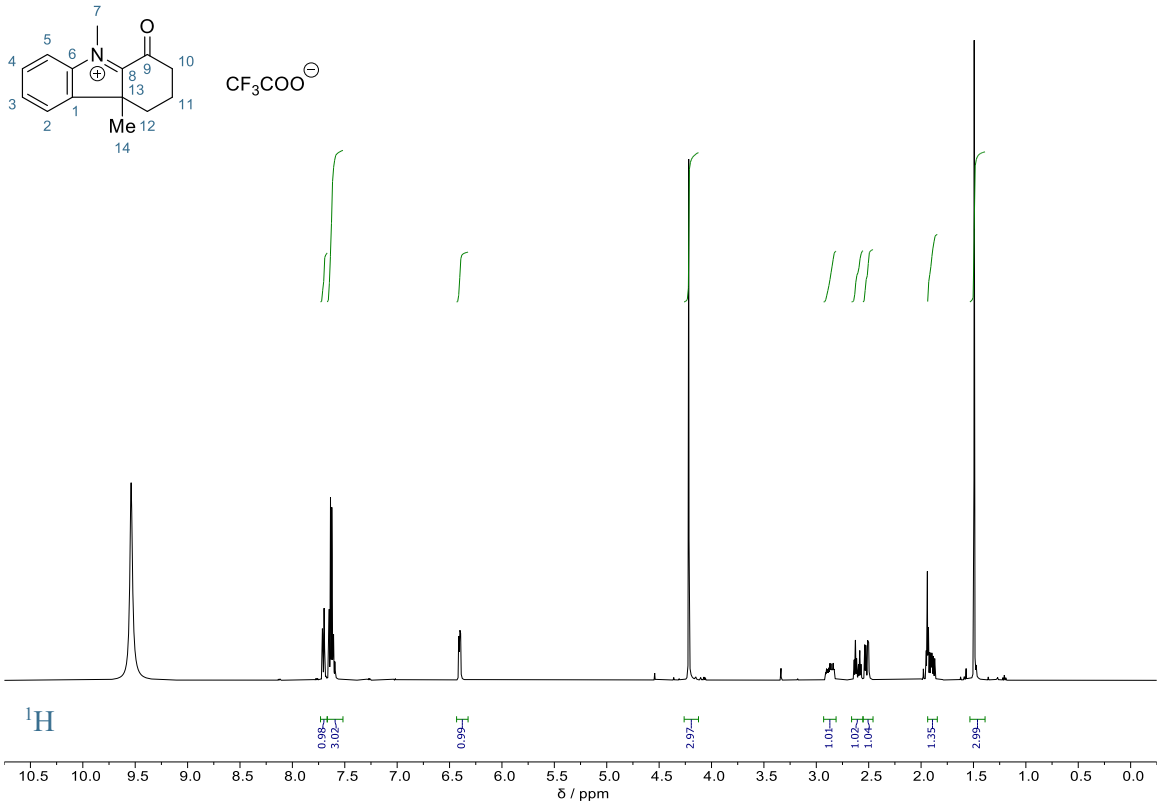
rac-9a-Hydroxy-4a,9-dimethyl-2,3,4,4a,9,9a-hexahydro-1*H*-carbazol-1-one, **11**

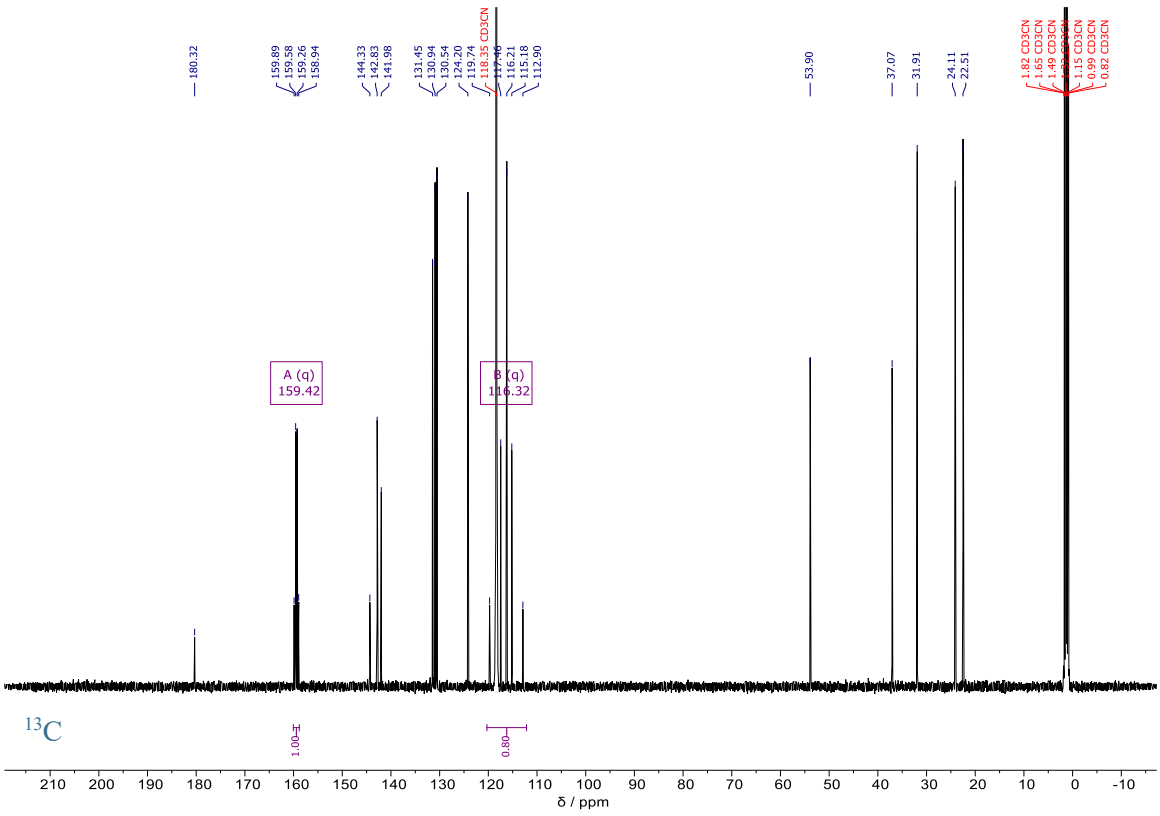




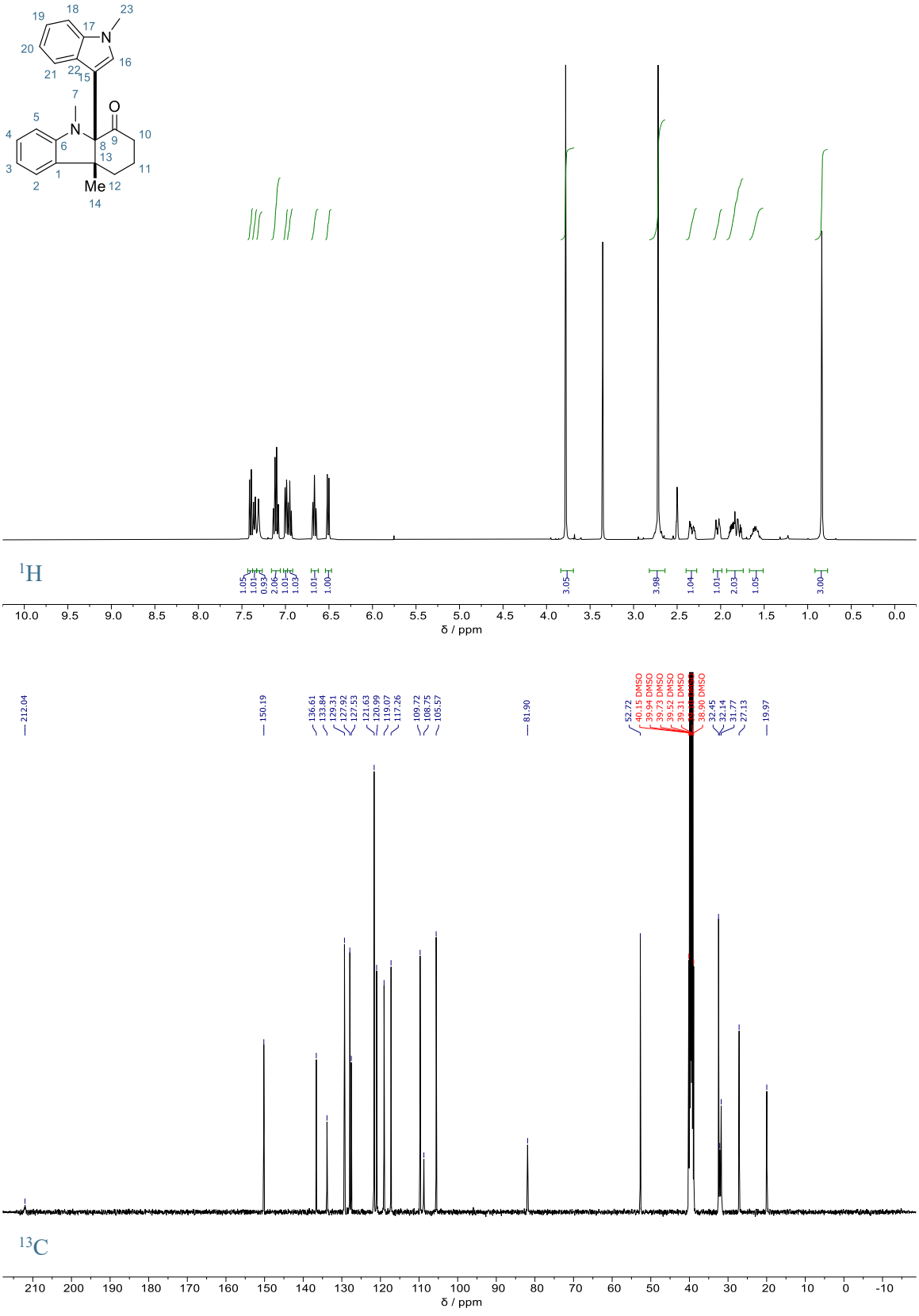


4a,9-Dimethyl-1-oxo-2,3,4,4a-tetrahydro-1*H*-carbazol-9-ium 2,2,2-trifluoroacetate, **12**

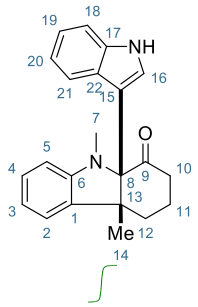


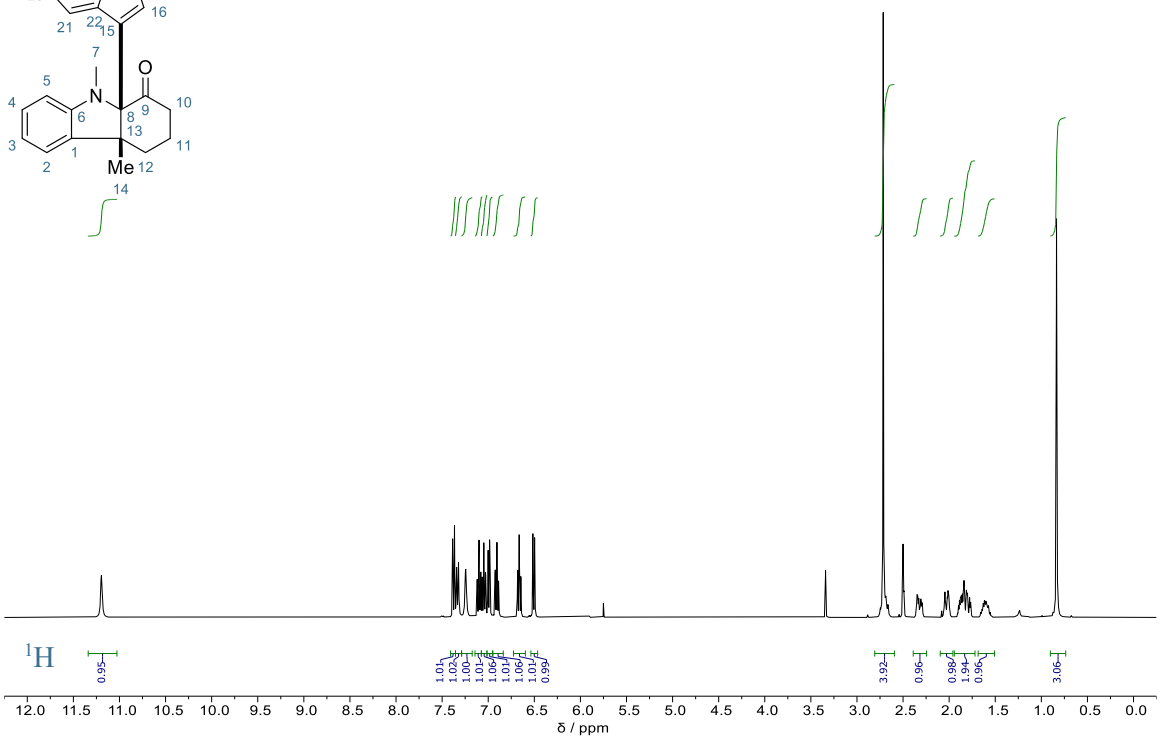


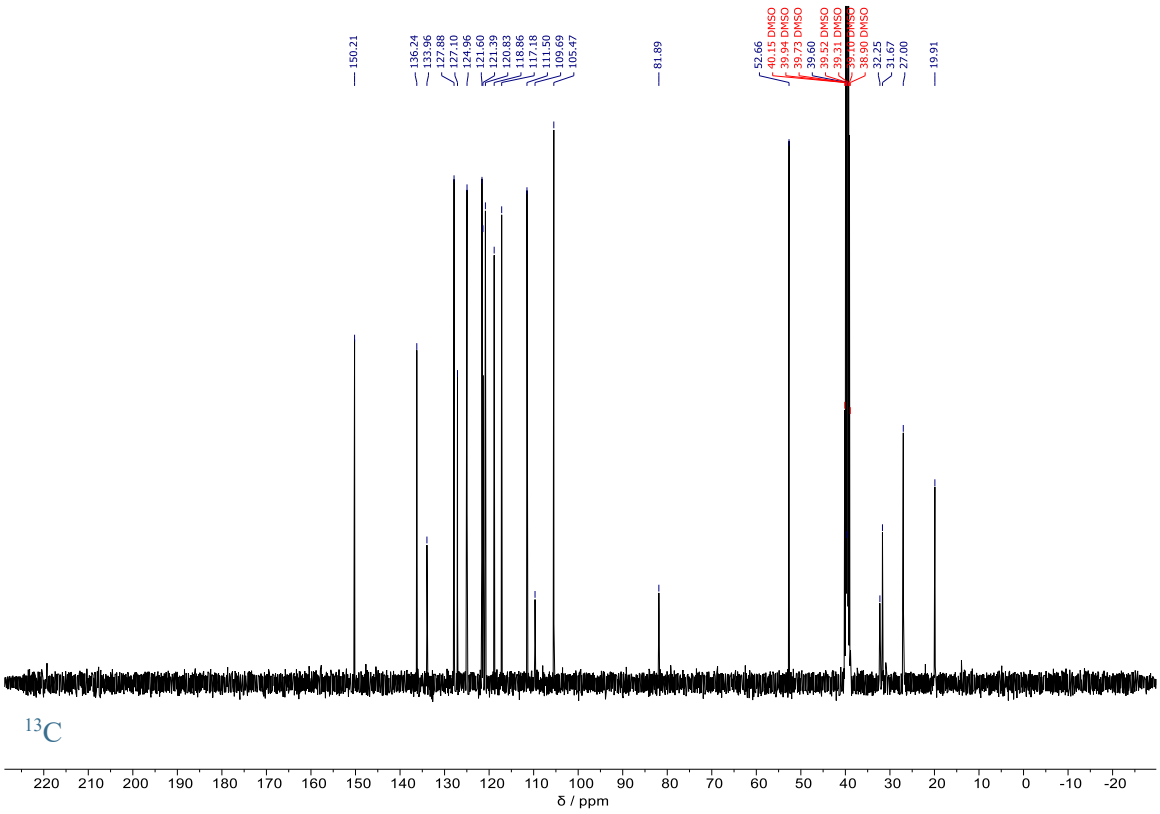
rac-4a,9-Dimethyl-9a-(1-methyl-1*H*-indol-3-yl)-2,3,4,4a,9,9a-hexahydro-1*H*-carbazol-1-one, **13**



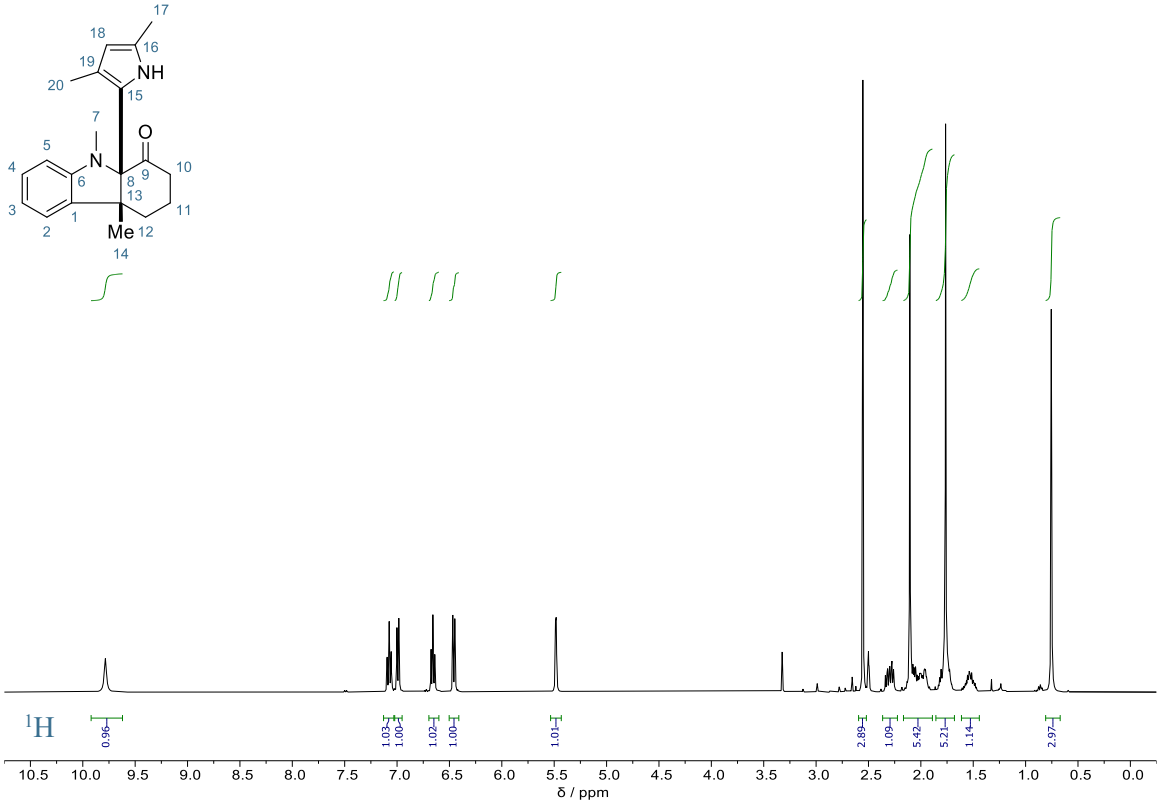
rac-9a-(1*H*-Indol-3-yl)-4a,9-dimethyl-2,3,4,4a,9,9a-hexahydro-1*H*-carbazol-1-one, **14**

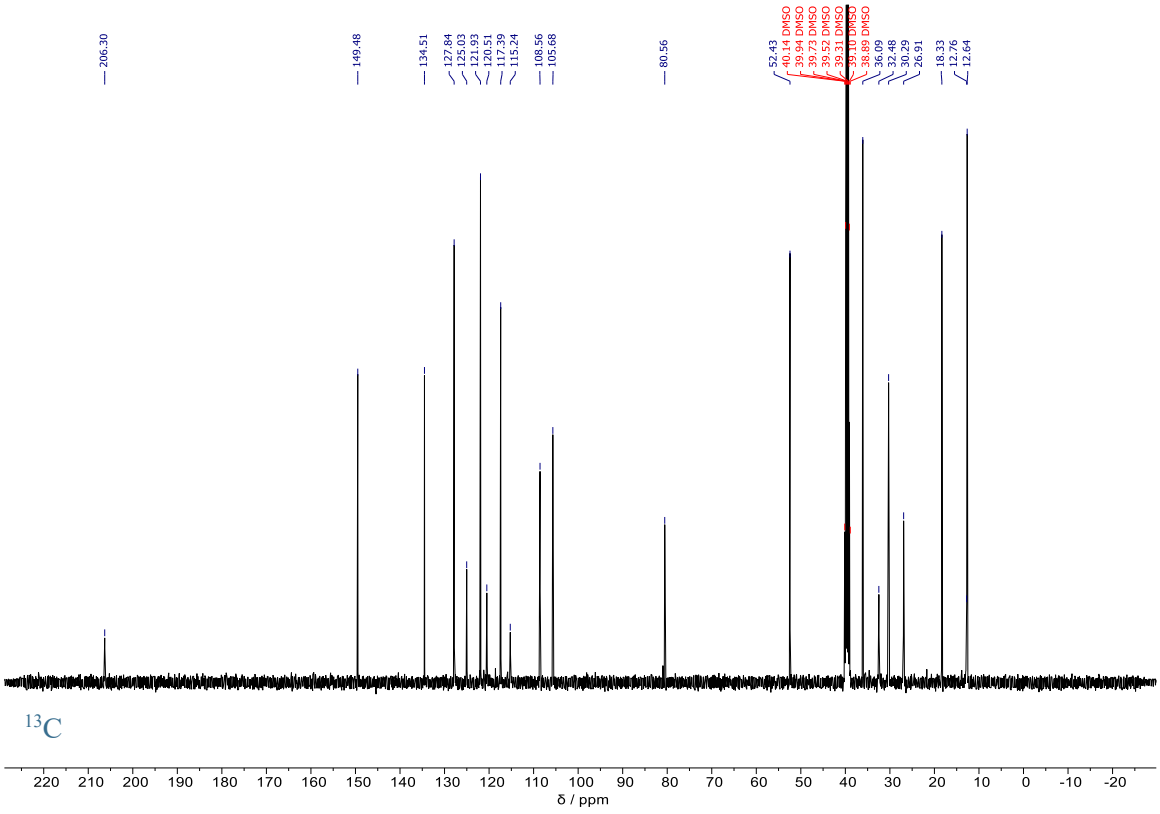




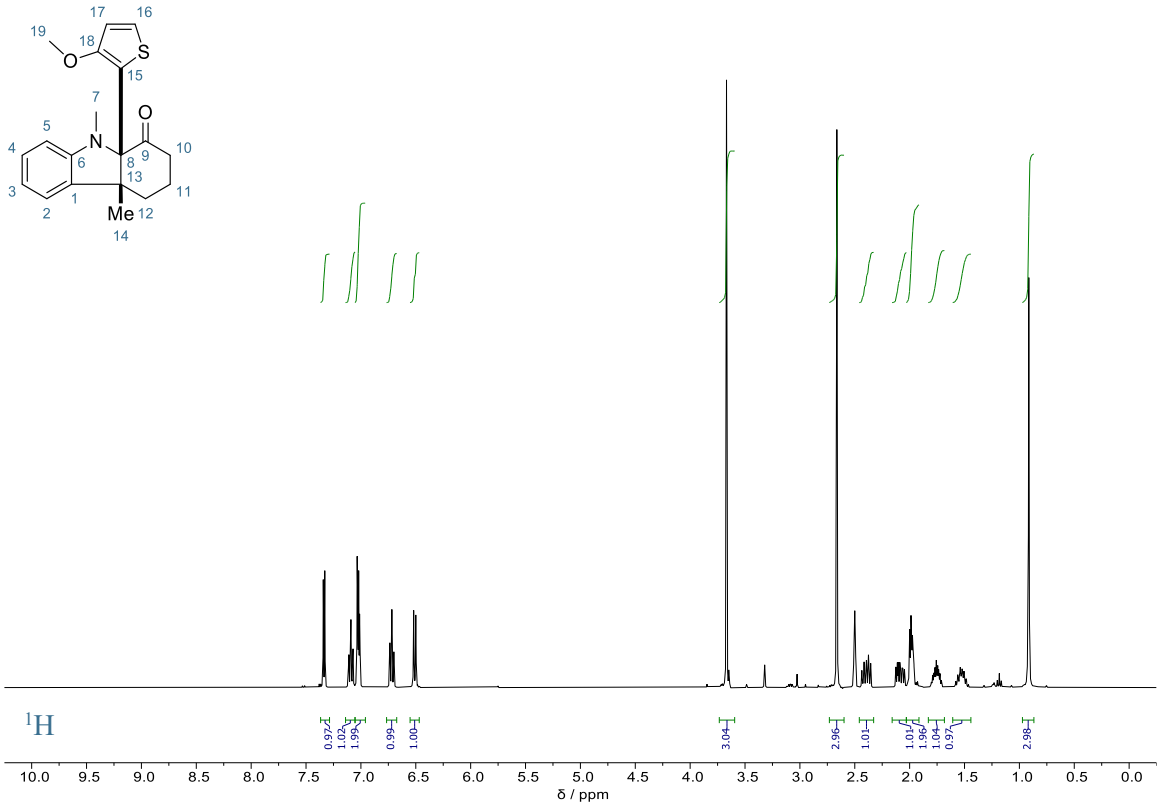


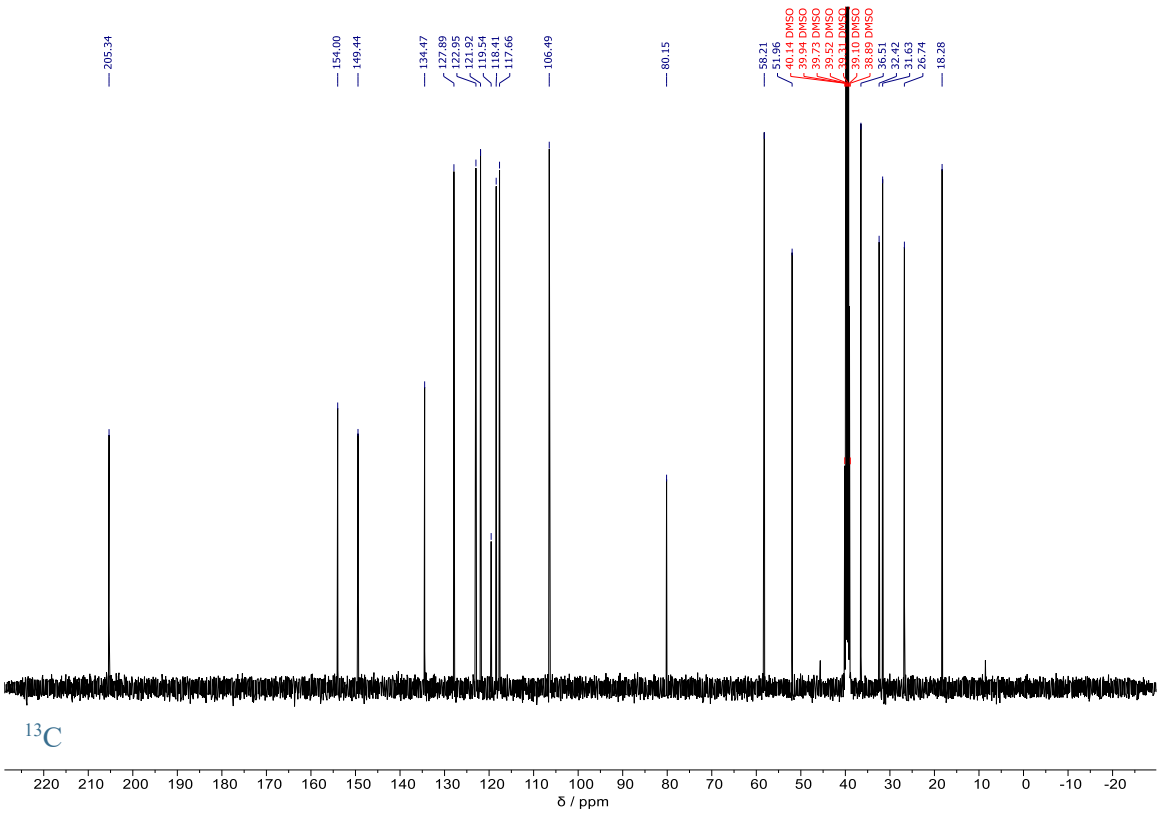
rac-9a-(3,5-Dimethyl-1*H*-pyrrol-2-yl)-4a,9-dimethyl-2,3,4,4a,9,9a-hexahydro-1*H*-carbazol-1-one, **15**





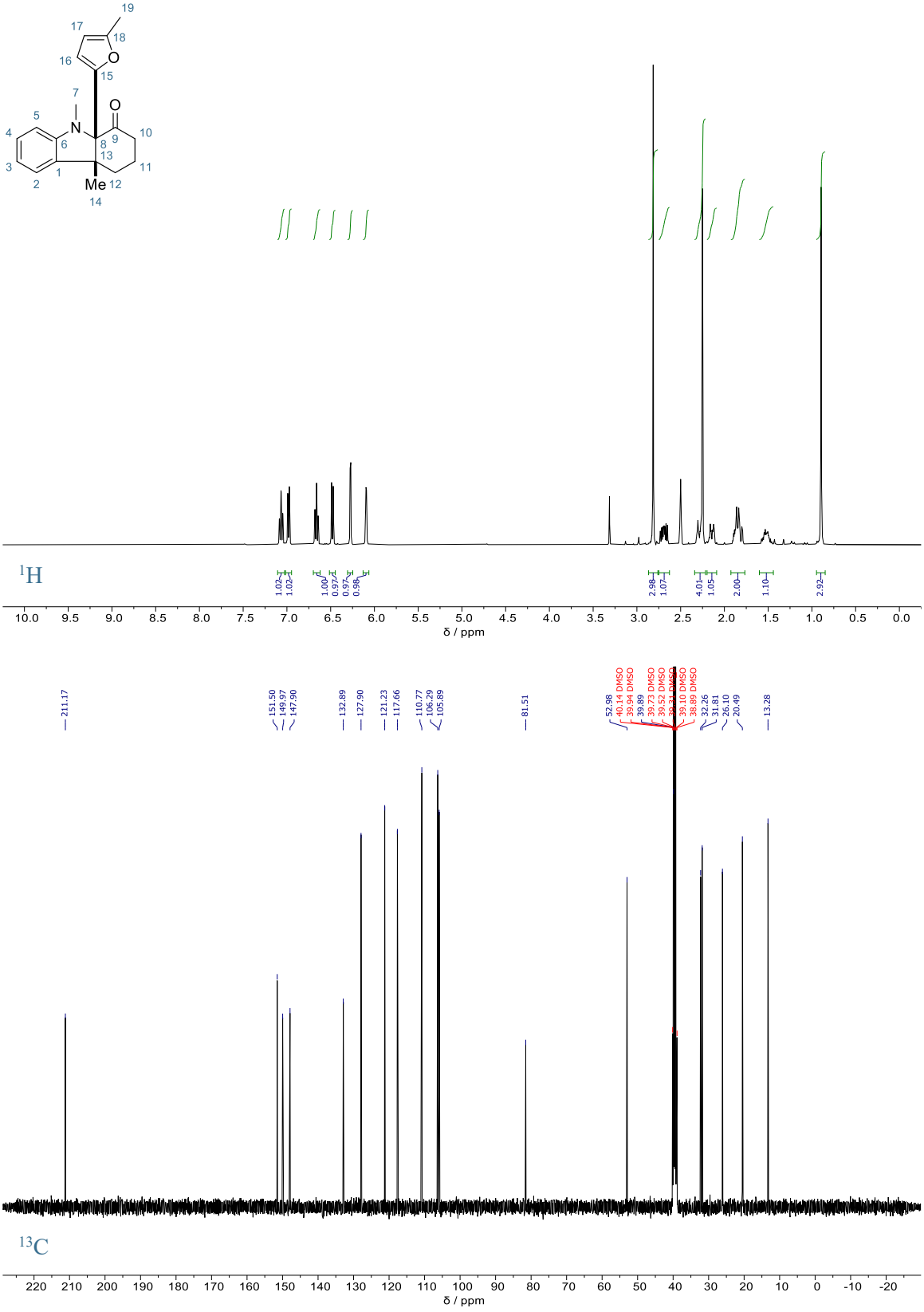
rac-9a-(3-Methoxythiophen-2-yl)-4a,9-dimethyl-2,3,4,4a,9,9a-hexahydro-1*H*-carbazol-1-one, **16**



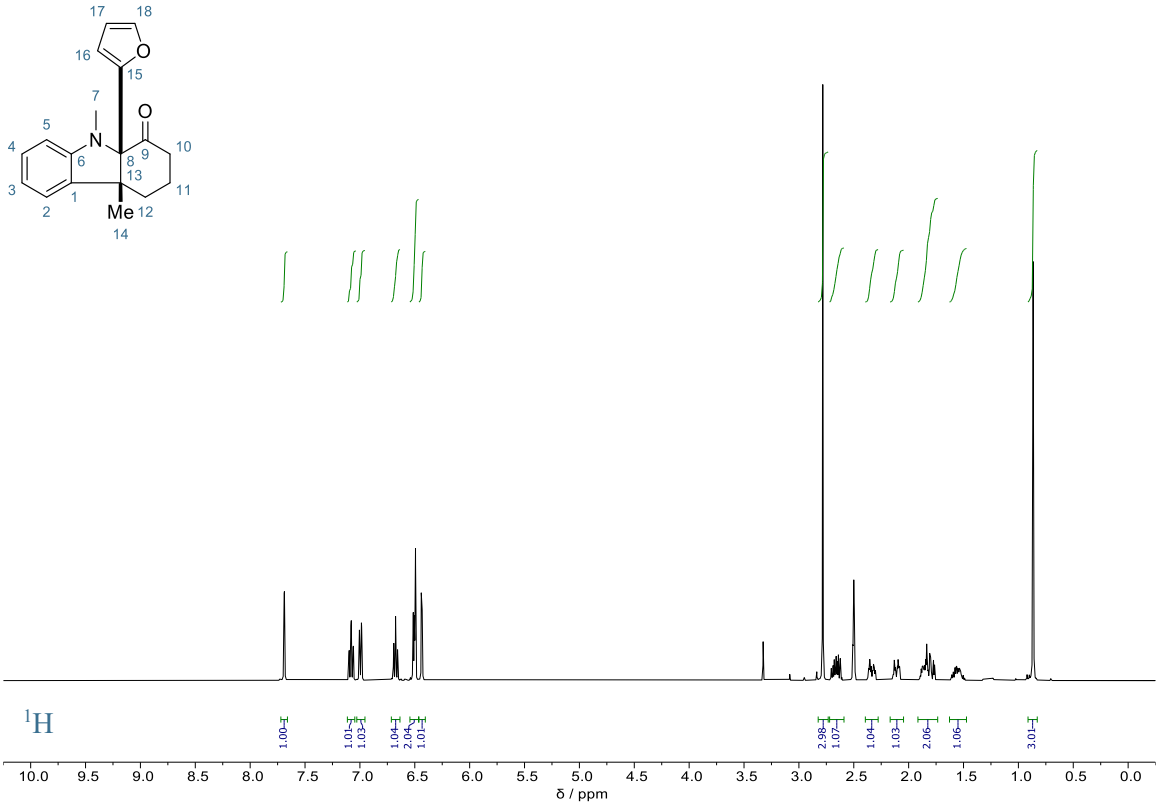


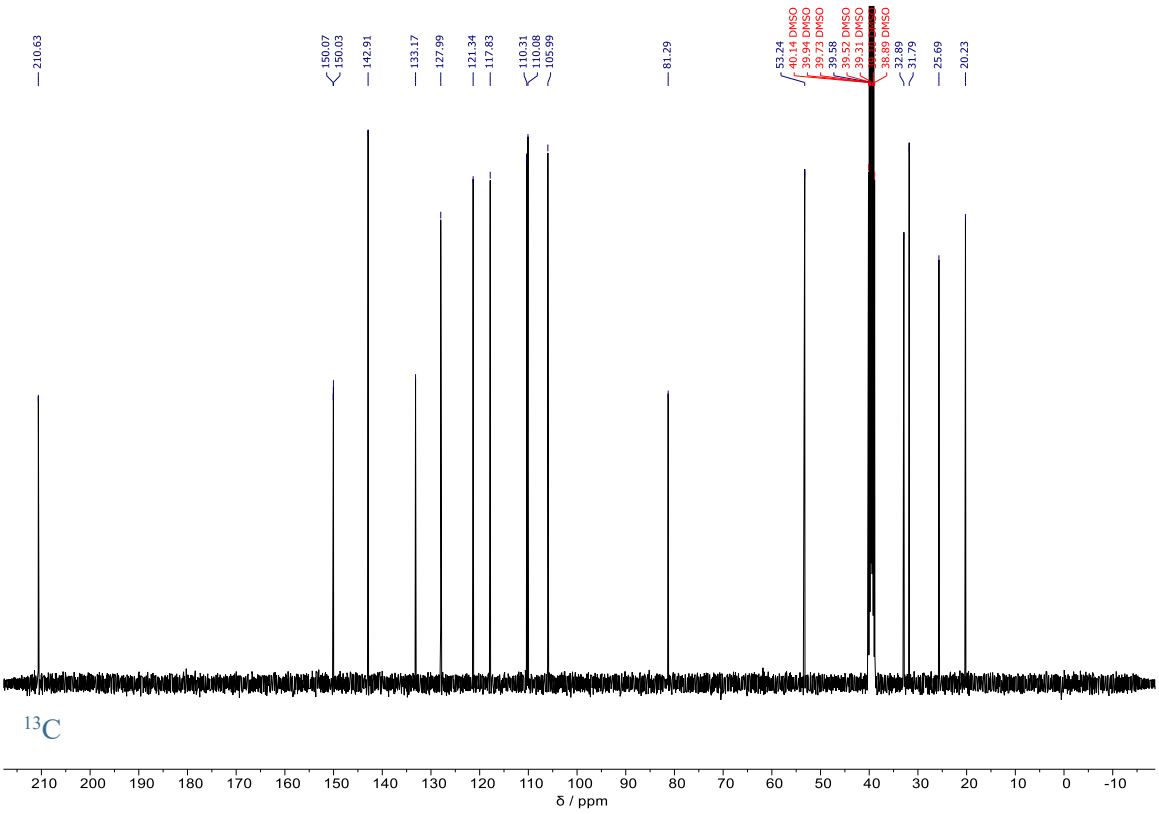
rac-4a,9-Dimethyl-9a-(5-methylfuran-2-yl)-2,3,4,4a,9,9a-hexahydro-1*H*-carbazol-1-one,

17

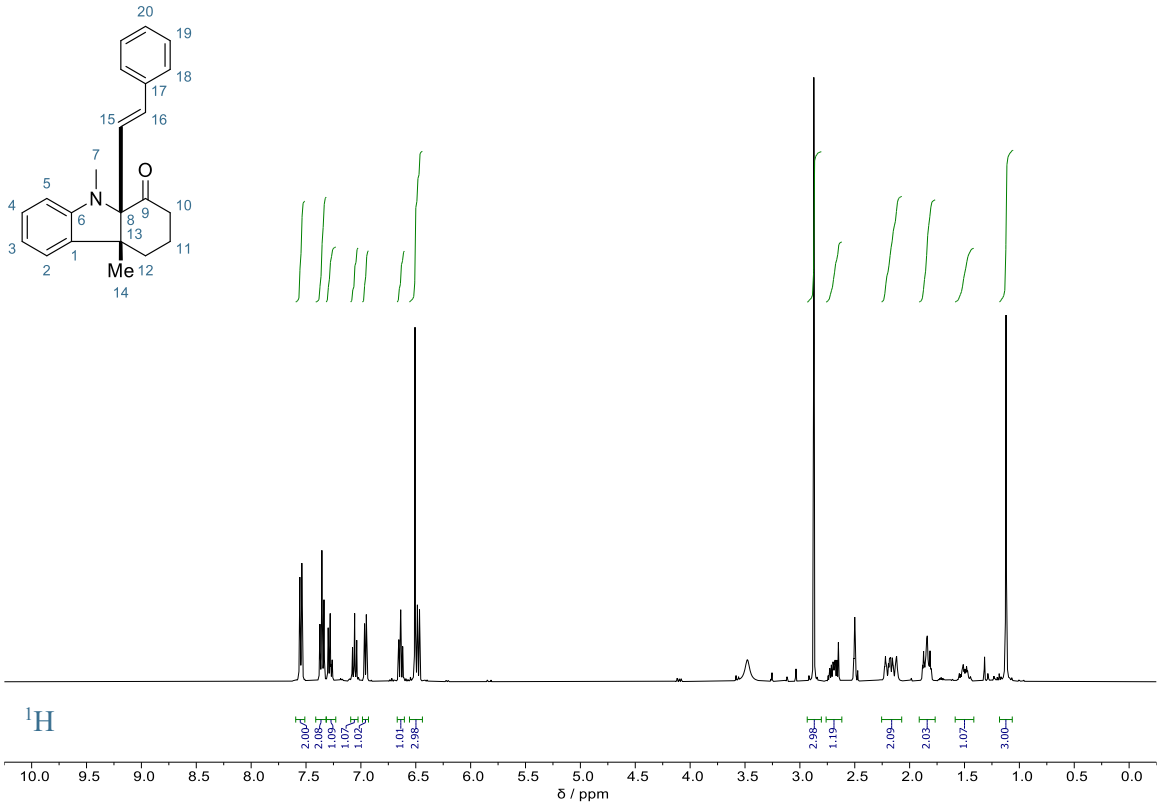


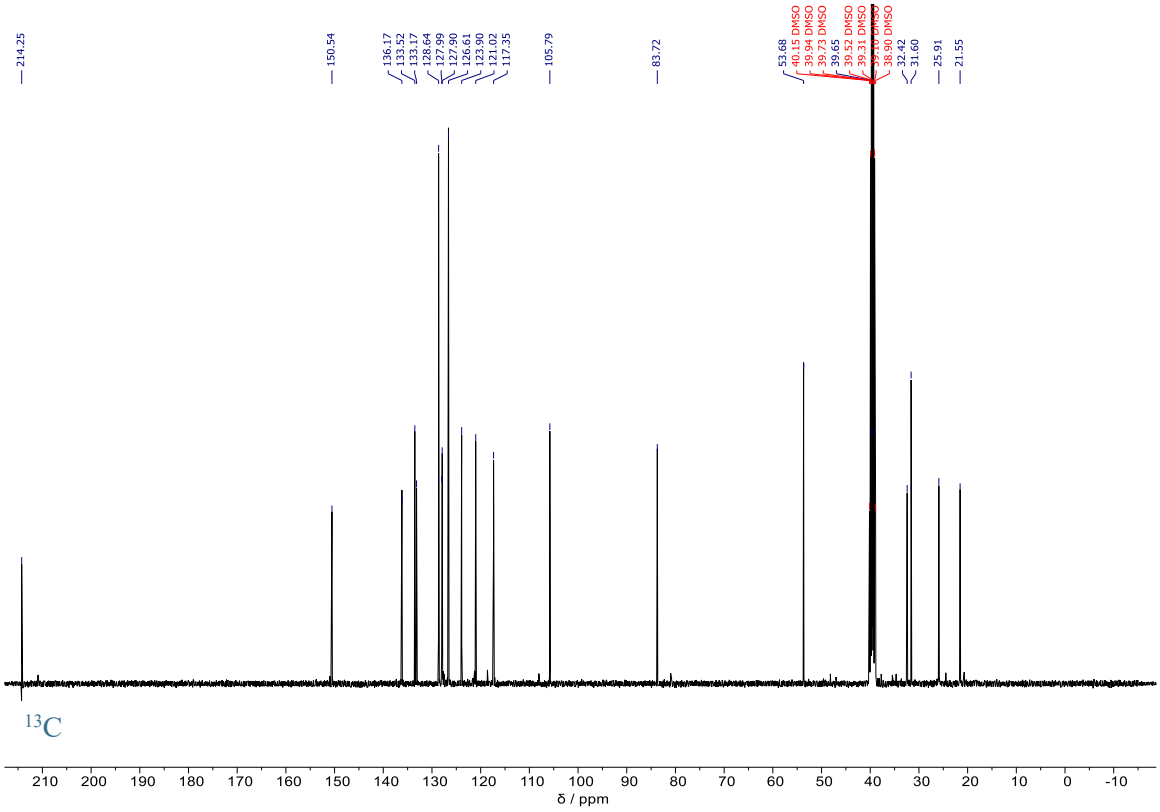
rac-9a-(Furan-2-yl)-4a,9-dimethyl-2,3,4,4a,9,9a-hexahydro-1*H*-carbazol-1-one, **18**



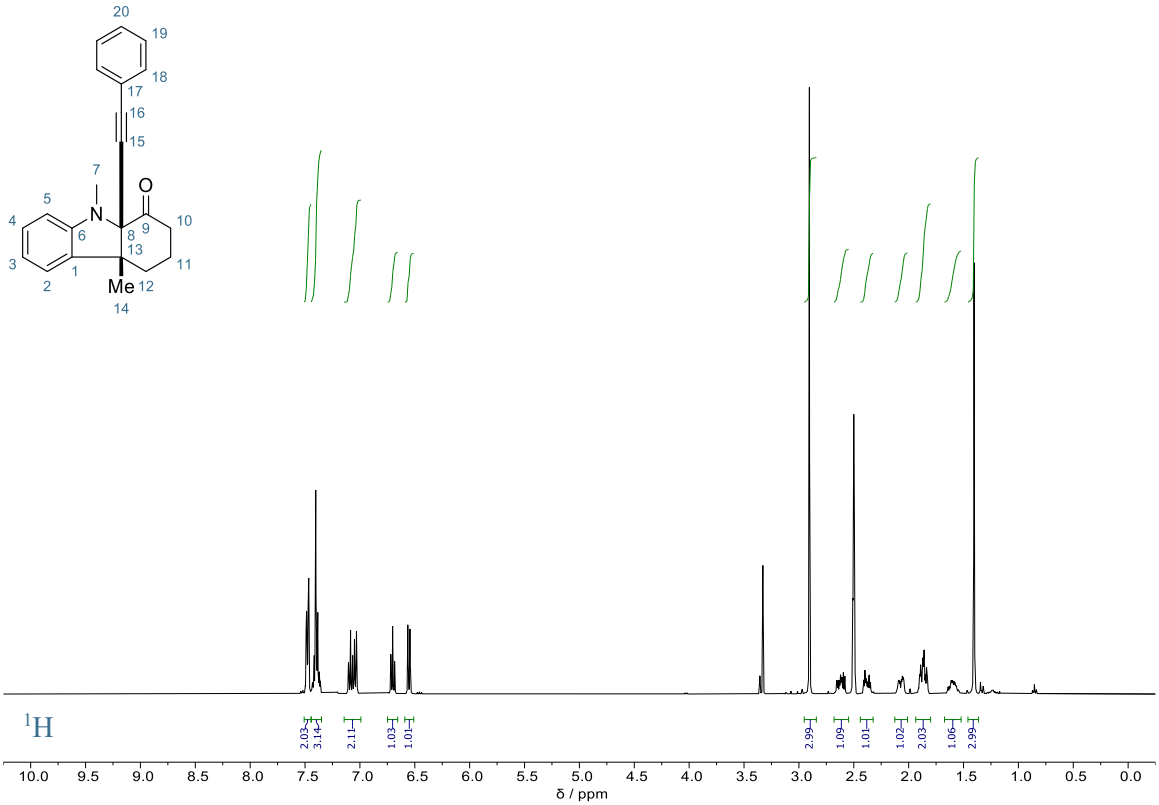


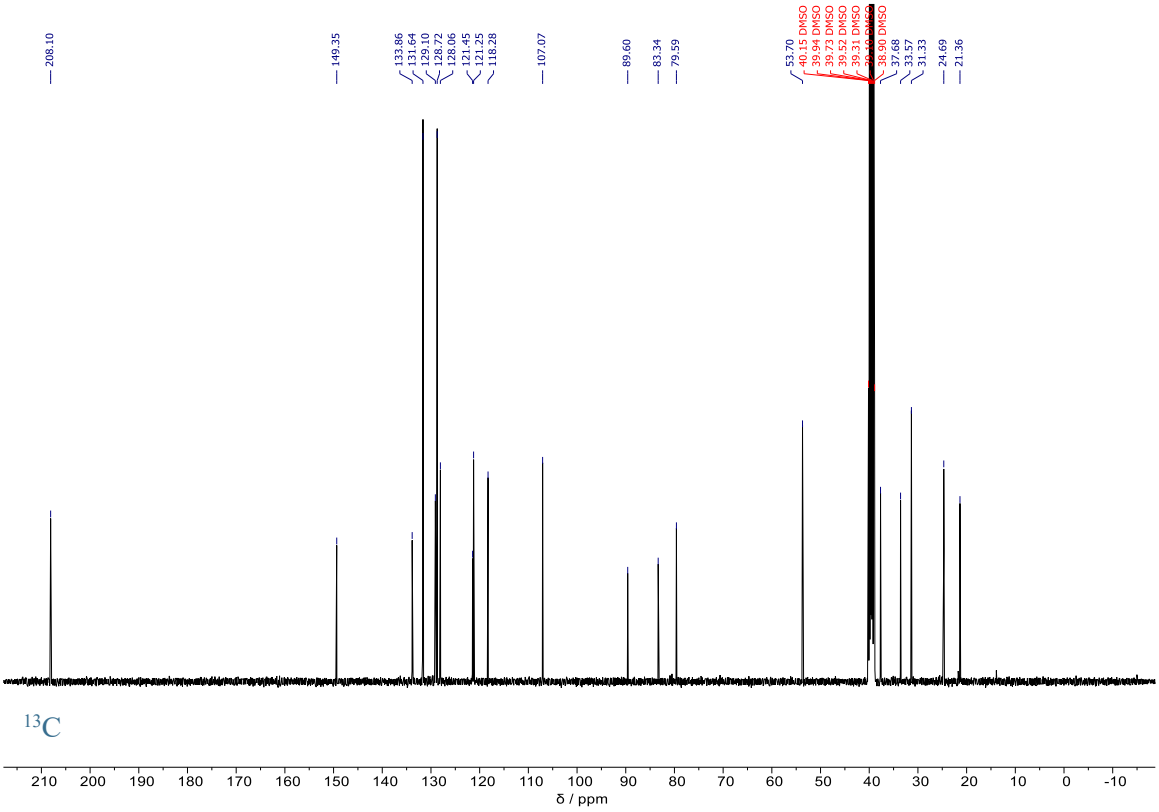
rac-4a,9-Dimethyl-9a-((*E*)-styryl)-2,3,4,4a,9,9a-hexahydro-1*H*-carbazol-1-one, **19**



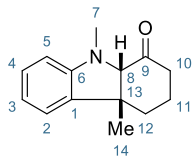


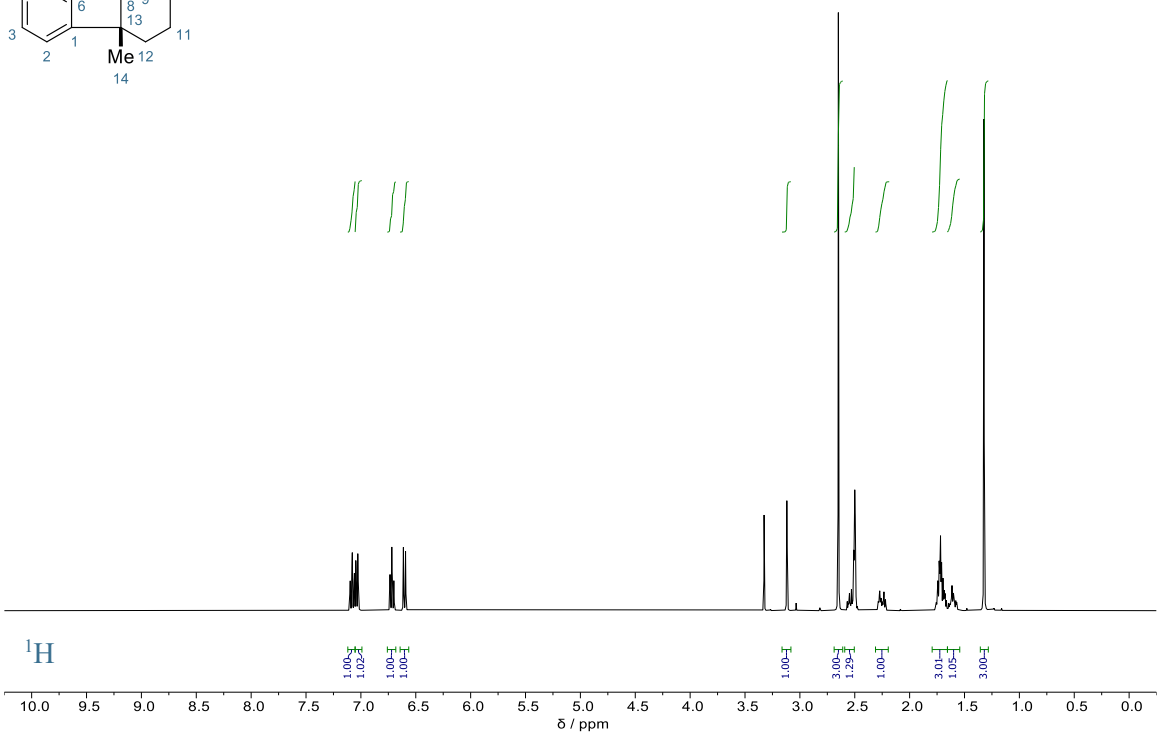
rac-4a,9-Dimethyl-9a-(phenylethynyl)-2,3,4,4a,9,9a-hexahydro-1*H*-carbazol-1-one, **20**

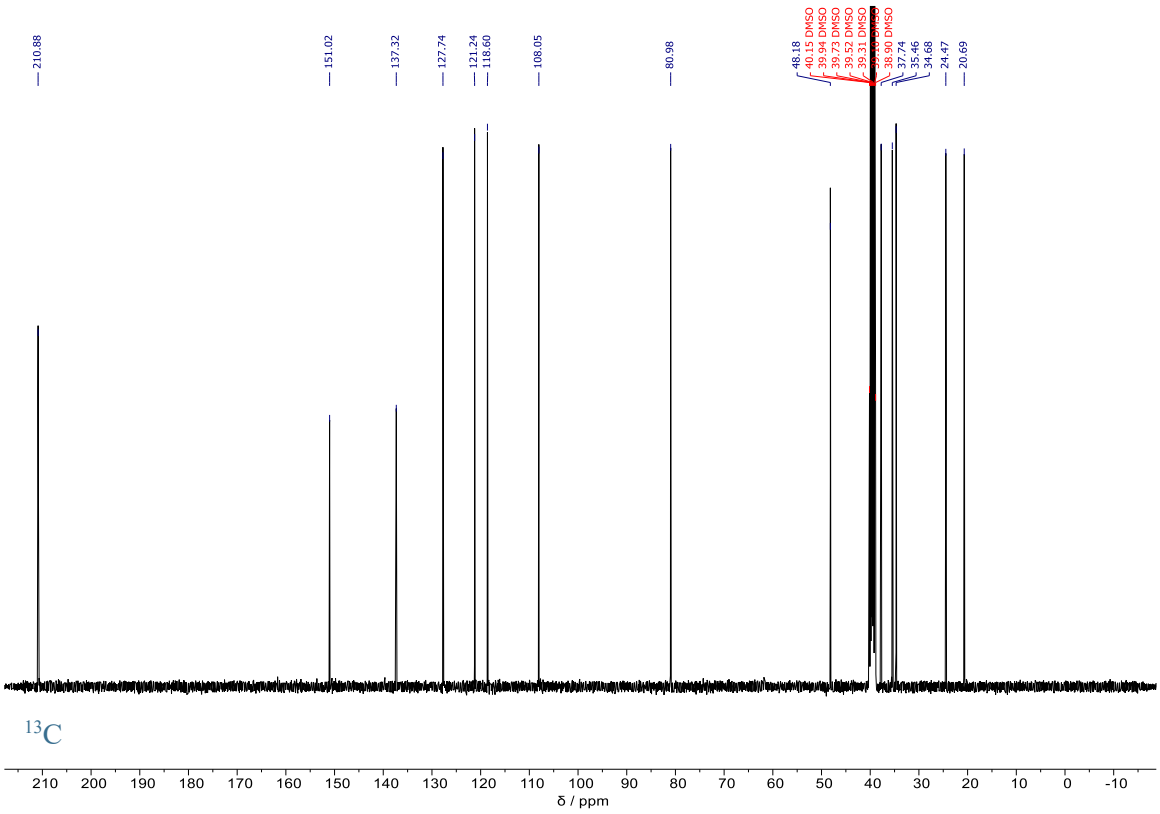




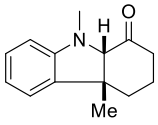
rac-4a,9-Dimethyl-2,3,4,4a,9,9a-hexahydro-1*H*-carbazol-1-one, **21**



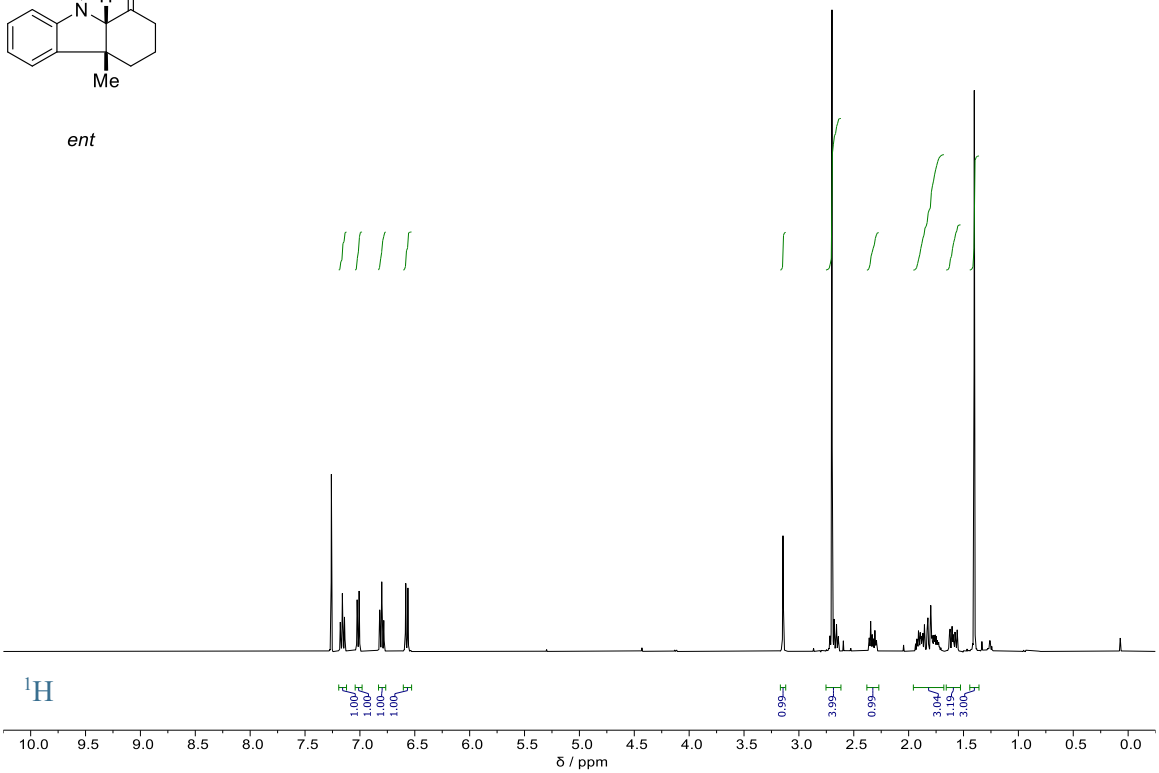




(–)-4a,9-Dimethyl-2,3,4,4a,9,9a-hexahydro-1*H*-carbazol-1-one, **(–)-21**

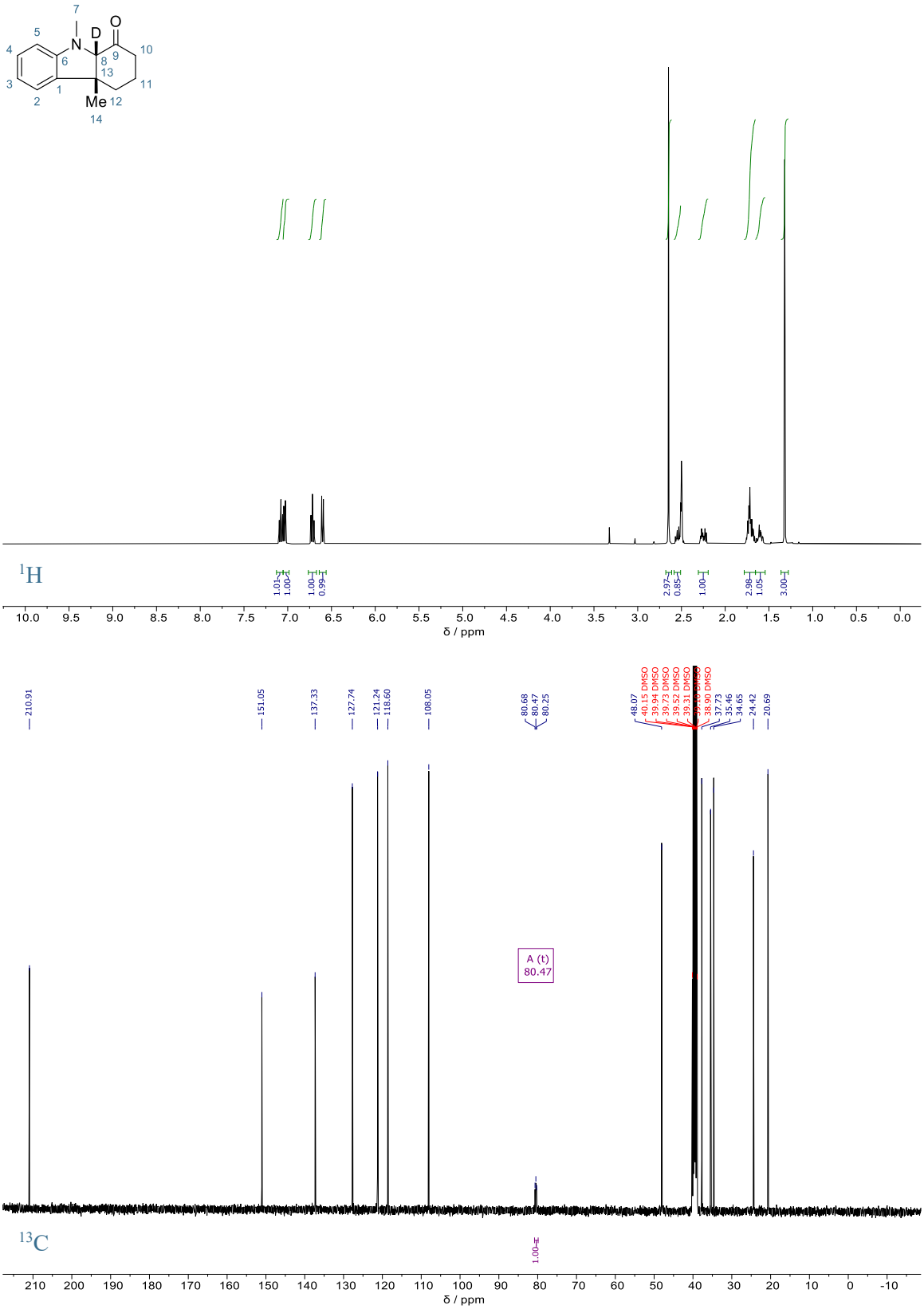


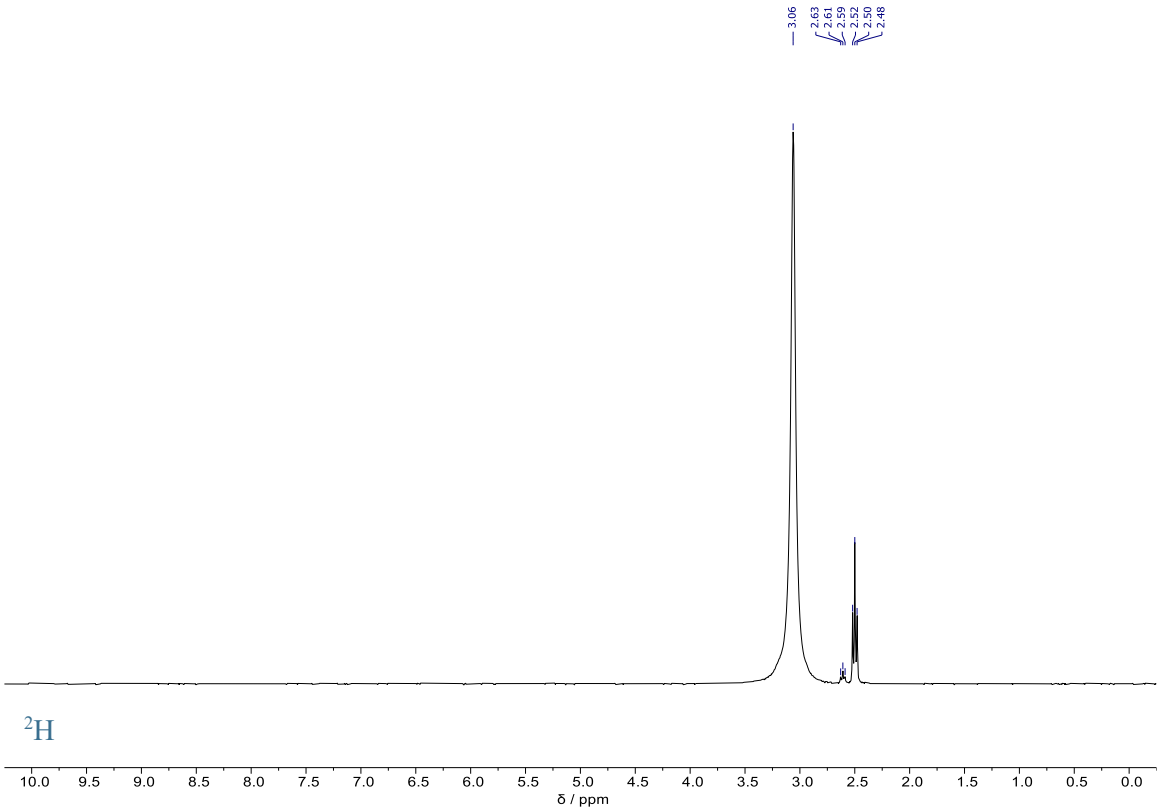
ent



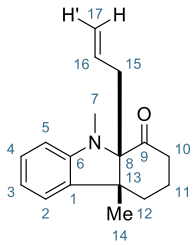
rac-4a,9-Dimethyl-2,3,4,4a,9,9a-hexahydro-1*H*-carbazol-1-one-9a-*d*, **22**

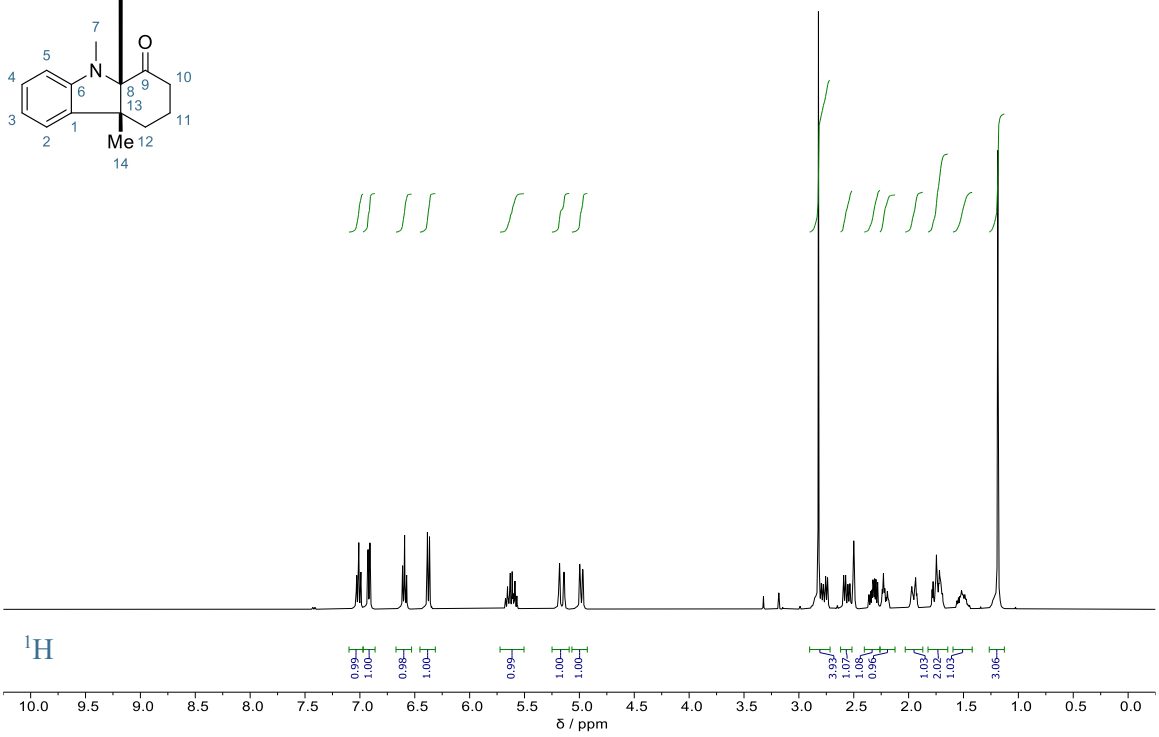
(^{1}H and ^{13}C in DMSO-d_6; ^{2}H in DMSO-h_6)



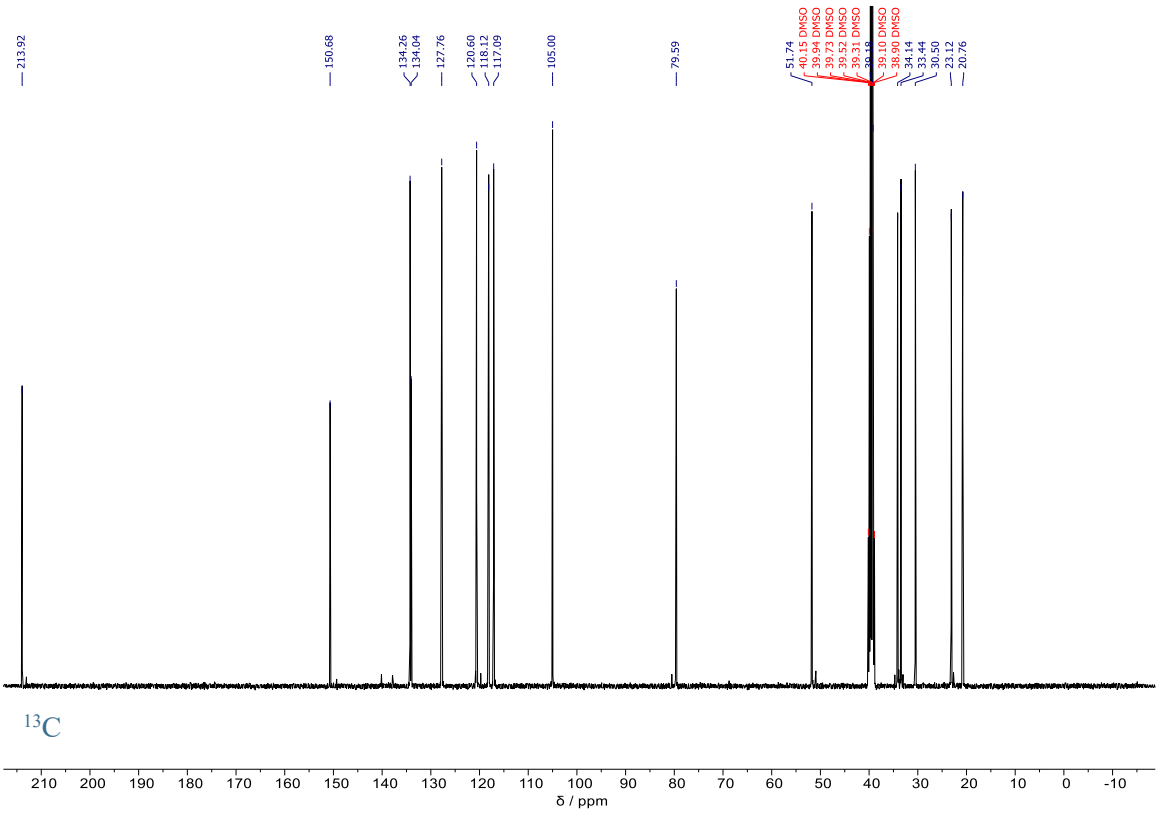

3.06
2.63
2.61
2.59
2.52
2.50
2.48
^{2}H
10.0 9.5 9.0 8.5 8.0 7.5 7.0 6.5 6.0 5.5 5.0 4.5 4.0 3.5 3.0 2.5 2.0 1.5 1.0 0.5 0.0
δ / ppm

rac-9a-Allyl-4a,9-dimethyl-2,3,4,4a,9,9a-hexahydro-1*H*-carbazol-1-one, **23**





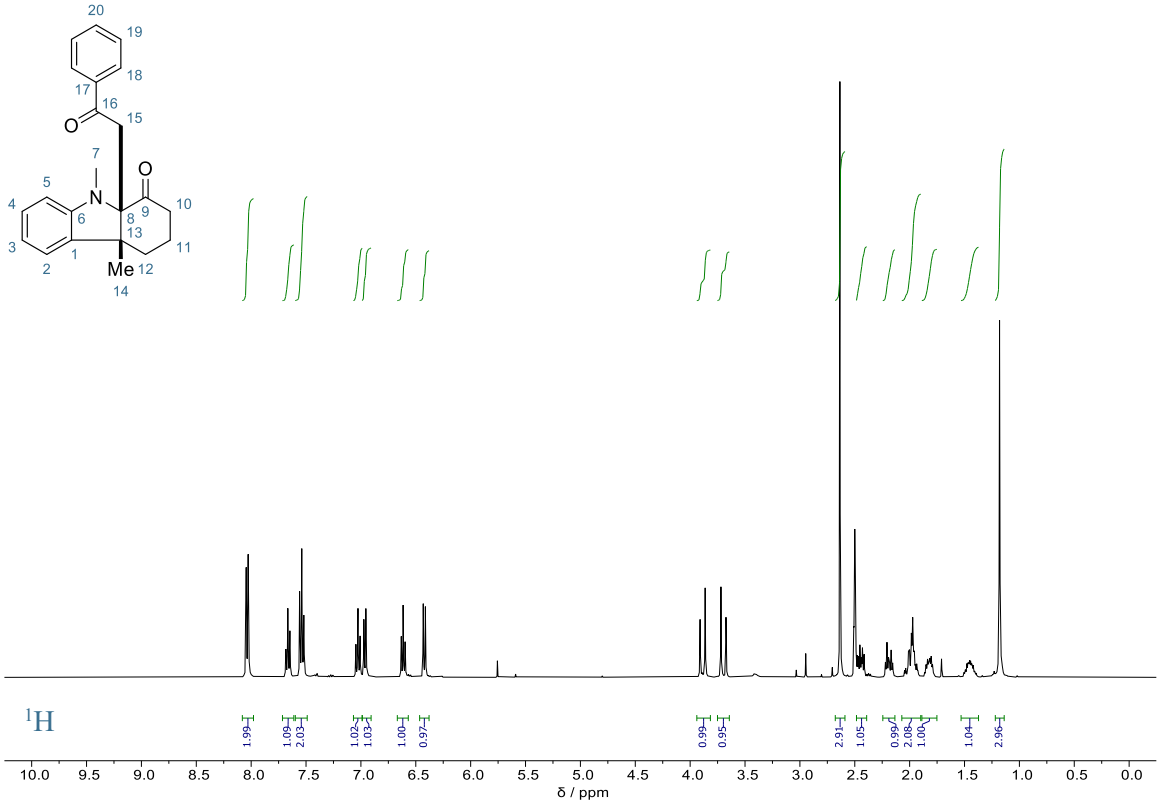
^{1}H

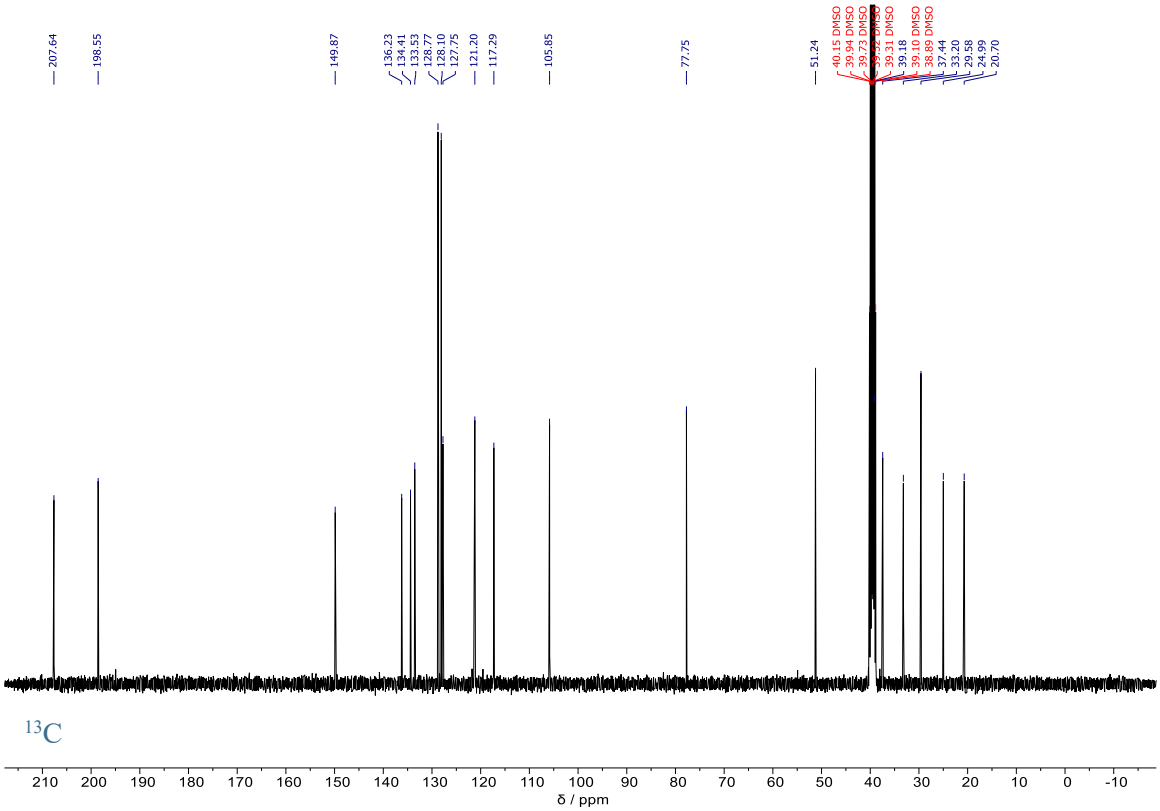


^{13}C

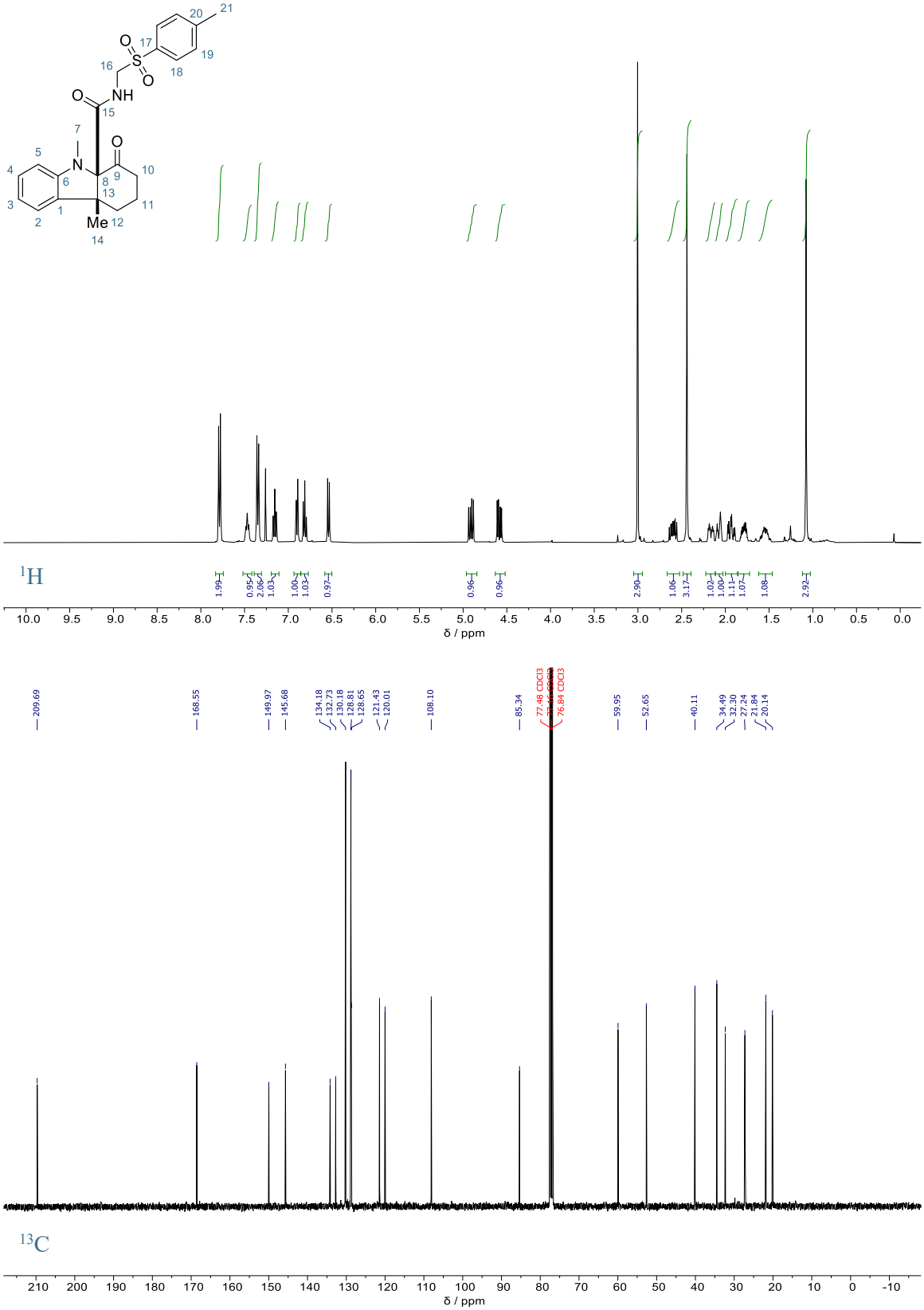
rac-4a,9-Dimethyl-9a-(2-oxo-2-phenylethyl)-2,3,4,4a,9,9a-hexahydro-1*H*-carbazol-1-one,

24

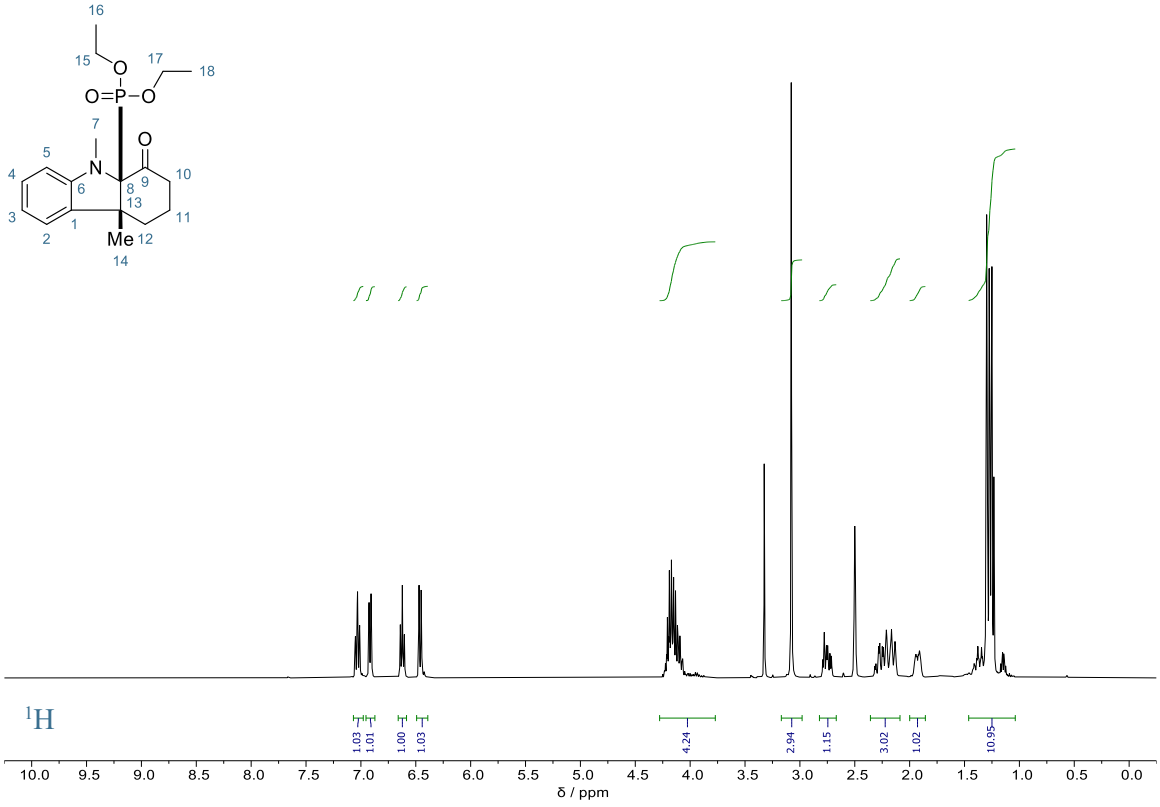


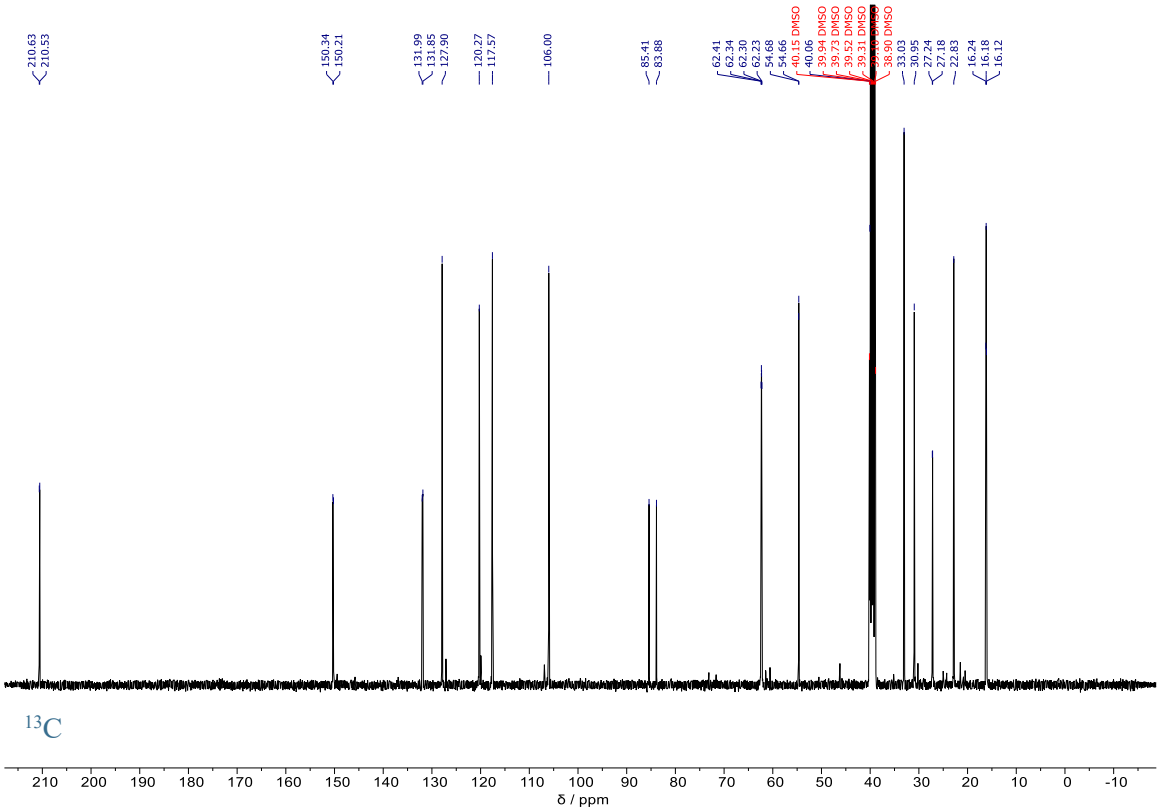


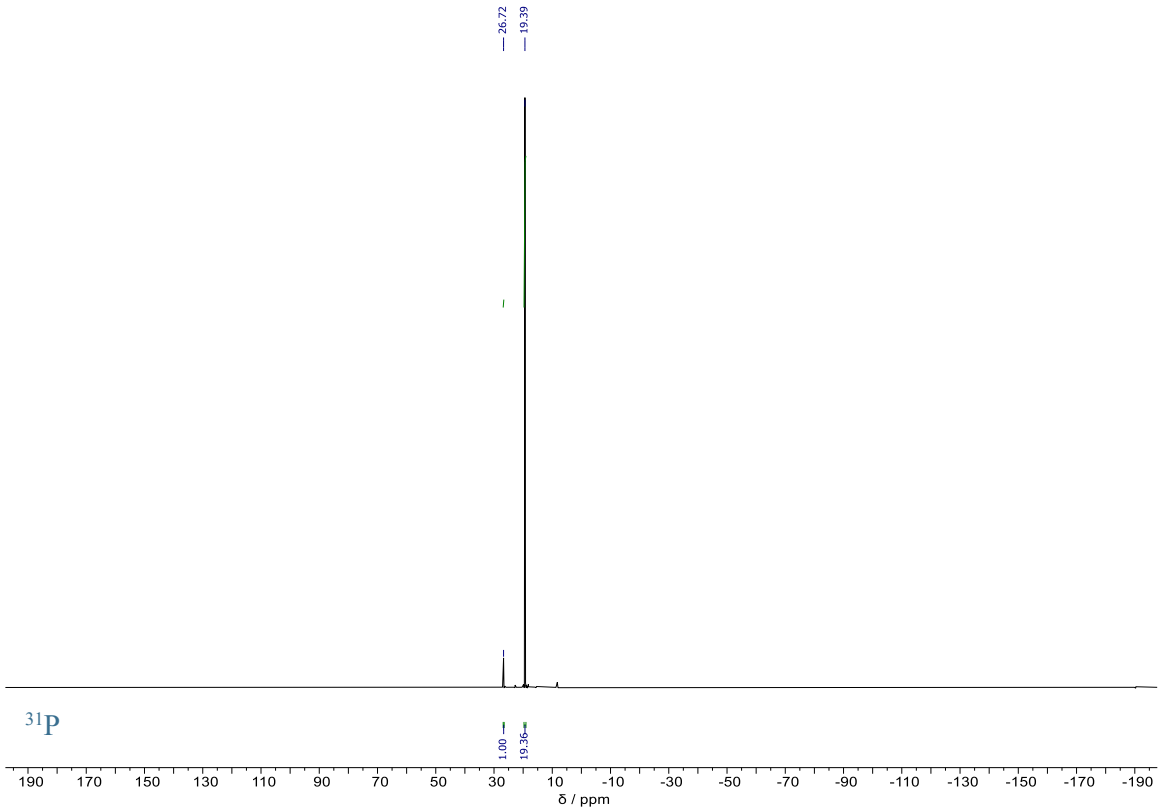
rac-4b,9-Dimethyl-8-oxo-*N*-(tosylmethyl)-4b,5,6,7,8,9-hexahydro-8a*H*-carbazole-8a-carboxamide, **25**



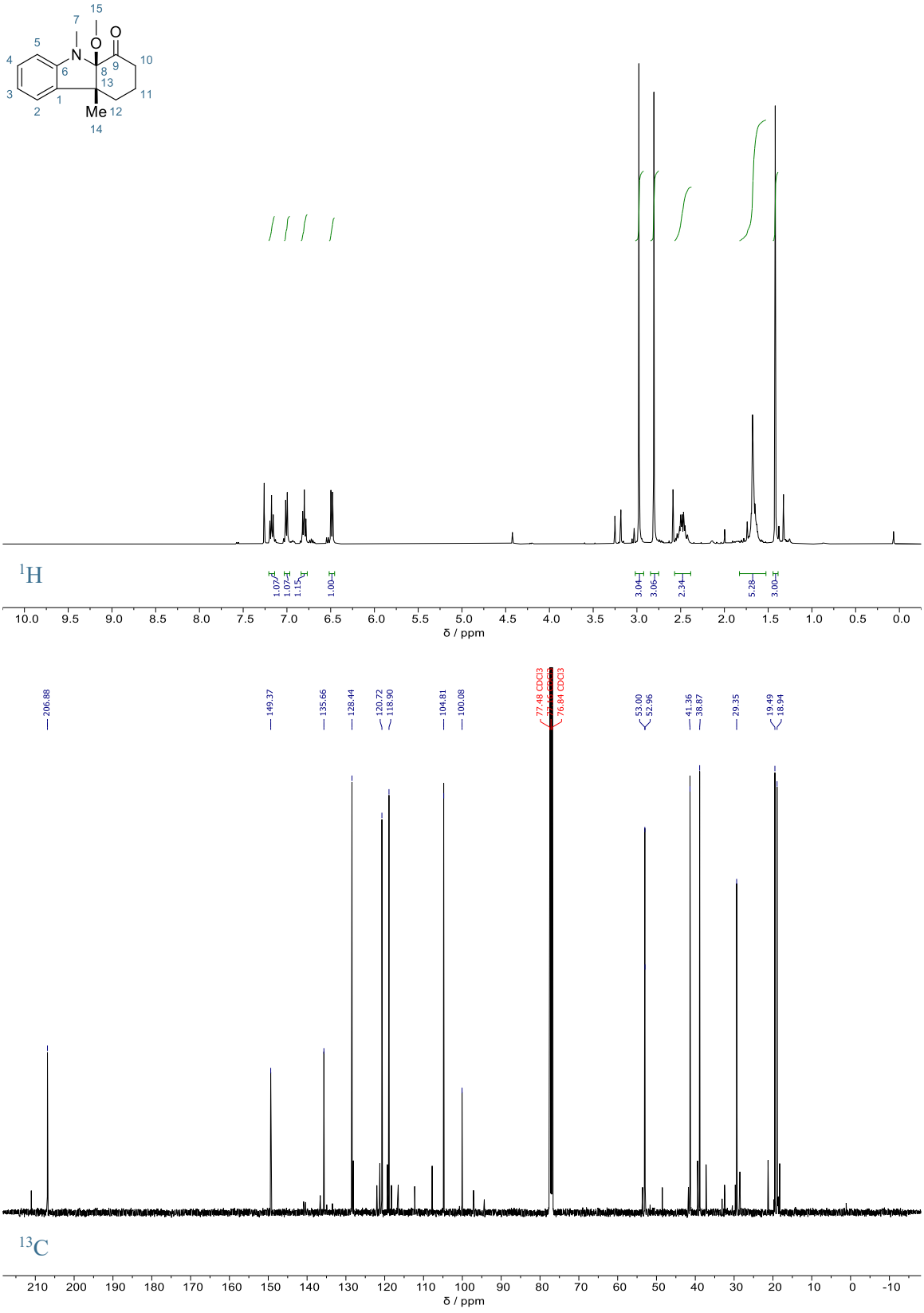
Diethyl (4b,9-dimethyl-8-oxo-4b,5,6,7,8,9-hexahydro-8a*H*-carbazol-8a-yl)phosphonate (racemate), **26**





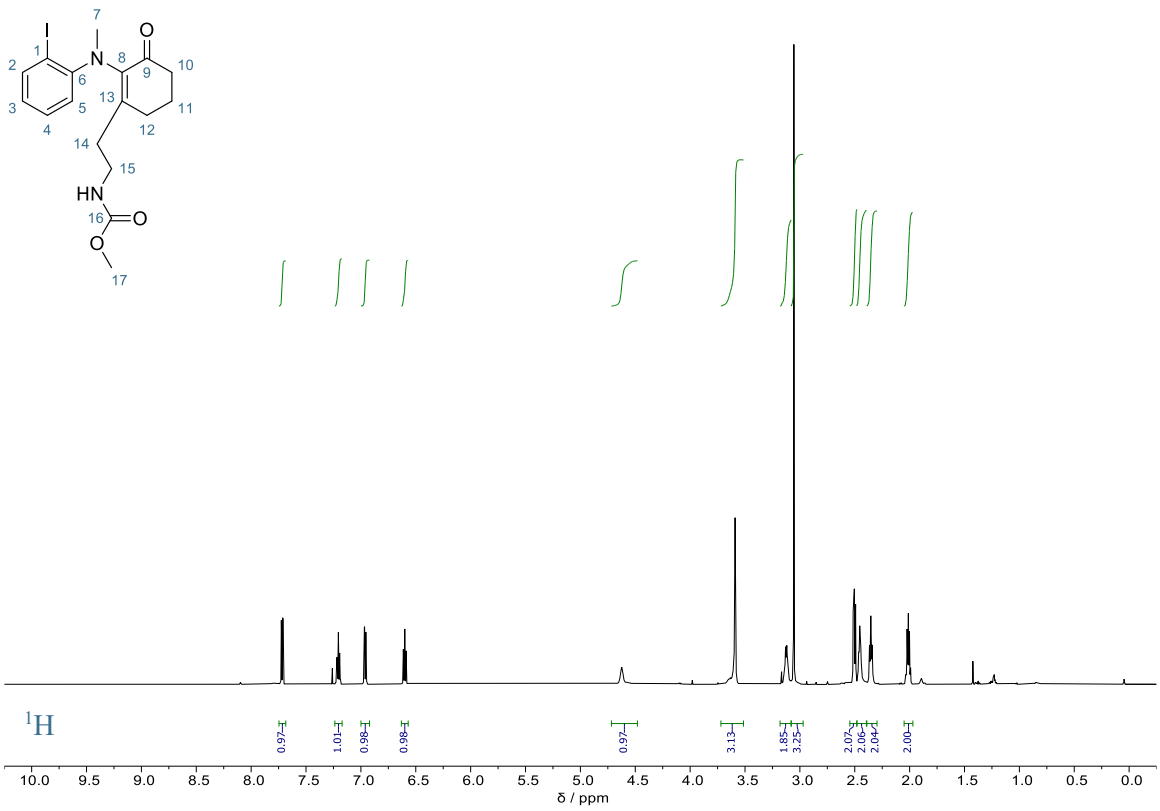

26.72
19.39
31P
1.00
19.36
190 170 150 130 110 90 70 50 30 10 -10 -30 -50 -70 -90 -110 -130 -150 -170 -190
δ / ppm

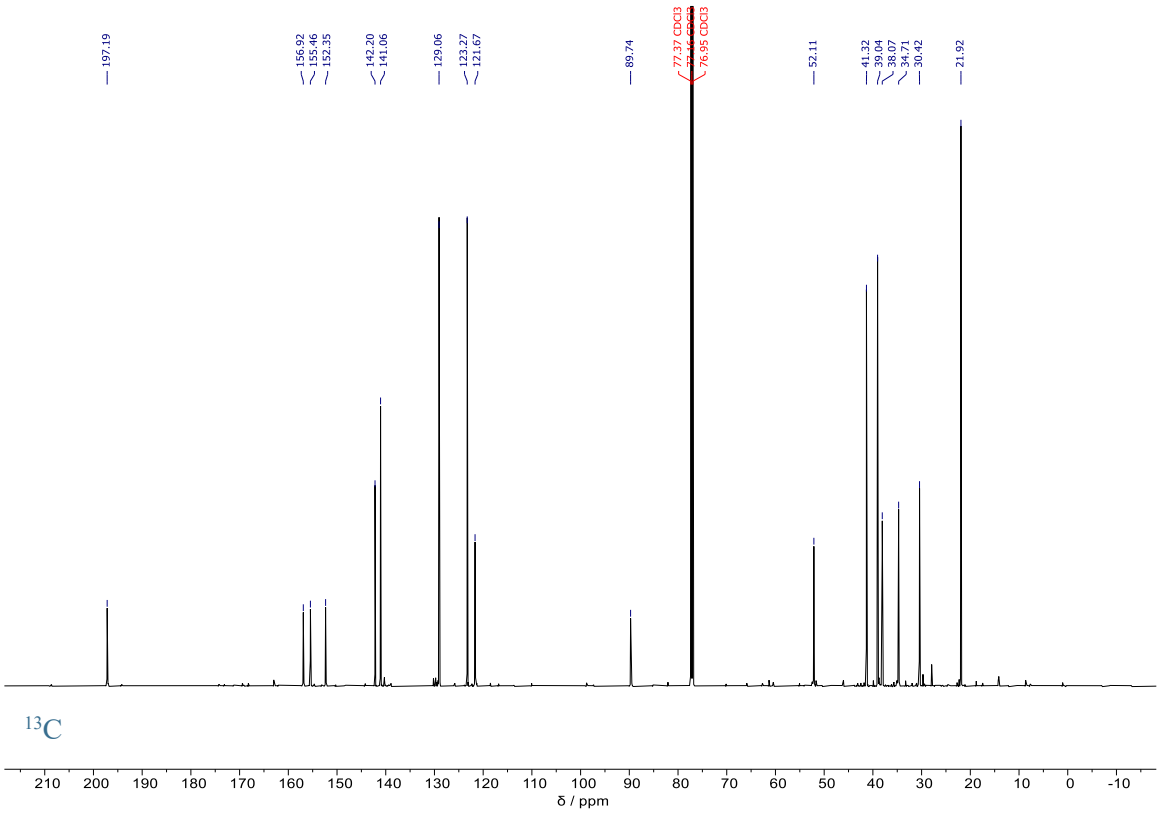
rac-9a-Methoxy-4a,9-dimethyl-2,3,4,4a,9,9a-hexahydro-1*H*-carbazol-1-one, **27**



Note: This compound was isolated and characterized without chromatographic purification owing to its instability on silica and alumina gels.

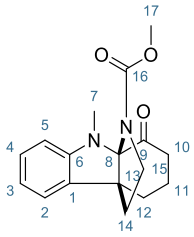
Methyl (2-(2-((2-iodophenyl)(methyl)amino)-3-oxocyclohex-1-en-1-yl)ethyl)carbamate, **28**

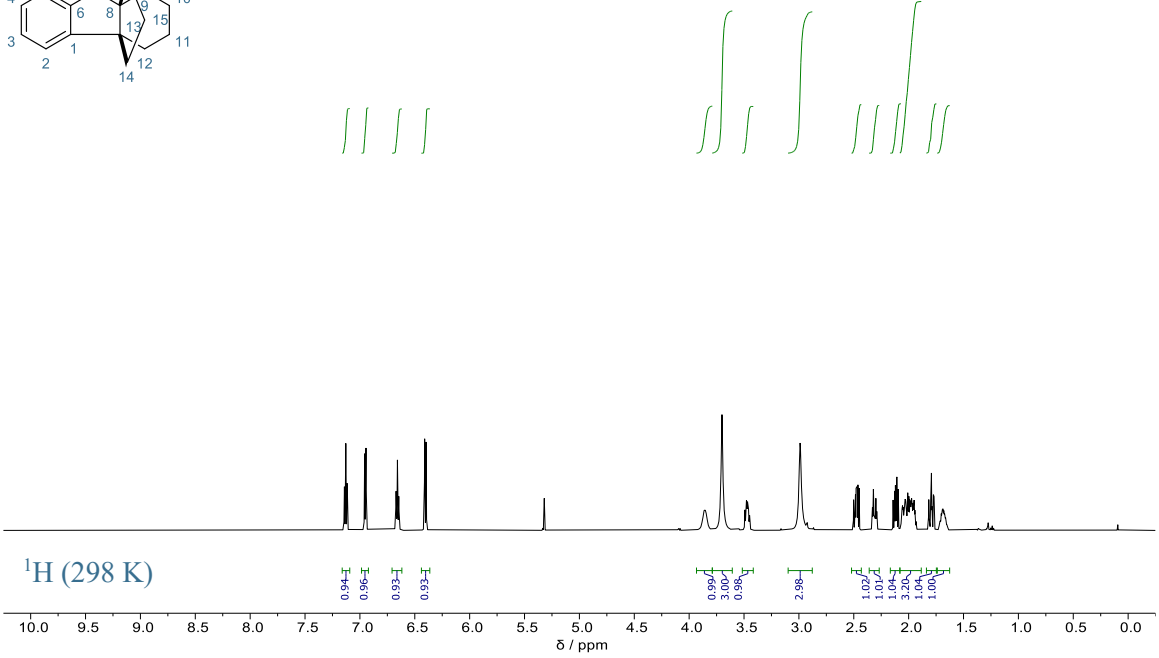


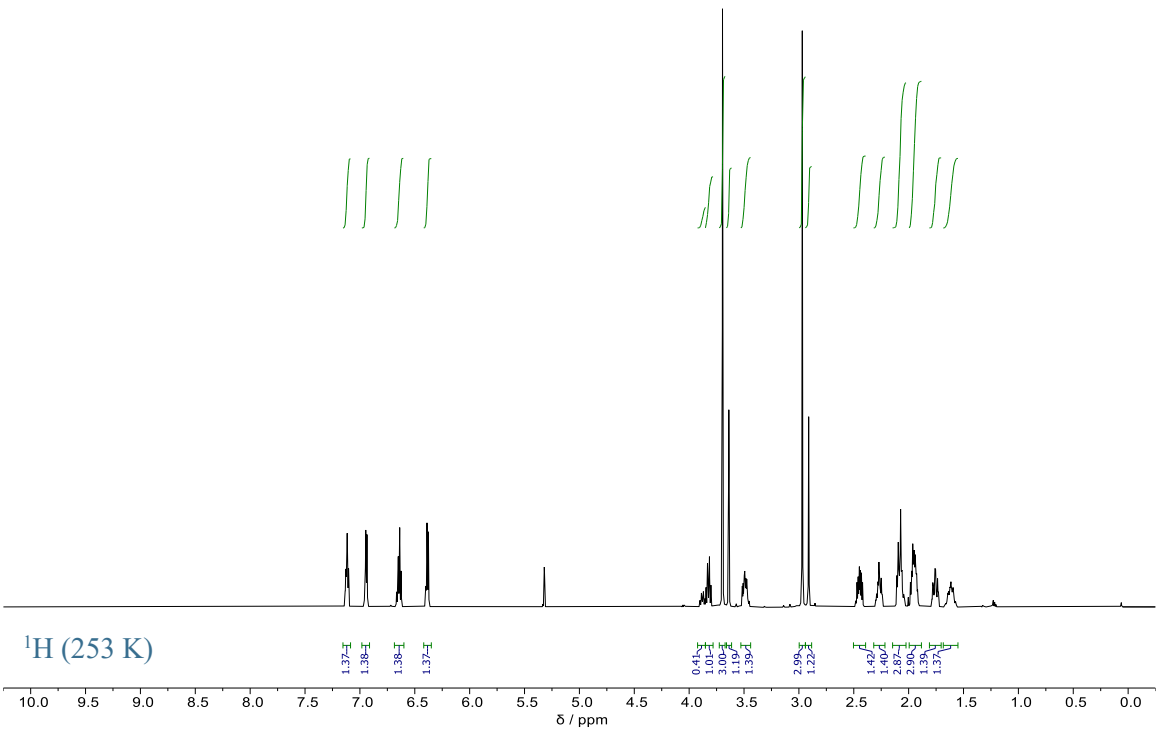


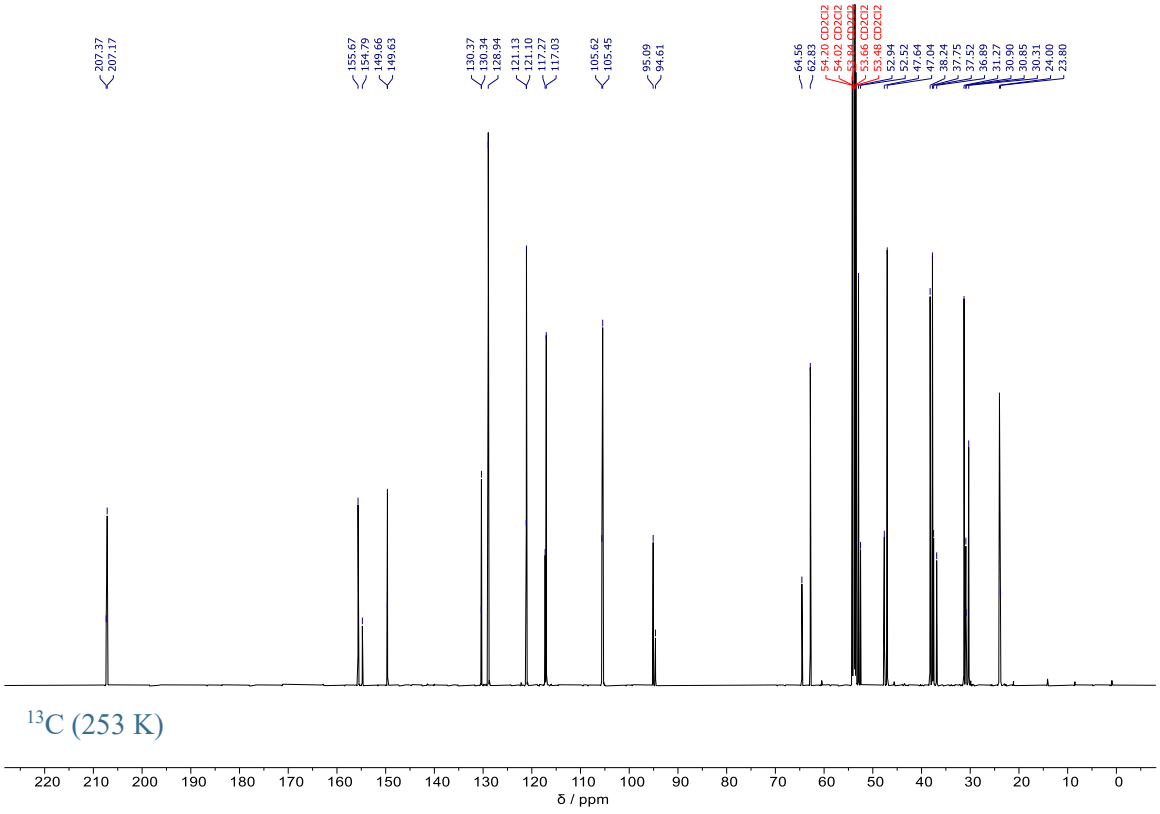
Methyl 9-methyl-8-oxo-5,6,7,8-tetrahydro-9*H*-8a,4b-(epiminoethano)carbazole-10-carboxylate (racemate), **29**

(^{1}H (298 K), ^{1}H (253 K) and ^{13}C (253 K) in CD_2Cl_2)



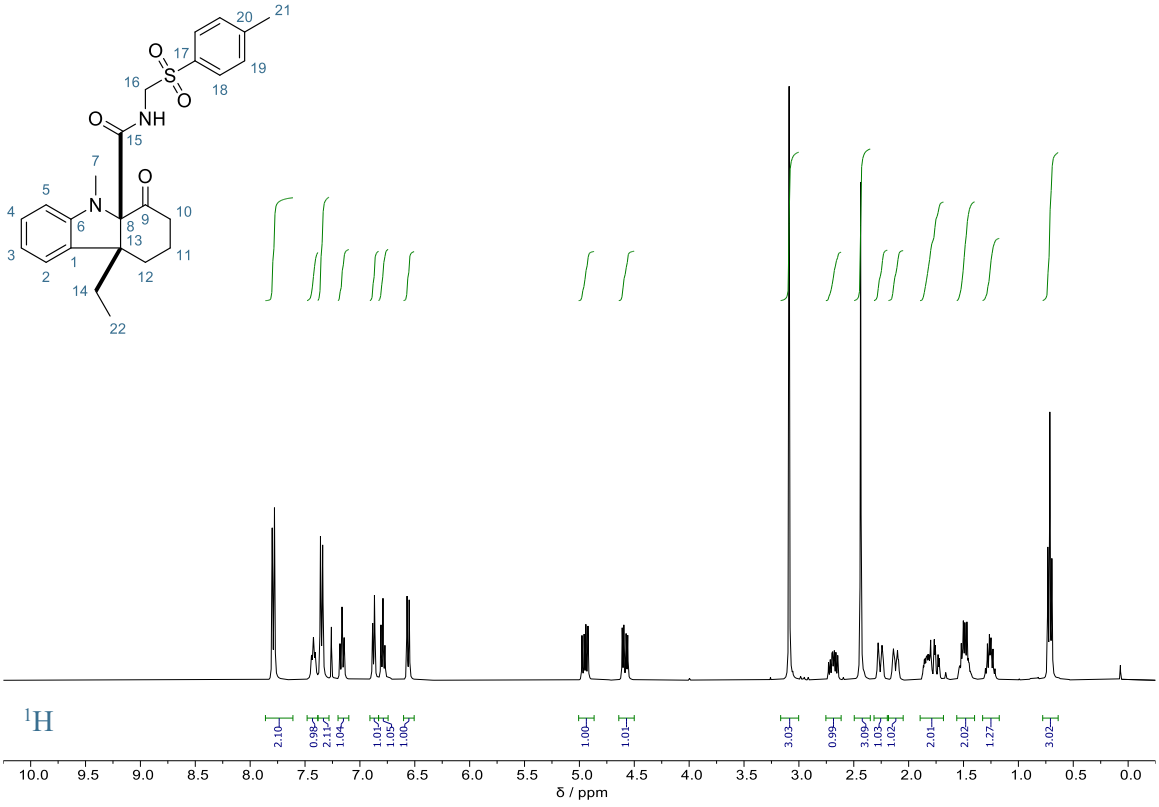


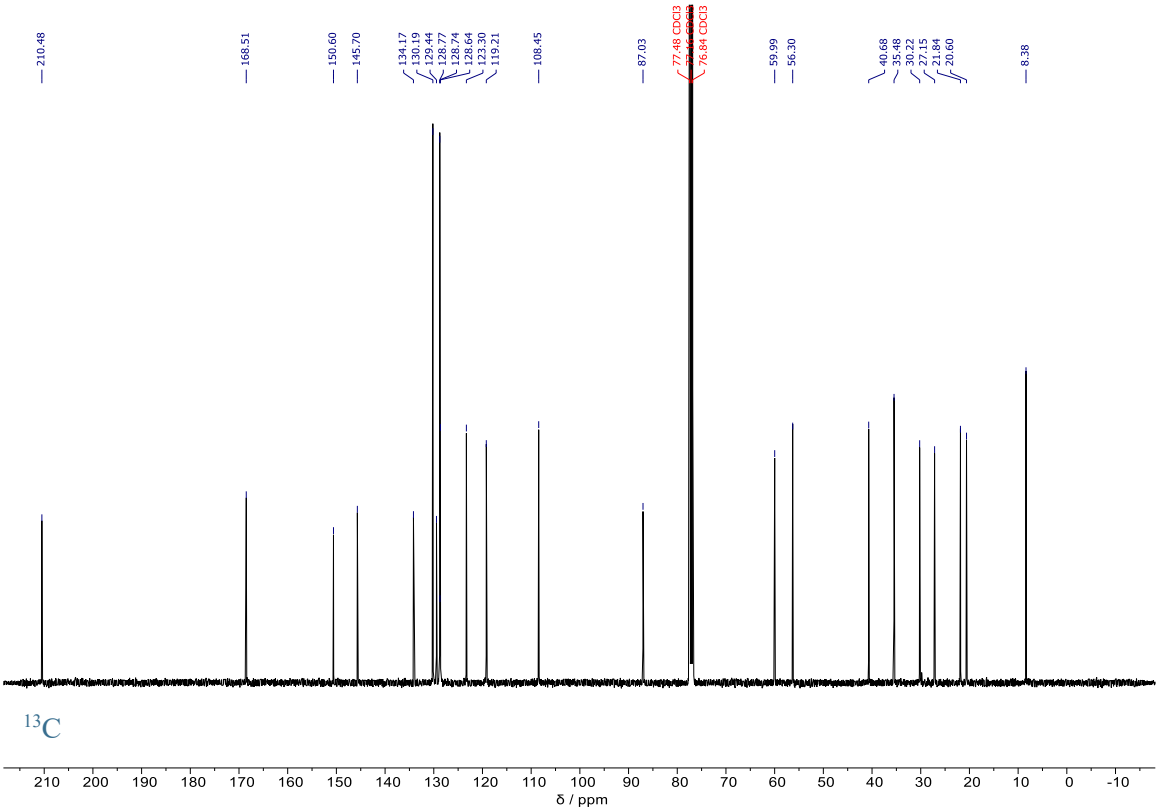



207.37
207.17
155.67
154.79
149.66
149.63
130.37
130.34
128.94
121.13
121.10
117.27
117.03
105.62
105.45
95.09
94.61
64.56
62.83
54.20 CD2Cl2
54.02 CD2Cl2
53.84 CD2Cl2
53.66 CD2Cl2
53.48 CD2Cl2
52.94
52.52
47.64
47.04
38.24
37.75
37.52
36.89
31.27
30.90
30.85
30.31
24.00
23.80
220 210 200 190 180 170 160 150 140 130 120 110 100 90 80 70 60 50 40 30 20 10 0
δ / ppm

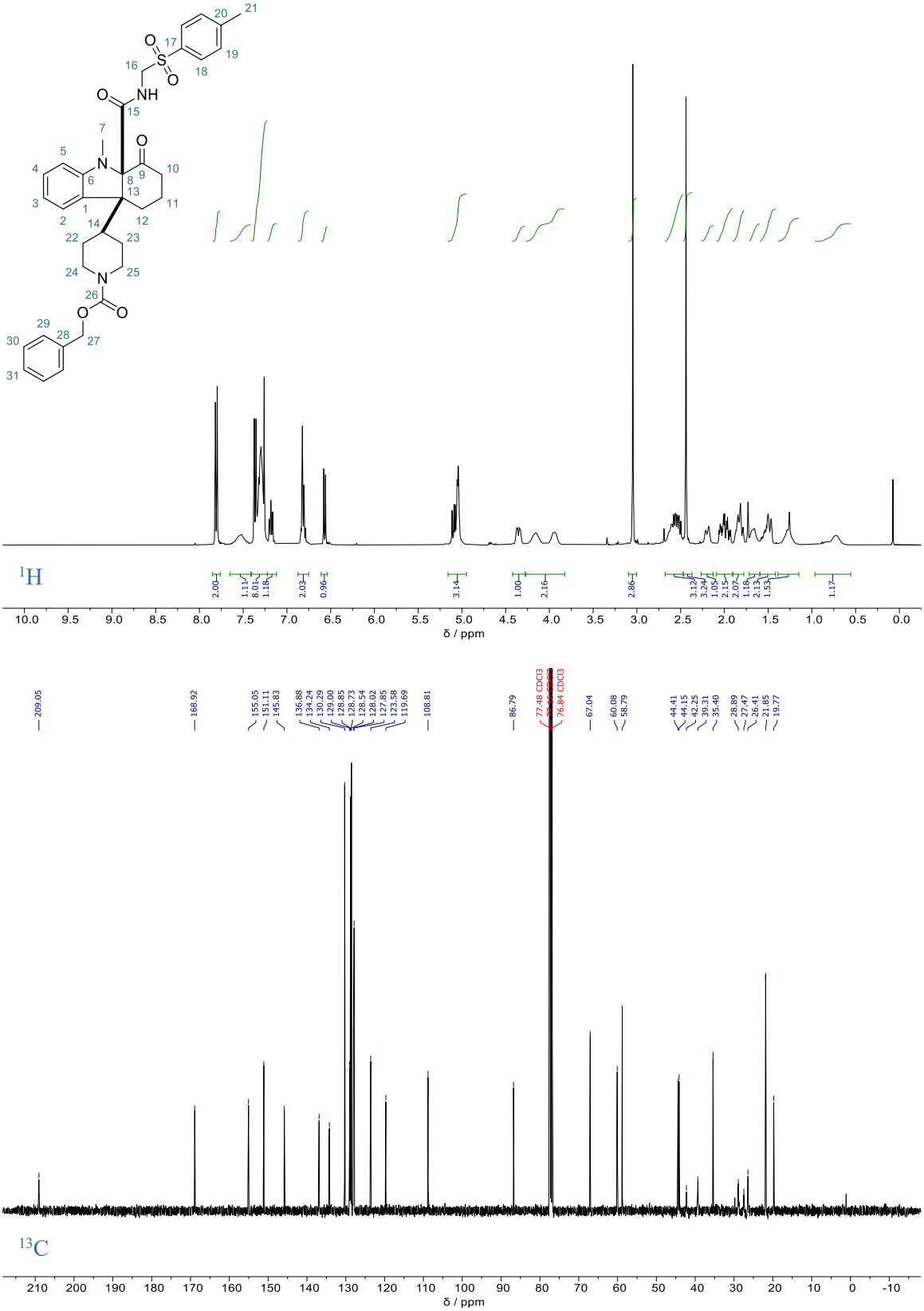
^{13}C (253 K)

rac-4b-ethyl-9-methyl-8-oxo-*N*-(tosylmethyl)-4b,5,6,7,8,9-hexahydro-8a*H*-carbazole-8a-carboxamide, **30**

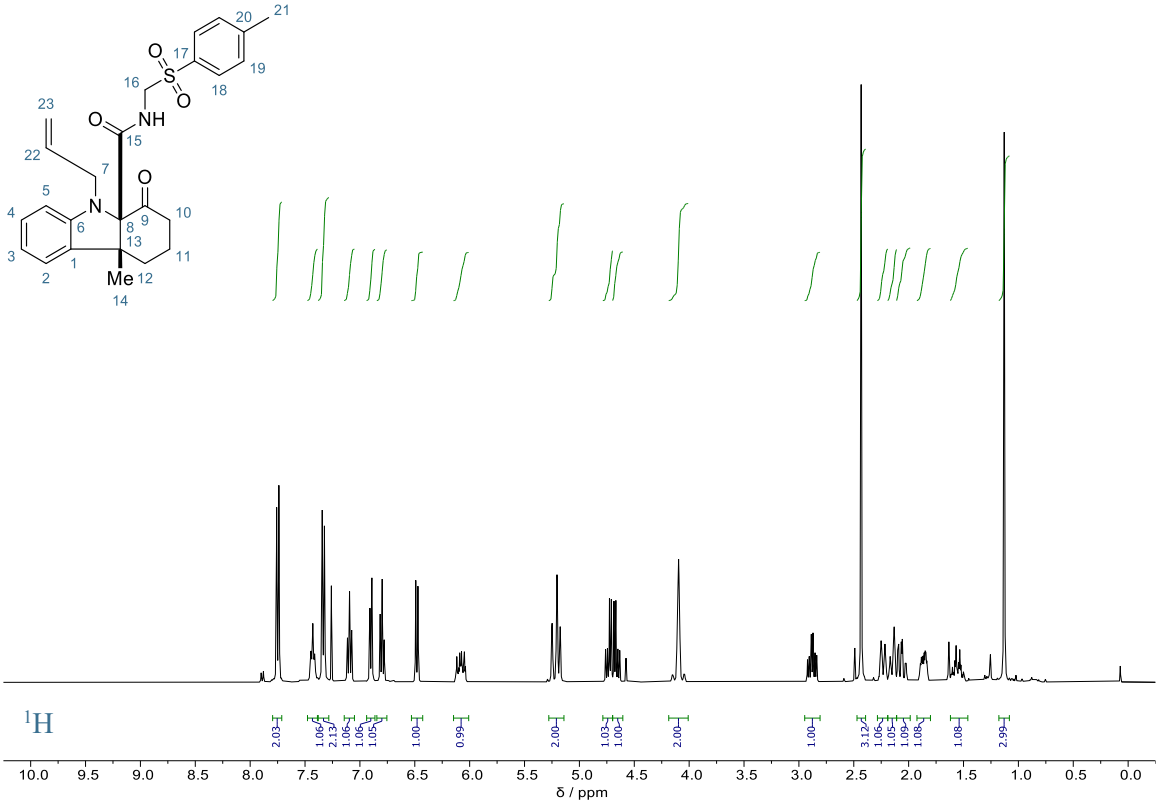


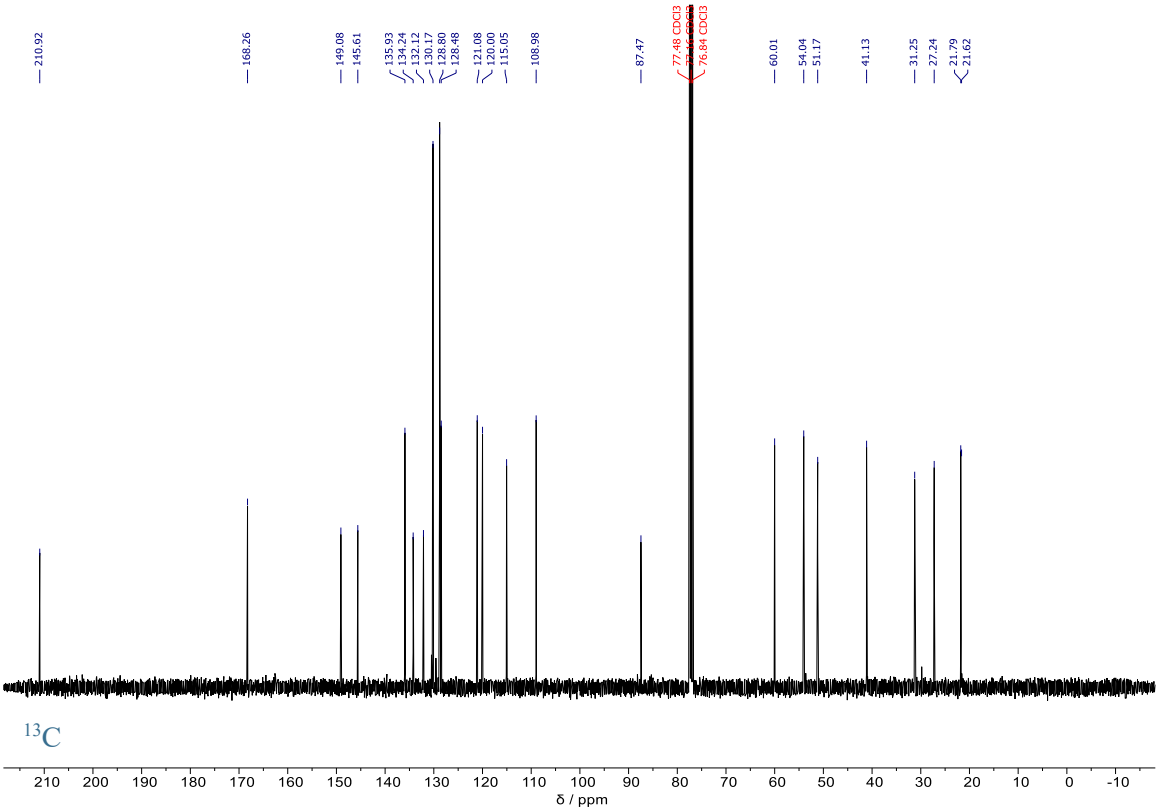


Benzyl 4-(9-methyl-1-oxo-9a-((tosylmethyl)carbamoyl)-1,2,3,4,9,9a-hexahydro-4a*H*-carbazol-4a-yl)piperidine-1-carboxylate (racemate), **31**

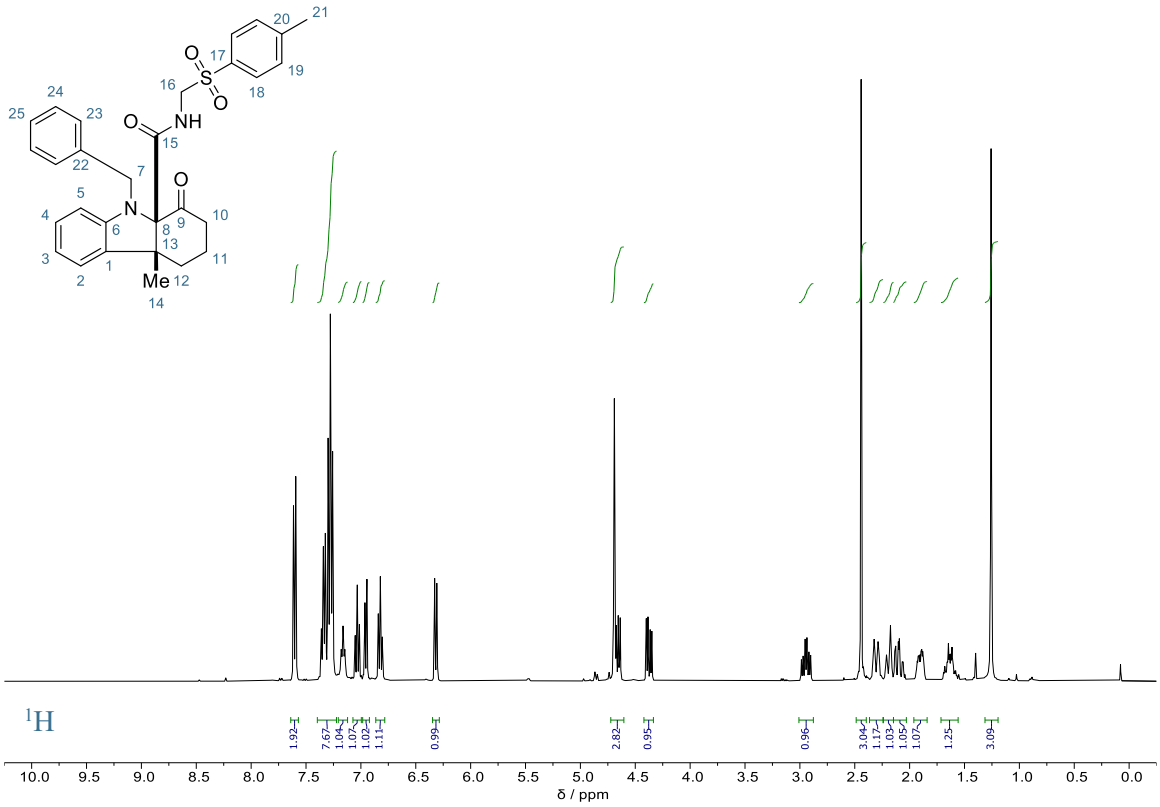


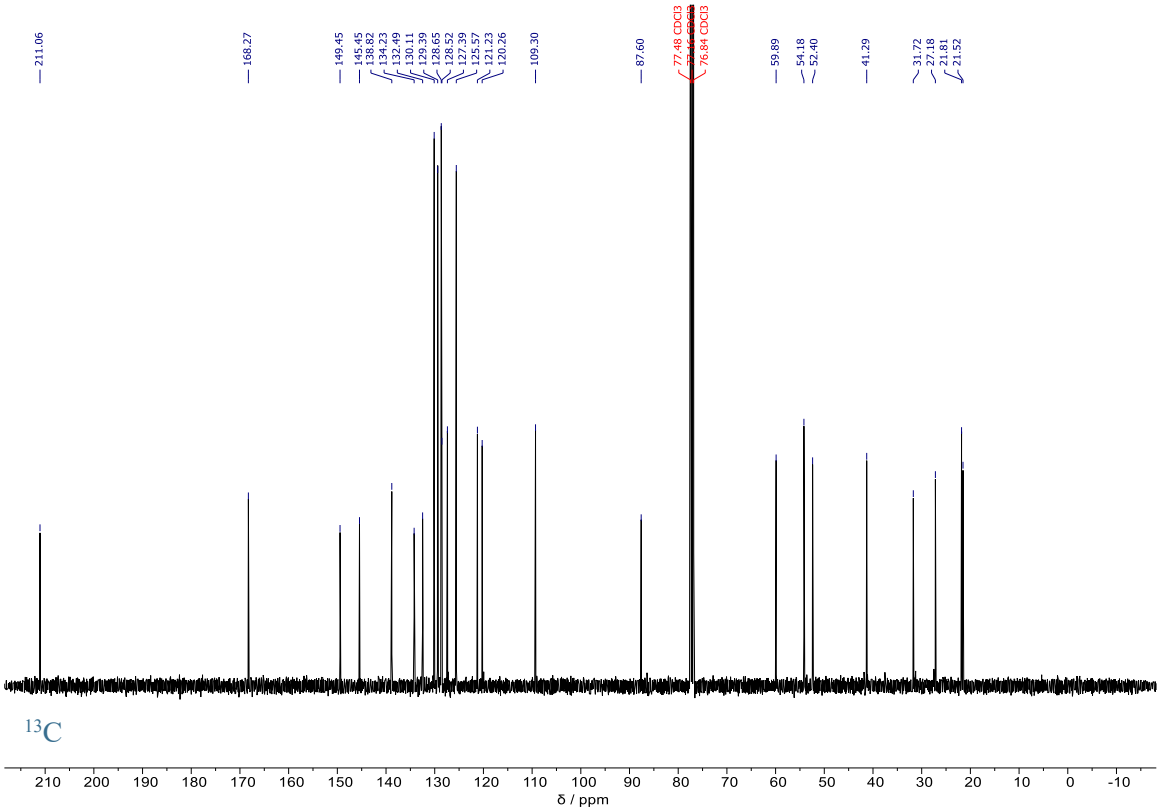
rac-9-Allyl-4b-methyl-8-oxo-*N*-(tosylmethyl)-4b,5,6,7,8,9-hexahydro-8a*H*-carbazole-8a-carboxamide, **32**



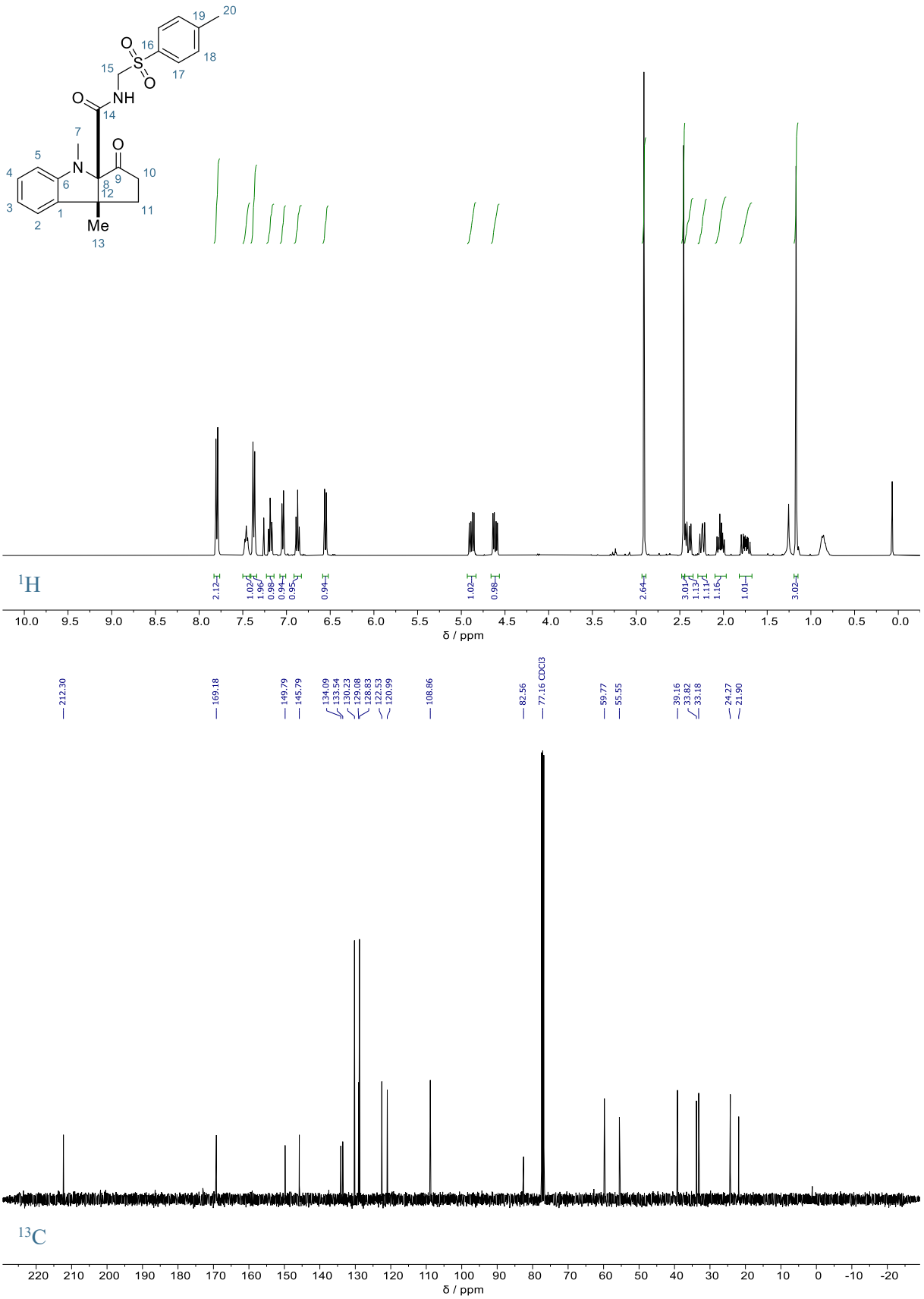


rac-9-Benzyl-4b-methyl-8-oxo-*N*-(tosylmethyl)-4b,5,6,7,8,9-hexahydro-8a*H*-carbazole-8a-carboxamide, **33**

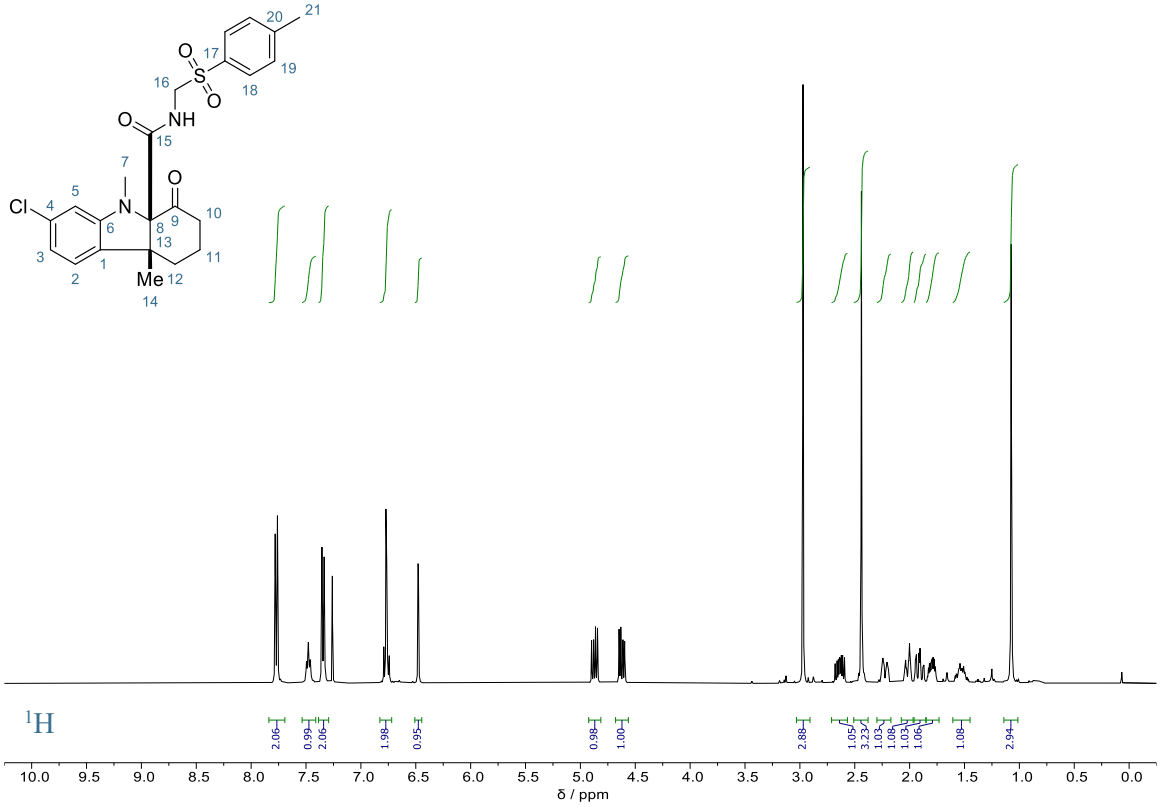


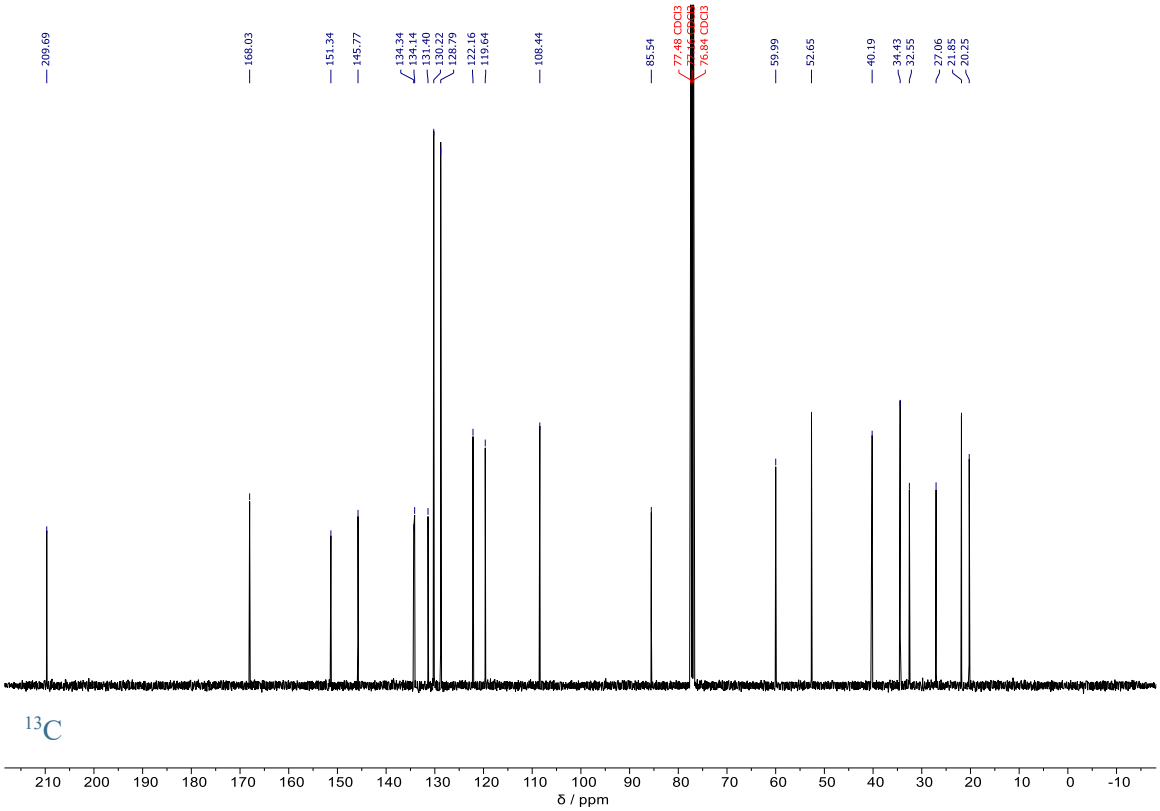


rac-4,8b-Dimethyl-3-oxo-*N*-(tosylmethyl)-2,3,4,8b-tetrahydrocyclopenta[b]indole-3a(1*H*)-carboxamide, **34**

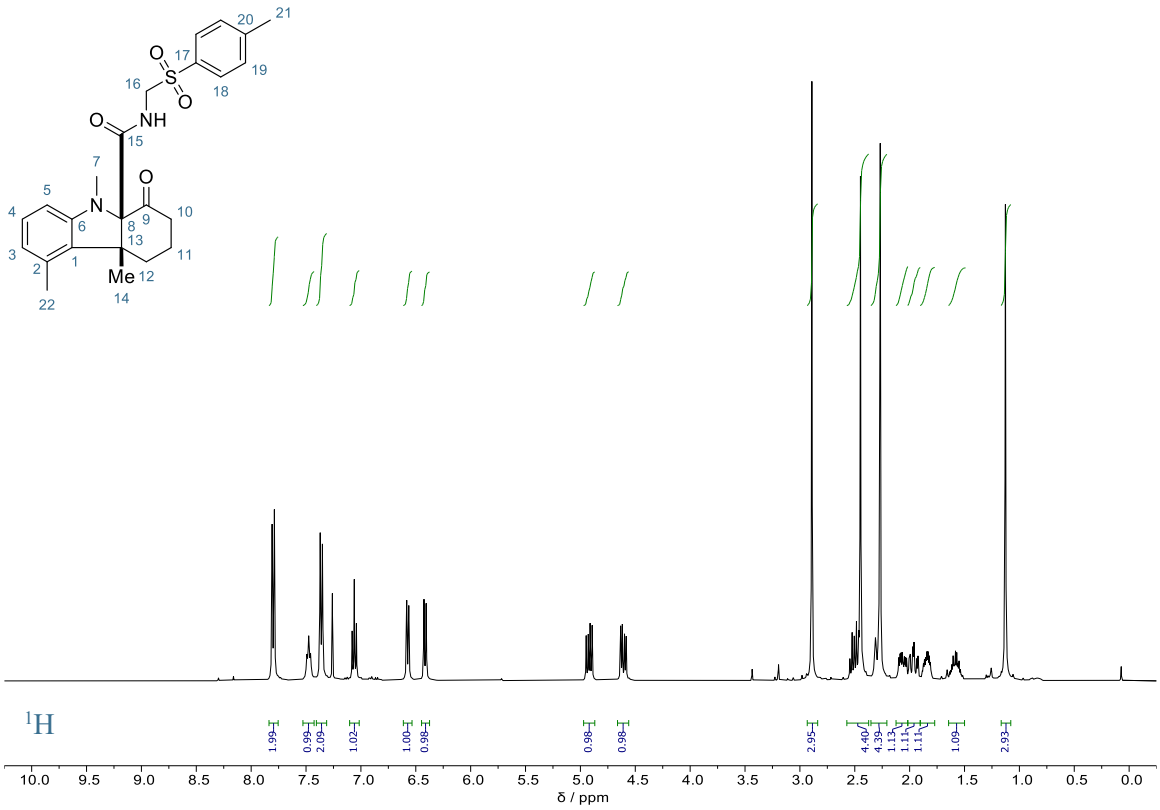


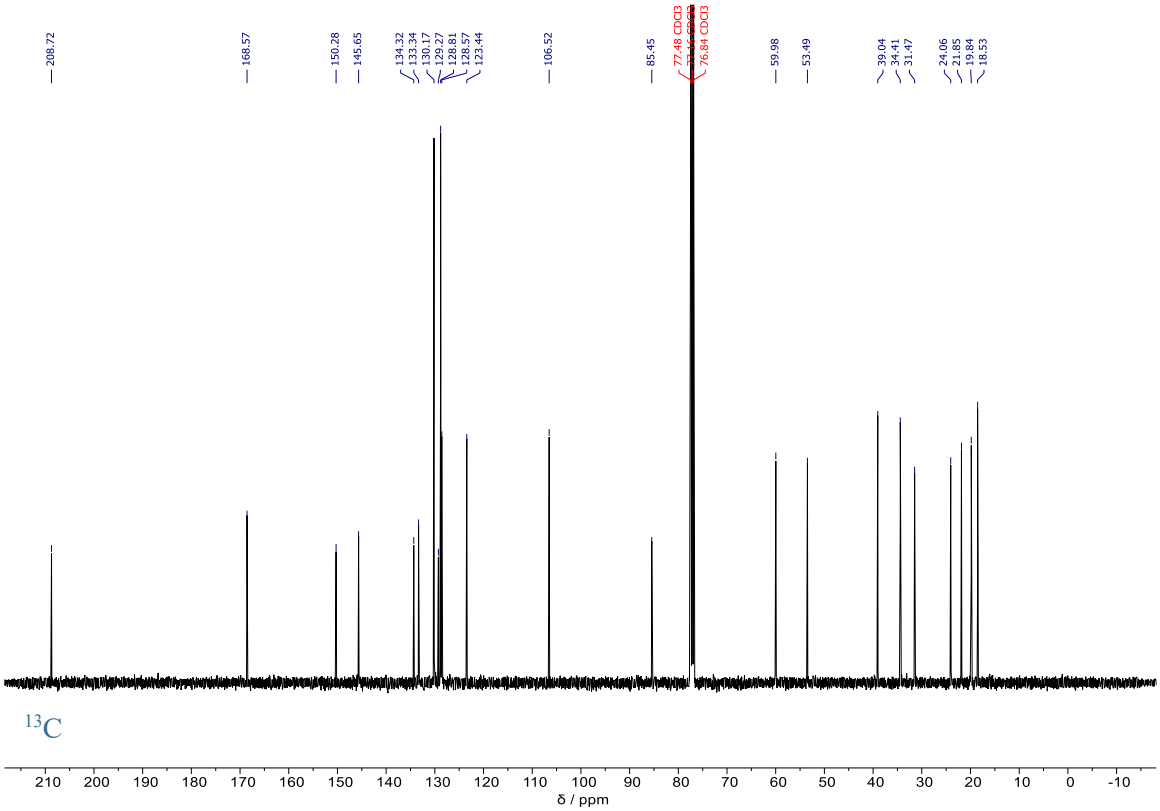
rac-2-Chloro-4b,9-dimethyl-8-oxo-*N*-(tosylmethyl)-4b,5,6,7,8,9-hexahydro-8a*H*-carbazole-8a-carboxamide, **35**



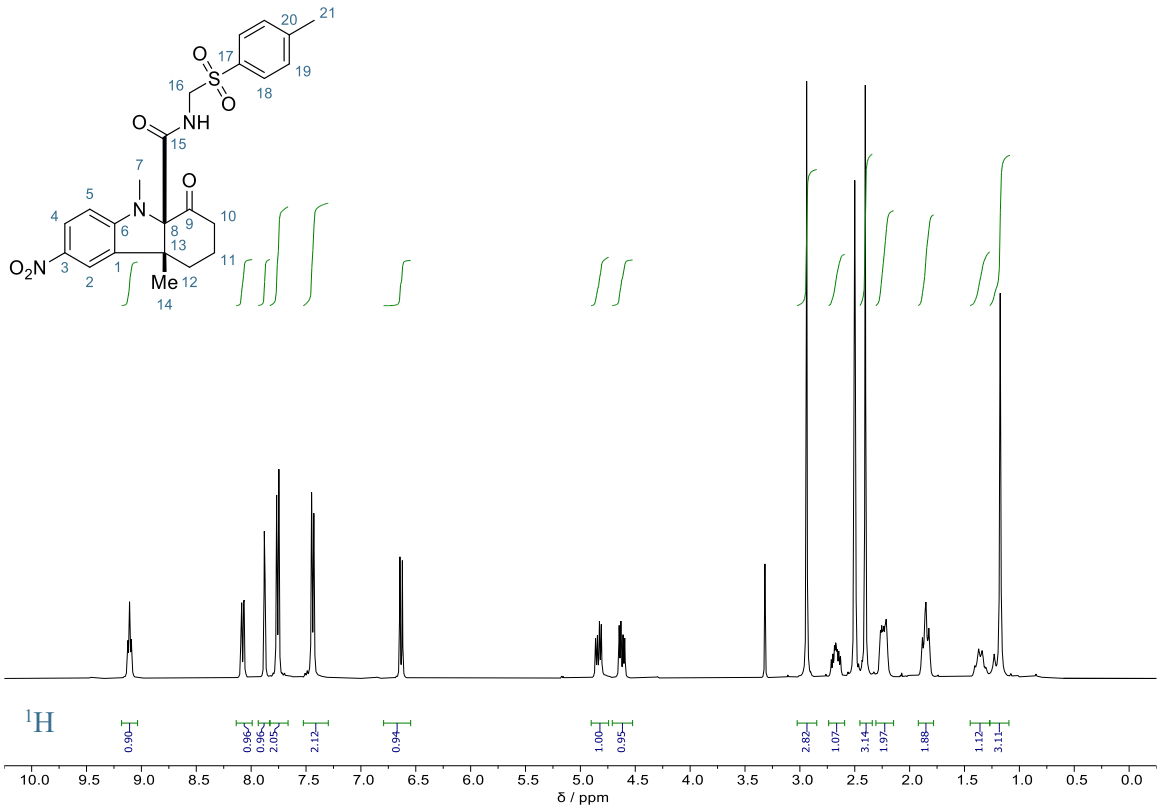


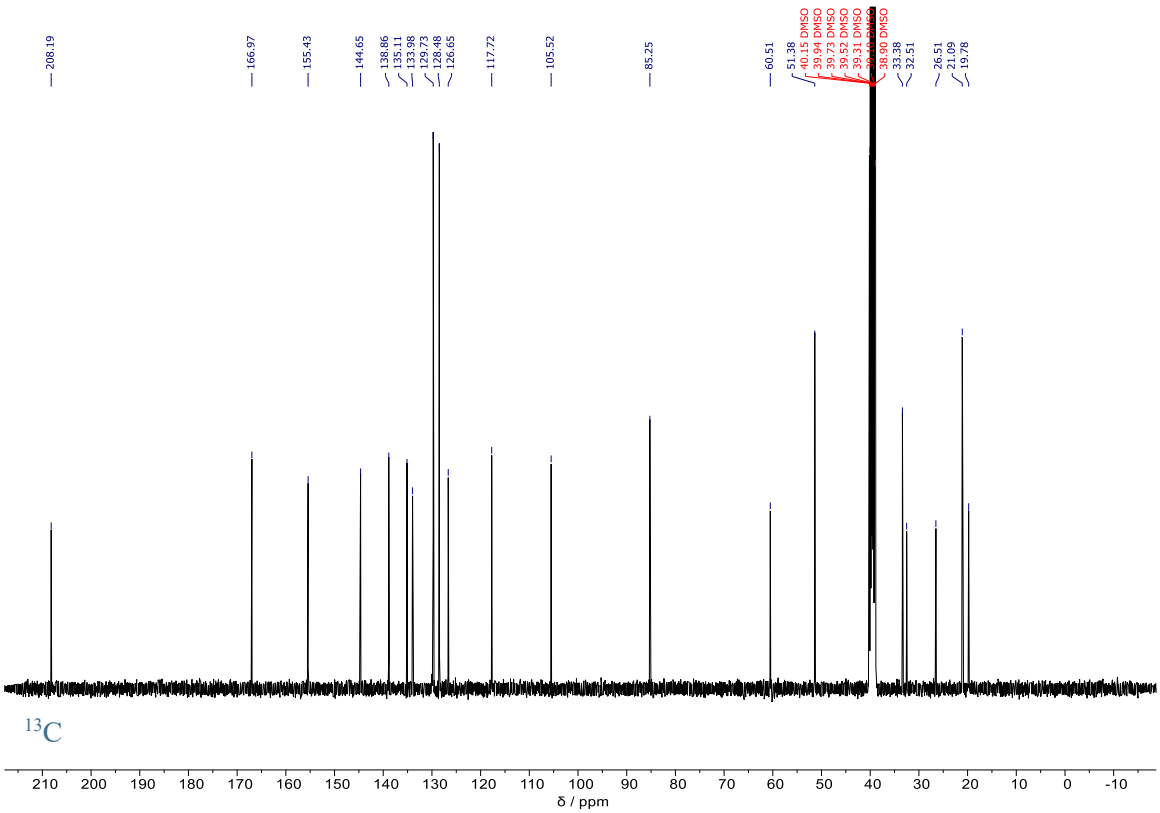
rac-4,4b,9-Trimethyl-8-oxo-*N*-(tosylmethyl)-4b,5,6,7,8,9-hexahydro-8a*H*-carbazole-8a-carboxamide, **36**



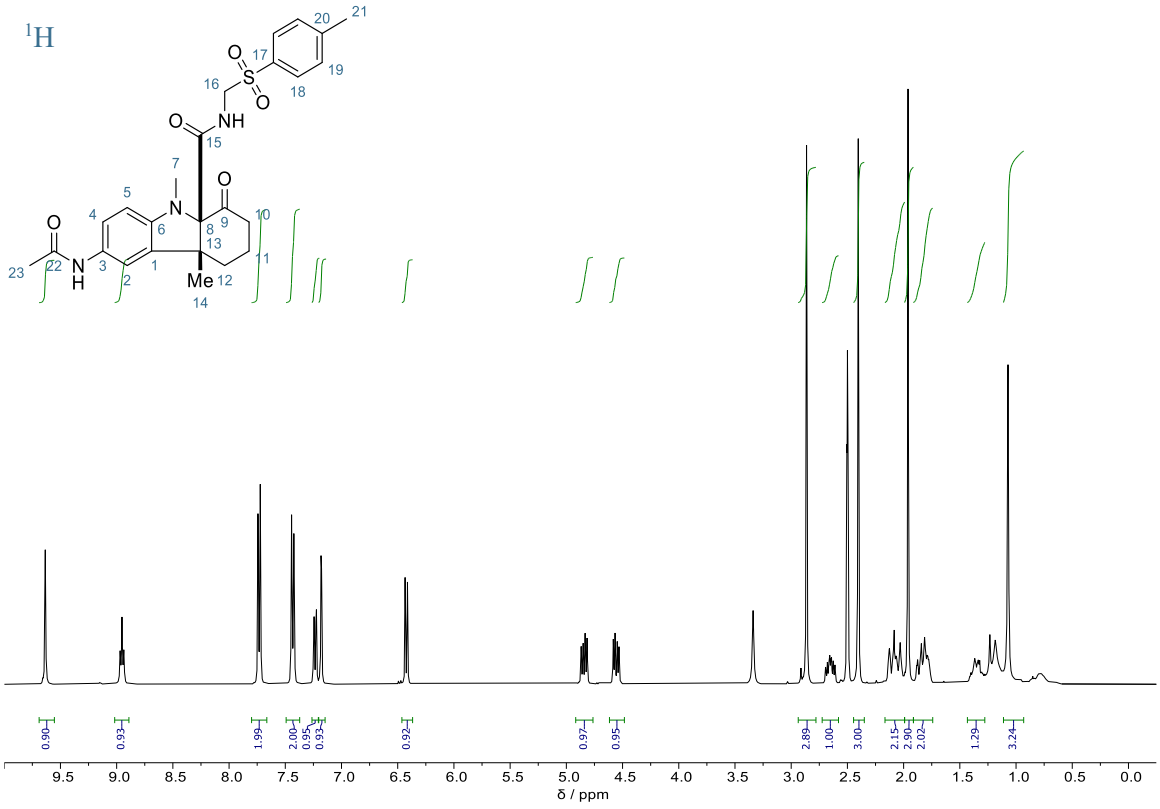


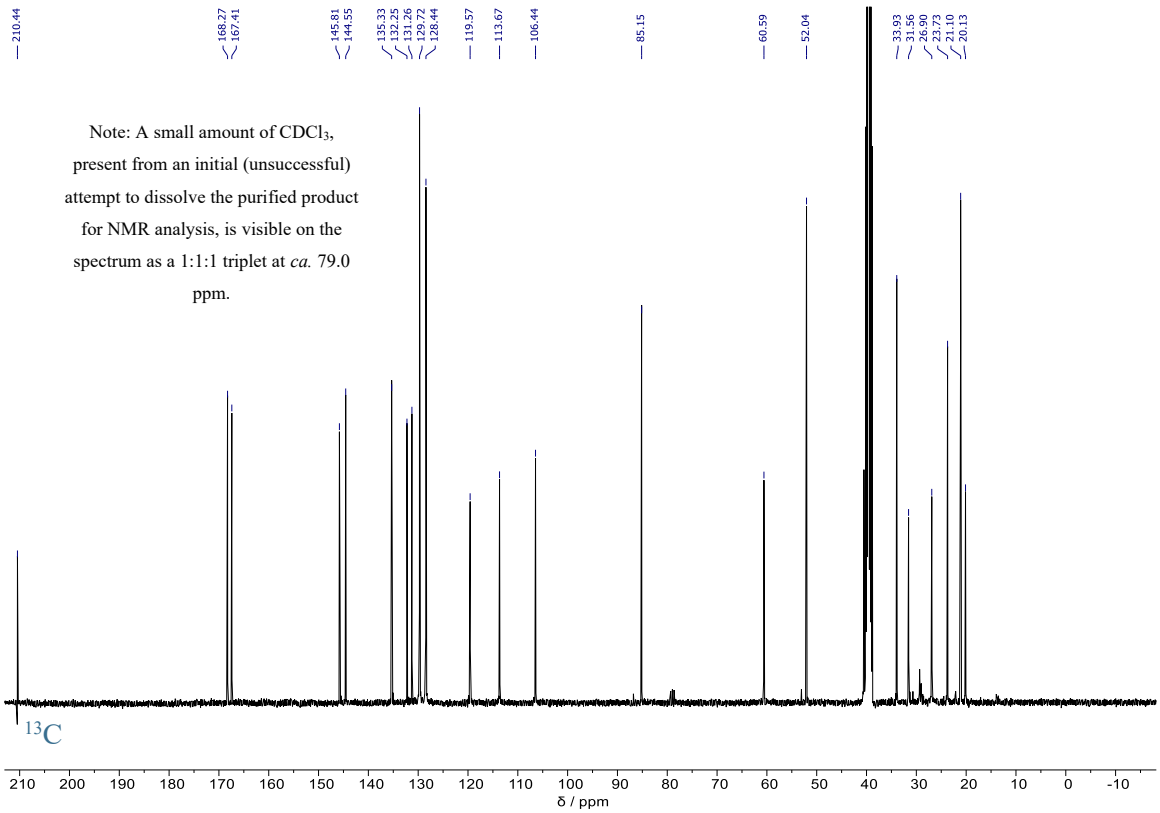
rac-4b,9-Dimethyl-3-nitro-8-oxo-*N*-(tosylmethyl)-4b,5,6,7,8,9-hexahydro-8a*H*-carbazole-8a-carboxamide, **37**





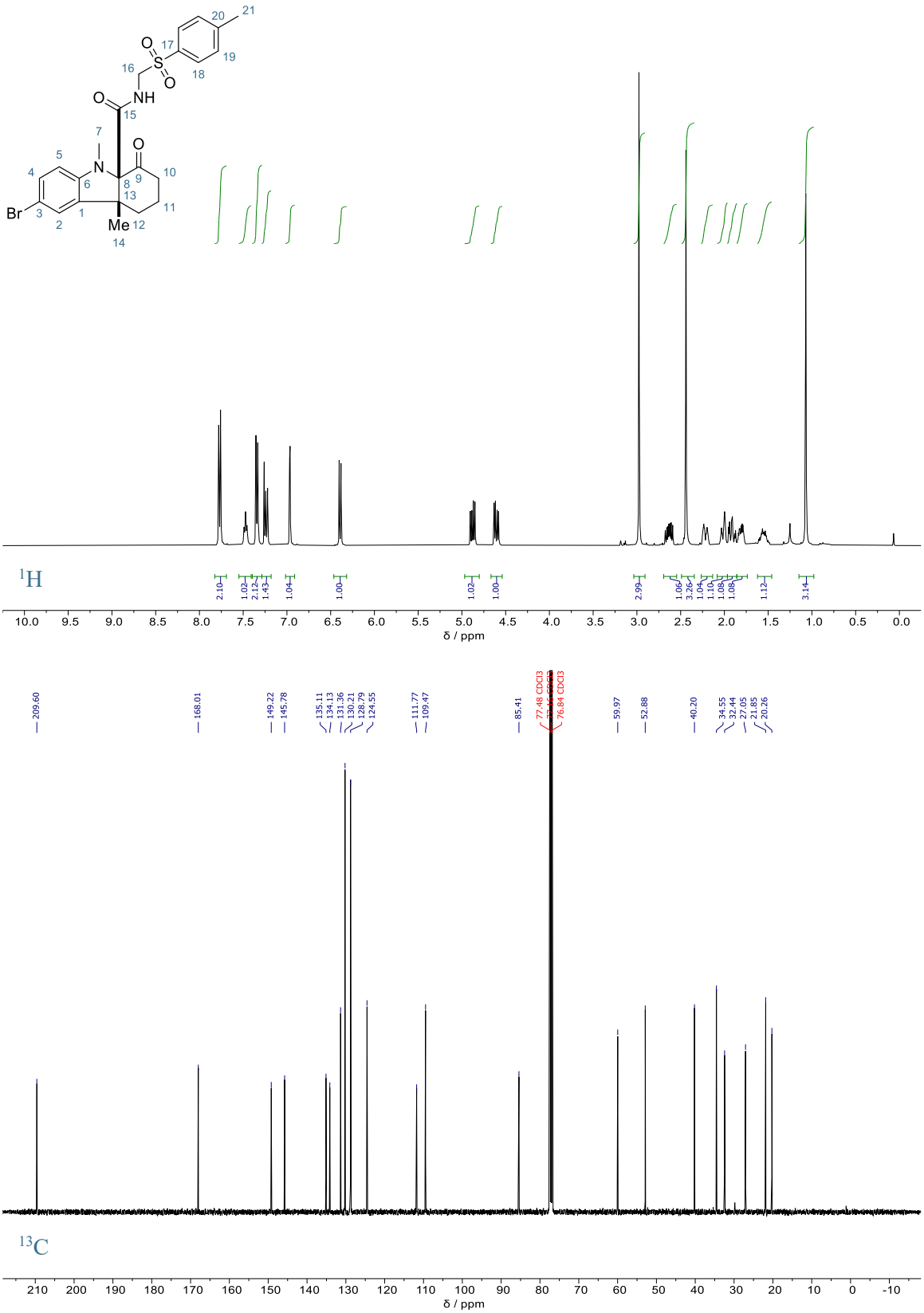
rac-3-Acetamido-4b,9-dimethyl-8-oxo-*N*-(tosylmethyl)-4b,5,6,7,8,9-hexahydro-8a*H*-carbazole-8a-carboxamide, **38**



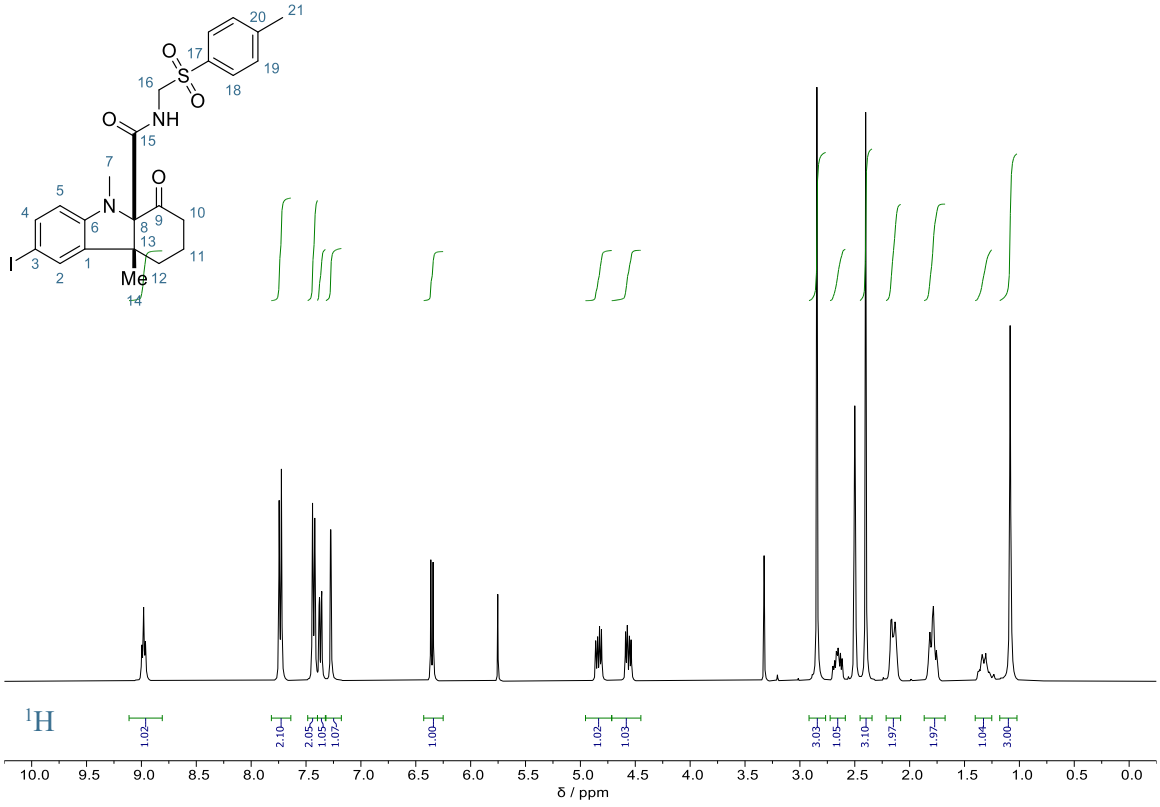


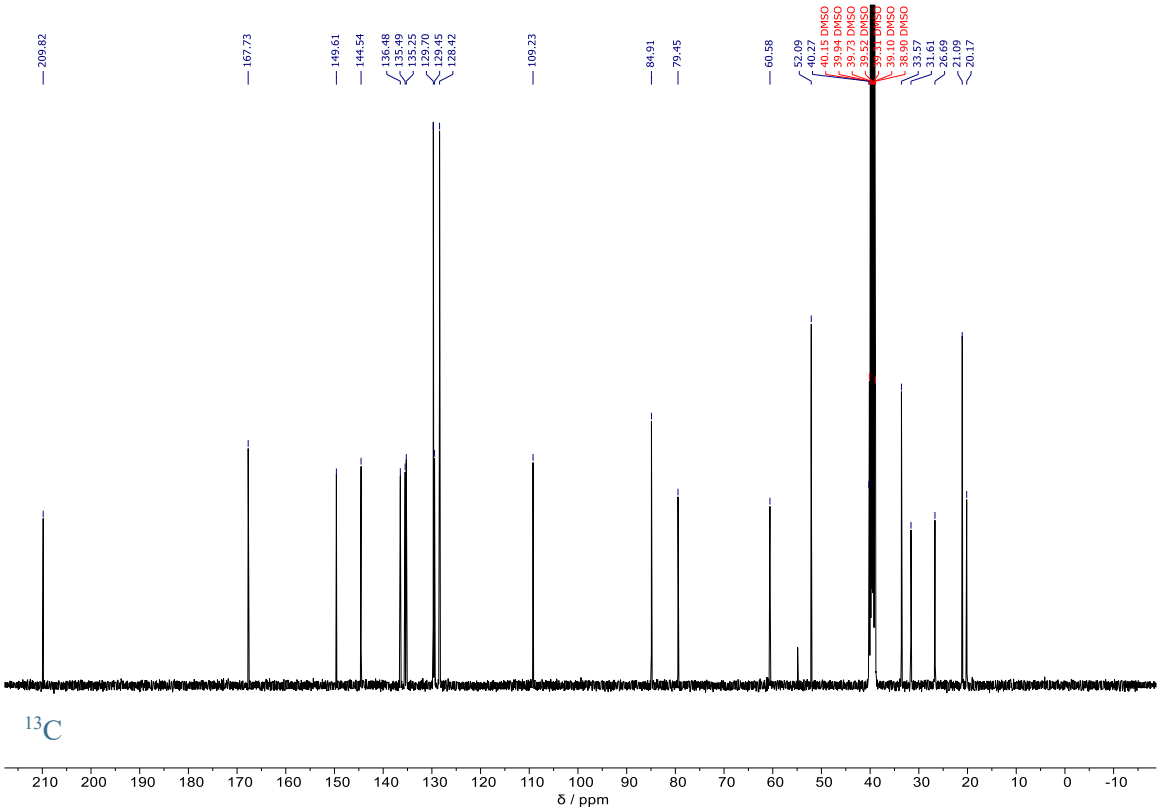
Note: A small amount of $CDCl_3$, present from an initial (unsuccessful) attempt to dissolve the purified product for NMR analysis, is visible on the spectrum as a 1:1:1 triplet at *ca.* 79.0 ppm.

rac-3-Bromo-4b,9-dimethyl-8-oxo-*N*-(tosylmethyl)-4b,5,6,7,8,9-hexahydro-8a*H*-carbazole-8a-carboxamide, **39**

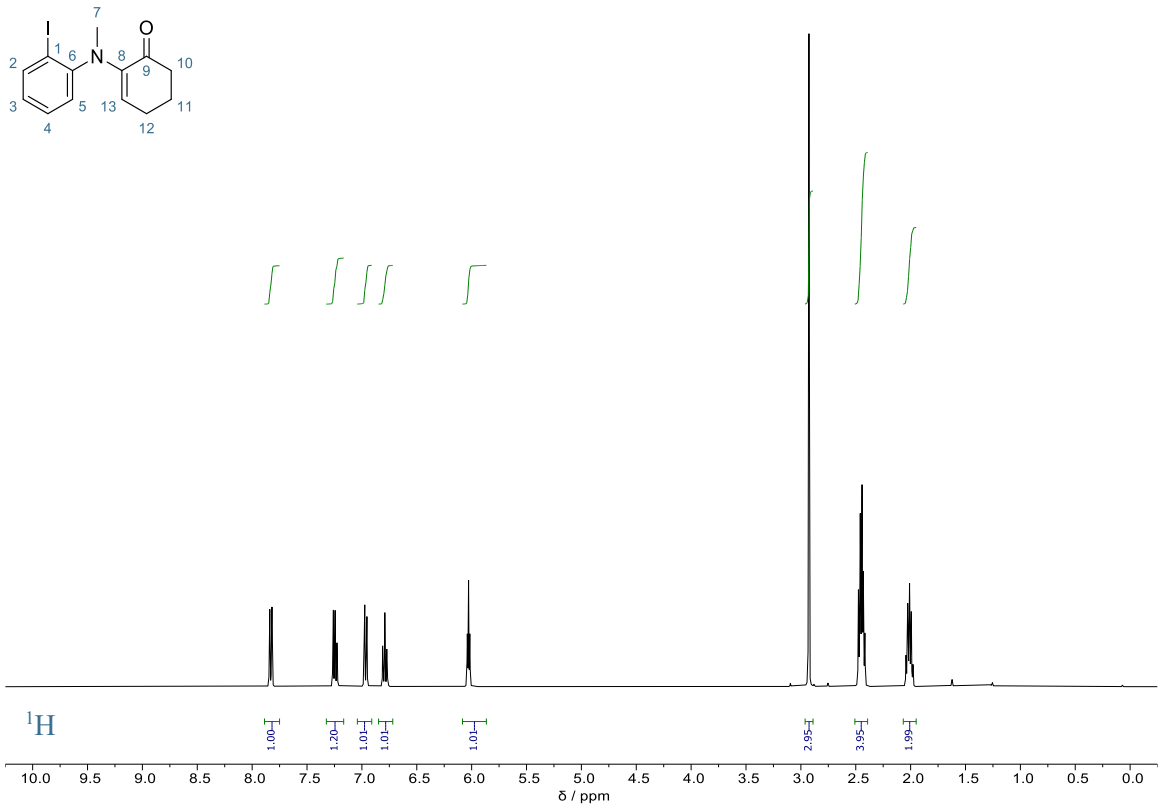


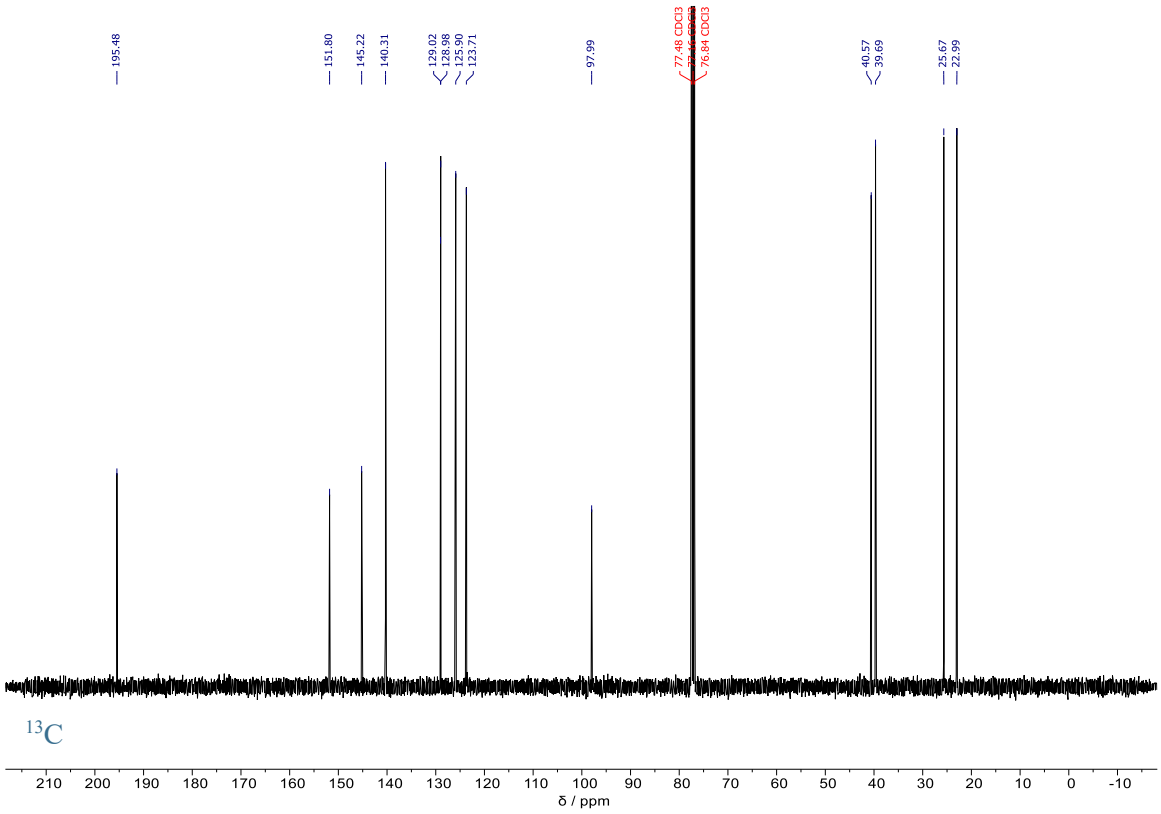
rac-3-Iodo-4b,9-dimethyl-8-oxo-*N*-(tosylmethyl)-4b,5,6,7,8,9-hexahydro-8a*H*-carbazole-8a-carboxamide, **40**



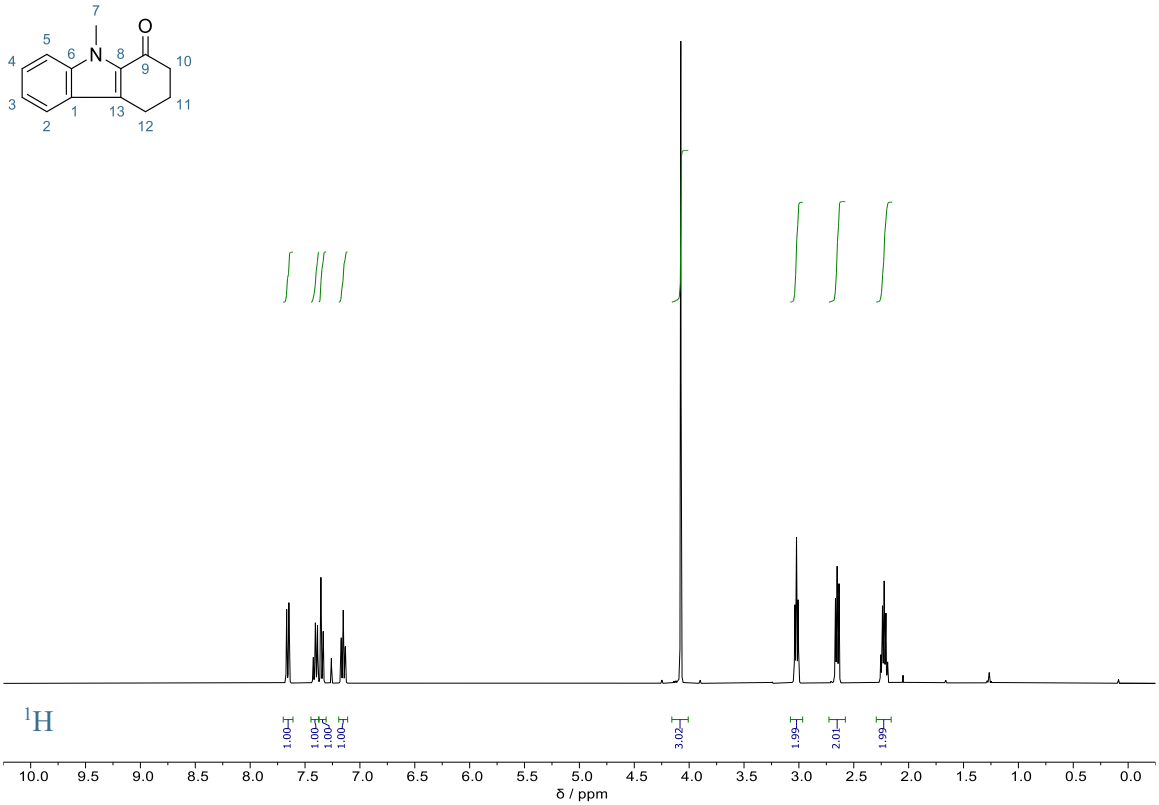


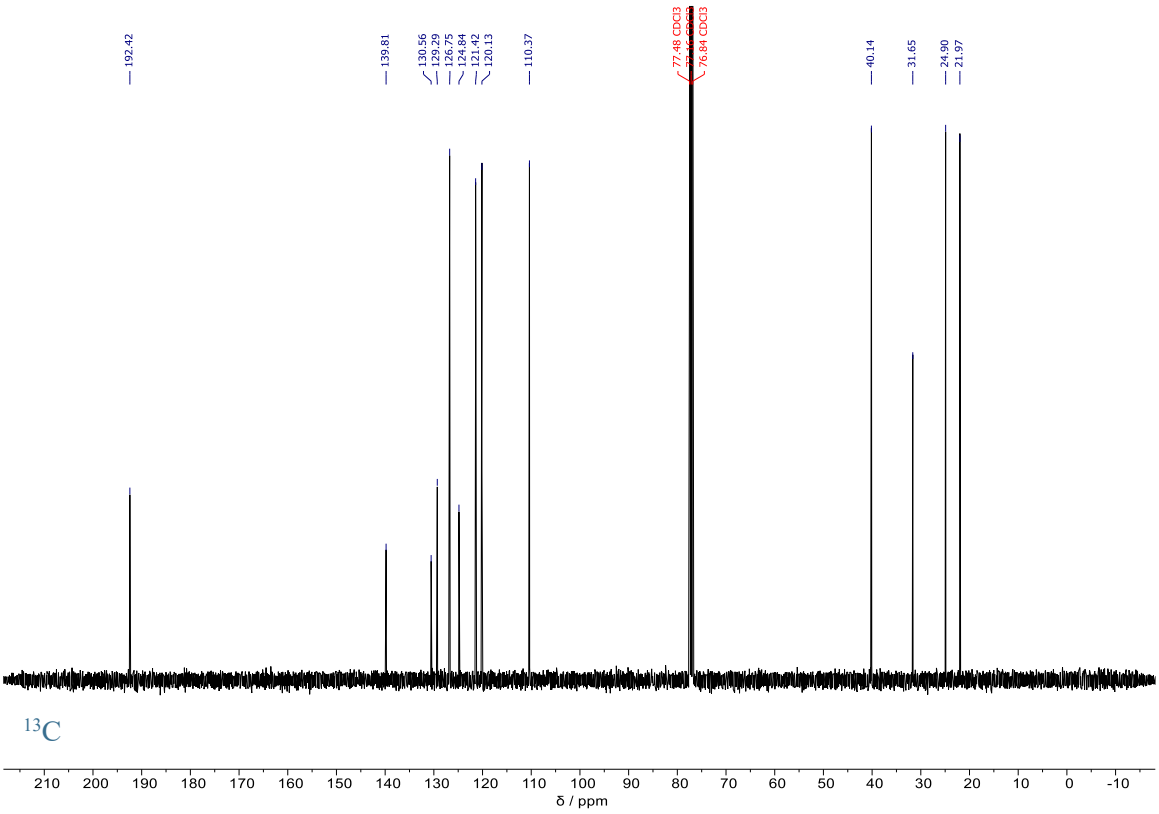
2-((2-Iodophenyl)(methyl)amino)cyclohex-2-en-1-one, **41**



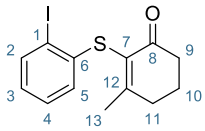


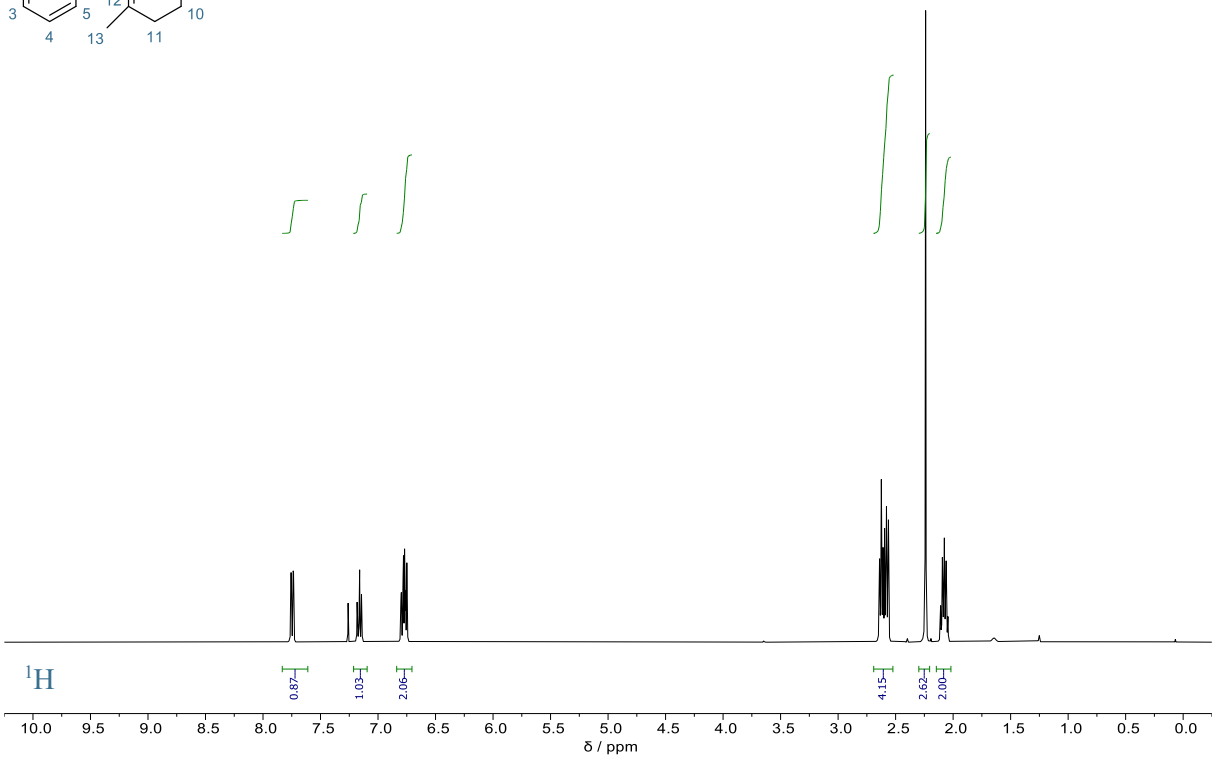
9-Methyl-2,3,4,9-tetrahydro-1*H*-carbazol-1-one, **42**



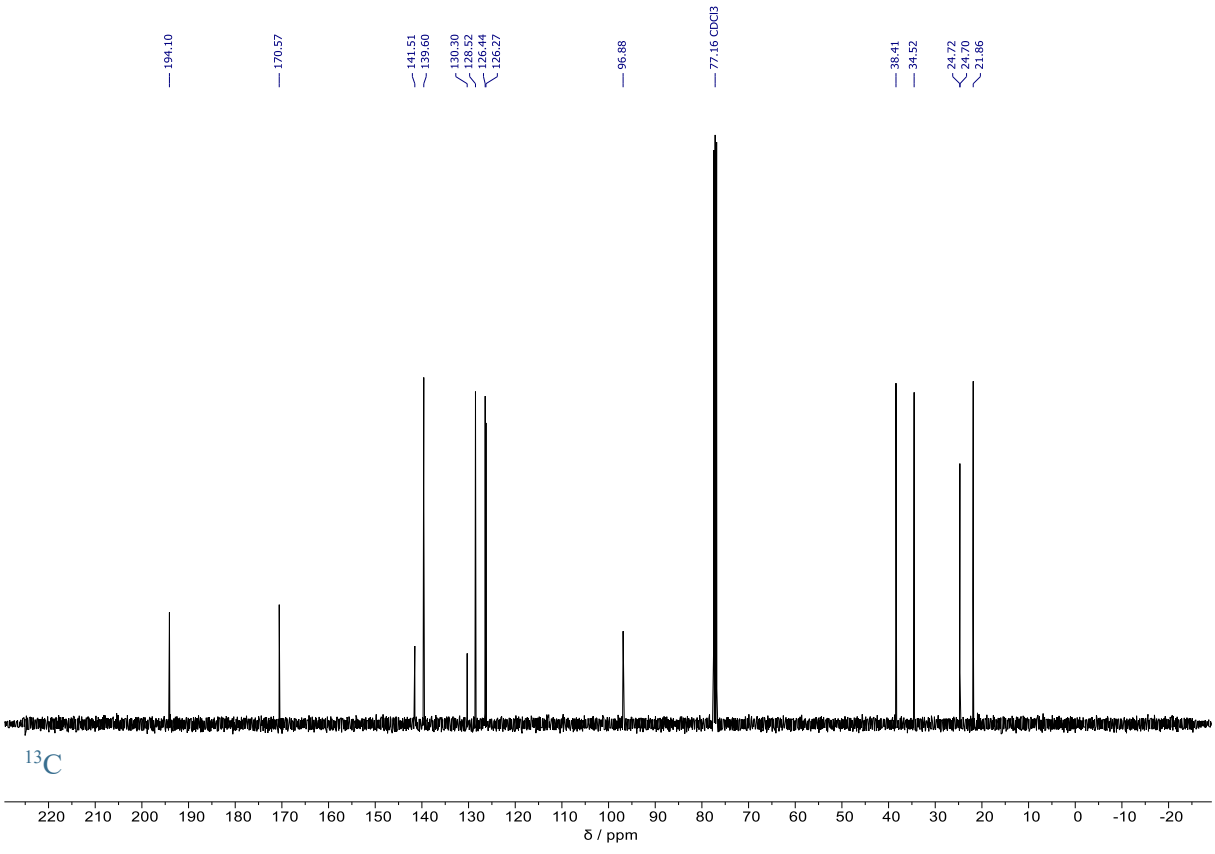


2-((2-Iodophenyl)thio)-3-methylcyclohex-2-en-1-one, **45**



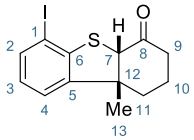


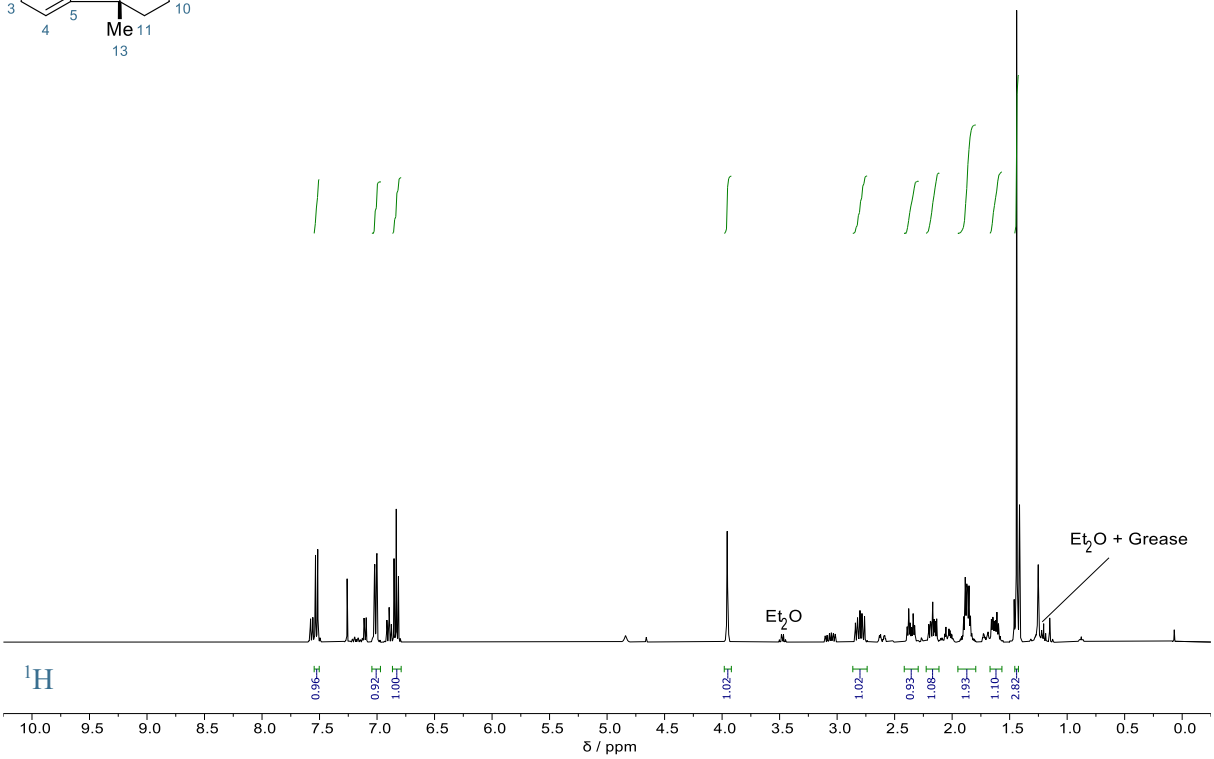
^{1}H

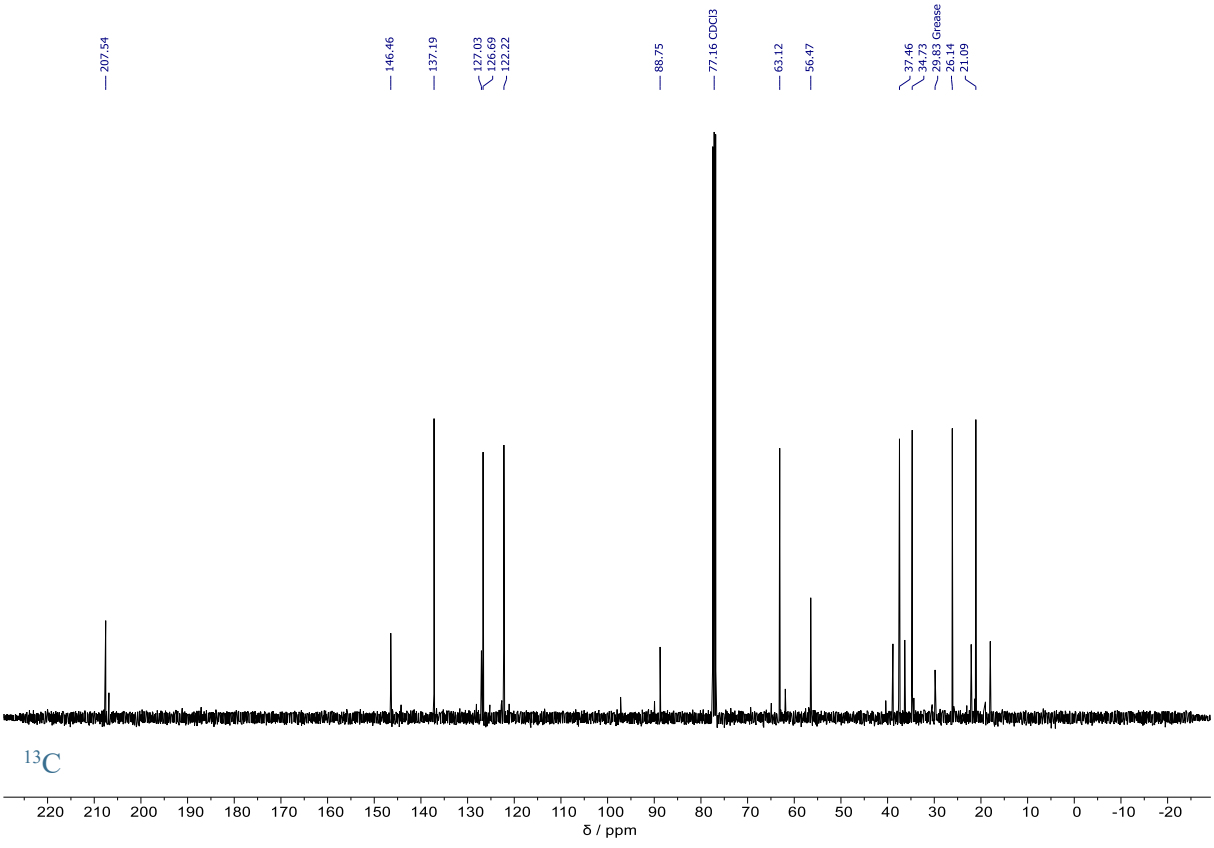


^{13}C

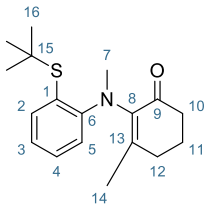
rac-6-Iodo-9b-methyl-2,3,4a,9b-tetrahydrodibenzo[b,d]thiophen-4(1*H*)-one, **46**

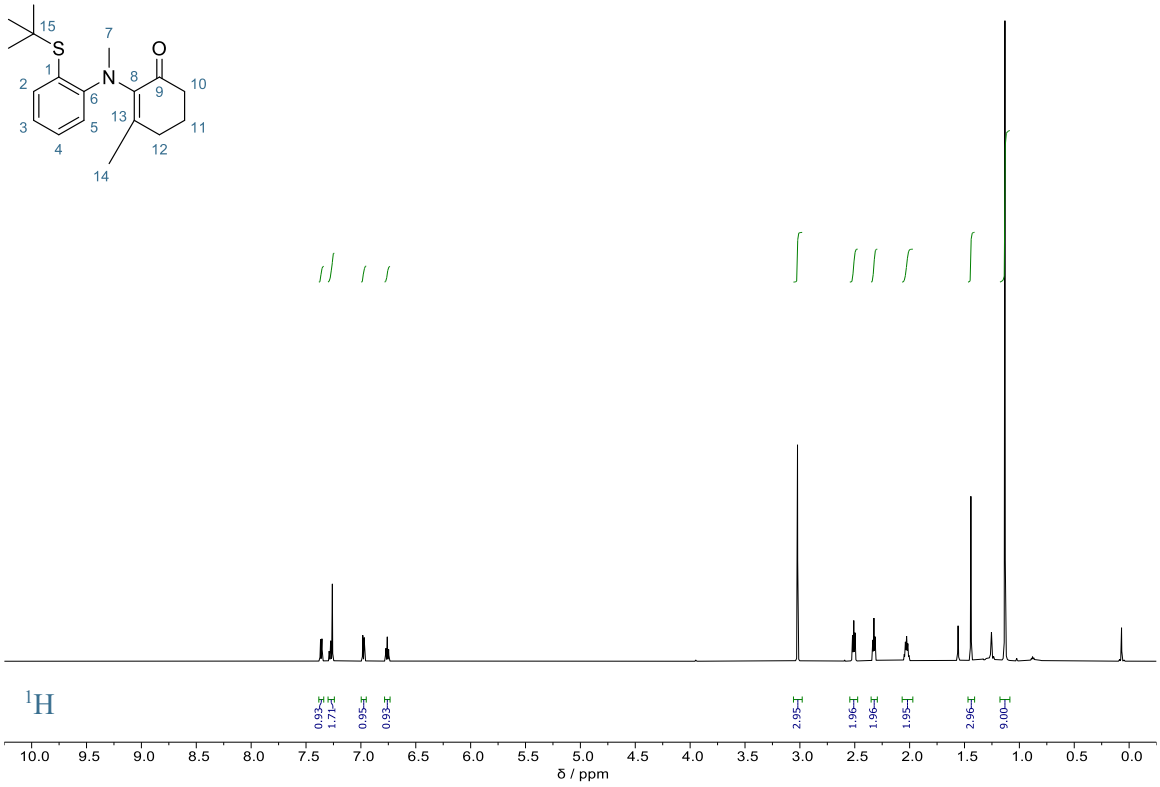


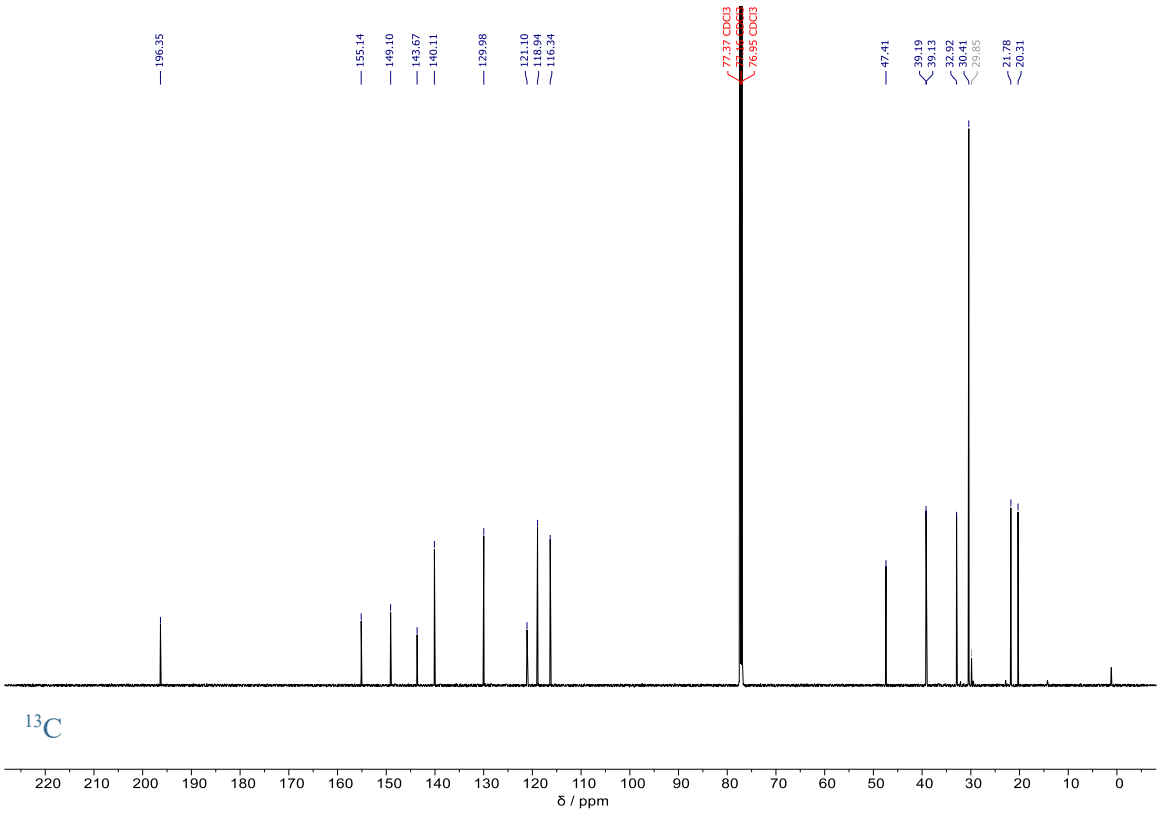




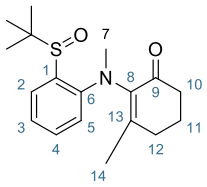
2-((2-(*tert*-Butylthio)phenyl)(methyl)amino)-3-methylcyclohex-2-en-1-one, **47**



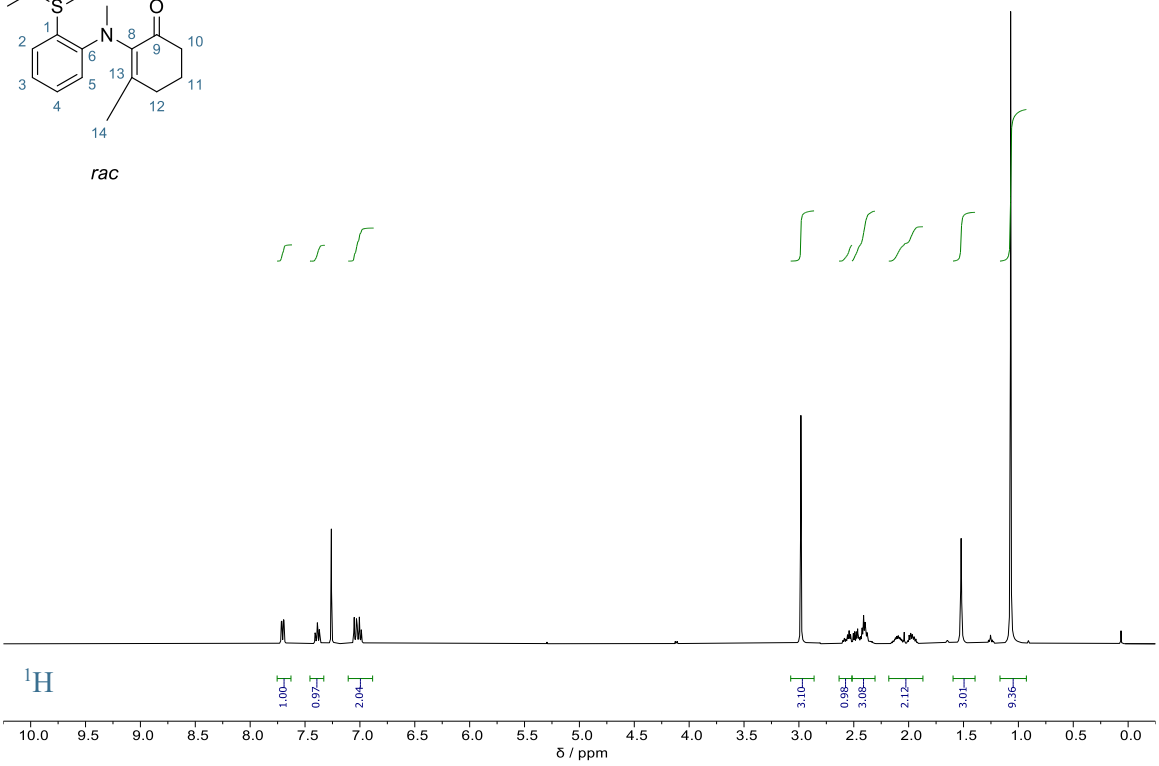


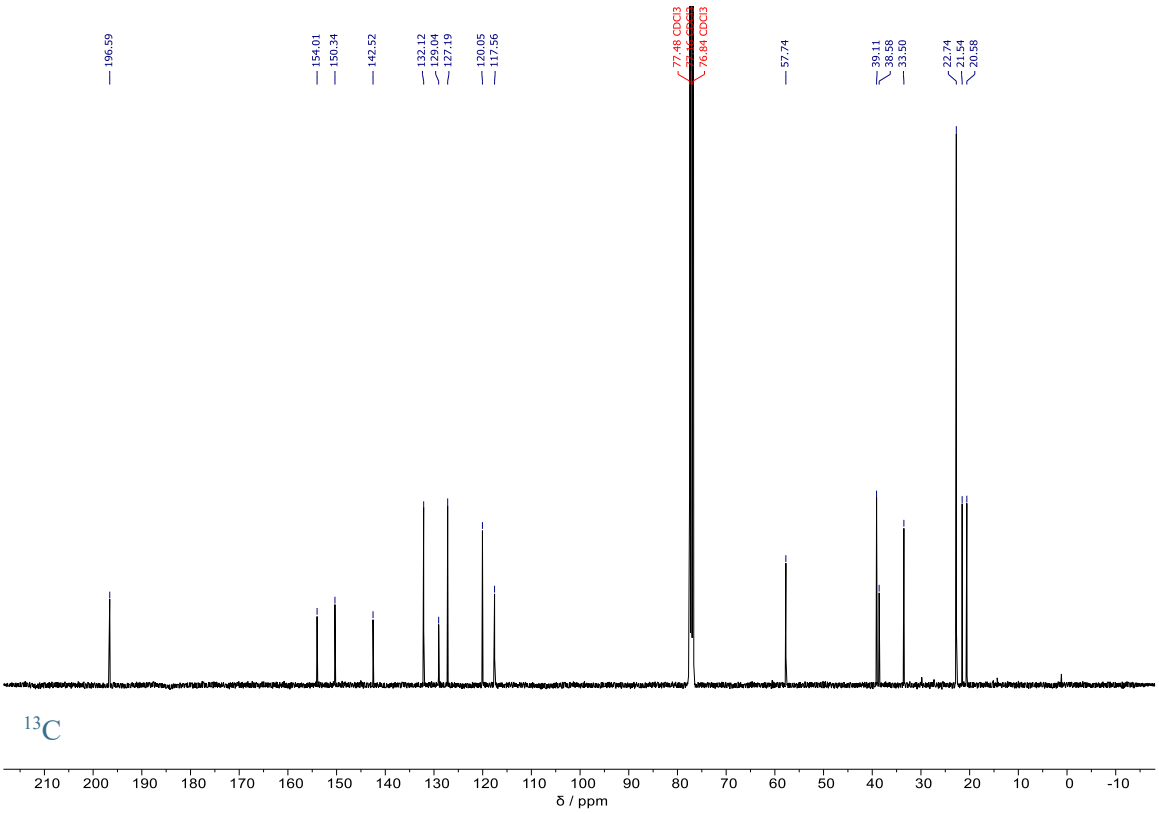


(±)-2-((2-(*tert*-Butylsulfinyl)phenyl)(methyl)amino)-3-methylcyclohex-2-en-1-one, **(±)-48**

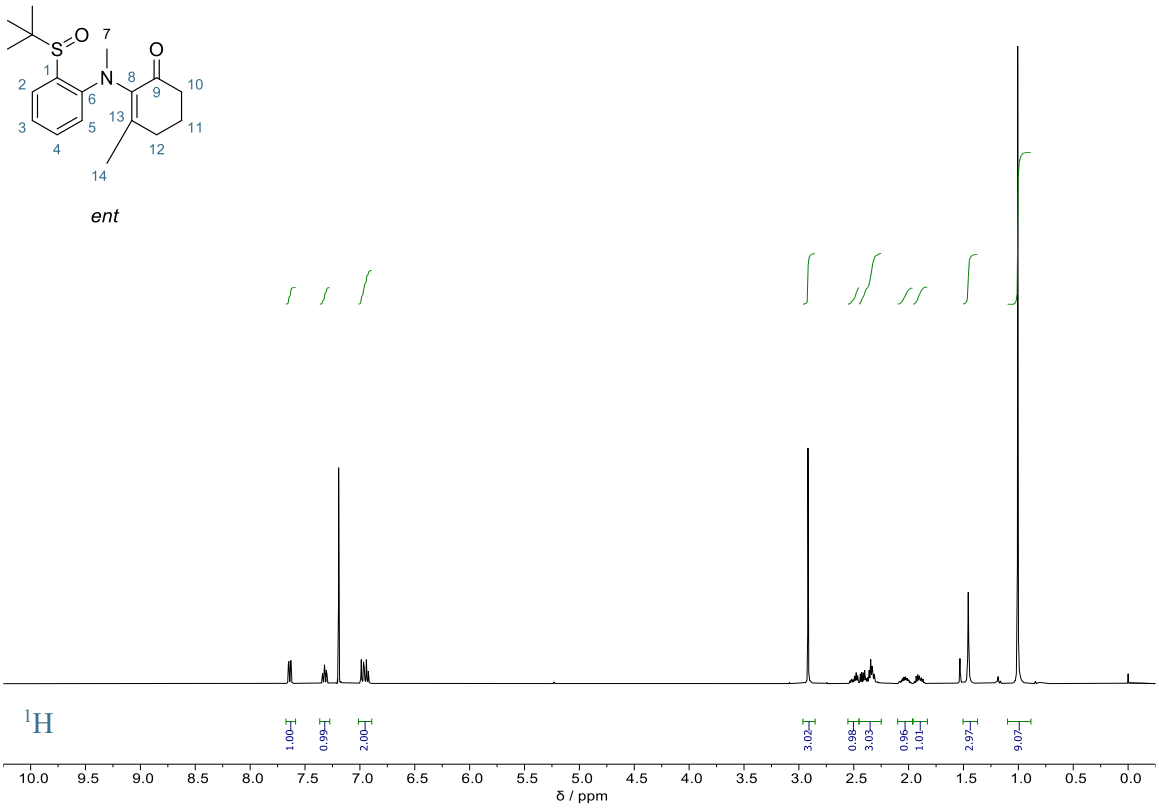


rac

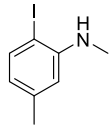


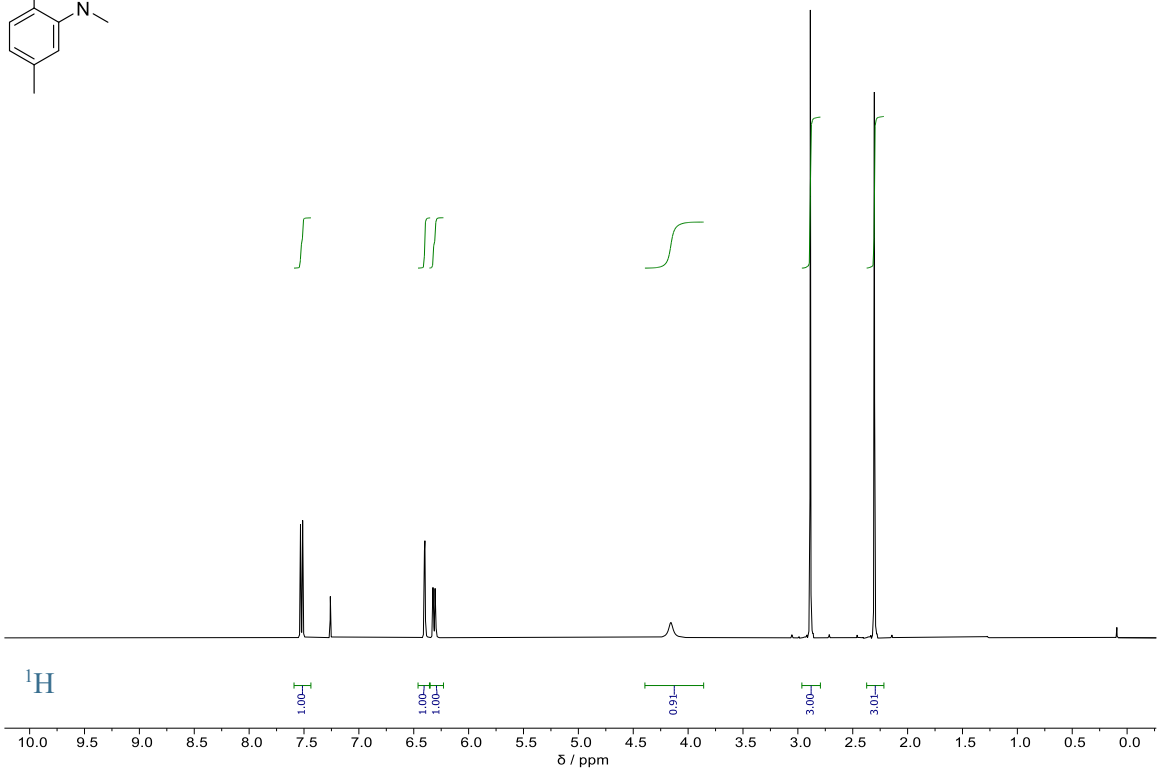


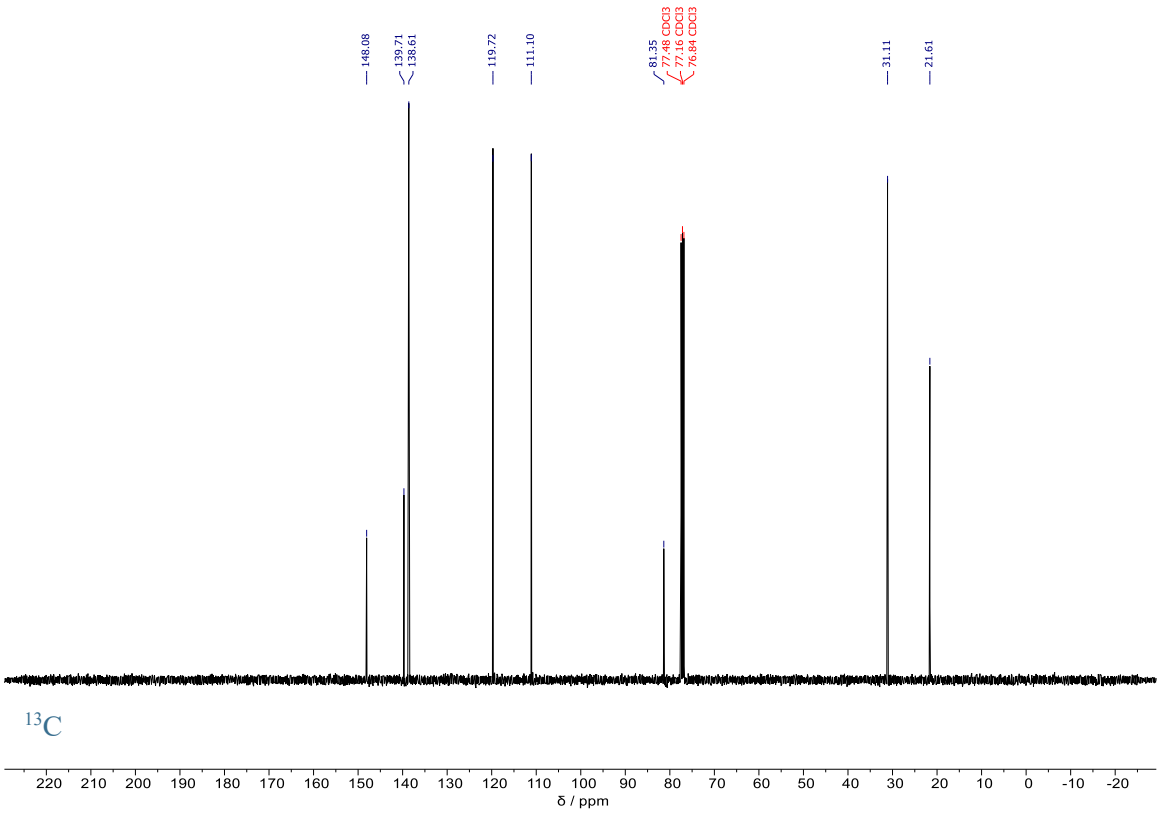
(+)-2-((2-(*tert*-Butylsulfinyl)phenyl)(methyl)amino)-3-methylcyclohex-2-en-1-one, **(+)-48**



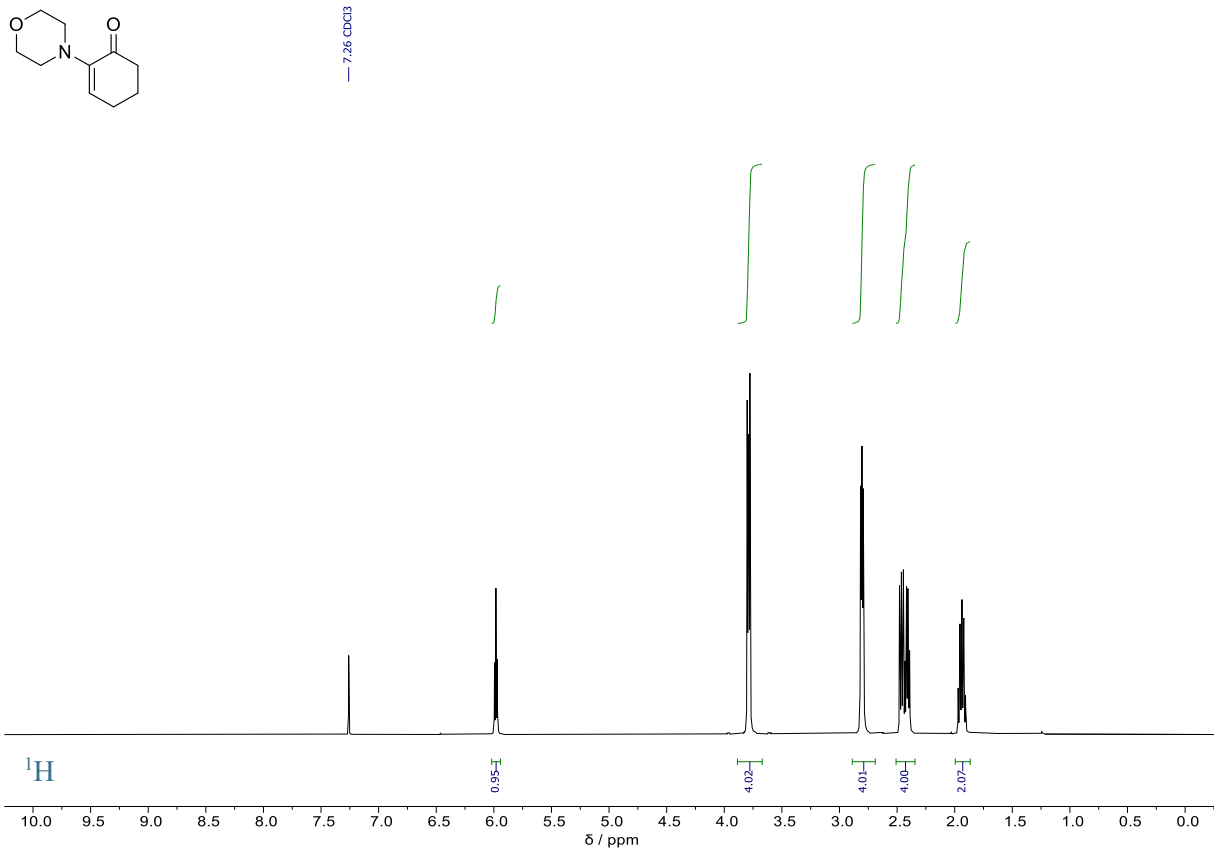
2-Iodo-*N*,5-dimethylaniline, **S1**

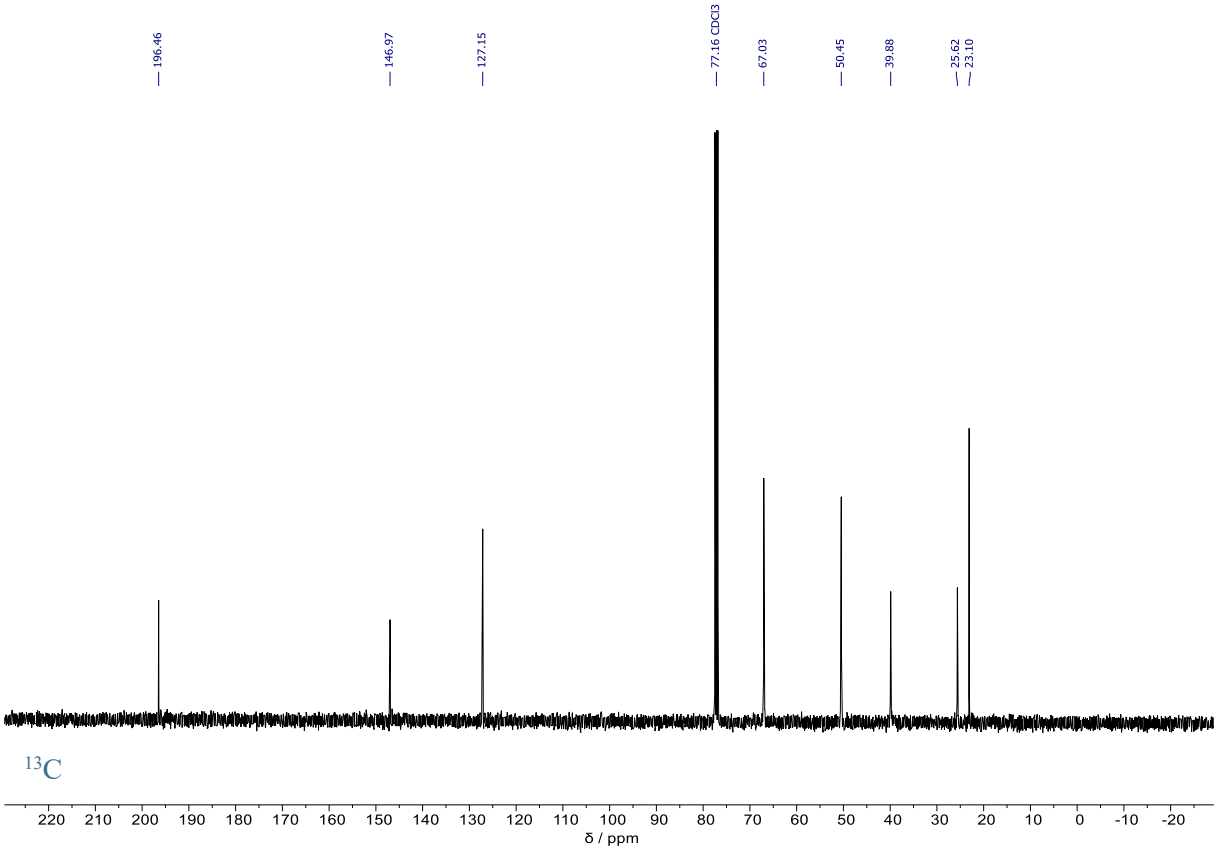




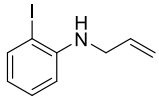


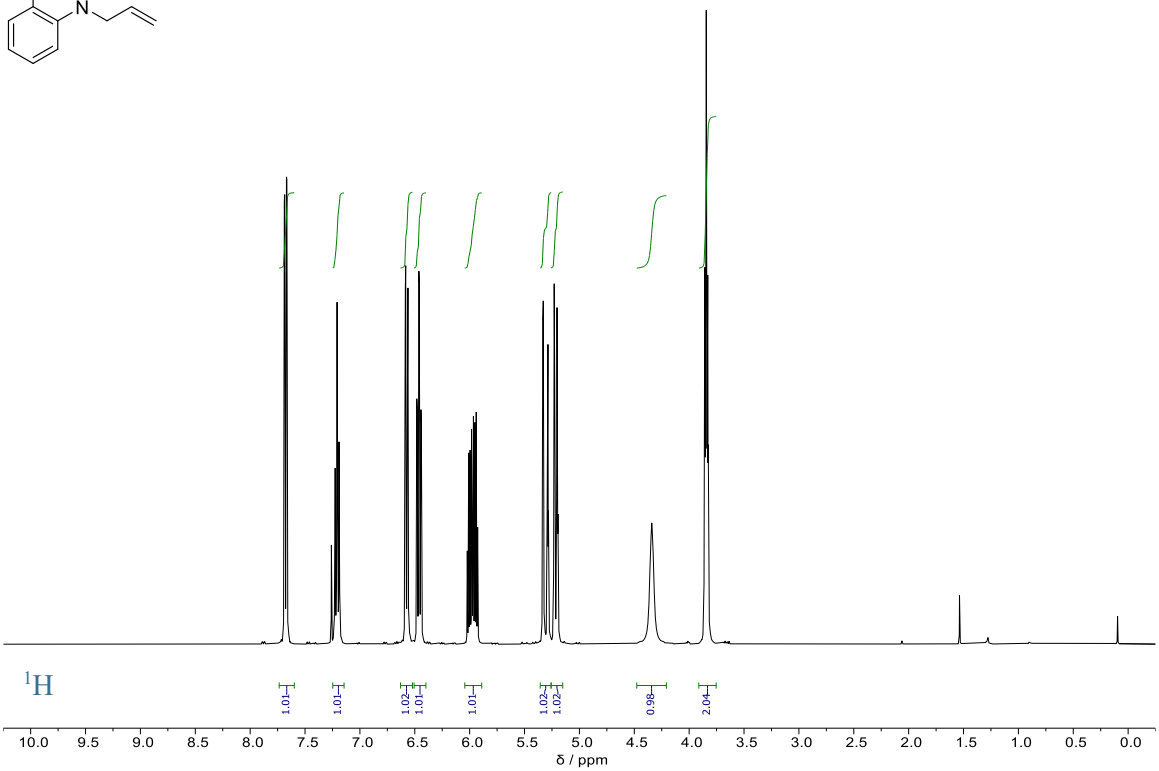
2-Morpholinocyclohex-2-en-1-one, **S2**



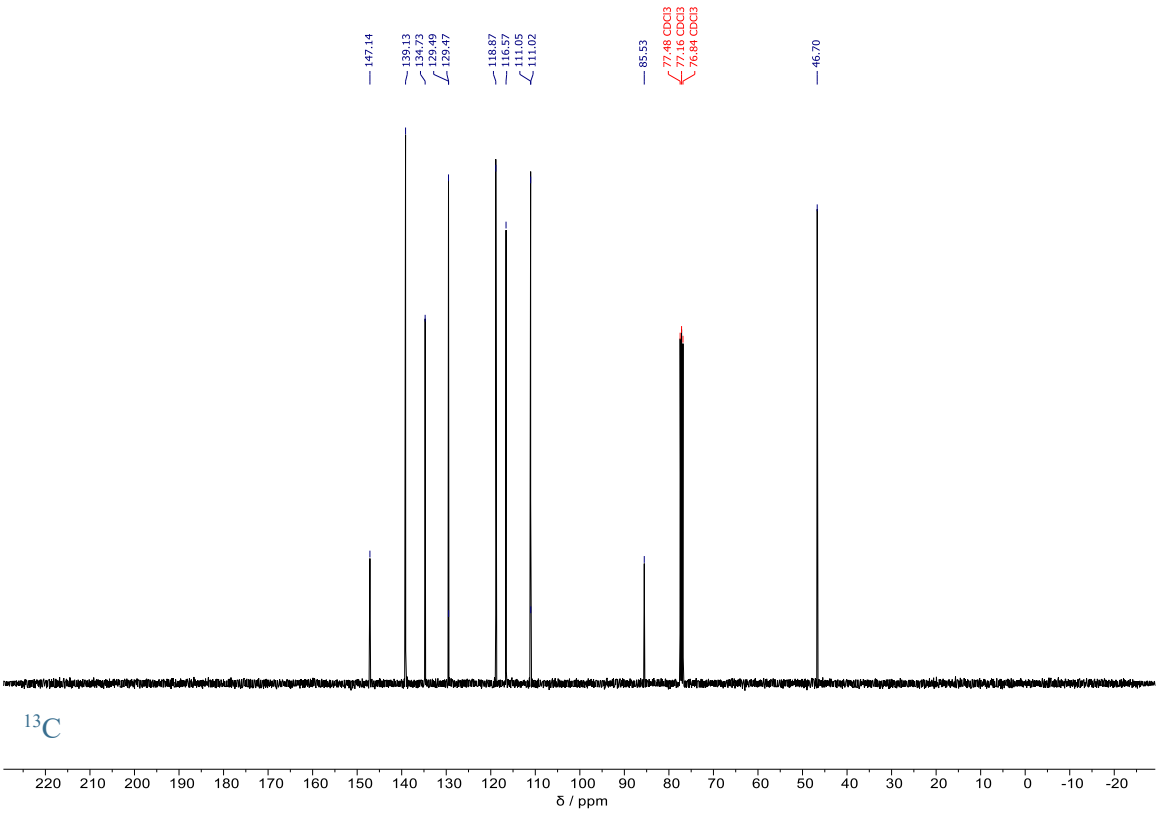


N-Allyl-2-iodoaniline, **S3**



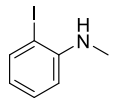


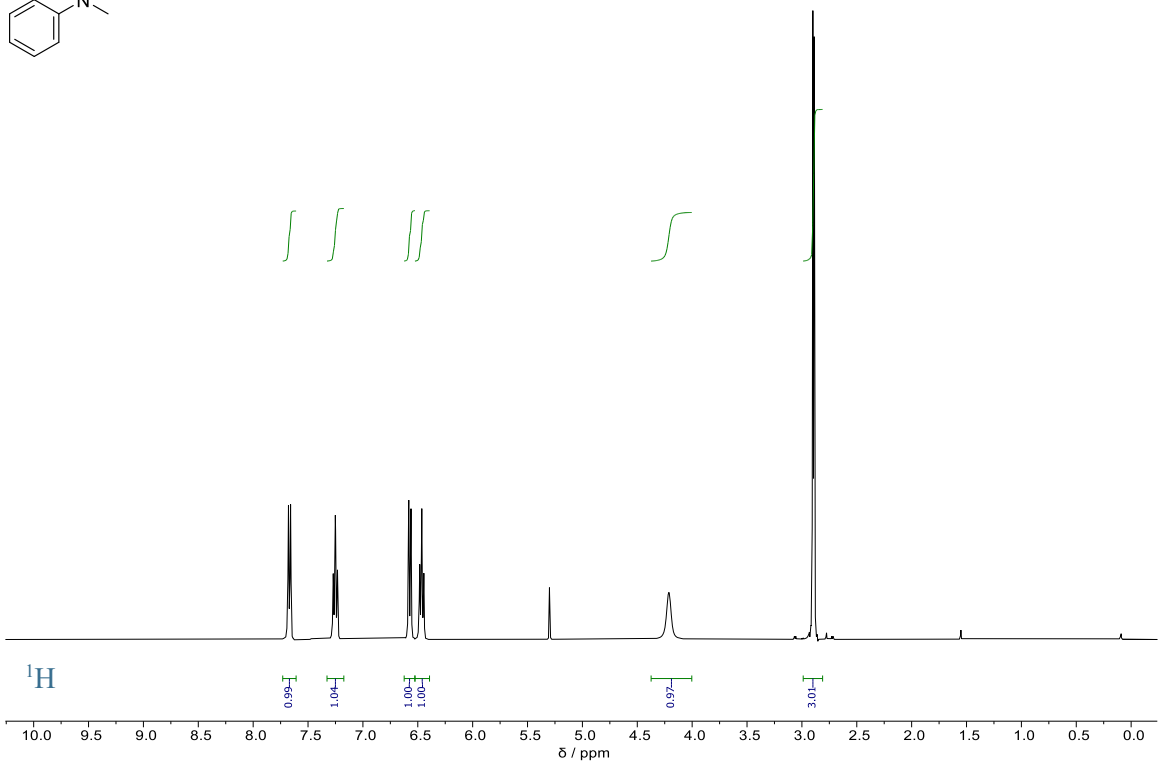
^{1}H

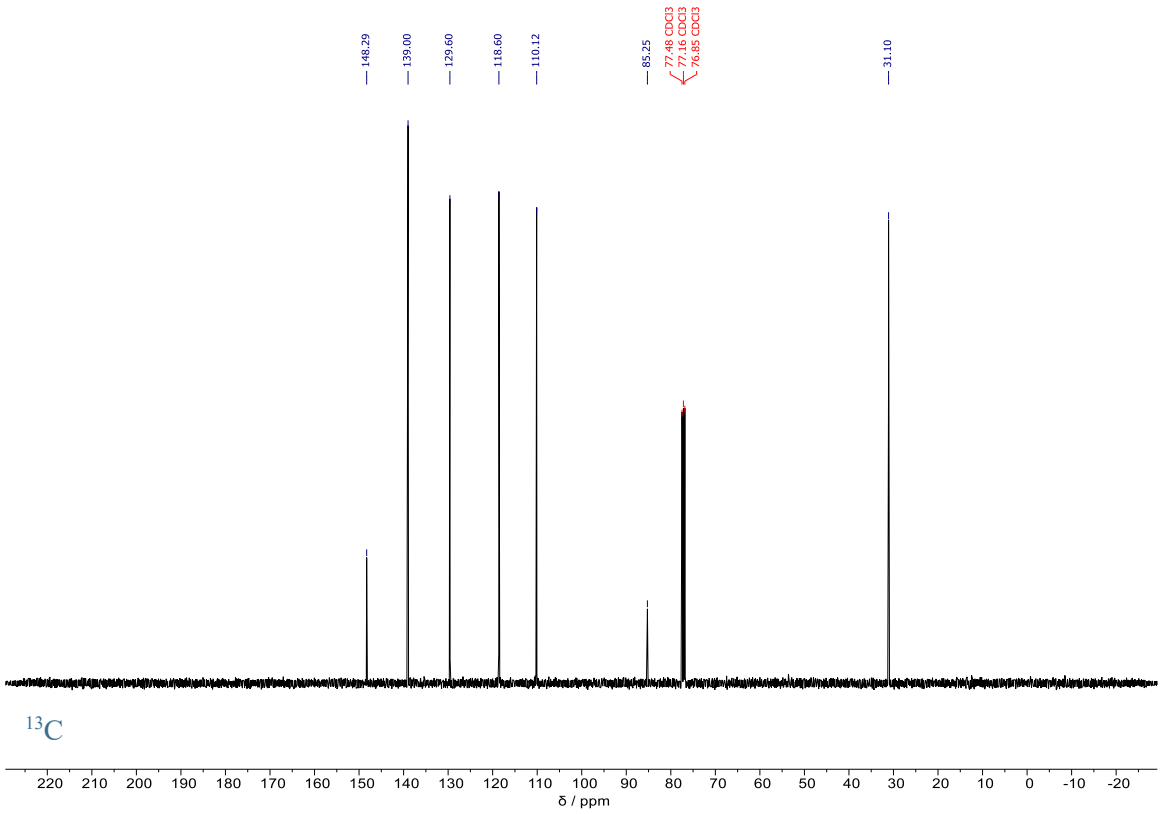


^{13}C

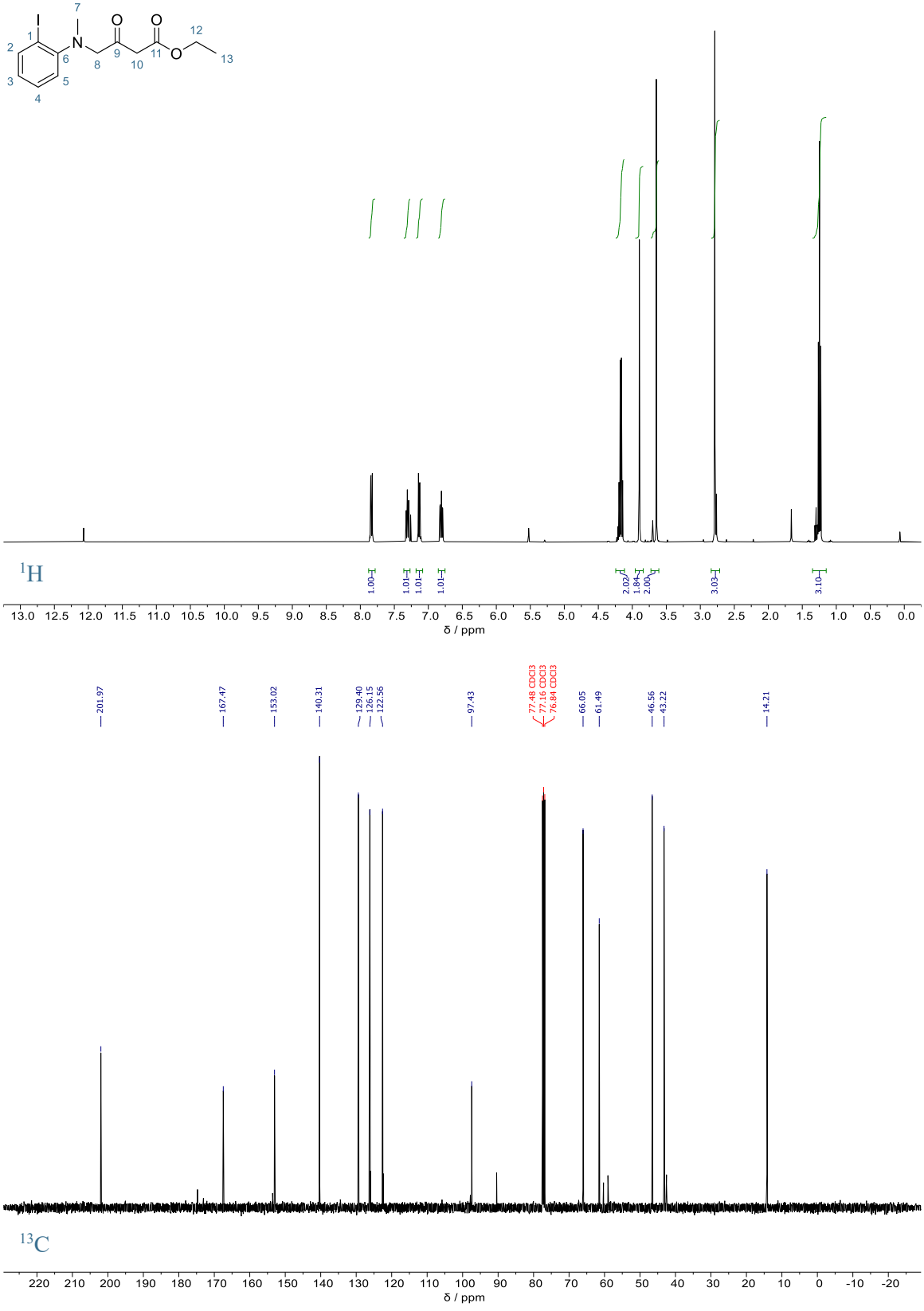
2-Iodo-*N*-methylaniline, **S4**





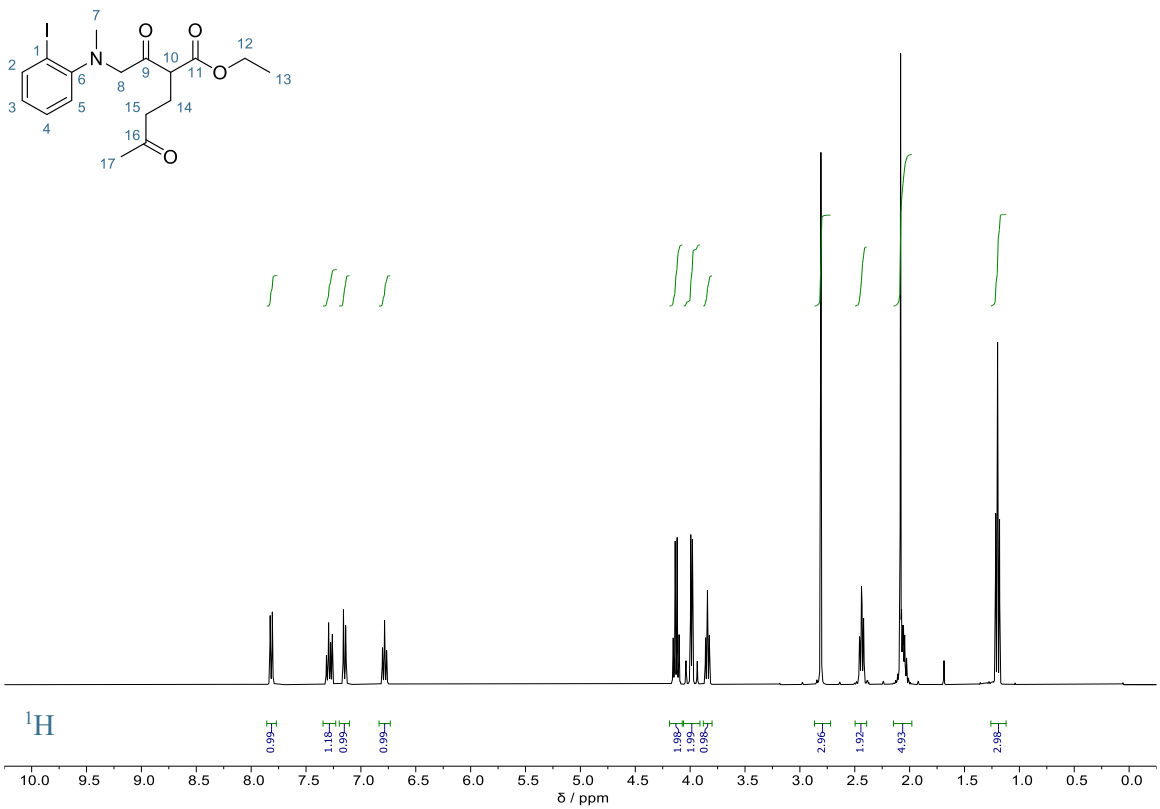


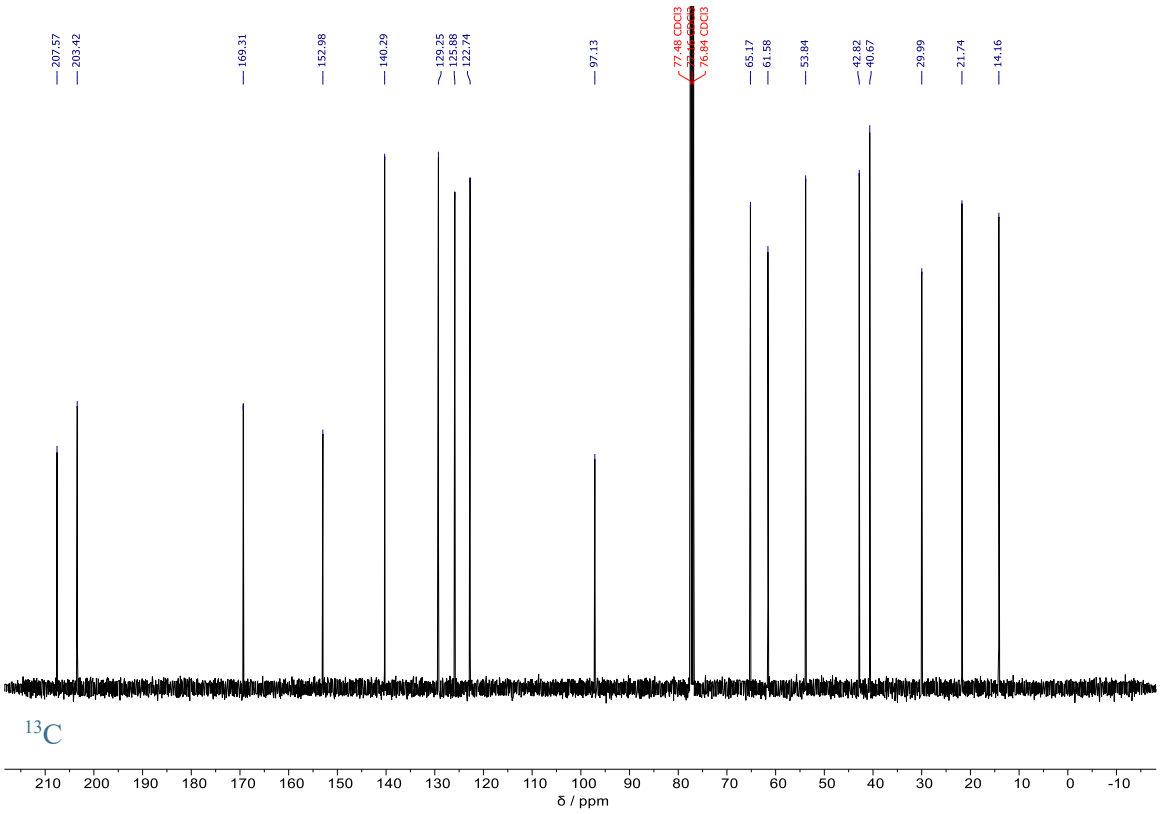
Ethyl 4-((2-iodophenyl)(methyl)amino)-3-oxobutanoate, **S5**



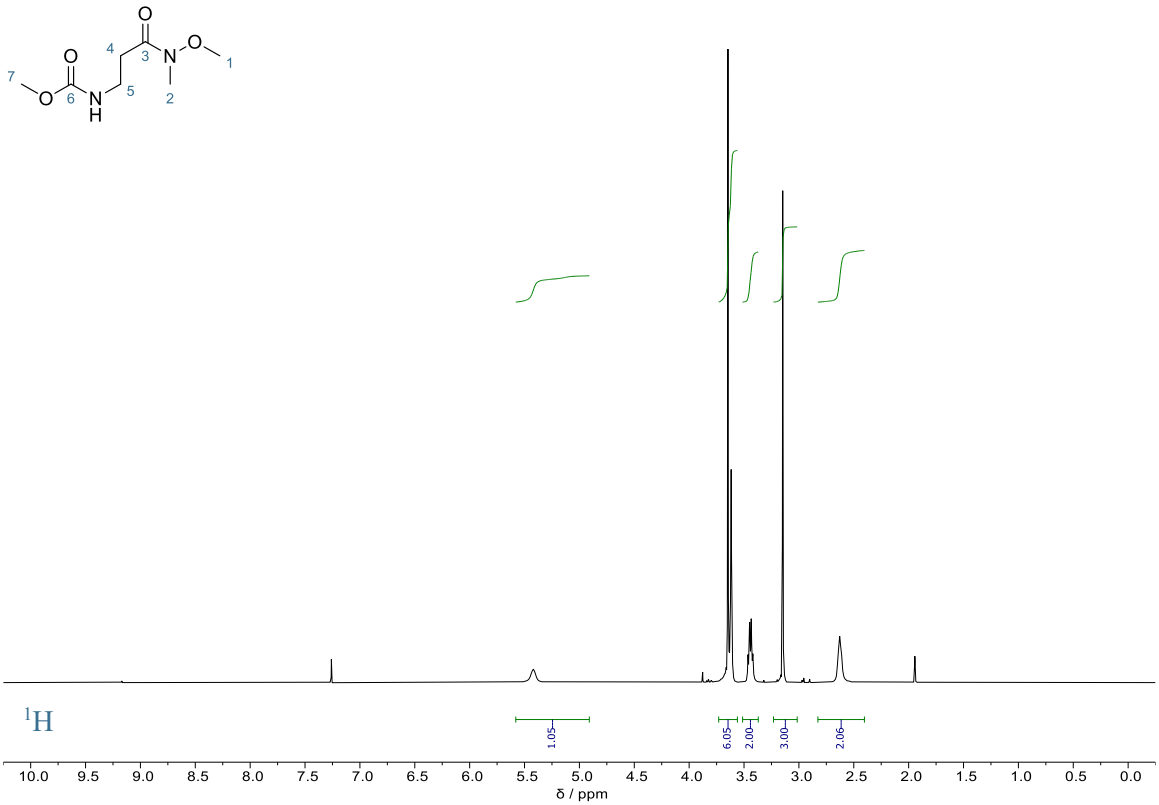
Note: A minor amount of the enol tautomer of this compound is visible on the ^{1}H and ^{13}C NMR spectra above.

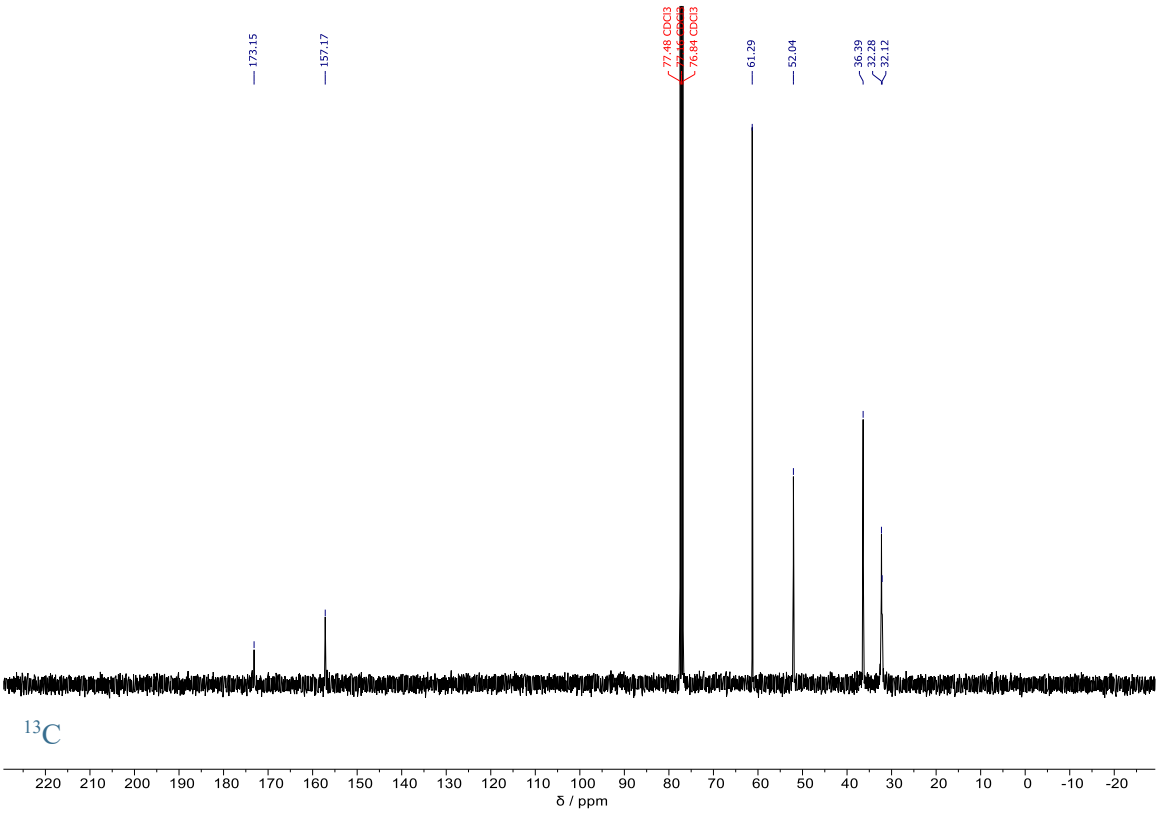
Ethyl 2-(*N*-(2-iodophenyl)-*N*-methylglycyl)-5-oxohexanoate, **S6**



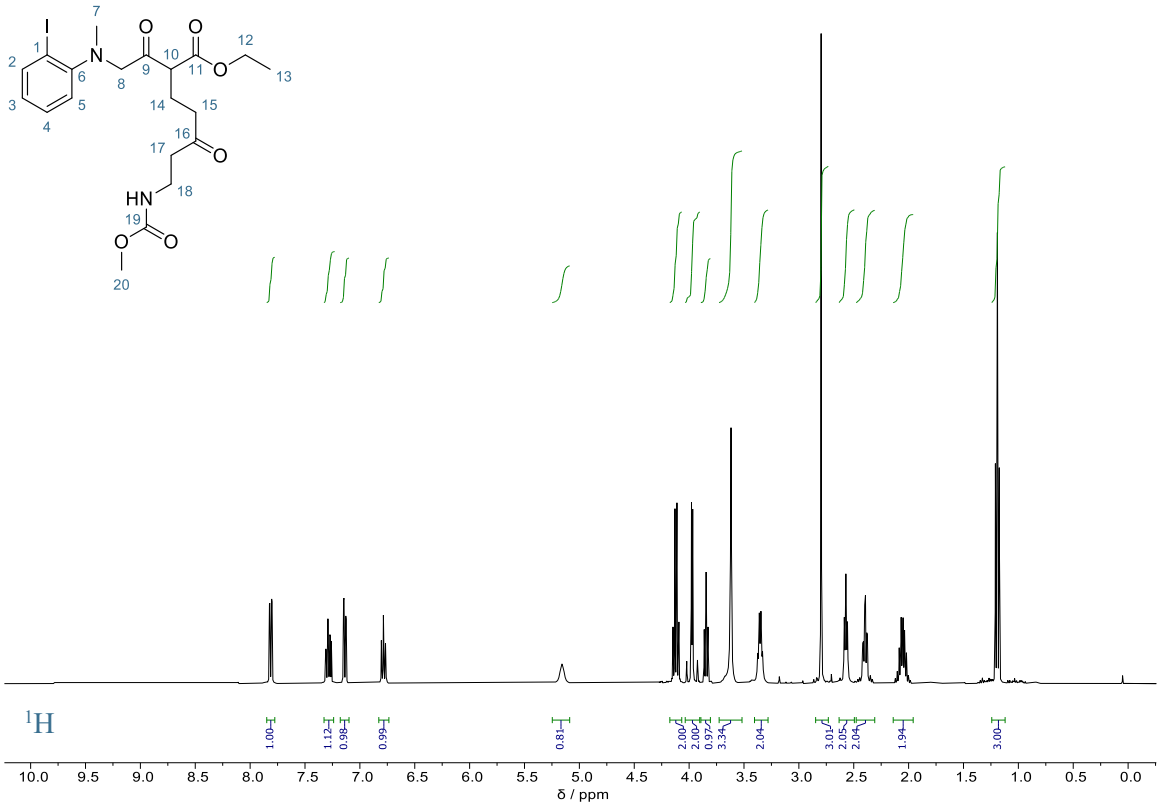


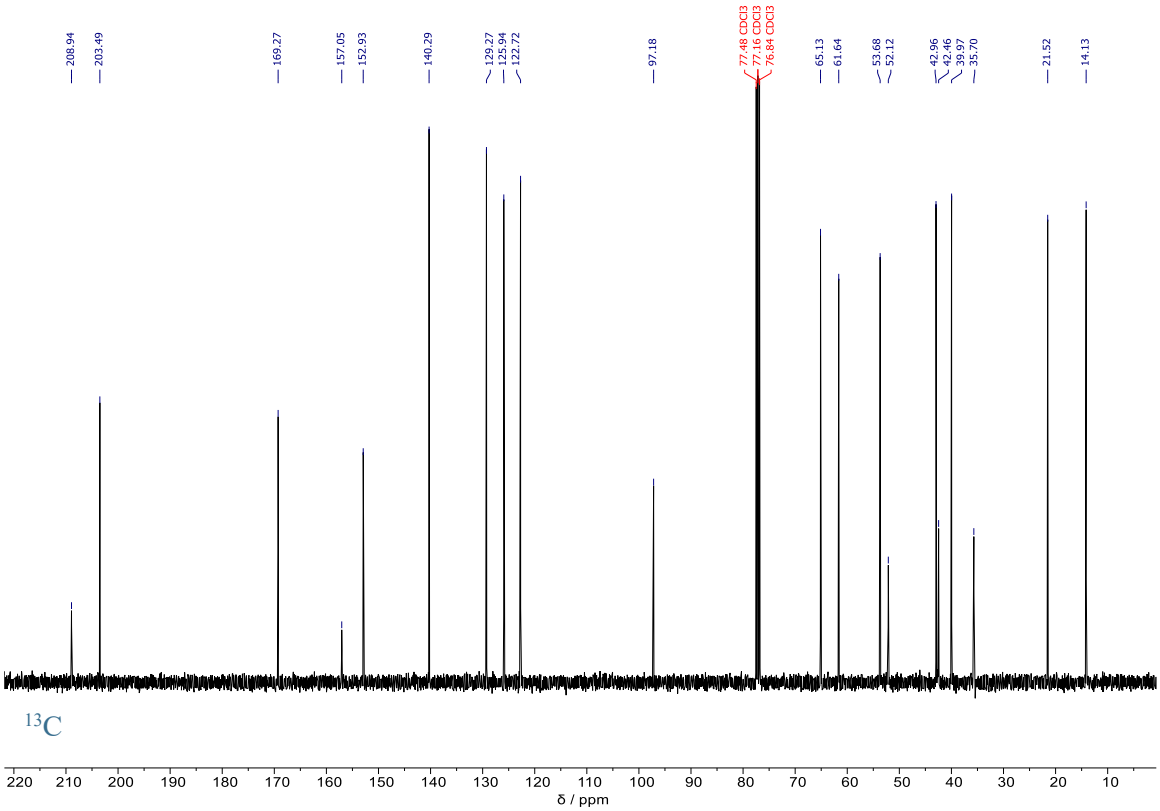
Methyl (3-(methoxy(methyl)amino)-3-oxopropyl)carbamate, **S9**



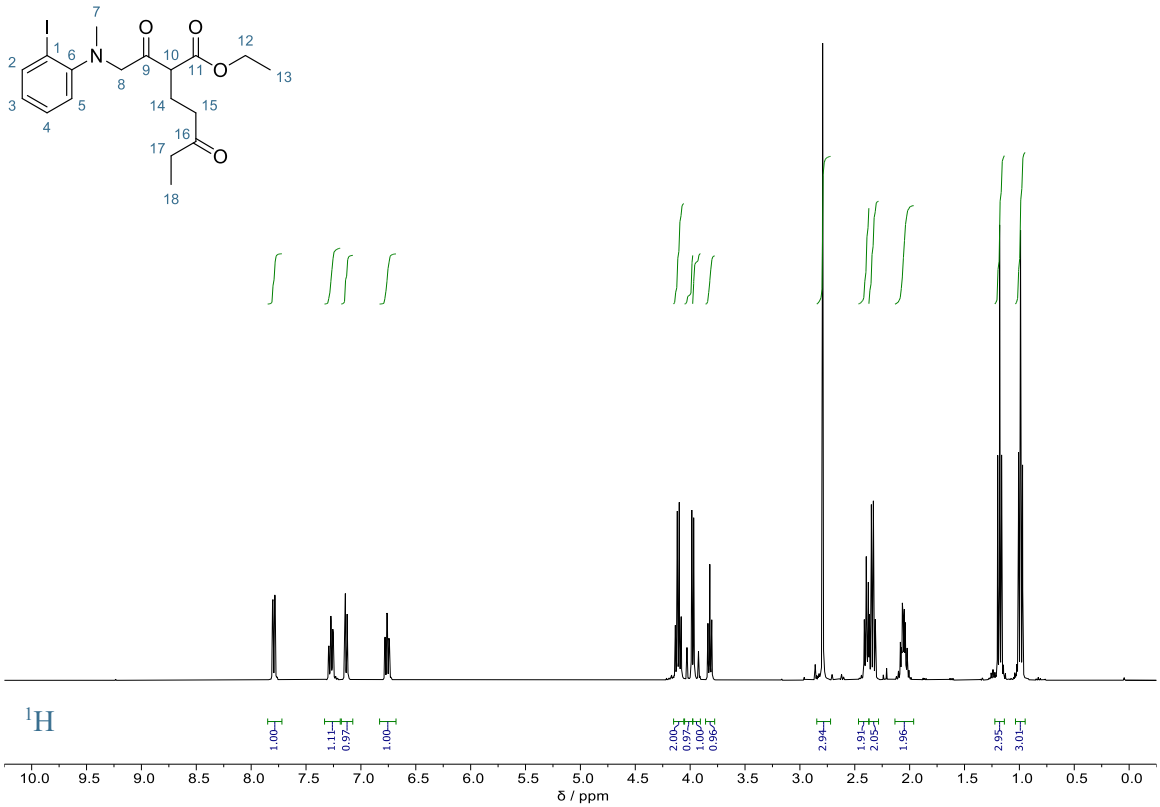


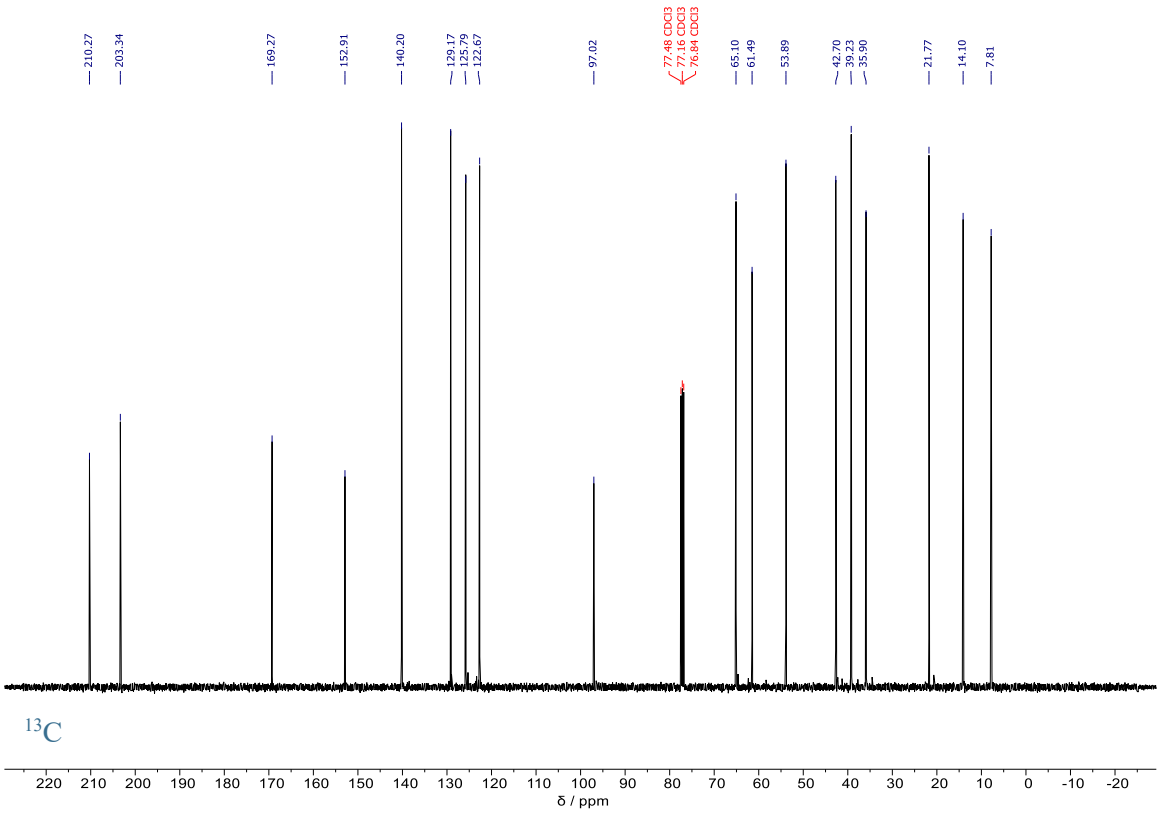
Ethyl 2-(*N*-(2-iodophenyl)-*N*-methylglycyl)-7-((methoxycarbonyl)amino)-5-oxoheptanoate, **S11**



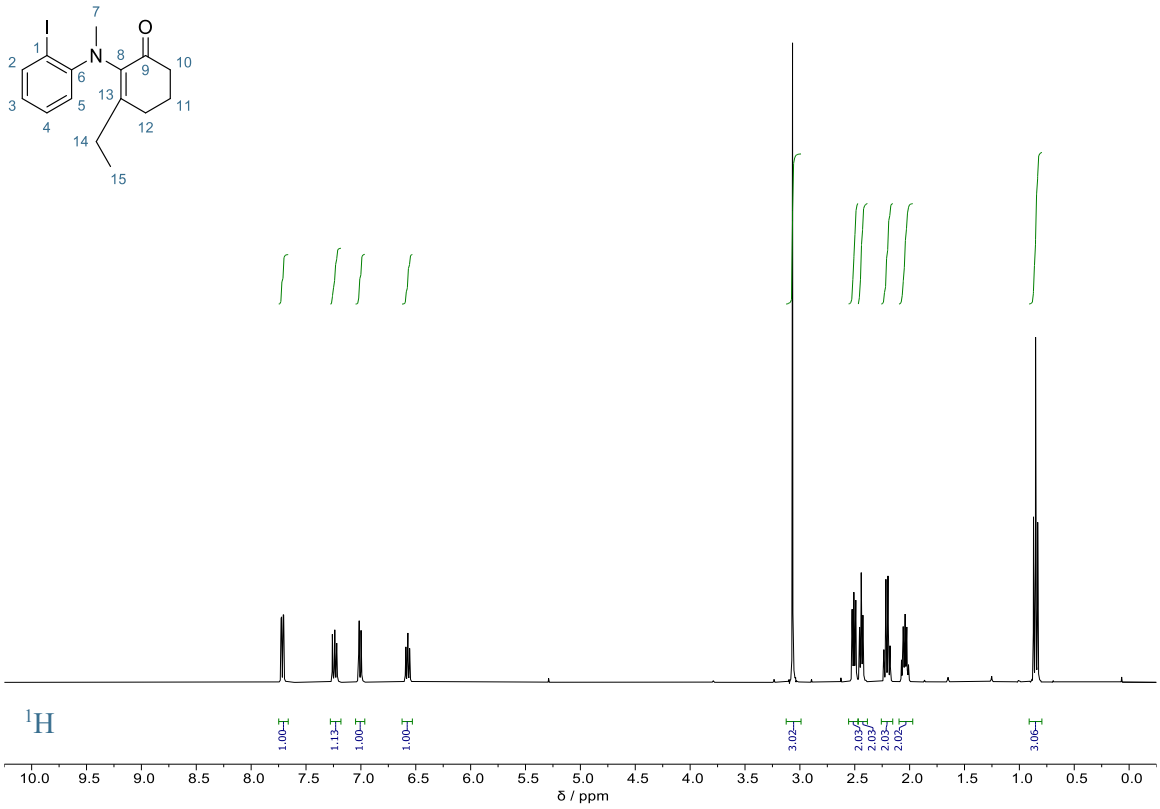


Ethyl 2-(*N*-(2-iodophenyl)-*N*-methylglycyl)-5-oxoheptanoate, **S12**

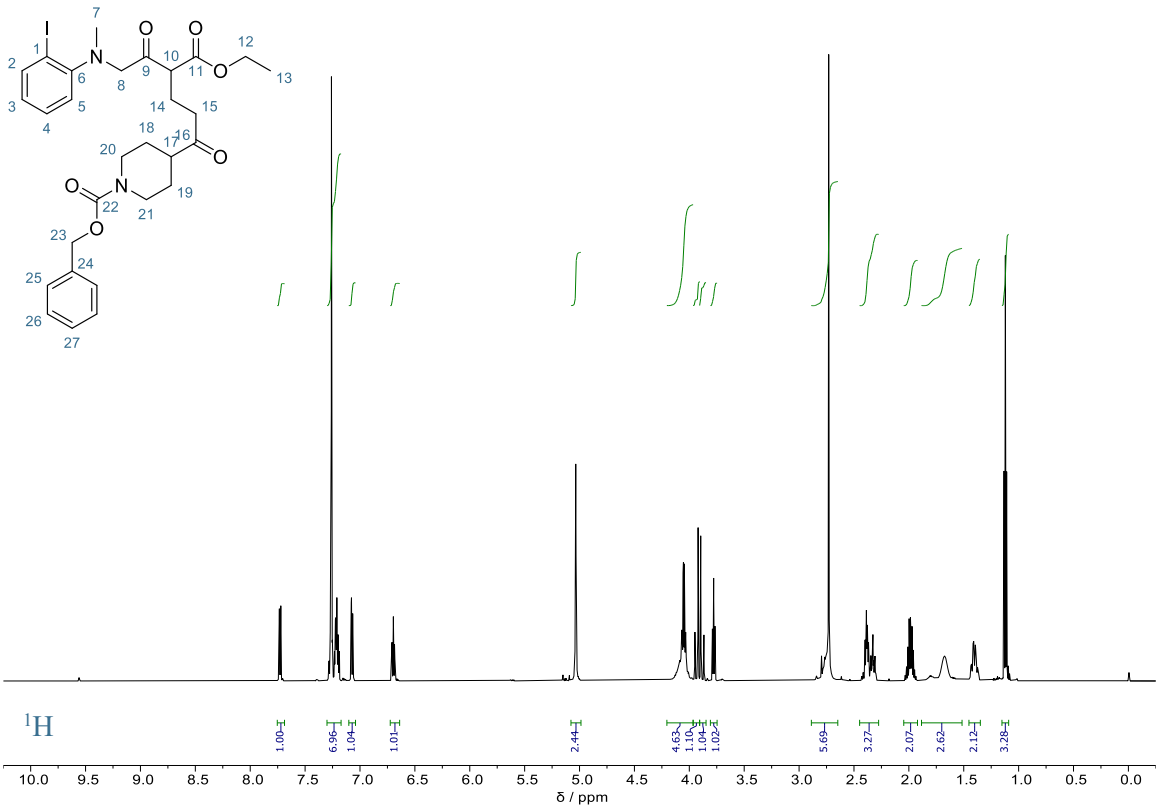


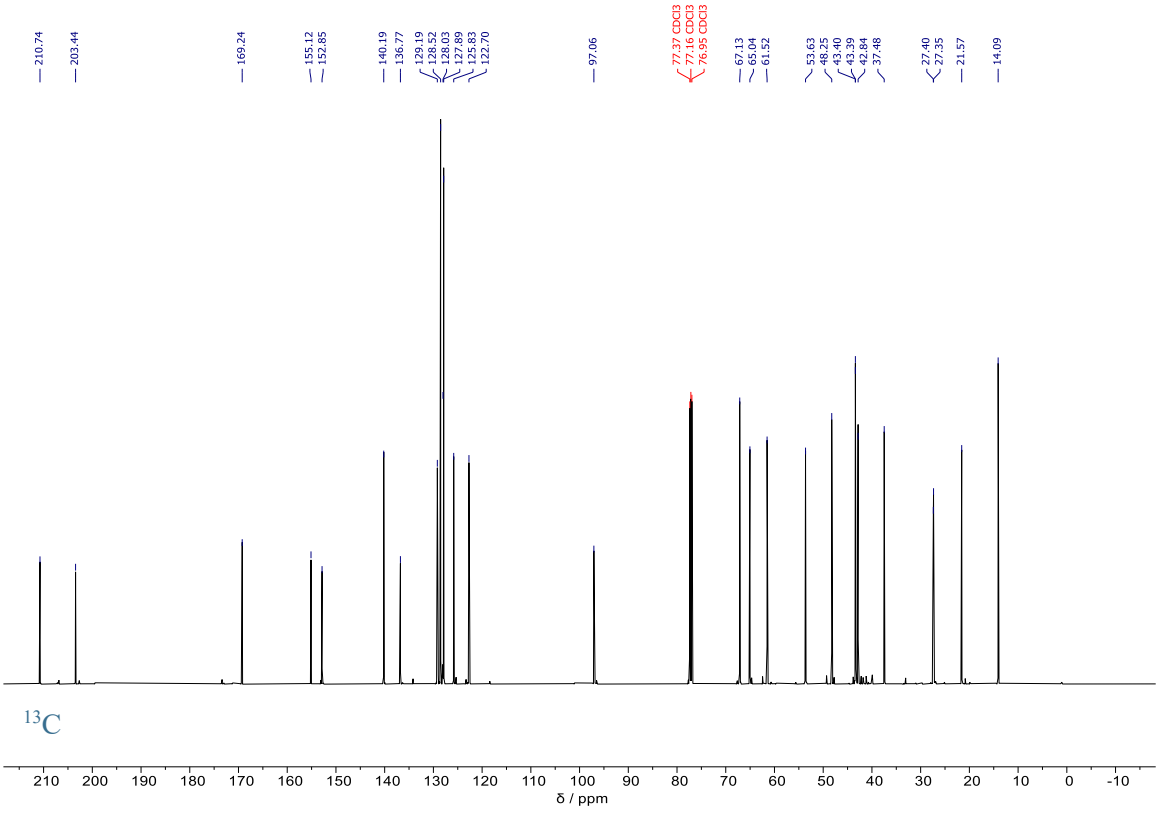


3-Ethyl-2-((2-iodophenyl)(methyl)amino)cyclohex-2-en-1-one, **S13**

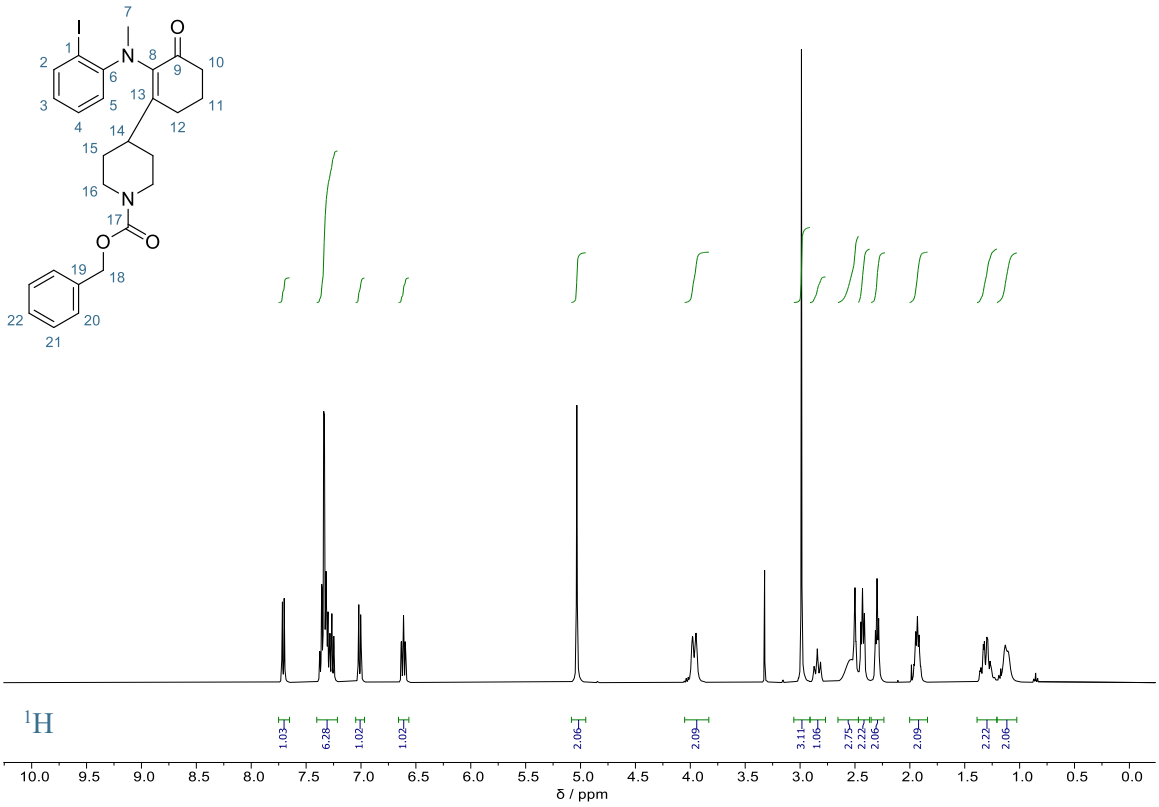


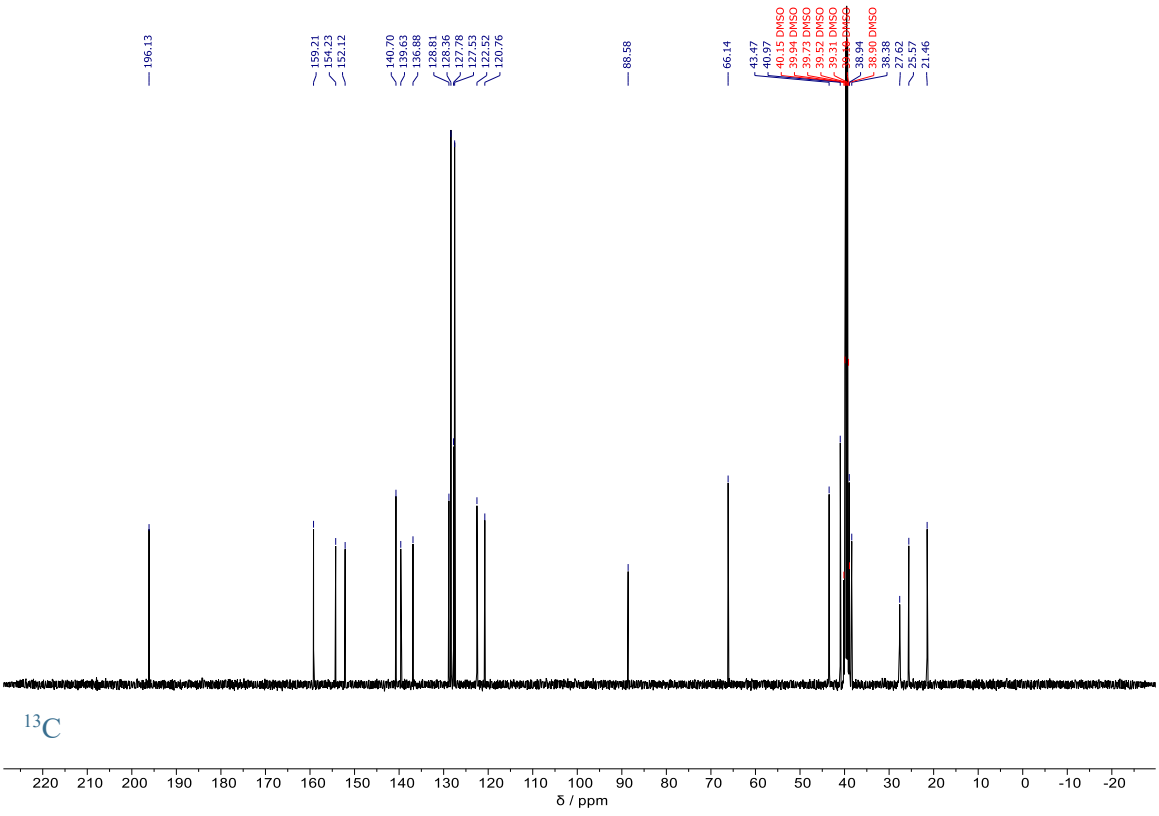
Benzyl 4-(4-(ethoxycarbonyl)-6-((2-iodophenyl)(methyl)amino)-5-oxohexanoyl)piperidine-1-carboxylate, **S16**



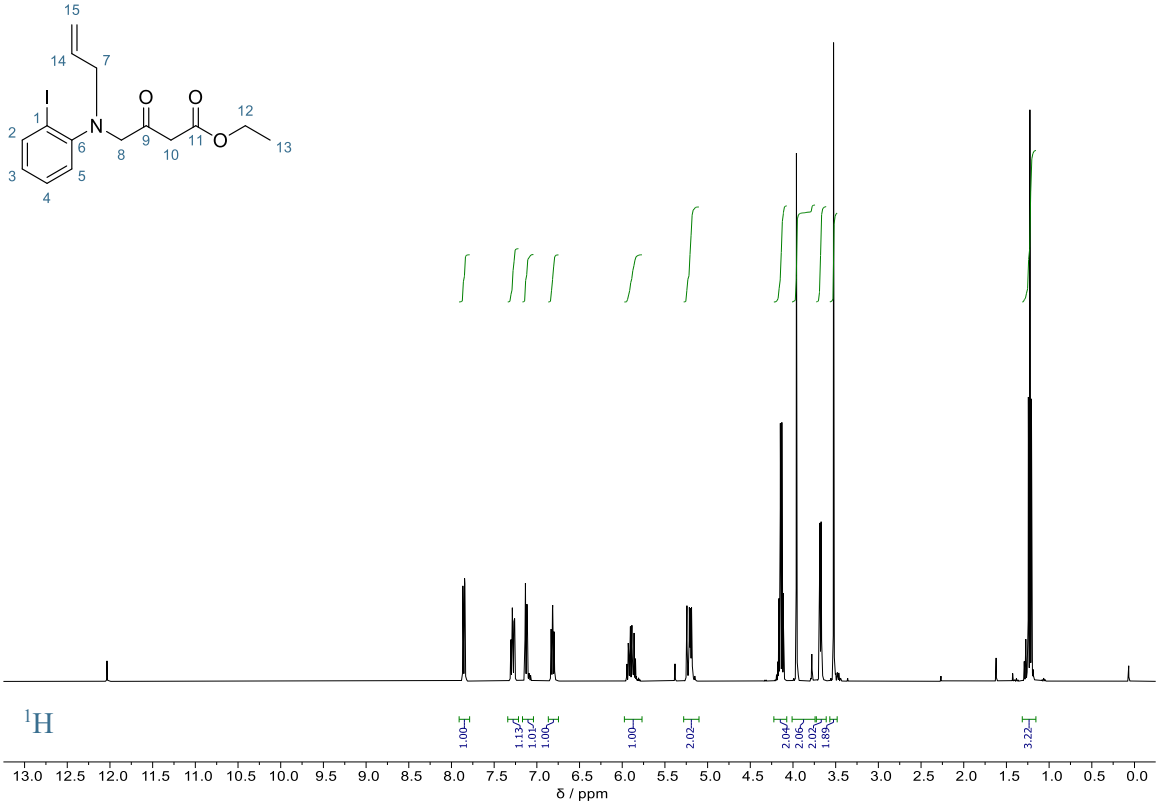


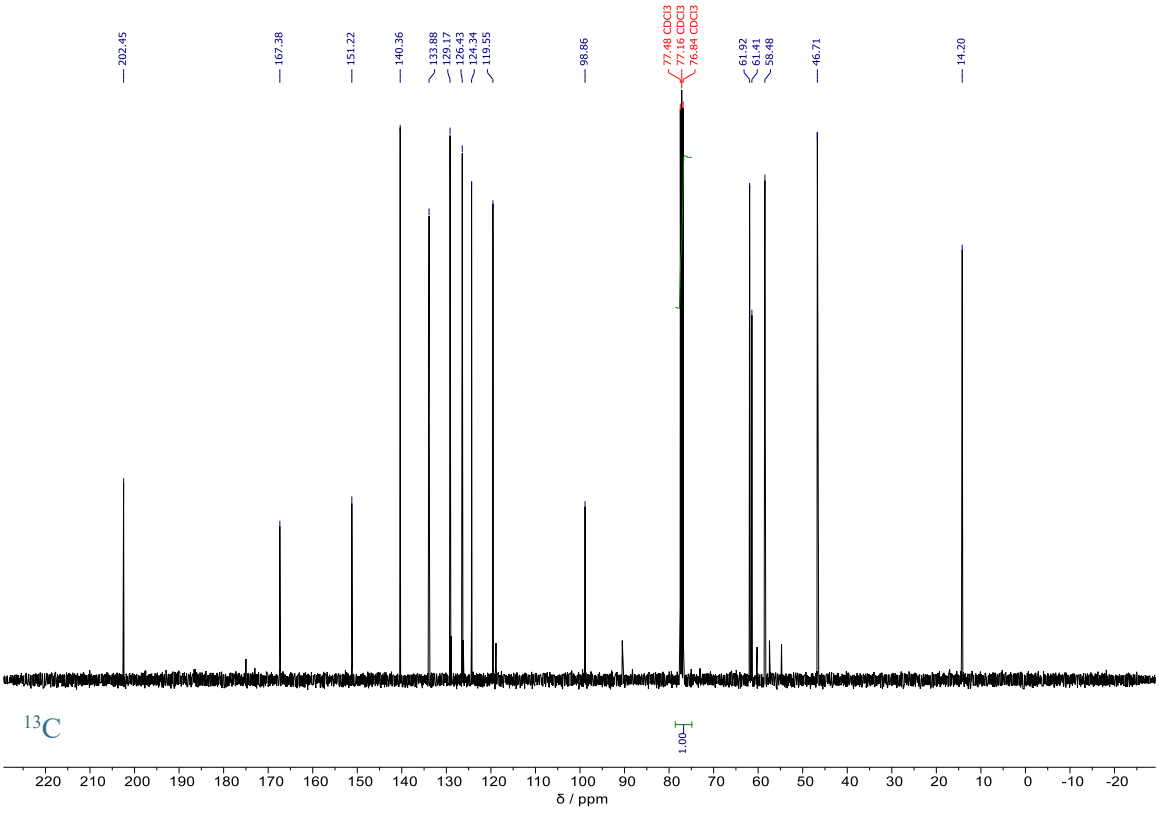
Benzyl 4-(2-((2-iodophenyl)(methyl)amino)-3-oxocyclohex-1-en-1-yl)piperidine-1-carboxylate, **S17**





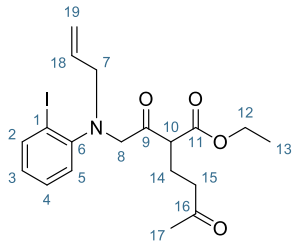
Ethyl 4-(allyl(2-iodophenyl)amino)-3-oxobutanoate, **S18**

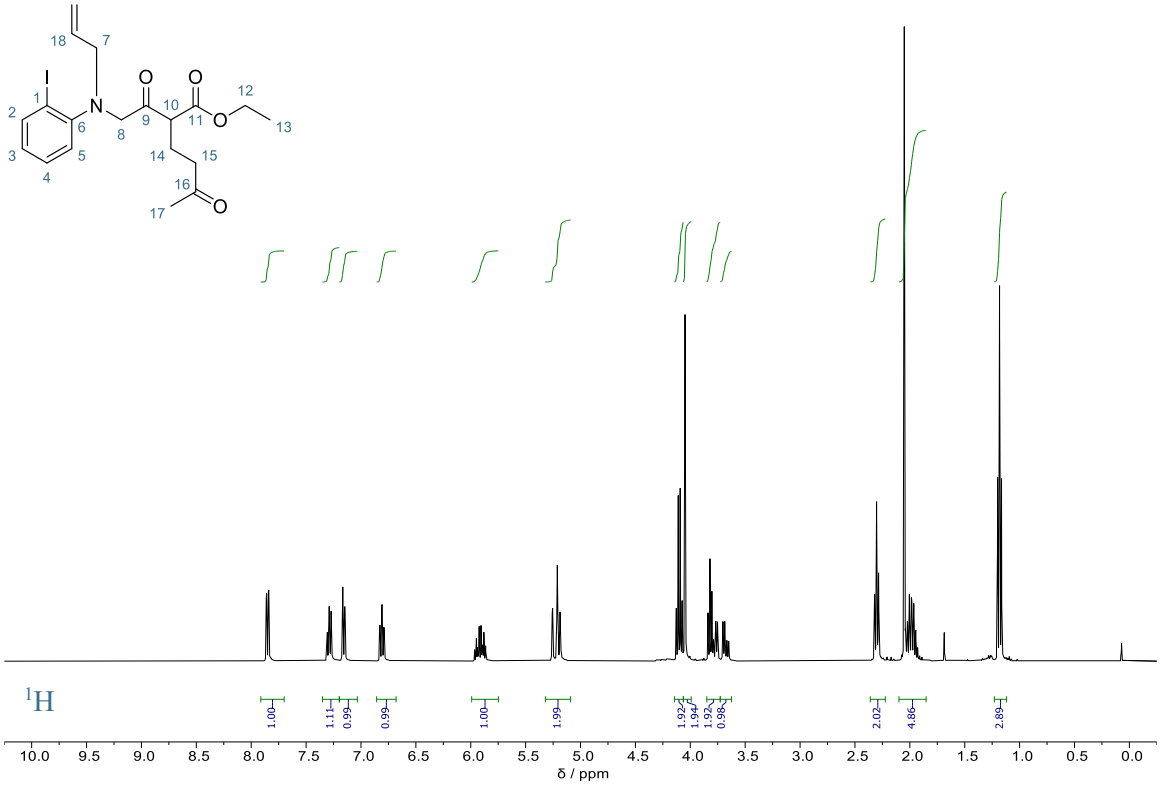


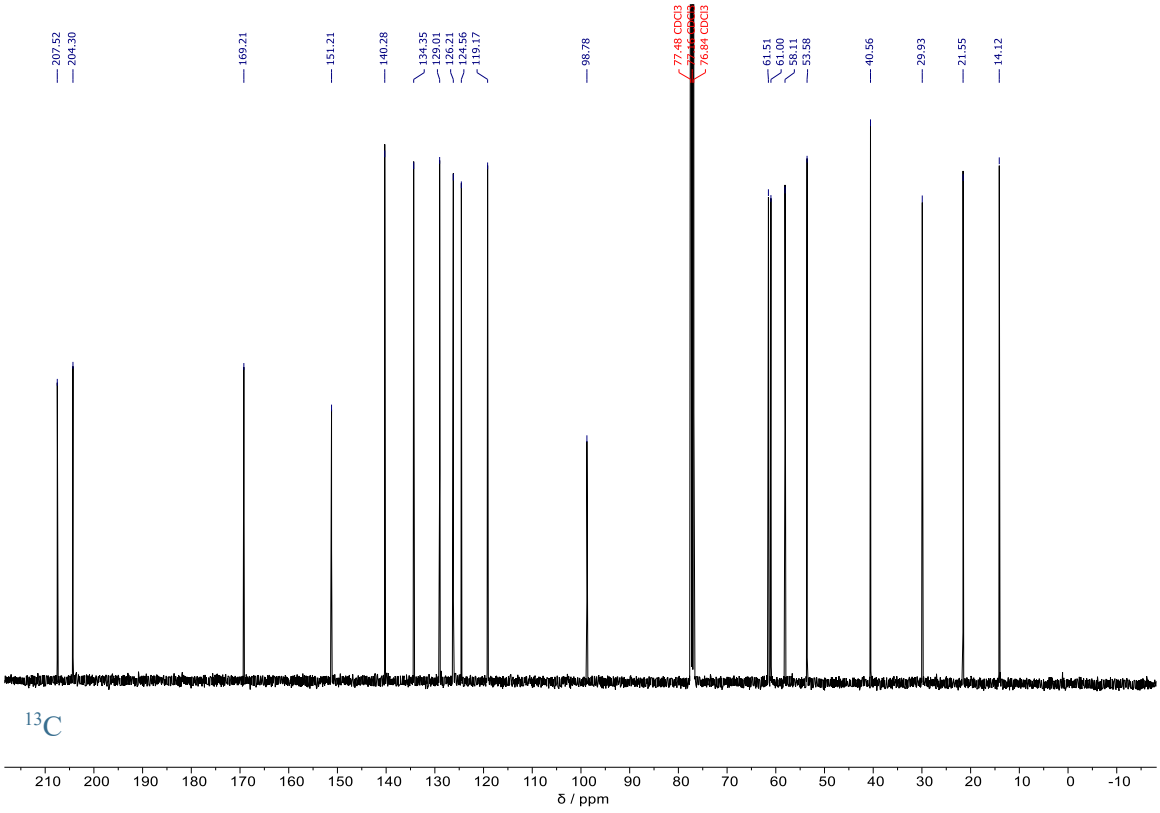


Note: A minor amount of the enol tautomer of this compound is visible on the ^{1}H and ^{13}C NMR spectra above.

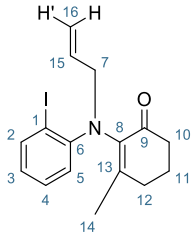
Ethyl 2-(*N*-allyl-*N*-(2-iodophenyl)glycyl)-5-oxohexanoate, **S19**

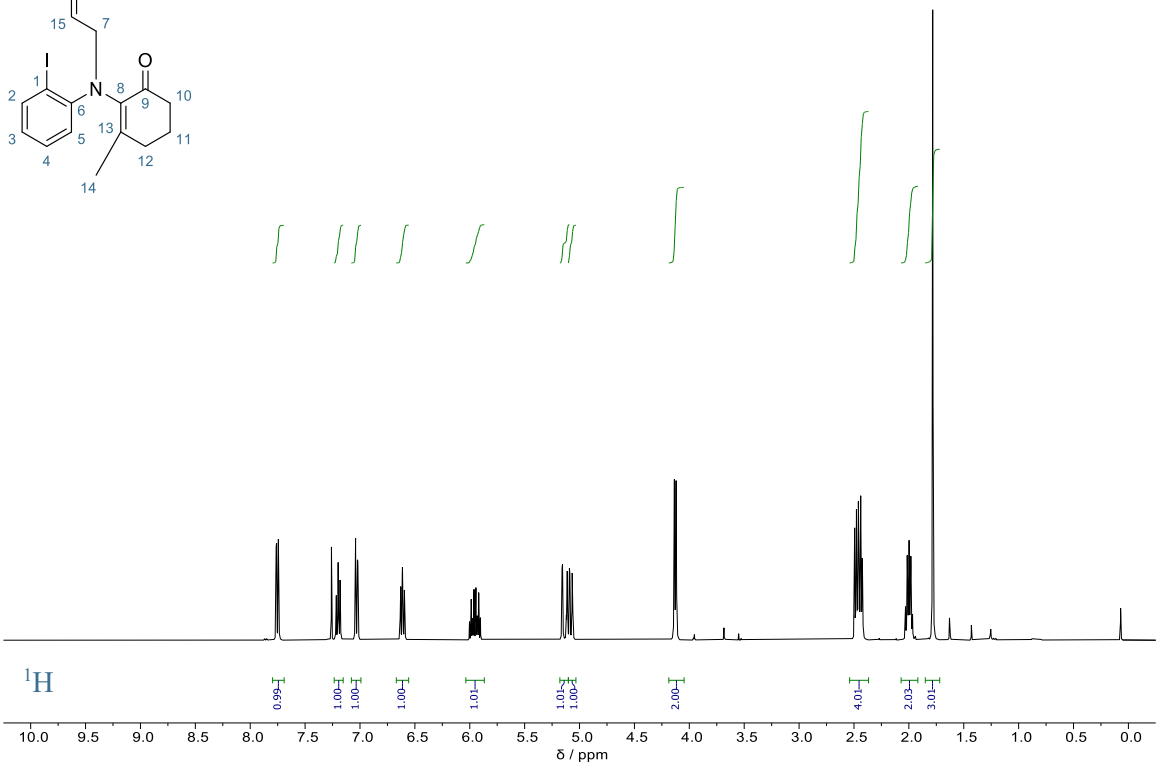


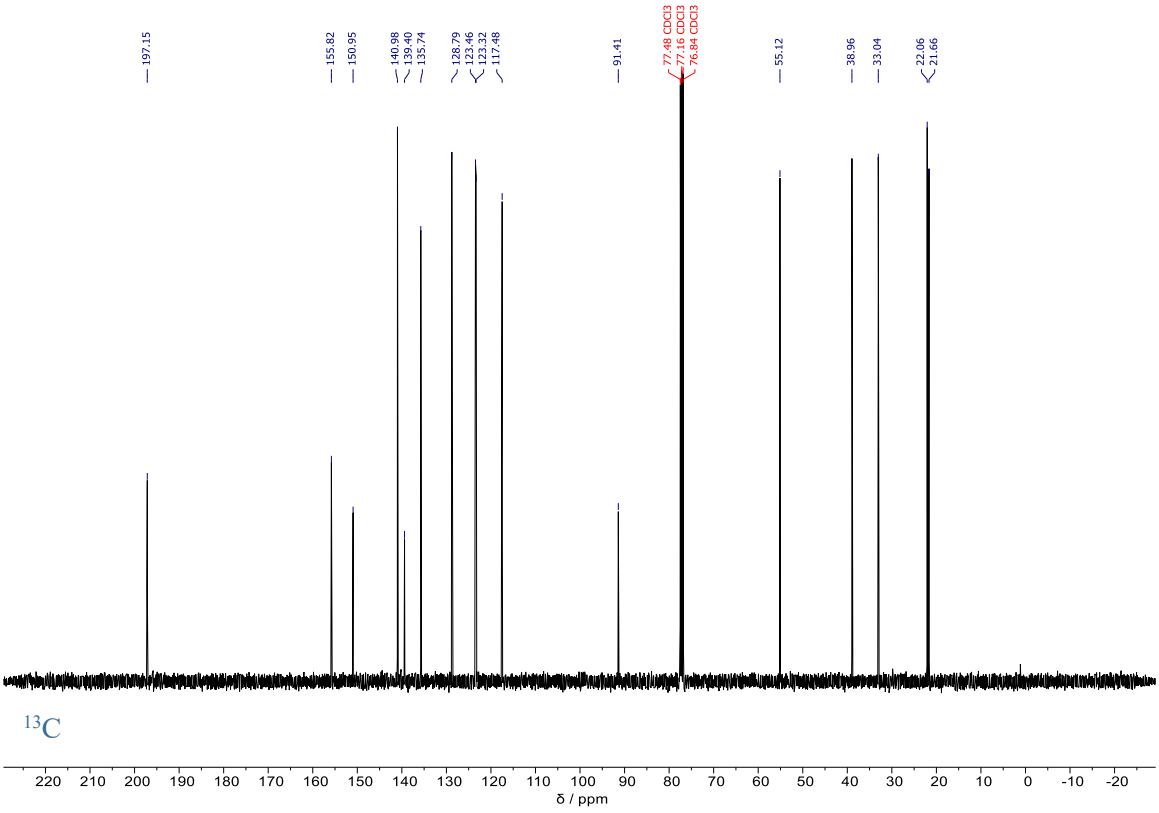




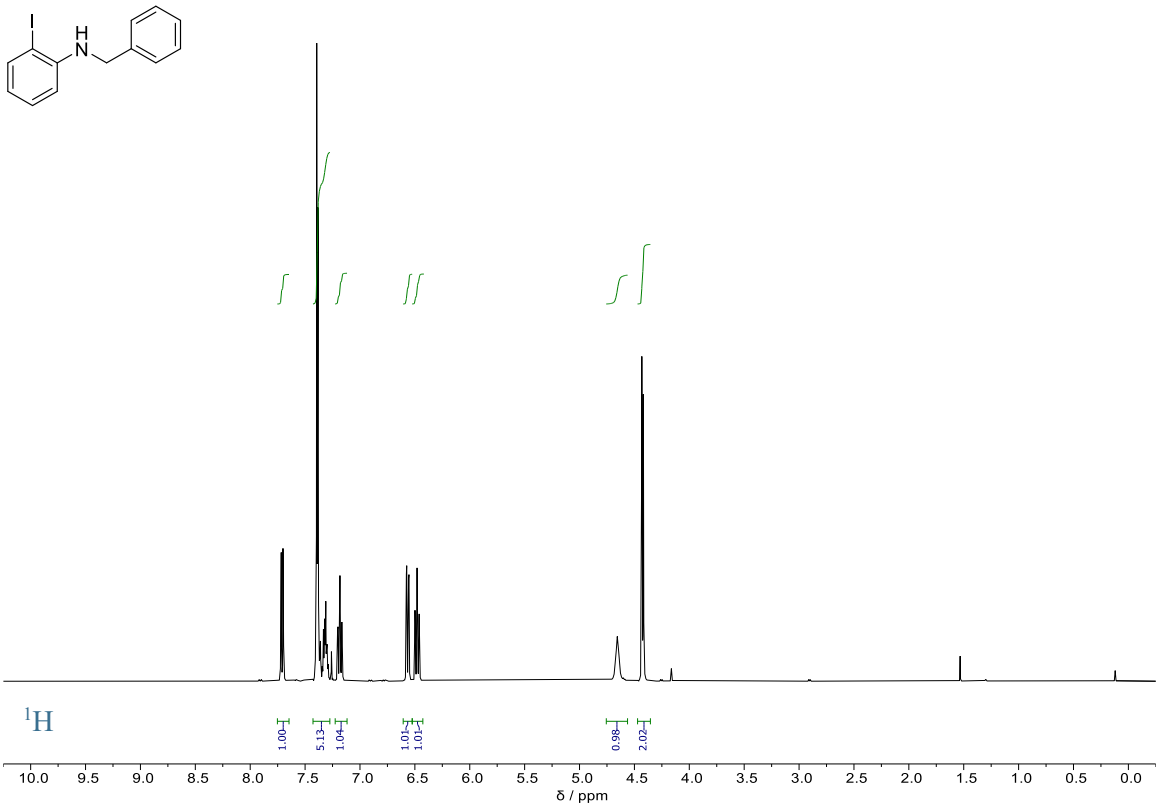
2-(Allyl(2-iodophenyl)amino)-3-methylcyclohex-2-en-1-one, **S20**

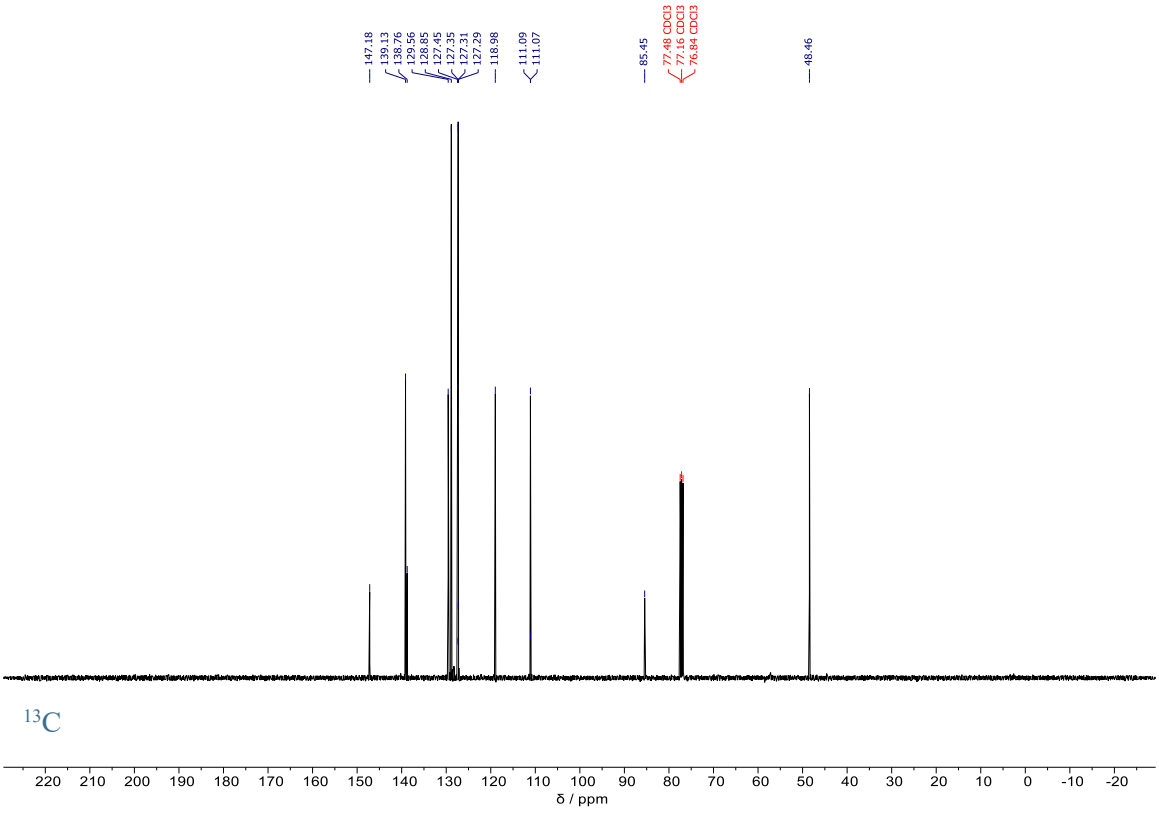




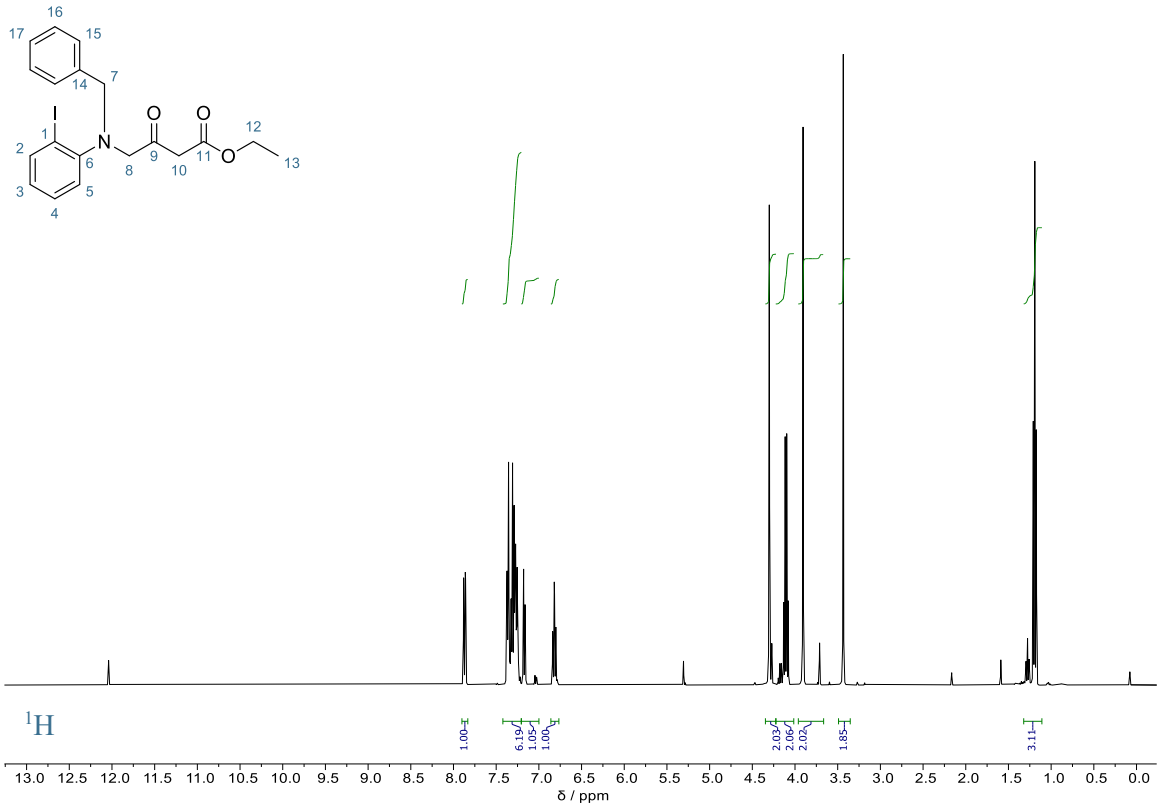


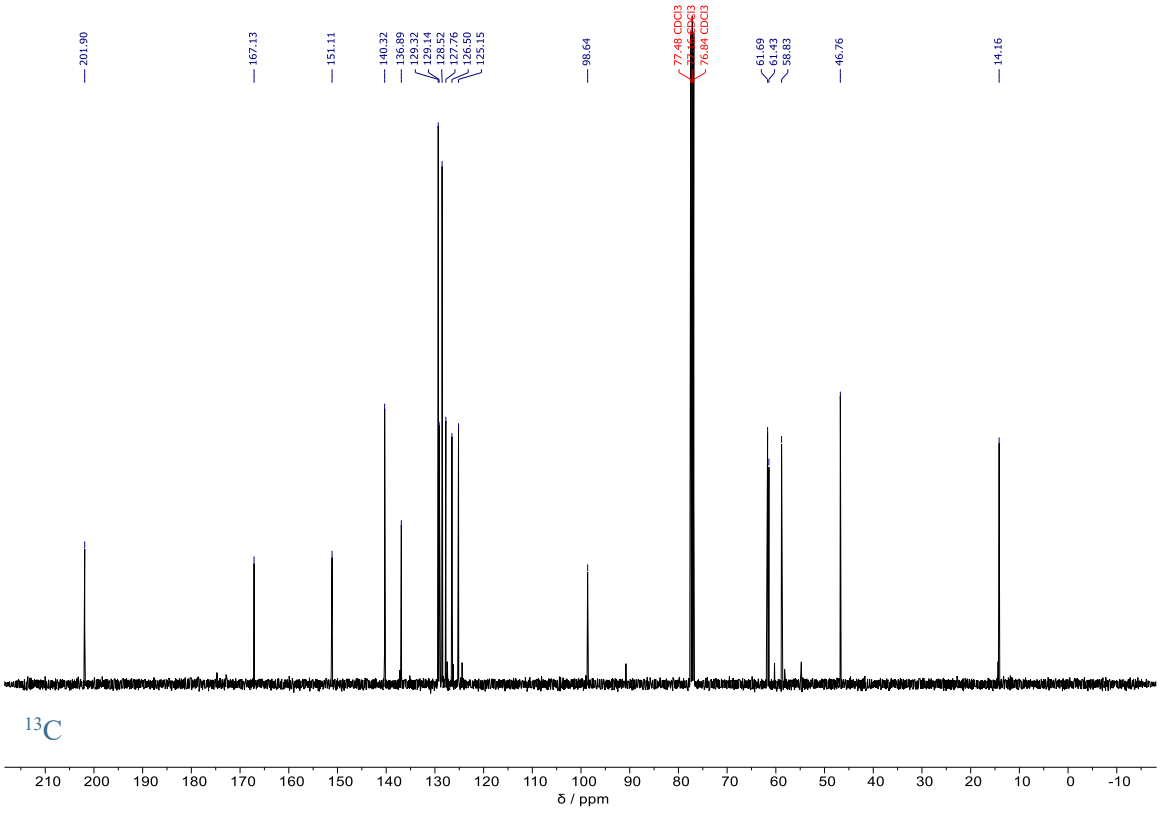
N-Benzyl-2-iodoaniline, **S21**





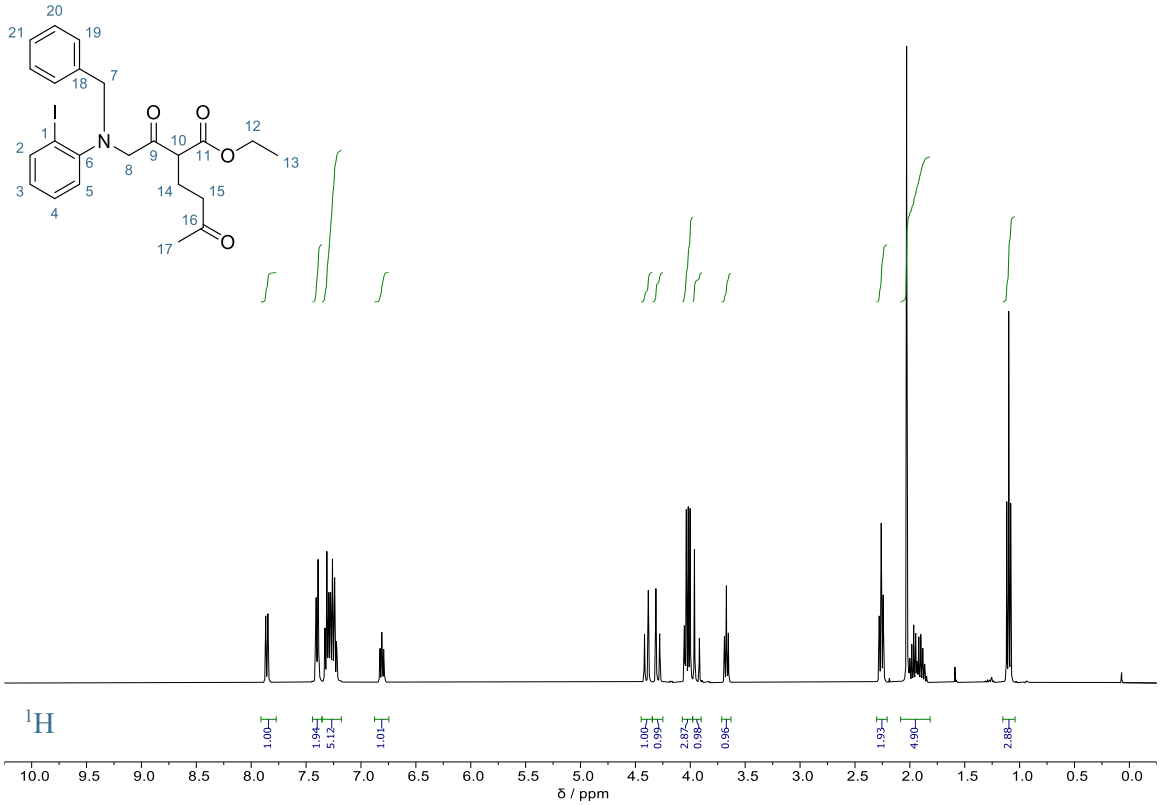
Ethyl 4-(benzyl(2-iodophenyl)amino)-3-oxobutanoate, **S22**

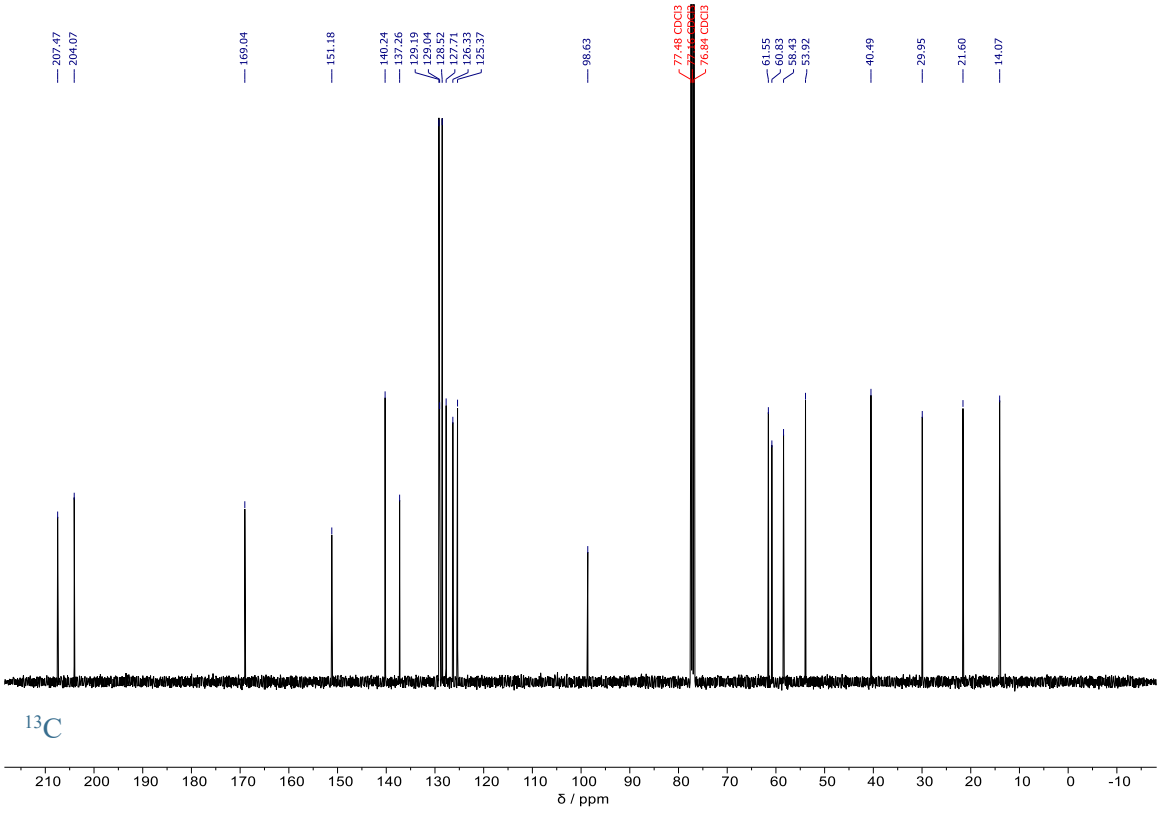




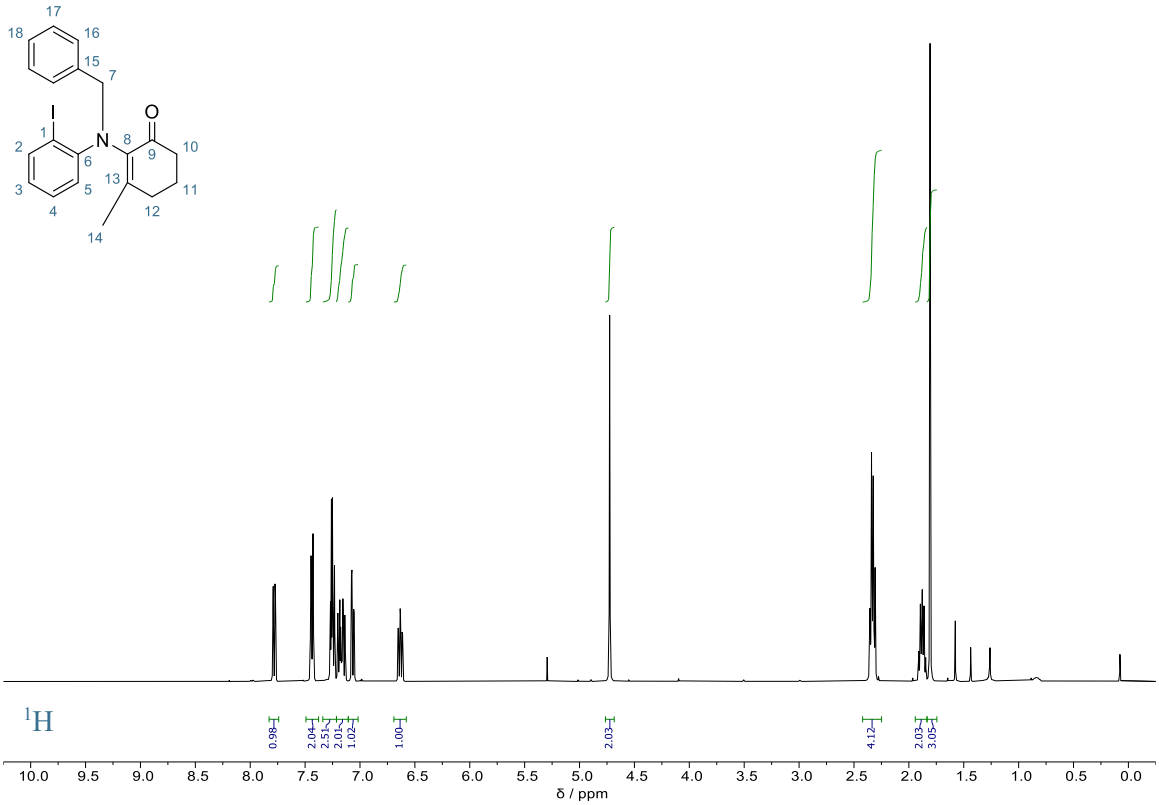
Note: A minor amount of the enol tautomer of this compound is visible on the ^{1}H and ^{13}C NMR spectra above.

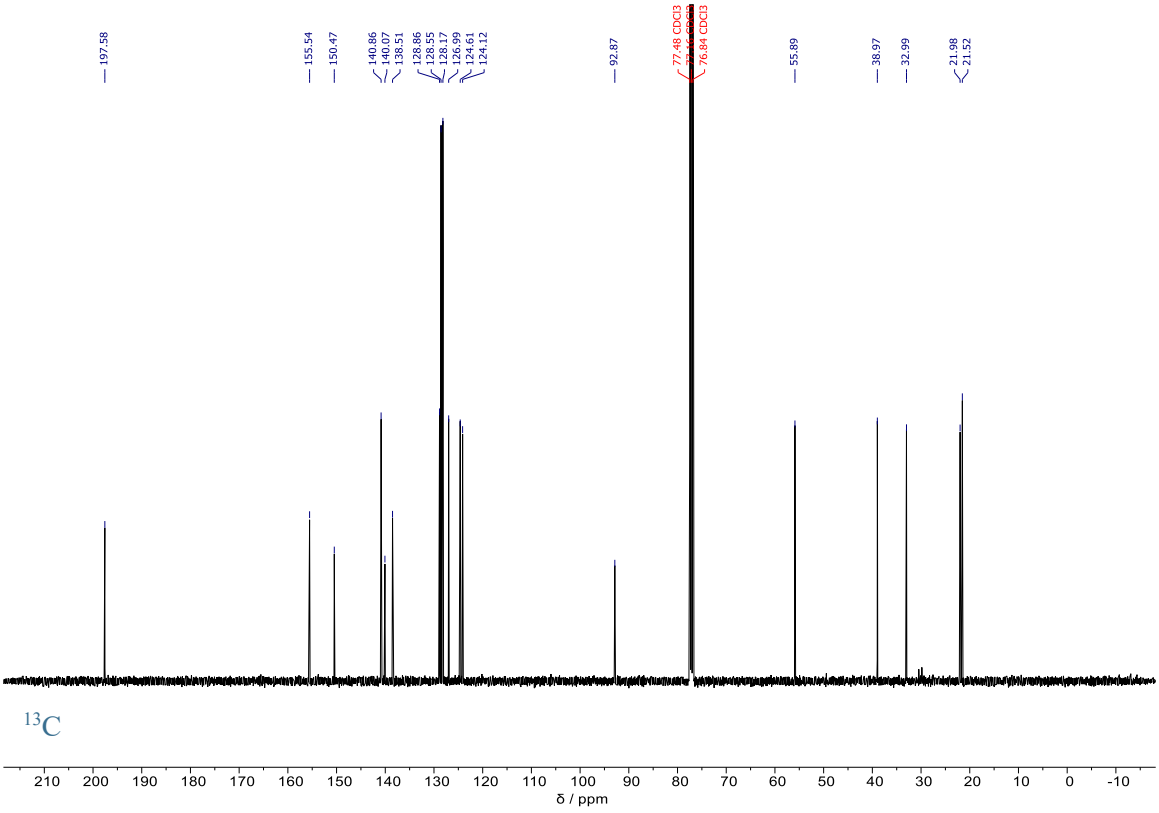
Ethyl 2-(*N*-benzyl-*N*-(2-iodophenyl)glycyl)-5-oxohexanoate, **S23**



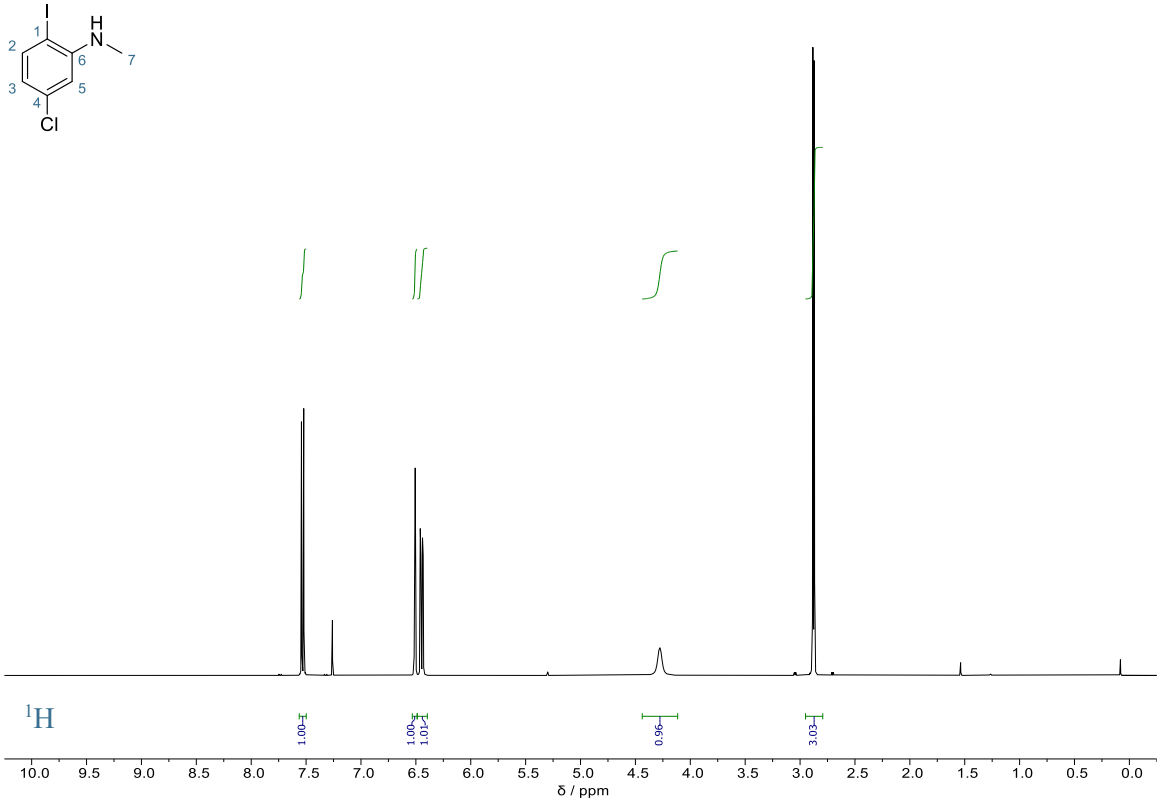


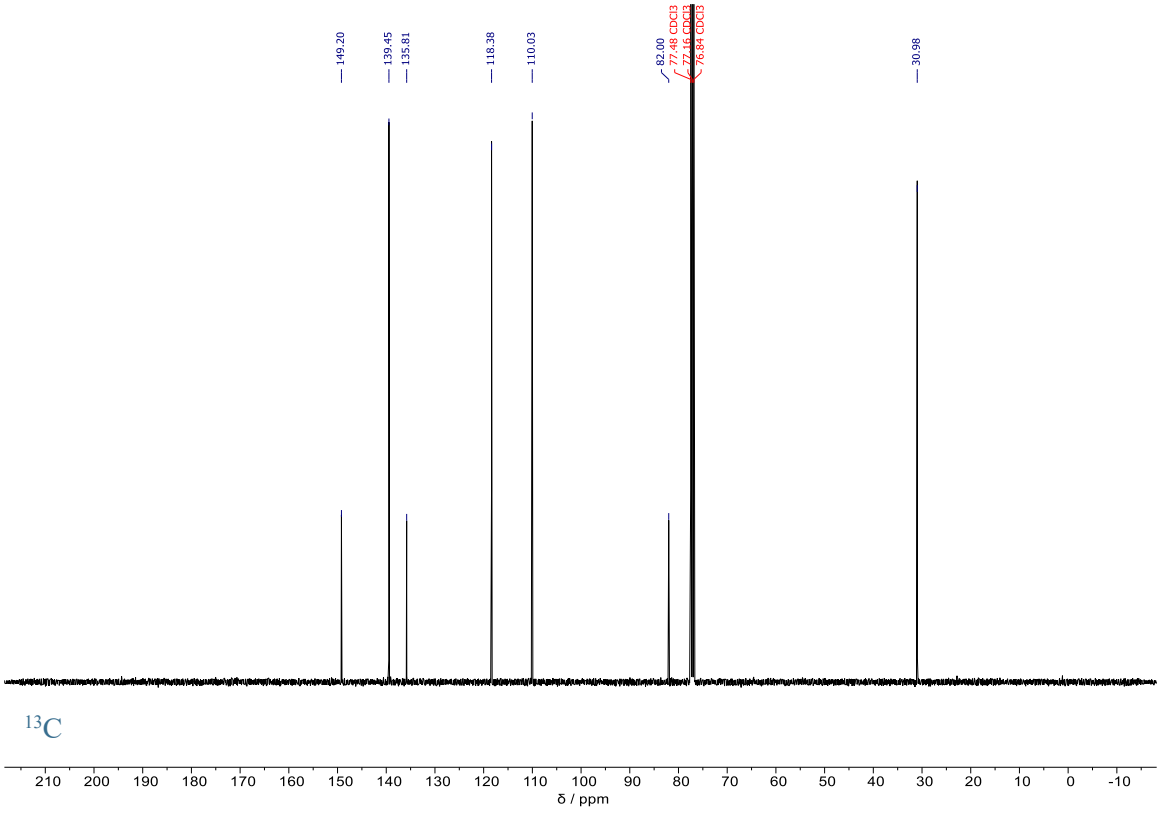
2-(Benzyl(2-iodophenyl)amino)-3-methylcyclohex-2-en-1-one, **S24**



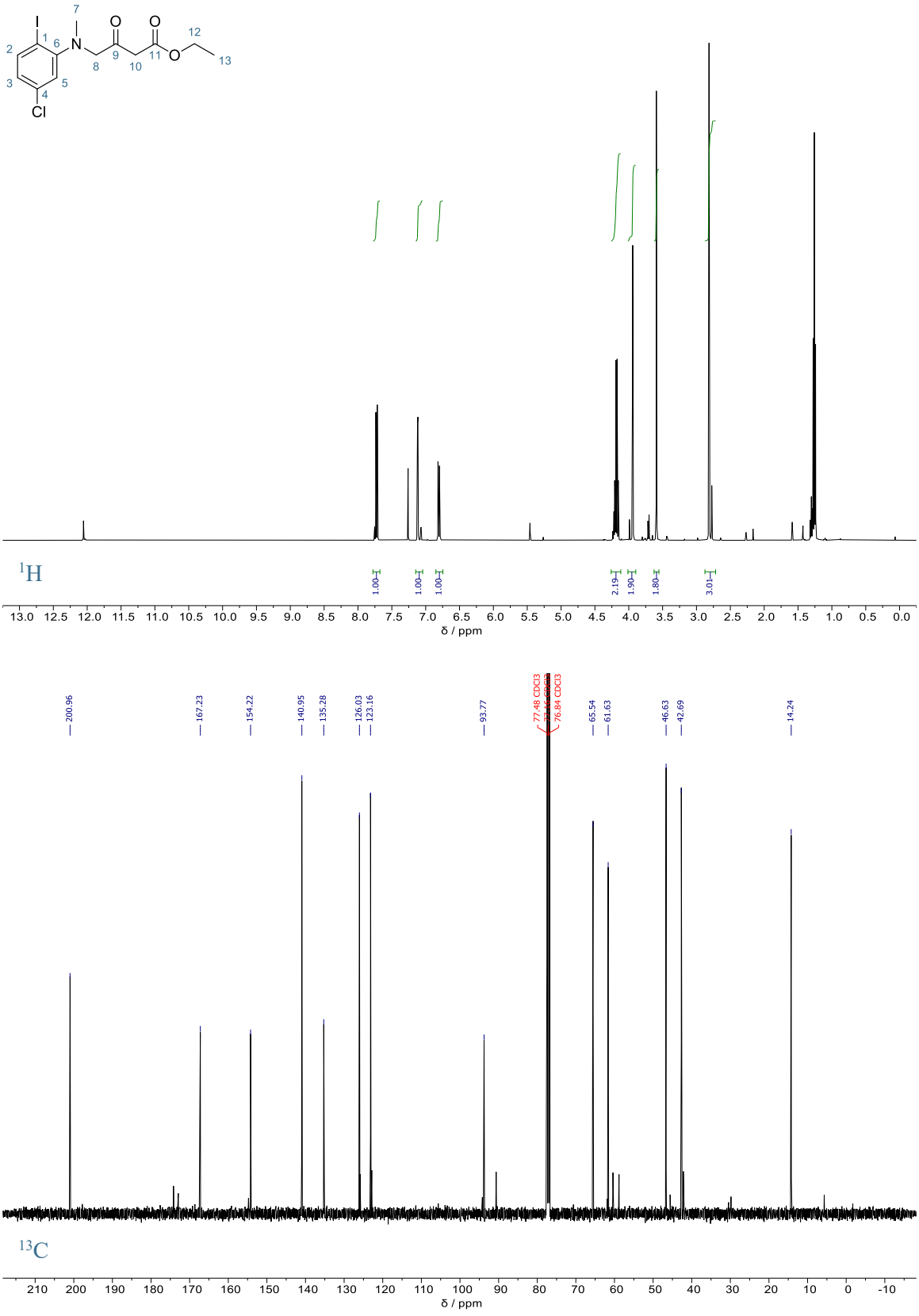


5-Chloro-2-iodo-*N*-methylaniline, **S25**



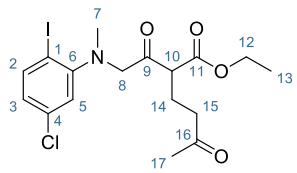


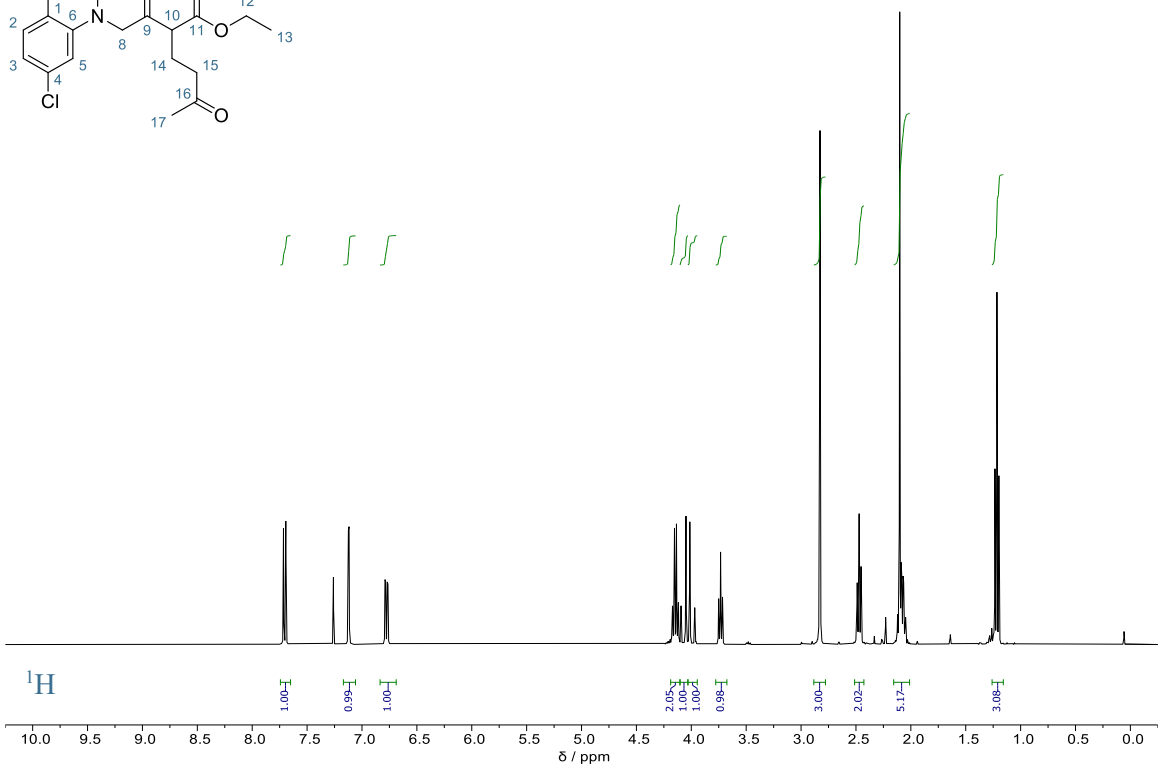
Ethyl 4-((5-chloro-2-iodophenyl)(methyl)amino)-3-oxobutanoate, **S26**

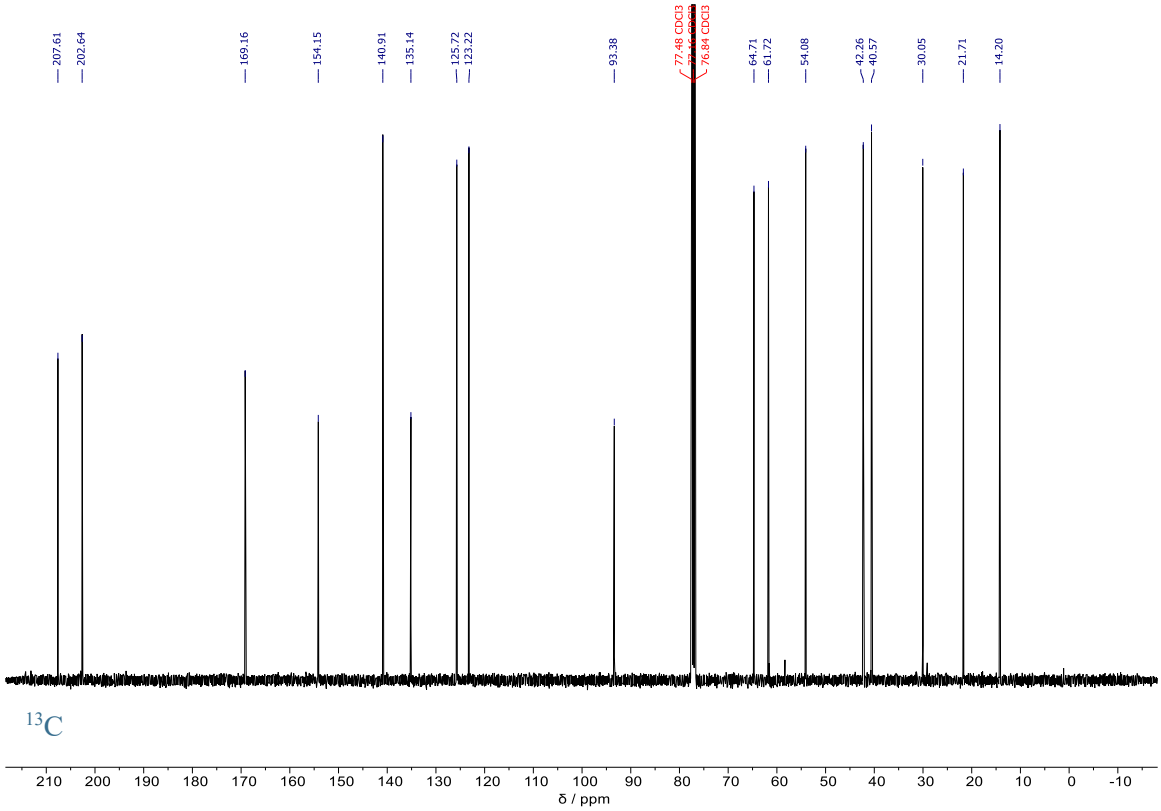


Note: A minor amount of the enol tautomer of this compound is visible on the ^{1}H and ^{13}C NMR spectra above.

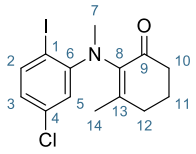
Ethyl 2-(*N*-(5-chloro-2-iodophenyl)-*N*-methylglycyl)-5-oxohexanoate, **S27**

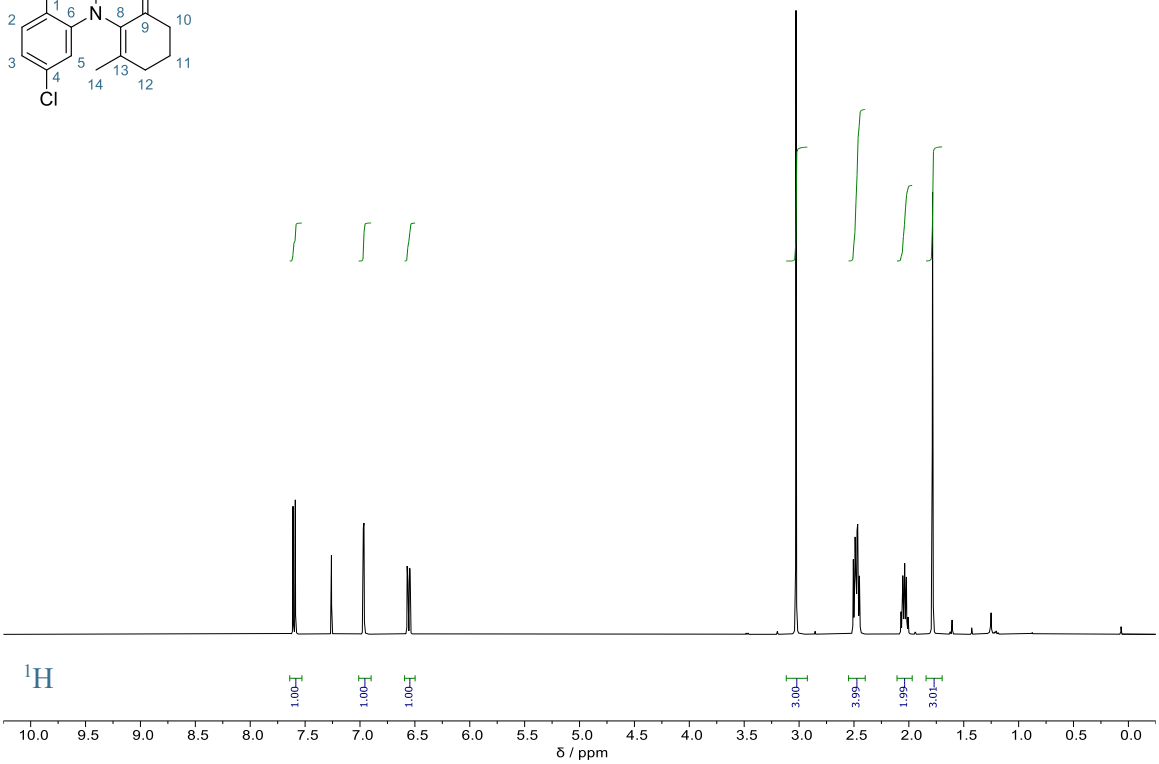


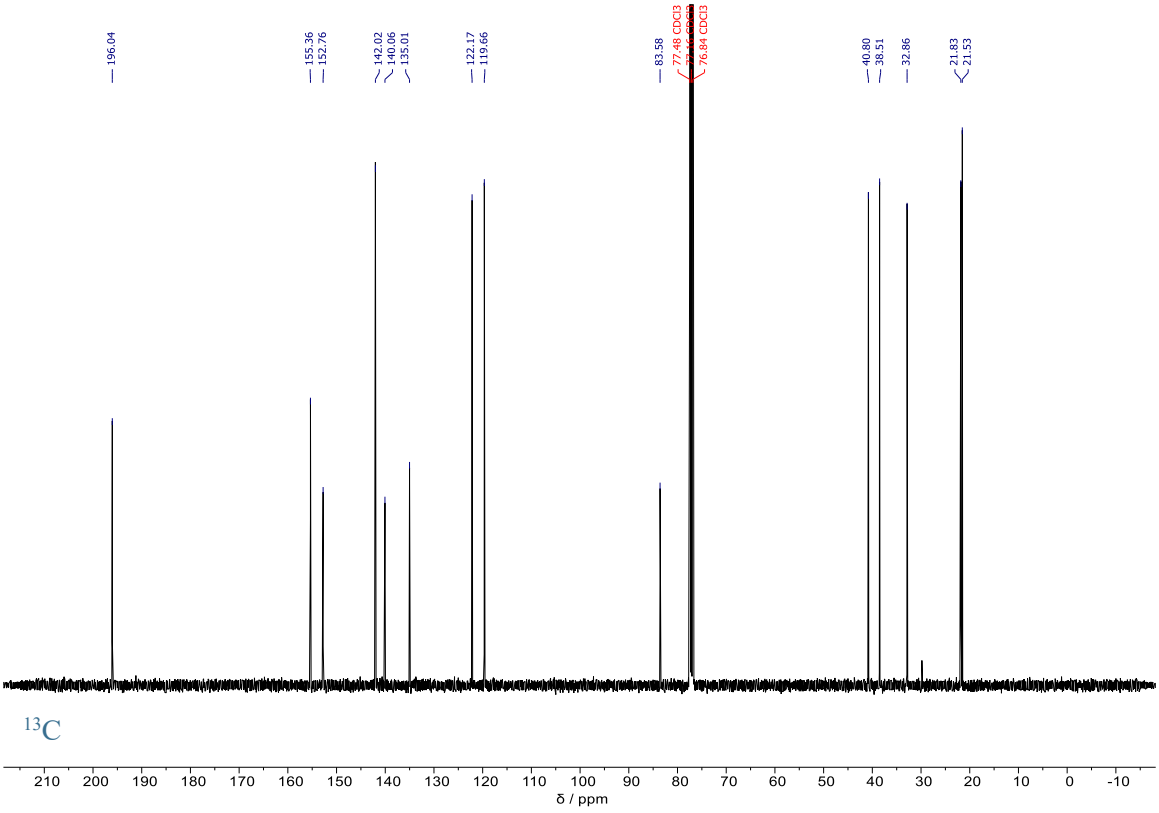




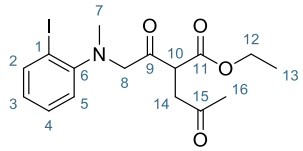
2-((5-Chloro-2-iodophenyl)(methyl)amino)-3-methylcyclohex-2-en-1-one, **S28**

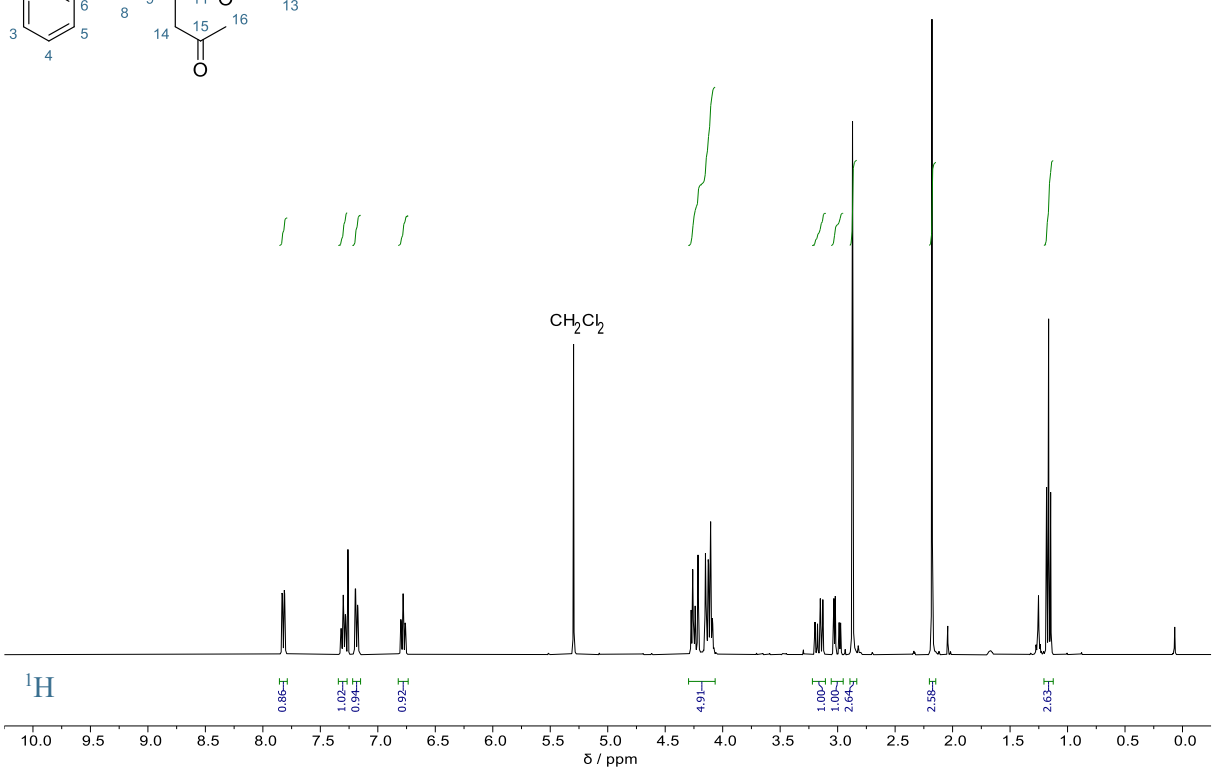


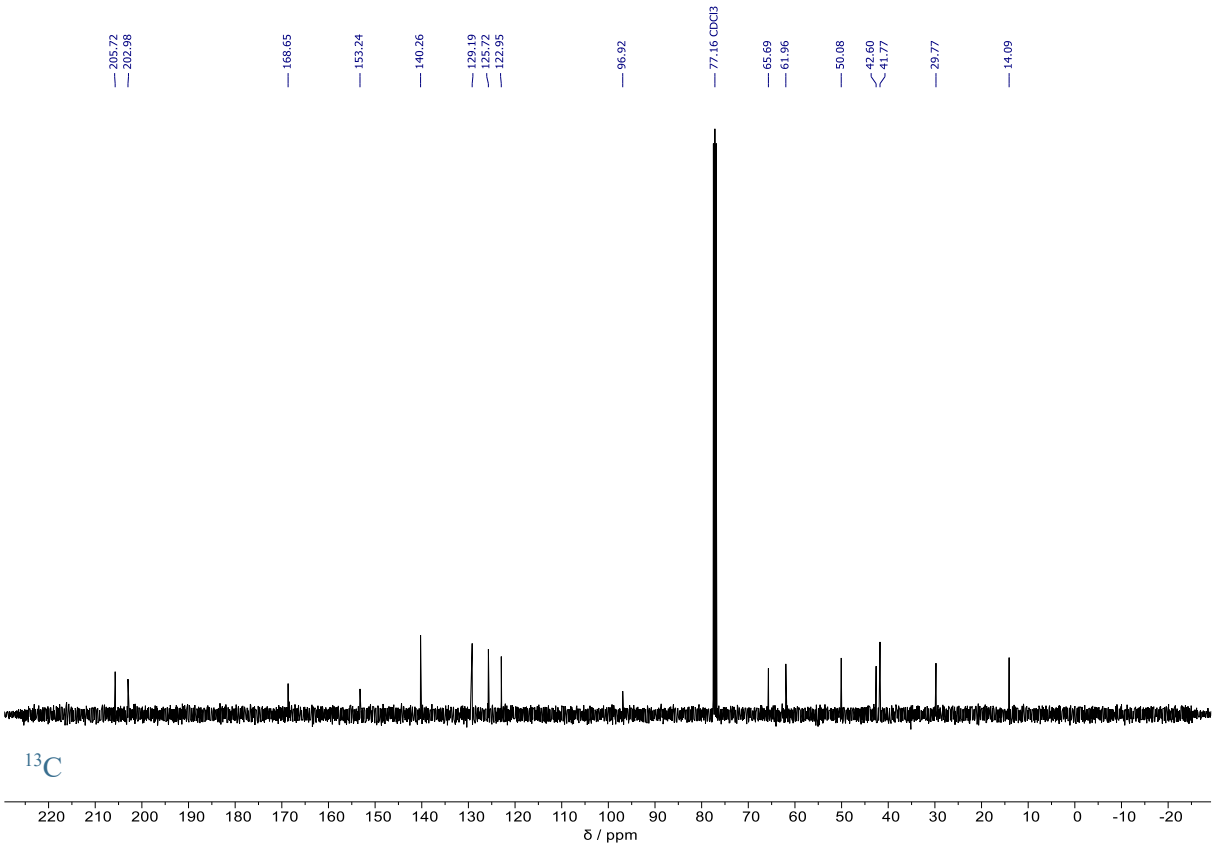




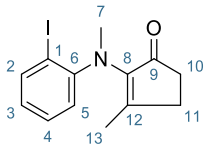
Ethyl 2-(*N*-(2-iodophenyl)-*N*-methylglycyl)-4-oxopentanoate, **S29**

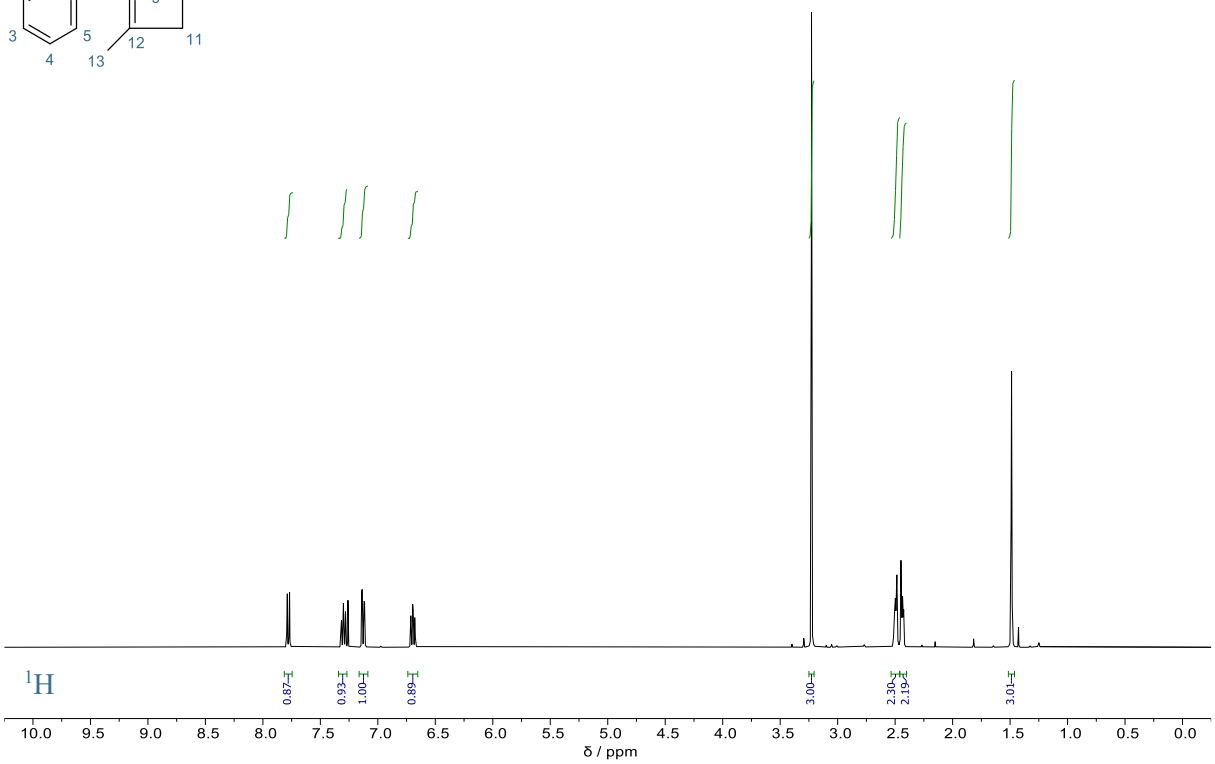


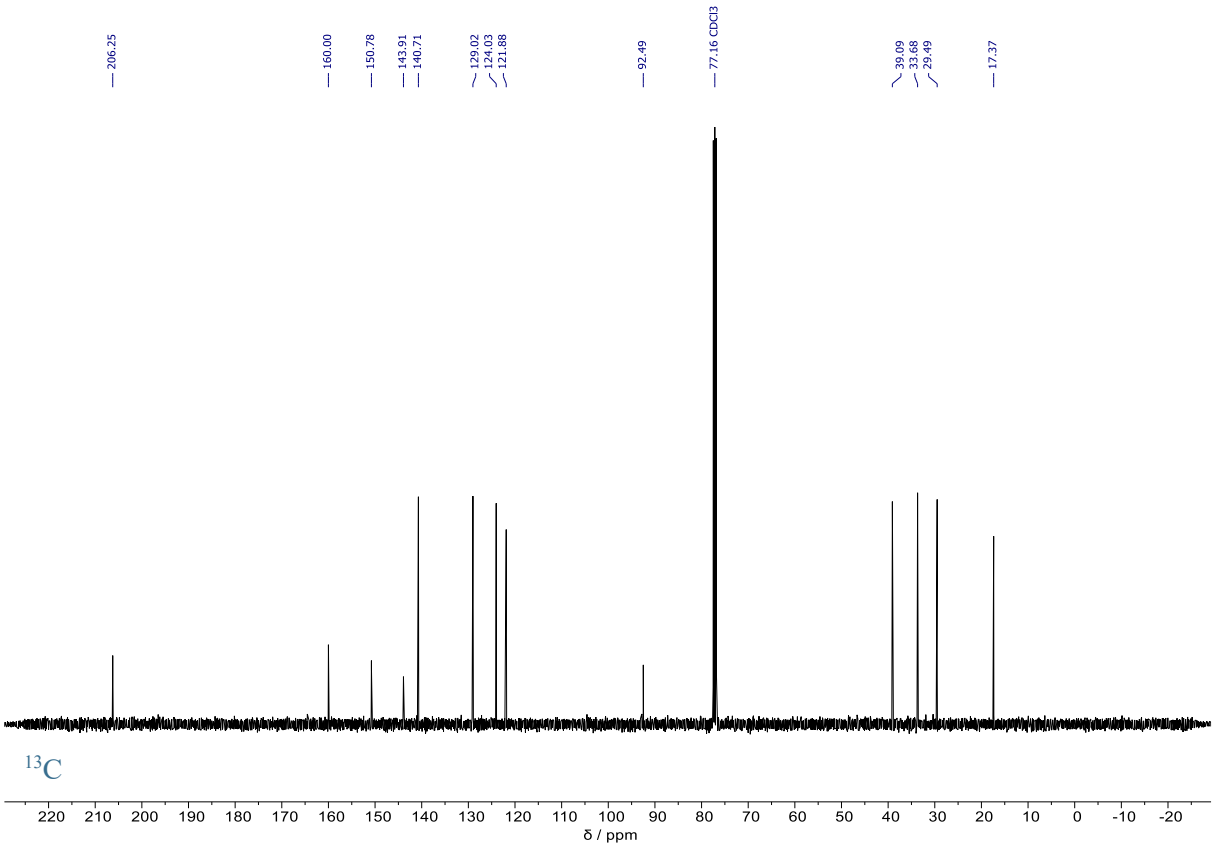




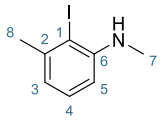
2-((2-Iodophenyl)(methyl)amino)-3-methylcyclopent-2-en-1-one, **S30**

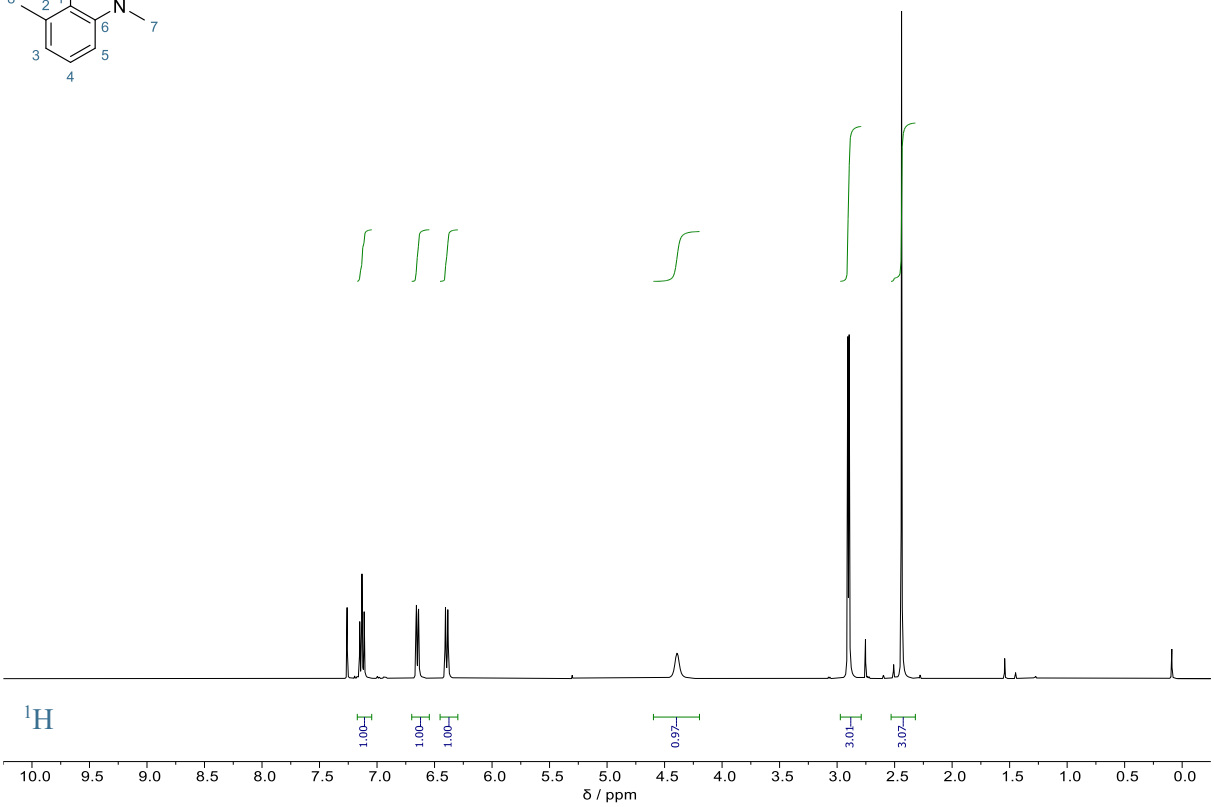




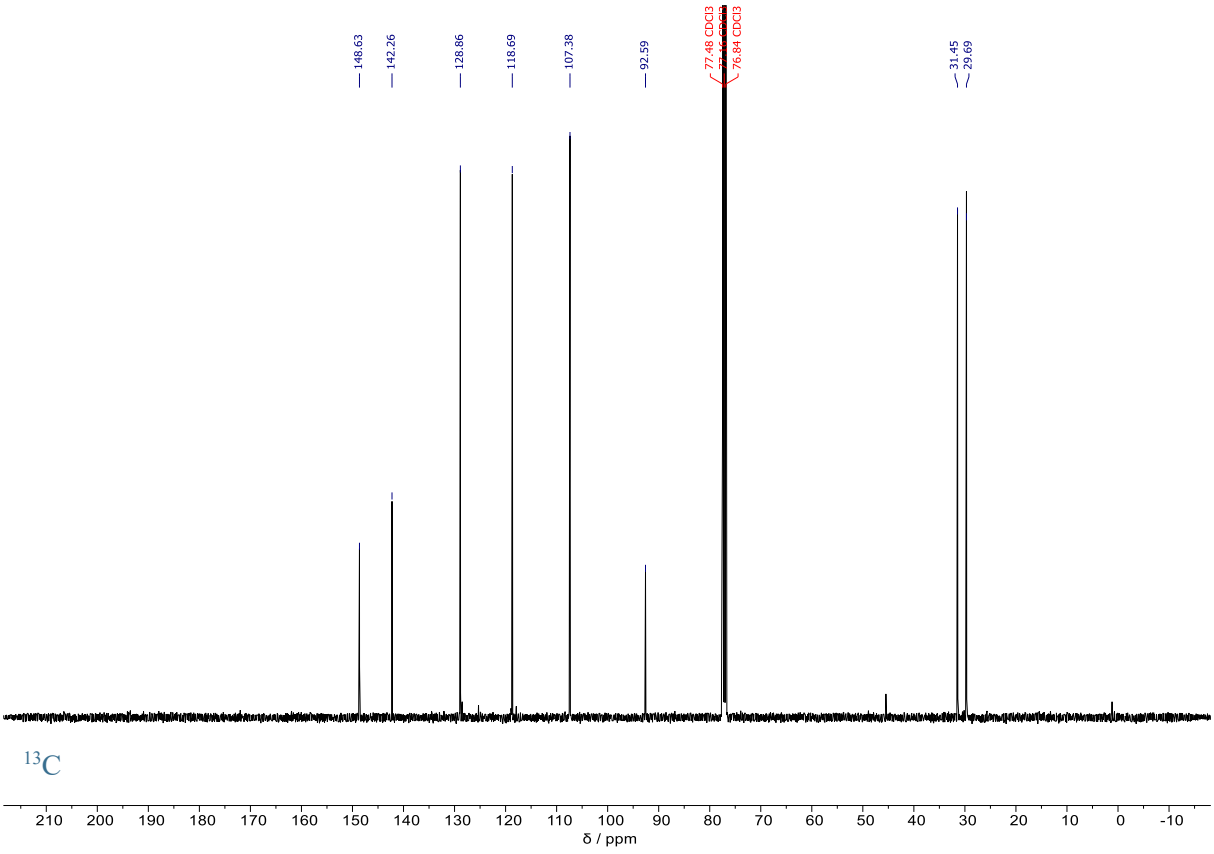


2-Iodo-*N*,3-dimethylaniline, **S31**



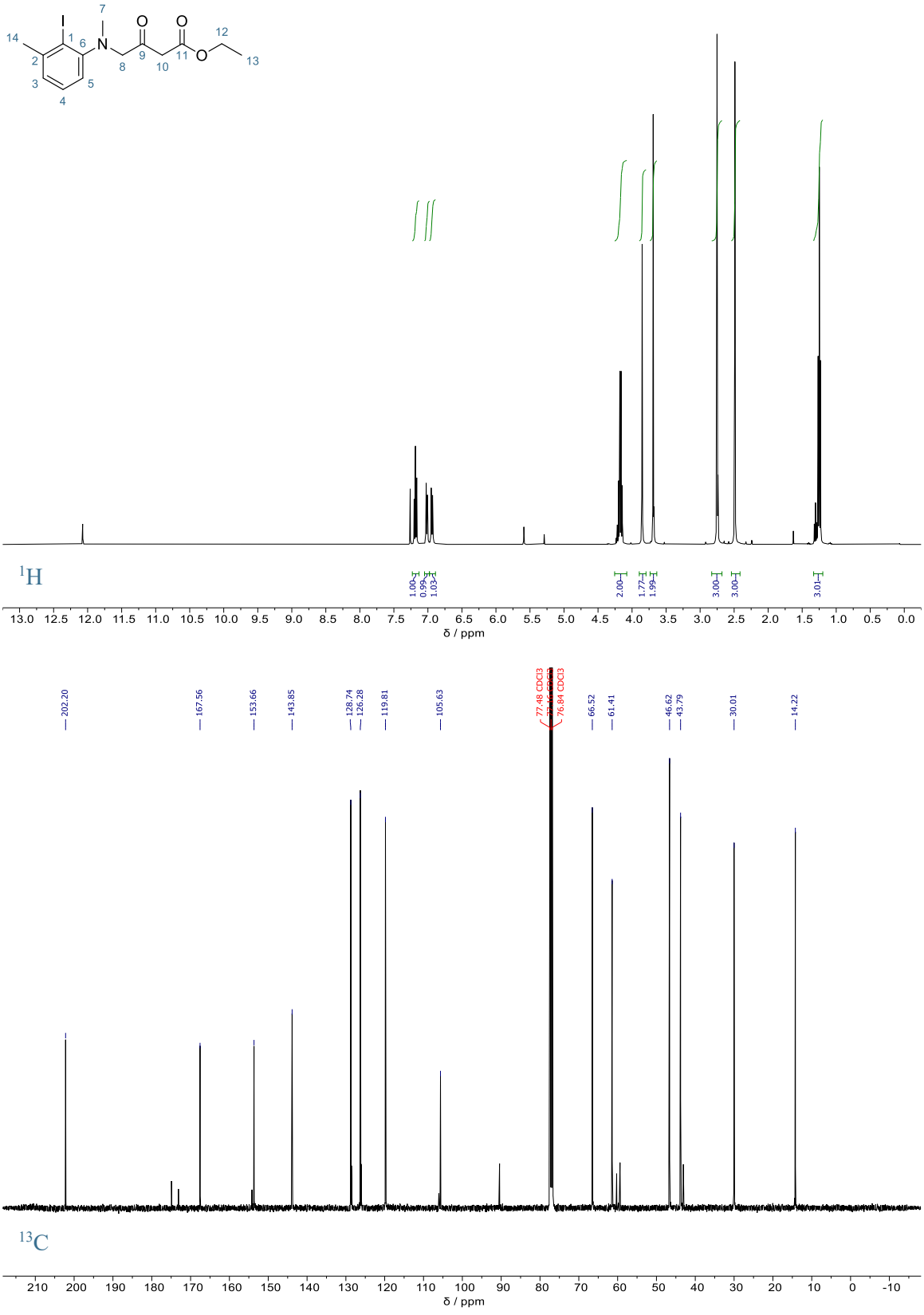


^{1}H



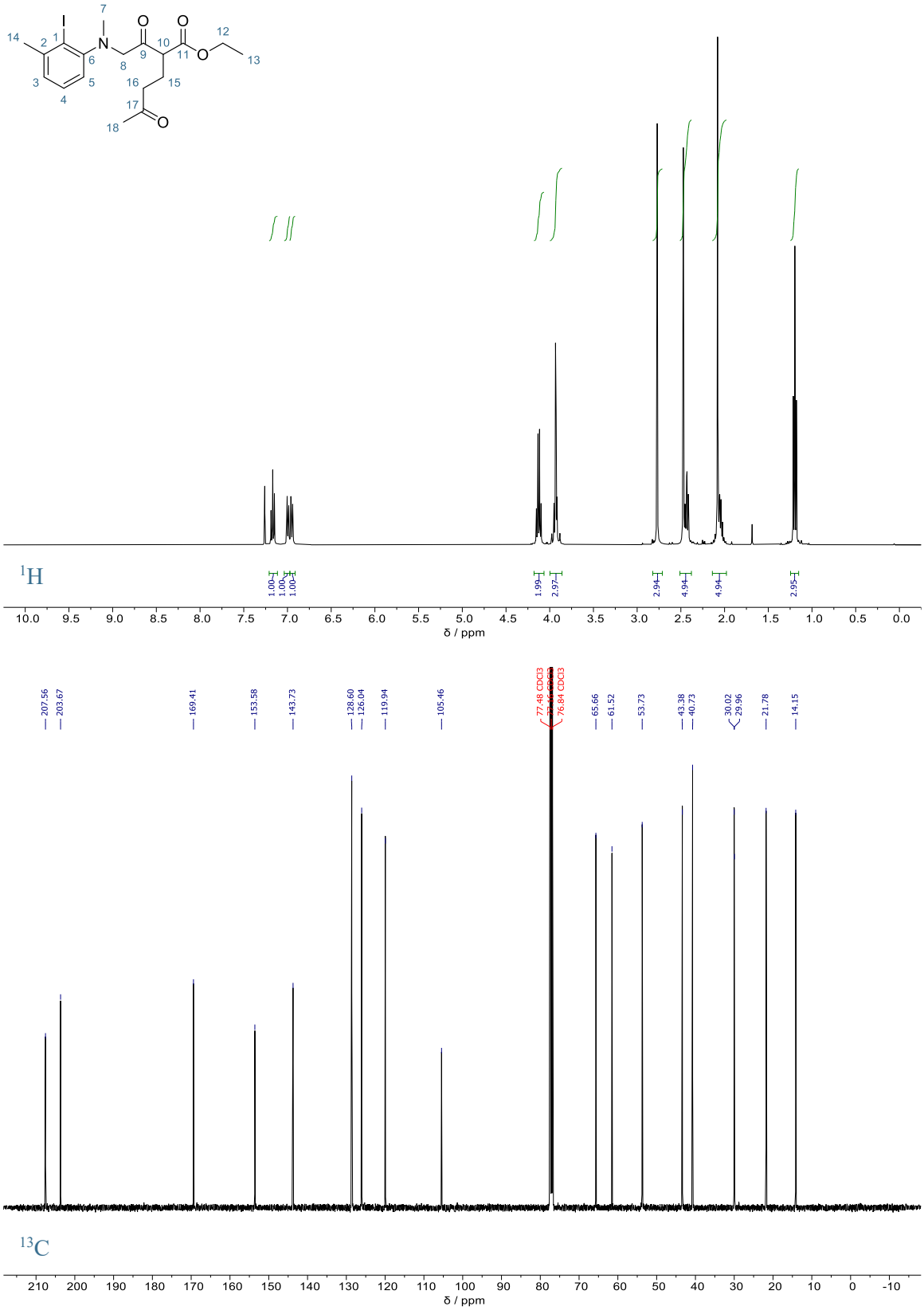
^{13}C

Ethyl 4-((2-iodo-3-methylphenyl)(methyl)amino)-3-oxobutanoate, **S32**

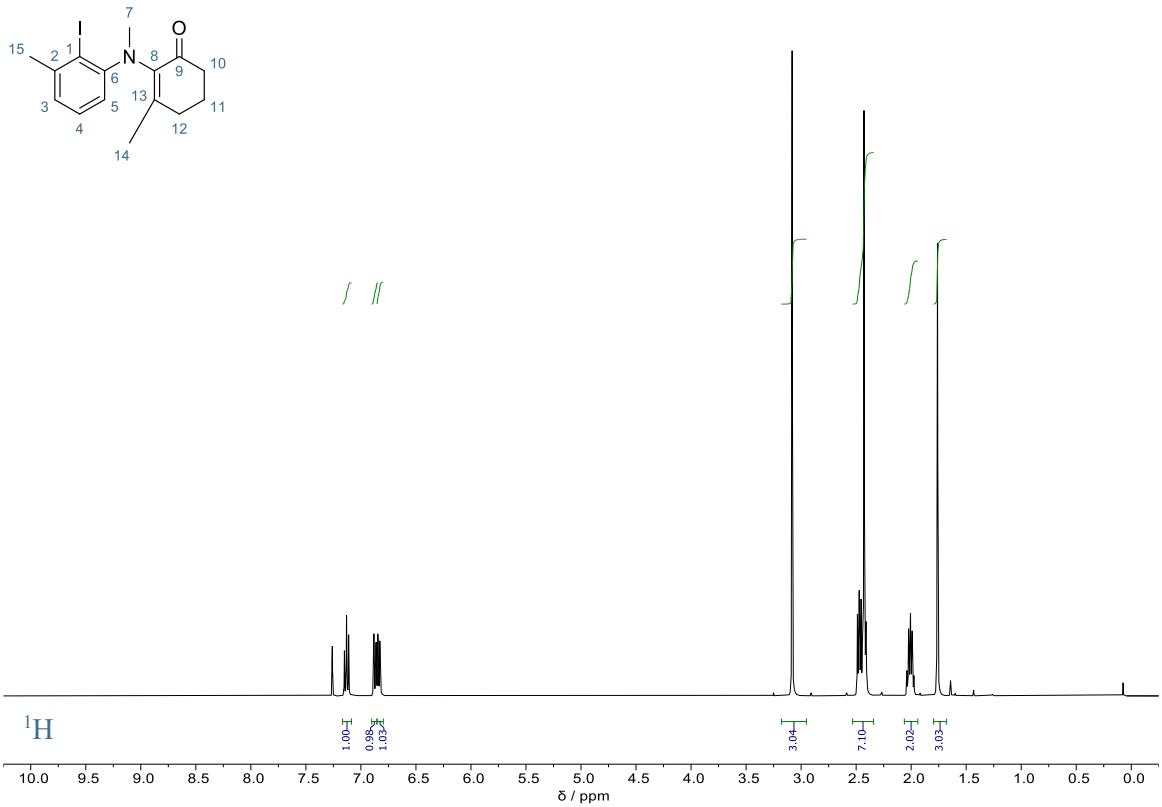


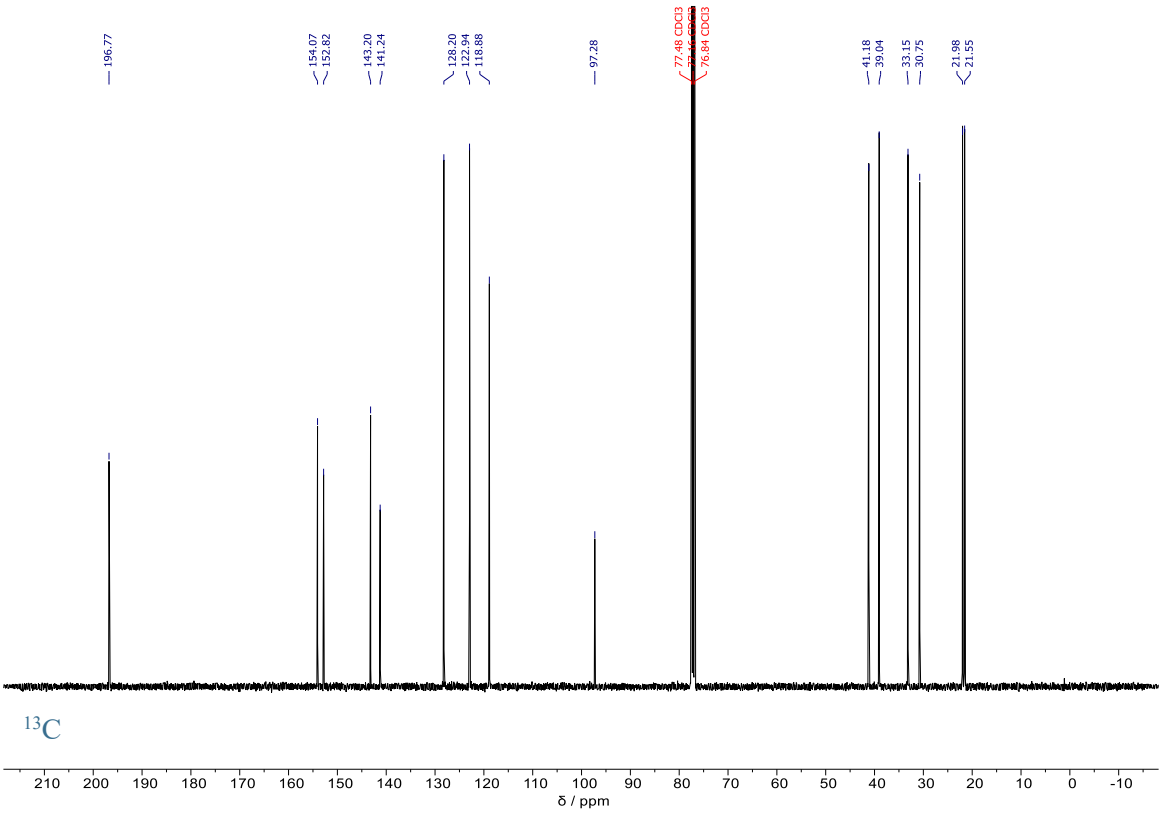
Note: A minor amount of the enol tautomer of this compound is visible on the ^{1}H and ^{13}C NMR spectra above.

Ethyl 2-(*N*-(2-iodo-3-methylphenyl)-*N*-methylglycyl)-5-oxohexanoate, **S33**

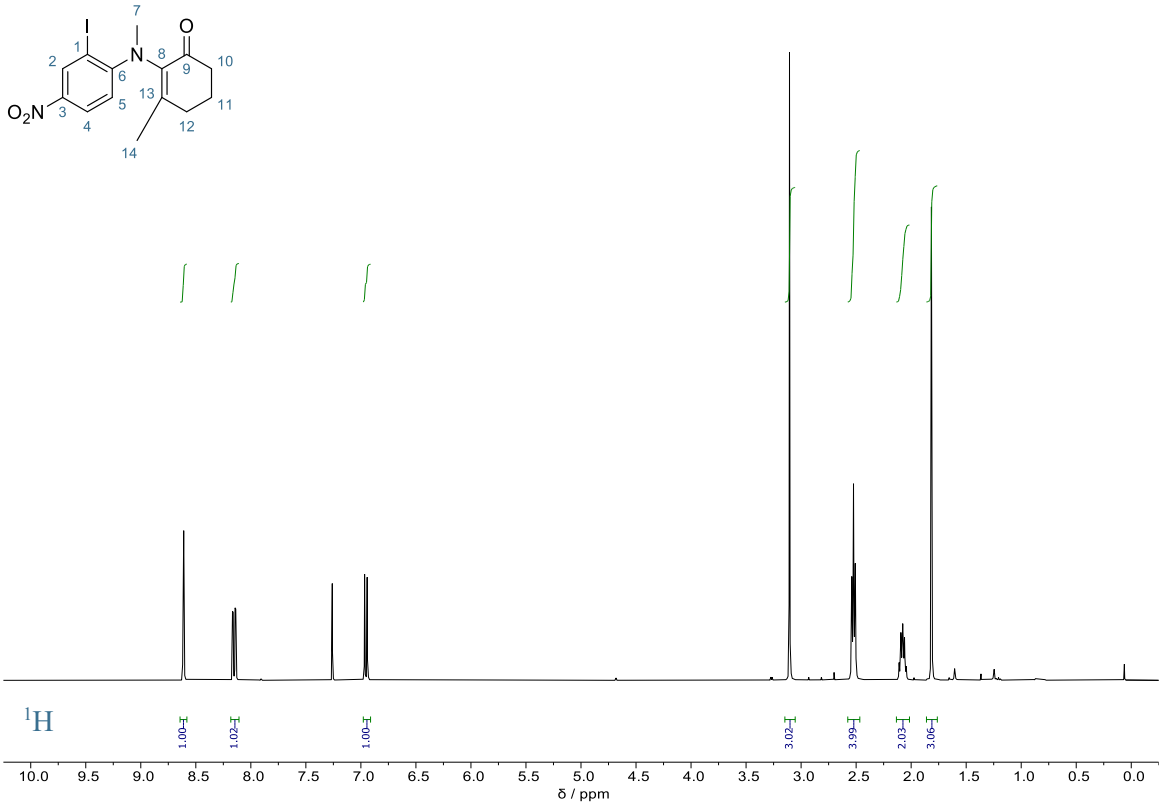


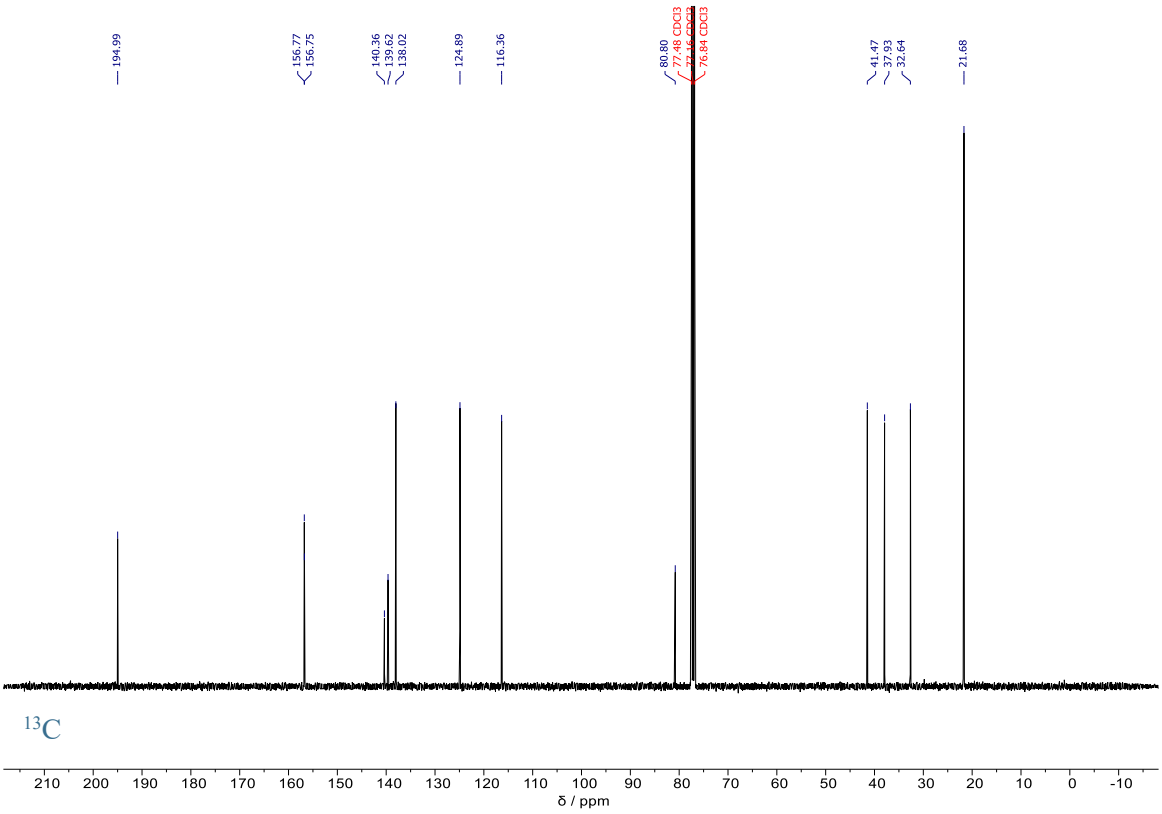
2-((2-Iodo-3-methylphenyl)(methyl)amino)-3-methylcyclohex-2-en-1-one, **S34**



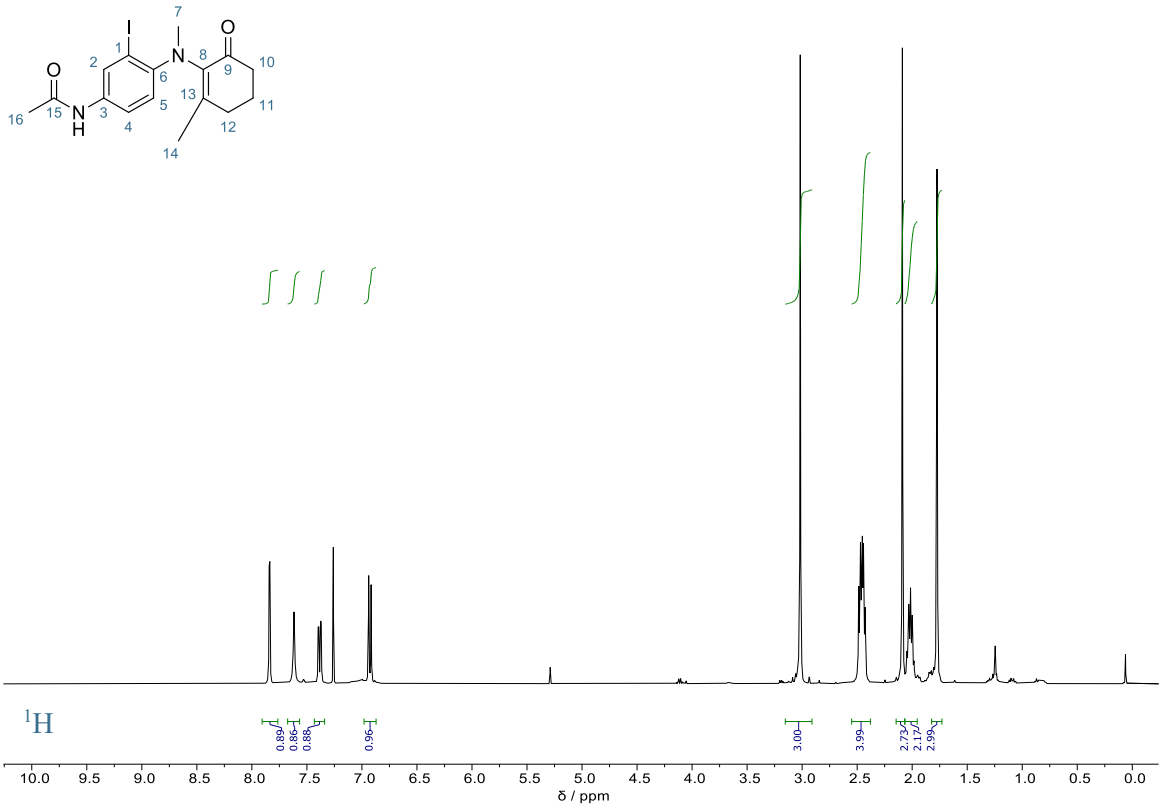


2-((2-Iodo-4-nitrophenyl)(methyl)amino)-3-methylcyclohex-2-en-1-one, **S35**

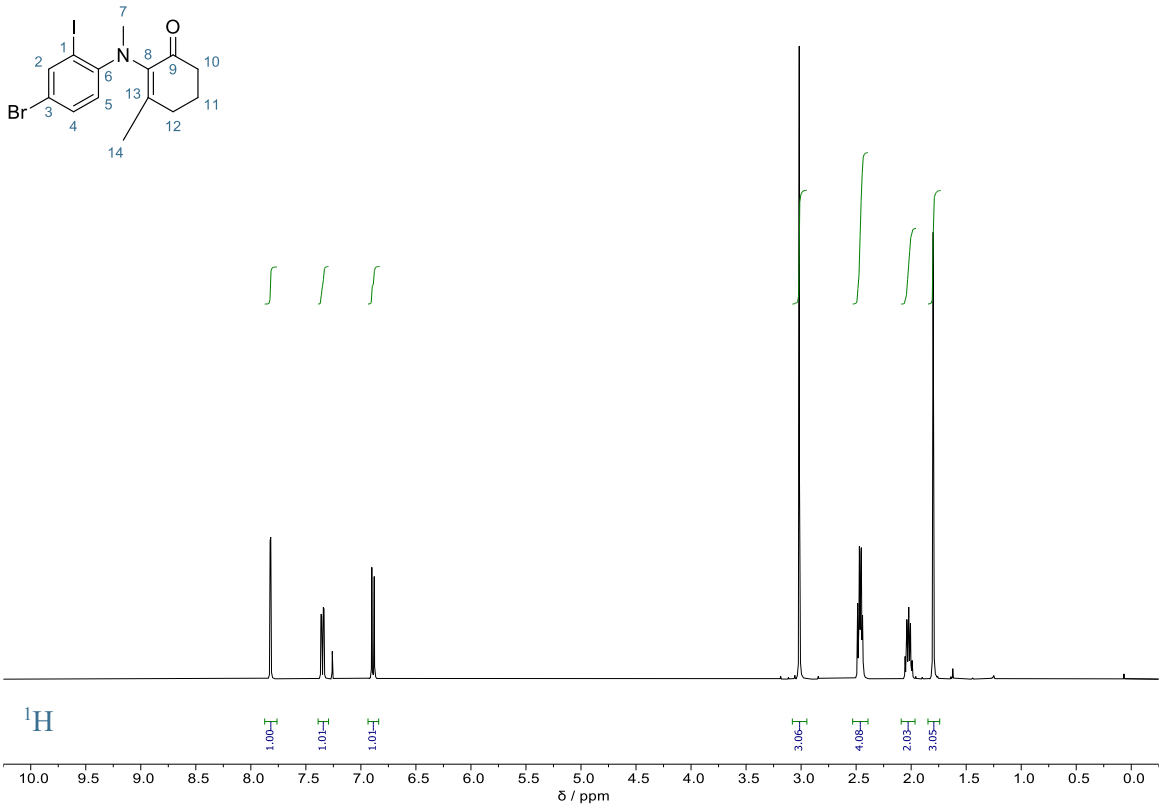


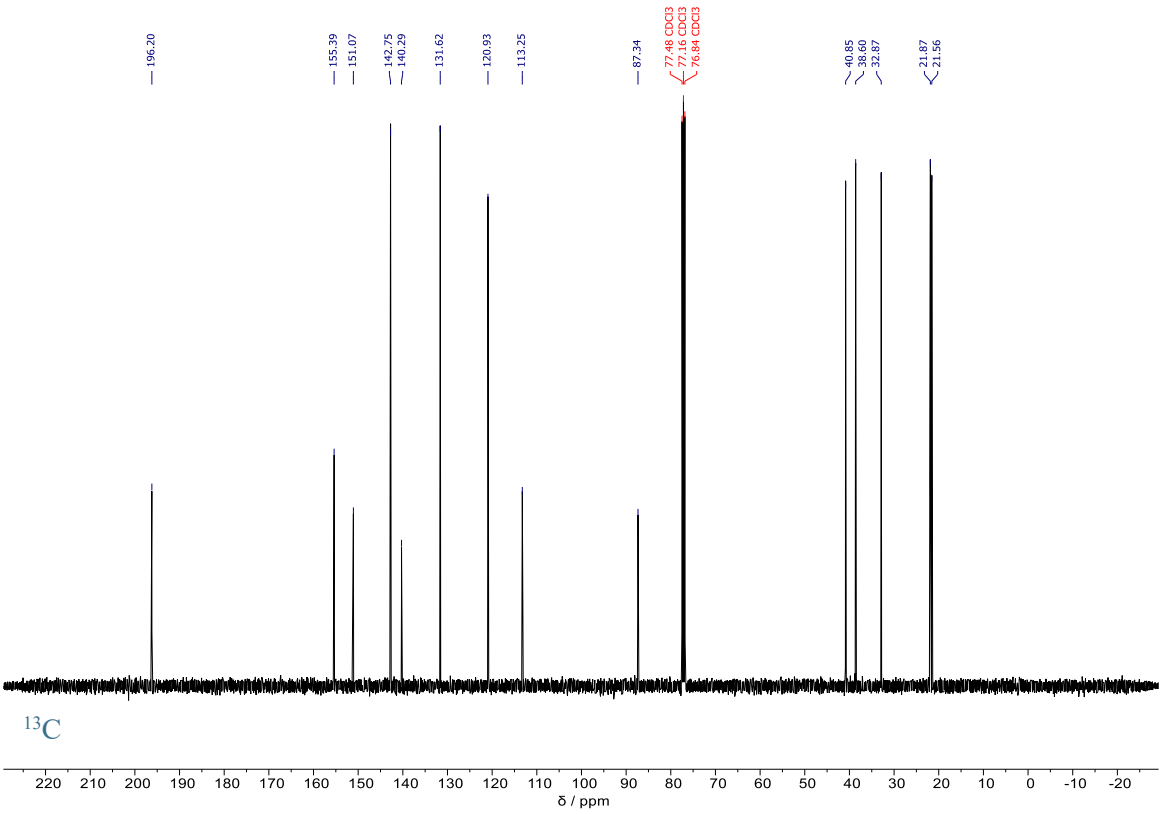


N-(3-Iodo-4-(methyl(2-methyl-6-oxocyclohex-1-en-1-yl)amino)phenyl)acetamide, **S36**

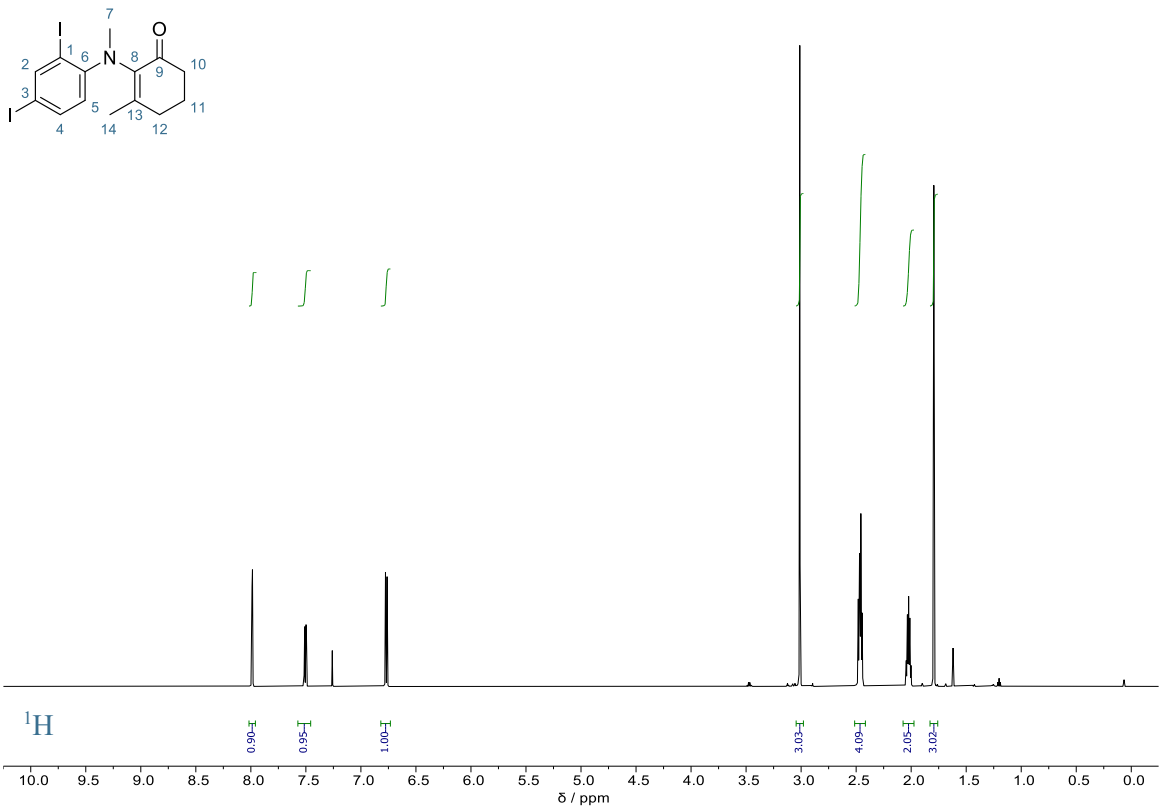


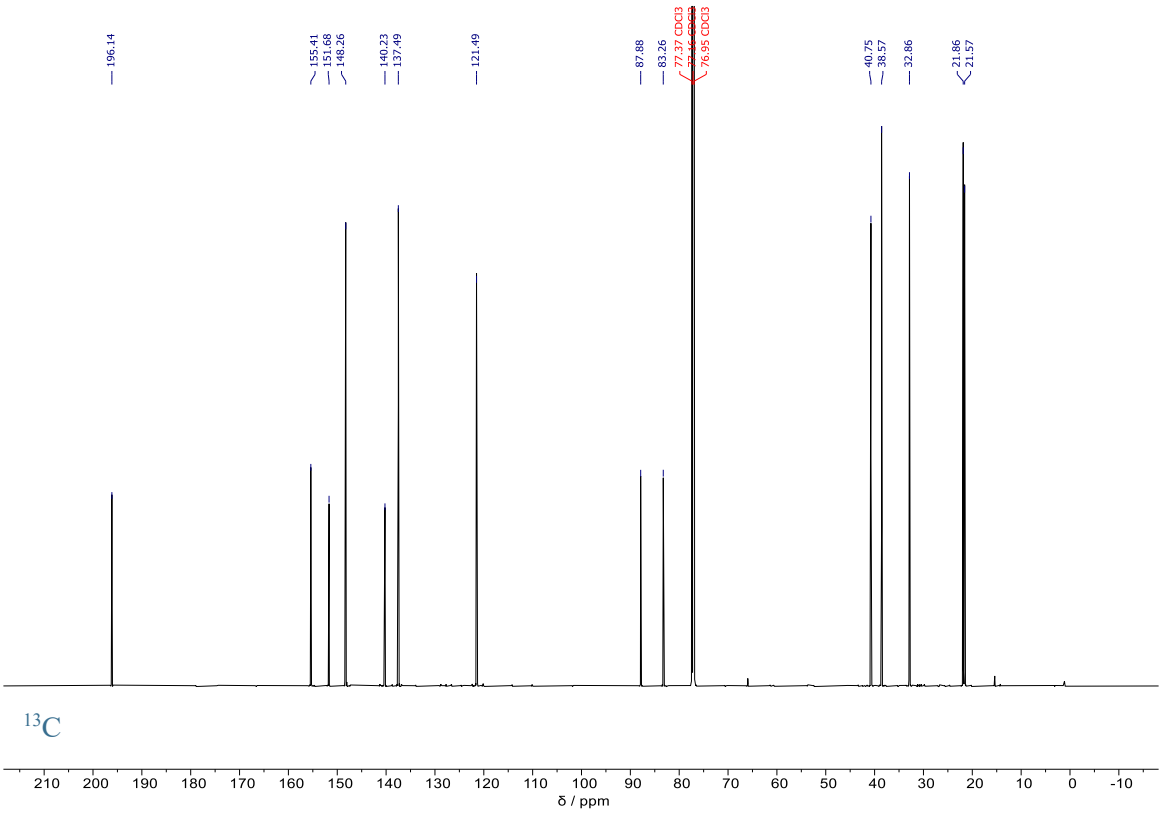
2-((4-Bromo-2-iodophenyl)(methyl)amino)-3-methylcyclohex-2-en-1-one, **S37**



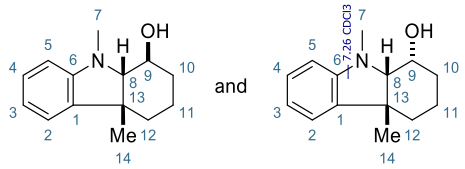


2-((2,4-Diiodophenyl)(methyl)amino)-3-methylcyclohex-2-en-1-one, **S38**

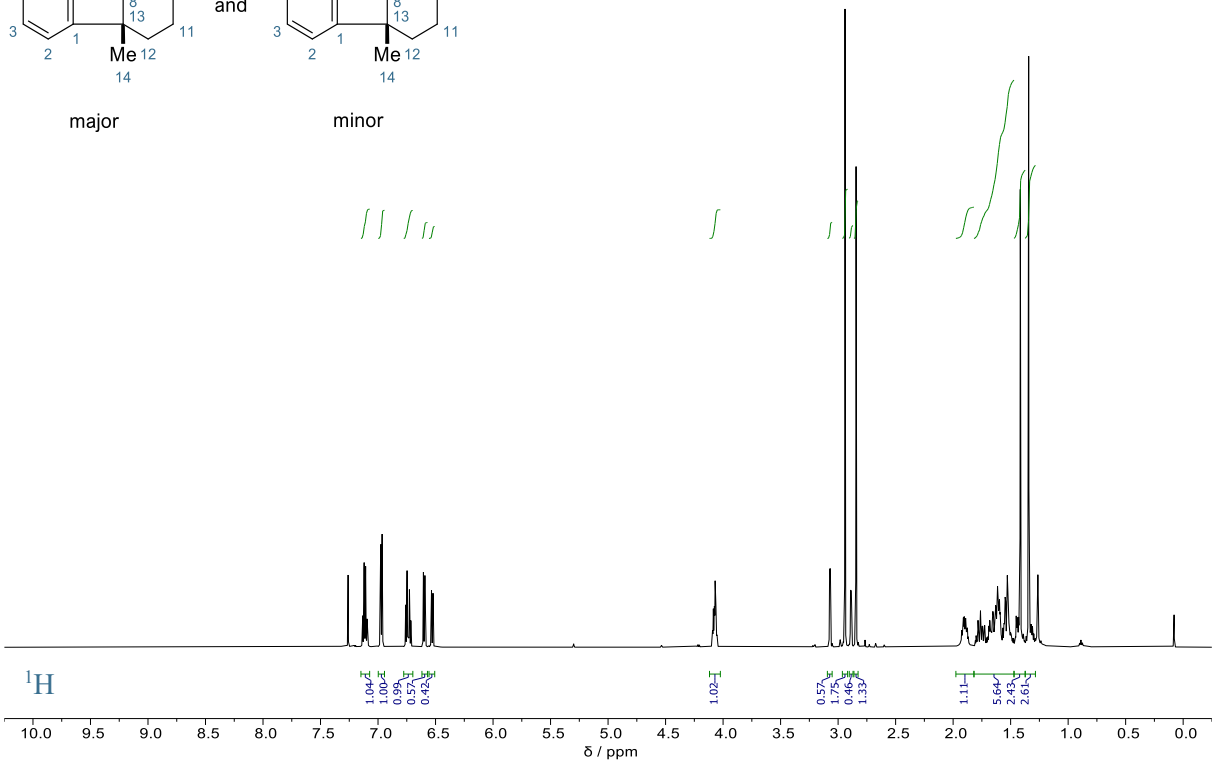


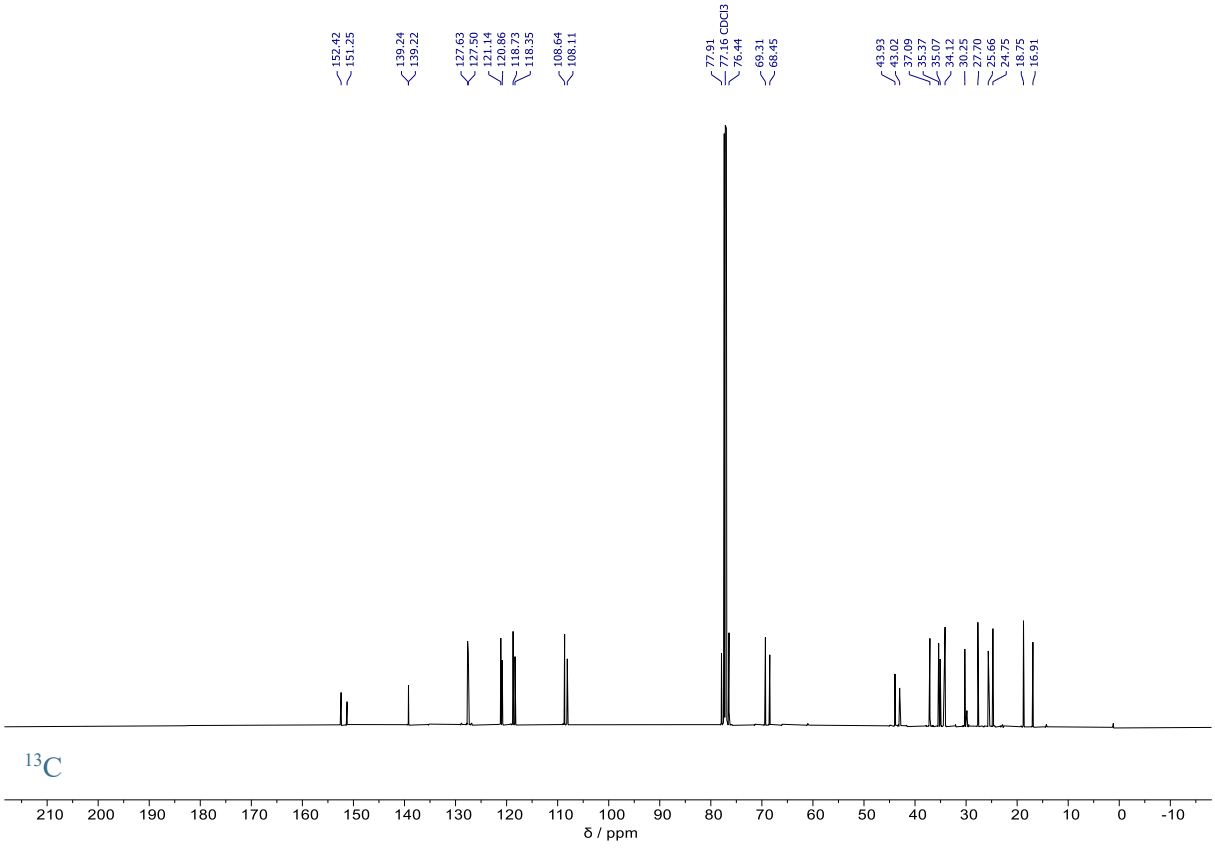


rac-4a,9-Dimethyl-2,3,4,4a,9,9a-hexahydro-1*H*-carbazol-1-ol, **S39**

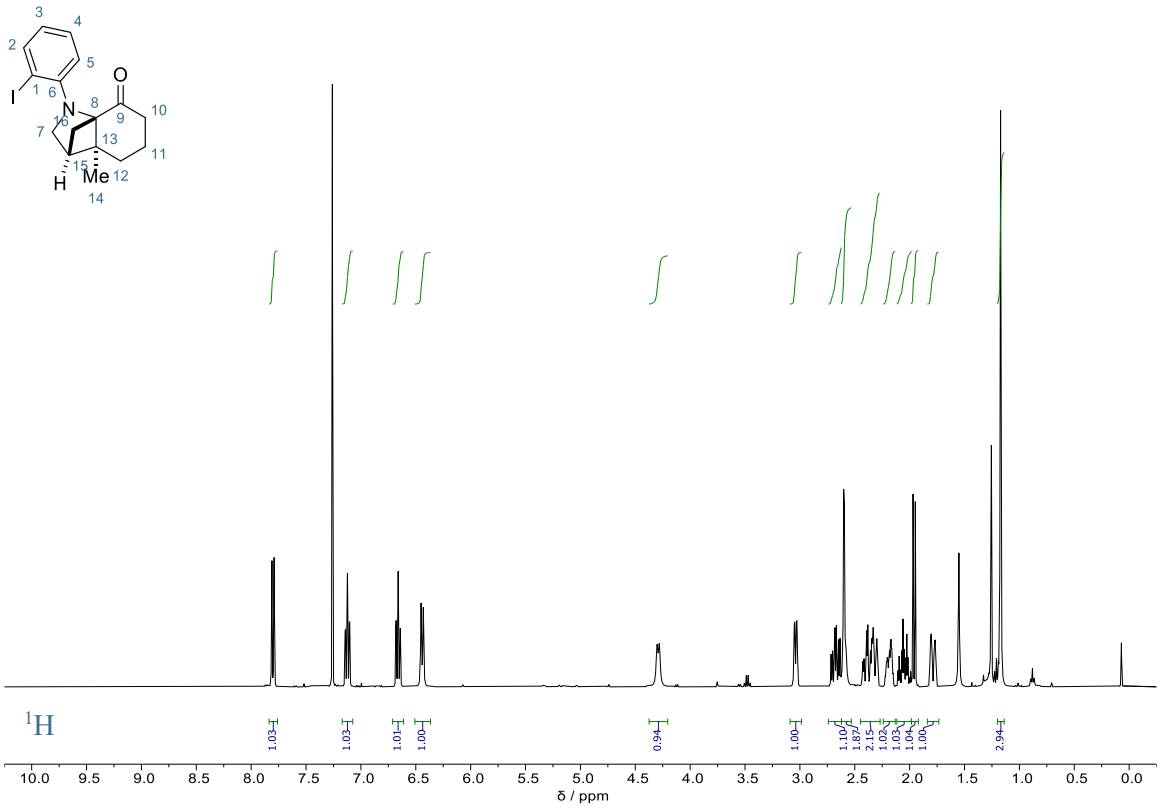


major and minor

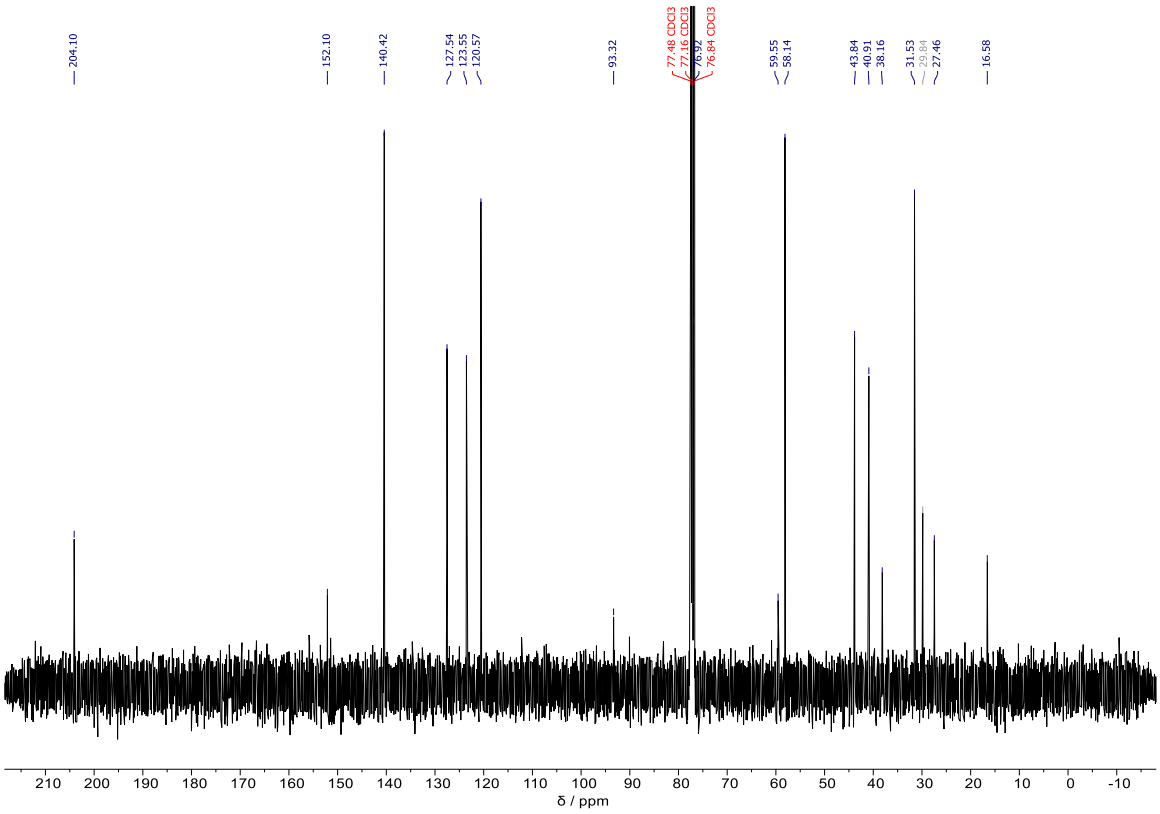




rac-1-(2-Iodophenyl)-3a-methylhexahydro-3,7a-methanoindol-7(1*H*)-one, **S41**

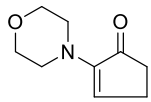


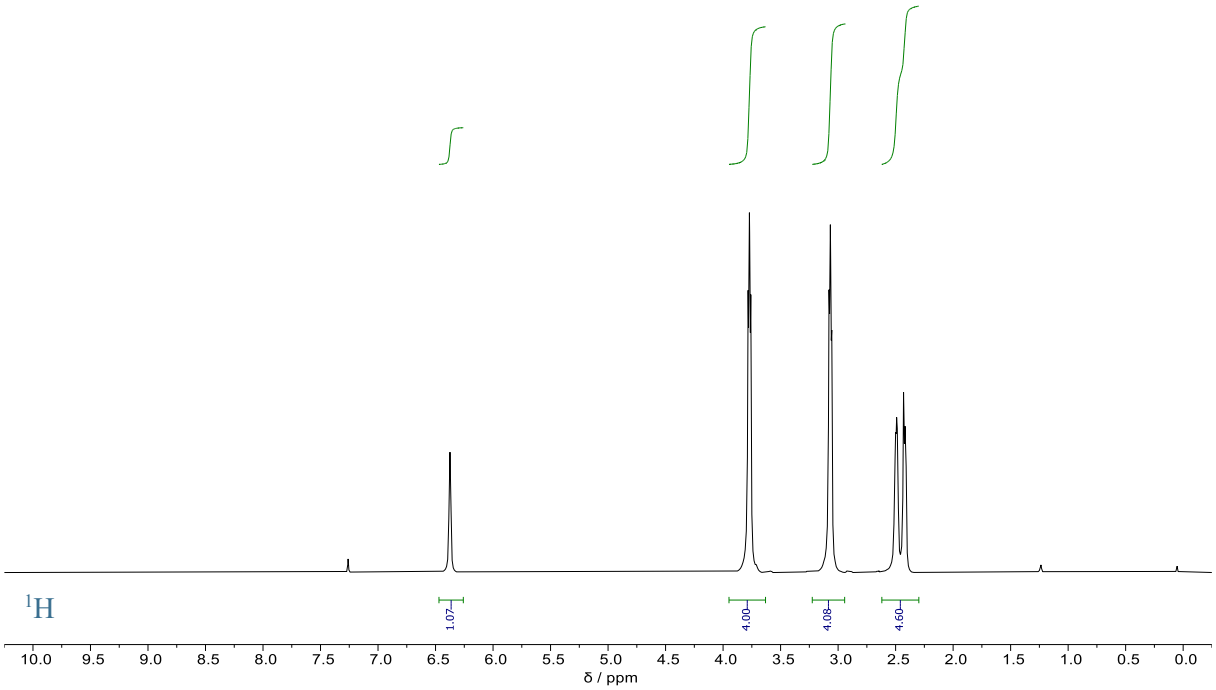
^{1}H

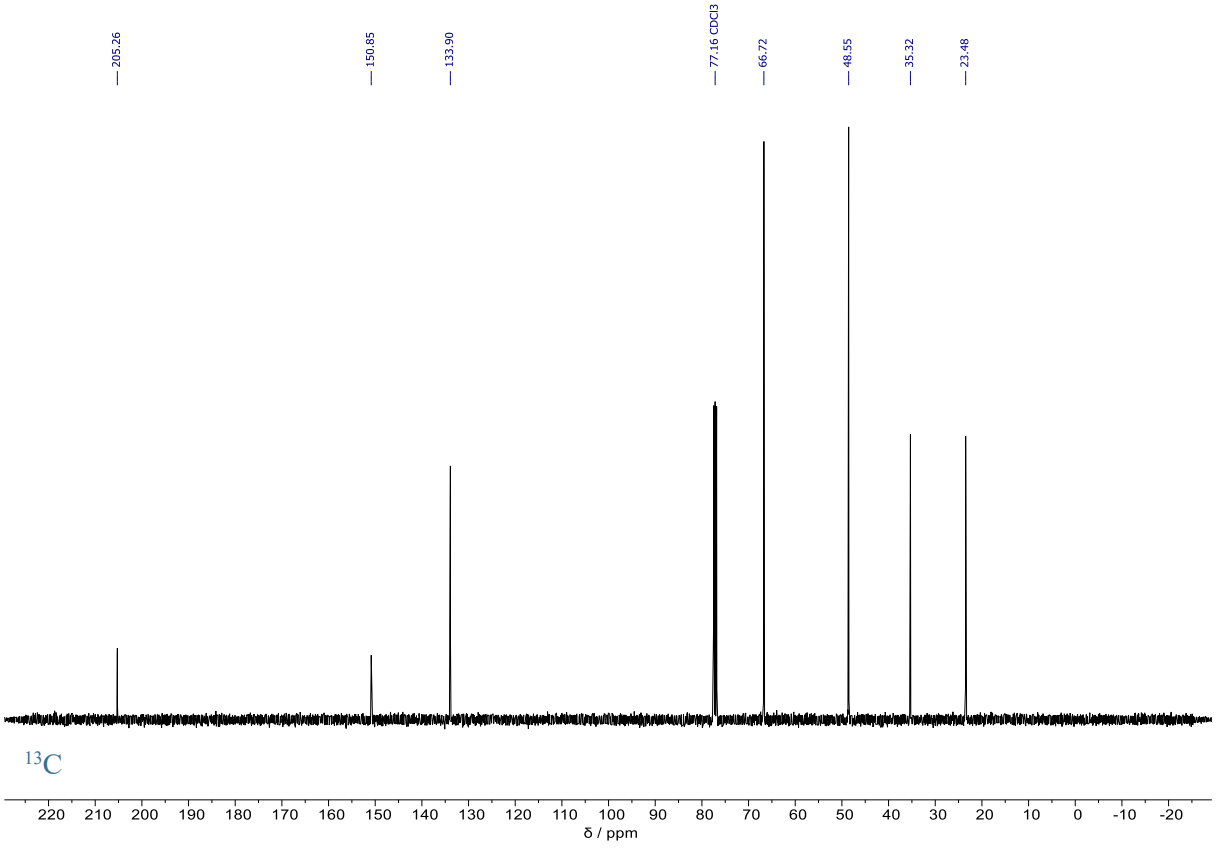


^{13}C

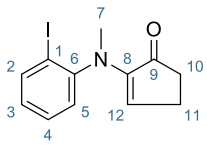
2-Morpholinocyclopent-2-en-1-one, **S42**

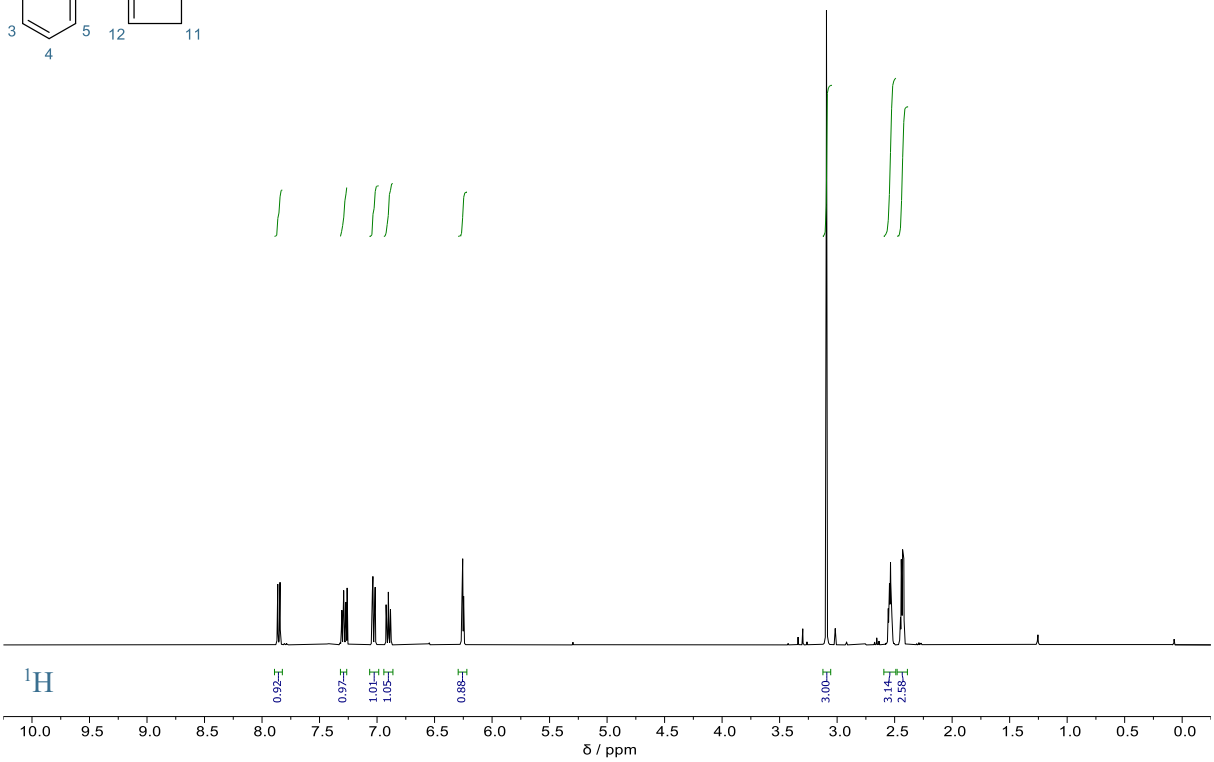


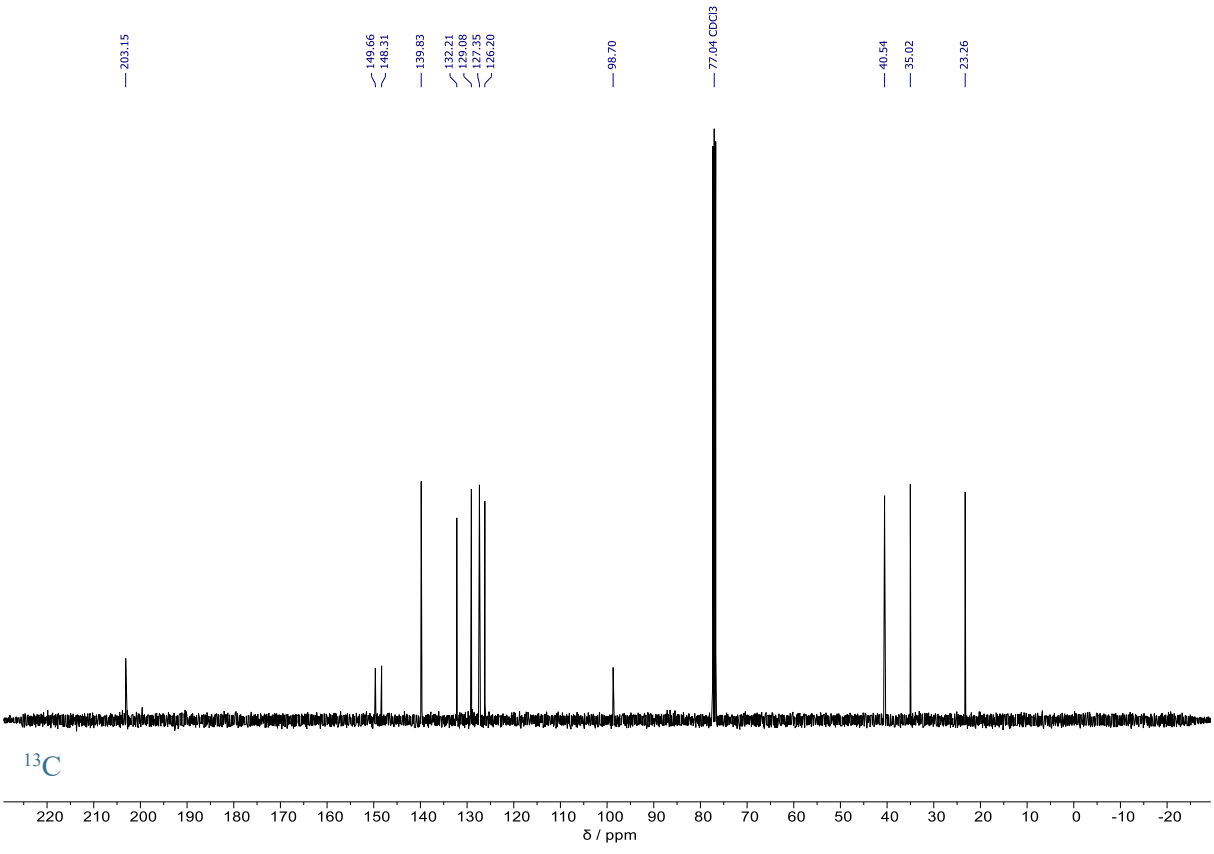




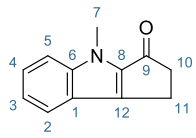
2-((2-Iodophenyl)(methyl)amino)cyclopent-2-en-1-one, **S43**

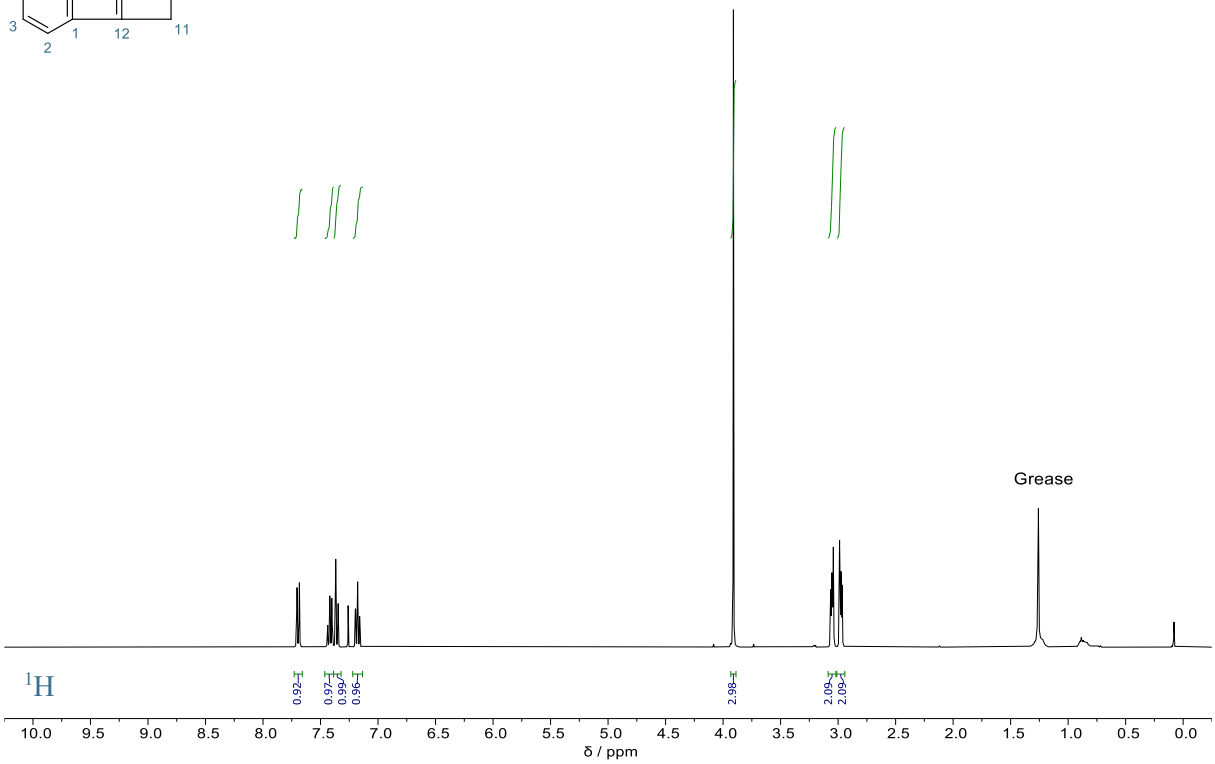


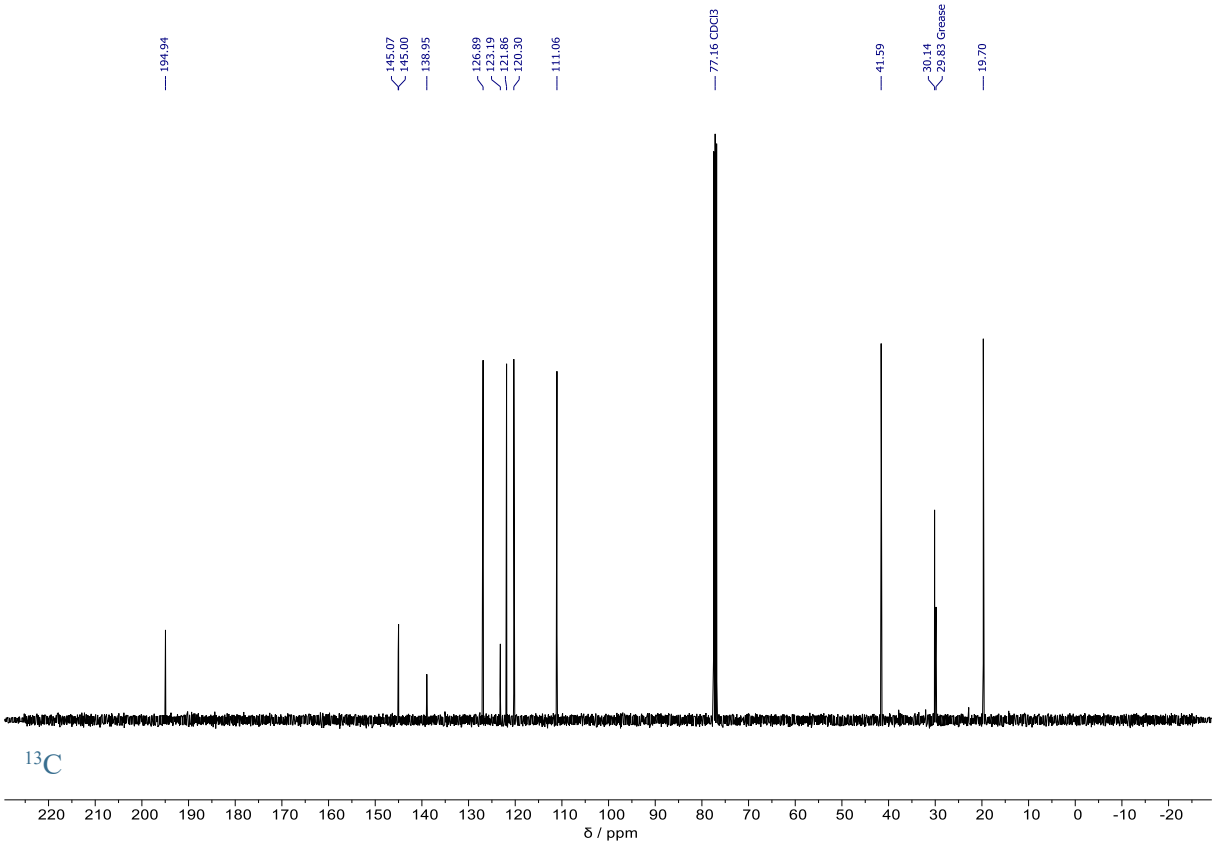




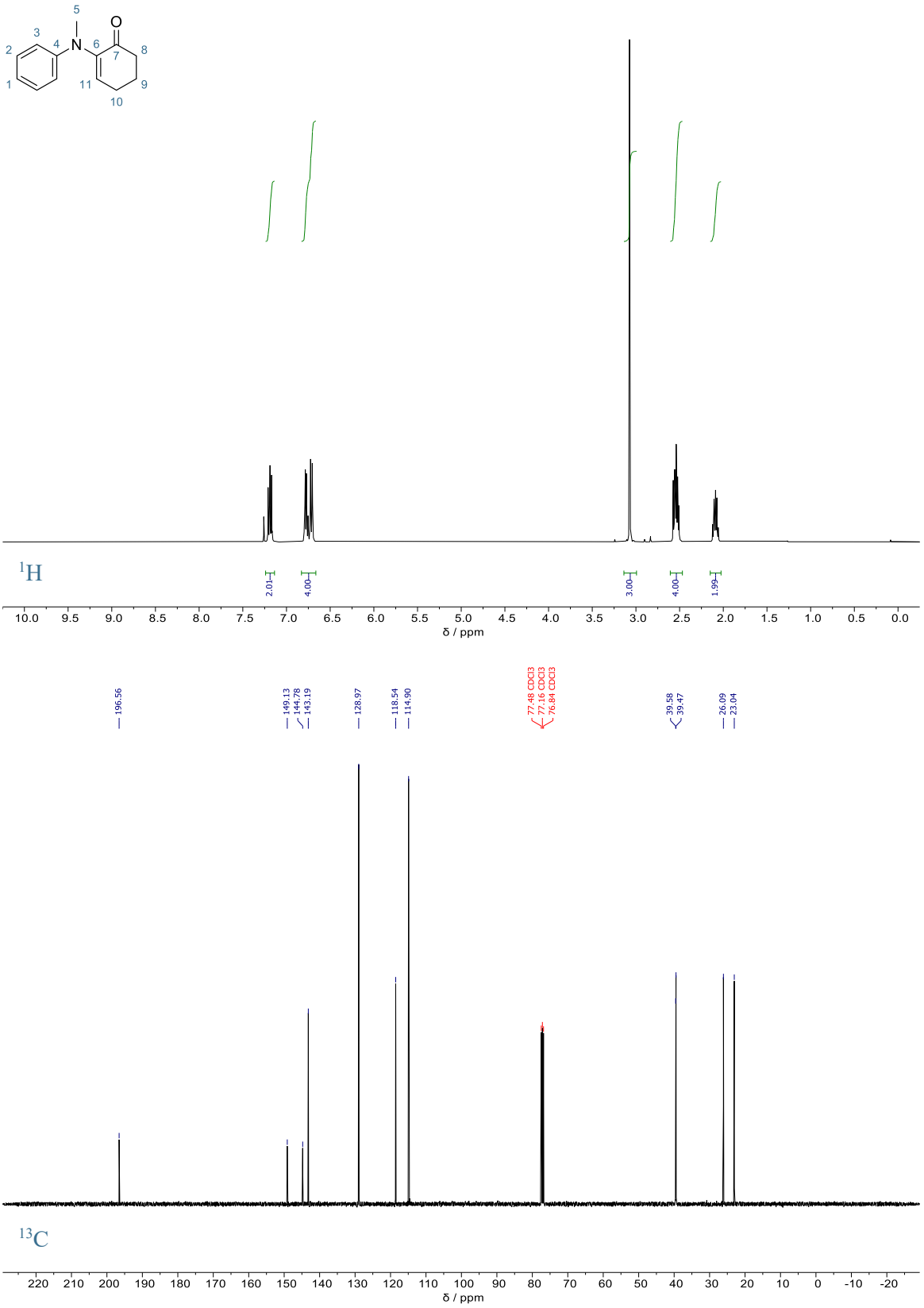
4-Methyl-1,4-dihydrocyclopenta[b]indol-3(2*H*)-one, **S44**



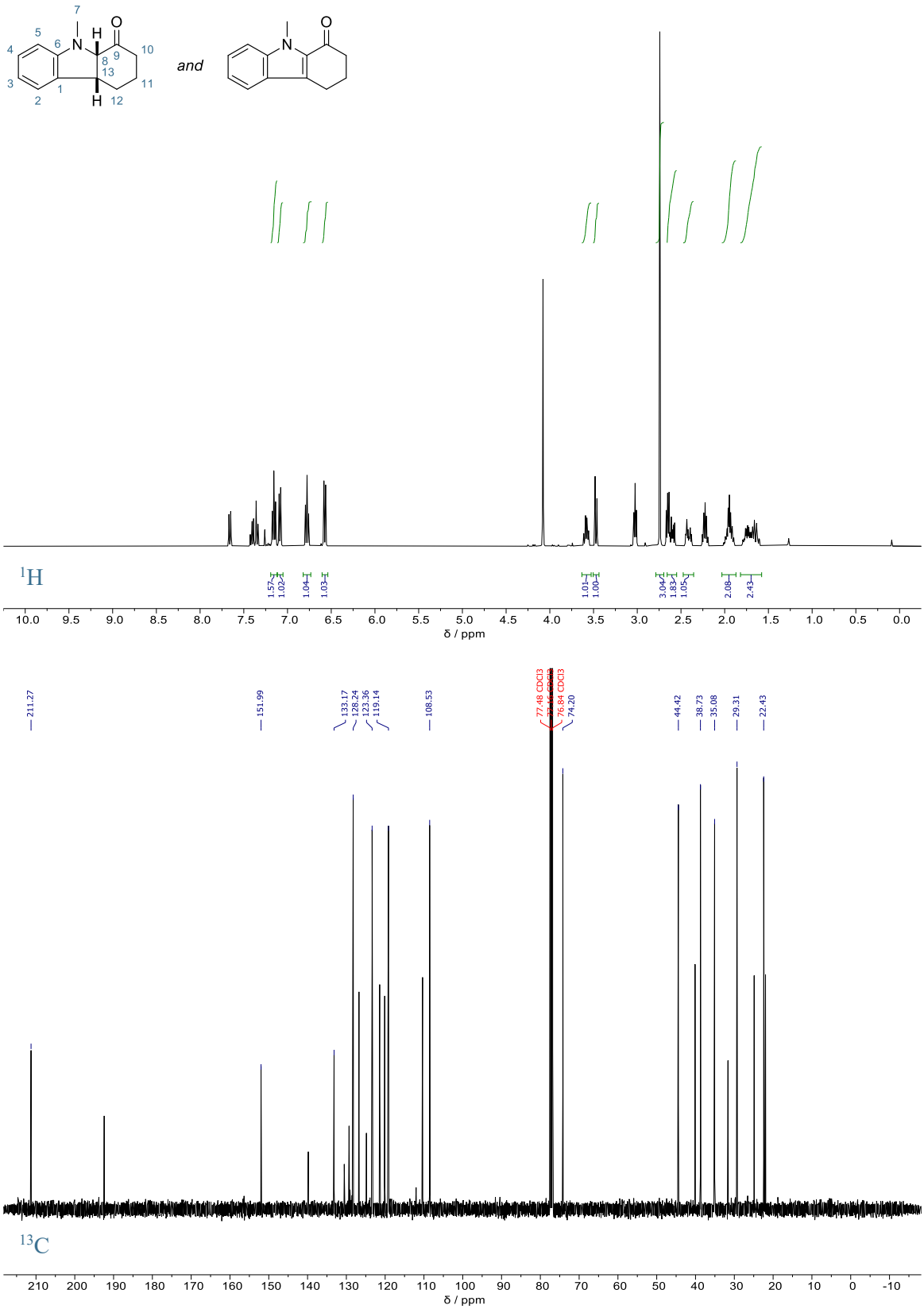




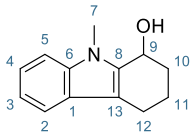
2-(Methyl(phenyl)amino)cyclohex-2-en-1-one, **S45**

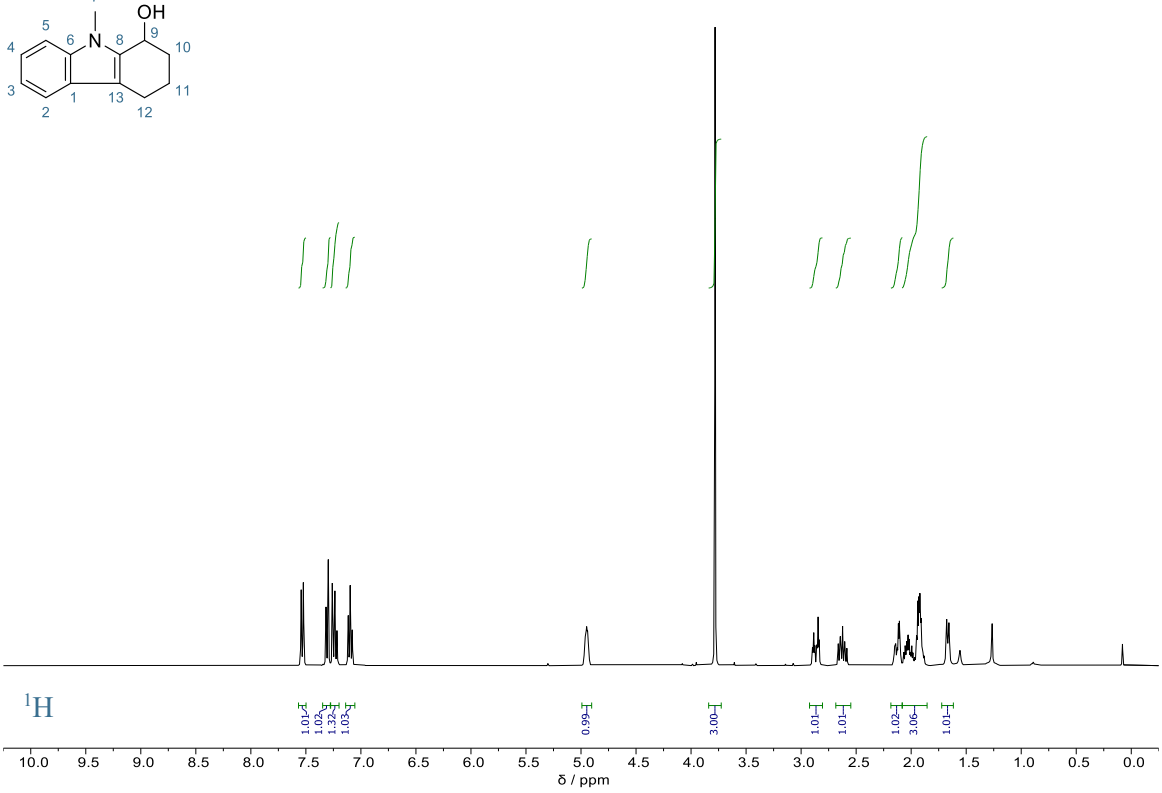


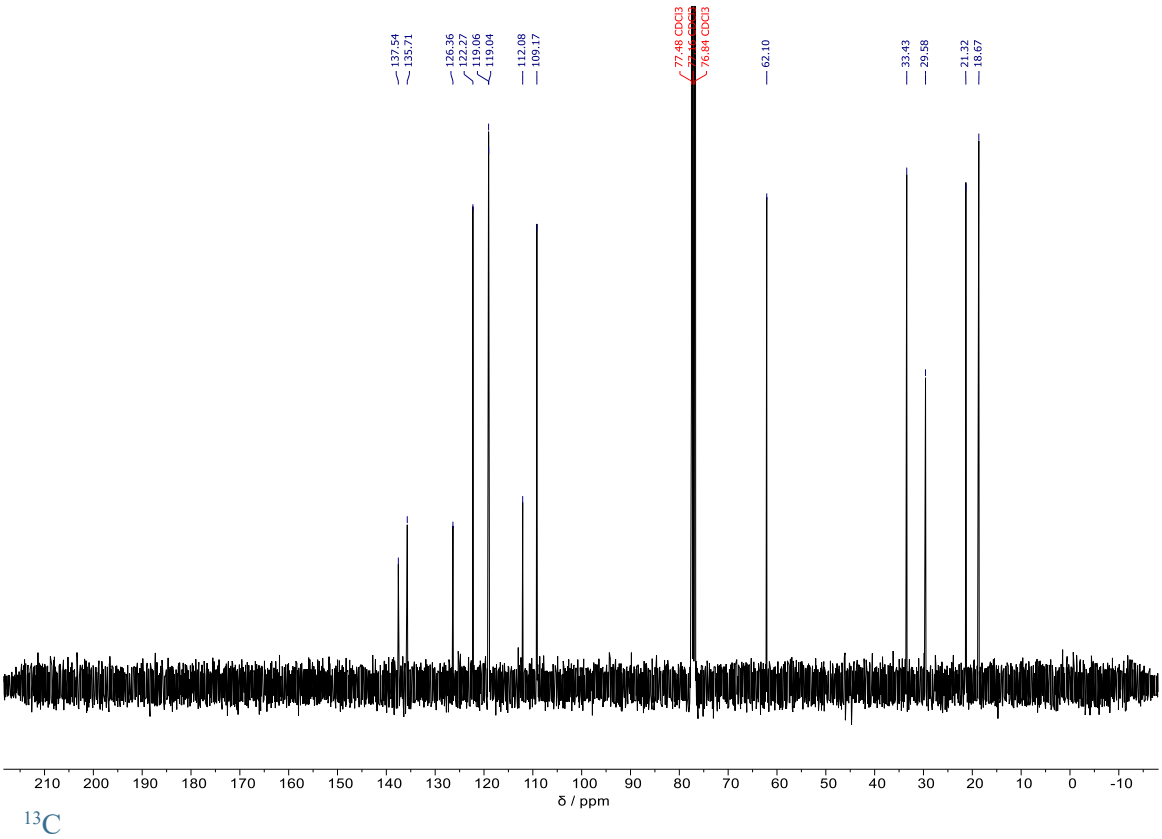
rac-9-Methyl-2,3,4,4a,9,9a-hexahydro-1*H*-carbazol-1-one, **S46**, *and* 9-methyl-2,3,4,9-tetrahydro-1*H*-carbazol-1-one, **42**



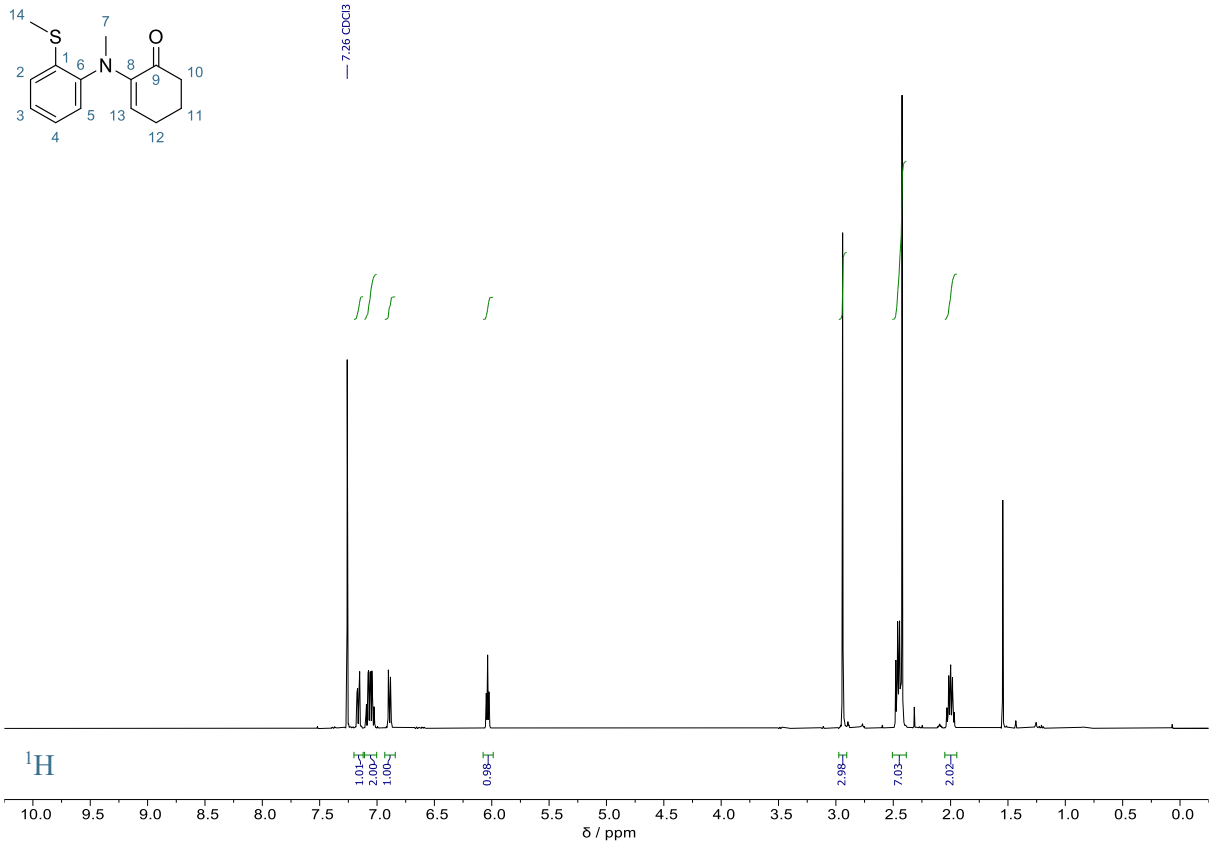
9-Methyl-2,3,4,9-tetrahydro-1*H*-carbazol-1-ol, **S47**

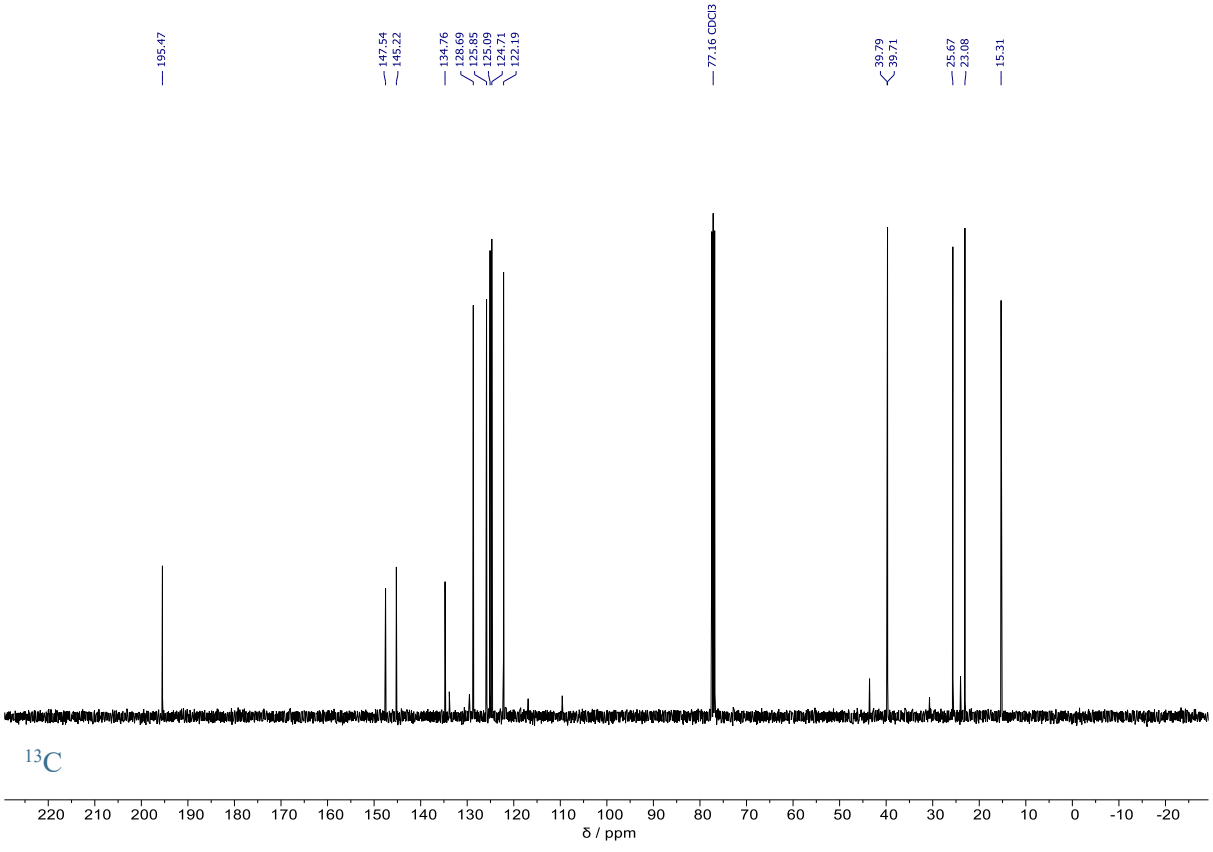






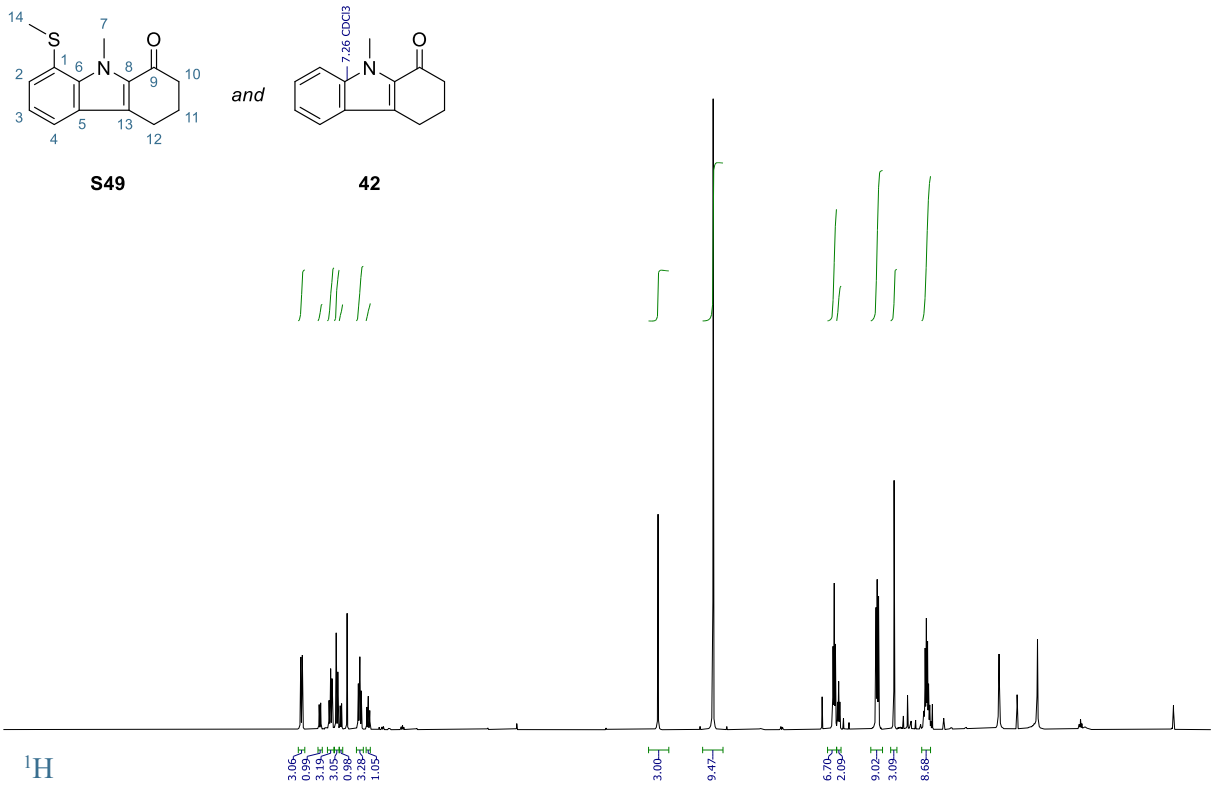
2-(Methyl(2-(methylthio)phenyl)amino)cyclohex-2-en-1-one, **S48**

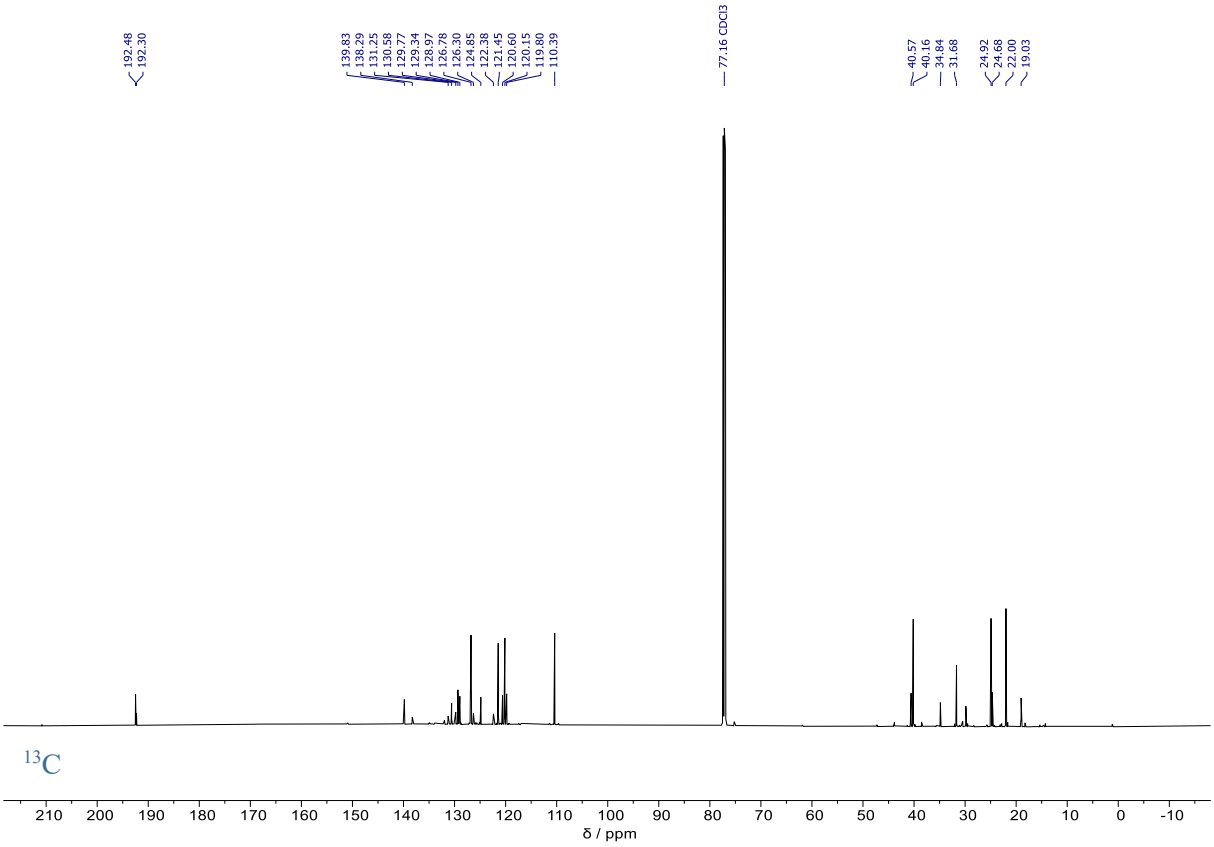




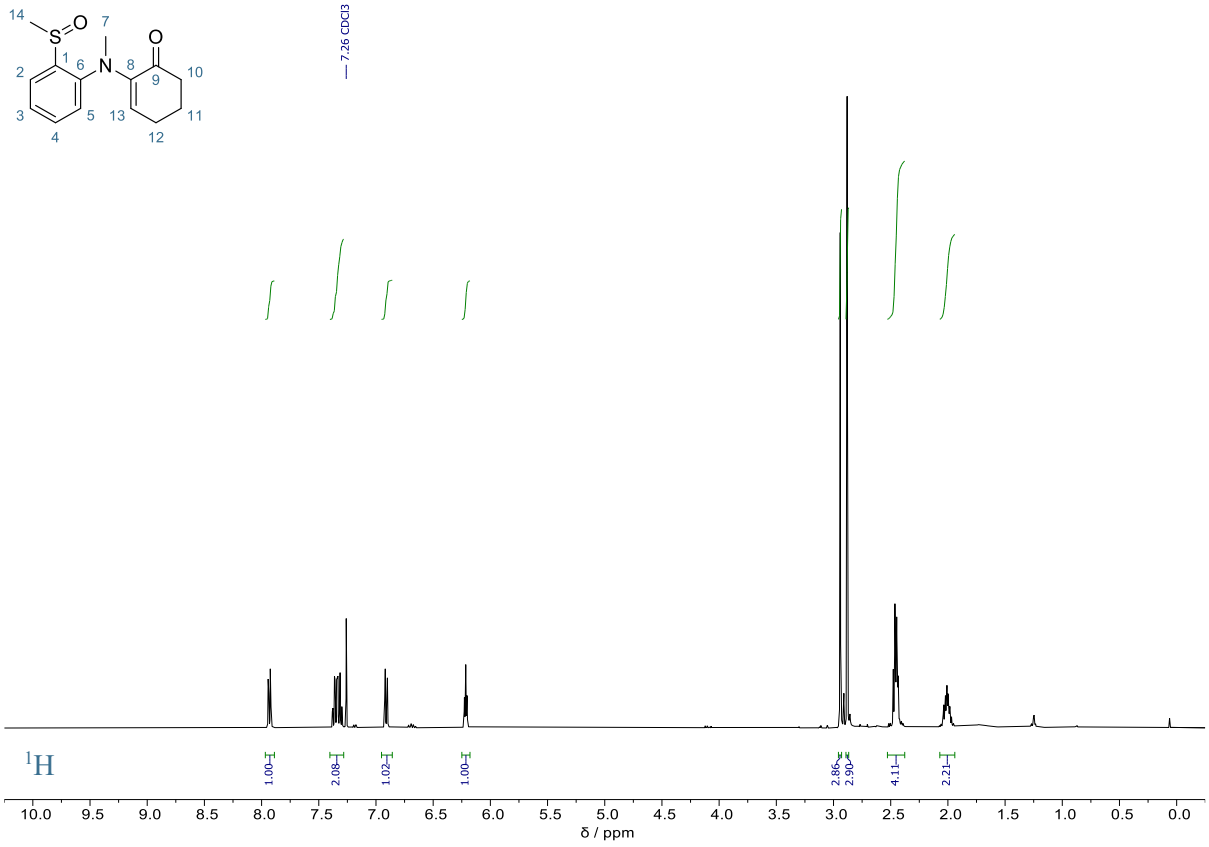
Note: This compound underwent partial degradation upon standing in $CDCl_3$ solution over a period of hours to days. The specific decomposition product that resulted from this process remains unidentified, but it can be detected as additional faint signals in the provided ^{13}C spectrum.

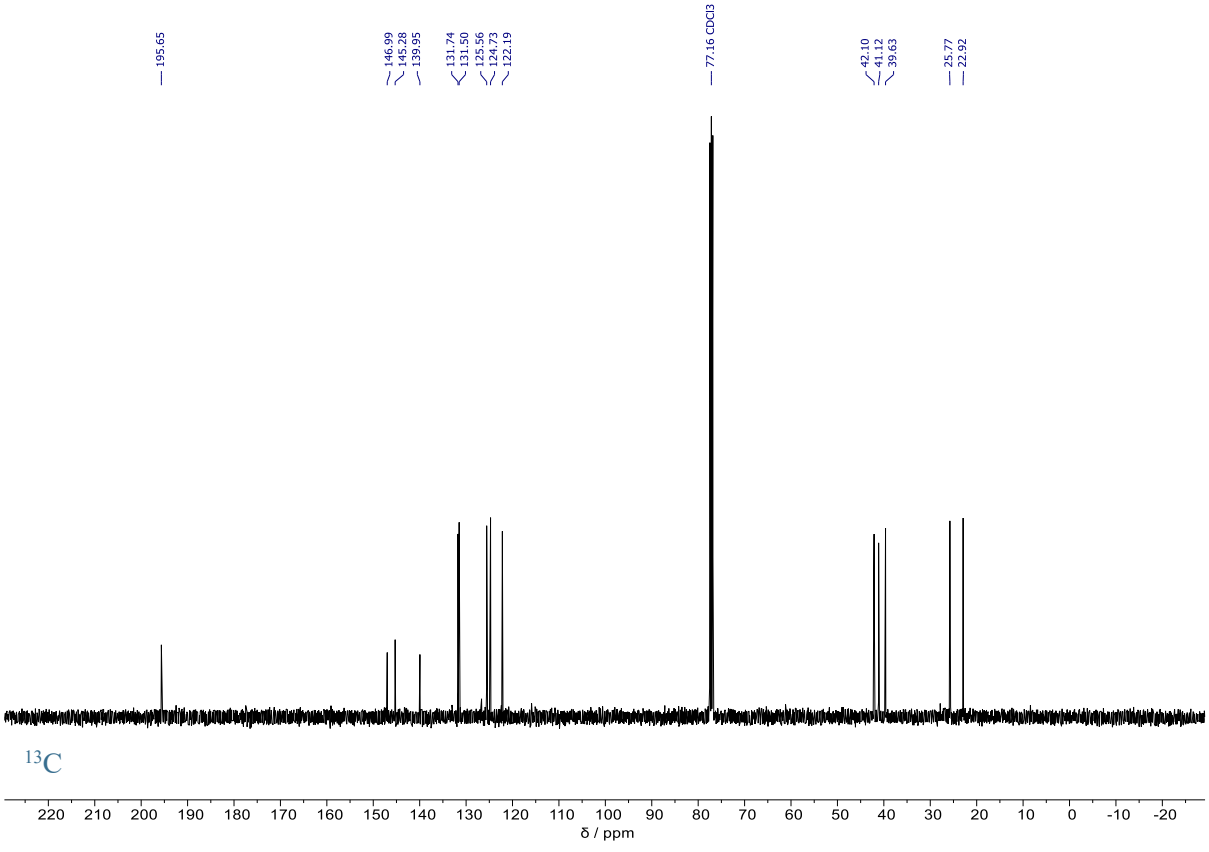
9-Methyl-8-(methylthio)-2,3,4,9-tetrahydro-1H-carbazol-1-one, **S49**, *and* 9-methyl-2,3,4,9-tetrahydro-1*H*-carbazol-1-one, **42**



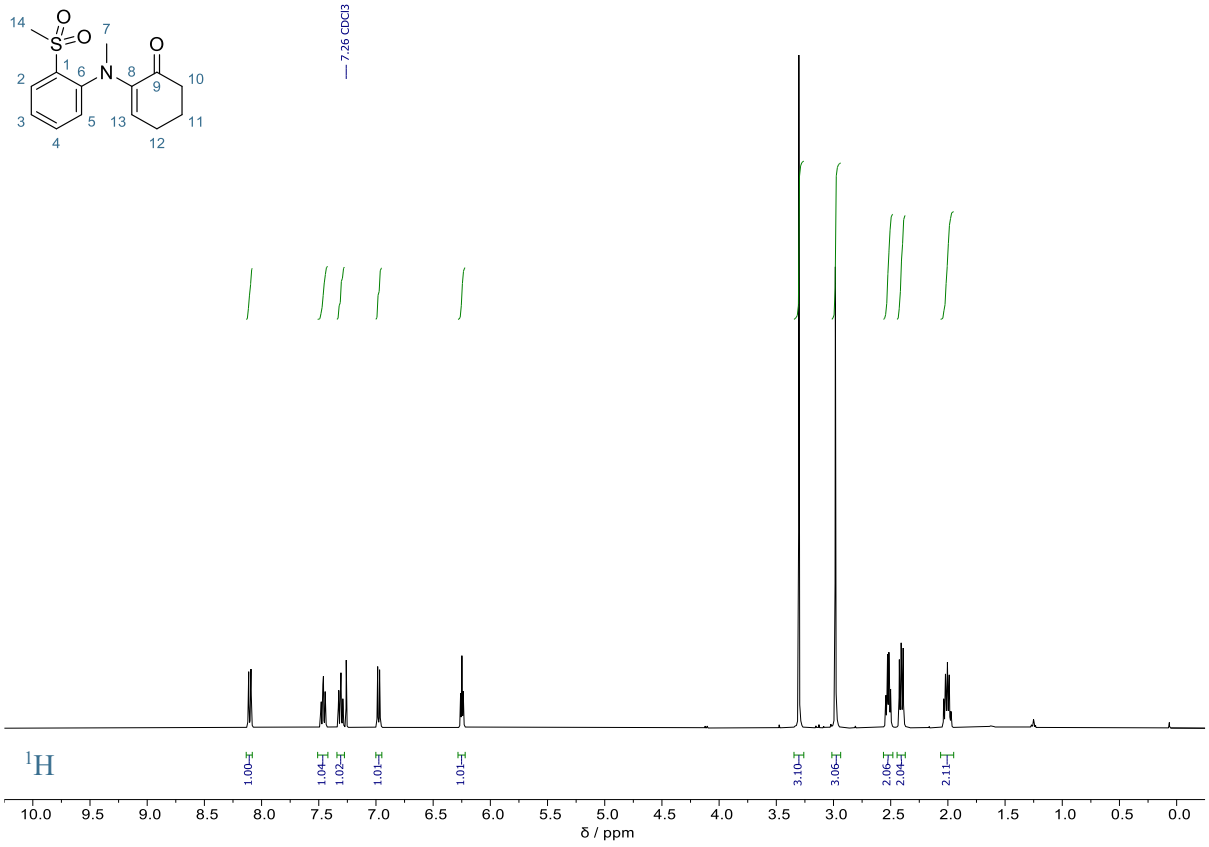


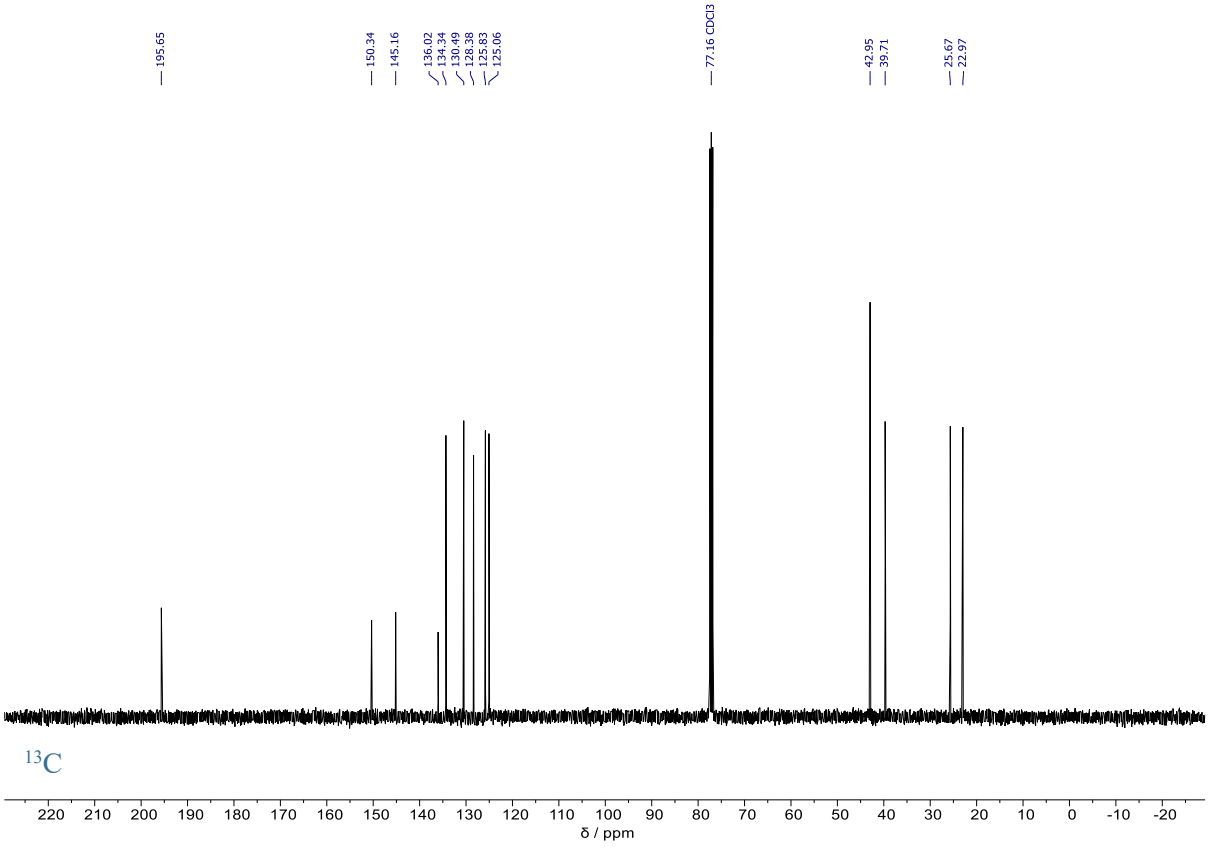
2-(Methyl(2-(methylsulfinyl)phenyl)amino)cyclohex-2-en-1-one, **S50**



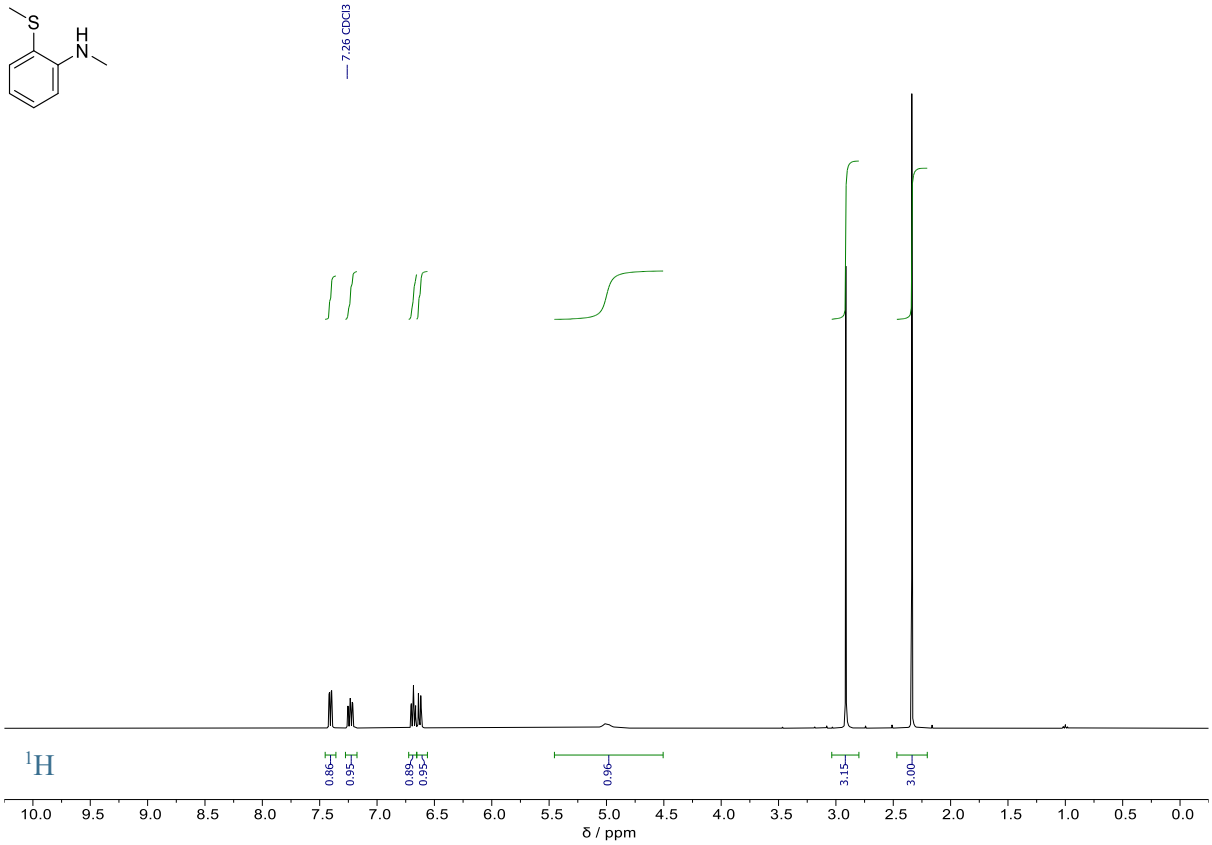


2-(Methyl(2-(methylsulfonyl)phenyl)amino)cyclohex-2-en-1-one, **S53**

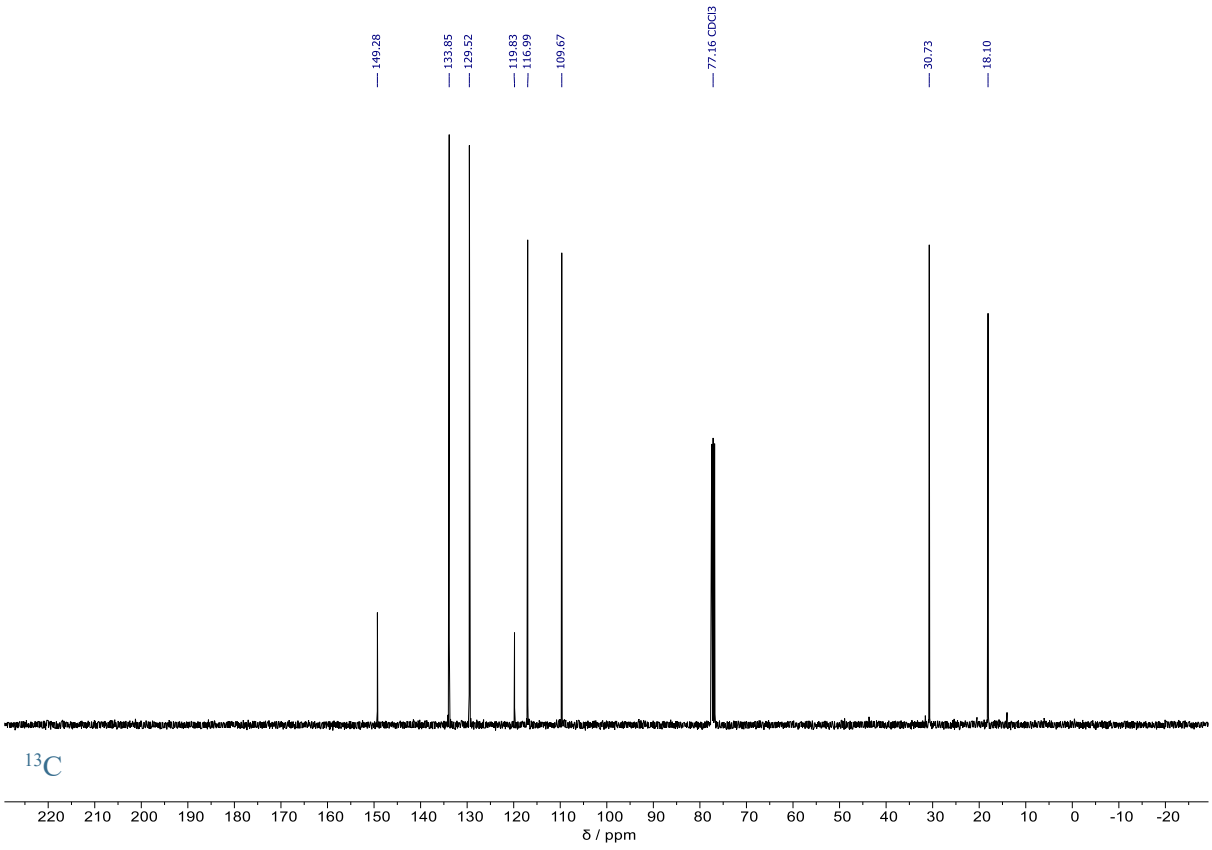




N-Methyl-2-(methylthio)aniline, **S56**

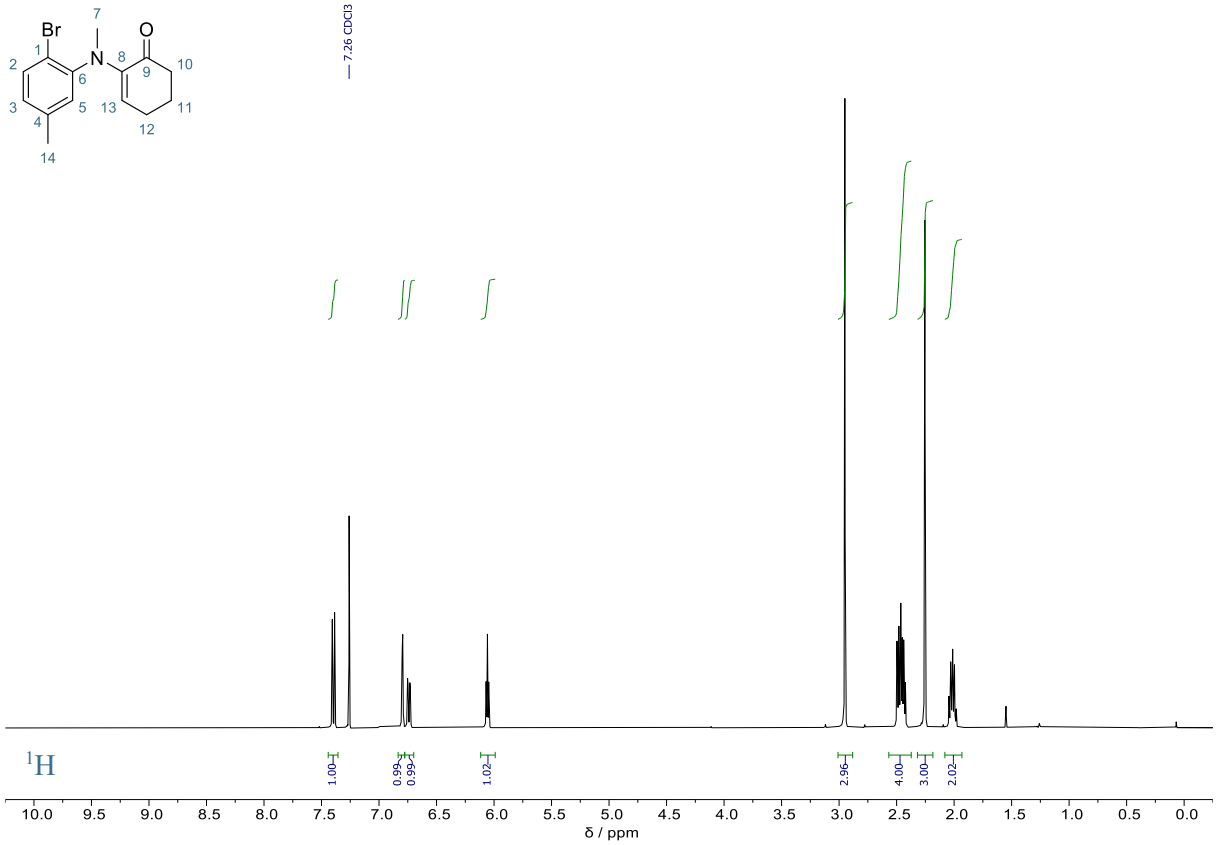


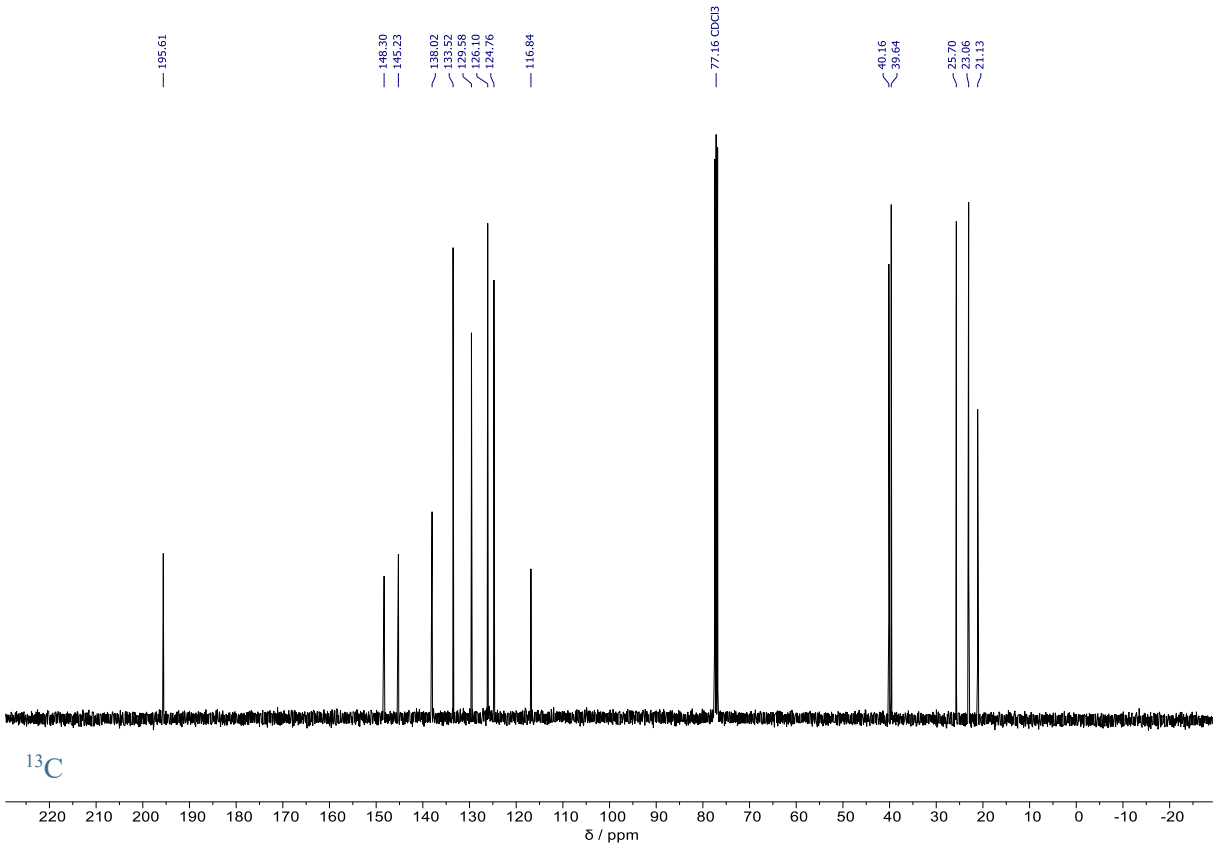
^{1}H



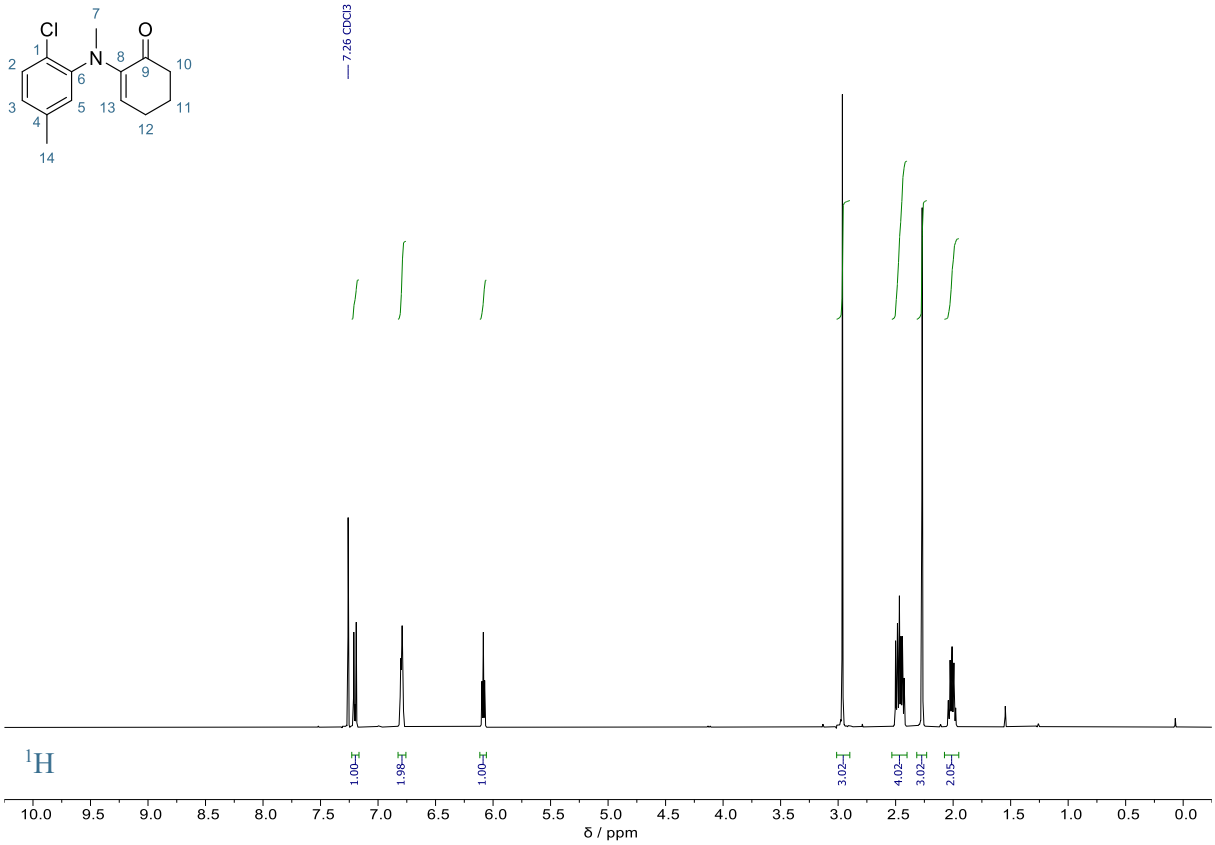
^{13}C

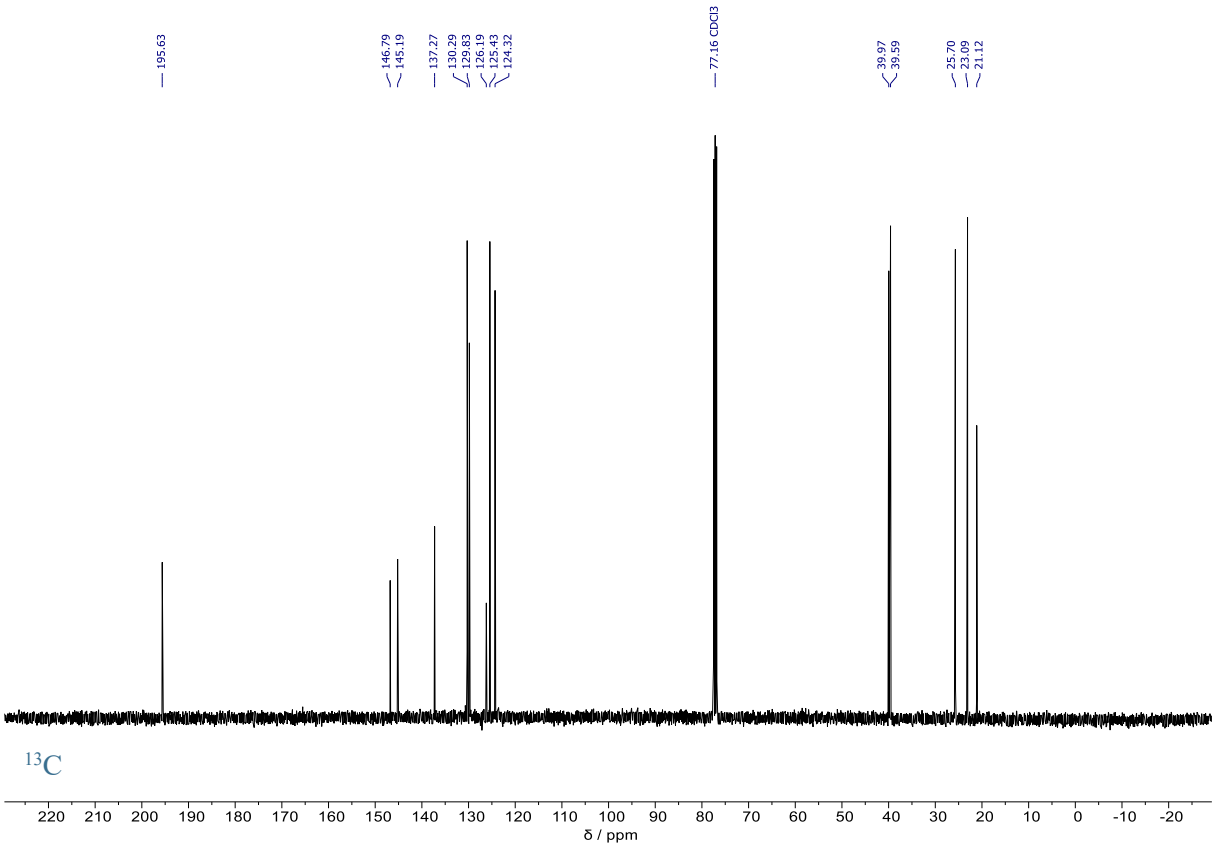
2-((2-Bromo-5-methylphenyl)(methyl)amino)cyclohex-2-en-1-one, **S57**



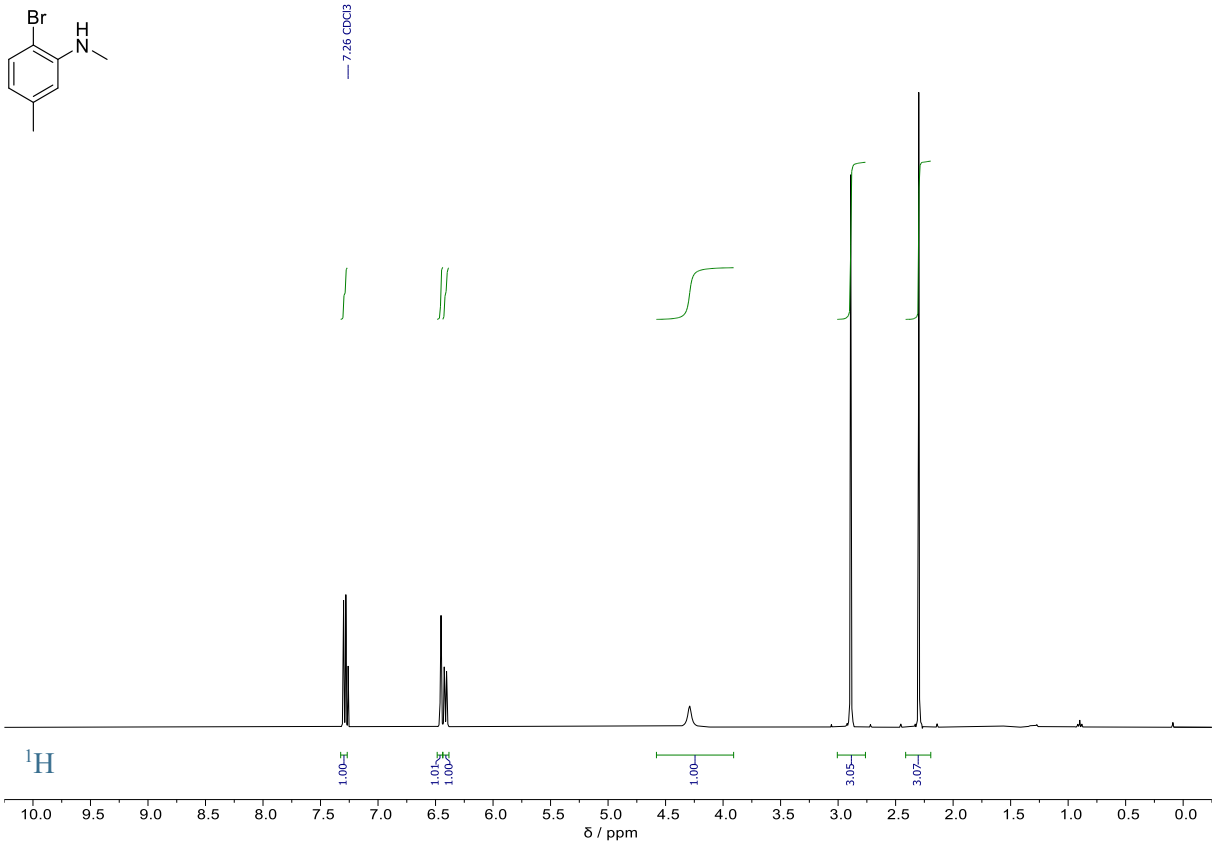


2-((2-Chloro-5-methylphenyl)(methyl)amino)cyclohex-2-en-1-one, **S58**

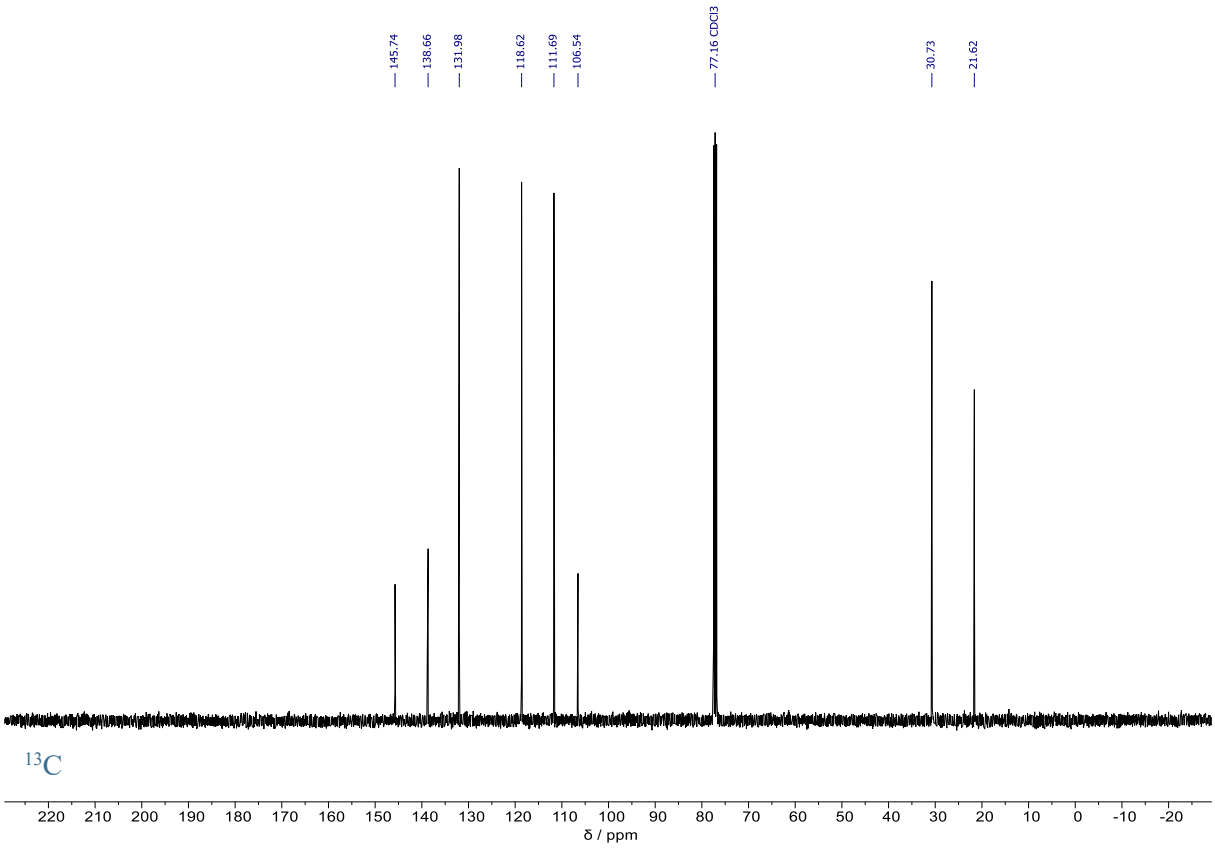




2-Bromo-*N*,5-dimethylaniline, **S59**

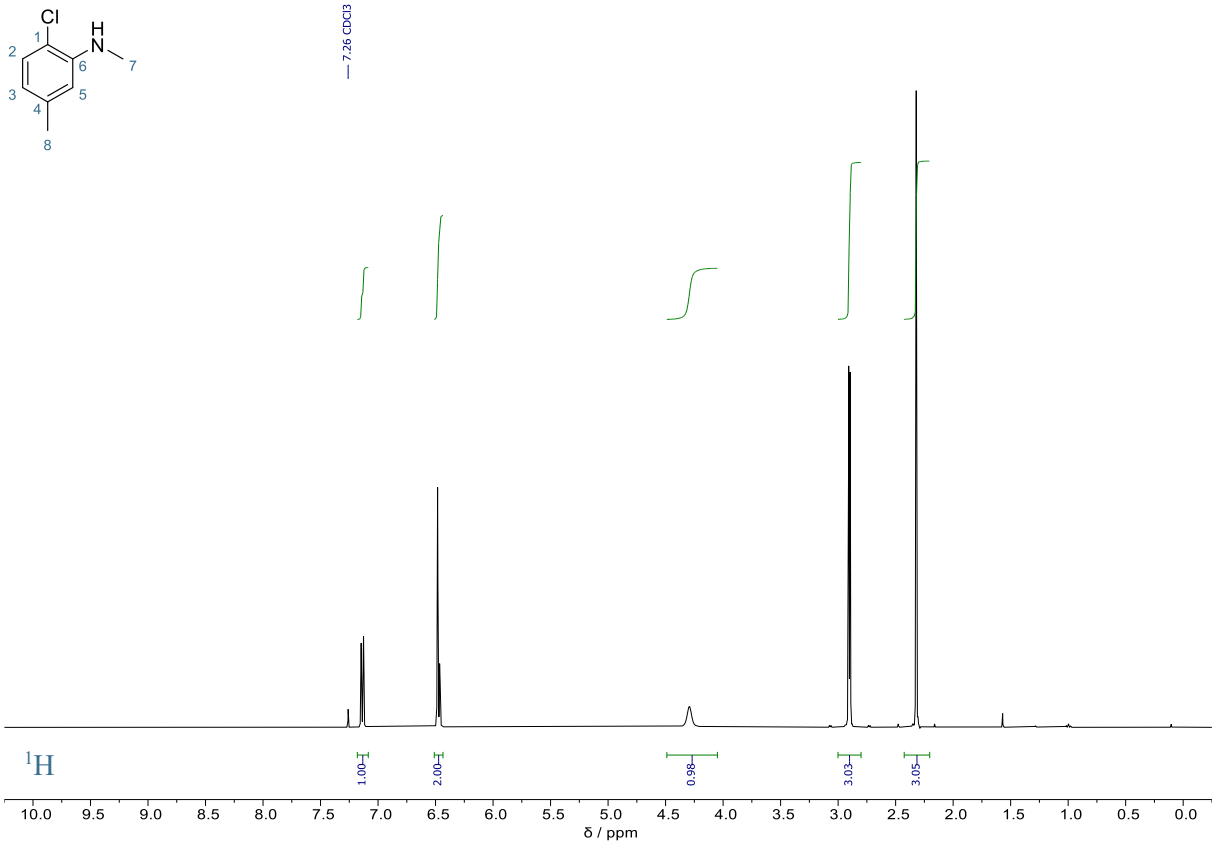


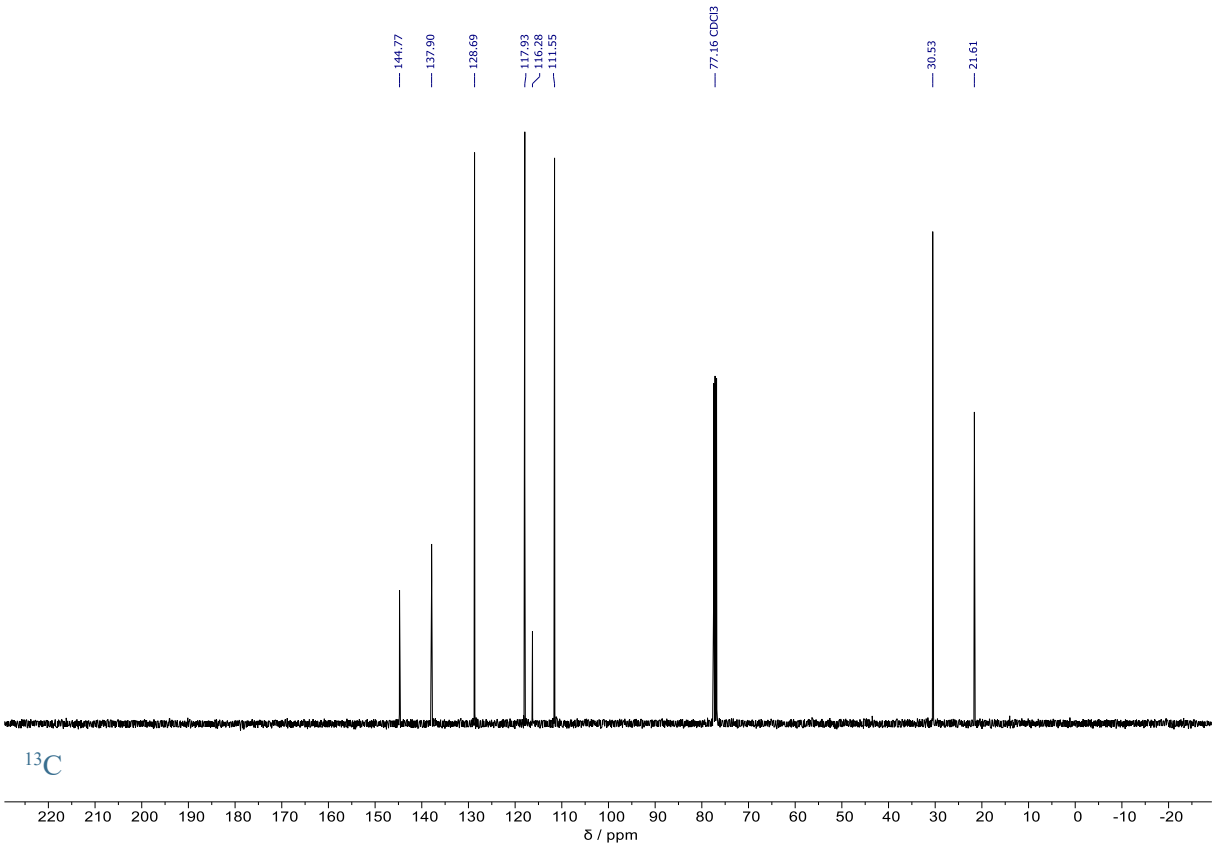
^{1}H



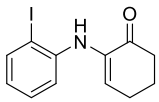
^{13}C

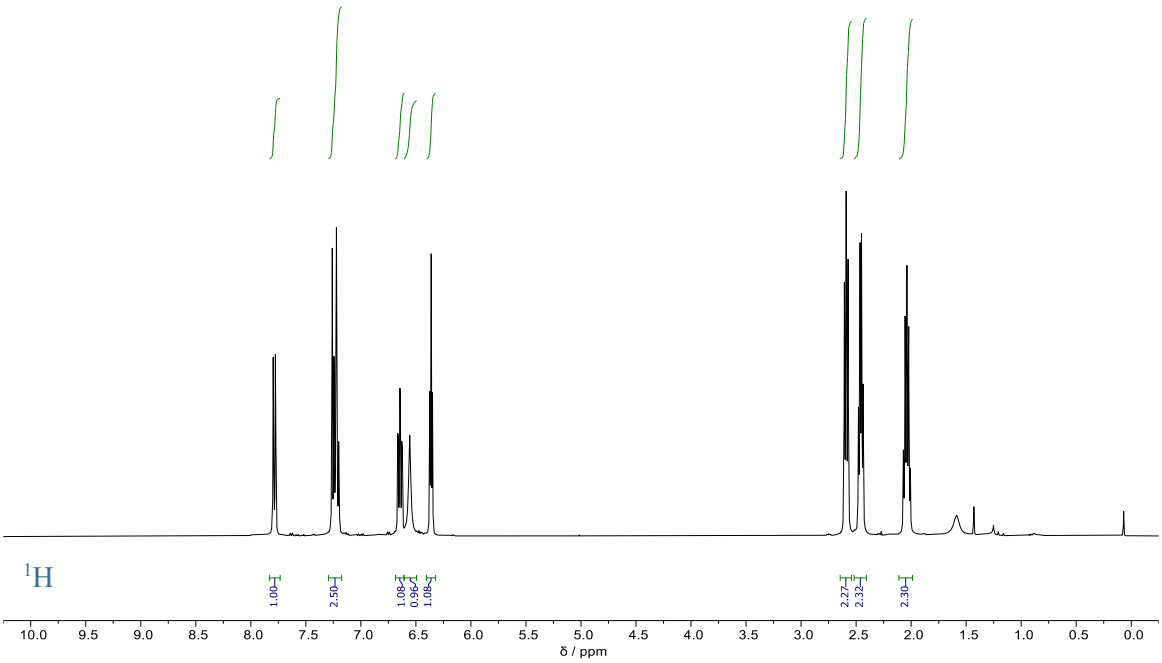
2-Chloro-*N*,5-dimethylaniline, **S60**



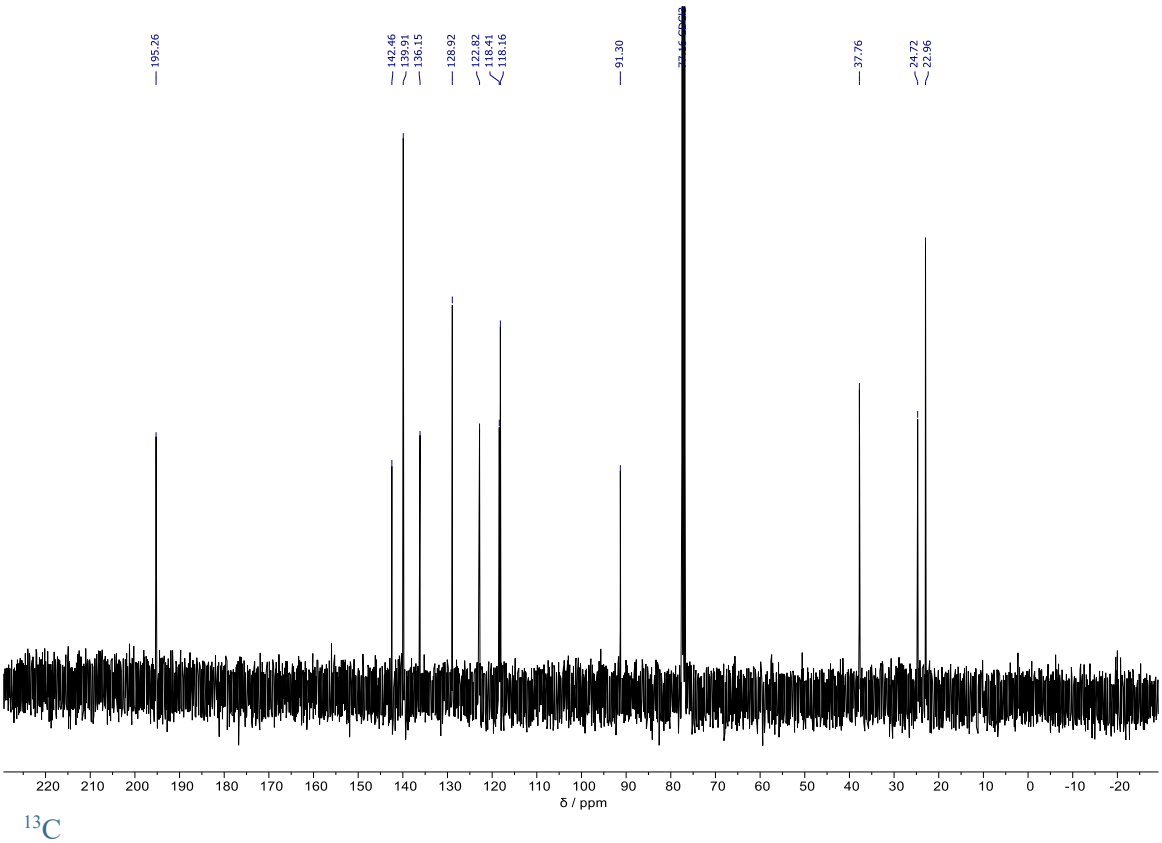


2-((2-Iodophenyl)amino)cyclohex-2-en-1-one, **S61**



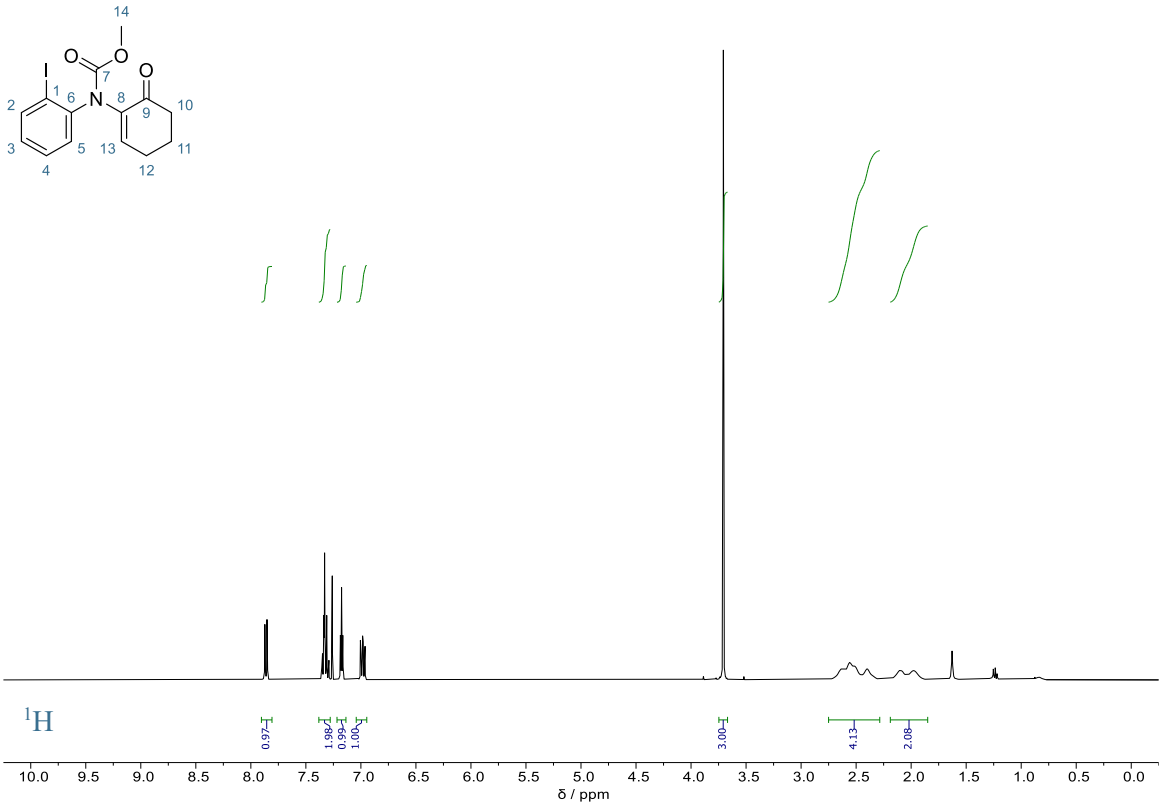


^{1}H

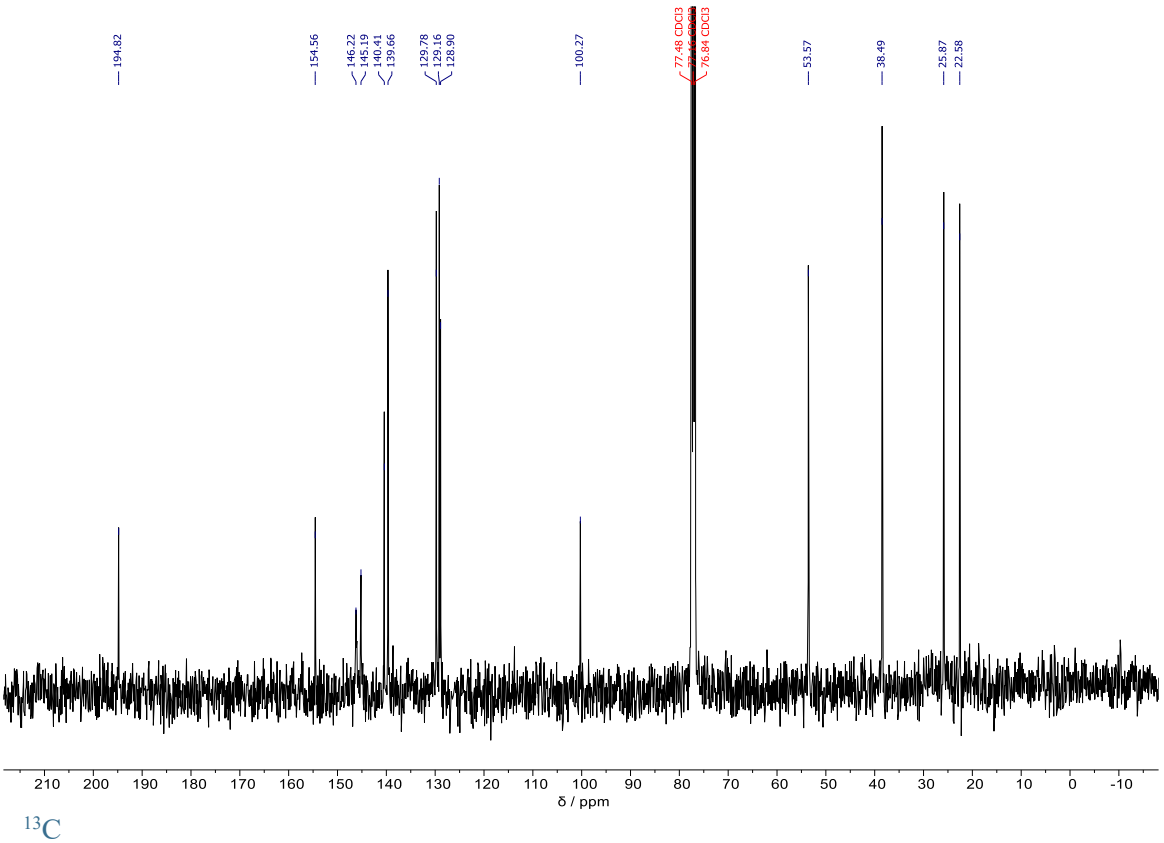


^{13}C

Methyl (2-iodophenyl)(6-oxocyclohex-1-en-1-yl)carbamate, **S62**

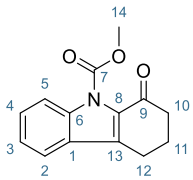


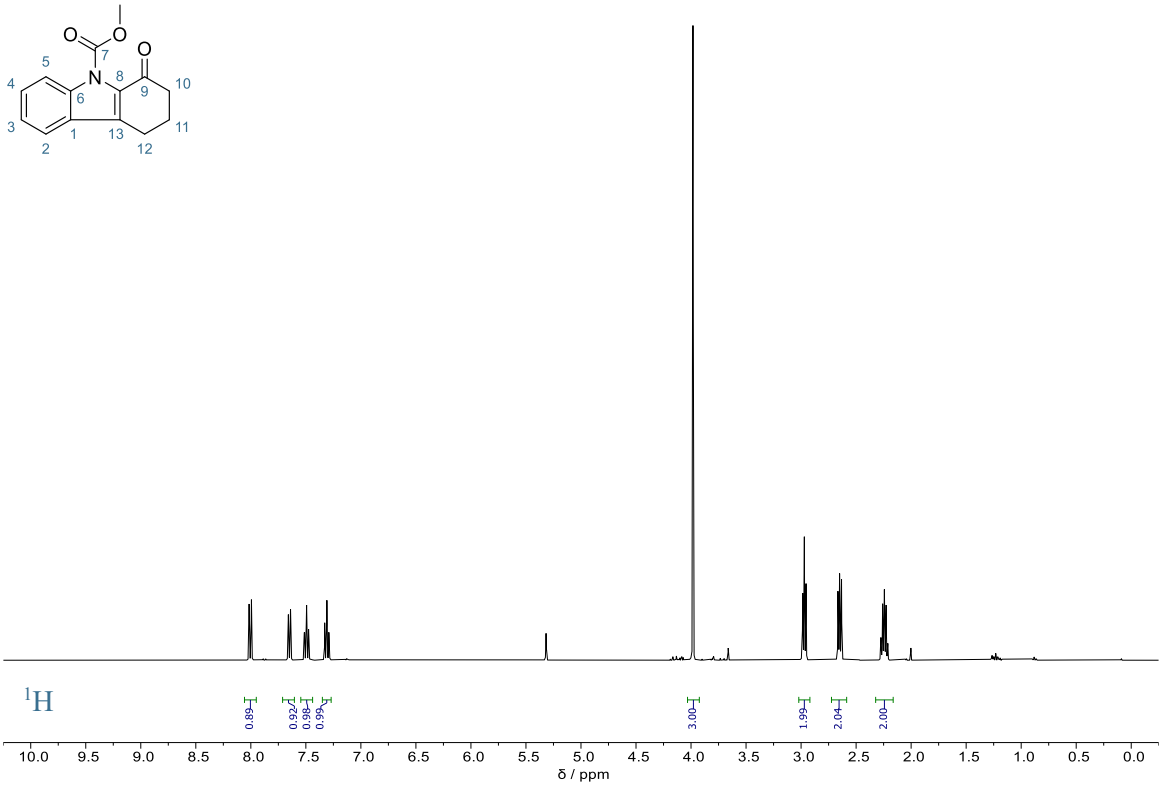
^{1}H

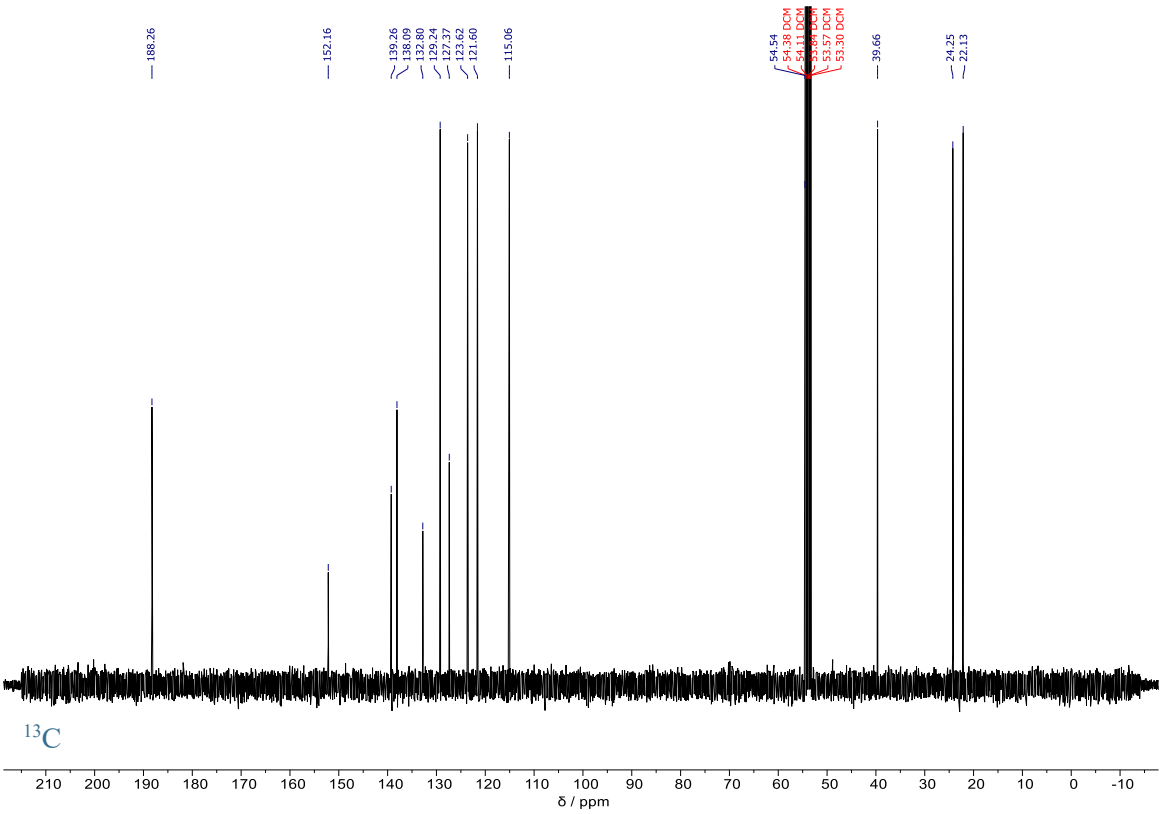


^{13}C

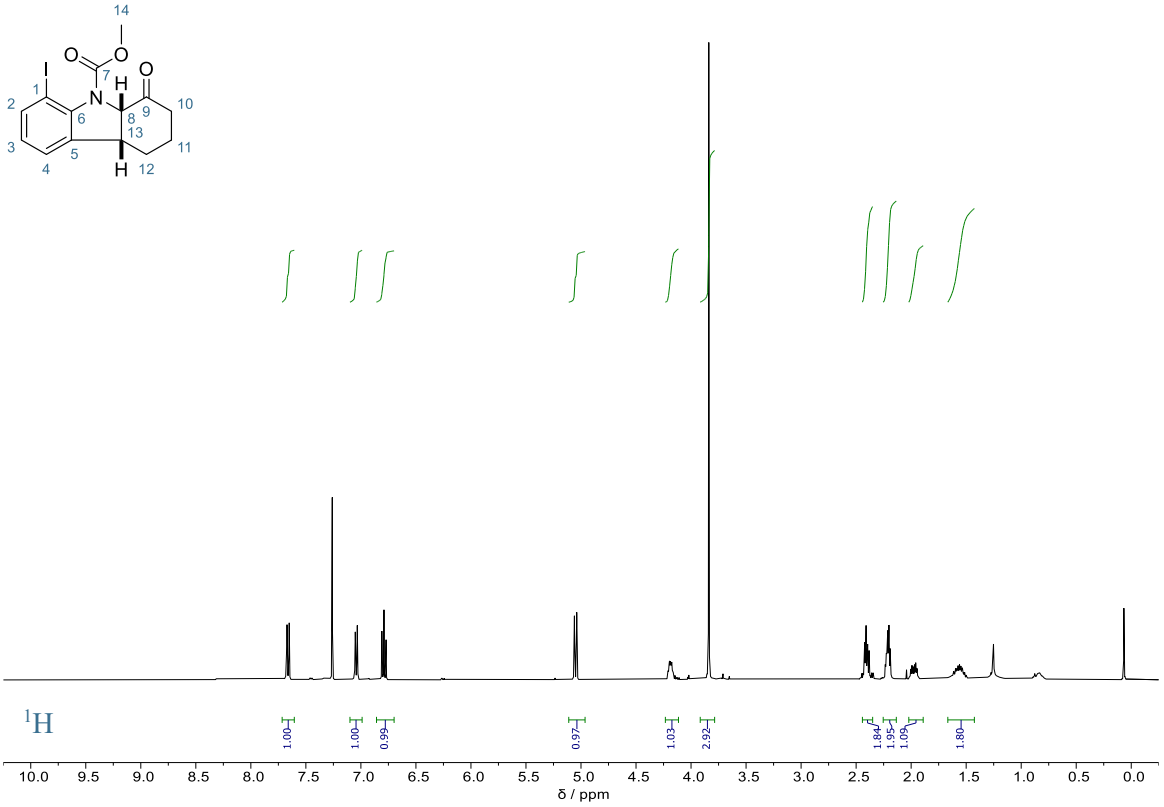
Methyl 1-oxo-1,2,3,4-tetrahydro-9*H*-carbazole-9-carboxylate, **S63**



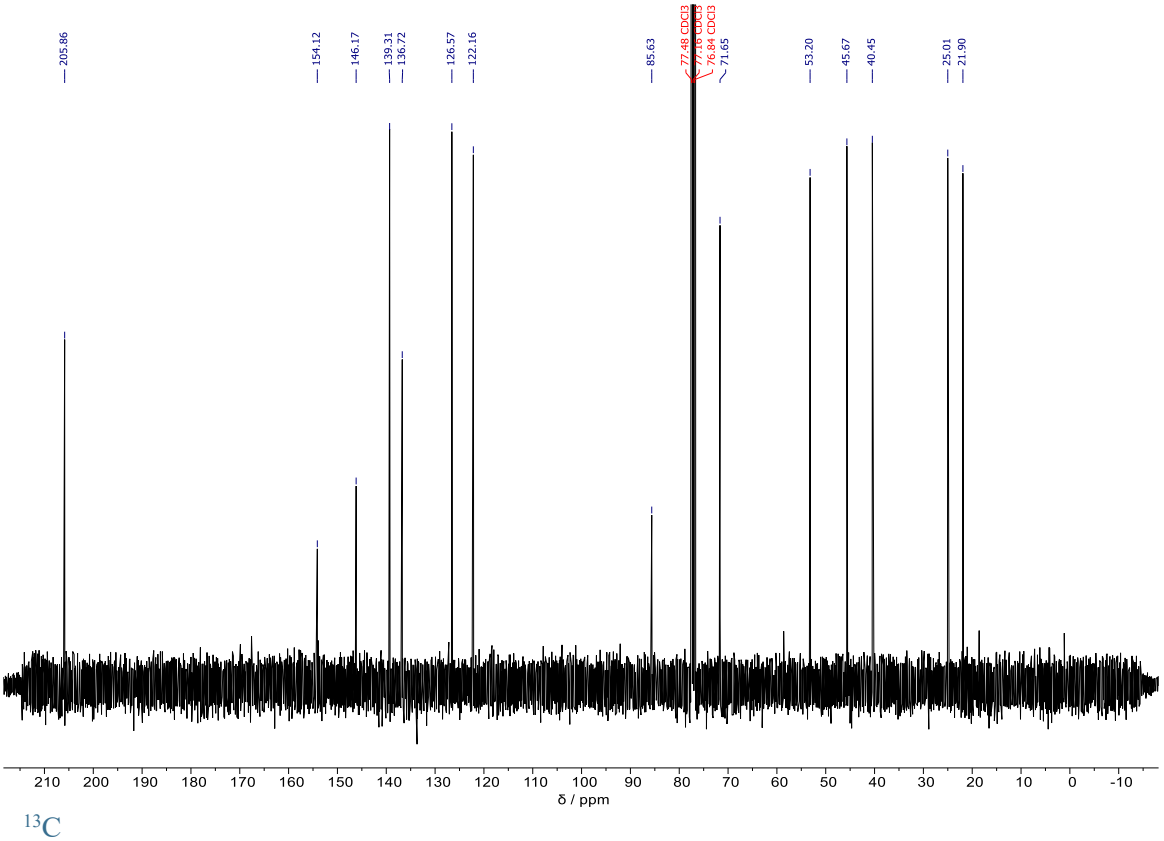




rac-Methyl 8-iodo-1-oxo-1,2,3,4,4a,9a-hexahydro-9*H*-carbazole-9-carboxylate, **S64**

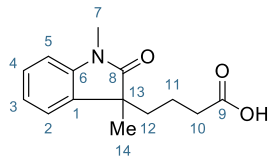


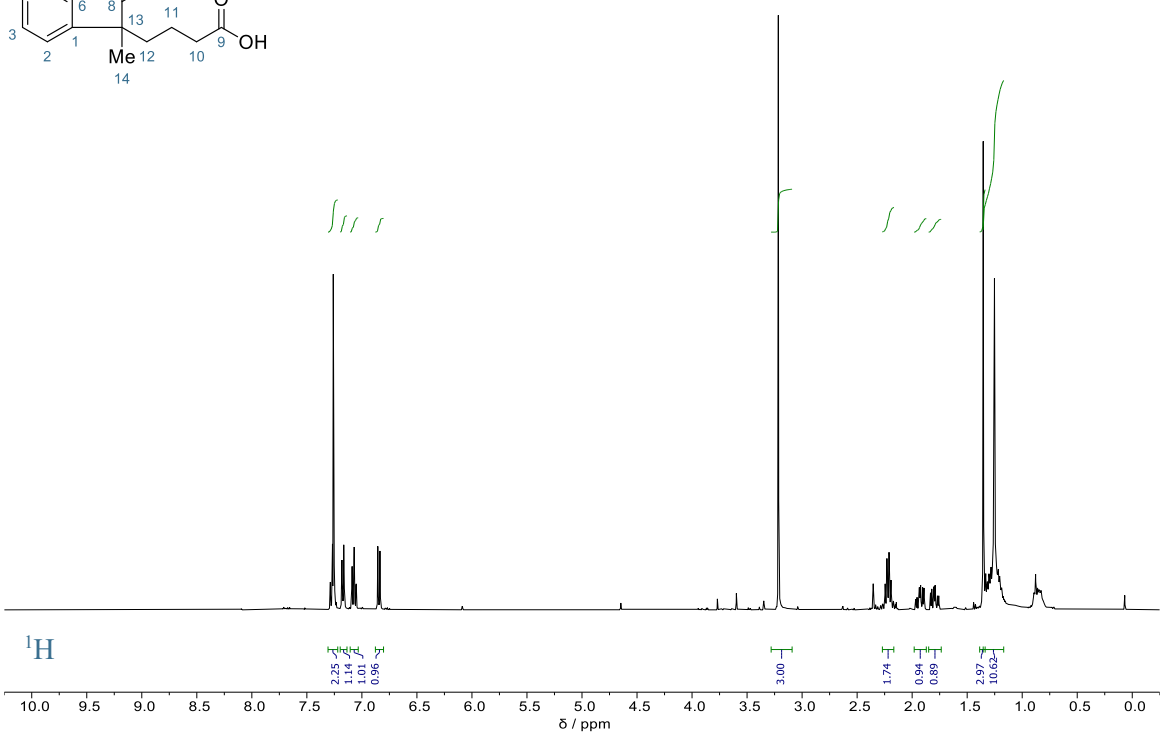
^{1}H



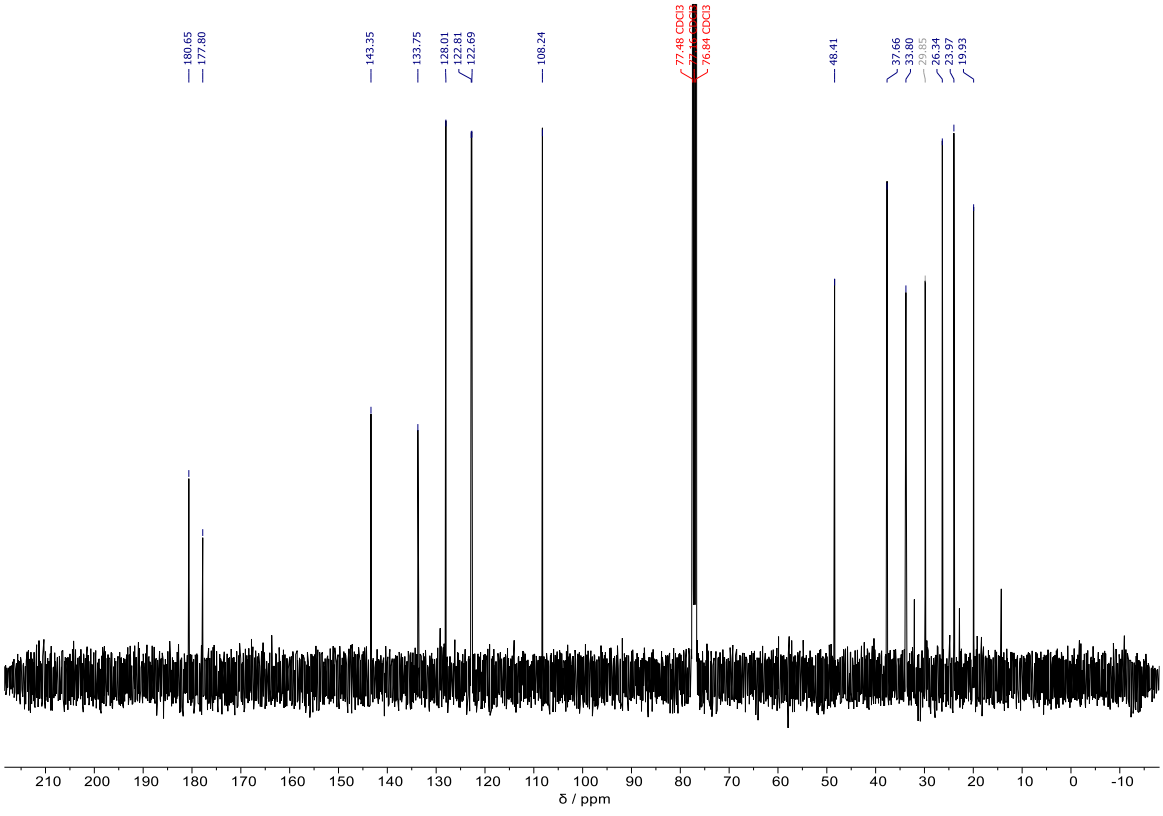
^{13}C

4-(1,3-Dimethyl-2-oxoindolin-3-yl)butanoic acid, **S65**





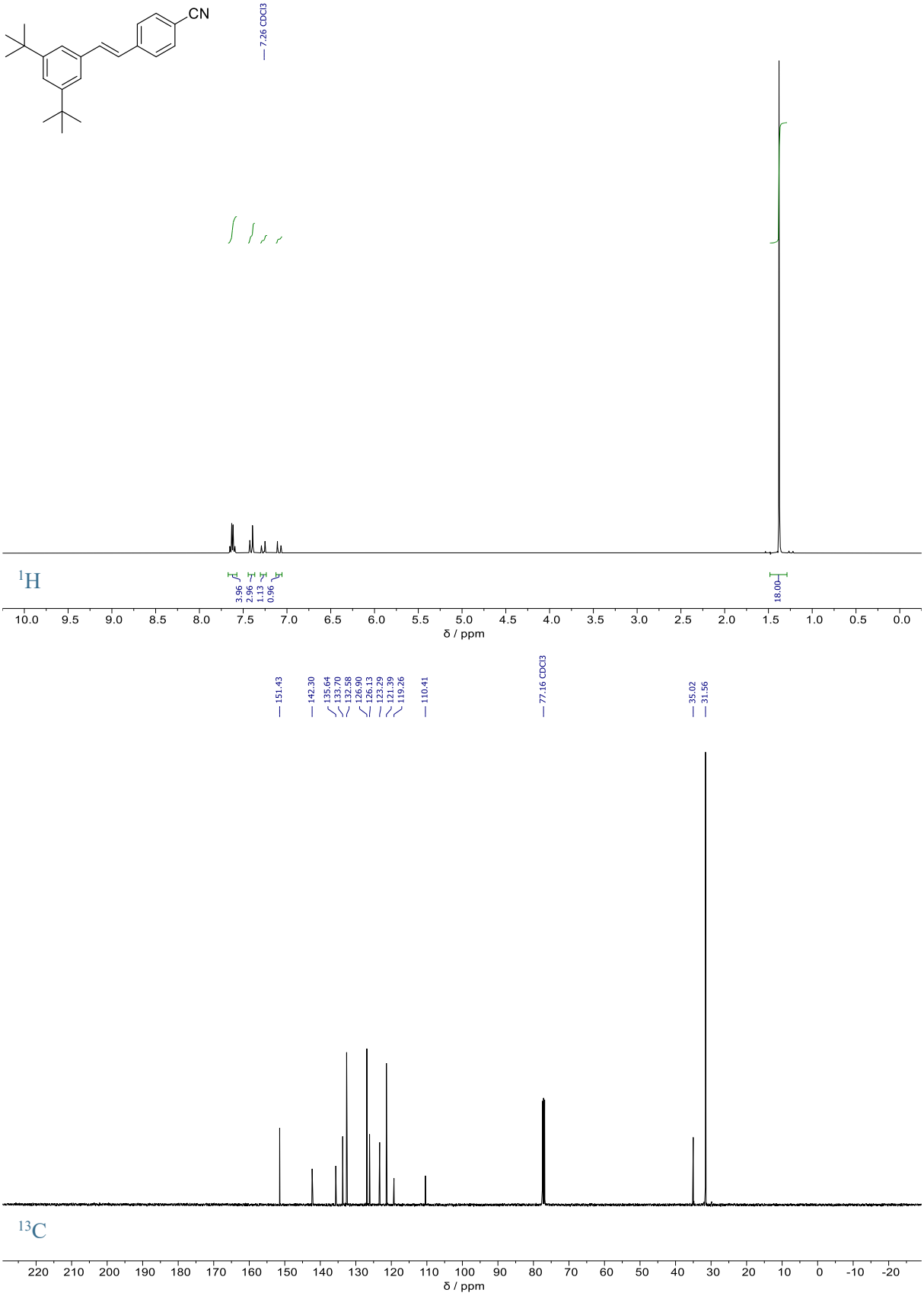
^{1}H



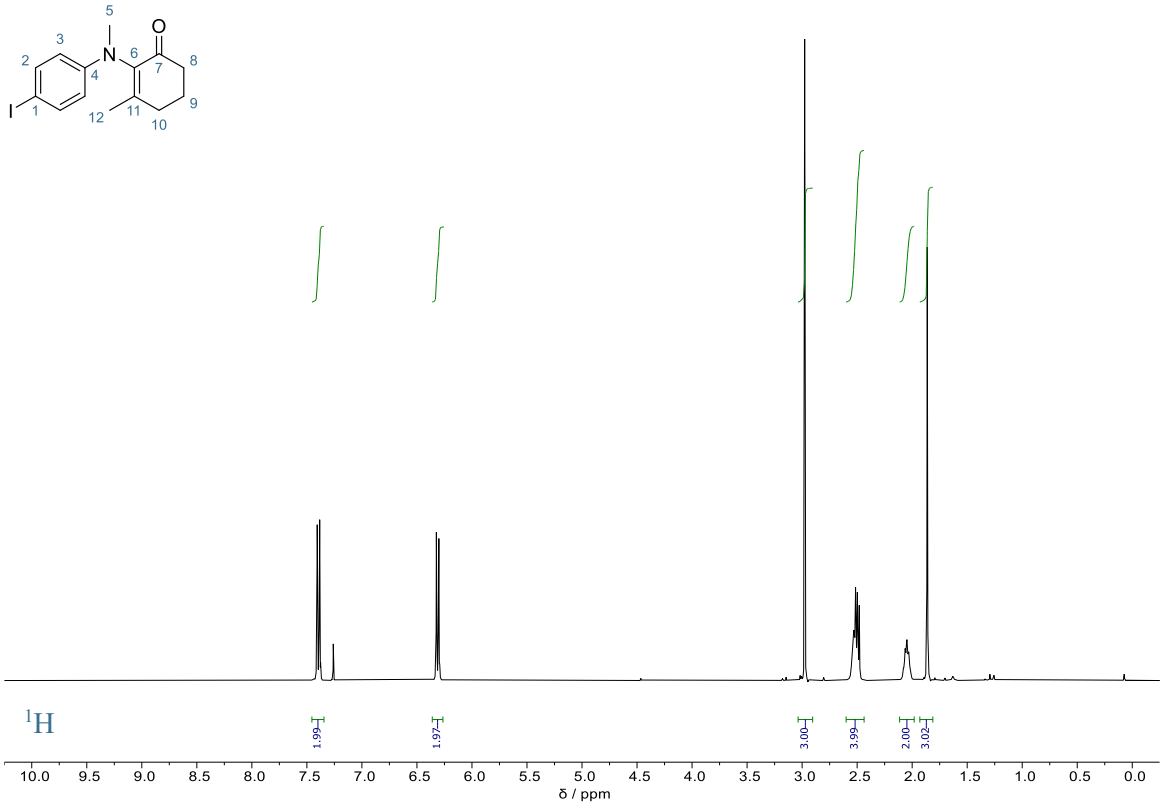
^{13}C

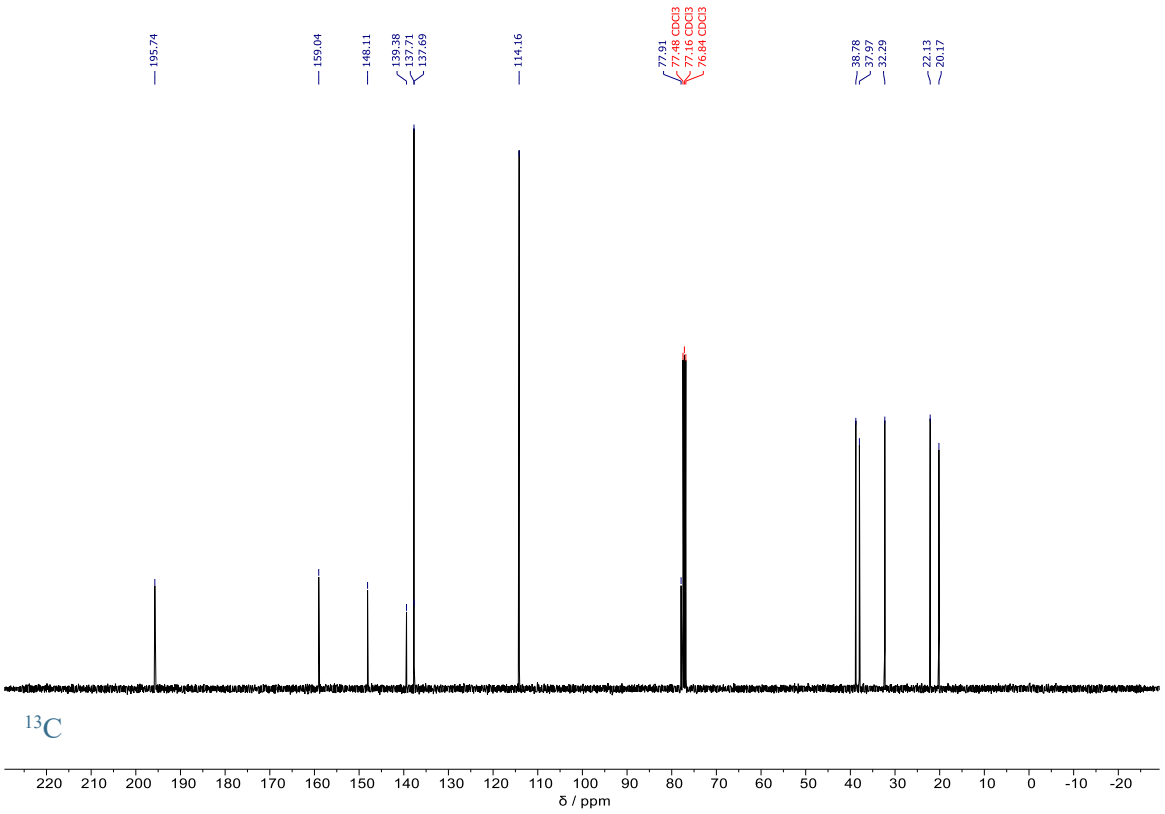
Note: Overlap with signals corresponding to $CHCl_3$ and grease led to over-estimation of certain integrals on the ^1H NMR spectrum above; full assignment of this side-product was enabled by multiplicity-edited HSQC and other 2D NMR experiments.

(*E*)-4-(3,5-Di-*tert*-butylstyryl)benzonitrile, **S66**

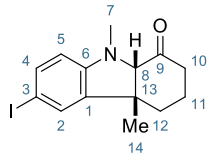


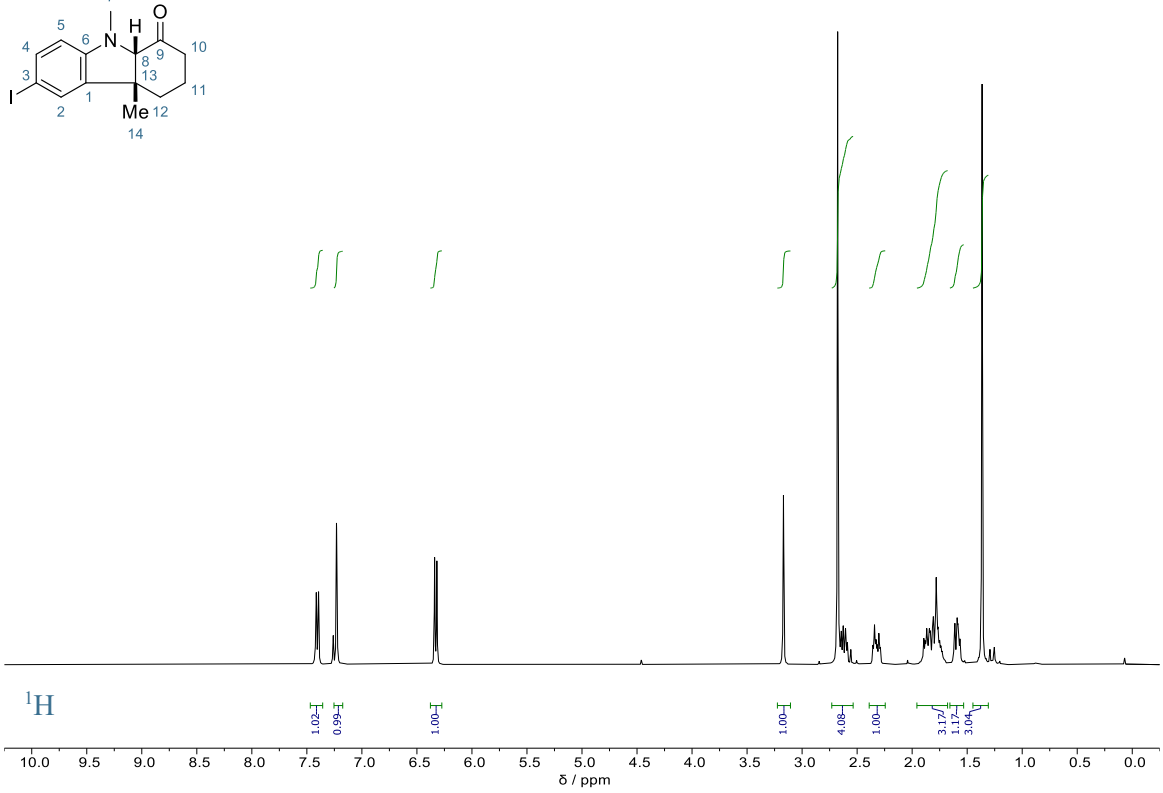
2-((4-Iodophenyl)(methyl)amino)-3-methylcyclohex-2-en-1-one, **S70**

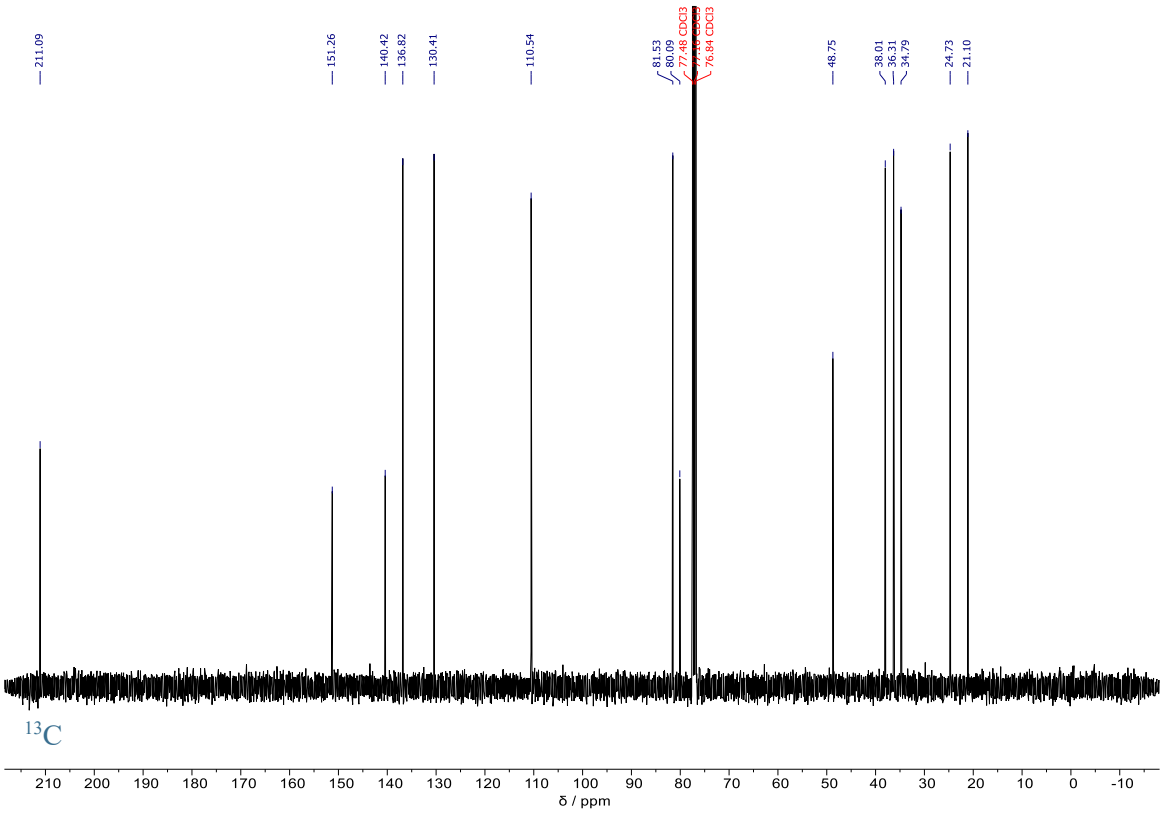




rac-6-Iodo-4a,9-dimethyl-2,3,4,4a,9,9a-hexahydro-1*H*-carbazol-1-one, **S71**

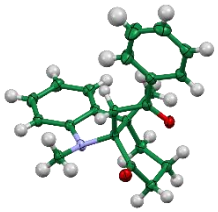






Data S4 – Crystal data and structural refinement

rac-4a,9-Dimethyl-9a-(2-oxo-2-phenylethyl)-2,3,4,4a,9,9a-hexahydro-1*H*-carbazol-1-one, **24**

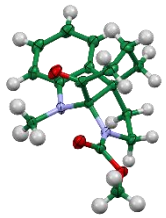


Colourless plates of diffraction quality were grown by vapour diffusion of cyclohexane into a solution of the product in tetrahydrofuran followed by slow evaporation of the resulting mixture.

Identification code	CCDC 2243733 (036OS21)	
Empirical formula	$C_{22}H_{23}NO_2$	
Formula weight	333.43	
Temperature	150 K	
Wavelength	1.54184 Å	
Crystal system	Triclinic	
Space group	P 1	
Unit cell dimensions	a = 9.8591(2) Å	α = 90°
	b = 12.4725(3) Å	β = 90°
	c = 14.9150(4) Å	γ = 90°
Volume	1732.29(7) $Å^3$	
Z	4	
Density (calculated)	1.278 Mg/m^3	
Absorption coefficient	0.641 mm^{-1}	
Crystal size	0.02 x 0.06 x 0.55 mm^3	
Theta range for data collection	4.652 to 76.646°.	
Index ranges	-12<=h<=12, -14<=k<=15, -18<=l<=18	
Reflections collected	41172	
Independent reflections	7210 [R(int) = 0.0560]	
Completeness to theta = 74.347°	99.7%	
Absorption correction	Multi-scan	

Refinement method	Full-matrix least-squares on F^2
Goodness-of-fit on F^2	1.0051
Final R indices [I>2sigma(I)]	R1 = 0.0428, wR2 = 0.1076
R indices (all data)	R1 = 0.0506, wR2 = 0.1146

Methyl 9-methyl-8-oxo-5,6,7,8-tetrahydro-9*H*-8a,4b-(epiminoethano)carbazole-10-carboxylate (racemate), **29**

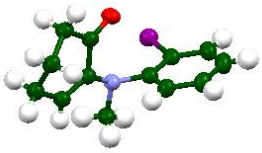


Colourless blocks of diffraction quality were grown by vapour diffusion of *n*-hexane into a solution of the product in dichloromethane.

Identification code	CCDC 2243732 (024OS21)	
Empirical formula	$C_{17}H_{20}N_2O_3$	
Formula weight	300.36	
Temperature	150 K	
Wavelength	1.54184 Å	
Crystal system	Orthorhombic	
Space group	P 2_1 2_1 2_1	
Unit cell dimensions	a = 8.39070(10) Å	α = 90°
	b = 11.82120(10) Å	β = 90°
	c = 15.2686(2) Å	γ = 90°
Volume	1514.43(3) $Å^3$	
Z	4	
Density (calculated)	1.317 Mg/m^3	
Absorption coefficient	0.739 mm^{-1}	
Crystal size	0.11 x 0.18 x 0.20 mm^3	
Theta range for data collection	4.731 to 76.584°.	
Index ranges	-10<=h<=10, -14<=k<=14, -19<=l<=16	
Reflections collected	35743	
Independent reflections	3171 [R(int) = 0.0463]	
Completeness to theta = 76.584°	99.6%	
Absorption correction	Multi-scan	
Refinement method	Full-matrix least-squares on F^2	

Goodness-of-fit on F^2	0.9983
Final R indices [I>2sigma(I)]	R1 = 0.0275, wR2 = 0.0715
R indices (all data)	R1 = 0.0288, wR2 = 0.0731

2-((2-Iodophenyl)(methyl)amino)cyclohex-2-en-1-one, **41**



Colourless needles of diffraction quality were grown by vapour diffusion of *n*-hexane into a solution of the product in dichloromethane.

Identification code	CCDC 2330002 (007mjh23)	
Empirical formula	$C_{13}H_{14}I_1N_1O_1$	
Formula weight	327.16	
Temperature	150 K	
Wavelength	1.54184 Å	
Crystal System	Monoclinic	
Space Group	P $2_1/c$	
Unit cell dimensions	a = 7.84780(10) Å	α = 90°
	b = 24.3054(2) Å	β = 106.1247(13)°
	c = 6.71110(10) Å	γ = 90°
Volume	1229.74(3) Å^3	
Z	4	
Density	1.77 Mg m^{-3}	
Absorption coefficient	20.282 mm^{-1}	
Crystal size	0.04 × 0.10 × 0.28 mm^3	
Theta range for data collection	3.622 to 76.086°	
Index ranges	-9<=h<=9, -30<=k<=30, -8<=l<=8	
Reflections collected	60035	
Independent reflections	2516 [R(int) = 0.034]	
Completeness to theta = 76.169°	99.8%	
Absorption correction	Multi-scan	
Refinement method	Full-matrix least squares on F^2	
Goodness-of-fit of F^2	0.9575	
Final R indices [I>2sigma(I)]	R1 = 0.0172, wR2 = 0.0463	

R indices (all data)	R1 = 0.0177, wR2 = 0.0467